

UNIVERSITAT DE BARCELONA

Epigenetic information contained in male germ cell chromatin-associated proteins and its potential impact on the reproductive function

Alberto de la Iglesia Rodríguez

ADVERTIMENT. La consulta d'aquesta tesi queda condicionada a l'acceptació de les següents condicions d'ús: La difusió d'aquesta tesi per mitjà del servei TDX (**www.tdx.cat**) i a través del Dipòsit Digital de la UB (**diposit.ub.edu**) ha estat autoritzada pels titulars dels drets de propietat intel·lectual únicament per a usos privats emmarcats en activitats d'investigació i docència. No s'autoritza la seva reproducció amb finalitats de lucre ni la seva difusió i posada a disposició des d'un lloc aliè al servei TDX ni al Dipòsit Digital de la UB. No s'autoritza la presentació del seu contingut en una finestra o marc aliè a TDX o al Dipòsit Digital de la UB (framing). Aquesta reserva de drets afecta tant al resum de presentació de la tesi com als seus continguts. En la utilització o cita de parts de la tesi és obligat indicar el nom de la persona autora.

ADVERTENCIA. La consulta de esta tesis queda condicionada a la aceptación de las siguientes condiciones de uso: La difusión de esta tesis por medio del servicio TDR (**www.tdx.cat**) y a través del Repositorio Digital de la UB (**diposit.ub.edu**) ha sido autorizada por los titulares de los derechos de propiedad intelectual únicamente para usos privados enmarcados en actividades de investigación y docencia. No se autoriza su reproducción con finalidades de lucro ni su difusión y puesta a disposición desde un sitio ajeno al servicio TDR o al Repositorio Digital de la UB. No se autoriza la presentación de su contenido en una ventana o marco ajeno a TDR o al Repositorio Digital de la UB (framing). Esta reserva de derechos afecta tanto al resumen de presentación de la tesis como a sus contenidos. En la utilización o cita de partes de la tesis es obligado indicar el nombre de la persona autora.

WARNING. On having consulted this thesis you're accepting the following use conditions: Spreading this thesis by the TDX (**www.tdx.cat**) service and by the UB Digital Repository (**diposit.ub.edu**) has been authorized by the titular of the intellectual property rights only for private uses placed in investigation and teaching activities. Reproduction with lucrative aims is not authorized nor its spreading and availability from a site foreign to the TDX service or to the UB Digital Repository. Introducing its content in a window or frame foreign to the TDX service or to the UB Digital Repository is not authorized (framing). Those rights affect to the presentation summary of the thesis as well as to its contents. In the using or citation of parts of the thesis it's obliged to indicate the name of the author.



UNIVERSITAT DE BARCELONA

Epigenetic information contained in male germ cell chromatin-associated proteins and its potential impact on the reproductive function

Doctoral Thesis

Alberto de la Iglesia Rodríguez

Barcelona, September 2022

Doctoral Thesis

Epigenetic information contained in male germ cell chromatin-associated proteins and its potential impact on the reproductive function

Doctoral Thesis report submitted by

Alberto de la Iglesia Rodríguez

To obtain the

Doctoral Degree by the University of Barcelona

within the

Doctoral Programme in Medicine and Translational Research of the Faculty of Medicine and Health Sciences, University of Barcelona

Work developed under the supervision of

Dr Rafael Oliva Virgili
Dr Judit Castillo Corullón

As part of the

Molecular Biology of Reproduction and Development Research Group, Genetics Unit, Department of Biomedical Sciences, Faculty of Medicine and Health Sciences, **University of Barcelona**, and August Pi i Sunyer Biomedical Research Institute (**IDIBAPS**)

In Barcelona, September 2022

Co-Supervisor	Co-Supervisor	Author
Dr Rafael Oliva Virgili	**Dr Judit Castillo Corullón**	**Alberto de la Iglesia Rodríguez**

0.

INDEX

INDEX

1 LIST OF ARTICLES THAT COMPRISE THE THESIS 9

2 SUMMARY 13

3 INTRODUCTION 21

3.1 Testicular and post-testicular events shaping the sperm cell 23
3.1.1 Spermatogenesis 23
3.1.2 The gradual but synergic process of nucleo-histone to nucleo-protamine transition 28
3.1.3 The orchestrated regulation of the nucleo-histone to nucleo-protamine transition 31
3.1.3.1 Posttraslational modifications of histones, histone variants, transition proteins, and protamines 31
3.1.3.2 Proteins modulating posttranslational modifications 32
3.1.3.1 Post meiotic gene expression program 36
3.1.4 Extra-testicular sperm maturation 40

3.2 The human mature sperm 42
3.2.1 Main parts of human mature sperm 42
3.2.2 Human mature sperm chromatin 42
3.2.2.1 Human sperm protamines 45
3.2.2.2 The structural organization of the nucleo-protamine 51

3.3 Sperm contribution to fertilization and beyond 54
3.3.1 Post-fertilization events: zygotic male pronuclear reprogramming 56

3.4 Male infertility 58
3.4.1 Evaluation of seminal parameters 59
3.4.2 Evaluation of testicular histology 60
3.4.2.1 Testicular tumors 62
3.4.3 Evaluation of unexplained male infertility 65
3.4.3.1 Protamine levels and male infertility 65
3.4.3.2 Sperm DNA fragmentation 66
3.4.3.3 Lifestyle and sociodemographic factors 67
3.4.4 Sperm selection for assisted reproduction techniques to overcome male infertility 69

4 HYPOTHESIS AND OBJECTIVES 71

4.1 Hypothesis 73

4.2 Objectives 75

5 RESULTS 77

5.1 CHAPTER 1. The impact of testicular pathologies and sperm quality on histone acylations regulating the nucleo-histone to nucleo-protamine transition 79
5.1.1 Work 1: Histone H4 acetylation is dysregulated in active seminiferous tubules adjacent to testicular tumours 81
5.1.2 Work 2: H4K5 butyrylation coexist with acetylation during human spermiogenesis and are retained in the mature sperm chromatin 107

5.2 CHAPTER 2: Layers of epigenetic information contained in the protein fraction of the nucleo-protamine domain 131
5.2.1 Work 3: Protamine Characterization by Top-Down Proteomics: Boosting Proteoform Identification with DBSCAN 133
5.2.2 Work 4: Alterations in the abundance of specific protamine proteoforms related to sperm chromatin packaging, obesity status, and age in men with unexplained infertility 159
5.2.3 Work 5: Protein-protein interaction analysis suggest additional regulatory roles for SRPK1 and PP1γ in male germ cell chromatin remodeling during mouse spermiogenesis 183

5.3 CHAPTER 3: Nanoscale insights into mature sperm chromatin reveals a fractal supramolecular structure which is altered in patients with double strand DNA breaks 215
5.3.1 Work 6: Nanoscale insights into human sperm chromatin through synchrotron light small-angle X-ray scattering (SAXS): fine-tuning the current model of paternal genome packaging *in vivo* 217

6 DISCUSSION 235

6.1 Acetylation and butyrylation marks on histone H4 as potential regulators of human male germ cells' chromatin remodeling 238

6.2 Epigenetic information contained in the less accessible fraction of the sperm chromatin: the role of protamine proteoforms and associated proteins 242

6.3 Nanoscale features of human sperm chromatin organization 247

7 CONCLUSIONS 251

8 REFERENCES 255

9 APPENDIX 289

10 ABBREVIATIONS 343

1.

LIST OF ARTICLES

The present thesis, written as a collection of articles, comprises **6 scientific works** that give answers to a total of 3 main objectives and the corresponding subobjectives. Two of the articles are already published, one is currently under revision, and 3 are included in form of manuscripts in preparation. Additionally, a review accepted for publication is included in the appendix.

Chapter 1

Barrachina F*, **de la Iglesia A***, Jodar M, Soler-Ventura A, Mallofré C, Rodriguez-Carunchio L, Goudarzi A, Corral JM, Ballescà JL, Castillo J, Oliva R. Histone H4 acetylation is dysregulated in active seminiferous tubules adjacent to testicular tumours. *Hum Reprod*. 2022 Jul 30;37(8):1712-1726. doi:10.1093/humrep/deac130.

***First author, IF 6.353, D1 (Obstetrics & Gynecology)**

de la Iglesia A, Jauregi P, Jodar M, Barrachina F, Ded L, Mallofré C, Rodríguez-Carunchio L, Corral JM, Ballescà JL, Komrskova K, Castillo C, Oliva R. H4K5 butyrylation coexist with acetylation during human spermiogenesis and are retained in the mature sperm chromatin. *Int J Mol Sci*, under revision.

First author, IF 6.208, Q1 (Biochemistry & Molecular Biology)

Chapter 2

Arauz-Garofalo G, Jodar M, Vilanova M, **de la Iglesia A,** Castillo J, Soler-Ventura A, Oliva R, Vilaseca M, Gay M. Protamine Characterization by Top-Down Proteomics: Boosting Proteoform Identification with DBSCAN. *Proteomes*. 2021 Apr 30;9(2):21. doi: 10.3390/proteomes9020021.

Fourth author, IF N/A (indexed in JCR), Q2 (Biochemistry, SJR)

Castillo J*, Gay M*, **de la Iglesia A***, Arauz-Garofalo G, Vilanova M, Corral JM, Guimerà M, Vilaseca M, Jodar M, Oliva R. Alterations in the abundance of specific protamine proteoforms related to sperm chromatin packaging, obesity status, and age in men with unexplained infertility. *Manuscript in preparation*.

***First author**

de la Iglesia A, Blanco M, Jodar M, Cocquet J, Castillo J, Oliva R. Protein-protein interaction analysis suggest additional regulatory roles for SRPK1 and PP1γ in male germ cell chromatin remodeling during mouse spermiogenesis. *Manuscript in preparation*.

First author

Chapter 3

de la Iglesia A, Huck-Iriart C, Malfois M, Leiva M, Jodar M, Guimerà M, Peralta S, Corral JM, Oliva R, Castillo J. Nanoscale insights into human sperm chromatin through synchrotron light small-angle X-ray scattering (SAXS): fine-tuning the current model of paternal genome packaging in vivo. *Manuscript in preparation*.

First author

Appendix

de la Iglesia A, Jodar M, Oliva R, Castillo J. Insights into the sperm chromatin and implications for male infertility from a protein perspective. *WIREs Mech Dis*[†]. 2022 Accepted for publication (12/9/2022).

First author

[†] Previously named Wiley Interdisciplinary Reviews-Systems Biology and Medicine (ISSN 1939-5094, **IF 7.288, Q1 in the category of Medicine, Research & Experimental**)

2.

SUMMARY

TÍTULO

"La información epigenética contenida en las proteínas asociadas a la cromatina de las células germinales masculinas y su posible impacto en la función reproductiva"

INTRODUCCIÓN

Contrario a la idea tradicional de que el gameto masculino es un simple portador del ADN paterno, los avances científicos de las últimas décadas han revelado que el espermatozoide aporta diferentes niveles de información epigenética al embrión. Así, las modificaciones postraduccionales (MPTs) de proteínas asociadas al DNA y la distribución diferencial del genoma paterno a lo largo de la cromatina, junto a una compleja población de ARNs no codificantes y proteínas con funciones de regulación génica, tendrían un impacto no solo en la fecundación si no también en el desarrollo embrionario preimplantacional. La cromatina espermática está formada principalmente por la asociación entre el ADN y dos tipos de proteínas diferentes, histonas y protaminas, que contienen MPTs específicas y presentan distintos estados de compactación del genoma, lo que da lugar a un nuevo concepto de marca epigenética exclusivo para esta célula. La relevancia y peculiaridades de la cromatina del gameto masculino han atraído interés a lo largo de los años, y se han realizado muchos esfuerzos para desentrañar todo lo que la confiere, no solo a nivel de espermatozoide maduro sino también durante la diferenciación de las espermátidas en la última fase de la espermatogénesis. Sin embargo, la cromatina de las células germinales masculinas es tan atractiva como compleja, requiriendo la adaptación de técnicas convencionales y la aplicación de otras nuevas para su estudio. A pesar de ello, se han conseguido identificar muchos factores importantes en la regulación y formación de la cromatina espermática, así como en la correcta transmisión de la información epigenética paterna al zigoto. Así, las MPTs de protaminas e histonas, tanto durante el desarrollo del gameto masculino como ya una vez madurados, y la estructura resultante tras la compactación de la cromatina espermática, surgen como rasgos interesantes a estudiar en mayor profundidad para descifrar su implicación en los casos de infertilidad masculina de origen desconocido.

HIPÓTESIS

La fracción proteica de la cromatina de las células germinales masculinas (histonas y protaminas, entre otras proteínas de la cromatina, y sus MPTs) podría tener un papel epigenético durante la maduración del espermatozoide y en eventos posteriores a la fertilización. Además, su alteración podría estar involucrada en diferentes patologías testiculares o infertilidad masculina de origen desconocido, e incluso tener un impacto sobre la conformación global (ultraestructura) de la cromatina espermática.

OBJETIVOS

La tesis doctoral tiene tres objetivos principales: 1) explorar MPTs de histonas involucradas en el proceso de transición de nucleo-histona a nucleo-protamina y su potencial epigenético, 2) Aumentar el conocimiento actual sobre las proteoformas de las protaminas, con especial atención en la fosforilación de las protaminas, y 3) Aplicar estrategias innovadoras al estudio de la cromatina espermática y errores de compactación, mediante el uso de dispersión de rayos X de ángulo pequeño (SAXS) con luz de sincrotrón para la caracterización del núcleo espermático a nivel de nanoescala. A su vez, el objetivo 1 se subdivide en 1a) describir alteraciones del patrón que sigue la acetilación global de la histona H4 durante la espermatogénesis en diferentes patologías testiculares, y 1b) caracterizar acilaciones específicas (acetilación y butirilación en H4K5) durante la espermatogénesis y en espermatozoide maduro, así como su relación con la calidad espermática. El objetivo 2 comprende 2a) definir el perfil normal de proteoformas de las protaminas mediante proteómica top-down e identificar alteraciones en las proteoformas de las protaminas en relación con infertilidad de origen desconocido, y 2b) explorar la red proteica interactiva de proteínas que modulan la fosforilación de las protaminas.

MÉTODOS

Se han utilizado una combinación de técnicas convencionales (recolección y procesamiento de muestras de semen humanas y de tejido testicular de ratón, inmunohistoquímica, inmunofluorescencia, western blot convencional, western blot Odyssey® de fluorescencia, extracción de RNA y RT-PCR, extracción y cuantificación de proteínas solubles, extracción, purificación, y análisis de proteínas básicas nucleares del espermatozoide, e inmunoprecipitación proteica), técnicas de alto rendimiento (proteómica top-down y bottom-up) y técnicas de alta resolución para la evaluación de ultraestructuras (SAXS con luz de sincrotrón), junto a análisis estadísticos exhaustivos para establecer las diferencias entre los diferentes grupos analizados.

RESULTADOS Y CONCLUSIONES PRINCIPALES

Los resultados que se incluyen en la presente tesis doctoral arrojan luz sobre la cromatina de las células germinales masculinas humanas y su potencial epigenético, tanto en el espermatozoide maduro como durante su proceso de diferenciación en el testículo. En el Capítulo 1 se describen MPTs en la histona H4 a nivel global y en el residuo específico Lys5 (H4K5), clave en el proceso de remodelación de la cromatina del espermatozoide humano durante la espermiogénesis, mostrando un patrón testicular característico que apoya su implicación en la regulación de esta etapa, de forma similar a la descrita en modelos de ratón. El comportamiento de la acetilación en H4 y H4K5 es bastante similar, mientras que la recientemente descrita butirilación en H4K5 presenta notables

diferencias que podrían tener impacto en la regulación temporal de la incorporación de protaminas a la cromatina (proceso conocido como transición nucleo-histona a nucleo-protamina). Por otro lado, hemos encontrado una alteración de la acetilación global en H4 en pacientes con patologías testiculares que no se observa cuando se estudia el residuo específico H4K5, lo que apunta a que pueda estar de alguna manera protegido frente a afectaciones testiculares, permaneciendo estable para favorecer la progresión de la espermatogénesis. Además, la forma en que la butirilación y la acetilación de H4K5 se retienen en el espermatozoide humano maduro apunta a una posible distribución diferencial de ambas MPTs a lo largo del genoma paterno, con posibles efectos en eventos posteriores a la fertilización. Entre las proteínas asociadas a la cromatina en el núcleo del espermatozoide, no sólo las histonas llevan MPTs, sino también las protaminas. En el Capítulo 2, el uso de un protocolo de análisis establecido por nuestro grupo para datos de proteómica top-down ha permitido la descripción fiable de proteoformas de protaminas en el espermatozoide humano. Su uso a nivel comparativo ha conseguido identificar abundancias alteradas de proteoformas de las protaminas en pacientes infértiles de origen desconocido en función del estado de protaminación de su cromatina, así como de su peso y edad. Los cambios asociados a obesidad o edad avanzada afectaron a proteoformas de protamina 1 (P1) modificadas post-traduccionalmente, principalmente por fosforilación. Mediante el estudio en testículo de ratón de las proteínas SRPK1 y PP1γ, involucradas en la fosforilación de las protaminas, se han revelado posibles papeles reguladores de ambas proteínas durante la espermiogénesis no descritos anteriormente, mediante su asociación con proteínas implicadas en regulación transcripcional y traslacional, así como en la remodelación de la cromatina de las células germinales. El estudio de proteoformas de protaminas en pacientes con una alteración en la abundancia relativa de protamina 1 (P1) y protamina 2 (P2) evidenciaron una acumulación de formas inmaduras de P2, lo que sugiere errores de procesamiento de su proteína precursora (Pre-P2). Sin embargo, como se detalla en el Capítulo 3, estas alteraciones no parecen traducirse en cambios estructurales de la cromatina a nivel nanoescala. A través del uso de dispersión de rayos X de ángulo pequeño (SAXS) utilizando luz de sincrotrón en núcleos de espermatozoides humanos normales, hemos detectado la presencia de una organización de la cromatina que se comporta de manera jerárquica en 2 niveles, en los que reorganizaciones supramoleculares de radio de giro ~67 nm surgen a partir de la agregación de pequeñas subunidades altamente compactadas, lisas y muy estables con radio equivalente ~7.7 nm. Aunque estas estructuras serian estables en presencia de un desequilibrio entre las abundancias relativas de protaminas, los agregados supramoleculares se afectarían por roturas de doble cadena de ADN, lo que apunta a una fuerte interconexión entre la estabilidad genómica y la arquitectura de la cromatina en el espermatozoide humano.

Así, los resultados derivados de esta tesis revelan características hasta ahora desconocidas sobre la composición y estructura de la cromatina de las células germinales masculinas, y refuerzan el potencial epigenético de la fracción proteica de la cromatina paterna en eventos más allá de la fertilización.

TITLE

"Epigenetic information contained in male germ cell chromatin-associated proteins and its potential impact on the reproductive function"

INTRODUCTION

Contrasting the traditional idea of the male gamete being a simple carrier of the paternal DNA, evidence in the last decades revealed that the sperm cell provides the embryo with different layers of epigenetic information, which is not limited to DNA methylation and non-coding RNAs but also involves the protein fraction of the sperm chromatin. Posttranslational modifications (PTMs) of chromatin-associated proteins, together with a complex population of proteins with gene regulatory roles, would also have an impact in fertilization and pre-implantation embryo development. Furthermore, the sperm chromatin, understood as the association between DNA and two different types of proteins, histones and protamines, both bearing PTMs, and resulting in two distinct genome compaction states, arises as a new concept of epigenetic mark that is exclusive for the male gamete. The relevance and peculiarities of sperm chromatin have attracted interest over the years, and many efforts have been made to disentangle it, not only in mature sperm but also during spermatid differentiation. However, male germ cells' chromatin is as attractive as challenging, and its study requires the adaptation of conventional techniques or application of new ones. Despite that, many important factors have been related with the regulation and formation of the sperm chromatin, as well as with the correct transmission of parental epigenetic information to the zygote. Thus, protamines, histones, and their PTMs, both during male gamete development and once matured, as well as the peculiarly compacted chromatin structure of mature sperm, emerge as interesting features to be further studied to increase the current knowledge on the epigenetic content of the protein fraction of sperm chromatin and its potential involvement in cases of unexplained male infertility.

HYPOTHESIS

The protein fraction of the germ cell's chromatin (histones and protamines, among other chromatin proteins, and their PTMs) could have an epigenetic role during sperm maturation and towards events beyond fertilization. In addition, its alteration could represent underlying causes of different testicular pathologies or unexplained human male infertility, and an impaired sperm chromatin state could have an impact towards the global sperm chromatin ultrastructure

OBJECTIVES

The objectives of this doctoral thesis are: 1) To explore histone PTMs involved in the process of nucleo-histone to nucleo-protamine transition and their epigenetic potential, 2) To increase the knowledge on protamine proteoforms, with a special focus on protamine phosphorylation, and 3) To apply innovative approaches to the study of the sperm chromatin and chromatin compaction defects through the use of small X-ray scattering (SAXS) with synchrotron light for the nanoscale characterization of the sperm nucleus.

Besides, objective 1 is subdivided into 1a) to describe alterations of a global histone H4 acetylation pattern during the spermatogenesis in different testicular affections, and 1b) to characterize specific novel acylations during spermatogenesis and in mature sperm (H4K5 acetylation and butyrylation) and their relationship with sperm quality. In turn, objective 2 comprises 2a) to define the normal profile of protamine PTMs through top-down proteomics and to identify alterations in the protamine proteoforms related with unexplained infertility and 2b) to explore the protein interactive networks of proteins modulating protamine phosphorylation.

METHODS

A combination of conventional approaches (human semen samples and mouse testicular tissue collection and processing, immunohistochemistry, immunofluorescence, conventional western blot, Odyssey® fluorescent western blot, RNA extraction and RT-PCR, soluble protein extraction and quantification, sperm basic nuclear protein extraction and analysis, and protein immunoprecipitation), high-throughput techniques (top-down y bottom-up proteomics), and high-resolution techniques for ultrastructural evaluation (SAXS with synchrotron light), were used, together with exhaustive statistical analyses to evaluate differences among the groups analyzed.

MAIN RESULTS AND CONCLUSIONS

The findings discussed in the present doctoral thesis shed new light into the chromatin of human male germ cells and its epigenetic potential, both during sperm testicular formation and in the mature sperm cell. Chapter 1 describes PTMs on histone H4 and the specific residue of Lys5 (H4K5), key regulator of the chromatin remodeling process taking place during spermiogenesis, showing a characteristic testicular pattern supporting their involvement in human spermiogenic regulation similar to that described in mouse models. The behavior of the well-characterized H4 and H4K5 acetylation along spermatogenesis present some similarities and remarkable differences to that of the recently described butyrylation on H4K5, which could impact the temporal regulation of the human nucleo-histone to nucleo-protamine (NH-NP) transition. Whereas global H4 acetylation was altered in patients with testicular pathologies, H4K5 seems to be somehow protected to external

perturbations, remaining stable. Besides, the way in which H4K5 butyrylation and acetylation are retained in human mature sperm point out a potential differential distribution alongside the paternal genome with potential effects in post-fertilization events.

Of note, protamines also bear PTMs. In Chapter 2, the data analysis pipeline for top-down proteomics set up by our team allowed the reliable description of protamine proteoforms in human sperm, evidencing altered abundance of some proteoforms in patients with biologically impaired chromatin and patients influenced by their lifestyle or demographic characteristics. Age- and weight-associated changes affected posttranslationally modified protamine 1 (P1) protamine proteoforms, mainly by phosphorylations. The study in the mouse testis of the protamine modulating proteins SRPK1 and PP1γ revealed potential role of both proteins not characterized so far in regulatory mechanisms during spermiogenesis, through their association with proteins participating in transcriptional and translational regulation, as well as in chromatin remodeling. Interestingly, when focusing on molecular characteristics of sperm chromatin maturity, as the relative levels of protamines, we observed an accumulation in protamine 2 (P2) immature forms at the proteoform level, suggesting potential P2 processing errors. However, as disclosed in Chapter 3, this alteration does not induce ultrastructural nanoscale changes in sperm chromatin. By applying Small-Angle X-ray Scattering (SAXS) using synchrotron light for the study of normal human sperm nuclei in solution, we described the presence of a 2-level chromatin organization in which supramolecular arrangements of radius ~67 nm arise from the aggregation of highly compacted, smooth, and very stable small subunits with radius ~7.7 nm. Strikingly, supramolecular aggregates were altered in patients with pathological levels of double strand DNA breaks, pointing out to strong interconnection between genomic stability and chromatin architecture.

Therefore, results derived from this doctoral tesis reveal male germ cell's chromatin features, both about its composition and structure, that support the epigenetic potential of the protein fraction of the paternal chromatin in events beyond fertilization.

3.

INTRODUCTION

3.1 Testicular and post-testicular events shaping the sperm cell

3.1.1 Spermatogenesis

Spermatogenesis is the complex process of cell differentiation involving marked genetic, structural, and functional changes, in which four haploid male gametes raise from a single diploid cell, the spermatogonia. The spermatogenic process takes place in the testis and starts when young males reach puberty. Its estimated mean duration is 64 days in humans, ranging from 42 to 76 days, and it comprises three well-characterized phases, illustrated in **Figure 1** (Bolcun-Filas & Handel, 2018; Goossens & Tournaye, 2013; Griswold, 2016; Heller & Clermont, 1963; Misell et al., 2006; Neto et al., 2016):

i) **Mitotic or proliferative phase**, in which A-type spermatogonia, diploid progenitors of the rest of spermatogenic cell types, undergo mitotic divisions to maintain the germ cell niche and promote male fertility throughout the life. According to their heterochromatin content, A-dark (A_d; quiescent, reserve stem cells) and A-pale (A_p; actively replicating, renewing stem cells) spermatogonia are distinguished. The contribution of different molecular factors drives A_p to either self-renew or differentiate into B-type spermatogonia, which divide mitotically once more to produce primary spermatocytes committed to enter meiosis.

ii) **Meiotic phase**, in which primary spermatocytes (4C in terms of DNA content, and 2N in terms of chromosome number) undergo two consecutive reductive meiotic divisions. A first meiotic division (Meiosis I) separates homologous chromosome pairs giving rise to two haploid secondary spermatocytes (1N, 2C), which consecutively go through a second meiotic division (Meiosis II) that produces two haploid round spermatids with half of the DNA content after segregation of sister chromatids (1N, 1C). Therefore, four haploid round spermatids are achieved from each diploid primary spermatocyte.

iii) **Spermiogenesis**, or **differentiation phase**, comprising the development of round spermatids into yet immature but hydrodynamically shaped testicular sperm without the need of any extra cellular division. This differentiation is achieved through very aggressive cellular processes, resulting in an elongation involving marked nuclear, cytoplasmic, and morphological changes. It includes the formation of the acrosome (arising from the Golgi apparatus) and flagellum, nuclear condensation through the process of nucleohistone to nucleoprotamine (NH-NP) transition (see Section 1.1.2 for more details), and cytoplasm loss, enabling a streamlining architechture (Hecht, 1998; Muciaccia et al., 2013; Neto et al., 2016; Oliva & Castillo, 2011; Oliva & Dixon, 1991). This extreme nuclear compaction and the loss of cytoplasm makes the sperm cells both transcriptionally and translationally silent.

Despite spermatogonial development begins at puberty, gametogenesis in humans starts early in embryo development, when primordial germ cells (PGCs), the first cells of the germ lineage, are originated in the epiblast from the inner cell mass. During fetal development, PGCs migrate towards the developing gonads in the genital ridge, where become gonocytes. In XY embryos properly expressing the sex determining region Y (*SRY*) gene on chromosome Y, which control sex-determining pathways, gonocytes will futher mature in the developing testis into pre-spermatogonia, which are blocked until birth. After birth, pre-spermatogonia migrate to the basement membrane to stablish the first pool of spermatogonial stem cells that will maintain spermatogenesis throught postpubertal life (Rijlaarsdam et al., 2014, Phillips et al., 2010).

In the postpubertal testis, male germ cells' differentiation specifically occurs inside seminiferous tubules, which are coiled structures delimited by a basal membrane that contain developing germ cells embedded in supporting somatic Sertoli cells, as represented in **Figure 1** (Bolcun-Filas & Handel, 2018; Griswold, 2016; Heller & Clermont, 1963; Misell et al., 2006; Neto et al., 2016). Sertoli cells' cytoplasm is constantly changing and spreads through ramifications all over the epithelium to maintain the correct progression of spermatogenesis, supplying the germ cells with the necessary factors (Chalmel et al., 2014).

Interestingly, developing male germ cells do not complete cytoplasmic divisions (cytokinesis), neither during mitosis nor meiosis. Therefore, big clones of differentiated daughter cells deriving from a single precursor (mature spermatogonium), are interconnected by cytoplasmic bridges, creating a syncytium. Cytoplasmic bridges remain until the final stage of testicular sperm maturation once they are released to the lumen of seminiferous tubules. This fact explains why mature sperm appear at the same time in any area of the seminiferous tubule. Contrary to the female gamete (the oocyte), the spermatozoon experiences most of its differentiation process during the last spermatogenic phase, after undergoing meiosis, as haploid cells. Thus, the importance of this syncytial organization relies on the fact that it creates a common cytoplasm that is shared between neighboring male germ cells, allowing haploid cells disposing all products of a complete diploid genome. This way, spermatozoa carrying Y chromosome can also benefit from essential proteins encoded by specific X chromosome genes, and vice-versa. As a result, diploid genome drive sperm differentiation in a similar way than oocytes. As differentiating, the sperm cell disposes of cellular components that will not be needed, such as ribosomes or Golgi apparatus, which together with other organelles will be eliminated through residual bodies that are still connected through cytoplasmic bridges. These residual bodies will be subsequently phagocyted by Sertoli cells (Bolcun-Filas & Handel, 2018; Griswold, 2016; Heller & Clermont, 1963; Misell et al., 2006; Neto et al., 2016).

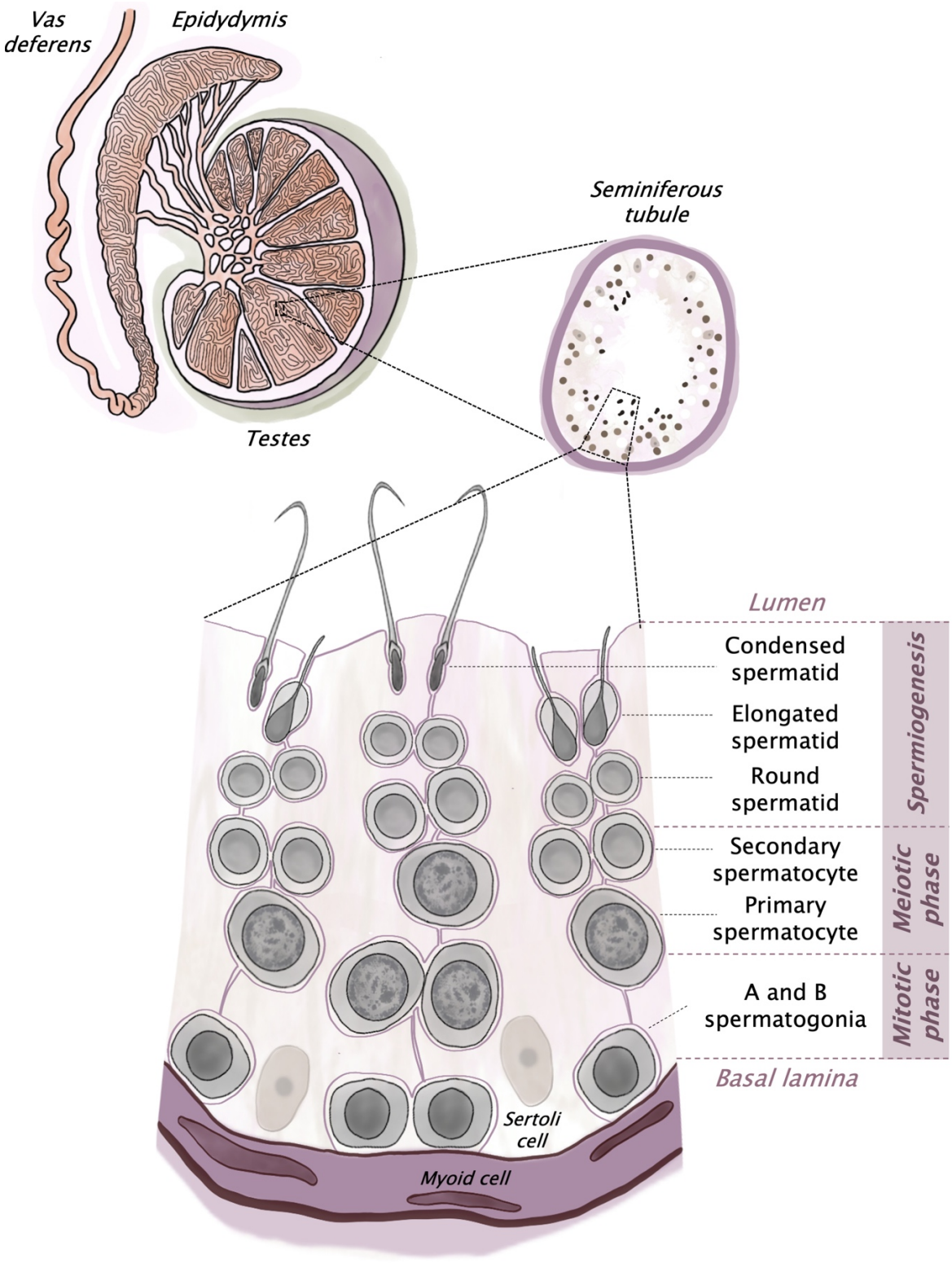


Figure 1. Male germ cell differentiation inside the testis. Spermatogenesis takes places in the testis, particularly inside seminiferous tubules, occurring from the basal lamina to the lumen. Developing male germ cells coexist with somatic supporting Sertoli cells. Once generated, testicular sperm are released to the lumen and travel through the rest of the male reproductive tract to complete their maturation. Illustration based on (R. Sharma & Agarwal, 2011).

Germ cells acquire a highly organized distribution within the seminiferous epithelium, with the less mature cells placed at the basal compartment. Thus, spermatogenesis spatially occurs from the basal part of the seminiferous tubule to the lumen, releasing the condensed spermatids to start post-testicular maturation (Griswold, 2016; Neto et al., 2016). it has been proposed that germ cells migrate throughout the human seminiferous epithelium according to a helical model, following organizational patterns based on spiral geometry, as represented in **Figure 2**. Therefore, a single cross-section of a seminiferous tubule will show multiple spermatogenic stages, opposite to the unique-stage model found in most mammals (Griswold, 2016; Muciaccia et al., 2013; Schulze & Rehder, 1984). Every 16 days, human spermatogonia start a new differentiation cycle, so different generations of germ cells are present in the seminiferous epithelium during the 64 days that take the whole spermatogenic process. This results in series of germ cell's repeating associations that have allowed their classification into 12 different seminiferous epithelium stages (**Figure 3**) (Muciaccia et al., 2013).

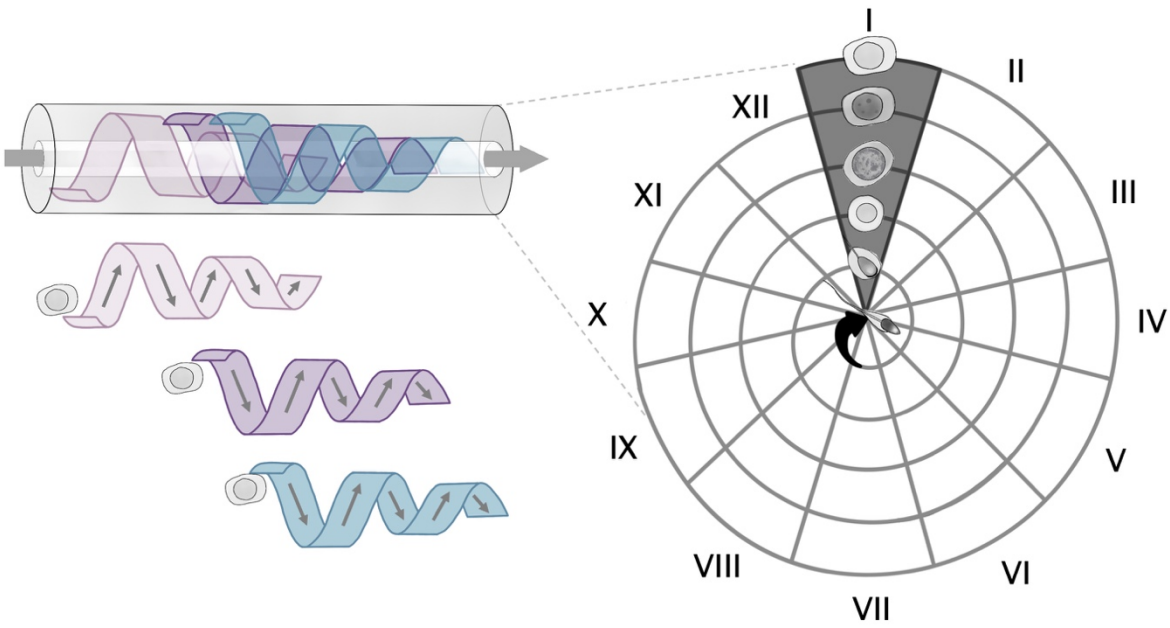


Figure 2. Helical model of human male germ cell development inside the seminiferous tubule. On the top left, a seminiferous tubule is represented. Inside, three hypothetical A-pale spermatogonia (represented below) commit to differentiation. Colored helixes represent differentiation direction (pink, purple, and blue). As a result, seminiferous tubule sections will contain different cell types organized according to different spermatogenic stages. Based on (Griswold, 2016; Schulze & Rehder, 1984).

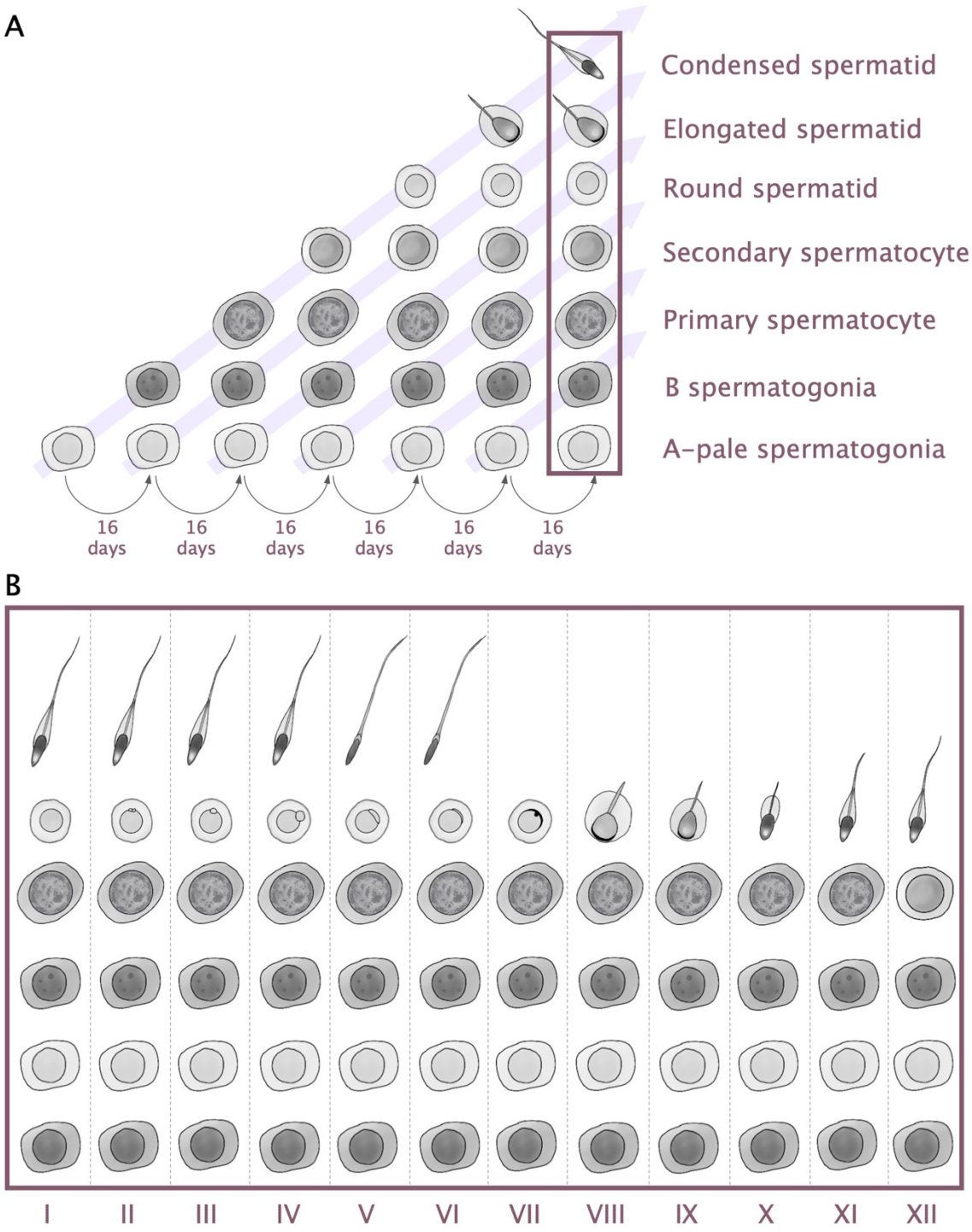


Figure 3. Cycle of the seminiferous epithelium and recurring associations of male germ cells in humans. A) Simplified representation of how the cycle of the seminiferous epithelium is derived. In humans, a spermatogonium commits to start differentiating every 16 days, much more frequently than a whole spermatogenic process (64 days). Therefore, at any point along the seminiferous tubule, germ cells at multiple differentiation stages coexist. Background grey arrows indicate male germ cell development progression, and curved arrows the periodicity of 16 days. **B**) The coexisting male germ cells resulting from single differentiation waves organize into cellular associations that repeat along the seminiferous tubule, allowing their classification into 12 different stages. Based on (Griswold, 2016; Muciaccia et al., 2013).

3.1.2 The gradual but synergic process of nucleo-histone to nucleo-protamine transition

Male germ cells undergo the NH-NP transition during spermiogenesis, a unique process of chromatin remodeling that gives rise to tightly compacted nuclei necessary to produce functional sperm (Christensen & Dixon, 1982; Grimes & Henderson, 1984; Hazzouri et al., 2000; Mezquita, 1985; Oliva et al., 1987; Oliva & Castillo, 2011; Oliva & Mezquita, 1982). It comprises a gradual replacement of the somatic cell-like core histones packaging the DNA by testis-specific histone variants, followed by transition proteins (TPs) 1 and 2 (TP1 and TP2, respectively) and, finally, by protamines (Balhorn, 2007; Barrachina et al., 2018; Castillo, de Mateo, et al., 2011; Gatewood et al., 1987; Kimmins & Sassone-Corsi, 2005; Oliva, 2006; Oliva & Dixon, 1991; Rathke et al., 2014). The process is represented in **Figure 4**. Whereas protamine 1 (P1) is synthetized as mature form, the different mature forms belonging to the family of protamine 2 (P2) arise from the proteolytic cleavage of a common P2 precursor (pre-P2) (Oliva, 2006); please refer to **Section 1.2.1** for further details. The outcome of this process consists of an 85-95% of the paternal human genome (92-98% in mouse) packed by protamines. This partial histone replacement gives rise to two differential chromatin regions that set the basis of one of the most interesting epigenetic marks contained in sperm cells: differential paternal genome distribution into the nucleo-histone domain, representing the most accessible fraction of the genome, and the nucleo-protamine domain, inaccessible and silenced (Arpanahi et al., 2009; Castillo, Amaral, Azpiazu, et al., 2014; S. Hammoud et al., 2009).

By incorporating histone variants and transition proteins, the nucleosome undergoes conformational changes which contribute to its destabilization, inducing open chromatin states that are needed to achieve proper chromatin remodeling. Besides expressing almost all histone variants present in somatic nuclei, male germ cells express additional unique testicular variants of H2A, H2B and H3, therefore containing the largest number of histone variants among all cell types (Barrachina et al., 2018; Boussouar et al., 2008; Ding et al., 2021; Hoghoughi et al., 2018). Testis-specific histone variants such as TH2A, TH2B, and H2BFWT, or other histone variants such as H3.3 and H3.4, present changes in their aminoacidic sequence compared to canonical histones that are responsible of the low-affinity binding to the DNA (Bonisch & Hake, 2012; Boulard et al., 2006; A. Li et al., 2005; Padavattan et al., 2017; Tachiwana et al., 2010; Ueda et al., 2017; Urahama et al., 2016). They have essential roles in male fertility since loss of TH2A and TH2B in mice has been related with impaired histone retention and sterility (Shinagawa et al., 2015), and depletion of the two H3.3 encoding genes (*H3f3a* and *H3f3b*) has been related with male subfertility and sterility in mouse, respectively (Tang et al., 2015; Yuen et al., 2014). Novel histone variants have been recently discovered in the testis, like H2B.K and H2B.N, without specific function yet, likely redundant but vital for unusual chromatin packing (Raman et al., 2022). In turn, TPs assist chromatin decondensation through DNA stabilization in a non-supercoiled state, acting

together with topoisomerases to diminish torsional stress, involved in DNA repair during chromatin remodeling (Akama et al., 1999; Lévesque et al., 1998; J. Singh & Rao, 1988). Formation and repair of transient double strand DNA (dsDNA) breaks are needed for a proper protamine incorporation. Phosphorylated histone variant H2A.X (γH2AX), marker of dsDNA breaks, is localized at the time of histone displacement presumed to be there as response to the arising dsDNA break formation in elongating spermatids (Jha et al., 2017; Leduc et al., 2008; Marcon & Boissonneault, 2004a). Interestingly, γH2AX is the only histone detected within the most attached protein fraction in the sperm chromatin (Castillo, Amaral, Azpiazu, et al., 2014), which may lead to think it could be retained in sperm after participating somehow in protamine incorporation.

While traditional approaches propose that the incorporation of histone variants, TPs, and protamines occurs in a purely sequential way (Balhorn, 2007; Bao & Bedford, 2016; Barrachina et al., 2018; Gaucher et al., 2012; Kimmins & Sassone-Corsi, 2005; J. D. Lewis et al., 2003; Meistrich et al., 2003; Oliva, 2006; Oliva & Castillo, 2011; Oliva & Dixon, 1991; Rathke et al., 2014), recent findings point out to a more synergic rather than sequential NH-NP process (Barral et al., 2017; Rezaei-Gazik et al., 2022). In fact, expression of spermatid-specific histone variant H2A.L.2 occurs concurrent to TPs, creating a nucleosome open conformation allowing TP loading into the chromatin. Depletion of H2A.L.2 is linked to aberrant TPs loading and pre-P2 processing (Barral et al., 2017). Furthermore, TPs and protamines seem to co-exist in late spermatids, when histones are still detectable (Meistrich et al., 2003; Zhao et al., 2004). Indeed, recent findings demonstrate that pre-P2 is spatiotemporally co-expressed with TPs, suggesting that they act together during NH-NP transition (Rezaei-Gazik et al., 2022). This is supported by recent evidence showing the essential role of the cleaved domain of pre-P2 (cP2) in P2 functionality, whose loss results in retained TP1-H2A.L.2 complexes in heterochromatin foci, indicating that cP2 is responsible of a correct interaction between P2 and TP1-H2A.L.2 complexes (Arévalo et al., 2022). Therefore, in normal conditions, H2A.L.2 mediate TPs loading into nucleosomes containing H2A.L.2-TH2B dimers, where TPs do not displace histones but rather generate an interface for protamine recruitment and processing, orientating protamines to finally displace histones (Arévalo et al., 2022; Barral et al., 2017). Indeed, depletion of cP2 domain induces a reduced P2 deposition into the chromatin, with part of P2 located at spermatid cytoplasm and residual bodies (Arévalo et al., 2022). Besides, TP2 loss causes pre-P2 accumulation, which would end up in altered levels of P2 family components (Zhao et al., 2001). Additionally, knockout mouse models of the genes coding for TP1 and TP2 (*Tnp1* or *Tnp2,* respectively) are subfertile, producing sperm with abnormal chromatin condensation. Of note, these mice seem to compensate the lack of one of the TPs by overexpressing the other one, so that only the simultaneous depletion of both genes would end in sterility (Shirley et al., 2004; Yu et al., 2000; Zhao et al., 2001). Interestingly, double *Tnp1-Tnp2* knockout mice generate testicular spermatids and few epididymal sperm, even though their chromatin compaction is impaired. This would support that protamines on their own

would be capable of histone replacement without the participation of transition proteins (Shirley et al., 2004). In fact, protamine extracts can compact DNA molecules of different lengths *in vitro* (Makita et al., 2011; Oliva et al., 1987; Oliva & Mezquita, 1986). Furthermore, gene-edited somatic cells expressing protamines achieved nuclear compaction in cell culture. P1 displace nucleosomes from somatic chromatin, leading to a spermatid-like nuclear compaction (Iuso et al., 2015). Strikingly, this P1-compacted somatic nucleus can be reversibly loosened by maternal histones after *in vitro* fertilization of an oocyte, producing embryos that progress until blastocyst stage (Iuso et al., 2015). Similarly, P2 condensation ability of somatic chromatin has been proved in somatic cells, observing fully condensed nuclei after 48h cell culture (Arévalo et al., 2022). All this evidence highlights the protamines as the main actors of histone displacement during spermiogenesis (Barral et al., 2017; Meistrich et al., 2003; Oliva et al., 1987; Oliva & Mezquita, 1986).

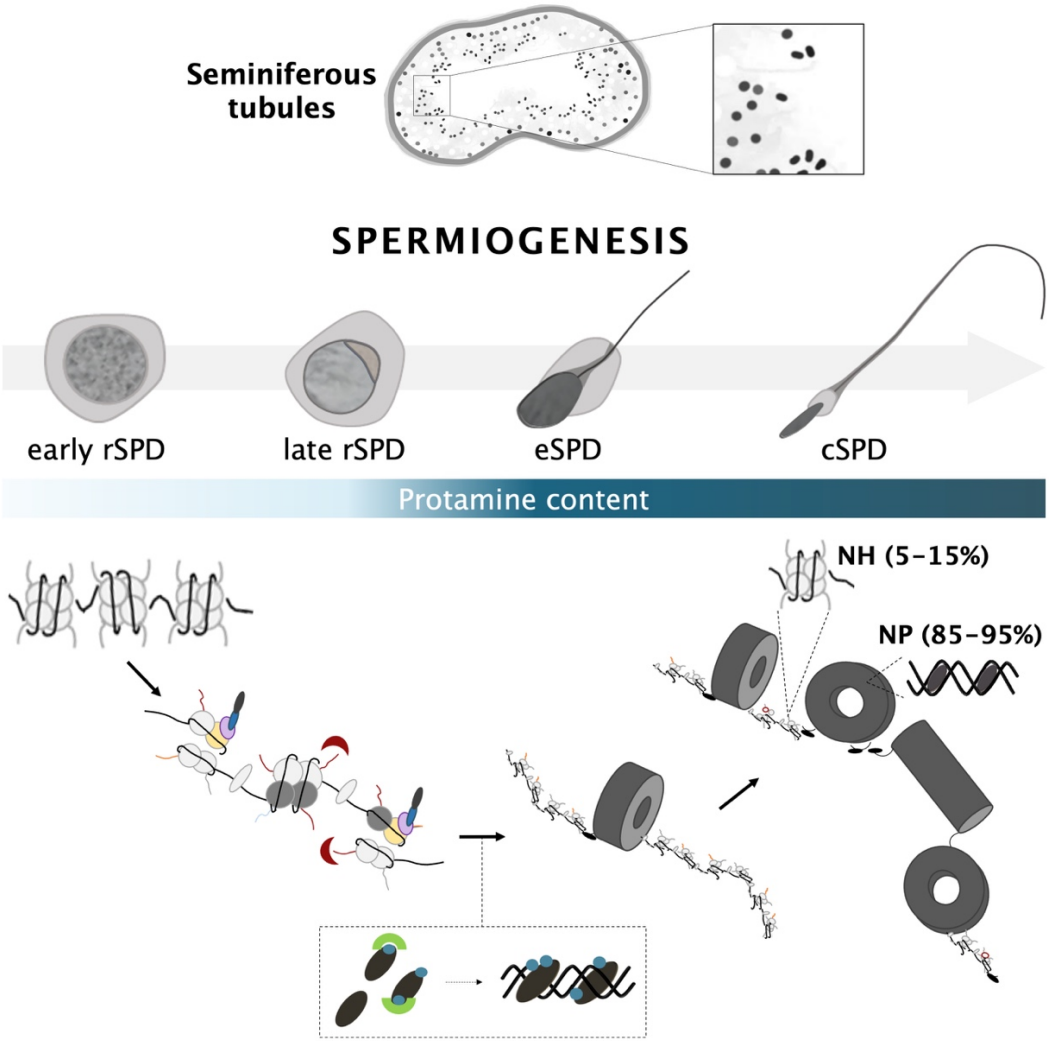


Figure 4. Nucleo-histone to nucleo-protamine transition. Histones (light grey) are replaced by H2A.L.2 (in yellow), other histone variants (dark grey), and transition proteins (purple), for the processing of immature protamine 2 (blue-grey). Other histone PTMs (represented as multi-coloured histone tails), and modulating proteins (moon-shaped, red) assist nucleosome removal. Protamine (elongated, dark grey) incorporation is facilitated by phosphorylation (blue dots) by kinases (in green), originating higher-order structures (toroids and rod-like structures, in dark grey).

3.1.3 The orchestrated regulation of the nucleo-histone to nucleo-protamine transition

Germ cell nuclear compaction is way more complex than the simple affinity of protamines to DNA thanks to their physicochemical properties, with a tight epigenetic regulation underlying the whole process of protamine incorporation. The regulation of the NH-NP transition comprises PTMs of the main proteins involved (histones, histone variants, transition proteins, and protamines), proteins that participate in recognition, addition, or removal of these PTMs, and a post-meiotic gene expression program, as discussed in the next section.

3.1.3.1 Posttraslational modifications of histones, histone variants, transition proteins, and protamines

A global histone H4 hyperacetylation wave is crucial for a proper NH-NP transition, neutralizing the positivity of histone tails, therefore destabilizing histone-DNA, and nucleosome-nucleosome interactions (Barrachina, de la Iglesia, et al., 2022; Hazzouri et al., 2000; Oliva & Mezquita, 1982). The first step towards nucleosome instability and histone eviction for large-scale chromatin remodeling consists of acetylation on H4 Lys 5 and 8 (H4K5K8ac). H4K5K8ac is recognized by the first bromodomain of the bromodomain-containing testis specific protein BRDT, which triggers the NH-NP transition (Dhar et al., 2012; Goudarzi et al., 2014; Her et al., 2021; Manterola et al., 2018; Morinière et al., 2009; Pivot-Pajot et al., 2003; Shang et al., 2007). Together with H4 hyperacetylation, a specific trimethylation of H3 Lys 79 (H3K79me3) wave precedes the NH-NP transition, more precisely prior TP1 incorporation, potentially contributing to its regulation (Dottermusch-Heidel et al., 2014). Residue-specific lysine acetylation of other histones, especially described for H3, contributes to the final global histone hyperacetylation state, destabilizing nucleosomes and favoring their removal (Grimes & Henderson, 1984; Hazzouri et al., 2000; Nair et al., 2008; Steilmann et al., 2011; Tan et al., 2011). In addition to inducing a relaxed nucleosomal conformation, histone PTMs also mark for subsequent proteasomal degradation after histone displacement, as it is the case of histone (poly)ubiquitination of core histones H2A and H2B (Baarends et al., 1999; Gou et al., 2017; Guo et al., 2018; Meng et al., 2019; Shmueli et al., 2021; X. Wang et al., 2019). PSMA8-containing proteasomes in the testis and enriched in haploid cells, known as spermatoproteasomes, also play a key role in degrading histones in acetylation-dependent manner (Gómez-H et al., 2019; Živković et al., 2022).

In recent years, little-known histone PTMs belonging to the group of acylations, have been identified in histones (Crespo et al., 2020; Sabari et al., 2017; Tan et al., 2011). Acylations such as propionylation, butyrylation, and crotonylation present similar physicochemical properties as histone acetylation, which would also induce open nucleosome conformation favoring gene expression and/or histone eviction (Sabari et al., 2017). Interestingly, butyrylation on H4K5 (coupled to either acetylation or butyrylation on K8) is not recognized by the first bromodomain of

BRDT, thus escaping the histone eviction. This could lead either to temporal regulation of histone replacement at specific nucleosomes during spermiogenesis, or histone retention of specific gene sequences in mature sperm (Goudarzi et al., 2016). These findings evidence the tight regulation of histone replacement by PTMs, highlighting the need of increasing the knowledge on the less characterized histone modifications and their role during spermiogenic chromatin remodeling, such as non-acetyl histone acylations. For instance, although it has not been confirmed as direct regulator of the NH-NP transition, crotonylation of H3K27 has been highly detected in post meiotic cells, concomitant to H4 hyperacetylation and histone removal, as well as retained in sperm, suggesting a comparable function to that of H4K5 or K8 butyrylation (Crespo et al., 2020). Interestingly, crotonylated H3K27 regulates the expression of spermiogenic-specific gene expression (such as TP2 and P1), acting in synergy with the same acetylated residue and associated with the highest gene expression (Crespo et al., 2020).

Apart from the epigenetic marks on canonical histones, histone variants and TPs also bear PTMs, affecting their binding affinity to DNA (Gupta et al., 2015, 2017; Hazzouri et al., 2000; Kwak & Dohmae, 2016; Mishra et al., 2015; Pentakota et al., 2014; Pradeepa et al., 2009; I. Singh & Parte, 2021). Of note, acetylated TP2 presents reduced ability to condense DNA (Pradeepa et al., 2009), suggesting that modified TPs may play a role during spermiogenesis, therefore contributing to establish the final sperm epigenome.

The epigenetic regulation of spermiogenesis through modification of specific protein residues also exists in protamines from different mammalian species (Arauz-Garofalo et al., 2021; Brunner et al., 2014; Castillo et al., 2015; Chirat et al., 1993; Pirhonen, Linnala-Kankkunen, & Mäenpää, 1994; Pruslin et al., 1987; Soler-Ventura et al., 2020). The main protamine PTM is phosphorylation, which regulates the binding affinity of the protamines to the DNA. The negative charge of the phosphate group leads to weaker affinity of phosphorylated protamines to the negatively charged DNA, compared to unmodified protamines (Willmitzer et al., 1977a, 1977b). Thus, while protamine phosphorylation would be necessary at earlier steps for incorporating protamines to DNA, subsequent dephosphorylation would be needed to achieve a tight sperm chromatin compaction (Itoh et al., 2019; Willmitzer et al., 1977a).

3.1.3.2 Proteins modulating posttranslational modifications

Modification of histones and other non-histone proteins, as well as amino acids susceptible of being postranslationally modified, provide binding sites for PTM regulating proteins. PTM-modulating proteins contain domains that specifically alter the posttranslational state of modifiable substrates. In other words, they recognize and modulate PTMs of other proteins, and have been described in many different contexts (Jenuwein & Allis, 2001; Ruthenburg et al., 2007; Seet et al., 2006; Strahl & Allis, 2000). It can be distinguished:

- **Writers**: proteins that incorporate concrete PTMs to the aminoacidic protein sequence.

- **Erasers**: proteins that remove PTMs from already modified amino acids.

- **Readers**: proteins containing domains that recognize PTMs from specific modified residues. Their binding event can expose a side chain of the protein to be more accessible (either for further modification or recognition).

Besides, modulating proteins can contain more than one active region. In that case, they are known as effectors, and their binding to posttraslationally modifiable substrates can exert other activities by the action of those additional functional domains. Effectors normally contain a reader domain, and among the possible additional functions they can recognize and further modify by PTMs introduction or removal (combined with writer or reader domains), remodel the chromatin fiber in ATP-dependent manner, stabilize a higher order chromatin structure, or gene expression regulation (Jenuwein & Allis, 2001; Ruthenburg et al., 2007; Seet et al., 2006; Strahl & Allis, 2000).

Regarding spermiogenic chromatin remodeling, NH-NP transition is mediated by the recruitment of histone acetyltransferases (HAT; writers of histone acetylation) as P300 and CBP by NUT to enhance H4K5/K8 acetylation (Shiota et al., 2018). Other HAT such as EPC1 and TIP60, components of NuA4 complex, are involved in histone hyperacetylation during spermiogenesis (Dong et al., 2017). Other histone acetylation readers and erasers (histone deacetylases) have been shown to contribute to the final histone acetylation state, and their deregulation has been related with male infertility and impaired chromatin compaction, as summarized in **Table 1**.

One of the main readers during spermiogenesis is BRDT, recognizing acetylated H4K5K8 to trigger and amplify the process of histone eviction, but also interacting with transcription factors in round spermatids to regulate expression of essential genes in this developmental stage (Her et al., 2021). Proteins modifying histone methylation have been also shown to control the expression of TPs and protamine genes (Eelaminejad et al., 2017; Z. Liu et al., 2010; Okada et al., 2007, 2010; Zuo et al., 2018). Details of these and additional examples can be found in **Table 1**.

Additionally, crosstalk among different histone PTMs and histone-modifying enzymes suggests a new layer of coordination on the NH-NP transition epigenetic control. Reduced gene expression of *Sly*, exclusive of post-meiotic male germ cells, deregulates not only DOT1L, a H3K79me3 methyltransferase, but also H4ac levels in elongated spermatids, leading to a global alteration of the chromatin compaction state (Moretti et al., 2017). DOT1L also recognizes ubiquitinated H2B, enhancing a noncatalytic function of this methyltransferase destabilizing the nucleosome, which

suggests an interplay between H3 methylation and H2B ubiquitination towards nucleosome removal (Jang et al., 2019).

Although protamines and their PTMs have been historically less studied than histones, some proteins modulating protamine phosphorylation are known. In the testis, SRSF protein kinase 1 (SRPK1) contributes to P1 phosphorylation, and Calcium/calmodulin-dependent protein kinase type IV (CAMK4) so does it in P2 (Papoutsopoulou et al., 1999; J. Y. Wu et al., 2000). Additional candidates phosphorylate protamines *in vitro*, such as c-AMP-dependent protein kinase A (PKA), which phosphorylates P1, and protein kinase C (PKC), which phosphorylates P2 (Pirhonen, Linnala-Kankkunen, & Mënpää, 1994). In terms of erasers, while no P1-specific phosphatases have been described yet, germ cell-specific isoform 2 of Serine/threonine-protein phosphatase PP1-gamma catalytic subunit (PP1γ2) is involved in removing phosphate groups from P2 (Itoh et al., 2019). Interestingly, the depletion of the chaperone needed for recruiting PP1γ2 to sperm chromatin in mice (HSPA4L) leads to infertility due to altered sperm head morphology, but the normal phenotype is rescued when P2 phosphorylation site is substituted by a non-phosphorylatable residue. This suggests that PP1γ2-mediated dephosphorylation is essential to achieve mouse fertility avoiding abnormal P2 phosphorylation levels in epididymal sperm (Itoh et al., 2019).

All studies mentioned above reinforces the idea of a highly orchestrated process of epigenetic regulation through a complex interplay between histone PTMs and histone-modyfying enzymes.

Table 1. Proteins modulating posttranslational modifications of histone and protamines expected to be involved in the regulation of the nucleohistone to nucleoprotamine transition.

Name	Molecular role	Description	References
BRD4	Bromodomain-containing protein, reader of histone acetylation	Acetylation reader, with preference for acetylated H4 over H3 in vivo. Associated with active genes in round spermatids. Differential gene expression through specific binding to residue-specific (H3K27) histone acetylation but not butyrylation, unlikely to bind crotonylation in the same residue. Potentially involved in nuclear proteins eviction linked to acrosome formation during spermiogenesis	(Bryant et al., 2015; Crespo et al., 2020; Ji et al., 2015; Vollmuth & Geyer, 2010)
BRDT	Bromodomain-containing protein, reader of histone acetylation	Reader of H4 acetylation. First bromodomain recognition of H4K5K8 is essential to trigger NH-NP transition, depletion leads to infertility (post-meiotic arrest). Gene expression regulation of post-meiotic genes	(Dhar et al., 2012; Gaucher et al., 2012; Her et al., 2021; Manterola et al., 2018; Pivot-Pajot et al., 2003; Shang et al., 2007)
CAMK4	Calcium/calmodulin-dependent kinase	Phosphorylates P2, depletion of Camk4 leads to infertility, impaired elongating spermatids with prolonged retention of Tnp2 and specific loss of P2	(J. Y. Wu et al., 2000)

CDYL	Chromodomain-containing protein, reader of histone methylation	Histone crotonylation regulator facilitating TP1 and PRM2 incorporation. Depletion of CDYL caused changes in histone methylation and acetylation profiles and altered gene expression, giving rise to teratozoospermia and progressive infertility in adulthood	(S. Liu et al., 2017; Xia et al., 2019)
DOT1L	Histone methyltransferase	Methyltransferase in the testis of H3K79, which precedes the NH-NP transition, more precisely prior TP1 incorporation	(Dottermusch-Heidel et al., 2014; Moretti et al., 2017)
EPC1	Component of NuA4 histone acetyltransferase (HAT) complex	Its depletion, together with TIP60, leads to impaired histone H4 hyperacetylation and subsequent histone replacement	(Dong et al., 2017)
HDAC3	Histone deacetylase	Inactivates meiotic program and activates postmeiotic genes during meiotic exit. Depletion of HDAC3 leads to infertility due to meiotic/early-stages round spermatids arrest, and increased H3 acetylation in spermatocytes and round spermatids. Coordinates gene expression program with SOX30	(Yin et al., 2021)
MRG15	Component of the NuA4 HAT complex	Recognizes methylated H3K36 and regulates alternative splicing mediated by polypyrimidine tract binding protein PTB, part of the HAT and HDAC complexes balancing histone acetylation	(Hayakawa et al., 2007; Iwamori et al., 2016)
P300	Histone acetyl-transferase	Involved in histone H4 hyperacetylation and essential for histone-to-protamine exchange. Acetylation of TP2 by p300 leads to significant reduction in its DNA condensation	(Pradeepa et al., 2009; Reynoird et al., 2010; Shiota et al., 2018)
PA200	Component of the proteasome, degradation of acetylated histones	Depletion leads to hypofertility with abnormal sperm, core histone retention in elongating spermatids due to defective acetylation-dependent histone proteasomal degradation. Its level of incorporation to the spermatoproteasome-containing PSMA8 subunit is 10-fold higher in spermatids than early spermatogenesis, key for proteasomal activity during spermiogenesis	(Khor et al., 2006; Qian et al., 2013; Živković et al., 2022)
PHF7	Ubiquitin ligase	E3-ubiquitin ligase for H3K14 in post-meiotic cells, required for histone to protamine transition. Stabilizes BRDT by attenuating BRDT ubiquitination	(Kim et al., 2020; X. Wang et al., 2019)
PP1γ2	Protein phosphatase	Dephosphorylates Ser56 of protamine 2 in mouse. HSPA4L-mediated chromatin localization of PP1γ2 is essential for fertility and maintenance of low oxidative stress levels during epidydymal transit	(Itoh et al., 2019)
SIRT1	Histone deacetylase	Loss of Sirt1 causes defects on H4 Lys5, 8, and 12 acetylation, and subsequent histone removal	(Bell et al., 2014)
SRPK1	Serine/Threonine kinase	Phosphorylation of protamine 1 in the testis, which favours protamine incorporation to the DNA	(Gou et al., 2020; Papoutsopoulou et al., 1999; Willmitzer et al., 1977b, 1977a)
TIP60	Catalytic subunit of NuA4 histone acetyltransferase (HAT) complex	Its depletion, together with Epc1, leads to impaired histone H4 hyperacetylation and subsequent histone replacement	(Dong et al., 2017)

3.1.3.1 Post meiotic gene expression program

The complex epigenetic regulation of the unique chromatin remodeling process during spermiogenesis goes beyond proteins and protein PTMs, as reviewed by others (Blanco & Cocquet, 2019; Moritz & Hammoud, 2022; T. Wang et al., 2019). The coordinated expression of key proteins governing the NH-NP transition, such as histone variants, TPs, protamines, and proteins modulating histone and protamine PTMs, is needed to properly develop the process.

A correct 3D conformation leading to differential chromatin accessibility is required for a fine-tuning of the post meiotic gene expression program. CTCF and its paralog BORIS, which are associated to nucleosomes that escape protamine replacement and are known to regulate gene expression through 3D chromatin organization, are essential to exit meiosis and activate post-meiotic genes. In fact, their depletion is related with abnormal histone retention, altered protamine incorporation, and male infertility (Hernández-Hernández et al., 2016; Rivero-Hinojosa et al., 2021). Additionally, transcription factors and modulators regulating the expression of the genes encoding protamines, histone variants, and TPs are crucial for chromatin compaction and fertility in mice, such as RFX2, SOX30, TAF7L, BRWD1, or CREM, as detailed in **Table 2** (Akinloye et al., 2007; Bai et al., 2018; Feng et al., 2017; Kistler et al., 2015; Kotaja et al., 2004; J. Li et al., 2020; Nagamori et al., 2006; Nantel et al., 1996; Y. Wu et al., 2016; Zhang et al., 2018; Zhou et al., 2013).

Apart from direct gene expression regulation, regulation at posttranscriptional level by ribonucleoproteins associated to mRNAs corresponding to TPs and P2 in mice has been recently identified in the testis, mediating the temporal gene expression regulation of the process (Phillips et al., 2019; Xu et al., 2014).

The process of NH-NP transition is also regulated through indirect pathways. For instance, the loss of the nuclear importin KPNA6 results in an impaired histone to protamine exchange and post meiotic gene expression program, even though the underlying cellular and molecular mechanisms have not been identified yet (N. Liu et al., 2021). Similarly, the helicases GRTH and CHD5 have a role on the transcription of key factors for histone replacement (Anbazhagan et al., 2020; Kavarthapu et al., 2019; Tsai-Morris et al., 2004). Moreover, CHD5 has been also found involved in the process of H4 hyperacetylation (W. Li et al., 2014; Zhuang et al., 2014).

Table 2. Proteins involved in the regulation of the nucleo-histone to nucleo-protamine transition as transcriptional or translational regulators of key proteins participating in the process.

Name	Molecular role	Description	References
ACT	Transcriptional regulator	Activator of CREM in the testis. KO mice present sperm with altered chromatin compaction and abnormal head shape	(Kotaja et al., 2004)
AURKC	Serine/threonine protein kinase	Depletion of AURKC is associated with compromised fertility in mice, with sperm evidencing impaired chromatin condensation. In infertile humans, single nucleotide deletions yield large-headed polyploid sperm	(Dieterich et al., 2007; Kimmins et al., 2007)
BNC1	Zinc-finger protein involved in transcription activation	Cooperates with TAF7L to regulate protamines and TPs during spermiogenesis development. Reduced gene expression in non-obstructive azoospermic men	(J. Li et al., 2020)
BRWD1	Bromodomain-containing transcriptional regulator	Key regulation of gene expression during postmeiotic sperm differentiation. Depletion causes infertility in mice, with decreased expresion of protamine 1 and TPs	(Pattabiraman et al., 2015; Philipps et al., 2008)
CB1 (CNR1)	G-protein coupled receptor for endogenous cannabinoids	Depletion leads to impaired histone removal by reducing H4 hyper-acetylation, increased TP2, and increased sperm DNA fragmentation during epidydymal transit. Promotes disulphide bond formation to ensure sperm chromatin condensation during epididymal transit	(Chioccarelli et al., 2010, 2020)
CHD5	Chromodomain helicase	Helicase whose depletion leads to infertility in mice, orchestrating histone H4 hyperacetylation, nucleosome eviction, DNA damage repair, as well as histone variants, TPs, and protamines expression	(W. Li et al., 2014; Zhuang et al., 2014)
CREM	CRE-binding transcriptional regulator	Abscence leads to postmeiotic arrest and impaired post-meiotic gene expression program, including protamines and TP1. Together with TISP40, regulate postmeiotic transcription. Recruit HIRA (histone chaperone) to CRE	(Nagamori et al., 2006; Nantel et al., 1996)
CTCF	Chromatin binding factor (transcriptional repressor)	Conditional depletion of CTCF in mouse spermatocytes causes infertility coupled with defects in chromatin compaction due to accelerated incorporation of protamine 1 to the DNA. Together with its testis-specific paralog BORIS, are associated with regions that escape histone eviction	(Hernández-Hernández et al., 2016; Rivero-Hinojosa et al., 2021)
DICER	dsRNA endoribonuclease, post-transcriptional gene silencing	Depletion leads to infertility with impaired spermatid elongation, reduced protamine 1 levels and H3 acetylation	(Korhonen et al., 2011)
DPY19L2	Acrosome development	Single nucleotide variants on DPY19L2 are associated with globozoospermia in humans, knockout mice infertile with impaired chromatin compaction, defective protamination, and histone retention. Essential for acrosome biogenesis	(Castaneda et al., 2021; Harbuz et al., 2011; Yassine et al., 2015)

GMCL1	Transcriptional regulator	Essential for fertility in mice, needed for expression of TPs and protamines and subsequent chromatin compaction and stablishment of nuclear structure in elongated spermatids	(Kimura et al., 2003)
GRTH	ATP-dependent RNA helicase	Essential for a properm spermiogenic development and gene expression of TPs, protamine 2, and TSSK6. Regulated by phosphorylation	(Anbazhagan et al., 2020; Kavarthapu et al., 2019; Tsai-Morris et al., 2004)
HIRA	Promotes replication-independent chromatin assembly	Histone H3.3 chaperone. HIRA is critical for DNA-synthesis-independent nucleosome assembly process, which could incorporate H3.3 to the nucleosome in spermiogenesis	(Nagamori et al., 2006; Ray-Gallet et al., 2002; Tagami et al., 2004; Wirbelauer et al., 2005)
KPNA6	Nuclear importin	Loss of function causes infertility, with incomplete sperm maturation, lower sperm count, and impaired histone to protamine exchange. Also leads to differential localization of BRWD1 and altered expression of RFX2 target genes	(N. Liu et al., 2021)
L3MBTL2	Polycomb protein	Its depletion causes a decrease in the histone acetylation levels in elongating spermatids and P1 deposition, leading to impaired chromatin condensation in sperm	(Meng et al., 2019)
LIS1	Component of platelet-activating factor acetylhydrolase 1b	Lack of LIS1 causes infertility in mice, with spermiogenesis arrest due to abnormal Tnp2 location, nuclear compaction, and acrosome formation	(Nayernia et al., 2003)
NSD2	Histone H3K36 methyltransferase	Catalyzes H3K36me2, depletion leads to aberrant spermiogenesis, increased H4K16ac potentially due to impaired PSMA8-dependent histone degradation, impaired EP300-induced H4K5/K8ac, histone retention, and enhanced protamine expression.	(Z. Li et al., 2022)
NUT	Universal oncogenic driver, involved in proliferation regulation	Triggers P300-dependent genome-wide histone H4 hyperacetylation, essential for histone to protamine exchange. NUT inactivation induces male sterility with spermatogenesis arrest at the histone-removal stage. NUT uses P300 and/or CBP to enhance acetylation of H4 at both K5 and K8	(Rousseaux et al., 2022; Shiota et al., 2018)
PABPC1	RNA binding protein	Ribonucleoprotein involved in protein translation regulation during spermiogenesis in mice, associated with sperm-specific mRNAs such as those of TPs and protamine 2	(Xu et al., 2014)
PIWI	Endoribonuclease repressing transposable elements	Required for fertility in mice, depletion leads to sperm abnormal chromatin compaction and histone retention. Single nucleotide variants found in humans are associated with azoospermia	(Gou et al., 2017)
PSMA8	Component of the testis-specific spermatoproteasome	Proteasomes containing PSMA8 subunit (spermatoproteasome) are predominants in spermatids. Promotes assembly of PA200 to the proteasome. Role on acetylation-dependent degradation of histones	(Gómez-H et al., 2019; Živković et al., 2022)
PYGO2	PHD finger protein involved in signal transduction	Depletion leads to infertility due to spermiogenesis arrest coupled to reduced gene expression of histone variants, TP2, and protamines. Single nucleotide polymorphisms in PYGO2 might be related with idiopathic oligozoospermia and azoospermia in humans	(Ge et al., 2015; Nair et al., 2008)

RFX2	Transcription factor	Knockout shows round spermatid arrest with cytoplasmic accumulation of TP2 the arrested cells, TP1 loss. Wu and colleagues show similar phenotype but without changes in TPs	(Kistler et al., 2015; Y. Wu et al., 2016)
SETD2	Histone H3K36 metyltransferase	H3K36me3 methyltransferase essential for protamine genes expression and spermiogenesis development in mice	(Zuo et al., 2018)
SLY	Regulator of gene expression	Sly-knockdown deregulates DOT1L (H3K79 methyltransferase) and H2A variants, showing decreased H4ac levels in elongating spermatids, and less protaminated chromatin, leading to alterations in postmeiotic chromatin structure and remodeling, as well to increased DNA oxidation	(El Kennani et al., 2018; Moretti et al., 2017; Riel et al., 2012)
SOX30	Transcription factor	Depletion in mice causes sterility due to post-meiotic arrest, decreased gene expression of histone variants, TP2, and protamines. Allows HDAC3 recruitment to genome binding sites to allow meiotic-to-postmeiotic transition	(Feng et al., 2017; X. Wang et al., 2019; Yin et al., 2021; Zhang et al., 2018)
TAF7L	Transcription factor	Depletion leads to infertility in mice due to postmeiotic arrest. Critical for gene expression of TPs, protamines and CAMK4. Cooperates with BNC1 to regulate a subset of spermiogenic genes. Single nucleotide variants are associated with oligozoospermia in men	(Akinloye et al., 2007; Y. Cheng et al., 2007; Gou et al., 2020; Ling et al., 2022; Zhou et al., 2013)
TARBP2	formation of the RNA induced silencing complex (RISC)	Postranslational activator of protamine 1 and 2 mRNAs. Mutant mice are sterile and evidence a mosaic expression of protamines 1 and 2, and prolonged retention of TP2 in later-stage elongated spermatids	(Braun, 2000; Lee et al., 1996; Zhong et al., 1999)
TISP40	leucine zipper-type transcription factor	Depletion causes abnormal histone retention. Heterodimeric with CREM increasing its binding ability to CRE, regulating postmeiotic transcription	(Nagamori et al., 2006; Nantel et al., 1996)
TSGA8	Testis specific protein with essential role in spermatogenesis and male fertility	Its loss leads to infertility, showing round spermatids altered chromosomal distribution, and nuclear malformation in elongating spermatids, together with altered gene expression program resulting in reduction of TP1 and protamine 1	(Kobayashi et al., 2021)
tsHMG	DNA-packaging factor of spermatids	Its phosphorylation by PKC is required for DNA binding and may modulate topoisomerase I-dependent supercoiling activity in spermatids	(Alami-Ouahabi et al., 1996; Baarends et al., 1999; Boissonneault & Lau, 1993)
TSSK6	Serine/Threonine kinase	Essential for fertility in mice, formation of gammaH2AX. Depletion causes increased histone retention, P2 precursor, and P2 intermediate forms in sperm	(Jha et al., 2017; Spiridonov et al., 2005)
ZFP628	Zinc-finger protein involved in transcription activation	TAF4B-interacting transcriptional cofactor whose depletion leads to infertility due to round spermatid arrest, causing reduced TPs and protamine mRNA levels	(Gustafson et al., 2020)

3.1.4 Extra-testicular sperm maturation

Testicular sperm are morphologically complete, but immotile and without fertilizing ability. Therefore, sperm maturation continues outside the testis during the transit through the male reproductive tract in contact with the fluids secreted by the epididymis and accessory sex glands that constitute the seminal plasma. The up to 2-weeks transit and storage of sperm cells in the epididymis gives rise to fully mature and motile ejaculated sperm cells with fertilizing potential (Dacheux & Dacheux, 2014; Gervasi & Visconti, 2017; Jodar et al., 2017; Orgebin-Crist, 1969; Schoysman & Bedford, 1986; Yoshida et al., 2018). Among the most remarkable changes that take place, sperm cells acquire forward progressive motility and the variation of sugars and lipids of the surface membrane, affecting membrane fluidity and preparing male gametes for later events. During epididymal transit and storage, sperm undergo changes of their proteomic composition which, together with protein post-traslational modifications (PTMs), activate different intracellular signaling cascades motivating sperm maturation. As transcriptionally and translationally silent cells, sperm proteomic changes during epididymal transit occurs through the incorporation of epididymal proteins through extracellular vesicles called epididymosomes, which can also contain RNAs and other molecules as cargo (Barrachina, Battistone, et al., 2022; Dacheux & Dacheux, 2014; Gervasi & Visconti, 2017; Jodar et al., 2017).

Like other aspects of sperm maturation, chromatin conformation neither finishes when immature sperm are released from the testis but continues through crucial events taking place in the epididymis, depicted in **Figure 5** (Yoshida et al., 2018). Generation of disulfide bonds needed to stabilize the sperm chromatin structure are promoted by the cannabinoid receptor 1 (CB1) in the epididymis (Chioccarelli et al., 2020). Of note, this protein plays a role in the NH-NP transition since CB1 depletion reduces H4 acetylation and increases TP2 in the testis and increases sperm DNA fragmentation levels along the epididymal transit, suggesting that disulfide bonds formation is essential for post-testicular chromatin stability and DNA integrity (Chioccarelli et al., 2010). Additional mechanisms of chromatin stabilization during epididymal transit have been described, such as protamine dephosphorylation and the release of zinc molecules from P2 that were acquired in the testis during protamine incorporation (Bianchi et al., 1992; Björndahl & Kvist, 2011; G. M. Dias et al., 2006; Gou et al., 2020; Itoh et al., 2019; Schneider et al., 2020). All this indicate that, even though the focus of the NH-NP transition has mostly been set on the testicular processes, attention should be also paid to the post-testicular events, which would contribute to the acquisition of the proper chromatin structure to protect the paternal genome from external damage.

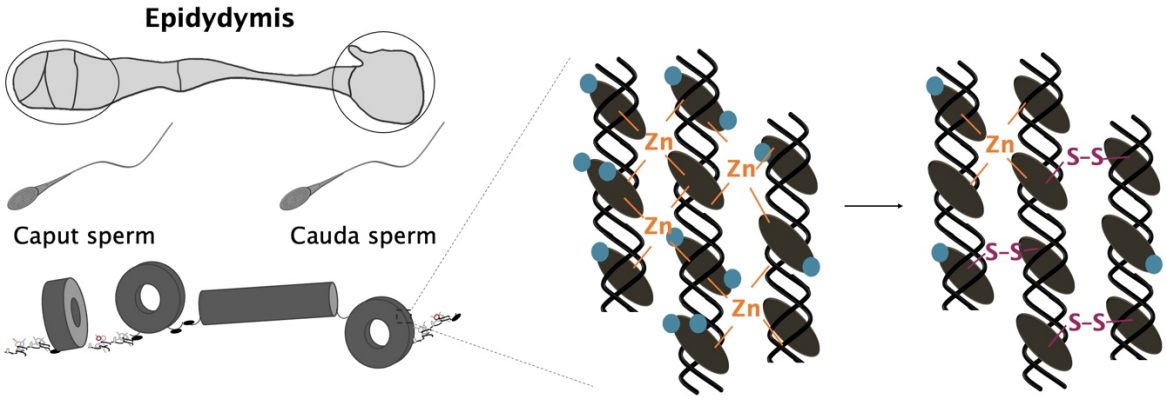


Figure 5. Epididymal events of chromatin stabilization. In the epididymis, zinc bridges (Zn, in orange) are partially lost, and the chromatin stabilizes through disulfide bonds (S-S, in magenta), coupled to a potential protamine dephosphorylation wave.

However, maturation is not fulfilled until sperm cells undergo capacitation during their journey through the female reproductive tract after ejaculation. The upcoming events are sequential, and the previous epididymal maturation events are prerequisite for sperm capacitation, contributing to gain fertilizing ability. In the female reproductive tract, capacitated sperm gain hyperactive motility. Molecular changes underlying these mechanisms have been described by our group and others, including changes in protein abundance and PTMs, membrane hyperpolarization, and increased activity of kinases, phosphatases and acetylases. In turn, capacitation is essential to achieve the potential to penetrate the zona pellucida and undergo acrosome reaction, a calcium-dependent process in which the acrosomal content (including hydrolytic enzymes such as acrosine and hyaluronidase) is released. Changes in sperm protein abundance after acrosome reaction have been also reported. Once fully mature, sperm can fuse with the oolemma, and finally fertilize the oocyte (Castillo, Bogle, et al., 2019; D. Y. Liu et al., 2007; Puga Molina et al., 2018). More information about sperm contribution to fertilization and beyond can be found in **Section 1.3**.

3.2 The human mature sperm

3.2.1 Main parts of human mature sperm

Once fully mature, the spermatozoon has a length of around 60 μm. As shown in **Figure 6**, it is divided in two main parts: head, with approximate length of 4–5 μm and width of around 3 μm; and tail or flagellum, presenting a diameter of 1–2 μm (Holstein et al., 2003; Kumar & Singh, 2021; Toshimori & Ito, 2003).

- **Head**: it comprises the sperm nucleus and the acrosome. According to the last WHO report, head dimensions correspond to median length = 4.1 μm, 95% CI 3.7–4.7 μm; and median width = 2.8 μm 95% CI 3.7–4.7 μm (World Health Organization, 2021). The nucleus contains the paternal genome highly packaged by protamines and retained histones, together with proteins, RNAs, and other epigenetic marks (see Section 1.3 for more details about the epigenetic potential of the sperm nucleus). Covering more than two third parts of the anterior part of the nucleus, the acrosome is a large secretory vesicle that holds hydrolytic enzymes for the spermatozoon to pierce the oocyte vestments.
- **Tail**: also named flagellum, is a specialized cilium with a complex structure that oversees sperm motility. It is attached to the posterior part of the head through the connecting piece, that contains the proximal (typical) and distal (atypical) centrioles. The distal centriole is the structure from which the axoneme arises, and in mature sperm is attached to the base of the axoneme. Sperm tail has three main parts: mid-piece, principal piece, and end piece. The mid-piece contains 70–100 mitochondria providing the energy source boosting sperm motility. The principal piece has a fibrotic sheath surrounding the axoneme. In turn, the end piece comprises the axoneme only surrounded by plasma membrane.

3.2.2 Human mature sperm chromatin

After the extensive nuclear remodeling during testicular and extra-testicular sperm maturation, the tightly packaged male gamete chromatin consists of an 85–95% protaminized DNA, and the 5–15% of the DNA remains associated to the retained histones. The non-randomly distributed sperm chromatin along the NP and NH domains evidences a differential accessibility in terms of chromatin-associated proteins, according to their affinity to the DNA. The nucleo-protamine domain, with the protamines being the structural proteins strongly attached to the DNA, represent the most condensed, therefore less inaccessible, fraction of the sperm chromatin. In contrast, the nucleo-histone domain, is easily accessible and is unattached together with a rich population of transcription factors and chromatin modifying proteins. This, plus the dual behavior of the nucleo-histone domain mainly enriched in intergenic regions and repetitive DNA associated to centromeric loci but also in developmental genes promoters, adds another layer of regulatory elements to the

complex structure of the human sperm chromatin (Arpanahi et al., 2009; Castillo, Amaral, & Oliva, 2014; Castillo, Amaral, Azpiazu, et al., 2014; Castillo et al., 2015; S. Hammoud et al., 2009; Luense et al., 2019; Okada & Yamaguchi, 2017; Oliva, 2006; Ozturk et al., 2021; Vavouri & Lehner, 2011). For a more detailed information about the specific distribution of the sperm chromatin into the nucleohistone and nucleoprotamine domains, please refer to **Annex 1** (**Section 3.1**).

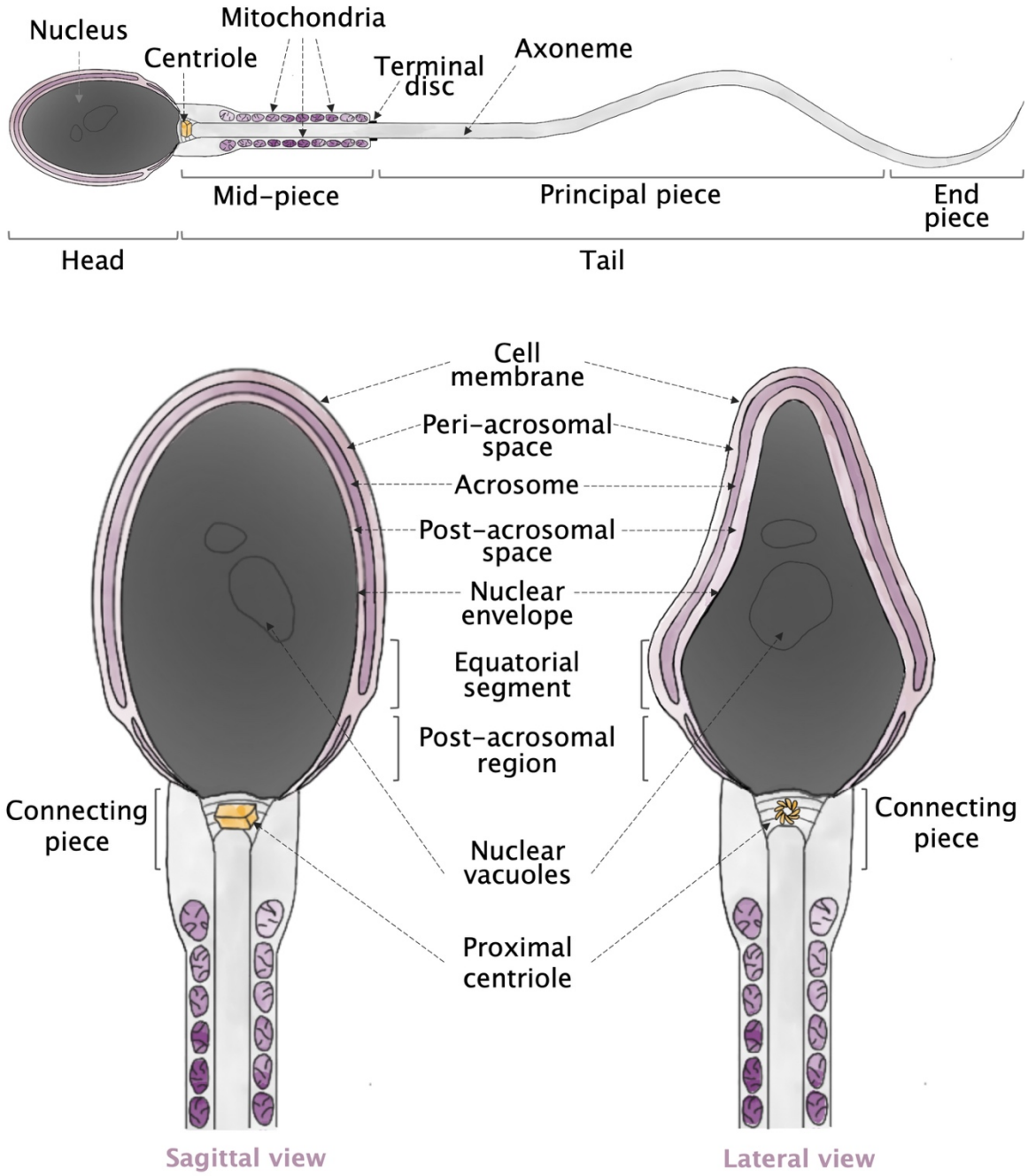


Figure 6. Diagram of mature sperm main parts. The sperm head contains the nucleus and acrosome. Tail is divided into mid-piece, principal piece, and end piece. Sperm head zooms below highlight specific structures, either from a sagittal (left) or lateral (right) point of view. Based on public domain images from *Wikimedia Commons, the free media repository*.

This differential chromatin accessibility has been recently studied applying novel 3D chromatin techniques, such as Hi-C, based in chromatin conformation capture, or ATAC-seq, based on Tn5 transposase. Interestingly, these approaches showed a distinct association of nucleosome-retained DNA, with presence of DNA bound to CTCF and cohesins in round spermatids and embryonic stem cells, and retention in intergenic regions that seems to not increase along spermatogenesis (Buenrostro et al., 2013; Y. H. Jung et al., 2017; Ke et al., 2017; Luense et al., 2019). In this regard, it is important to remark the detection in the mature sperm cell of predetermined enhancers and super-enhancers associated to elements involved in the 3D organization of the chromatin that are functional in embryonic and adult tissues (Y. H. Jung et al., 2017). Interestingly, sperm genomic 3D organization revealed many similarities to that of somatic cells as fibroblasts or embryonic stem cells, divided in different compartments (A and B compartments, respectively associated to active and repressive chromatin regions), and partially conserving topologically associated domains (TADs) (Battulin et al., 2015; Y. H. Jung et al., 2017; Ke et al., 2017; Luo et al., 2020; Vara et al., 2019; Y. Wang et al., 2019). Nonetheless, sperm possess more long-range interactions (> 2Mb), most of them between TADs, that could contribute to either establishing the highly compacted state or maintaining it. Indeed, 3D conformation of sperm from species without protamines lack TADs, resembling mitotic chromosomes (Gibcus et al., 2018; Wike et al., 2021). This A-B and TADs compartmentalization correlates with retained histones in sperm. Some controversy arises from the use of current 3D-chromatin technologies in such compacted (therefore unaccesible) mammalian sperm, which would potentially bias the results from the real *in vivo* genomic architecture (Moritz & Hammoud, 2022).

This genomic distribution not seen in any somatic cell type, leads to the unique chromatin structure arising from the protamine incorporation, giving the sperm cell very particular properties that are essential for a proper sperm function.

3.2.2.1 Human sperm protamines

Despite more than 6,000 different proteins having been identified, protamines represent a major part of the male gamete nuclear protein content due to their highly relevant function (Castillo et al., 2018). They compact the DNA in a semi crystalline structure that allows sperm to achieve a hydrodynamic shape needed to reach the oocyte, as well as to protect the paternal genome from external damage during its journey (Barrachina et al., 2018; Oliva, 2006; Oliva & Castillo, 2011). The protamine packaging capacity is higher than that of histones thanks to the extreme physicochemical properties of the protamines, which are very small in size, extremely basic, and can form inter- and intramolecular disulfide bonds to stabilize the nucleo-protamine structure (Balhorn, 2007; Oliva, 2006). Therefore, while a nucleosome compacts around 200 bp of DNA, the structural unit formed by the union of protamines and DNA is estimated to contain at least 50,000 bp (Castillo, Amaral, & Oliva, 2014).

A notable number of different protamine proteoforms have been identified in the human and mouse spermatozoa, understanding as proteoforms all the different molecular forms of a protein product encoded by a single gene (including changes due to genetic variants, different products from alternative RNA splicing, and PTMs) (Arauz-Garofalo et al., 2021; Brunner et al., 2014; Castillo et al., 2015; Soler-Ventura et al., 2020). In mammals, two different protamines have been described: protamine 1 (P1) and protamine 2 family (P2) (Balhorn, 2007; Barrachina et al., 2019; Jodar & Oliva, 2014; Oliva, 2006; Oliva & Castillo, 2011). In humans, P1 is translated from a single gene, *PRM1*, as a mature protein of 6,823 Da, with 51 amino acids and a 47.1% of arginine, which confers an extremely positive charge (pI=12.08; UniProtKB database https://www.uniprot.org/). Human P2, in contrast, is translated from *PRM2* gene as a precursor (pre-P2) of 102 amino acids that is processed by proteolysis in the N-terminal part giving rise to three mature components: HP2 (the most abundant one), HP3, and HP4 (Jodar & Oliva, 2014; Oliva, 2006). Interestingly, the human mature sperm not only contains P2 mature forms, but also retain pre-P2 and other immature proteoforms (HPI1, HPI2, HPS1, and HPS2) generated by proteolysis that slightly differ in amino acid number in the N-terminal part, whose function has not been revealed yet (de Mateo, Ramos, de Boer, et al., 2011; Soler-Ventura et al., 2020). There is evidence at protein level of another isoform generated by alternative splicing named P2 isoform 2, containing 140 amino acids. It differs from pre-P2 by the incorporation of 50 amino acids between positions 91 and 102 of the canonical sequence (Soler-Ventura et al., 2020). Of note, an RNA corresponding to an additional splice variant, the P2 isoform 3, has been also reported, but not detected at protein level (Soler-Ventura et al., 2020). Both P2 isoforms generated by alternative splicing seem to be only conserved among higher primates but not in other mammals such as mice and rats, and no specific function has been suggested for any of them yet (Soler-Ventura et al., 2020). In global, a high diversity on protamine amino acid sequences exists in the human sperm, comprised in **Figure 7**, raising the question of whether they result from a simple inefficient processing of the precursor, they respond to the need of

redundancy to ensure protamine function, or there is any proteoform-specific functional implication still unknown.

The complexity of the protamine proteoform composition in the sperm cell is even higher when considering post-translational modifications. As indicated in the previous **Section 1.1.3.1**, protamine phosphorylation is required for a proper protamine incorporation into the sperm chromatin (Gou et al., 2020; Papoutsopoulou et al., 1999; Willmitzer et al., 1977a, 1977b; J. Y. Wu et al., 2000). Apart from its role on regulating the NH-NP transition, phosphorylated protamine residues are present in sperm cell from different mammalian species (Arauz-Garofalo et al., 2021; Brunner et al., 2014; Castillo et al., 2015; Chirat et al., 1993; Pirhonen, Linnala-Kankkunen, & Mäenpää, 1994; Pruslin et al., 1987; Soler-Ventura et al., 2020). Our team has recently determined the most complete protamine phosphorylation proteoforms profile in normal human spermatozoon so far, by adapting mass spectrometry (MS) approaches and proteoform identification algorithms to the special properties of the protamines (Arauz-Garofalo et al., 2021; Soler-Ventura et al., 2020). Proteoforms bearing one, two, or three phosphate groups were detected for P1, while P2 was identified with one or two phosphorylations. Of note, pre-P2 showed the highest incorporation of phosphate groups, since mono-, di-, tri- and tetra-phosphorylated proteoforms were identified (Soler-Ventura et al., 2020). Several target residues have been characterized, some of them observed in different studies despite the challenges behind residue-specific characterization of protamine PTMs, such as S9 and S11 in P1 or S37 and S59 for P2 (Chirat et al., 1993; Hornbeck et al., 2015; Soler-Ventura et al., 2020). From those, P1S9 and P2S59 have been also identified in mouse protamine homolog sequences, increasing the interest on protamine PTMs functional role in the male gamete (Brunner et al., 2014). Mouse protamines also bear acetylation and methylation, either as alone or in combination, proving that protamines can bear multiple PTMs in a single molecule (Brunner et al., 2014).

The study of protamine proteoforms through conventional proteomic analysis is challenging due to their very particular physical-chemical properties (very small size, sequence rich in arginine and cysteines, extreme basicity, and highly similar P2 proteoforms). In fact, standardized bottom-up MS methodology relying on trypsin digestion to arginine and lysine residues is not straightforward. To overcome this, the already published works on human and mouse protamine proteoforms applied variations to conventional techniques, such as bottom-up MS after digestion with different proteolytic enzymes combined with top-down proteomics (Brunner et al., 2014; Soler-Ventura et al., 2020). Top-down proteomics arises as an interesting option to study protamine proteoforms since it is based on intact protein analysis, allowing the identification of proteoform microheterogeneity, identifying complex proteoforms like truncated forms, sequence variations, or combinations of multiple PTMs.



Figure 7. Human protamines amino acid sequences. PRM1 and PRM2 genes encoding protamine 1 (P1) and protamine 2 family (P2), respectively, are represented in purple. P2 family is generated by proteolysis from a common precursor (pre-P2), generating mature forms (HP2, HP3, HP4), and intermediate forms (HPI1, HPI2, HPS1, and HPS2). Intermediate forms together with pre-P2, comprise P2 immature forms. Arginines are highlighted in blue, cysteines in orange. Lilac undercolour indicates phosphorylation sites. Purple lines in pre-P2 mark proteolytic sites of mature and intermediate P2 forms. Numbers in P2 mature and immature forms indicate the starting amino acid with respect to pre-P2 sequence. Based on Oliva, 2006; de Mateo et al., 2011b; Jodar and Oliva, 2014; Soler-Ventura et al., 2020.

Several mouse models have been generated to increase the knowledge and relevance of protamine proteoforms in sperm function and proper chromatin conformation (Cho et al., 2001, 2003; Takeda et al., 2016). First studies based on the generation of chimeric mice showed that haploinsufficiency of mouse protamine 1 or protamine 2 genes (*Prm1* or *Prm2*, respectively) resulted in male infertility (Cho et al., 2001, 2003; Takeda et al., 2016). However, the recent application of cutting-edge gene edition using CRISPR/Cas9 technology, whose precision and efficiency avoids disturbing gene structure or regulatory DNA sequences, has rapidly changed the paradigm, as described below (summarized in **Table 3**).

- **Protamine 1 KO models**: Targeted disruption of both alleles of *Prm1* induced infertility with dramatic alterations of epididymal sperm. Sperm were immotile and presented head defects, damaged membrane, and disrupted acrosome. Impaired sperm chromatin integrity was accompanied by almost completely fragmented DNA. The sperm chromatin and membrane integrity were impaired already in the testis. In contrast, depletion of one *Prm1* allele led to subfertility (decreased pregnancy rate resulting in reduced litter size), and although sperm motility was drastically impaired, the sperm showed no head morphological defects and better chromatin integrity. Both $Prm1^{-/-}$ and $Prm1^{+/-}$ mice accumulated pre-P2 and showed flagellum defects (Merges et al., 2022).

- **Protamine 2 KO models**: In contrast to what has been observed in $Prm1^{+/-}$ mice, the loss of just one allele of *Prm2* was tolerated and the mice were fertile. The disruption of both *Prm2* alelles was the only condition resulting in infertility, exhibiting a very similar phenotype to $Prm1^{-/-}$ mice (Schneider et al., 2016, 2020). Sperm evaluation of targeted $Prm2^{-/-}$ mice revealed normal epididymal sperm counts but with very drastic flagellar and acrosomal morphological alterations, resulting in immotile sperm (Schneider et al., 2016). However, testicular sperm did not apparently show morphological alterations, suggesting that sperm defects in $Prm2^{-/-}$ mice are acquired during epididymal transit (Schneider et al., 2020). In fact, Prm2-deficient testicular sperm showed a success rate to develop blastocyst after ICSI like that of wild-type testicular sperm. Upregulation of Prm1 expression is observed in deficient $Prm2^{-/-}$ mice to compensate the loss of Prm2, but even though it seems enough to properly package the testicular sperm DNA, it is insufficient to generate a functional epididymal spermatozoa. It has been suggested that Prm2 incorporates zinc in its structure to stabilize the sperm chromatin in the testis (Bianchi et al., 1992; Björndahl & Kvist, 2011), that are released during sperm epididymal maturation (G. M. Dias et al., 2006). Recent findings have proposed that zinc released by Prm2 is incorporated into

the structure of the antioxidant protein SOD1 in the epididymis, conferring stability and ensuring an optimal antioxidant activity inside spermatozoa during sperm maturation. Therefore, the loss of Prm2 could result in a low antioxidant capability of the epididymal sperm that might promote alterations in sperm DNA, membranes, and morphology (Schneider et al., 2020)(Schneider et al., 2020).

- **Protamine 2 precursor KO models**: Not only gene editing of mature protamines revealed interesting phenotypes. Depletion of the cleaved part of pre-P2 (cP2 domain) in one or both alleles ($Prm2^{+/\Delta c}$ and $Prm2^{-/\Delta c}$, respectively) results in immotile and inviable sperm, similar to $Prm2^{-/-}$ and $Prm1^{-/-}$ spermatozoa (Arévalo et al., 2022). Additionally, testicular sperm from $Prm2^{+/\Delta c}$ and $Prm2^{-/\Delta c}$ transgenic mice already show DNA fragmentation that increase throughout epididymal transit, contrasting with the phenotype observed in $Prm2^{-/-}$ mice. These different results could be explained by a disruption of the synergistic process of NH-NP mediated by H2A.L.2-TP complexes potentially induced by the loss of cP2, which may end with a random incorporation of P2 in the sperm chromatin (Arévalo et al., 2022). Non-specific binding of protamines to DNA lead to strong DNA hypercondensation, which could result in strand breaks in testicular spermatozoa. Moreover, it seems that TPs are retained in sperm chromatin in absence of cP2, therefore avoiding P1 and P2 incorporation. Strong oxidative DNA damage in cauda epididymis and complete epididymal sperm DNA fragmentation were reported in both $Prm2^{+/\Delta c}$ and $Prm2^{-/\Delta c}$ mice. Of note, the $Prm2^{-/\Delta c}$ model displayed a more severe phenotype, showing not only alterations on sperm motility and morphology, but also reduced sperm counts.

Table 3. Sperm evaluation and fertility status of the available protamine-deficient mouse models.

	Generation of mice mutants	Sperm concentration	Sperm motility	Sperm morphology	Sperm DNA damage	Fertility	Others	References
Chimeras Prm1$^{+/-}$	Disruption of 1 allele coding sequence (*Prm1* or *Prm2*) in ESC by homologous recombination and ESC injection into blastocysts	Normal	Reduced	Flagellum tightly wrapped around the head or with elongated heads having a reduced ventral flexure	Altered sperm chromatin integrity, higher sperm DNA fragmentation	No sire produced	Only P1 protein was reduced. Abnormally processed P2	(Cho et al., 2001, 2003)
Chimeras Prm2$^{+/-}$							P1 and mature P2 were reduced. Abnormally processed P2	
Prm1$^{+/-}$	*Prm1*-deficient chimeric female carrying *Prm1*-deficient oocytes	Normal	Reduced	Abnormal morphology mainly in the tail	Altered sperm chromatin integrity, higher sperm DNA fragmentation	No (natural mating/IVF) except IVF with zona-free oocytes	Enhanced acrosome reaction and reduced mitochondrial membrane potential. Reduced P1 and mature P2. Abnormally processed P2	(Takeda et al., 2016)
Prm1$^{+/-}$	CRISPR/Cas9 mediated gene-editing in zygotes	Normal	Drastically decreased	Normal (no drastic head defects)	Low but detectable DNA fragmentation	Subfertile (low pregnancy rate, reduced litter size)	Accumulation of P2 precursor. Impaired flagellar structure.	(Merges et al., 2022)
Prm1$^{-/-}$		Normal	Immotile	Head (lose of hooked-shape, smaller, elliptic, thinner), membrane, acrosome, deffects	Altered sperm chromatin integrity. Almost all DNA is fragmented, some part remains intact	No sire produced	Accumulation of P2 precursor, increased histone retention, defects on chromatin hypercondensation. Impaired flagellar structure and membrane	
Prm2$^{+/-}$	CRISPR/Cas9 mediated gene-editing in oocytes	Normal	Normal	Normal	Normal	Fertile	Reduced P2	(Schneider et al., 2016, 2020)
Prm2$^{-/-}$		Normal	Immotile	No acrosome, midpiece wrapped around sperm head	Altered sperm chromatin integrity, fully fragmented DNA	No sire produced	No P2 and upregulation of P1. Declined viability	
Prm2$^{+/\Delta c}$	CRISPR/Cas9 mediated gene-editing in oocytes	Normal	Drastically decreased	Slimmer less-hooked or smaller hookless nucleus	Completely fragmented DNA	Infertile	Drastic viability decrease. Switched P1/P2 ratio, pre-P2 accumulation. Impaired nuclear P2 eviction	(Arévalo et al., 2022)
Prm2$^{-/\Delta c}$		Reduced	Drastically decreased	Similar but more severe nuclear defects than Prm2$^{+/\Delta c}$	Completely fragmented DNA, even more severe	Infertile	Drastically decreased viability. Pronounced switch of P1/P2 ratio. Additional P2 signal in spermatid cytoplasm and residual bodies.	
Prm1$^{S9A/+}$	CRISPR/Cas9 mediated Knock-in Mutations in specific P1 ph-sites	Normal	NA	Normal	Normal DNA compaction	Fertile	-	(Gou et al., 2020)
Prm1$^{S43A/+}$		Normal	NA	Normal	Normal DNA compaction	Fertile		
Prm1$^{S9S43A/+}$		Slightly reduced	NA	Normal	Normal DNA compaction	Drastic Reduced		
Prm2$^{S56A/A}$	CRISPR/Cas9 mediated Knock-in mutations in specific P2 ph-sites	NA	NA	NA	NA	Fertile	-	(Itoh et al., 2019)
Prm2$^{S56D/D}$		NA	NA	NA	NA	Fertile		

3.2.2.2 The structural organization of the nucleo-protamine

The first steps towards understanding the sperm chromatin structure were based on microscopy observations of the extremely condensed nucleus and the determination of protamine and DNA chemical composition. More than a century ago, the characterization of "protamin" (extremely basic nature) and "nuclein" (later identified as DNA, with acidic nature) extracted from salmon sperm, suggested strong electrostatic interactions underlying the highly condensed sperm nuclear structure (Dahm, 2005a; Miescher, 1874).

A deeper study on sperm protamines showed high inter-species variability, since either mature sperm from many vertebrates do not have protamines or, when present, the aminoacidic sequences show low homology. This variability contrasted with the extremely well-conserved somatic chromatin based on histone packaging (Kasinsky et al., 1987, 2011; Mezquita, 1985; Oliva & Dixon, 1991; Soler-Ventura et al., 2018; Subirana, 1983), which probably motivated that, despite protamines were one of the first proteins to be isolated, the detailed study of the NP structure, composition, and function started much later than that of the NH (Bloch, 1969; Dixon, 1972).

The nucleo-histone structure was elucidated by a combination of electron microscopy techniques, evidencing a "beads on a string" image, combined by determination of nucleosomal elementary size from partial micrococcal nuclease chromatin digestion and size determination of the generated DNA fragments, as shown in **Figure 8** (Subirana et al., 1985). Nucleosome crystallization allowed determining its high-resolution structure by X-ray diffraction (Azorin et al., 1980; Subirana, 1997), which has not been achieved so far for the nucleo-protamine. Thus, the available information and models on the nucleo-protamine structure, either extracted *in vivo* or reconstituted *in vitro,* are based on the combination of a wide range of microscopic techniques and X-ray diffraction in solution.

The study of human, mouse, and rooster sperm through electron and/or atomic force microscopy evidenced a combination of toroidal structures (external diameter = 50-160 nm, width = 40-55 nm) and *rod-like* structures (thickness = 40-55 nm, length = 160-350nm), summarized in **Figure 8** (Allen et al., 1993, 1997; Ausió et al., 2014; Balhorn, 2007; Hud et al., 1993, 1995; Vilfan et al., 2006). Remarkably, similar toroidal structures were obtained *in vitro* upon DNA condensation with purified protamines and other cations (Conwell et al., 2003; Conwell & Hud, 2004; DeRouchey & Rau, 2011).

At the finest structure, derived from X-ray diffraction of tRNA-protamine crystals, led to propose a model where protamine molecules would bind the minor groove of tRNA double helical portion (Warrant & Kim, 1978). However, tRNA-based results are not necessarily extrapolated to infer the DNA-protamine complex structure. In fact, *in vitro* reconstituted nucleo-protamine in solution or native sperm chromatin analyzed by X-ray diffraction suggest that protamine molecules would align along the DNA, binding to the major groove, favored by most of the

studies (**Figure 8**) (Balhorn, 1982; Fita et al., 1983; Vilfan et al., 2004). Complementary, molecular dynamics simulations and free energy calculations with full atomistic details indicate that protamine molecules located in the major groove rather use the DNA backbone as binding site, representing the best compromise between enthalpy and entropy (Mukherjee et al., 2021). These linear complexes of DNA and protamine have also been proposed to associate side-by-side in a close-packed hexagonal arrangement (**Figure 8**) (Allen et al., 1993; Balhorn, 1982; Fita et al., 1983; Hud & Downing, 2001; Hud & Vilfan, 2005; Sartori Blanc et al., 2001). Accurate measurements using small angle X-ray scattering (SAXS) concluded that in this hexagonal lattice, the equilibrium interaxial spacing (D_{int}, representing the actual distance between DNA helices) is 30.1 A° for bull sperm nuclei and 29.2 A° for salmon sperm nuclei, both in solution at near physiological salt conditions (150 mM NaCl), without reducing agent and at a temperature of 20ºC (**Figure 8**) (Hutchison et al., 2017). A different approach based on infrared spectroscopy of DNA complexed with salmon and squid protamines concluded found large amounts of defined protamine secondary structure stabilized by intramolecular hydrogen bonds, efficiently promoting tight hexagonal packing of the DNA molecules (Roque et al., 2011).

Inter- and intra-molecular disulfide bonds and formation of zinc bridges are an additional layer of stabilization in cysteine-containing protamines, in addition to the strong electrostatic interactions derived from the positively charged arginine residues in protamine sequence and the negatively charged phosphates of the DNA backbone (Balhorn, 2007; Björndahl & Kvist, 2011; Hutchison et al., 2017; Vilfan et al., 2004). As discussed in previous sections, this tightly packaged structure condenses most of the sperm DNA, is non-randomly distributed along the genome, and intercalates with regions retaining histones and nucleosomes, providing an epigenetic richness which is transferred to the oocyte upon fertilization (Castillo, Amaral, Azpiazu, et al., 2014; Castillo et al., 2015; Gatewood et al., 1987; S. Hammoud et al., 2009; Oliva, 2006).

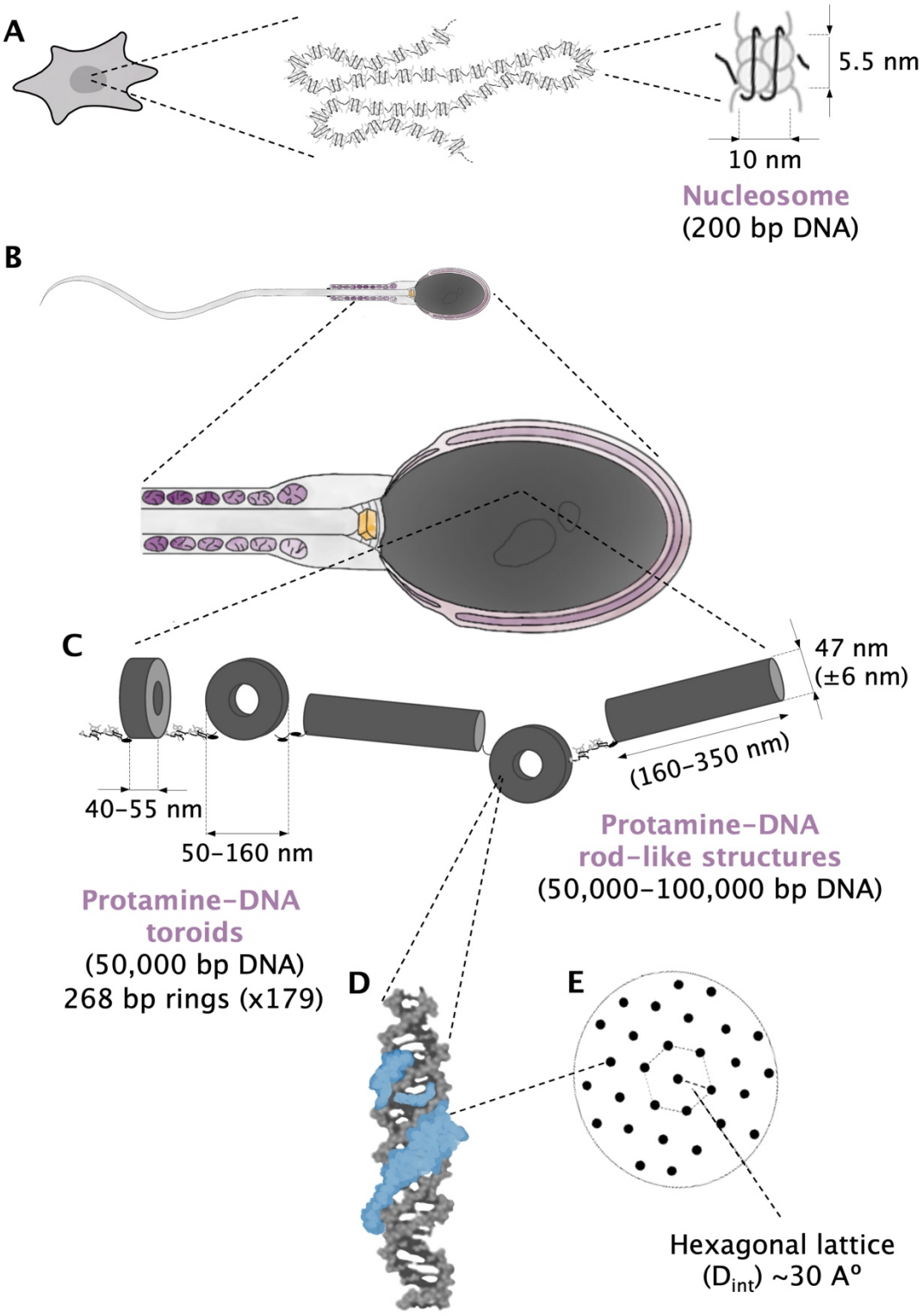


Figure 8. Current model of mammalian nucleo–protamine structure. Representations of (**A**) somatic human cell and (**B**) nucleo–histone structure. (**C**) Human spermatozoon and enlarged section of head and midpiece. (**D**) Current model of nucleoprotamine structure formed by toroidal structures and rod–like nucleo–protamine structures. (**E**) Favoured model of protamines would longitudinally locate in the major groove of DNA. (**F**) Linear complexes of DNA and protamine associate side–by–side in close–packed hexagonal arrangements with interaxial spacing (Dint) representing the actual distance between DNA helices is 30 A°.

3.3 Sperm contribution to fertilization and beyond

The classical perspective of the sperm being a simple carrier of the paternal DNA has been maintained until a couple of decades ago (Dahm, 2005b; Maruyama & Singson, 2006; Miescher, 1874). However, the application of high-throughput technologies ('omics') has allowed to provide evidence that the male gamete contains a wide set of layers of information, much more than half of the DNA of a new individual. When fertilizing, the sperm cell provides a DNA containing different epigenetic marks such as DNA methylation (S. Hammoud et al., 2010; Siklenka et al., 2015), histones and protamines' PTMs (Arauz-Garofalo et al., 2021; Brunner et al., 2014; Brykczynska et al., 2010; Carrell et al., 2008; Castillo et al., 2015; Siklenka et al., 2015; Soler-Ventura et al., 2020), and genes differentially distributed into the nucleohistone and the nucleoprotamine domains (Arpanahi et al., 2009; Brykczynska et al., 2010; Carone et al., 2014; Castillo, Amaral, & Oliva, 2014; Castillo, Amaral, Azpiazu, et al., 2014; Erkek et al., 2013; S. Hammoud et al., 2009; Y. H. Jung et al., 2017; Luense et al., 2019; Ozturk et al., 2021; Saida et al., 2011; Samans et al., 2014; Yamaguchi et al., 2018). All these epigenetic marks coexist with a complex population of RNAs and proteins, some of them being essential for early embryogenesis and future offspring health (Amaral et al., 2014; Castillo, Amaral, & Oliva, 2014; Castillo, Amaral, Azpiazu, et al., 2014; Castillo et al., 2018; de Mateo, Castillo, et al., 2011; Jodar et al., 2013, 2015). They are summarized in **Figure 9**.

In terms of sperm chromatin epigenetic potential, whereas the study has mostly been approached through DNA methylation analysis (S. Hammoud et al., 2010; Laurentino et al., 2016; Leitão et al., 2020; Siklenka et al., 2015), the advances on the description of the sperm proteome have revealed that the male gamete carries a substantial number of nuclear proteins with epigenetic roles, involved in gene expression regulation modulating transcription, biogenesis of non-coding RNAs, and the stablishment of DNA and histone marks (Castillo, Amaral, & Oliva, 2014; Castillo, Amaral, Azpiazu, et al., 2014; Castillo et al., 2015, 2018). To fully understand the impact of the proteomic contribution to the zygote and developing embryo, it is important to consider that the sperm cell is the product of the spermatogenesis and extra-testicular maturation, highly complex differentiation processes involving changes at many different levels (genetic, proteomic, chromatin, biochemical, structural), which has already been formerly discussed in sections 1.1.1 and 1.1.2. Therefore, some of the sperm proteins could represent spermatogenic leftovers required for spermatogenesis or extra-testicular maturation, while some others have a direct implication in oocyte fertilization. However, recent findings suggest that the sperm proteome also contains groups of proteins with the potential to be post-translationally modified that are delivered to the embryo, which could have a role immediately after fertilization and during pre-implantation embryo development (Castillo et al., 2018).

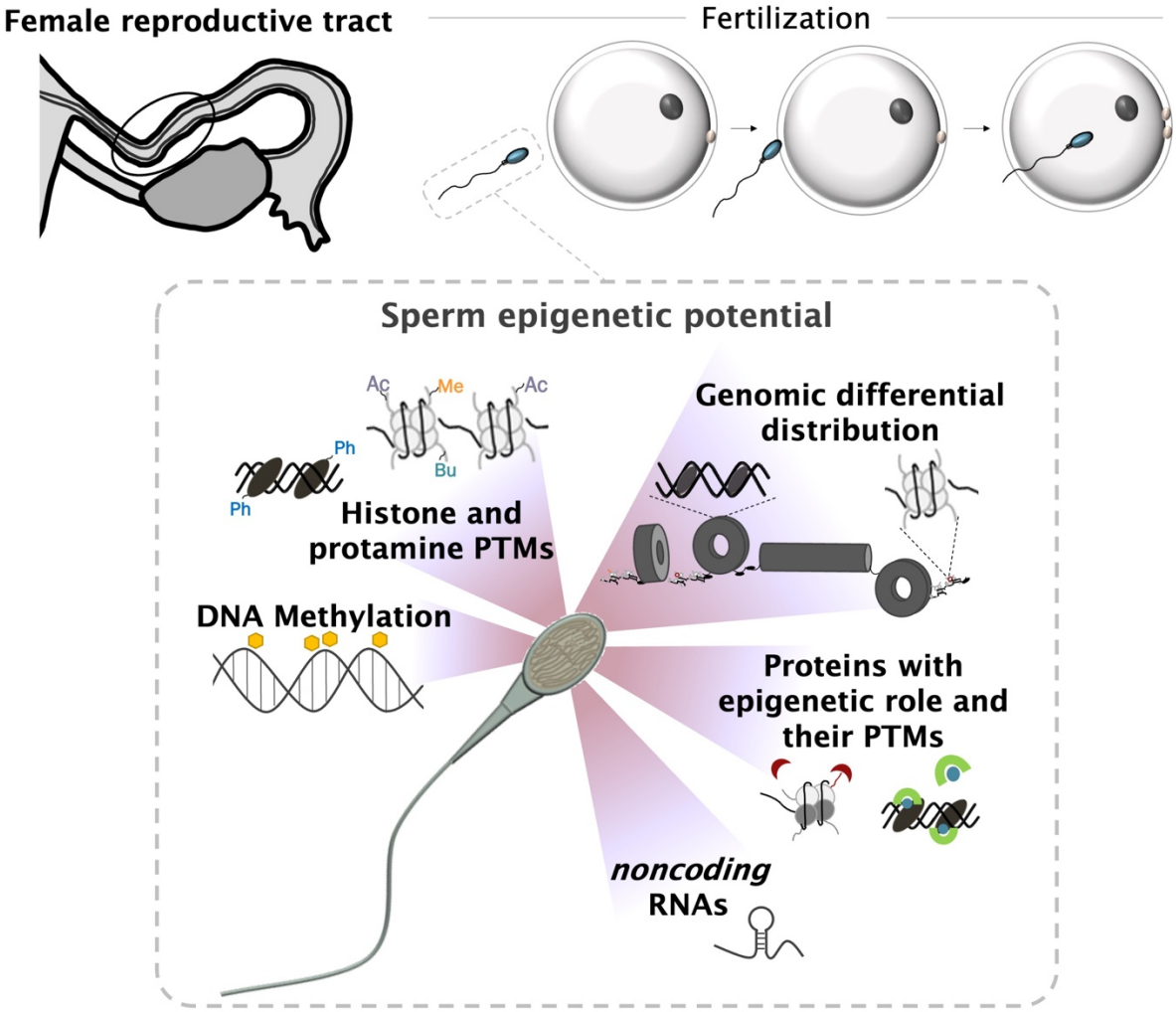


Figure 9. Sperm epigenetic potential. Depiction of the different layers of epigenetic information contained in mature sperm nucleus at fertilization in the female reproductive tract, comprising a complex set of epigenetic marks.

3.3.1 Post-fertilization events: zygotic male pronuclear reprogramming

After fertilizing the oocyte, the sperm nucleus coexists independently with the oocyte nucleus within the zygotic cytoplasm. Even though both sperm and oocyte nuclei contain haploid genomes, they are extremely different in terms of chromatin state. The highly compacted sperm nucleus that was acquired during spermiogenesis and extra-testicular sperm maturation, which is transcriptionally and translationally inert, must be epigenetically reprogrammed through protamine removal and histone incorporation to allow embryonic genome activation to start the pre-implantation embryo development (Collas & Poccia, 1998; Okada & Yamaguchi, 2017).

Like its spermatogenic mirroring process of NH-NP, the process of nucleoprotamine to nucleohistone (NP-NH) transition is highly coordinated. The protein family of nucleoplasmins are essential for male pronuclear decompaction (Philpott & Leno, 1992). Interestingly, besides nucleoplasmins, some key players involved in the NH-NP transition or in its epigenetic regulation have been found crucial for the reverse process of protamine-to-histone (NP-NH) transition in the zygote, represented in **Figure 10**. SRPK1-mediated protamine phosphorylation accelerates the process of male pronuclear decompaction by recruiting nucleoplasmin to H3.3 retained nucleosomes, which has been suggested as starting point of protamine removal (Gou et al., 2020). Moreover, phosphorylated protamines would recruit HIRA to deposit H3.3 into newly generated free DNA regions, essential for *de novo* nucleosome assembly and required for a proper nuclear envelope formation in the zygote (Gou et al., 2020; Inoue & Zhang, 2014; Lin et al., 2014; van der Heijden et al., 2005). ASF1 assists the load of H3.3-H4 dimers on HIRA, before their incorporation into paternal chromatin (Horard et al., 2018). Other histone variants such as TH2A, TH2B, and H2A.X, and histone PTMs such as H3K4 methylation mediated by the methyltransferase Mll3/4 also play a crucial role in paternal genome reprogramming guiding genome-wide chromatin transitions (Aoshima et al., 2015; Montellier et al., 2013; Nashun et al., 2010; Shinagawa et al., 2014).

These finding also suggest a coordinated epigenetic regulation of the process, that somehow resembles to that of the NH-NP transition. Therefore, it could be thought that impairments on the nucleo-protamine structure derived from either inefficient nuclear compaction, poor structural stabilization during extra-testicular maturation, or altered composition of sperm protamine proteoforms, could also impact the de-protaminization rhythms in the zygote and have potential effects on paternal nuclear reprogramming and beyond.

The study of this reverse process could be of high interest as a model to find new regulators of the spermiogenic process. For example, H4R3 methylation plays a role in the de-protaminization of the male pronucleus (Hatanaka et al., 2017) but its potential role during spermiogenesis is yet unknown. However, recent findings

identify H3 arginine methylation during spermiogenesis, prior to phosphorylation of H3T3 by Haspin, but with unknown function (Soupsana et al., 2021). Also, H3 arginine dimethylation in the core histone weakens its affinity to the DNA (Casadio et al., 2013). It is known that arginine methylation in the histone tail is related with transcriptional activation (i.e., open chromatin states), and H4R3me2 promotes subsequent acetylation of H4 histone tails by P300 in HeLa cells (H. Wang et al., 2001). H4 arginine methylation is indeed regulated by crosstalk of its modulating proteins with with other H4 coil PTMs, such as acetylated/butyrylated K5 or phosphorylated S1, (Fulton et al., 2022), which is involved in histone accessibility and mitotic chromatin compaction and is essential for a histone deacetylation after DNA-breaks repairs (Krishnamoorthy et al., 2006; Utley et al., 2005). This may lead us think of a role of histone arginine methylation on nucleosome destabilization during spermiogenesis coordinated with acetylation, phosphorylation, and proteins modulating them.

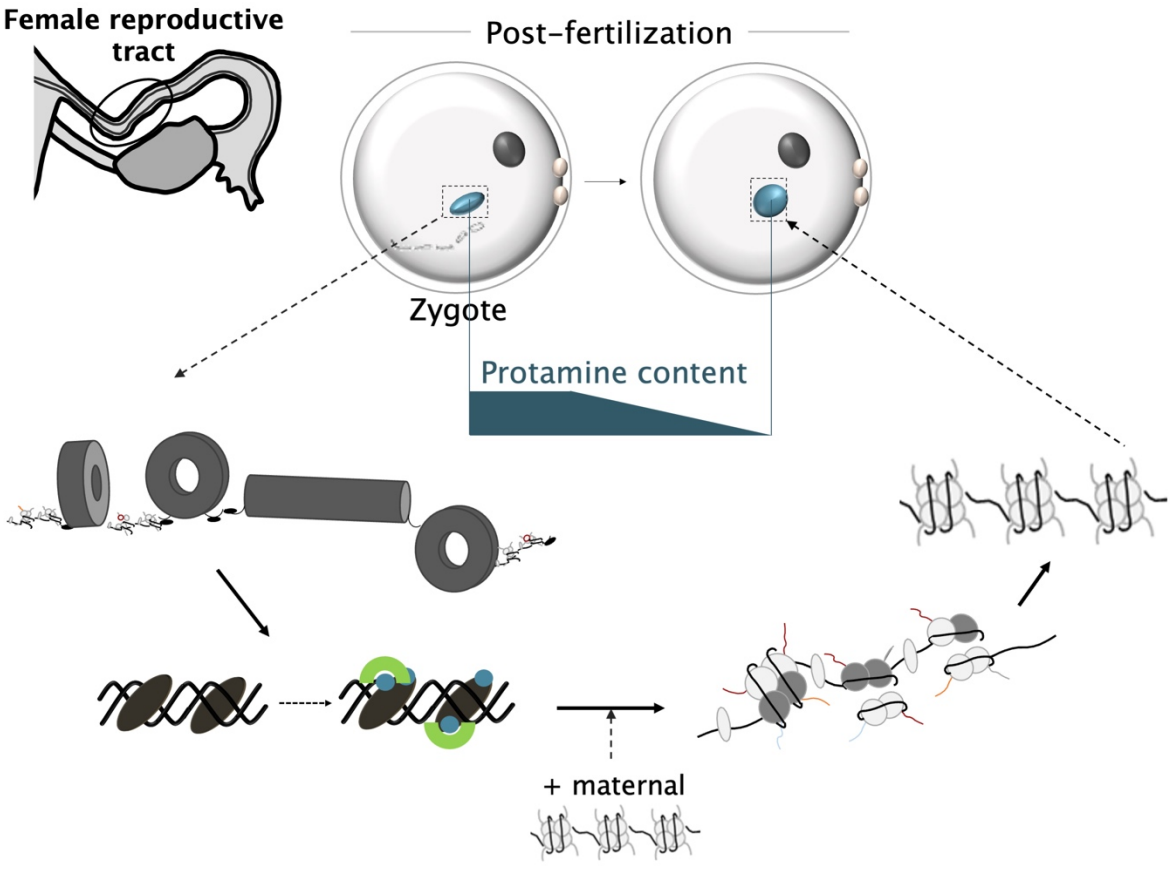


Figure 10. Male pronuclear remodeling. The process of nucleo-protamine to nucleo-histone transition happens in the zygote, where some proteins that were needed to achieve a proper NH-NP transition in the testis play a role in reprogramming the male genome.

3.4 Male infertility

According to definitions by the World Health Organization (WHO), infertility, in terms of the couple, refers to the "*disease of the male or female reproductive system defined by the failure to achieve pregnancy after at least one year of regular unprotected sexual intercourses*" (World Health Organization, 2022). This condition affects around 186 million people globally, corresponding to an approximate 12% of couples seeking for a child, and a general decline of global fertility cases from 4.7 to 2.4 live births between the last 7 decades is reported (Agarwal et al., 2021; Mascarenhas et al., 2012; Murray et al., 2018; Skakkebaek et al., 2019). Among all cases, male factor is present in the 50% of the couples (20–30% solely, beyond 20% contributory), and different studies evidence a negative trend in sperm quality in the last 60 years (Agarwal et al., 2021; Levine et al., 2017; Lv et al., 2021; Salonia et al., 2021; Tiegs et al., 2018).

Among the possible known causes of male infertility, a wide variety of alterations are included, such as anatomical defects as varicocele, primary spermatogenic failure, obstructions and ejaculation failure, genital tract infections, genetic disorders, endocrine alterations, and immune problems, among others (Jungwirth et al., 2019; Minhas et al., 2021; Tiegs et al., 2018). Despite thorough diagnostic workups have been stablished including evaluation of clinical history, physical exploration, semen analysis, and hormonal profile, the cause of infertility remains elusive in about 50% male infertility causes (Agarwal et al., 2021). The so-called infertility of unknown origin is referred as idiopathic male infertility when there is a reduction of semen quality with no apparent reason, or as unexplained infertility when seminal parameters are considered normal (see **Table 4** in **Section 1.4.1**) (Agarwal et al., 2021; J. H. Jung & Seo, 2014; Jungwirth et al., 2019; Minhas et al., 2021; Sansone et al., 2018). Apart for sociodemographic factors, such as delay in childbearing, that could underly global fertility rates, other factors including lifestyle, environment, and toxic habits can affect the quality and development of gametes and embryo and are considered risk factors for idiopathic male infertility. Besides the direct potential effects on male reproductive health, they can be transmitted to the offspring via genetic and epigenetic alterations (Agarwal et al., 2021; Balawender & Orkisz, 2020; R. Sharma et al., 2013; Tiegs et al., 2018).

The global trends on male reproductive health decline evidence several common symptoms that are englobed within the concept of testicular dysgenesis syndrome. This condition includes increasing incidence of testicular cancer, low semen quality and potential decline over the time, spermatogenic impairments, high possibility and increasing frequencies of cryptorchidism (undescended testis), hypospadias, different spectra of sex development, and growing demand of assisted reproduction techniques (ART) (Skakkebæk et al., 2001; Skakkebaek et al., 2016a). Genetic, epigenetic, and environmental factors could have a role in the etiology underlying this syndrome. Several signs of this syndrome that manifest during adulthood have a potential origin during fetal development in the mother's uterus suggesting that environmental exposure of the fetal testis might contribute to the

phenotype. Indeed, recent findings point out that environmental exposures are the most important factors in the observe declined trends, rather than genetic susceptibility, even though it is still multifactorial (Skakkebaek et al., 2016a, 2019).

Facing male infertility and testicular dysgenesis syndrome diagnosis, evaluation of seminal parameters and testicular histology are performed, respectively. However, these approaches are insufficient in cases of unknown etiology, to whom complementary unconventional analyses that are not part of the infertility clinic routines have been proposed. In these cases, ART are the only available treatment, together with hormonal and non-hormonal empirical therapies and changes in lifestyle.

3.4.1 Evaluation of seminal parameters

The first step towards the evaluation of male fertility is the analysis of the seminal parameters, known as seminogram. The guidelines for seminal parameters' evaluation by the WHO have been recently updated in their 6th Edition of the *WHO Laboratory Manual for the Examination and Processing of Human Semen*, and the cutoff values (shown in **Table 4**) continue evolving over the years, reflecting the general decrease in semen quality (World Health Organization, 2021). Patients presenting all seminal parameters over the threshold values are known as normozoospermic.

Table 4. Seminal parameters cutoff according to the 5th and 6th editions of the WHO Laboratory Manual for the Examination and Processing of Human Semen. The numbers indicate the reference normal values (5th percentile of the distribution of semen examination results) and the 95% confident interval is expressed in brackets. Values under references lead to different types of seminal alterations.

	WHO Manual 5th Edition (2010)	WHO Manual 6th Edition (2021)	Seminal alteration
Semen volume (mL)	1.5 (1.4–1.7)	1.4 (1.3–1.5)	Hypospermia (<1.4) Aspermia (0)
Sperm concentration (10^6/mL)	15 (12–16)	16 (15–18)	Oligozoospermia (<16)
Total sperm count (10^6/mL)	39 (33–46)	39 (35–40)	Criptozoospermia (<0.1) Azoospermia (0)
Sperm progressive motility (%)	32 (31–34)	30 (29–31)	Asthenozoospermia
Sperm total motility (PR+NP, %)	40 (38–42)	42 (40–43)	
Normal forms (%)	4 (3–4)	4 (3.9–4)	Teratozoospermia
Vitality (%)	58 (55–63)	54 (50–56)	Necrozoospermia

PR = progressive, NP = non-progressive

Alterations in one or more seminal parameters lead to different types of seminal alterations and are associated with male infertility, which are gathered in **Table 4**. When the semen volume is reduced, the patient can present either hypospermia, or aspermia if there is no ejaculate, normally caused by retrograde ejaculation. If the sperm concentration is under the reference value, the patient exhibits oligozoospermia. When concentration is under 5 million of sperm per mL (Mz/mL), the phenotype is generally classified as severe oligozoospermia. If no sperm are observed in fresh preparations during the seminal evaluation, but they are seen in a centrifuged pellet, the patient present criptozoospermia (normally <0.1 Mz/mL). In case they are neither observed after centrifugation (sperm concentration of 0 Mz/mL), the patient displays azoospermia. Low percentage in either progressive (motility type A: the sperm moves forward; and B: sperm moves without a specific direction) or total (motility A, B, and C: the sperm moves but does not displace, known as non-progressive) sperm motility leads to asthenozoospermia. Low sperm motility can sometimes be related with low vitality levels, known as necrozoospermia. Percentage of normal forms under the threshold is named teratozoospermia. All of them can have different etiology and can be either pure phenotypes or combinations, leading to more complex phenotypes.

Other alterations, such as haemospermia (also known as hematospermia), the presence of erythrocytes in the ejaculate, or leukospermia (also known as leukocytospermia or pyospermia), which is the presence of leucocytes in the ejaculate over 10% with respect to total sperm count, are also related with poor semen quality and could be indicators of problems in the male reproductive tract (Agarwal et al., 2021; World Health Organization, 2021).

3.4.2 Evaluation of testicular histology

Apart from the basic male infertility evaluation through clinical history, physical exploration, semen analysis, and hormonal profile, testicular biopsies provide important information for further categorization of men with low or zero sperm production, helping to find a diagnostic or guide the fertility treatment (Cerilli et al., 2010; Male Infertility Best Practice Policy Committee of the American Urological Association & Practice Committee of the American Society for Reproductive Medicine, 2006; McLachlan et al., 2007). The causes can have their origin at three different levels:

i) Pretesticular, defined as extragonadal endocrine disorders affecting spermatogenesis through failures in hormonal stimulation or direct suppression.

ii) Testicular, or primary defects of the testes that can be either congenital or appear after disease processes or environmental aggresions.

iii) Post-testicular, which mostly are obstructions of the ducts further to the testes.

The etiology of male infertility due to testicular dysfunction can have its origin on congenital disorders, either by chromosomal abnormalities affecting sexual and autosomal chromosomes that cause numerical or structural aberrations, or by monogenic cause through single nucleotide variants. Developmental factors, such as undescended testis, are also associated with spermatogenic failure. In other cases, the testicular failure is acquired throughout life, after genitourinary infections, varicocele, gonadotoxic cancer treatments, or intake of medications that can impact testicular function. Also, exposure to environmental hazards or adverse lifestyle factors underly testicular failures. However, the cause is still unknown in a relevant percentage of the cases (Cerilli et al., 2010; A. Sharma et al., 2021).

Among the current European Association of Urology recommendations for the report of a testicular biopsy (Cerilli et al., 2010; Male Infertility Best Practice Policy Committee of the American Urological Association & Practice Committee of the American Society for Reproductive Medicine, 2006; McLachlan et al., 2007), the following testicular alterations can be distinguished (illustrated in **Figure 11**):

a) Sertoli-cell only syndrome (SCOS): total absence of germ cells inside the seminiferous tubules (germ cell aplasia), respecting the tubular architecture and supporting cells, being Sertoli cells the only intratubular cell type observed. Testicular histology resembles to a prepubertal stage and interstitial Leydig cells are observed.

b) Spermatogenic arrest (SA): spermatogenesis stops developing after a determined germ cell type. It is more frequent at the primary spermatocyte level due to meiotic impairments but can happen at any other cell type. The arrest can be total, if it happens uniformly throughout all seminiferous tubule sections (therefore named maturation arrest), or partial, if some seminiferous tubule sections with complete spermatogenesis are observed.

c) Hypospermatogenesis (HP): full spermatogenesis occurs, but the total number of germ cells is decreased. Although it may exist in all tubules, variability across tubules is common, including some SCOS-like pattern.

d) Hyalinization of seminiferous tubule: total absence of cells in the seminiferous tubules, it is also known as tubular sclerosis. Hyalinization can be intra or peritubular, usually accompanied by fibrosis and accumulation of membrane-like material in the basement. Some Leydig cells may remain in the interstitium.

The evaluation of the testicular biopsy helps to discriminate between primary testicular failures or blockages. When the azoospermic patient's testicular histology displays a normal and complete spermatogenesis, it is suggestive of an obstructive azoospermia. However, non-obstructive azoospermia (primary testicular failure)

entails a more challenging diagnostic. Apart from spermatogenic defects, testicular biopsies are diagnostic tools currently used to characterize other testicular pathologies, such as testicular tumors. The presence of testicular tumors is not exclusive or other pathologies, and can also be accompanied by spermatogenic alterations, giving rise to male infertility cases of complex diagnosis.

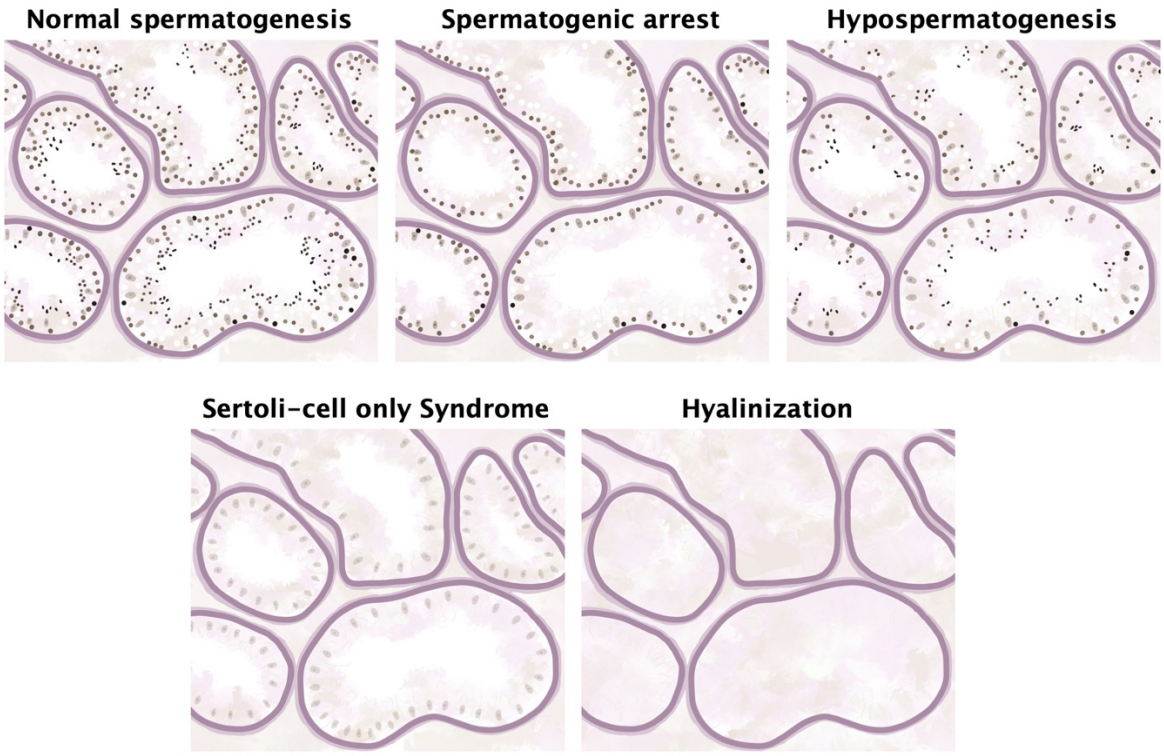


Figure 11. Illustrations of testicular biopsies representing different spermatogenic alterations compared with normal spermatogenesis.

3.4.2.1 Testicular tumors

Testicular cancer is the most common cancer in the adolescent and young adults (AYA) population in many countries, comprising the reproductive age. Therefore, fertility preservation of testicular tissue prior gonadotoxic treatments such as chemotherapy or radiotherapy is common among these patients (Saltzman & Cost, 2018). The incidence of testicular tumors has increased during the last decades and continues rising, representing 1% of adult neoplasms and a 5% of urological tumors. According to their development and epigenetic features, testicular tumors can be classified according to the WHO latest update in 2016 in pathological classification (Moch et al., 2016; Williamson et al., 2017), gathered in the EAU Guidelines on Testicular Cancer (Laguna et al., 2022), as shown in **Table 5**. Among them, the predominant histology is the so-called testicular germ cell tumors (TGCT). They can either be related or not to a precursor intratubular lesion named germ cell neoplasia *in situ* (GCNIS). The key underlying pathogenicity of those

derived from GCNIS arises from impaired fetal differentiation of gonocytes into spermatogonia due to a combination of genetic and environmental factors that lead to insufficient activity of testicular somatic cell niche, resulting in arrested differentiation and prolonged expression of pluripotency genes. The derived cells are called delayed gonocytes or pre-GCNIS cells, which acquire secondary genomic changes becoming invasive tumor cells (GCNIS) at the time they adapt to post-pubertal testis niche, either proliferating to seminomas or re-programming to non-seminoma subtypes. Germ cell tumors non-related to GCNIS such as spermatocytic tumors arise after birth, from germ cells acquiring gain-of-function genetic variants in genes that promote spermatogonial survival or proliferation, at least in a subset of cases. The pathogenesis of testicular germ cell tumors is represented in **Figure 12** (Rajpert-De Meyts et al., 2016; Skakkebaek et al., 2016b).

Table 5. Histological classification of the testicular tumors according to reccomendations of the WHO latest update in 2016 in pathological classification (Moch et al., 2016; Williamson et al., 2017), gathered in the EAU Guidelines on Testicular Cancer (Laguna et al., 2022)

1. Germ cell tumors	**4. Sex cord/stromal tumors**
Germ cell neoplasia in situ (GCNIS)	Leydig cell tumor
	Malignant Leydig cell tumor
2. Germ cell tumors derived from GCNIS	Sertoli cell tumor
Seminoma	Malignant Sertoli cell tumor
Embryonal Carcinoma	Large cell calcifying Sertoli cell tumor
Teratoma, post-pubertal type	Intratubular large cell hyalinizing Sertoli cell neoplasia
Teratoma with somatic malignant components	Granulosa cell tumor
Yolk salk tumor, post-pubertal type	Adult type
Trophoblastic tumors	Juvenile type
Mixed germ cell tumors	Thecoma/fibroma group of tumors
	Other sex cord/gonadal stromal tumors
3. Germ cell tumors unrelated to GCNIS	Mixed
Spermatocytic tumor	Unclassified
Yolk sac tumor, pre-pubertal type	Tumors containing both germ cell and sex cord/gonadal stromal
Mixed germ cell tumor, pre-pubertal type	Gonadoblastoma
5. Miscellaneous non-specific stromal tumors	
Ovarian epithelial tumors	Tumors of paratesticular structures
Tumors of the collecting ducts and rete testis	Adenomatoid tumor
Adenoma	Mesothelioma (epithelioid, biphasic)
Carcinoma	Epididymal tumors
Papillary cystadenoma	Crystadenoma of the epididymis
Mesenchymal tumors of the spermatic cord and testicular adnexae	Adenocarcinoma of the epidydymis

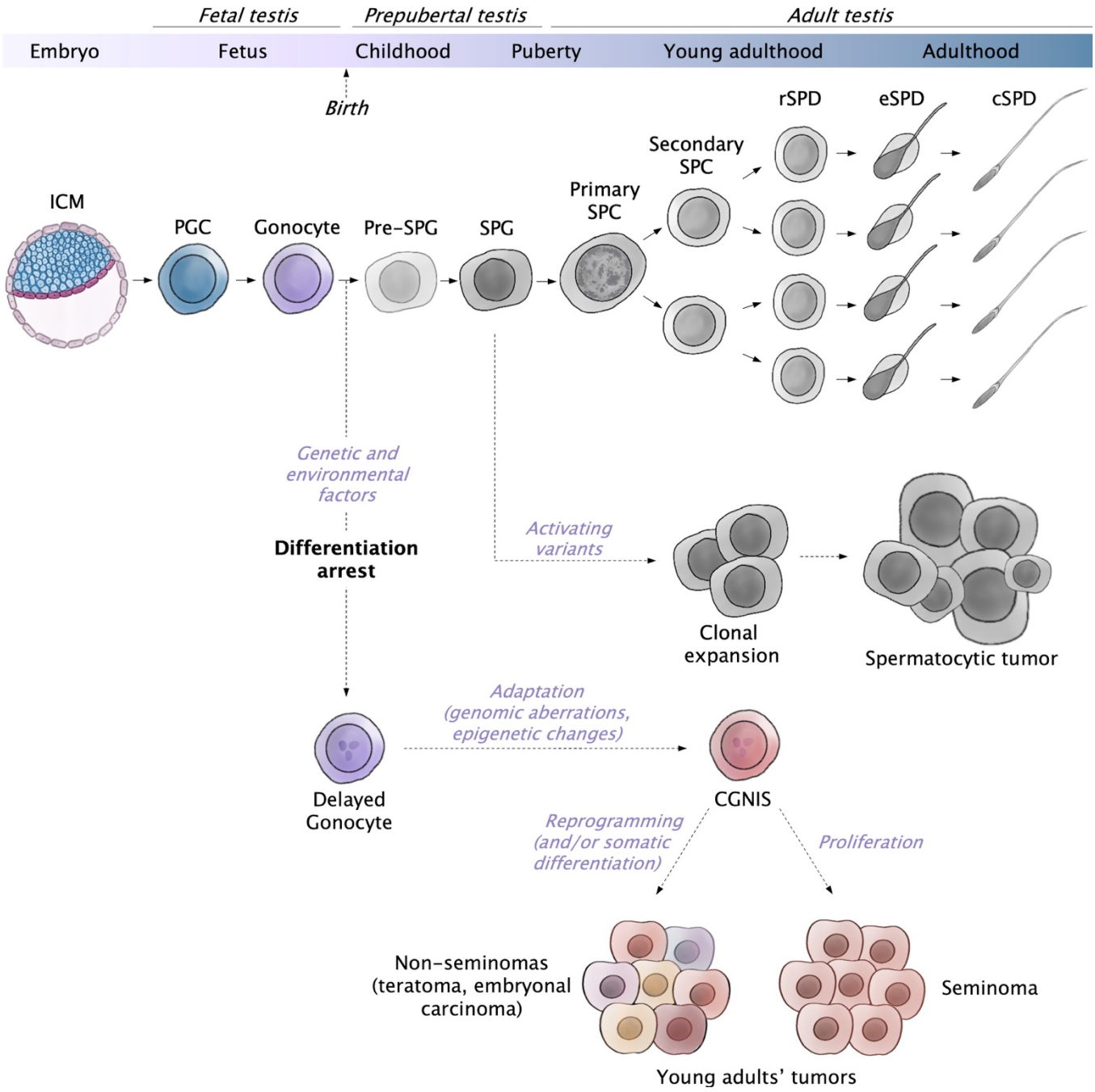


Figure 12. Pathogenesis of testicular germ cell tumors in young adults according to germ cell origin. Normal germ cell differentiation is shown on the top (colored cell types expressing embryonic pluripotency factors). Tumours of young adults (seminomas and non-seminomas) are preceded by germ cell neoplasia in situ (GCNIS), derived from arrested gonocytes that failed to differentiate into spermatogonia. Gradual acquisition of secondary genomic and epigenetic changes lead to malignant germ cells while adapting to the post-pubertal testis niche. Spermatocytic tumour of old men is caused by gain-of-function mutations in genes promoting spermatogonial survival or proliferation. ICM: inner cell mass; PGC: primordial germ cell. Based on Rajpert-de Meyst et al.,, 2016; Skakkaebaek et al., 2016.

3.4.3 Evaluation of unexplained male infertility

In the daily routine practice of the assisted reproduction clinics, female factor is evaluated in a very extensive manner, contrasting with a much simpler evaluation of the male that mostly relies on the study of semen quality. Therefore, in cases of infertility in which female factor has been discarded, and male physical exploration, hormonal profile, and seminogram are normal, a problem arises from the lack of complementary tools to evaluate male infertility. In these cases, ART are started anyways, somehow blindly. Therefore, in recent years, research has focused on finding underlying causes of unexplained male infertility at the molecular level, since knowing the exact cause of infertility will contribute to develop better approaches and to increase success rates. Among the potential causes, those that involve transmission of paternal information, either at genetic or epigenetic level, have attracted special interest, such as protamine levels, sperm DNA damage, or lifestyle and sociodemographic factors.

3.4.3.1 Protamine levels and male infertility

Sperm chromatin maturity has been investigated as underlying cause behind cases of unexplained infertility. One of the most used approaches to traditionally evaluate sperm chromatin status and male infertility has been the determination of relative P1 and P2 protein levels. It has been proposed that mature sperm from fertile men contain similar abundance of P1 and P2 components at protein level, suggesting a reference P1/P2 ratio around 1 (Balhorn et al., 1988; de Yebra et al., 1993; Mengual et al., 2003; Nanassy et al., 2011). Alterations on the P1/P2 ratio, as well as on the individual abundance of P1 and P2, have been associated with increased DNA damage, lower success rates of ART, and altered seminal parameters (sperm count, motility, and morphology), as summarized in (Jodar & Oliva, 2014) and (Soler-Ventura et al., 2018).

Not only protein alterations on mature P1 and P2, but also on pre-P2 seem to compromise human male fertility, either due to the incomplete processing of pre-P2 or the total absence of mature P2 (Carrell & Liu, 2001; de Mateo et al., 2009; de Mateo, Ramos, de Boer, et al., 2011; Rezaei-Gazik et al., 2022), with negative impact on DNA integrity, ART outcomes and seminal parameters (Rezaei-Gazik et al., 2022; Soler-Ventura et al., 2018). Increased retention of pre-P2 in sperm has been recently reported to be associated with fertilization failure, as well as to impaired nucleosome disassembly during spermatogenesis (Rezaei-Gazik et al., 2022), which could explain the origin of the observed sperm defects.

Overall, these findings reinforce a role of protamines towards producing fully functional sperm, achieving ART success, and post-fertilization events, evidencing that alterations on the relative amount between P1 and P2, as well as on pre-P2 processing, direct impact male fertility status. Indeed, patients with incorrect protamination are more prone to be vulnerable to reactive oxygen species (ROS) attack and is related with increased DNA damage (Carrell et al., 2007b; Castillo,

Simon, et al., 2011). However, it is important to remark that the threshold for the P1/P2 ratio has been defined using conventional techniques based on acid-urea polyacrylamide gel electrophoresis (acid-urea PAGE), which limits the quantification to the main bands corresponding to P1 and P2. Therefore, this approach does not encompass the whole population of protamine proteoforms that has been described through mass spectrometry (Arauz-Garofalo et al., 2021; Soler-Ventura et al., 2020), which could explain the variability on the P1/P2 levels detected among studies (Ni et al., 2016).

In a similar manner, phosphorylated proteoforms can neither be evaluated by conventional acid-urea PAGE approaches. However, it would be important to start considering protamine phosphorylation levels when evaluating unexplained cases of male infertility since altered levels of SRPK1, kinase phosphorylating P1, have been related with patients with low pregnancy rate, suggesting a link between protamine phosphorylation and ART outcome (Azpiazu et al., 2014). Indeed, while some redundancy apparently exists among protamine phosphorylation sites, a minimum phosphorylation level must be reached for proper sperm functionality. The creation or depletion of a new single phosphorylation site might not have a real effect in fertility status based on results derived from transgenic mouse models with knock-in mutations affecting phosphorylated sites of P1 and P2 showing no adverse defects (Gou et al., 2020; Itoh et al., 2019). However, simultaneous disruption of 2 phosphorylation sites led to drastic fertility decline (Gou et al., 2020). In contrast to phosphorylation redundancy, a correct protamine dephosphorylation is crucial for fertility, at least for P2. Dephosphorylation of P2 at Ser56 is impaired causes infertility and sperm morphology defects, and the phenotype is rescued when the residue is modified with an amino acid that is not susceptible to be phosphorylated (Itoh et al., 2019). All this information is summarized in **Table 3**, **Section 1.2.2.1**. Therefore, this suggests that searching for alterations on protamine PTMs rather than in unmodified residues could provide more answers about the impact of protamines in male fertility.

3.4.3.2 Sperm DNA fragmentation

A growing number of studies links sperm DNA fragmentation with unexplained male infertility and unsuccessful reproductive outcomes (Agarwal et al., 2020; Nicopoullos et al., 2019; Simon et al., 2019). It has been shown that DNA damage is independent from semen quality, being detected in semen samples from infertile normozoospermic men (Muratori et al., 2015). Indeed, it has become a useful biomarker for the evaluation of male infertility since it has been described a high sperm DNA fragmentation, especially dsDNA breaks, associated with altered early embryogenesis increasing the risk of gestational failure during the first trimester. Whereas dsDNA breaks are associated with pregnancy loss, single strand DNA (ssDNA) breaks are linked to fertilization failure (Carrell et al., 2003; S. E. M. Lewis & Simon, 2010; McQueen et al., 2019; Yifu et al., 2020). Findings also suggest an impact of sperm DNA fragmentation on the epigenetic state of the zygotic male

pronucleus, which could reflect errors during paternal nuclear reprogramming (Rajabi et al., 2018). The relation between DNA fragmentation and sperm chromatin condensation seems clear. A poorly condensed sperm chromatin is less prone to protect the paternal DNA, therefore more sensitive to nucleases and to DNA breaks (Cortés-Gutiérrez et al., 2014; Muratori & de Geyter, 2019). Oxidative stress is associated with sperm DNA fragmentation because the different lesions on the DNA caused by the reactive oxygen species (ROS) can result in structural damage of the DNA strands. However, only intense DNA oxidation is considered a potential cause of DNA breaksnot (Agarwal et al., 2008; Aitken et al., 2010; Makker et al., 2009; Rashki Ghaleno et al., 2021). Despite oxidative stress is considered one of the most common factors associated with DNA fragmentation, there are other multiple causes, such as incorrect chromatin remodeling, nuclease activity, exposure to external factors such as radiation or toxic compounds, or advanced age (Aitken et al., 2010; Castillo, Simon, et al., 2011; Maione et al., 1997; Sakkas & Alvarez, 2010). Sperm DNA fragmentation have been measured through many different approaches, including SCSA, TUNEL, SCD and COMET assays (Cissen et al., 2016; Hamilton & Assumpção, 2020). Nowadays, the COMET assay is considered the most simple and sensitive method to measure ssDNA and dsDNA breaks, using an electrophoretic migration as a basic method to determine the presence and intensity of the DNA breaks in single cells (Simon et al., 2017).

3.4.3.3 Lifestyle and sociodemographic factors

Factors as delay in the time of conception, not only of females but also males, or obesity derived not only from genetic predisposition but from current dietary trends and increasing sedentarism, are related with male infertility of unknown cause (Agarwal et al., 2021; Mascarenhas et al., 2012; Tiegs et al., 2018).

Advanced paternal age

Despite the attention have been historically paid on retarded maternal age as risk factor for reproductive outcome, male age has recently become one of the main topics of study in the field of male infertility. Advanced paternal age is reported to affect seminal parameters, sperm genetics, and reproductive success with or without implication of ART. However, it is complicated to define purely age-derived effects not affected by age-related co-morbidities, and the latest studies report no effect on sperm parameters, supporting that healthy ageing is indeed associated with normal reproductive function (Laurentino et al., 2020; Pohl et al., 2021). However, beyond these normal seminal parameters, one of the clearest effects of paternal age in the germline is the rise in *de novo* mutations, derived from the multiple mitotic divisions throughout life and endorsed by the hypothesis of *selfish spermatogonial selection*, that would suggest that *de novo* mutations would offer the germ cells a selective advance, therefore promoting their expansion. To maintain a constant spermatogenic activity, the spermatogonia increase proliferation but with decreased

spermatogenic efficiency, leading to loss of quiescence in the spermatogonial stem cells' niche. There are multiple effects in sperm, such as telomeric elongation, increased DNA fragmentation, and changes of the DNA methylation pattern (Jenkins et al., 2018; Pohl et al., 2021). The sperm of aged males carry DNA methylation alterations, some of them at genes associated with diverse psychological conditions, evidencing a disturbed sperm epigenome that could be contributing to the appearance of offspring disorders (Jenkins et al., 2014). Indeed, the transgenerational effect of age-associated changes in DNA methylation has been described in mouse models (Milekic et al., 2015). Therefore, a clear pattern of changes in the germline, intrinsic to ageing and affecting sperm cells, is present in ageing men with good reproductive and overall health status, which could underlie fertility issues (Laurentino et al., 2016, 2020). These molecular alterations support that advanced paternal age could be a risk factor for miscarriage and increased rate of mental disorders and mutations in the offspring (Agarwal et al., 2021; du Fossé et al., 2020; Jenkins et al., 2018; Kong et al., 2012; Mazur & Lipshultz, 2018).

Obesity

The increase in obesity rates, measured through the body mass index (BMI), is associated with poor semen quality and male infertility. Despite the parameters to characterize the obese patient might be revisited, the current standards stablish BMI between 18-24,9 as normal weight, 25-29,9 refers to overweight, and above 30 is considered obesity. Obesity can affect spermatogenesis at many levels, either thermal, endocrine, epigenetic, or others external factors as sexual dysfunction, sleep apnea, stress, or inflammation, with an impact in sperm epigenome that can be transmitted to the subsequent generations and affect the newborn's health (Craig et al., 2017; Fullston et al., 2012, 2013; McPherson et al., 2014; Pepin et al., 2022; Soubry et al., 2013). Despite an increased risk of reduced seminal parameters is reported as BMI rises, many obese men present a normal seminogram (Alshahrani et al., 2016; A. O. Hammoud et al., 2008). Although no apparent alterations are observed at the semen analysis level, sperm from obese normozoospermic patients carry DNA methylation alterations at imprinted genes and altered expression of sncRNAs, specifically Piwi-interacting RNAs (piRNAs), that play an essential role in spermatogenesis regulation (Donkin et al., 2016; Soubry et al., 2016). Histone marks are altered in mouse obese models, either repressive or active, correlating with deregulation of histone-modifying enzymes (Deshpande et al., 2021; Palmer et al., 2011). Despite no effect on histone positioning withing the human sperm genome was reported (Donkin et al., 2016), different sperm histone H3 occupancy at regulatory genes has been observed in mouse model (Terashima et al., 2015). This evidences the clear connection already reported between metabolic processes and gene regulation through chromatin remodeling (Berger & Sassone-Corsi, 2016). Interestingly, DNA methylation changed after weight loss induced by bariatric surgery in human obese males. The changes were observed shortly after the surgery and maintained over time, suggesting that epigenetic changes may occur during the

latest stages of sperm maturation (Donkin et al., 2016). Similarly, recent findings evidence that human seminal parameters are increased after diet-induced weight loss and maintained through exercise, which may result in improved fertility through yet unknown molecular mechanisms (Andersen et al., 2022). All this evidences the impact that lifestyle can have on male fertility.

3.4.4 Sperm selection for assisted reproduction techniques to overcome male infertility

The current clinical approach to tackle men with unexplained infertility mostly relies in ART together with changes in lifestyle such as weight loss, physical activity, and stop smoking habits, sometimes accompanied by observational hormonal or non-hormonal treatments (Agarwal et al., 2021). *In vitro* fertilization (IVF) and intra-cytoplasmic sperm injection (ICSI) represent some of the most used reproductive techniques to treat the infertile couples. Before ICSI, sperm selection procedures to select the best spermatozoa are used to overcome the intrinsic high heterogeneity in terms of sperm quality of the semen sample. Among the different sperm selection approaches, 1-layer (50%), 2-layers (40% and 80%), or 3-layers (50%, 70%, and 90%) density gradient centrifugation, often followed by swim-up, are routinely used to select the 'best quality' sperm cells. However, these techniques mainly rely on sperm motility, leaving behind the rest of sperm molecular features, which could be responsible at more or less extent of the low success of ART cycles in Europe (65-70% failure rate per cycle) (de Geyter et al., 2018). Besides, infertile couples normally face several attempts of ART cycles, evidencing a current need to properly characterize the currently existing tools to optimize and personalize their use, but also to find new ones to increase the success rate of ART cycles.

Density gradient centrifugation helps to recover a population of normal morphology and intact DNA in teratozoospermic patients (Xue et al., 2014). Sperm chromatin maturity should be one of the main aspects to evaluate after sperm selection, due to the evidences reported about its impact on reproductive outcomes (Agarwal et al., 2020; Simopoulou et al., 2016). Results comparing the best quality sperm population after density gradient centrifugation in normozoospermic infertile patients with unselected sperm suggest changes in chromatin proteins and PTMs relevant for the NH-NP transition during spermiogenesis, such as H4K8ac and TH2B (de Mateo, Ramos, van der Vlag, et al., 2011). A reduction of DNA fragmentation with no effect in P1/P2 ratio has been reported after density gradient centrifugation (Castillo, Simon, et al., 2011; Chiamchanya et al., 2010), but in some studies this trend is not observed in all patients, with a subgroup evidencing increased DNA damage after sperm preparation (Castillo, Simon, et al., 2011; Muratori et al., 2016). Recent findings point out that sperm DNA fragmentation determination in the viable sperm population is a better indicator to assess the effect of selection rather than analyzing the total sperm population, observing an increased DNA fragmentation in

viable spermatozoa after a density gradient centrifugation or swim-up (Muratori et al., 2019).

Some alternatives to select the best spermatozoa have been proposed to the use of density gradient centrifugation followed by ICSI, but they are time-consuming and implicate the use of non-standard equipment in the IVF lab plus, like intracytoplasmic morphologically selected sperm injection (IMSI). The most recent trend is the use of microfluidics devices for sperm selection, whose reduced sample manipulation and preparation time suggest their upcoming incorporation in the reproductive clinics to replace the density gradient centrifugation (Nosrati et al., 2017). Preliminary approaches suggest promising results (Gode et al., 2020; Quinn et al., 2018), but larger studies evaluating complementary indicators of sperm chromatin maturity are needed to prove their efficiency over the existing methods.

4.

HYPOTHESIS & OBJECTIVES

4.1 Hypothesis

Growing evidence support that the function of the spermatozoa is much wider than being a simple carrier of the paternal DNA. Indeed, the sperm cell provides the embryo with epigenetic marks not only limited to DNA methylation, but also including additional layers of epigenetic information with the potential of being implicated in fertilization and pre-implantation embryo development. Besides the complex population of non-coding RNAs and a group of proteins with epigenetic roles contained in the sperm nucleus, the sperm chromatin itself, understood as the association between DNA and different types of proteins providing distinct compaction properties, arises as a new concept of sperm epigenetic mark.

The relevance of sperm chromatin and its peculiarities have attracted interest over the years, and many efforts have been made to disentangle it. However, sperm chromatin somehow represents both sides of the same coin since the peculiarities that make it a highly attractive field of study are the ones that make its study very challenging, requiring adaptation of conventional techniques for the study of somatic chromatin or application of new ones. Despite that, the successful application of many different techniques has revealed many factors that have gained importance due to their potential role in the proper regulation, formation of the sperm chromatin, and proper transmission of epigenetic paternal information to the zygote. Among them, protamine and histone PTMs, both during male gamete development and once matured, together with the resulting sperm chromatin structure, need to be further studied, as well as their relationship with cases of unexplained male infertility.

Therefore,

the hypothesis of the present doctoral thesis is that the protein fraction of the germ cell's chromatin (histones and protamines, among other chromatin proteins, and their PTMs) could have an epigenetic role during sperm maturation and towards events beyond fertilization. In addition, its alteration could represent underlying causes of different testicular pathologies or unexplained human male infertility, and an impaired sperm chromatin state could have an impact towards the global sperm chromatin ultrastructure.

4.2 Objectives

1) **To explore histone PTMs involved in the process of nucleo-histone to nucleo-protamine transition and their epigenetic potential**

    a) To describe alterations of a global histone H4 acetylation pattern during the spermatogenesis in different testicular affections

    b) To characterize specific novel acylations during spermatogenesis and in mature sperm (H4K5 acetylation and butyrylation) and their relationship with sperm quality

2) **To increase the knowledge on protamine proteoforms, with a special focus on protamine phosphorylation**

    a) To define the normal profile of protamine PTMs through top-down proteomics and to identify alterations in the protamine proteoforms related with unexplained infertility

    b) To explore the protein interactive networks of proteins modulating protamine phosphorylation

3) **Application of innovative approaches to the study of the sperm chromatin and chromatin compaction defects: small X-ray scattering (SAXS) with synchrotron light for the nanoscale characterization of the sperm nucleus**

5.

RESULTS

5.1 CHAPTER 1. The impact of testicular pathologies and sperm quality on histone acylations regulating the nucleo-histone to nucleo-protamine transition

Comprising the following scientific works:

Barrachina F*, **de la Iglesia A***, Jodar M, Soler-Ventura A, Mallofré C, Rodriguez-Carunchio L, Goudarzi A, Corral JM, Ballescà JL, Castillo J, Oliva R. Histone H4 acetylation is dysregulated in active seminiferous tubules adjacent to testicular tumours. Hum Reprod. 2022 Jul 30;37(8):1712-1726. doi:10.1093/humrep/deac130.

***First author, IF 6.353, D1 (Obstetrics & Gynecology)**

de la Iglesia A, Jauregi P, Jodar M, Barrachina F, Ded L, Mallofré C, Rodríguez-Carunchio L, Corral JM, Ballescà JL, Komrskova K, Castillo C, Oliva R. H4K5 butyrylation coexist with acetylation during human spermiogenesis and are retained in the mature sperm chromatin. Int J Mol Sci, under revision.

First author, IF 6.208, Q1 (Biochemistry & Molecular Biology)

5.1.1 Work 1: Histone H4 acetylation is dysregulated in active seminiferous tubules adjacent to testicular tumours

Published as:

Barrachina F[1,††], **de la Iglesia A[1†]**, Jodar M[1,2], Soler-Ventura A[1], Mallofré C[3], Rodriguez-Carunchio L[3,4], Goudarzi A[5,§], Corral JM[6,7], Ballescà JL[1,7], Castillo[1#], Oliva R[1,2#]. Histone H4 acetylation is dysregulated in active seminiferous tubules adjacent to testicular tumours. *Hum Reprod*. 2022 Jul 30;37(8):1712-1726.

[1] Molecular Biology of Reproduction and Development Research Group, Department of Biomedical Sciences, Faculty of Medicine and Health Sciences, Institut d'Investigacions Biomèdiques August Pi i Sunyer (IDIBAPS), Fundació Clínic per a la Recerca Biomèdica, Universitat de Barcelona, Barcelona, Spain.

[2] Biochemistry and Molecular Genetics Service, Hospital Clinic, Barcelona, Spain.

[3] Department of Pathology, Hospital Clínic, Barcelona, Spain.

[4] Faculty of Medicine, University of Vic-Central University of Catalonia (UVic-UCC), Barcelona, Spain.

[5] CNRS UMR 5309, INSERM U1209, Université Grenoble Alpes, Institute for Advanced Biosciences, Grenoble, France.

[6] Department of Urology, IDIBAPS, Hospital Clínic, Barcelona, Spain.

[7] Institute of Gynaecology, Obstetrics and Neonatology, Hospital Clínic, Barcelona, Spain.

[†] The authors consider that the first two authors should be regarded as joint First Authors

[†] Current affiliation: Program in Membrane Biology, Nephrology Division, Department of Medicine, Massachusetts General Hospital and Harvard Medical School, Boston, MA, United States

[§] Current affiliation: Department of Clinical Biochemistry, School of Medicine, Shahid Beheshti University of Medical Sciences, Tehran, Iran

[*] Corresponding authors

PMID: 35678707 DOI: 10.1093/humrep/deac130

Human Reproduction, pp. 1–15, 2022
https://doi.org/10.1093/humrep/deac130

human reproduction

ORIGINAL ARTICLE *Andrology*

Histone H4 acetylation is dysregulated in active seminiferous tubules adjacent to testicular tumours

Ferran Barrachina [1,8,†], Alberto de la Iglesia [1,†], Meritxell Jodar [1,2], Ada Soler-Ventura [1], Carme Mallofré [3], Leonardo Rodriguez-Carunchio [3,4], Afsaneh Goudarzi [5,9], Juan Manuel Corral [6,7], Josep Lluís Ballescà[1,7], Judit Castillo [1,*], and Rafael Oliva [1,2,*]

[1]Molecular Biology of Reproduction and Development Research Group, Department of Biomedical Sciences, Faculty of Medicine and Health Sciences, Institut d'Investigacions Biomèdiques August Pi i Sunyer (IDIBAPS), Fundació Clínic per a la Recerca Biomèdica, Universitat de Barcelona, Barcelona, Spain [2]Biochemistry and Molecular Genetics Service, Hospital Clinic, Barcelona, Spain [3]Department of Pathology, Hospital Clínic, Barcelona, Spain [4]Faculty of Medicine, University of Vic-Central University of Catalonia (UVic-UCC), Barcelona, Spain [5]CNRS UMR 5309, INSERM U1209, Université Grenoble Alpes, Institute for Advanced Biosciences, Grenoble, France [6]Department of Urology, IDIBAPS, Hospital Clínic, Barcelona, Spain [7]Institute of Gynaecology, Obstetrics and Neonatology, Hospital Clínic, Barcelona, Spain [8]Present address: Program in Membrane Biology, Nephrology Division, Department of Medicine, Massachusetts General Hospital and Harvard Medical School, Boston, MA, USA [9]Present address: Department of Clinical Biochemistry, School of Medicine, Shahid Beheshti University of Medical Sciences, Tehran, Iran

*Correspondence address. Molecular Biology of Reproduction and Development Research Group, Department of Biomedical Sciences, Faculty of Medicine and Health Sciences, Institut d'Investigacions Biomèdiques August Pi i Sunyer (IDIBAPS), Fundació Clínic per a la Recerca Biomèdica, Universitat de Barcelona, Barcelona, Spain and Biochemistry and Molecular Genetics Service, Hospital Clinic, Barcelona, Spain. E-mail: roliva@ub.edu (R.O.) https://orcid.org/0000-0003-4876-2410; Molecular Biology of Reproduction and Development Research Group, Department of Biomedical Sciences, Faculty of Medicine and Health Sciences, Institut d'Investigacions Biomèdiques August Pi i Sunyer (IDIBAPS), Fundació Clínic per a la Recerca Biomèdica, Universitat de Barcelona, Barcelona, Spain. E-mail: juditcastillo@ub.edu (J.C.) https://orcid.org/0000-0002-9407-2675

Submitted on March 23, 2021; resubmitted on April 26, 2022; editorial decision on May 20, 2022

STUDY QUESTION: Is histone H4 acetylation (H4ac) altered in the seminiferous tubules of patients affected by testicular tumours?

SUMMARY ANSWER: A considerable dysregulation of H4ac was detected in the cells of the seminiferous tubules adjacent to testicular tumours of different aetiology and prior to any treatment, while no comparable alterations were observed in patients with disrupted spermatogenesis.

WHAT IS KNOWN ALREADY: Altered H4ac levels have been associated with a variety of testicular pathological conditions. However, no information has been available regarding potential alterations in the spermatogenic cells adjacent to the neoplasia in testicular tumour patients.

STUDY DESIGN, SIZE, DURATION: A retrospective analysis using testicular sections from 33 men aged between 21 and 74 years old was performed. Three study groups were defined and subjected to double-blind evaluation: a control group with normal spermatogenesis (n = 6), patients with testicular tumours (n = 18) and patients with spermatogenic impairments (n = 8). One additional sample with normal spermatogenesis was used as a technical internal control in all evaluations.

PARTICIPANTS/MATERIALS, SETTING, METHODS: Immunohistochemistry against H4ac and, when needed, Placental-like alkaline phosphatase and CD117, was performed on testicular sections. The H4ac H-score, based on the percentage of detection and signal intensity, was used as the scoring method for statistical analyses. Protein expression data from the Human Protein Atlas were used to compare the expression levels of predicted secreted proteins from testicular tumours with those present in the normal tissue.

MAIN RESULTS AND THE ROLE OF CHANCE: We revealed, for the first time, a dramatic disruption of the spermatogenic H4ac pattern in unaffected seminiferous tubule cells from different testicular tumour patients prior to any antineoplastic treatment, as compared to controls ($P < 0.05$). Since no similar alterations were associated with spermatogenic impairments and the *in silico* analysis revealed proteins potentially secreted by the tumour to the testicular stroma, we propose a potential paracrine effect of the neoplasia as a mechanistic hypothesis for this dysregulation.

[†]The authors consider that the first two authors should be regarded as joint First Authors.

© The Author(s) 2022. Published by Oxford University Press on behalf of European Society of Human Reproduction and Embryology. All rights reserved.
For permissions, please email: journals.permissions@oup.com

Downloaded from https://academic.oup.com/humrep/advance-article/doi/10.1093/humrep/deac130/6604813 by UNIVERSITAT DE BARCELONA. Biblioteca user on 31 July 2022

LIMITATIONS, REASONS FOR CAUTION: Statistical analyses were not performed on the hypospermatogenesis and Leydig cell tumour groups due to limited availability of samples.

WIDER IMPLICATIONS OF THE FINDINGS: To the best of our knowledge, this is the first report showing an epigenetic alteration in cells from active seminiferous tubules adjacent to tumour cells in testicular tumour patients. Our results suggest that, despite presenting spermatogenic activity, the global epigenetic dysregulation found in the testicular tumour patients could lead to molecular alterations of the male germ cells. Since testicular tumours are normally diagnosed in men at reproductive age, H4ac alterations might have an impact when these testicular tumour patients express a desire for fatherhood.

STUDY FUNDING/COMPETING INTEREST(S): This work was supported by the European Union Marie Curie European Training Network actions and by grants to R.O. from the 'Ministerio de Economía y Competividad (Spain)' (fondos FEDER 'una manera de hacer Europa', PI13/00699, PI16/00346 and PI20/00936) and from EU-FP7-PEOPLE-2011-ITN289880. J.C. was supported by the Sara Borrell Postdoctoral Fellowship, Acción Estratégica en Salud, CD17/00109. J.C. is a Serra Húnter fellow (Universitat de Barcelona, Generalitat de Catalunya). F.B. has received grants from the Ministerio de Educación, Cultura y Deporte para la Formación de Profesorado Universitario (Spain) (FPU15/02306). A.d.l.I. is supported by a fellowship of the Ministerio de Economía, Industria y Competitividad (Spain) (PFIS, FI17/00224). M.J. is supported by the Government of Catalonia (Generalitat de Catalunya, pla estratègic de recerca i innovació en salut, PERIS 2016-2020, SLT002/16/00337). The authors have no conflicts of interest to declare.

TRIAL REGISTRATION NUMBER: N/A.

Key words: histone H4 acetylation / immunohistochemistry / spermatogenesis / testicular tumour / epigenetics / epigenetic dysregulation / fertility preservation

Introduction

The spermatogenesis is a tightly regulated cellular process, in which the diploid spermatogonia (SPG) differentiate into highly specialized haploid cells, the spermatozoa. Histone variants and histone marks play a crucial role in the chromatin dynamics which occur during this process and are required to achieve spermatozoa with fertilization potential (de Mateo *et al.*, 2011; Hammoud *et al.*, 2011; Oliva and Ballescà, 2012; Azpiazu *et al.*, 2014; Castillo *et al.*, 2014, 2015; Barrachina *et al.*, 2018a). Specifically in mammals, a hyperacetylation of the core histones occurs during the last stage of the spermatogenesis, spermiogenesis, leading to the process of chromatin reorganization known as the nucleohistone-to-nucleoprotamine (NH-NP) transition (Christensen and Dixon, 1982; Oliva and Mezquita, 1982; Grimes and Henderson, 1984; Oliva *et al.*, 1987; Hazzouri *et al.*, 2000; Oliva and Castillo, 2011). The impact of histone acetylation relies on the specific modification of lysine residues within the N-terminal domains, which neutralizes the positive charge of the histone tails, destabilizes the histone binding to the DNA, affects the nucleosome-nucleosome interactions, modifies chromatin compaction, and acts as an epigenetic mark. The NH-NP transition is a gradual process triggered when a wave of histone H4 hyperacetylation recruits the Bromodomain-containing testis-specific protein (Pivot-Pajot *et al.*, 2003; Gaucher *et al.*, 2012; Goudarzi *et al.*, 2014). Histones are firstly replaced by testis-specific histone variants, and subsequently by transition proteins, then ultimately by the small and extremely basic protamines, giving rise to tightly packed nucleoprotamine toroidal structures (Oliva and Dixon, 1991; Kimmins and Sassone-Corsi, 2005; Oliva, 2006; Balhorn, 2007; Oliva and Castillo, 2011; Rathke *et al.*, 2014; Bao and Bedford, 2016; Barrachina *et al.*, 2018b). Of note, when a complete NH-NP transition occurs, 5–15% of the histones are retained in the human sperm nucleus and are mainly associated with developmental genes and gene promoters, among other specific genomic sites (Gatewood *et al.*, 1987; Oliva, 2006; Balhorn, 2007; Arpanahi *et al.*, 2009; Hammoud *et al.*, 2009; Castillo *et al.*, 2014, 2015; Torres-Flores and Hernández-Hernández, 2020).

In human testes, histone H4 hyperacetylation has been detected in SPG, round spermatids (rSPD), elongating spermatids (eSPD) and the supporting Sertoli cells (SC) (Sonnack *et al.*, 2002; Faure *et al.*, 2003; Kleiman *et al.*, 2008). The maximum peak of histone H4 acetylation (H4ac) seems to occur in eSPD, when the NH-NP transition is taking place. This pattern has been found to be highly conserved among several distant species such as stallion, rat, mouse, birds, rainbow trout and the fruit fly (Oliva and Mezquita, 1982; Christensen *et al.*, 1984; Grimes and Henderson, 1984; Meistrich *et al.*, 1992; Wolf *et al.*, 1993; Hazzouri *et al.*, 2000; Ketchum *et al.*, 2018). Interestingly, after a normal spermatogenic process, histone H4ac has been also detected in the remaining nucleosomes of mature human sperm (Gatewood *et al.*, 1990; Paradowska *et al.*, 2012). Published results support that H4ac is involved in the proper development of the spermatogenic process. For instance, altered levels of H4ac have been detected in testicular sections of patients with disrupted spermatogenesis (Sonnack *et al.*, 2002; Faure *et al.*, 2003; Kleiman *et al.*, 2008). Additionally, increased H4ac levels have also been found in SC from men with a mixed phenotype of Sertoli cell-only syndrome (SCOS) and testicular tumour. However, due to the absence of germ cells, no potential alterations in the spermatogenesis of men with testicular tumours were reported (Faure *et al.*, 2003).

Fertility preservation is common in testicular tumour patients since it is normally diagnosed among the adolescent and young adults population, comprising the reproductive age (Saltzman and Cost, 2018). Clinical guidelines state that these patients should be offered semen cryopreservation and pre-treatment fertility assessment, with strong recommendations for discussing sperm banking prior to orchidectomy or radio/chemotherapy treatments, which can damage fertility (Meistrich, 2013; Moody *et al.*, 2018; Oktay *et al.*, 2018; Laguna *et al.*, 2020). However, this option is not always available in testicular tumour patients presenting male subfertility (Peng *et al.*, 2009; Williams *et al.*,

Downloaded from https://academic.oup.com/humrep/advance-article/doi/10.1093/humrep/deac130/6604813 by UNIVERSITAT DE BARCELONA. Biblioteca user on 31 July 2022

2009; Fraietta *et al.*, 2010). By pursuing possible fertility preservation options for these patients, less invasive surgical methods have been developed as an alternative to the classical intervention of radical orchiectomy either in the treatment or initial evaluation of a testicular tumour (Picton *et al.*, 2015). Indeed, techniques such as the testis-sparing surgery and the oncological testicular sperm extraction coupled with orchiectomy are currently offered (Giannarini *et al.*, 2010; Borghesi *et al.*, 2015; Suzuki *et al.*, 2015; Luján *et al.*, 2016; Tsutsumi *et al.*, 2017; Hamano *et al.*, 2018; Kuroda *et al.*, 2018). However, whether the adjacent testicular tumour affects the epigenetic profile of spermatogenic cells from intact seminiferous tubules has not been explored so far. Nonetheless, recent evidence points out that sperm used for fertility preservation in testicular tumour patients might contain molecular alterations even before the initiation of the anti-tumour treatment (Dias *et al.*, 2020).

In the present study, we aimed to update the spermatogenic H4ac pattern during human spermatogenesis based on a detailed spermatogenic classification system, as well as to shed new light on the potential alterations of the spermatogenic H4ac pattern in patients affected by different testicular pathologies. To that end, we have evaluated the H4ac levels in the seminiferous tubules of (i) patients with normal spermatogenesis, (ii) testicular tumour patients displaying spermatogenic activity adjacent to the neoplasia and (iii) patients with spermatogenic impairments. Since this is the first report assessing H4ac levels in the intact seminiferous tubules adjacent to the tumour tissue, our results provide novel and useful information towards the identification of the potential epigenetic risks underlying fertility preservation of apparently healthy male germ cells from testicular tumour patients.

Materials and methods

Biological material

Human testicular biopsies (n = 33) were provided by the Departments of Pathology from the Hospital Clínic de Barcelona (Barcelona, Spain) and the Hospital Universitari de Vic (Vic, Spain). All patients signed informed consent in accordance with the Declaration of Helsinki. Samples were used following the appropriate ethical guidelines, and the Internal Review Board and the Clinical Research Ethics Committee of the corresponding hospitals approved the biological material storing and processing. Testicular biopsies were obtained from infertile patients with azoospermia or severe oligozoospermia, related or not with spermatogenic defects, and patients with testicular tumours. Three main groups of the study were established (Fig. 1): (i) control patients with histologically normal spermatogenesis corresponding to the male partners of couples undergoing assisted reproduction studies (one post-vasectomy individual, two patients with obstructive azoospermia due to cystic fibrosis genotypes, and three azoospermic patients), showing all germ cell types and spermatogenic stages (n = 6); (ii) patients with testicular neoplasia (n = 18); and (iii) azoospermic or severe oligozoospermic infertile patients with altered spermatogenesis (n = 8). The second group was subdivided according to the type of testicular tumour, as follows: seminoma (SEM; n = 4), spermatocytic tumour (SPCT; n = 3), embryonal carcinoma (EmCA; n = 5), teratoma (TER; n = 4) and non-malignant Leydig cell tumour (LCT; n = 2). The third group was subdivided according to the type of spermatogenic alteration into patients with SCOS (n = 3), hypospermatogenesis (Hp; n = 2) and spermatogenic arrest (SA; n = 3). Two of the SA patients with presented spermatocyte (SPC) arrest (one with complete arrest and the other one with partial arrest) and the third showed evidence of a partial arrest in rSPD. In addition to the groups above, one sample corresponding to a patient with normal spermatogenesis was used as a technical internal control in all evaluations. A detailed description of the number of subjects and the clinical histological evaluation is shown in Fig. 1.

Testicular tissue processing and paraffin-embedding

Samples were fixed prior to paraffin-embedding in either Bouin's fixative or 4% Formol, depending on the sample size (biopsies or orchiectomy specimens, respectively), for histopathologic evaluation or other procedures. Following the hospital's routine procedures, biopsies were fixed in Bouin solution for 3–4 h, and surgical specimens were fixed in 4% Formol for 24–48 h (detailed individual information is included in Supplementary Table SI). After fixation, the specimens were processed in a fluid-transfer advanced automatic tissue processor and paraffin-embedded to make the blocks. The tissue was covered in molten paraffin in a mold, and the paraffin was cooled down until it solidifyied. The block was cut into 4 µm-sections using a microtome.

Testicular histopathological evaluation

The histopathological evaluation of testicular sections was exhaustively performed by an anatomopathologist. The haematoxylin-eosin-stained sections from each patient were reviewed to histologically identify spermatogenic defects (Cerilli *et al.*, 2010) and/or testicular tumours, following the World Health Organization (WHO) guidelines (Moch *et al.*, 2016). When needed, the tumour diagnosis was confirmed by checking the expression of the appropriate biomarkers. Ultrasound evaluation was monitored to discard the presence of testicular microlithiasis (Leblanc *et al.*, 2018). The presence of either complete or partial spermatogenic activity in the seminiferous tubules adjacent to the tumour tissue was a strict inclusion criterion for the group of patients with testicular tumours. After histopathological confirmation, additional testicular sections from each patient were used for further immunohistochemical analyses.

Immunohistochemistry

Immunohistochemistry (IHC) was performed on paraffin-embedded testicular sections, as described previously (Barrachina *et al.*, 2019). Testicular tissue samples were randomly grouped in different runs, and an internal positive control was included in each of them to check the overall intensity of the different runs. This internal positive control corresponded to a section obtained from an orchitectomy specimen of 4.5 cm showing normal spermatogenesis and no presence of testicular tumour (Supplementary Table SI). Note that due to the size of the surgical material, the internal positive control was fixed in 4% formol and showed the same H4ac pattern as the samples from the control group fixed in Bouin (Fig. 2). Therefore, we discarded any potential bias related with the tissue fixation method. The presence of the

Downloaded from https://academic.oup.com/humrep/advance-article/doi/10.1093/humrep/deac130/6604813 by UNIVERSITAT DE BARCELONA. Biblioteca user on 31 July 2022

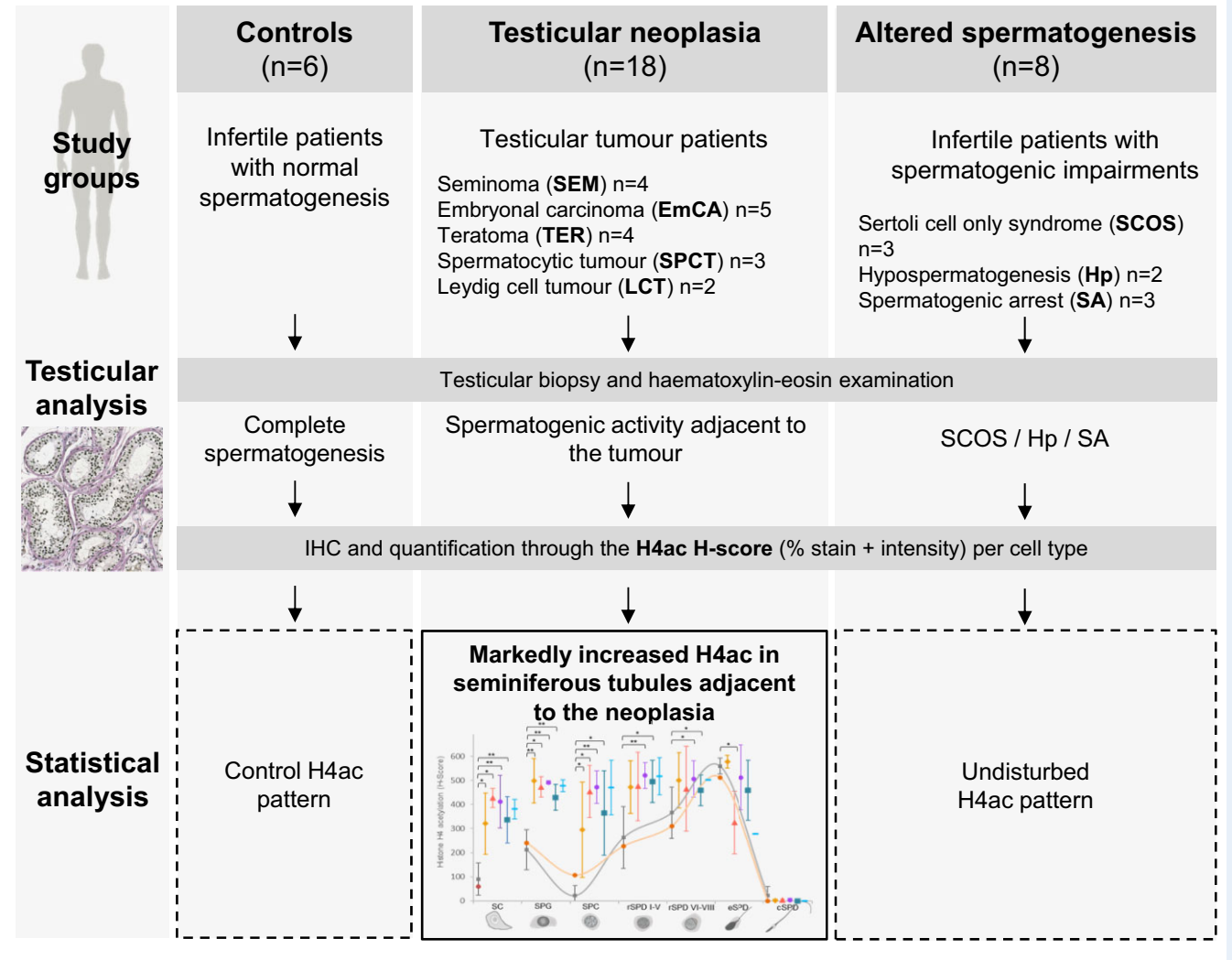


Figure 1. Overall strategy used for the characterization and statistical comparison of the spermatogenic histone H4 acetylation (H4ac) pattern between the different groups of study through the immunohistochemical H4ac H-score. The study groups and types of patients are indicated at the top of the figure. See Supplementary Table SI for detailed individual information of each sample included in the present study. The methodological approach and the main conclusion are shown in the middle and bottom of the figure, respectively.

normal spermatogenic H4ac pattern in the internal positive control was verified in all IHC runs.

Sections were dewaxed in toluene and rehydrated through graded series of ethanol to water with 0.3% hydrogen peroxide incubation. Subsequently, antigen retrieval was performed with 10 mM sodium citrate (pH 6.0) at 99.5°C for 20 min. Slides were then blocked with PBS-5% skim milk for 30 min at room temperature (RT) and incubated with Avidin/Biotin Blocking Kit (Vector Laboratories, Burlingame, CA, USA). The sections were incubated overnight at 4°C with the primary antibody. A polyclonal anti-acetyl histone H4 antibody (5 µg/ml; #06-598, Millipore, Billerica, MA, USA), detecting histone H4 acetylated on lysines 5, 8, 12 and 16 was used to analyse the presence of H4ac. Regarding our aim of evaluating global H4ac, we considered using an antibody able to detect several acetylated residues in the same protein sequence rather than an antibody against a single specific residue. However, we also confirmed the H4ac IHC staining using an alternative monoclonal antibody against the specific acetylation of the H4K5 residue (dil 1:100, #PTM-163, PTM BIO LLC, Chicago, IL, USA), obtaining similar results (data not shown). Negative controls without primary antibody were included. Afterwards, sections were incubated with a biotinylated goat anti-rabbit secondary antibody (Vector Laboratories, Burlingame, CA, USA) and an avidin-biotin-peroxidase detection kit (Vectastain ABC Elite Kit, Vector Laboratories, Burlingame, CA, USA). Colour development was achieved by reaction with diaminobenzidine (DAB, 3,3′-diaminobenzidine tetrahydrochloride) and sections were additionally counterstained with haematoxylin and Periodic Acid-Schiff's (PAS) reagent (Sigma-Aldrich, St. Louis, MO, USA). Sections were dehydrated in ethanol, cleared in toluene, and mounted in Eukitt Mounting Medium (Sigma-Aldrich, St. Louis, MO, USA) to finally be analysed by a transmission light microscope

Downloaded from https://academic.oup.com/humrep/advance-article/doi/10.1093/humrep/deac130/6604813 by UNIVERSITAT DE BARCELONA. Biblioteca user on 31 July 2022

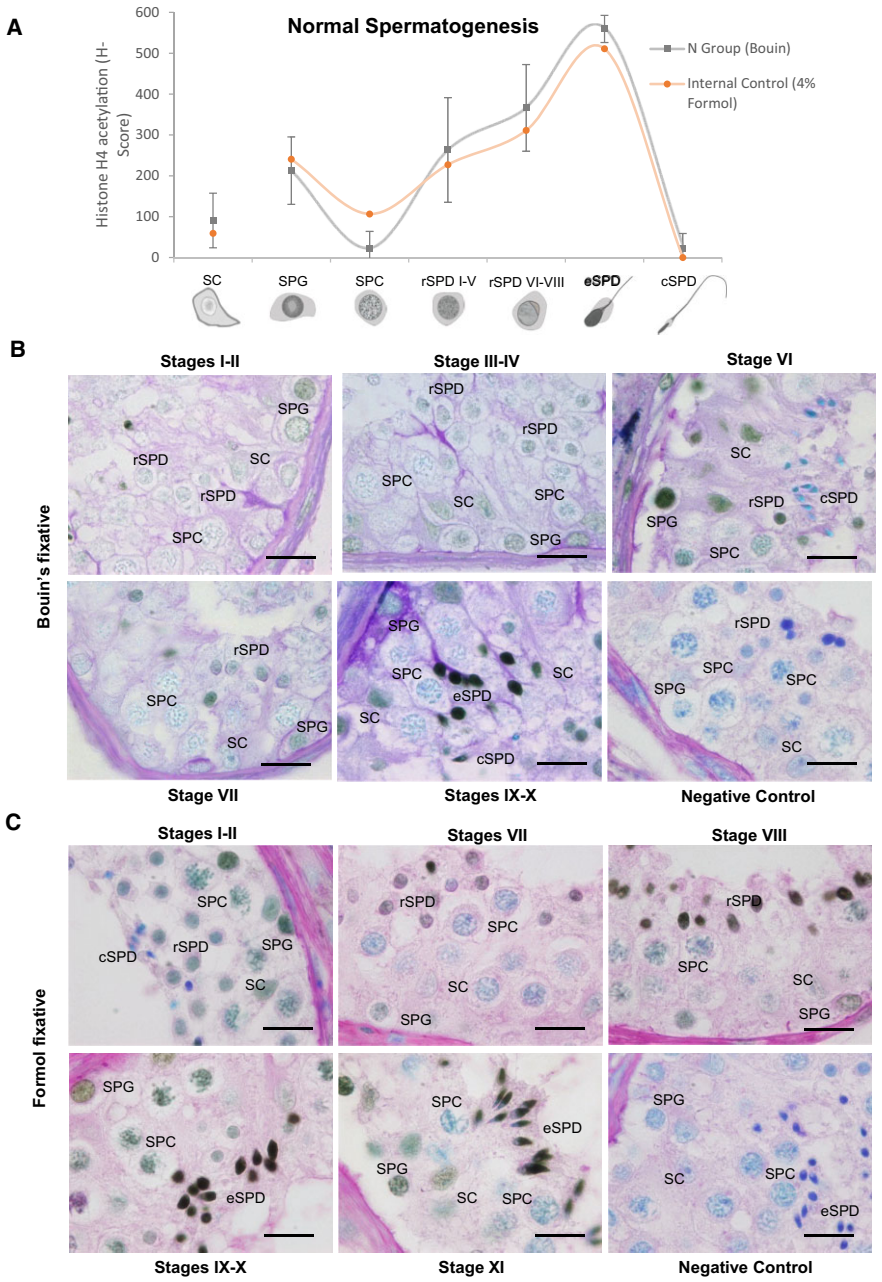


Figure 2. Histone H4 acetylation (H4ac) levels in patients with normal spermatogenesis. (**A**) Immunohistochemistry (IHC) results according to the analysed testicular cell type. Mean H4ac H-scores are shown with error bars corresponding to the standard deviation. The progress of the spermatogenic H4ac pattern during normal spermatogenesis (using Bouin's fixative) and the internal technical control (using fixation with 4% formol) are represented with a soft line (in grey and orange, respectively). (**B**) Microscopy images of seminiferous tubule sections from a biopsy of a patient with normal spermatogenesis fixed with Bouin's fixative. Representative images show the different spermatogenic stages with positive H4ac IHC detection (brown colour). (**C**) Microscopy images of seminiferous tubule sections from the internal technical control displaying normal spermatogenesis, which was obtained from an orchiectomy specimen and fixed with 4% Formol. Representative images show the different spermatogenic stages with positive H4ac IHC detection (brown colour). Note that, regardless the fixative used, a similar staining pattern was obtained in B and C. Tissues were counterstained with PAS-haematoxylin. Scale bars = 10 µm. cSPD, condensing spermatids; eSPD, elongating spermatids; rSPD I–V, early-stages (I–V) round spermatids; rSPD VI–VIII, late-stages (VI–VIII) round spermatids; SC, Sertoli cells; SPC, spermatocytes; SPG, spermatogonia.

Downloaded from https://academic.oup.com/humrep/advance-article/doi/10.1093/humrep/deac130/6604813 by UNIVERSITAT DE BARCELONA. Biblioteca user on 31 July 2022

(Olympus BX50, Olympus, Tokyo, Japan) (Barrachina et al., 2019). For the testicular tumour groups, consecutive histological sections to those used for H4ac staining were used to identify neoplastic areas in SEM (n = 2) and EmCA (n = 2) patients (Fig. 1). Specifically, the routine germ cell tumour markers Placental-like alkaline phosphatase (PLAP) (0.15 µg/µl, PLAP-NB10 clone, #760-2664, F. Hoffmann-La Roche Ltd, Basilea, Switzerland) and CD117 (0.1 µg/µl, CD117-EP10 clone, #790-7061, F. Hoffmann-La Roche Ltd, Basilea, Switzerland) were used (Iczkowski et al., 2008). PLAP and CD117 IHC stainings were performed using Ventana's automated staining platform BenchMark ULTRA IHC/ISH System (Ventana Medical Systems Inc., Oro Valley, AZ, USA), following the manufacturer's recommendations.

Spermatogenic stage classification and IHC evaluation

The classification of testicular cells and spermatogenic stages of the seminiferous tubules sections was based on a published classification of human spermatogenesis (Muciaccia et al., 2013). This classification includes 12 different stages of human spermatogenesis (expressed in Roman numerals), based on the position of the testicular cells along the seminiferous epithelium, the cell morphology, and the acrosome development. For each patient, up to 30 seminiferous tubule sections at different stages were analysed. In the biopsies from testicular tumour patients, we evaluated the neoplasia in situ and the seminiferous tubule sections adjacent to the tumour.

The IHC assessment was achieved by two independent operators using PAS–haematoxylin staining, blinded to the experimental procedures. The method selected for the H4ac scoring system was the H-score (Fedchenko and Reifenrath, 2014), with minor modifications. Specifically, the H-score was determined by adding the proportion of cells presenting each level of intensity (expressed in percentage) multiplied by the intensity (expressed in ordinal values), as follows:

$$\text{H} - \text{score} = (\%_{\text{intensity } 0} \times 0) + (\%_{\text{intensity } 1} \times 1) + (\%_{\text{intensity } 2} \times 2) + [\ldots]$$

This scoring method normally comprises a semi-quantitative scale of intensity detection corresponding to ordinal values from 0 to 3. Due to the good signal obtained with the antibody used, we could broaden the intensity scale, establishing values from 0 to 6. Thus, 0 corresponded to 'no signal', 1 to 'weak', 2 to 'mild-weak', 3 to 'mild', 4 to 'mild-strong', 5 to 'strong' and 6 to 'very strong' signals. Because of that, our H-score presents a dynamic range from 0 to 600. A minimum of 30 seminiferous tubular sections were analysed per subject. Since the intensity of the signal within cells belonging to the same specific cell type was homogeneous along the seminiferous tubule section, the mean intensity of each cell type was calculated and used for H-score determination. Thus, H-score for each testicular cell type analysed per seminiferous tubule section was provided for each individual patient (Fig. 1). The results corresponding to the different sample groups were expressed as the mean H4ac H-score ± SD.

Statistical analysis

Data analysis was conducted in RStudio software version 1.2.5033 (RStudio Team, 2019) and the *car* package (Fox and Weisberg, 2019) and using GraphPad Prism version 7.0 for Windows (GraphPad Software, La Jolla, CA, USA, www.graphpad.com). Normal distribution was assessed by Shapiro–Wilk normality test followed by Levene's homoscedasticity test. According to the distribution of each dataset, either a multiple Student's *t*-test or Mann–Whitney *U* was performed between normal and pathological groups for each testicular cell type, and between consecutive spermatogenic cell types, in order to establish the spermatogenic H4ac pattern. *P*-values <0.05 were considered statistically significant. Statistical limitations were considered due to the low number of patients in some studied groups, and only groups formed by at least three patients were included in the statistical analysis. Principal component analysis (PCA) was performed considering H4ac H-scores in the different cell types as variables, including patients with complete spermatogenesis (therefore presenting values of H4ac H-score for all variables analysed) from normal and tumour groups.

In silico prediction of testicular tumour secreted proteins

Proteins secreted by the testicular tumour were predicted using protein expression data from the Human Protein Atlas version 20.0 (Uhlen et al., 2017). Briefly, the list of proteins expressed in the testicular tumour was retrieved from the Pathology dataset (release date 6 February 2021) and filtered according to the available set of predicted secreted proteins (https://v20.proteinatlas.org/search/protein_class:Predicted+secreted+proteins). Only those proteins expressed at high and medium levels with enhanced, approved or supported reliability in the majority of testicular tumour patients included in the dataset were considered for further analyses. Subsequently, protein expression data in the normal testicular tissue were collected and compared with the levels of the corresponding predicted testicular tumour secreted proteins. To infer the functional involvement of the predicted secreted proteins, we determined the enrichment on Gene Ontology (GO) Biological Process and Molecular Function annotations enclosed in the Gene Ontology Consortium Database (http://www.geneontology.org/). *P*-values <0.05 after Bonferroni correction were considered significant. Pathway enrichment analysis was also conducted using Reactome (Jassal et al., 2020), in which *P*-values <0.05 after false-discovery rate correction were considered significant.

Results

Characterization of the histone H4ac levels in the testicular cells of patients with normal spermatogenesis

Histological sections (testicular biopsies fixed in Bouin's fixative) from individuals displaying normal spermatogenesis (controls) were subjected to IHC analysis after morphological confirmation by an anatomopathologist. The H4ac H-score values for each cell type are shown in Table I (mean value ± SD), while the graphical overview of the spermatogenic H4ac pattern during normal spermatogenesis, together with representative images of the H4ac immunolabelling, are shown in Fig. 2. According to the H4ac H-score, SPG displayed intermediate levels of H4ac (212.7 ± 82.5), which decreased to minimum levels at the SPC stage (22.4 ± 41.5, $P < 0.01$, Supplementary Fig. S1) and were restored after meiosis ($P < 0.01$, Fig. 2, Supplementary Fig. S1, Table I).

Downloaded from https://academic.oup.com/humrep/advance-article/doi/10.1093/humrep/deac130/6604813 by UNIVERSITAT DE BARCELONA. Biblioteca user on 31 July 2022

Table I Comparative immunohistochemical levels of histone H4 acetylation in the seminiferous tubule sections from each group of patients included in the study.

Group	Testicular histology	H4ac H-score (mean ± SD)						
		SC	SPG	SPC	rSPD I–V	rSPD VI–VIII	eSPD	cSPD
Infertile patients with normal spermatogenesis (Controls)	Normal spermatogenesis (N)	90.7 ± 66.9	212.7 ± 82.5	22.4 ± 41.5	263.4 ± 128.0	366.3 ± 106.0	559.5 ± 33.3	22.2 ± 36.8
Infertile patients with altered spermatogenesis	Sertoli cell-only syndrome (SCOS)	153.2 ± 81.1	–	–	–	–	–	–
	Hypospermatogenesis (Hp)	55.5 ± 8.9	152.1 ± 21.6	0.3 ± 0.4	84.0 ± 45.8	248.7 ± 257.5	531.4 ± 21.2	50.1 ± 70.9
	Spermatogenic arrest (SA)	34.0 ± 27.1	109.2 ± 64.6	0.6 ± 1.0	112.5 ± 123.5	162.6 ± 17.8	358.5 ± 153.2	14.1 ± 3.8
Testicular tumour patients	Seminoma (SEM)	320.9 ± 126.5*	498.6 ± 91.9**	295.2 ± 198.5*	472.4 ± 109.5	500.1 ± 115.4	578.0 ± 25.9	2.1 ± 4.2
	Embryonal carcinoma (EmCA)	411.5 ± 109.3**	491.4 ± 6.3**	472.1 ± 67.6**	520.2 ± 52.9**	506.0 ± 75.3*	512.4 ± 134.9	3.8 ± 6.6
	Teratoma (TER)	336.3 ± 96.0**	429.6 ± 54.3**	364.5 ± 174.8*	495.0 ± 87.5*	459.5 ± 63.7*	459.5 ± 124.4	0.0 ± 0.0
	Spermatocytic Tumour (SPCT)	426.8 ± 39.0*	473.0 ± 42.3*	454.2 ± 107.8*	475.0 ± 141.9	465.4 ± 175.9	325.0 ± 129.7*	2.8 ± 4.8
	Leydig cell tumour (LCT)	381.0 ± 40.7	477.6 ± 24.6	470.1 ± 113.3	516.6 ± 77.2	502.8	279.0	0.0

Results are expressed as the mean H-score ± SD.
cSPD, condensing spermatids; eSPD, elongating spermatids; rSPD I-V, early-stages (I-V) round spermatids; rSPD VI–VIII, late-stages (VI–VIII) round spermatids; SC, Sertoli cells; SPC, spermatocytes; SPG, spermatogonia.
*$P < 0.05$, **$P < 0.01$, resulting from the comparison with the control group with normal spermatogenesis (N). Note that the Hp and LCT groups were not considered for statistical analysis due to the limited sample availability.

Specifically, early-stages (stages I to V) round spermatids (rSPD I–V) showed intermediate H4ac levels (263.4 ± 128.0), followed by a non-significative trend towards higher levels in later-stages (stages VI to VIII) round spermatids (rSPD VI–VIII; 366.3 ± 106.0), reaching a maximum in eSPD (559.5 ± 33.3, $P < 0.01$). Finally, the H4ac levels dramatically decreased to minimum levels in condensed spermatids (cSPD; 22.2 ± 36.8, $P < 0.01$). In the non-spermatogenic SC, H4ac was detected with an H-score of 90.7 ± 66.9 (Fig. 2, Table I). Of note, the same H4ac spermatogenic pattern was described for the internal technical control fixed with 4% Formol (Fig. 2A and C), discarding any variability in the detection of the H4ac levels due to the fixation method (Oosterhuis *et al.*, 2011). Individual H4ac H-scores for each patient included in this study are shown in Supplementary Table SI.

The spermatogenic histone H4ac pattern is dramatically impaired in seminiferous tubules adjacent to testicular tumours

Testicular tumour patients stratified by tumour type into five groups of the study were included in the analysis. According to the tumour origin, three groups comprised patients affected by germ cell tumours derived from germ cell neoplasia *in situ* (GCNIS) (SEM, EmCA and TER), one group included patients affected by a germ cell tumour unrelated to GCNIS (SPCT), and the last one was formed by patients affected by a sex cord-stromal tumour (LCT). Spermatogenic activity in seminiferous tubules adjacent to tumour areas was detected for all neoplasias included in this study (Fig. 3, Table I). All of the samples showed a global H4ac dysregulation with increased levels in all germ cell types from SPG to rSPD VI–VIII, as well as in SC (Fig. 3A, Table I). Consequently, the characteristic gradual increase of H4ac associated with normal spermatogenesis was not detected in this group of patients with testicular tumours (Fig. 3A, Supplementary Fig. S1). Conversely, eSPD and cSPD displayed discrete reductions of the H4ac levels. Of note, the most dramatic differences were found in the stage of SPC, showing remarkably higher levels of H4ac compared with the minimum levels found in the control group (295.2 ± 198.5 for SEM, 454.2 ± 107.8 for SPCT, 472.1 ± 67.6 for EmCA and 364.5 ± 174.8 for TER versus 22.4 ± 41.5 for the N group; Table I).

H4ac H-scores of all of the cell types analysed in the LCT group revealed a similar behaviour compared with the rest of the groups of patients with testicular tumours. However, the LCT group was not considered for statistical analysis due to the limited number of available samples (Table I). Individually detailed information about the H4ac H-scores is shown in Supplementary Table SI, and representative images of the altered H4ac found in the different subtypes of testicular tumour patients are shown in Fig. 3B. PCA supports these findings, with principal components 1 and 2 explaining the 77.98% of the variability of our data (60.89% and 17.09%, respectively) and separating control and tumour groups into two independent clusters (Fig. 3C). Interestingly, all patients affected by a tumour were clustered together

Downloaded from https://academic.oup.com/humrep/advance-article/doi/10.1093/humrep/deac130/6604813 by UNIVERSITAT DE BARCELONA. Biblioteca user on 31 July 2022

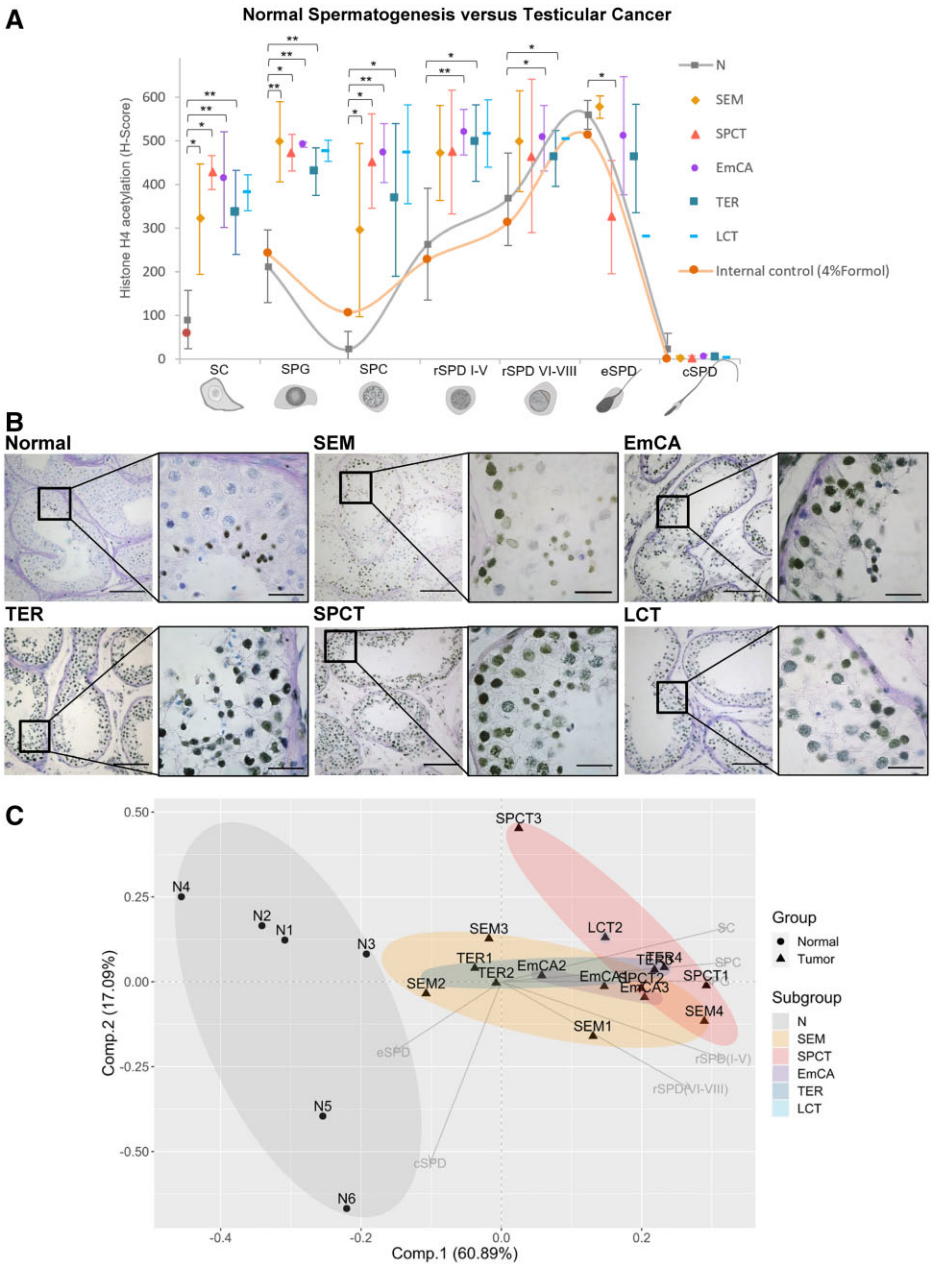


Figure 3. Immunohistochemistry analyses of H4ac on testicular biopsies from patients with testicular tumours. (**A**) H4ac H-scores (mean value ± SD) for each testicular cell type analysed in controls and testicular tumour patients. The pattern of H4ac in normal spermatogenesis (N) and the internal technical control are represented with a soft line (in grey and orange, respectively). (**B**) Representative images of H4ac IHC detection (brown colour) in seminiferous tubule sections from testicular biopsies of patients with normal spermatogenesis (Normal), Teratoma (TER), Seminoma (SEM), Embryonal carcinoma (EmCA), Leydig cell tumour (LCT) and Spermatocytic tumour (SPCT). Increased H4ac levels are observed in the seminiferous tubule cells from testicular tumour patients compared with the control group (normal spermatogenesis). Tissues were counterstained with PAS-haematoxylin. Scale bars = 125 µm (main images, left), 25 µm (magnifications, right). (**C**) Principal component analysis (PCA) of controls ('Normal', round dots) and patients affected by a tumour ('Tumour', triangles). Principal component 1 (Comp.1, *x* axis) and principal component 2 (Comp.2, *y* axis) explain 60.89% and 17.09% of the variability of our data, respectively. Grey arrows scaled to the origin indicate the strength (loadings) of each variable. The tumour group, independently of the type of tumour, presents high H4ac H-scores in early spermatogenic stages and somatic Sertoli cells. Individual patients are shown as listed in Supplementary Table SI, and only patients with complete spermatogenesis were considered for the analysis. PC1 = 0.45SC + 0.43SPG + 0.454SPC + 0.444rSPD (I–V) + 0.378rSPD (VI–VIII) − 0.216eSPD − 0.143cSPD. PC2 = 0.224SC − 0.318rSPD (I–V) − 0.442rSPD (VI–VIII) − 0.291eSPD − 0.75cSPD. *$P < 0.05$, **$P < 0.01$. cSPD, condensing spermatids; eSPD, elongating spermatids; rSPD I–V, early-stages (I–V) round spermatids; rSPD VI–VIII, late-stages (VI–VIII) round spermatids; SC, Sertoli cell; SPC, spermatocyte; SPG, spermatogonia.

Downloaded from https://academic.oup.com/humrep/advance-article/doi/10.1093/humrep/deac130/6604813 by UNIVERSITAT DE BARCELONA. Biblioteca user on 31 July 2022

independently of the type of tumour, and were characterized by high values of the variables corresponding to early spermatogenesis (SPG, SPC and rSPD) and somatic SC.

In order to determine whether similar H4ac alterations might be also found in presence of non-tumour dysregulations, we evaluated the spermatogenic H4ac pattern in testicular tissue from infertile patients with spermatogenic impairments (Supplementary Fig. S2A, Table I). Although the H4ac H-score of all germ cell types associated with the Hp and SA phenotypes tended to be lower than in the control group, the characteristic gradual increase of H4ac from SPG to post-meiotic germ cells observed in the patients with normal spermatogenesis was maintained (Supplementary Fig. S2A). Representative images comparing H4ac immunolabelling between infertile men showing normal spermatogenesis and patients with spermatogenic impairments are shown in Supplementary Fig. S2B–E. Detailed information about the H4ac H-score per individual patient is specified in Supplementary Table SI.

The impaired spermatogenic histone H4ac pattern of testicular tumour patients is not dependent on the presence of seminiferous tubules with pre-invasive GCNIS

We further explored whether H4ac dysregulated levels detected in the different cell types within the seminiferous tubules adjacent to the tumour tissue might be due to the presence of a pre-invasive GCNIS. To that end, we investigated the presence of pre-invasive GCNIS in biopsies from all testicular tumour groups through IHC detection of PLAP and CD117 (Supplementary Fig. S3). No seminiferous tubules containing pre-invasive GCNIS were observed in SPCT, TER or LCT patients. In contrast, pre-invasive GCNIS was identified in localized areas of the testis biopsy in patients with EmCA and SEM. Considering that the same altered H4ac spermatogenic pattern is observed in patients with and without pre-invasive GCNIS, and that H4ac levels were thoroughly studied all along the testis biopsy, we can confirm that the global H4ac alteration observed is independent of the presence or not of pre-invasive GCNIS in seminiferous tubules with spermatogenic activity. In order to confirm this fact, we selected a representative SEM patient to analyse H4ac levels in seminiferous tubules with and without pre-invasive GCNIS, and found similarly altered H4ac spermatogenic levels (Table II).

The potential secretory effect of the testicular germ cell tumours as a mechanistic hypothesis behind the altered intratubular spermatogenic H4ac pattern

By analysing the data contained in the Human Protein Atlas Database, 71 proteins were predicted to be secreted by testicular germ cell tumours (Fig. 4, Supplementary Table SII). The Gene Ontology enrichment analyses revealed an overrepresentation of biological processes and molecular functions related to cell communication and signal transduction ($P < 0.05$ after Bonferroni correction; Supplementary Fig. S4A and B). Furthermore, the Reactome analysis resulted in an overrepresentation of metabolic pathways involved in cell signalling (Supplementary Fig. S4C). Of note, pathways involved in immune system signalling through cytokines (interleukins and TNFs), signalling by growth factors and phosphorylation-mediated signal transduction were also enriched. Some of the proteins predicted to be secreted by the testicular cancer were not detected or were expressed at low levels in the healthy testicular tissue (Supplementary Table SII).

Discussion

The role of histone H4ac in nucleosome destabilization and chromatin remodelling during the spermatogenic process is well established and highly conserved among different species (Christensen and Dixon, 1982; Oliva and Mezquita, 1982; Grimes and Henderson, 1984; Hazzouri *et al.*, 2000). In the present study, we reported that the spermatogenic H4ac pattern during normal human spermatogenesis is in agreement with the results previously reported by others (Sonnack *et al.*, 2002; Faure *et al.*, 2003; Kleiman *et al.*, 2008). As a novelty, we further defined the H4ac levels among different subtypes of post-meiotic cells, such as the early-stages round spermatids (stages I to V), late-stage round spermatids (stages VI to VIII), elongated spermatids (stages IX to XI) and condensed spermatids. We detected the highest H4ac levels in eSPD, preceded by a gradual increase starting from early-stages rSPD. These results might be reflecting the hyperacetylation wave that triggers the NH-NP transition observed in the post-meiotic cells during spermiogenesis (Christensen and Dixon, 1982; Oliva and Mezquita, 1982; Grimes and Henderson, 1984; Oliva *et al.*, 1987, 1990; Hazzouri *et al.*, 2000). Similarly, the dramatic drop of H4ac levels detected in cSPD was coherent with the small proportion of histones that remain associated with the sperm genome after

Table II Comparative histone H4 acetylation levels in seminiferous tubules with and without pre-invasive germ cell neoplasia *in situ* (GCNIS) from a seminoma patient (SEM3).

	H4ac H-score				
Testicular histology	**SPG**	**SPC**	**rSPD**	**eSPD**	**cSPD**
N group (mean value)	212.7	22.4	314.9	559.5	22.2
Seminiferous tubules without pre-invasive GCNIS	376.8 (30)	210.0 (30)	342.6 (21)	533.4 (9)	19.2 (21)
Seminiferous tubules with pre-invasive GCNIS	446.4 (30)	199.8 (29)	337.8 (21)	600.0 (11)	0.0 (17)

Immunohistochemistry results are expressed through the H4ac H-score. The number of tubular sections showing each of the analysed cell types is indicated in brackets. H-score mean values are shown for the control group (N).
cSPD, condensing spermatids; eSPD, elongating spermatids; rSPD, round spermatids; SPC, spermatocytes; SPG, spermatogonia.

Downloaded from https://academic.oup.com/humrep/advance-article/doi/10.1093/humrep/deac130/6604813 by UNIVERSITAT DE BARCELONA. Biblioteca user on 31 July 2022

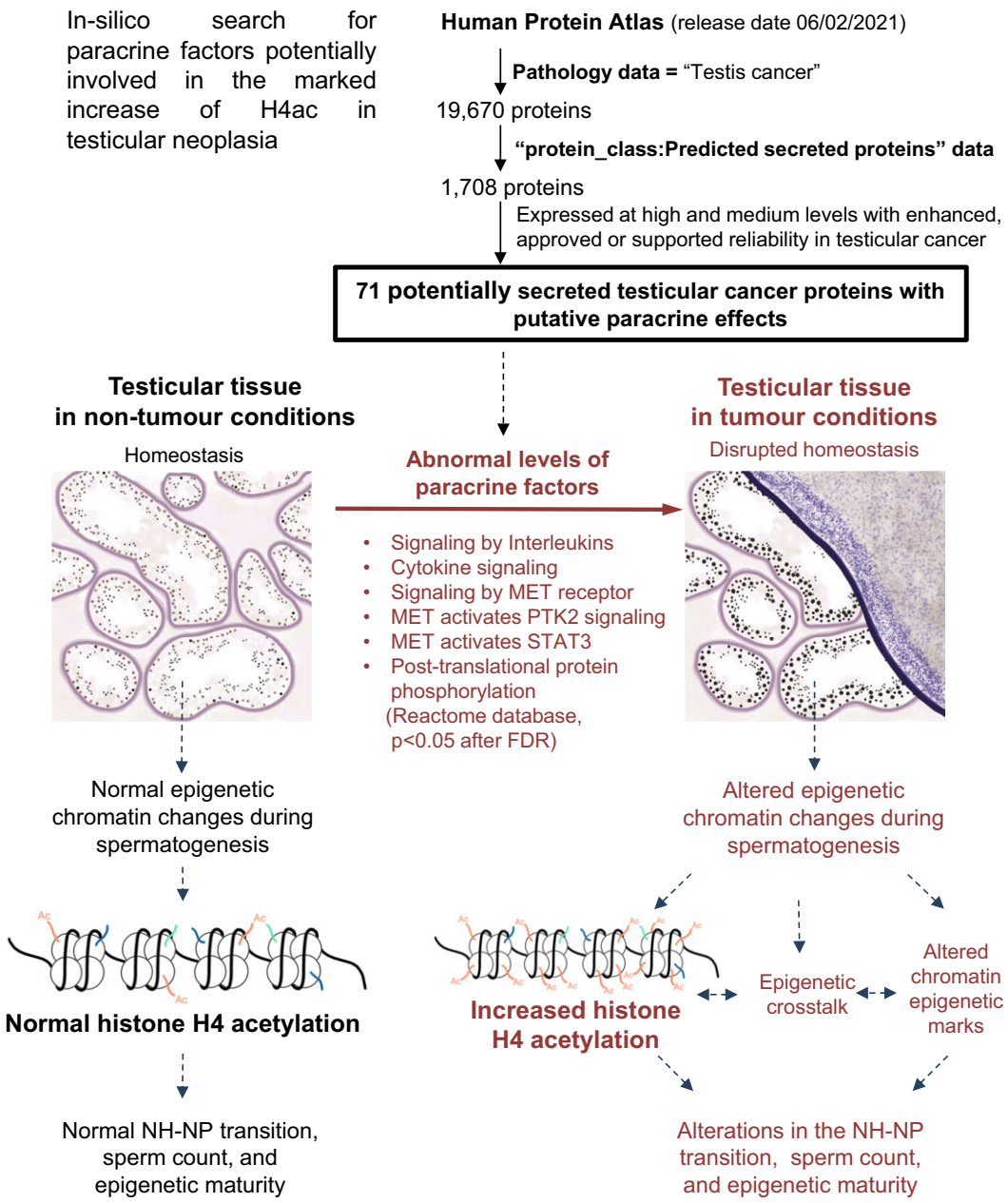


Figure 4. Pipeline of the explanatory mechanistic hypothesis behind the altered H4ac levels found in the testicular cancer patients. Pathology data and predicted secreted proteins from the Human Protein Atlas (http://v20.proteinatlas.org) allowed us to identify 71 potentially secreted testicular cancer proteins with putative paracrine effects associated with signalling pathways involving cytokines and growth factors activating signal transduction through phosphorylation cascades. A schematic representation of the testicular tissue in both non-tumour (left side) and tumour (right side) conditions is shown. In non-cancerous conditions, normal epigenetic regulation of the spermatogenic process is carried out in the healthy seminiferous tubules, leading to a normal gene expression pattern and a proper NH-NP transition. In presence of testicular cancer, the homeostatic state would be potentially impaired due to the secretion of paracrine factors from the tumour, leading to an increase of the H4ac levels in the different cell types. The altered H4ac levels could be also promoted by an epigenetic crosstalk of other potentially altered histone marks and through their effectors. The global epigenetic dysregulation during the spermatogenesis could give rise to altered gene expression patterns and a disrupted chromatin remodelling, resulting in an altered epigenetic cargo of the germ cells that would be further used for fertility preservation purposes. H4ac, histone H4 acetylation; NH-NP, nucleohistone to nucleoprotamine transition.

Downloaded from https://academic.oup.com/humrep/advance-article/doi/10.1093/humrep/deac130/6604813 by UNIVERSITAT DE BARCELONA. Biblioteca user on 31 July 2022

completion of the spermiogenesis (Gatewood *et al.*, 1987; Oliva, 2006; Balhorn, 2007; Castillo *et al.*, 2014; Rathke *et al.*, 2014). The normal spermatogenic H4ac pattern was observed in all control biopsies fixed with Bouin's fixative, as well as in the internal technical control from an orchiectomy specimen fixed with 4% formol, discarding any technical bias caused by the fixative used. In our analysis, SPG showed intermediate levels of H4ac, which differs from the previously reported high levels of H4ac for this specific cell type (Sonnack *et al.*, 2002; Faure *et al.*, 2003). Our slightly lower values could be explained by the use of different antibodies or due to the refinement of the scoring method applied herein. Indeed, we used an H-score method establishing a much broader dynamic range of intensities of up to six different levels. In any case, the detection of H4ac levels in SPG was expected since this modification is physiologically required as part of the replicative and transcriptionally active mitotic state in the normal spermatogenic process (Jan *et al.*, 2017; Hermann *et al.*, 2018). However, this normal H4ac pattern is completely disturbed in the presence of testicular tumour, showing a marked increase in the H4ac levels of both germ and somatic cells in apparently healthy seminiferous tubules adjacent to the tumour. Of note, increased H4ac levels in SC of SEM and EmCA patients were previously described by Faure *et al.* (2003). However, since the testicular tumour patients selected for their study also presented SCOS, no information was available regarding the spermatogenic cells adjacent to the testicular tumours (Faure *et al.*, 2003). It is interesting to highlight that in germ cells altered H4ac levels were mainly detected in early stages of spermatogenesis, while later spermatogenic cell types, such as eSPD and cSPD, displayed slightly lower H4ac levels in the testicular tumour patients compared with the normal spermatogenic pattern. These higher H4ac levels in SPG and SPC, together with the loss of the gradual increase of the H4ac levels in post-meiotic cells found in normal spermatogenesis, might lead to a premature nucleosome destabilization and histone displacement, therefore leading to an early loss of H4 hyperacetylation in the later stages of spermatogenesis (Christensen and Dixon, 1982; Oliva and Mezquita, 1982; Grimes and Henderson, 1984; Oliva *et al.*, 1987, 1990; Hazzouri *et al.*, 2000). It has been described by others that chromatin epigenetic impairments during spermatogenesis are linked to decreased H4ac levels in later stages of the spermatogenesis (eSPD) and, consequently, to defective histone retention and chromatin remodelling (Moretti *et al.*, 2017). With that, the observed H4ac alteration during the spermatogenesis in testicular tumour patients could be related to a subsequent defective retention of histone epigenetic marks in mature sperm, potentially leading to the transmission of altered epigenetic modifications and affecting events beyond fertilization.

Even though some EmCA and LCT patients showed an arrest at the rSPD or eSPD stage, our results suggest that the effect produced by the tumour itself is stronger than the one produced by the spermatogenic impairment, since their altered pattern is similar to that of tumour patients with complete spermatogenesis. Additionally, H4ac staining was positive in all tumour cells, which is in accordance with previous observations describing that germ cell neoplasia harbours a general abundance of epigenetic marks associated with active chromatin states (Omisanjo *et al.*, 2007; Almstrup *et al.*, 2010; Kristensen *et al.*, 2012; van der Zwan *et al.*, 2014; Rajpert-De Meyts *et al.*, 2015). This could create a globally altered environment in the testicular stroma with a potential effect on the seminiferous tubule cells.

Because of the above findings, we further sought to decipher whether the altered spermatogenic H4ac pattern found in the testicular tumour groups was caused by an intrinsic neoplastic state of the seminiferous tubule cells. Theoretically, no direct effect of the neoplasia in the seminiferous tubule cells of patients with LCT, a tumour without a germ-cell-related origin, might be expected. Indeed, we discarded the presence of pre-invasive GCNIS in LCT patients through IHC staining of PLAP and CD117. However, H4ac H-scores of LCT patients seem to indicate an altered spermatogenic H4ac pattern similar to that in other tumour subgroups. Of note, this would point to the tumour environment as responsible for the epigenetic alteration within the seminiferous tubules. In the case of germ cell tumours, the presence of seminiferous tubules with pre-invasive GCNIS was discarded in the SPCT and TER groups, but the SEM and EmCA groups included patients with tubules presenting pre-invasive GCNIS and spermatogenic activity. Despite that, similar altered H4ac profiles were observed in all tumour groups, and even between patients with or without pre-invasive GCNIS. Additionally, our extensive evaluation of the H4ac levels covered all areas of the biopsy. All these facts indicate that the impaired H4ac epigenetic profile was observed independently of the presence of pre-invasive GCNIS in active seminiferous tubules. Indeed, the analysis of seminiferous tubules with and without pre-invasive GCNIS showed a similar H4ac alteration in a representative SEM patient. These striking observations may indicate that cells from apparently normal seminiferous tubules would be affected by the surrounding tumour regardless of their origin.

Taking all this together, we suggest a potential paracrine effect of the testicular tumour on the adjacent seminiferous tubules responsible for the global dysregulation of the H4ac levels. The simple presence of a neoplasia could impair the homeostasis in the testicular stroma, causing a dysregulation of the interstitial protein levels, finally leading to an impaired cell signalling (Fig. 4). We hypothesize that the tumour secretes small proteins or paracrine signals that could impair the intercellular communication causing an altered signal transduction, therefore producing a dysregulation of intracellular signalling cascades and altering nuclear gene expression in the intratubular cells. In fact, our *in silico* prediction of the testicular cancer protein secretome, despite being limited to testicular germ cell tumours, suggests that some of the proteins expressed at higher levels in the tumour are not detectable, or are expressed at lower levels, in the healthy testicular tissue, supporting the existence of a potential paracrine disruption of the cell signalling. Indeed, we found an overrepresentation of pathways that could be supporting the paracrine communication between the tumour and seminiferous tubule cells, such as ligand-receptor pathways, including cytokine signalling and growth factors, as well as phosphorylation-mediated signal transduction. Since infiltration of immune cells is common in testicular tumours and contributes to the tumour microenvironment composition, some cytokines and chemokines that are normally protective could have a negative impact on testicular function and physiology (Loveland *et al.*, 2017). Furthermore, immune cell infiltration is associated with a disruption of the blood–testis barrier in the affected seminiferous tubules, allowing the permeabilization of small molecules (Pérez *et al.*, 2013). Through the binding to surface receptors, the dysregulation of intracellular phosphorylation cascades directly involved in the male germ cell development would carry out changes in gene activity that could be related to changes on H4ac levels. For example, bone morphogenetic protein 6 (BMP6) has been

Downloaded from https://academic.oup.com/humrep/advance-article/doi/10.1093/humrep/deac130/6604813 by UNIVERSITAT DE BARCELONA. Biblioteca user on 31 July 2022

related to the regulation of Hippo signalling, which is known to regulate cell survival and proliferation. Remarkably, some of the proteins involved in this pathway are essential for a proper development of spermatogenesis (Pulkkinen et al., 2020). Also hepatocyte growth factor is related to the activation of intracellular signalling cascades through the JAK/STAT pathways and associated kinase activities, one of the major pathways that maintain stem cell activity and identity in the testis niche (Zhang et al., 2018). JAK/STAT proteins have been also related to epigenetic effectors in the maintenance of the germ cell status (Tarayrah et al., 2015). In addition, histones are phosphorylated in specific residues by kinases, and the crosstalk with other histone post-translational modifications can affect histone acetylation levels. In fact, not only histones but also histone modifiers (acetyltransferases and deacetylases) are phosphorylated (Baek, 2011). Therefore, H4ac levels could be affected by the crosstalk between kinases involved in phosphorylation cascades and other nuclear cofactors, such as effectors of histone acetylation or other histone marks (Baek, 2011; Moretti et al., 2017). However, the interpretation of our *in silico* prediction is limited by the scarce availability of gene expression data in testicular tumours, which is not sorted by tumour subtypes. Because of that, we would like to emphasize that this mechanistic hypothesis can orientate future research in the field, but has to be experimentally confirmed. Indeed, this common global increase of H4ac levels found in all types of tumours might rely on mechanisms that could vary according to their intrinsic differences in their cellularity and secretory patterns. As detailed in Supplementary Table SI, we have analysed specimens with variable tumour size representing different proportions of the total surgical material, and the increase in the H4ac levels in patients affected by testicular tumours are coherent among all of them. However, the reported results correspond to a partial representation of the testicle that always included the tumour (except for patient TER1). To that extent, we could hypothesize this secretory effect in a representative part of the testicle, but without the possibility to check the whole organ. To the best of our practice, within the tissue section, the evaluation of the H4ac levels was performed in seminiferous tubules from different areas, to avoid any bias, and we observed similar patterns regardless the distance to the tumour.

Nowadays, the simple production of spermatozoa or the presence of testicular germ cells are sufficient for fertility preservation before starting the antineoplastic therapy (Meistrich, 2013; Moody et al., 2018; Oktay et al., 2018; Laguna et al., 2020). However, the molecular evaluation presented in this work indicates that the spermatogenic cells in seminiferous tubules adjacent to the tumour, and potentially the resulting spermatozoa, might present an impaired epigenetic state. Therefore, these alterations may affect post-fertilization events or transmit altered epigenetic information to the progeny. In fact, recent evidence has pointed out alterations of the semen quality and mature sperm protein profile from testicular tumour patients before any reproductive toxic treatment (Suzuki et al., 2015; Bruno et al., 2018; Dias et al., 2020; Xavier et al., 2021). Testicular microlithiasis, a condition associated with an increased risk of developing testis tumour, is also associated with reduced sperm count (Barbonetti et al., 2019; Anvari Aria et al., 2020). Alterations in sperm DNA methylation have been reported associated with oligozoospermia and some sperm tumour patients (Bruno et al., 2018; Åsenius et al., 2020). Thus, it should be important to be aware of the potential imprinting alterations when sperm banking or testicular tissue cryopreservation are performed before or coupled to the orchiectomy or the tumour treatment (Giannarini et al., 2010; Borghesi et al., 2015; Suzuki et al., 2015; Luján et al., 2016; Tsutsumi et al., 2017; Hamano et al., 2018; Kuroda et al., 2018).

To the best of our knowledge, this is the first report providing evidence of epigenetic alterations of the testicular tissue with spermatogenic activity adjacent to testicular tumours. Despite the relatively low number of patients evaluated and the use of a semi-quantitative technique, a global dysregulation of H4ac was found in the spermatogenic cells near all of the different subtypes of testicular tumours assessed. Our findings pinpoint a common characteristic of testicular tumour patients that might be considered regarding fertility preservation purposes. Further studies and cohort validations will contribute to determining the magnitude and potential consequences of this epigenetic risk underlying fertility preservation for testicular tumour patients.

Supplementary data

Supplementary data are available at *Human Reproduction* online.

Data availability

The data underlying this article are available in the article and in its online supplementary material.

Acknowledgements

The authors acknowledge the technical support provided by the facility of Advanced Optical Microscopy (Casanova) from the Scientific and Technological Centers of the Universitat de Barcelona (CCiTUB).

Authors' roles

F.B., A.d.l.I., M.J., J.C. and R.O. participated in the study design. C.M., L.R-C., J.L.B. and J.M.C. were involved in the clinical evaluation of the patients. F.B., A.d.l.I., A.S.-V. and A.G. executed the study. F.B., A.d.l.I., M.J., J.C. and R.O. analysed the results. F.B., A.d.l.I., M.J., J.C. and R.O. drafted the manuscript. All authors critically reviewed and approved the final version of the manuscript.

Funding

This work was supported by the European Union Marie Curie European Training Network actions and by grants to R.O. from the 'Ministerio de Economía y Competividad (Spain)' (fondos FEDER 'una manera de hacer Europa', PI13/00699, PI16/00346 and PI20/00936) and from EU-FP7-PEOPLE-2011-ITN289880. J.C. was supported by the Sara Borrell Postdoctoral Fellowship, Acción Estratégica en Salud, CD17/00109. J.C. is a Serra Húnter fellow (Universitat de Barcelona, Generalitat de Catalunya). F.B. has received grants from the Ministerio de Educación, Cultura y Deporte para la Formación de Profesorado Universitario (Spain) (FPU15/02306). A.d.l.I. is supported by a fellowship of the Ministerio de Economía, Industria y Competitividad (Spain) (PFIS, FI17/00224). M.J. is supported by the Government of Catalonia

Downloaded from https://academic.oup.com/humrep/advance-article/doi/10.1093/humrep/deac130/6604813 by UNIVERSITAT DE BARCELONA. Biblioteca user on 31 July 2022

(Generalitat de Catalunya, pla estratègic de recerca i innovació en salut, PERIS 2016-2020, SLT002/16/00337).

Conflict of interest

The authors declare no conflict of interest.

References

Almstrup K, Nielsen JE, Mlynarska O, Jansen MT, Jørgensen A, Skakkebæk NE, Rajpert-De Meyts E. Carcinoma *in situ* testis displays permissive chromatin modifications similar to immature foetal germ cells. *Br J Cancer* 2010;**103**:1269–1276.

Anvari Aria S, Nordström Joensen U, Bang AK, Priskorn L, Nordkap L, Andersson A, Jørgensen N. Testicular microlithiasis on scrotal ultrasound in 4850 young men from the general population: associations with semen quality. *Andrology* 2020;**8**:1736–1743.

Arpanahi A, Brinkworth M, Iles D, Krawetz SA, Paradowska A, Platts AE, Saida M, Steger K, Tedder P, Miller D. Endonuclease-sensitive regions of human spermatozoal chromatin are highly enriched in promoter and CTCF binding sequences. *Genome Res* 2009;**19**:1338–1349.

Åsenius F, Danson AF, Marzi SJ. DNA methylation in human sperm: a systematic review. *Hum Reprod Update* 2020;**26**:841–873.

Azpiazu R, Amaral A, Castillo J, Estanyol JM, Guimerà M, Ballescà JL, Balasch J, Oliva R. High-throughput sperm differential proteomics suggests that epigenetic alterations contribute to failed assisted reproduction. *Hum Reprod* 2014;**29**:1225–1237.

Baek SH. When signaling kinases meet histones and histone modifiers in the nucleus. *Mol Cell* 2011;**42**:274–284.

Balhorn R. The protamine family of sperm nuclear proteins. *Genome Biol* 2007;**8**:227.

Bao J, Bedford MT. Epigenetic regulation of the histone-to-protamine transition during spermiogenesis. *Reproduction* 2016;**151**:R55–R70.

Barbonetti A, Martorella A, Minaldi E, D'Andrea S, Bardhi D, Castellini C, Francavilla F, Francavilla S. Testicular cancer in infertile men with and without testicular microlithiasis: a systematic review and meta-analysis of case-control studies. *Front Endocrinol (Lausanne)* 2019;**10**:164.

Barrachina F, Anastasiadi D, Jodar M, Castillo J, Estanyol JM, Piferrer F, Oliva R. Identification of a complex population of chromatin-associated proteins in the European sea bass (*Dicentrarchus labrax*) sperm. *Syst Biol Reprod Med* 2018a;**64**:502–517.

Barrachina F, Jodar M, Delgado-Dueñas D, Soler-Ventura A, Estanyol JM, Mallofré C, Ballescà JL, Oliva R. Stable-protein pair analysis as a novel strategy to identify proteomic signatures: application to seminal plasma from infertile patients. *Mol Cell Proteomics* 2019;**18**:S77–S90.

Barrachina F, Soler-Ventura A, Oliva R, Jodar M. Sperm nucleoproteins (histones and protamines). In: Zini A, Agarwal A (eds). *A Clinician's Guide to Sperm DNA and Chromatin Damage*. Cham: Springer International Publishing, 2018b, 31–51.

Borghesi M, Brunocilla E, Schiavina R, Gentile G, Dababneh H, Mora L, Della Prete C, del Franceschelli A, Colombo F, Martorana G et al Role of testis sparing surgery in the conservative management of small testicular masses: oncological and functional perspectives. *Actas Urol Esp* 2015;**39**:57–62.

Bruno C, Blagoskonov O, Barberet J, Guilleman M, Daniel S, Tournier B, Binquet C, Choux C, Fauque P. Sperm imprinting integrity in seminoma patients? *Clin Epigenet* 2018;**10**:125.

Castillo J, Amaral A, Azpiazu R, Vavouri T, Estanyol JM, Ballesca JL, Oliva R. Genomic and proteomic dissection and characterization of the human sperm chromatin. *Mol Hum Reprod* 2014;**20**:1041–1053.

Castillo J, Estanyol J, Ballescà J, Oliva R. Human sperm chromatin epigenetic potential: genomics, proteomics, and male infertility. *Asian J Androl* 2015;**17**:601–609.

Cerilli LA, Kuang W, Roger D. A practical approach to testicular biopsy interpretation for male infertility. *Arch Pathol Lab Med* 2010;**134**:1197–1204.

Christensen ME, Dixon GH. Hyperacetylation of histone H4 correlates with the terminal, transcriptionally inactive stages of spermatogenesis in rainbow trout. *Dev Biol* 1982;**93**:404–415.

Christensen ME, Rattner JB, Dixon GH. Hyperacetylation of histone H4 promotes chromatin decondensation prior to histone replacement by protamines during spermatogenesis in rainbow trout. *Nucleic Acids Res* 1984;**12**:4575–4592.

de Mateo S, Castillo J, Estanyol JM, Ballescà JL, Oliva R. Proteomic characterization of the human sperm nucleus. *Proteomics* 2011;**11**:2714–2726.

Dias T, Agarwal A, Pushparaj P, Ahmad G, Sharma R. Reduced semen quality in patients with testicular cancer seminoma is associated with alterations in the expression of sperm proteins. *Asian J Androl* 2020;**22**:88–93.

Faure AK, Pivot-Pajot C, Kerjean A, Hazzouri M, Pelletier R, Péoc'h M, Sèle B, Khochbin S, Rousseaux S. Misregulation of histone acetylation in Sertoli cell-only syndrome and testicular cancer. *Mol Hum Reprod* 2003;**9**:757–763.

Fedchenko N, Reifenrath J. Different approaches for interpretation and reporting of immunohistochemistry analysis results in the bone tissue—a review. *Diagn Pathol* 2014;**9**:221.

Fox J, Weisberg S. *An R Companion to Applied Regression*. Thousand Oaks, CA: Sage, 2019.

Fraietta R, Spaine DM, Bertolla RP, Ortiz V, Cedenho AP. Individual and seminal characteristics of patients with testicular germ cell tumors. *Fertil Steril* 2010;**94**:2107–2112.

Gatewood J, Cook G, Balhorn R, Bradbury E, Schmid C. Sequence-specific packaging of DNA in human sperm chromatin. *Science* 1987;**236**:962–964.

Gatewood JM, Cook GR, Balhorn R, Schmid CW, Bradbury EM. Isolation of four core histones from human sperm chromatin representing a minor subset of somatic histones. *J Biol Chem* 1990;**265**:20662–20666.

Gaucher J, Boussouar F, Montellier E, Curtet S, Buchou T, Bertrand S, Hery P, Jounier S, Depaux A, Vitte A-L et al Bromodomain-dependent stage-specific male genome programming by BRDT. *EMBO J* 2012;**31**:3809–3820.

Giannarini G, Dieckmann K-P, Albers P, Heidenreich A, Pizzocaro G. Organ-sparing surgery for adult testicular tumours: a systematic review of the literature. *Eur Urol* 2010;**57**:780–790.

Goudarzi A, Shiota H, Rousseaux S, Khochbin S. Genome-scale acetylation-dependent histone eviction during spermatogenesis. *J Mol Biol* 2014;**426**:3342–3349.

Downloaded from https://academic.oup.com/humrep/advance-article/doi/10.1093/humrep/deac130/6604813 by UNIVERSITAT DE BARCELONA. Biblioteca user on 31 July 2022

Grimes SR, Henderson N. Hyperacetylation of histone H4 in rat testis spermatids. *Exp Cell Res* 1984;**152**:91–97.

Hamano I, Hatakeyama S, Nakamura R, Fukuhara R, Noro D, Seino H, Yoneyama T, Hashimoto Y, Koie T, Yokoyama Y et al Onco-testicular sperm extraction (Onco-TESE) from a single testis with metachronous bilateral testicular cancer: a case report. *Basic Clin Androl* 2018;**28**:1.

Hammoud SS, Nix DA, Hammoud AO, Gibson M, Cairns BR, Carrell DT. Genome-wide analysis identifies changes in histone retention and epigenetic modifications at developmental and imprinted gene loci in the sperm of infertile men. *Hum Reprod* 2011;**26**:2558–2569.

Hammoud SS, Nix DA, Zhang H, Purwar J, Carrell DT, Cairns BR. Distinctive chromatin in human sperm packages genes for embryo development. *Nature* 2009;**460**:473–478.

Hazzouri M, Pivot-Pajot C, Faure A-K, Usson Y, Pelletier R, Sèle B, Khochbin S, Rousseaux S. Regulated hyperacetylation of core histones during mouse spermatogenesis: involvement of histone-deacetylases. *Eur J Cell Biol* 2000;**79**:950–960.

Hermann BP, Cheng K, Singh A, Roa-De La Cruz L, Mutoji KN, Chen I-C, Gildersleeve H, Lehle JD, Mayo M, Westernströer B et al The mammalian spermatogenesis single-cell transcriptome, from spermatogonial stem cells to spermatids. *Cell Rep* 2018;**25**:1650–1667.e8.

Iczkowski KA, Butler SL, Shanks JH, Hossain D, Schall A, Meiers I, Zhou M, Torkko KC, Kim SJ, MacLennan GT. Trials of new germ cell immunohistochemical stains in 93 extragonadal and metastatic germ cell tumors. *Hum Pathol* 2008;**39**:275–281.

Jan SZ, Vormer TL, Jongejan A, Röling MD, Silber SJ, Rooij DG, de Hamer G, Repping S, Pelt AMM, van et al Unraveling transcriptome dynamics in human spermatogenesis. *Development* 2017;**144**:3659–3673.

Jassal B, Matthews L, Viteri G, Gong C, Lorente P, Fabregat A, Sidiropoulos K, Cook J, Gillespie M, Haw R et al The reactome pathway knowledgebase. *Nucleic Acids Res* 2020;**48**:D498–D503.

Ketchum CC, Larsen CD, McNeil A, Meyer-Ficca ML, Meyer RG. Early histone H4 acetylation during chromatin remodeling in equine spermatogenesis. *Biol Reprod* 2018;**98**:115–129.

Kimmins S, Sassone-Corsi P. Chromatin remodelling and epigenetic features of germ cells. *Nature* 2005;**434**:583–589.

Kleiman SE, Bar-Shira Maymon B, Hauser R, Botchan A, Paz G, Yavetz H, Yogev L. Histone H4 acetylation and AZFc involvement in germ cells of specimens of impaired spermatogenesis. *Fertil Steril* 2008;**89**:1728–1736.

Kristensen DG, Mlynarska O, Nielsen JE, Jacobsen GK, Rajpert-De Meyts E, Almstrup K. Heterogeneity of chromatin modifications in testicular spermatocytic seminoma point toward an epigenetically unstable phenotype. *Cancer Genet* 2012;**205**:425–431.

Kuroda S, Kondo T, Mori K, Yasuda K, Asai T, Sanjo H, Yakanaka H, Takeshima T, Kawahara T, Kato Y et al Successful onco-testicular sperm extraction from a testicular cancer patient with a single testis and azoospermia. *Clin Exp Reprod Med* 2018;**45**:44–47.

Laguna MP, Albers P, Algaba F, Bokemeyer C, Boormans BL Fischer S, Fizazi K, Gremmels H, Nicol D, Nicolai N. *European Association of Urology Guidelines. 2020 Edition*. Arnhem, The Netherlands: European Association of Urology Guidelines Office, 2020.

Leblanc L, Lagrange F, Lecoanet P, Marçon B, Eschwege P, Hubert J. Testicular microlithiasis and testicular tumor: a review of the literature. *Basic Clin Androl* 2018;**28**:8.

Loveland KL, Klein B, Pueschl D, Indumathy S, Bergmann M, Loveland BE, Hedger MP, Schuppe H-C. Cytokines in male fertility and reproductive pathologies: immunoregulation and beyond. *Front Endocrinol (Lausanne)* 2017;**8**:307.

Luján S, Guzman-Ordaz D, Rogel R, Broseta E, Pellicer A, Boronat F. ONCO-TESE: Obtaining spermatozoa after radical orchiectomy for testicular tumour and azoospermia. *Actas Urol Esp* 2016;**40**:64–67.

Meistrich ML. Effects of chemotherapy and radiotherapy on spermatogenesis in humans. *Fertil Steril* 2013;**100**:1180–1186.

Meistrich ML, Trostle-Weige PK, Lin R, Allis CD, Bhatnagar YM. Highly acetylated H4 is associated with histone displacement in rat spermatids. *Mol Reprod Dev* 1992;**31**:170–181.

Moch H, Cubilla AL, Humphrey PA, Reuter VE, Ulbright TM. The 2016 WHO classification of tumours of the urinary system and male genital organs—part A: renal, penile, and testicular tumours. *Eur Urol* 2016;**70**:93–105.

Moody JA, Ahmed K, Horsfield C, Pedersen MRV, Yap T, Shabbir M. Fertility preservation in testicular cancer—predictors of spermatogenesis. *BJU Int* 2018;**122**:236–242.

Moretti C, Serrentino M-E, Ialy-Radio C, Delessard M, Soboleva TA, Tores F, Leduc M, Nitschké P, Drevet JR, Tremethick DJ et al SLY regulates genes involved in chromatin remodeling and interacts with TBL1XR1 during sperm differentiation. *Cell Death Differ* 2017;**24**:1029–1044.

Muciaccia B, Boitani C, Berloco BP, Nudo F, Spadetta G, Stefanini M, Rooij D, Vicini E. Novel stage classification of human spermatogenesis based on acrosome development. *Biol Reprod* 2013;**89**:60.

Oktay K, Harvey BE, Partridge AH, Quinn GP, Reinecke J, Taylor HS, Wallace WH, Wang ET, Loren AW. Fertility preservation in patients with cancer: ASCO clinical practice guideline update. *J Clin Oncol* 2018;**36**:1994–2001.

Oliva R. Protamines and male infertility. *Hum Reprod Update* 2006;**12**:417–435.

Oliva R, Ballescà JL. Altered histone retention and epigenetic modifications in the sperm of infertile men. *Asian J Androl* 2012;**14**:239–240.

Oliva R, Bazett-Jones D, Mezquita C, Dixon GH. Factors affecting nucleosome disassembly by protamines in vitro. Histone hyperacetylation and chromatin structure, time dependence, and the size of the sperm nuclear proteins. *J Biol Chem* 1987;**262**:17016–17025.

Oliva R, Bazett-Jones DP, Locklear L, Dixon GH. Histone hyperacetylation can induce unfolding of the nucleosome core particle. *Nucleic Acids Res* 1990;**18**:2739–2747.

Oliva R, Castillo J. Proteomics and the genetics of sperm chromatin condensation. *Asian J Androl* 2011;**13**:24–30.

Oliva R, Dixon GH. Vertebrate protamine genes and the histone-to-protamine replacement reaction. *Prog Nucleic Acid Res Mol Biol* 1991;**40**:25–94.

Oliva R, Mezquita C. Histone H4 hyperacetylation and rapid turnover of its acetyl groups in transcriptionally inactive rooster testis spermatids. *Nucleic Acids Res* 1982;**10**:8049–8059.

Omisanjo OA, Biermann K, Hartmann S, Heukamp LC, Sonnack V, Hild A, Brehm R, Bergmann M, Weidner W, Steger K. DNMT1

Downloaded from https://academic.oup.com/humrep/advance-article/doi/10.1093/humrep/deac130/6604813 by UNIVERSITAT DE BARCELONA. Biblioteca user on 31 July 2022

and HDAC1 gene expression in impaired spermatogenesis and testicular cancer. *Histochem Cell Biol* 2007;**127**:175–181.

Oosterhuis JW, Stoop H, Dohle G, Boellaard W, van Casteren N, Wolffenbuttel K, Looijenga LHJ. A pathologist's view on the testis biopsy. *Int J Androl* 2011;**34**:e14–e20.

Paradowska AS, Miller D, Spiess A-N, Vieweg M, Cerna M, Dvorakova-Hortova K, Bartkuhn M, Schuppe H-C, Weidner W, Steger K. Genome wide identification of promoter binding sites for H4K12ac in human sperm and its relevance for early embryonic development. *Epigenetics* 2012;**7**:1057–1070.

Peng X, Zeng X, Peng S, Deng D, Zhang J. The association risk of male subfertility and testicular cancer: a systematic review. *PLoS One* 2009;**4**:e5591.

Pérez CV, Theas MS, Jacobo PV, Jarazo-Dietrich S, Guazzone VA, Lustig L. Dual role of immune cells in the testis. *Spermatogenesis* 2013;**3**:e23870.

Picton HM, Wyns C, Anderson RA, Goossens E, Jahnukainen K, Kliesch S, Mitchell RT, Pennings G, Rives N, Tournaye H et al; ESHRE Task Force On Fertility Preservation In Severe Diseases. A European perspective on testicular tissue cryopreservation for fertility preservation in prepubertal and adolescent boys. *Hum Reprod* 2015;**30**:2463–2475.

Pivot-Pajot C, Caron C, Govin J, Vion A, Rousseaux S, Khochbin S. Acetylation-dependent chromatin reorganization by BRDT, a testis-specific bromodomain-containing protein. *Mol Cell Biol* 2003; **23**:5354–5365.

Pulkkinen HH, Kiema M, Lappalainen JP, Toropainen A, Beter M, Tirronen A, Holappa L, Niskanen H, Kaikkonen MU, Ylä-Herttuala S et al BMP6/TAZ-Hippo signaling modulates angiogenesis and endothelial cell response to VEGF. *Angiogenesis* 2020;**24**:129–144.

Rajpert-De Meyts E, Nielsen JE, Skakkebaek NE, Almstrup K. Diagnostic markers for germ cell neoplasms: from placental-like alkaline phosphatase to micro-RNAs. *Folia Histochem Cytobiol* 2015; **53**:177–188.

Rathke C, Baarends WM, Awe S, Renkawitz-Pohl R. Chromatin dynamics during spermiogenesis. *Biochim Biophys Acta* 2014;**1839**: 155–168.

RStudio Team. RStudio: Integrated Development Environment for R. In RStudio I. Boston, MA: RStudio, Inc., 2019.

Saltzman AF, Cost NG. Adolescent and young adult testicular germ cell tumors: special considerations. *Adv Urol* 2018;**2018**:1–8.

Sonnack V, Failing K, Bergmann M, Steger K. Expression of hyperacetylated histone H4 during normal and impaired human spermatogenesis. *Andrologia* 2002;**34**:384–390.

Suzuki K, Shin T, Shimomura Y, Iwahata T, Okada H. Spermatogenesis in tumor-bearing testes in germ cell testicular cancer patients. *Hum Reprod* 2015;**30**:2853–2858.

Tarayrah L, Li Y, Gan Q, Chen X. Epigenetic regulator Lid maintains germline stem cells through regulating JAK-STAT signaling pathway activity. *Biol Open* 2015;**4**:1518–1527.

Torres-Flores U, Hernández-Hernández A. The interplay between replacement and retention of histones in the sperm genome. *Front Genet* 2020;**11**:780.

Tsutsumi S, Kawahara T, Takeshima T, Chiba S, Uemura K, Otani M, Shimokihara K, Hayashi Y, Mochizuki T, Takamoto D et al Onco-testicular sperm extraction (onco-TESE) for bilateral testicular tumors: two case reports. *J Med Case Rep* 2017;**11**:139.

Uhlen M, Zhang C, Lee S, Sjöstedt E, Fagerberg L, Bidkhori G, Benfeitas R, Arif M, Liu Z, Edfors F et al A pathology atlas of the human cancer transcriptome. *Science* 2017;**357**:eaan2507.

van der Zwan YG, Rijlaarsdam MA, Rossello FJ, Notini AJ, de Boer S, Watkins DN, Gillis AJ, Dorssers LC, White SJ, Looijenga LH. Seminoma and embryonal carcinoma footprints identified by analysis of integrated genome-wide epigenetic and expression profiles of germ cell cancer cell lines. *PLoS One* 2014;**9**:e98330.

Williams DH, Karpman E, Sander JC, Spiess PE, Pisters LL, Lipshultz LI. Pretreatment semen parameters in men with cancer. *J Urol* 2009;**181**:736–740.

Wolf KW, Jeppesen P, Mitchell A. Spermatid nucleus of *Megaselia scalaris* loew (insecta, diptera, phoridae): a study using anti-histone antibodies, scanning electron microscopy, and a centromere-specific oligonucleotide. *Mol Reprod Dev* 1993;**35**:272–276.

Xavier R, Carvalho RC, de Fraietta R. Semen quality from patients affected by seminomatous and non-seminomatous testicular tumor. *Int Braz J Urol* 2021;**47**:495–502.

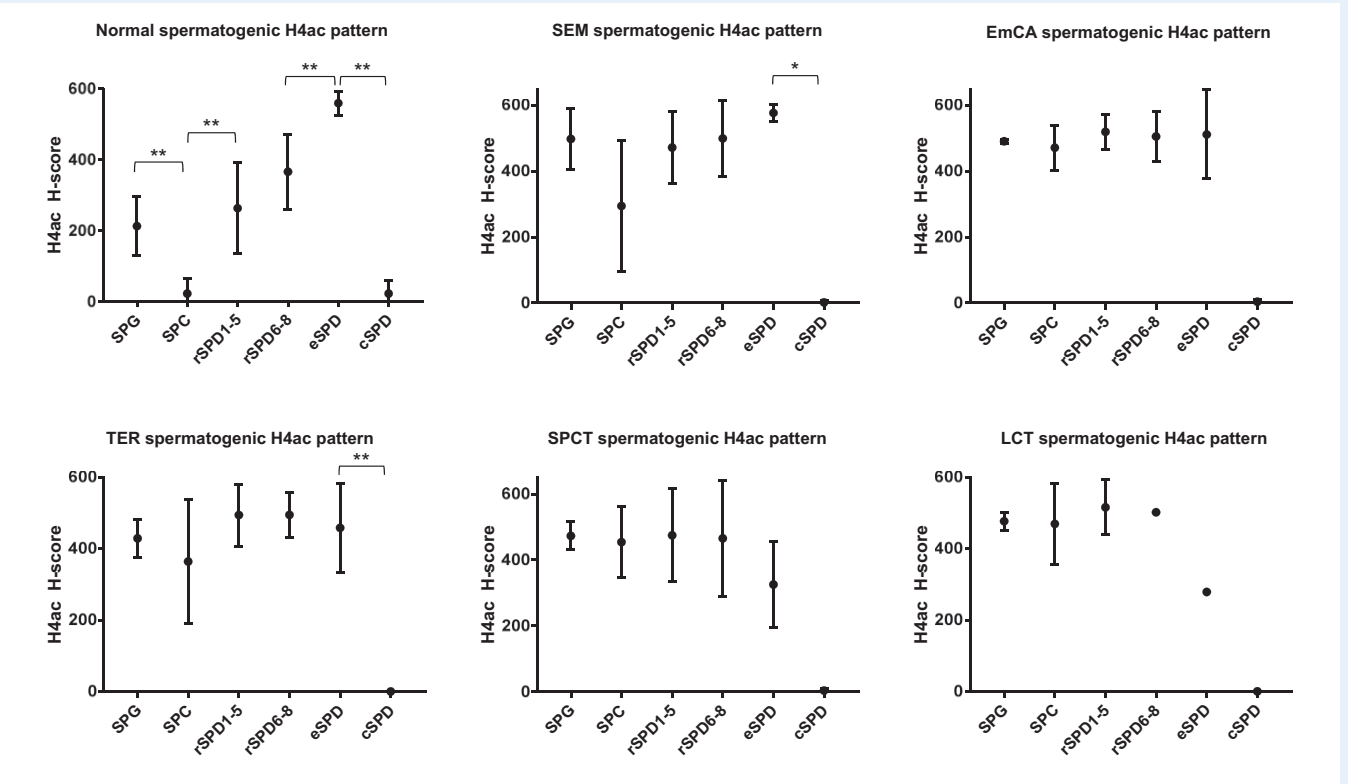
Zhang Y, Xia M, Jin K, Wang S, Wei H, Fan C, Wu Y, Li X, Li X, Li G et al Function of the c-Met receptor tyrosine kinase in carcinogenesis and associated therapeutic opportunities. *Mol Cancer* 2018; **17**:45.

Downloaded from https://academic.oup.com/humrep/advance-article/doi/10.1093/humrep/deac130/6604813 by UNIVERSITAT DE BARCELONA. Biblioteca user on 31 July 2022

Human Reproduction, pp. 1–1, 2022
https://doi.org/10.1093/humrep/deac130

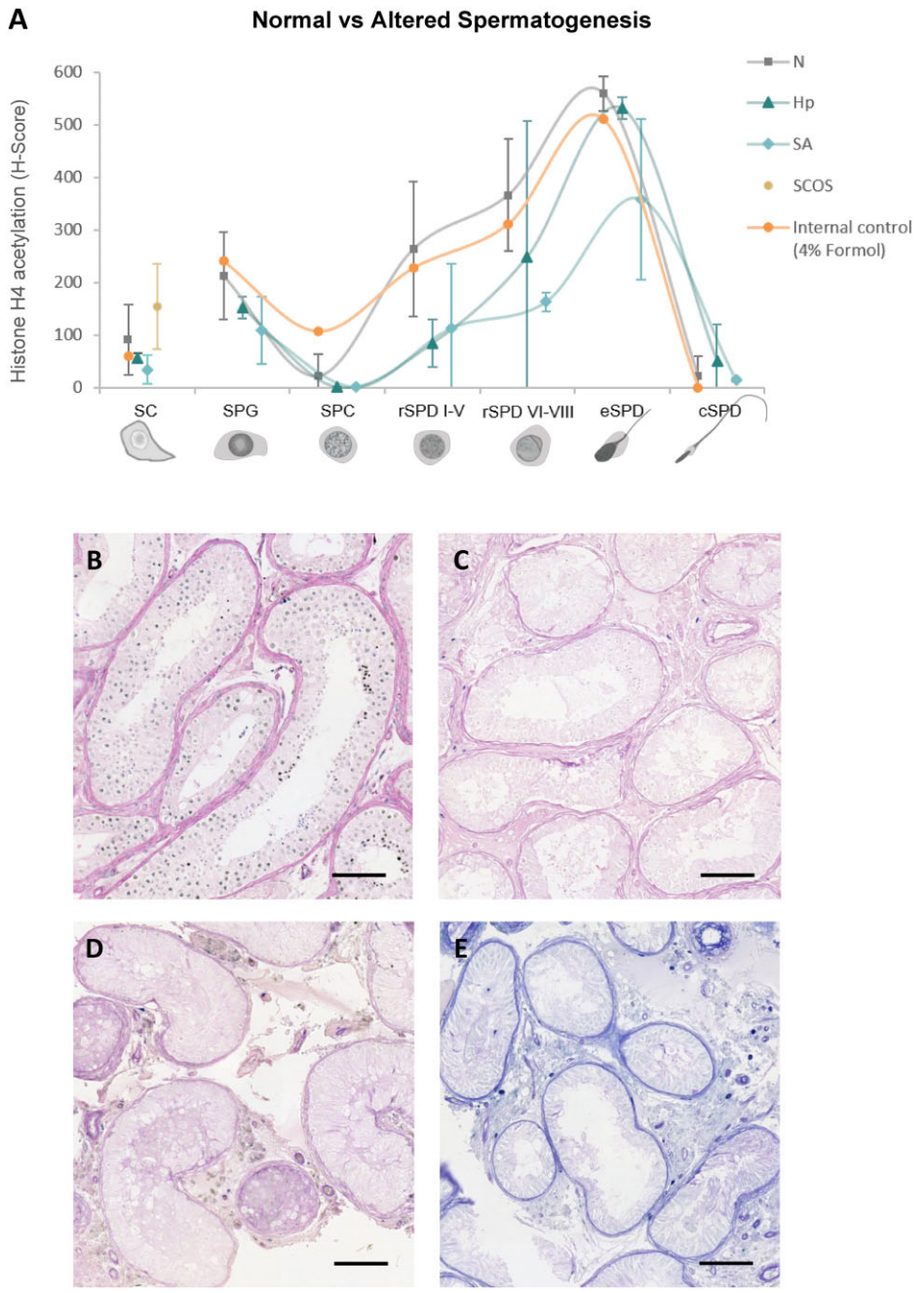
human reproduction

SUPPLEMENTARY DATA



Supplementary Figure S1. Comparative IHC spermatogenic H4ac patterns in patients with normal spermatogenesis and patients affected by testicular tumours. The H4ac pattern described in patients with normal spermatogenesis (upper left), characterized by the significant changes observed along the spermatogenesis, is lost in the spermatogenesis of patients affected by the different types of testicular tumours. H4ac H-scores (mean value ± SD) are shown for each testicular cell type analysed in controls and testicular tumour patients. *$P < 0.05$, **$P < 0.01$. cSPD, condensing spermatids; EmCA, embryonal carcinoma; eSPD, elongating spermatids; LCT, leydig cell tumour; rSPD, round spermatids; SC, Sertoli cell; SEM, seminoma; SPC, spermatocyte; SPCT, spermatocytic tumour; SPG, spermatogonia; TER, teratoma.

Human Reproduction, pp. 1–1, 2022
https://doi.org/10.1093/humrep/deac130

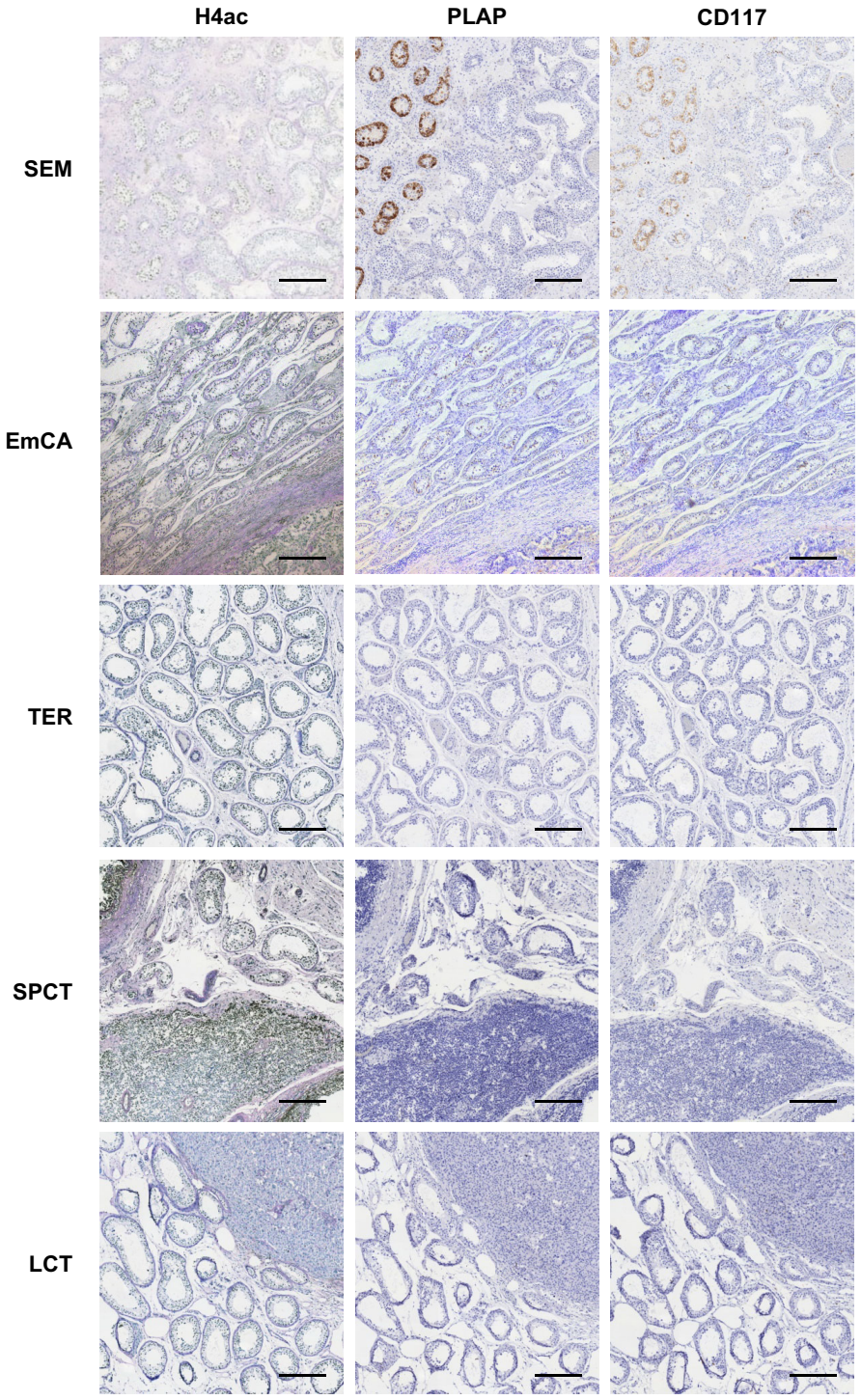


Supplementary Figure S2. IHC analyses of H4ac on testicular biopsies from patients with spermatogenic impairments. (**A**) H4ac H-scores (mean value ± SD) corresponding to each testicular cell type analysed in the groups of patients with normal (N) and altered spermatogenesis (hypospermatogenesis, Hp; spermatogenic arrest, SA; and Sertoli cell-only Syndrome, SCOS). The progress of the spermatogenic H4ac pattern in normal spermatogenesis (N) and the internal technical control are represented with a soft line (in grey and orange, respectively). (**B**–**E**) Representative images of H4ac IHC detection (brown colour) in seminiferous tubule sections from testicular biopsies of patients with normal and altered spermatogenesis: Normal spermatogenesis (**B**), hypospermatogenesis (**C**), spermatogenic arrest (**D**) and Sertoli cell-only Syndrome (**E**). No significant differences were found compared to the control group. The spermatogenic cells from patients with spermatogenic impairments (in Hp and SA, when available) displayed the gradual increase in the H4ac levels observed in patients with normal spermatogenesis. Tissues were counter-stained with PAS-haematoxylin. Scale bars = 100 µm. cSPD, condensing spermatids; eSPD, elongating spermatids; rSPD I-V, early-stages (I–V) round spermatids; rSPD VI–VIII, late-stages (VI–VIII) round spermatids; SC, Sertoli cell; SPC, spermatocyte; SPG, spermatogonia.

Human Reproduction, pp. 1–1, 2022
https://doi.org/10.1093/humrep/deac130

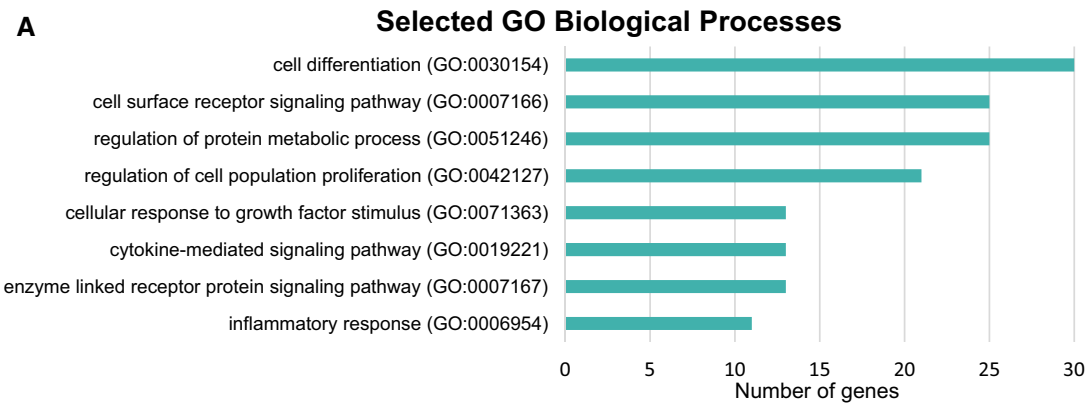
human reproduction

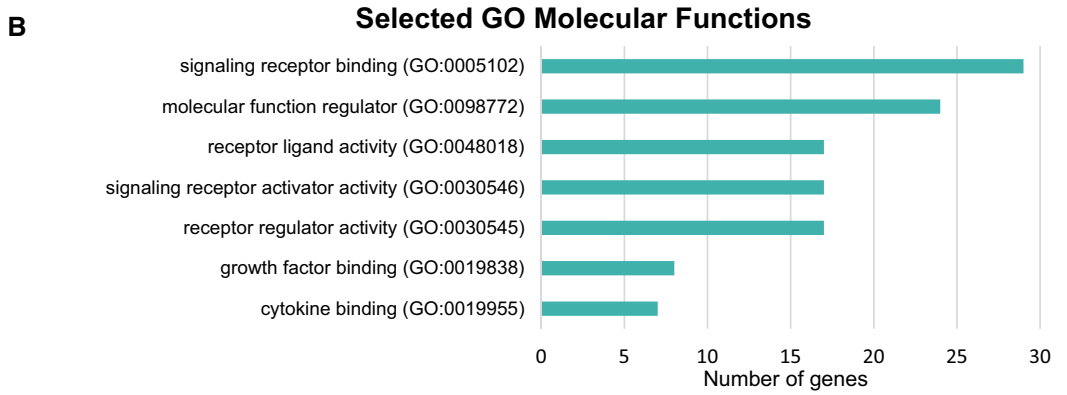
SUPPLEMENTARY DATA

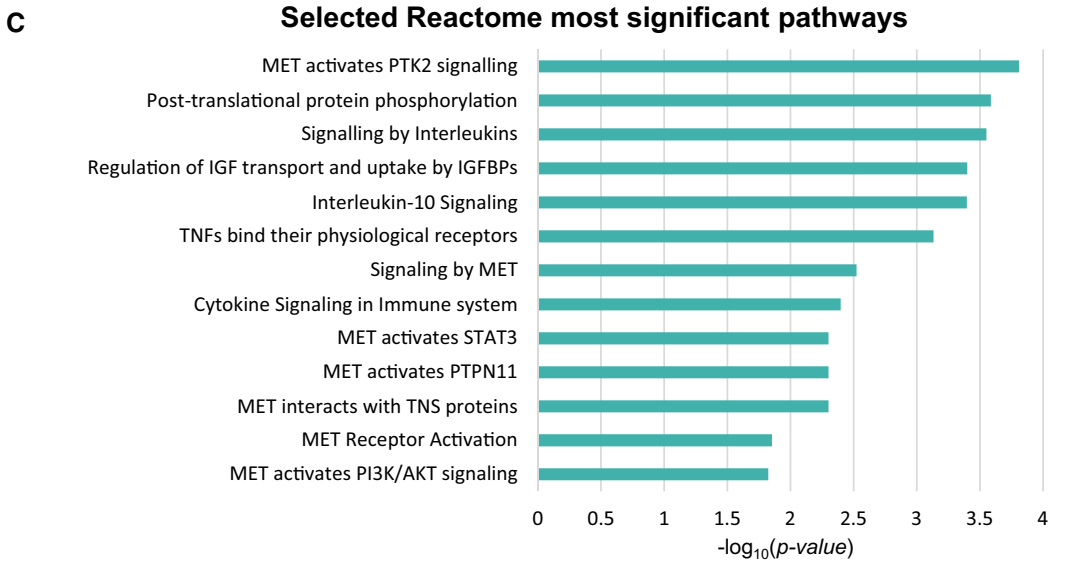


Supplementary Figure S3. The impaired spermatogenic histone H4 acetylation pattern of testicular tumour patients is not dependent on the presence of seminiferous tubules with pre-invasive germ cell neoplasia *in situ* (GCNIS). Consecutive testicular sections were immunohistochemically stained with H4ac, PLAP and CD117 in patients with seminoma (SEM), embryonal carcinoma (EmCA), teratoma (TER), spermatocytic tumour (SPCT) and Leydig cell tumour (LCT). PLAP and CD117 stainings allowed the discernment of the seminiferous tubules containing pre-invasive GCNIS, evidencing a positive pattern in SEM and EmCA. The increased H4ac levels in the seminiferous tubules observed in all groups of testicular cancer patients is independent of the presence or not of pre-invasive GCNIS. Tissues were counterstained with PAS-haematoxylin. Scale bars = 200 µm.

Human Reproduction, pp. 1–1, 2022
https://doi.org/10.1093/humrep/deac130







Supplementary Figure S4. Implications of the potential paracrine effect of the tumour on the healthy testicular tissue. Representation of a selection of enriched Gene Ontology (GO) annotations for biological processes (**A**) and molecular functions (**B**) identified in the predicted subset of secreted testicular tumour proteins ($P < 0.05$ after Bonferroni correction). The number of proteins identified corresponding to each GO annotation is represented in the *X* axis. (**C**) Selection of significantly enriched pathways associated with the testicular tumour predicted secretome after Reactome analysis ($P < 0.05$ after FDR correction). The horizontal axis represents the -$\log_{10}$(*P*-value) for each pathway.

Supplementary Table SI. Immunohistochemical results of histone H4 acetylation in testicular sections from control patients (Normal spermatogenesis), patients with altered spermatogenesis (Sertoli cell-only syndrome, hypospermatogenesis, spermatogenic arrest) and patients with different testicular tumors (seminoma, spermatocytic tumor, embryonal carcinoma, teratoma and Leydig cell tumor). Results are expressed according to the testicular cell type analyzed. H-score is expressed per patient, and summarized per group as mean ± SD. The number of evaluated tubular sections presenting each of the analyzed cell types is indicated in brackets. Complementary sample information such as age, type of fixative used for each specimen, size of the biopsy and tumor size is shown. Data corresponding to the IHC internal control is included at the bottom of the "Normal spermatogenesis (N)" group.

Group of study & Patient ID	Histone H4 acetylation (H-Score)							acH4 detection	Sample information			
	SC	SPG	SPC	rSPD (I-V)	rSPD (VI-VIII)	eSPD	cSPD	CANCER CELLS	Patient Age	Fixative	Size of the biopsy	Tumor size
Normal spermatogenesis (N)												
N1	78.6 (28)	182.4 (28)	0.0 (26)	266.4 (3)	327.0 (11)	540.0 (15)	0.0 (7)	-	30	Bouin	0.9 cm	-
N2	96.0 (26)	242.4 (26)	0.0 (26)	127.2 (12)	325.2 (16)	600.0 (3)	0.0 (6)	-	35	Bouin	0.6 cm	-
N3	214.8 (29)	304.2 (29)	31.2 (29)	292.8 (12)	379.8 (9)	558.6 (10)	3.0 (8)	-	35	Bouin	1.0 cm	-
N4	37.8 (29)	110.4 (29)	0.0 (31)	100.2 (15)	212.4 (15)	600.0 (7)	0.0 (16)	-	34	Bouin	0.6 cm	-
N5	27.6 (29)	136.8 (30)	0.0 (29)	386.4 (15)	525.0 (15)	525.0 (4)	40.2 (15)	-	42	Bouin	0.4 cm	-
N6	89.4 (29)	300.0 (30)	103.2 (29)	407.4 (13)	428.4 (13)	533.4 (3)	90.0 (10)	-	50	Bouin	0.7 cm	-
Mean ± SD	**90.7 ± 66.9**	**212.7 ± 82.5**	**22.4 ± 41.5**	**263.4 ± 128.0**	**366.3 ± 106.0**	**559.5 ± 33.3**	**22.2 ± 36.8**					
Internal control	*59.4 (32)*	*240.6 (32)*	*106.7 (30)*	*227.3 (11)*	*311.1 (9)*	*511.1 (9)*	*0.0 (9)*	-	*64*	*Formol*	*4.5 cm*	-
Sertoli cell-only syndrome (SCOS)												
SCOS1	80.4 (31)	-	-	-	-	-	-	-	34	Bouin	0.5 cm	-
SCOS2	240.6 (30)	-	-	-	-	-	-	-	39	Bouin	0.8 cm	-
SCOS3	138.6 (30)	-	-	-	-	-	-	-	33	Bouin	0.7 cm	-
Mean ± SD	**153.2 ±81.1**	-	-	-	-	-	-					
Hypospermatogenesis (Hp)												
HP1	61.8 (20)	136.8 (24)	0.6 (21)	51.6 (9)	430.8 (6)	546.6 (6)	100.2 (6)	-	32	Bouin	1.5 cm	-
HP2	49.2 (25)	167.4 (25)	0.0 (24)	116.4 (17)	66.6 (3)	516.6 (6)	0.0 (3)	-	40	Bouin	0.4 cm	-
Mean ± SD	**55.5 ±8.9**	**152.1 ± 21.6**	**0.3 ± 0.4**	**84.0 ± 45.8**	**248.7 ± 257.5**	**531.4 ± 21.2**	**50.1 ± 70.9**					
Spermatogenic arrest (SA)												
SA1 - total SPC arrest	42.6 (35)	113.4 (29)	1.8 (32)	-	-	-	-	-	39	Bouin	0.5 cm	-
SA2 - partial SPC arrest	3.6 (26)	42.6 (21)	0.0 (20)	25.2 (4)	175.2 (4)	466.8 (6)	16.8 (6)	-	40	Bouin	0.7 cm	-
SA3 - partial rSPD arrest	55.8 (27)	171.6 (28)	0.0 (27)	199.8 (20)	150.0 (4)	250.2 (2)	11.4 (9)	-	29	Bouin	0.5 cm	-
Mean ± SD	**34.0 ± 27.1**	**109.2 ± 64.6**	**0.6 ± 1.0**	**112.5 ± 123.5**	**162.6 ± 17.8**	**358.5 ± 153.2**	**14.1 ± 3.8**					
Seminoma (SEM)												
SEM1	279.6 (29)	568.8 (29)	271.2 (28)	525.0 (16)	600.0 (2)	600.0 (1)	0.0 (7)	Positive	52	Formol	7.0 cm	1.5 cm
SEM2	166.8 (27)	446.4 (28)	84.0 (25)	400.2 (12)	400.2 (4)	561.6 (13)	8.4 (12)	Positive	36	Formol	5.0 cm	2.0 cm
SEM3	376.8 (30)	396.0 (24)	262.2 (29)	364.2 (14)	400.2 (4)	550.2 (10)	0.0 (9)	Positive	36	Formol	10.0 cm	0.4 cm
SEM4	460.2 (25)	583.2 (30)	563.4 (30)	600.0 (17)	600.0 (5)	600.0 (10)	0.0 (9)	Positive	49	Formol	6.5 cm	3.8 cm
Mean ± SD	**320.9 ± 126.5***	**498.6 ± 91.9****	**295.2 ± 198.5***	**472.4 ± 109.5**	**500.1 ± 115.4**	**578.0 ± 25.9**	**2.1 ± 4.2**					
Embryonal carcinoma (EmCA)												
EmCA1	405.0 (21)	489.6 (19)	471.6 (14)	499.8 (7)	499.8 (4)	600.0 (5)	0.0 (5)	Positive	27	Formol	7.0 cm	4.0 cm
EmCA2	229.2 (30)	483.6 (31)	470.4 (27)	510.0 (10)	400.2 (2)	580.2 (3)	0.0 (6)	Positive	35	Formol	6.8 cm	6.8 cm
EmCA3	437.4 (29)	488.4 (29)	363 (26)	552.6 (14)	550.2 (4)	357.0 (9)	11.4 (8)	Positive	36	Formol	4.3 cm	1.2 cm
EmCA4	475.8 (15)	499.8 (21)	537.6 (4)	450.0 (4)	480.0 (3)	-	-	Positive	21	Formol	4.0 cm	2.0 cm
EmCA5	510 (20)	495.6 (28)	517.8 (16)	588.6 (9)	600.0 (3)	-	-	Positive	26	Formol	4.0 cm	2.6 cm
Mean ± SD	**411.5 ± 109.3****	**491.4 ± 6.3****	**472.1 ± 67.6****	**520.2 ± 52.9****	**506.0 ± 75.3***	**512.4 ± 134.9**	**3.8 ± 6.6**					
Teratoma (TER)												
TER1	233.4 (30)	410.4 (29)	292.8 (28)	400.2 (17)	420.0 (5)	577.8 (9)	0.0 (15)	No visible cells	38	Formol	5.0 cm	0.9 cm
TER2	276.0 (29)	439.8 (30)	151.8 (28)	442.8 (7)	471.6 (7)	543.6 (16)	0.0 (4)	Positive	37	Formol	6.0 cm	2.7 cm
TER3	409.8 (20)	498.6 (29)	486.6 (25)	553.8 (13)	525.0 (3)	407.4 (10)	0.0 (15)	Positive	34	Formol	7.0 cm	4.1 cm
TER4	426.0 (23)	369.6 (23)	526.8 (15)	583.2 (12)	566.4 (4)	309.0 (11)	0.0 (7)	Positive	21	Formol	3.2 cm	3.0 cm
Mean ± SD	**336.3 ± 96.0****	**429.6 ± 54.3****	**364.5 ± 174.8***	**495.0 ± 87.5***	**459.5 ± 63.7***	**459.5 ± 124.4**	**0.0 ± 0.0**					
Spermatocytic Tumor (SPCT)												
SPCT1	471.6 (21)	495.0 (21)	554.4 (11)	583.2 (12)	600.0 (3)	400.2 (3)	0.0 (4)	Positive	71	Formol	12.0 cm	5.5 cm
SPCT2	400.2 (27)	499.8 (29)	468.0 (21)	527.4 (12)	529.8 (3)	399.6 (12)	8.4 (8)	Positive	74	Formol	9.0 cm	5.0 cm
SPCT3	408.6 (12)	424.2 (23)	340.2 (20)	314.4 (7)	266.4 (3)	175.2 (4)	0.0 (3)	Positive	37	Formol	5.0 cm	3.5 cm
Mean ± SD	**426.8 ± 39.0***	**473.0 ± 42.3***	**454.2 ± 107.8***	**475.0 ± 141.9**	**465.4 ± 175.9**	**325.0 ± 129.7***	**2.8 ± 4.8**					
Leydig cell tumor (LCT)												
LCT1	409.8 (25)	495.0 (25)	550.2 (15)	571.2 (7)	-	-	-	Positive	37	Formol	7.5 cm	2.4 cm
LCT2	352.2 (27)	460.2 (28)	390.0 (21)	462.0 (9)	502.8 (5)	279.0 (9)	0.0 (4)	Positive	49	Formol	4.5 cm	2.1 cm
Mean ± SD	**381.0 ±40.7**	**477.6 ± 24.6**	**470.1 ± 113.3**	**516.6 ± 77.2**	**502.8**	**279.0**	**0.0**					

SC: Sertoli cells; SPG: spermatogonia; SPC: spermatocytes, rSPD I-V: early-stages (I-V) round spermatids; rSPD VI-VIII: late-stages (VI-VIII) round spermatids; eSPD: elongating spermatids, cSPD: condensing spermatids. *p<0.05, **p<0.01 resulting from the comparison with the control group(N). Note that the Hp and LCT groups were not considered for statistical analysis due to the limited sample availability, nor the internal control.

Supplementary Table SII. List of *in silico* predicted testicular tumor secreted proteins. Num
about the different protein expression levels ("High", "Medium", "Low" or "ND" - not detect
per number of patients in the testicular tumor column. Comparison with the protein expres
testis is detailed per testicular cell type (NA is typed when information was not available).

		Testicular cancer				Normal test
Gene name	**Uniprot ID**	**High**	**Medium**	**Low**	**ND**	**Testicular cell type**
ADAMTSL4	Q6UY14	0	10	2	0	Cells in seminiferous ducts Leydig cells
AFP	P02771	2	5	4	0	Cells in seminiferous ducts Leydig cells
AIMP1	Q12904	1	11	0	0	Elongated or late spermatids Leydig cells Pachytene spermatocytes Peritubular cells Preleptotene spermatocytes Round or early spermatids Sertoli cells Spermatogonia
ALB	P02768	0	9	2	0	Cells in seminiferous ducts Leydig cells
APOO	Q9BUR5	1	5	5	0	Elongated or late spermatids Leydig cells Pachytene spermatocytes Peritubular cells Preleptotene spermatocytes Round or early spermatids Sertoli cells Spermatogonia
BMP6	P22004	0	11	0	0	Cells in seminiferous ducts Leydig cells
C14orf93	Q9H972	9	1	1	0	Cells in seminiferous ducts Leydig cells
C1orf54	Q8WWF1	5	6	0	0	Cells in seminiferous ducts Leydig cells
CFB	P00751	1	7	4	0	Cells in seminiferous ducts Leydig cells
CHRD	Q9H2X0	3	4	3	2	Elongated or late spermatids Leydig cells Pachytene spermatocytes Peritubular cells Preleptotene spermatocytes Round or early spermatids Sertoli cells Spermatogonia
COL18A1	P39060	1	7	0	3	Cells in seminiferous ducts Leydig cells
COL1A2	P08123	0	7	3	0	Cells in seminiferous ducts Leydig cells
COPA	P53621	0	7	4	1	Elongated or late spermatids Leydig cells Pachytene spermatocytes Peritubular cells Preleptotene spermatocytes Round or early spermatids Sertoli cells Spermatogonia
CP	P00450	3	7	2	0	Cells in seminiferous ducts Leydig cells
CPB2	Q96IY4	0	12	0	0	Cells in seminiferous ducts Leydig cells
CRTAP	O75718	10	0	0	0	Cells in seminiferous ducts Leydig cells
CX3CL1	P78423	10	0	0	0	Cells in seminiferous ducts Leydig cells
DMP1	Q13316	0	11	1	0	Cells in seminiferous ducts Leydig cells
ECM2	O94769	0	6	5	0	Cells in seminiferous ducts Leydig cells
EDIL3	O43854	2	10	0	0	Cells in seminiferous ducts Leydig cells
ENTPD5	O75356	0	9	2	0	Cells in seminiferous ducts Leydig cells
ENTPD6	O75354	10	2	0	0	Cells in seminiferous ducts Leydig cells
FAM3C	Q92520	4	6	2	0	Elongated or late spermatids Leydig cells Pachytene spermatocytes Peritubular cells Preleptotene spermatocytes Round or early spermatids Sertoli cells Spermatogonia
FGF19	O95750	1	8	2	1	Cells in seminiferous ducts Leydig cells
FSTL3	O95633	3	6	0	0	Cells in seminiferous ducts Leydig cells
HAPLN3	Q96S86	1	6	2	1	Cells in seminiferous ducts Leydig cells
HGF	P14210	0	11	0	0	Cells in seminiferous ducts Leydig cells
HSPG2	P98160	1	7	3	0	Cells in seminiferous ducts Leydig cells

IL15	P40933	3	6	3	0	Cells in seminiferous ducts Leydig cells
IL15RA	Q13261	0	8	3	0	Cells in seminiferous ducts Leydig cells
IL1R1	P14778	2	7	2	1	Cells in seminiferous ducts Leydig cells
ITIH3	Q06033	3	5	1	2	Cells in seminiferous ducts Leydig cells
ITIH5	Q86UX2	1	9	0	1	Cells in seminiferous ducts Leydig cells
IZUMO4	Q1ZYL8	1	10	1	0	Elongated or late spermatids Leydig cells Pachytene spermatocytes Peritubular cells Preleptotene spermatocytes Round or early spermatids Sertoli cells Spermatogonia
JAM3	Q9BX67	1	7	3	1	Cells in seminiferous ducts Leydig cells
LAMB2	P55268	2	10	0	0	Elongated or late spermatids Leydig cells Pachytene spermatocytes Peritubular cells Preleptotene spermatocytes Round or early spermatids Sertoli cells Spermatogonia
LAMC1	P11047	5	3	0	4	Elongated or late spermatids Leydig cells Pachytene spermatocytes Peritubular cells Preleptotene spermatocytes Round or early spermatids Sertoli cells Spermatogonia
LTBP4	Q8N2S1	3	4	1	3	Cells in seminiferous ducts Leydig cells
MANF	P55145	2	5	5	0	Cells in seminiferous ducts Leydig cells
MET	P08581	0	6	5	0	Cells in seminiferous ducts Leydig cells
METRN	Q9UJH8	2	8	0	0	Cells in seminiferous ducts Leydig cells
MIF	P14174	2	8	2	0	Cells in seminiferous ducts Leydig cells
MMP11	P24347	0	10	1	0	Cells in seminiferous ducts Leydig cells
NELL1	Q92832	0	6	2	1	Cells in seminiferous ducts Leydig cells
NMB	P08949	0	6	3	2	Cells in seminiferous ducts Leydig cells
NRP1	O14786	0	8	3	1	Cells in seminiferous ducts Leydig cells
PDGFB	P01127	0	11	1	0	Elongated or late spermatids Leydig cells Pachytene spermatocytes Peritubular cells Preleptotene spermatocytes Round or early spermatids Sertoli cells Spermatogonia
PLTP	P55058	0	6	4	1	Cells in seminiferous ducts Leydig cells
PODNL1	Q6PEZ8	0	8	2	0	Elongated or late spermatids Leydig cells Pachytene spermatocytes Peritubular cells Preleptotene spermatocytes Round or early spermatids Sertoli cells Spermatogonia
PON1	P27169	0	7	5	0	Cells in seminiferous ducts Leydig cells
PON2	Q15165	3	6	1	0	Elongated or late spermatids Leydig cells Pachytene spermatocytes Peritubular cells Preleptotene spermatocytes Round or early spermatids Sertoli cells Spermatogonia
PRTN3	P24158	3	4	1	3	Cells in seminiferous ducts Leydig cells
PTK7	Q13308	0	5	4	0	Elongated or late spermatids Leydig cells Pachytene spermatocytes Peritubular cells Preleptotene spermatocytes Round or early spermatids Sertoli cells Spermatogonia

PTX3	P26022	2	8	1	1	Elongated or late spermatids Leydig cells Pachytene spermatocytes Peritubular cells Preleptotene spermatocytes Round or early spermatids Sertoli cells Spermatogonia
RGMA	Q96B86	0	10	1	0	Cells in seminiferous ducts Leydig cells
RNPEP	Q9H4A4	3	8	0	0	Cells in seminiferous ducts Leydig cells
RSPRY1	Q96DX4	0	10	2	0	Cells in seminiferous ducts Leydig cells
SCGB1D2	O95969	7	4	1	0	Cells in seminiferous ducts Leydig cells
SDC4	P31431	0	11	0	0	Elongated or late spermatids Leydig cells Pachytene spermatocytes Peritubular cells Preleptotene spermatocytes Round or early spermatids Sertoli cells Spermatogonia
SEMA3A	Q14563	0	9	2	1	Cells in seminiferous ducts Leydig cells
SERPINA6	P08185	1	7	2	1	Elongated or late spermatids Leydig cells Pachytene spermatocytes Peritubular cells Preleptotene spermatocytes Round or early spermatids Sertoli cells Spermatogonia
SERPINA7	P05543	1	8	3	0	Cells in seminiferous ducts Leydig cells
SHE	Q5VZ18	2	6	2	1	Cells in seminiferous ducts Leydig cells
SPOCK2	Q92563	0	10	2	0	Elongated or late spermatids Leydig cells Pachytene spermatocytes Peritubular cells Preleptotene spermatocytes Round or early spermatids Sertoli cells Spermatogonia
SRPX2	O60687	0	9	2	0	Cells in seminiferous ducts Leydig cells
TIMP2	P16035	0	10	1	0	Elongated or late spermatids Leydig cells Pachytene spermatocytes Peritubular cells Preleptotene spermatocytes Round or early spermatids Sertoli cells Spermatogonia
TNFRSF1A	P19438	0	7	4	0	Cells in seminiferous ducts Leydig cells
TNFRSF1B	P20333	2	8	2	0	Cells in seminiferous ducts Leydig cells
TNFSF13B	Q9Y275	0	9	2	0	Cells in seminiferous ducts Leydig cells
TSKU	Q8WUA8	1	6	5	0	Elongated or late spermatids Leydig cells Pachytene spermatocytes Peritubular cells Preleptotene spermatocytes Round or early spermatids Sertoli cells Spermatogonia
TXNDC16	Q9P2K2	12	0	0	0	Cells in seminiferous ducts Leydig cells

5.1.2 Work 2: H4K5 butyrylation coexist with acetylation during human spermiogenesis and are retained in the mature sperm chromatin

Submitted as:

de la Iglesia A[1], Jauregi P[1], Jodar M[1,2], Barrachina F[1,†], Ded L[3], Mallofré C[4], Rodríguez-Carunchio L[4,5], Corral JM[1,6,7], Ballescà JL[1,7], Komrskova K[3,8], Castillo J[1,*], Oliva R[1,2,*]. H4K5 butyrylation coexist with acetylation during human spermiogenesis and are retained in the mature sperm chromatin. *Int J Mol Sci*. 2022. *Under revision*.

[1] Molecular Biology of Reproduction and Development Research Group, Department of Biomedical Sciences, Faculty of Medicine and Health Sciences, Institut d'Investigacions Biomèdiques August Pi i Sunyer (IDIBAPS), Fundació Clínic per a la Recerca Biomèdica, Universitat de Barcelona, Barcelona, Spain.

[2] Biochemistry and Molecular Genetics Service, Hospital Clinic, Barcelona, Spain.

[3] Laboratory of Reproductive Biology, Institute of Biotechnology, Czech Academy of Sciences, BIOCEV, Vestec, Czech Republic.

[4] Department of Pathology, Hospital Clínic, Barcelona, Spain.

[5] Faculty of Medicine, University of Vic – Central University of Catalonia (UVic-UCC), Barcelona, Spain.

[6] Department of Urology, IDIBAPS, Hospital Clínic, Barcelona, Spain.

[7] Clinic Institute of Gynaecology, Obstetrics and Neonatology, Hospital Clínic, Barcelona, Spain.

[8] Department of Zoology, Faculty of Science, Charles University, Prague, Czech Republic

[†] Current affiliation: Program in Membrane Biology, Nephrology Division, Department of Medicine, Massachusetts General Hospital and Harvard Medical School, Boston, MA, United States

[*] Corresponding authors

International Journal of
Molecular Sciences

MDPI

Article

H4K5 butyrylation coexist with acetylation during human spermiogenesis and are retained in the mature sperm chromatin

Alberto de la Iglesia [1], Paula Jauregi [1], Meritxell Jodar [1,2], Ferran Barrachina [1,†], Lukas Ded [3], Carme Mallofré [4], Leonardo Rodríguez-Carunchio [4,5], Juan Manuel Corral [1,6,7], Josep Lluís Ballescà [1,7], Katerina Komrskova [3,8], Judit Castillo [1,*], Rafael Oliva [1,2,*]

[1] Molecular Biology of Reproduction and Development Research Group, Institut d'Investigacions Biomèdiques August Pi i Sunyer (IDIBAPS), Fundació Clínic per a la Recerca Biomèdica, Departament de Biomedicina, Facultat de Medicina i Ciències de la Salut, Universitat de Barcelona (UB), Barcelona, Spain
[2] Biochemistry and Molecular Genetics Service, Hospital Clínic, Barcelona, Spain
[3] Laboratory of Reproductive Biology, Institute of Biotechnology, Czech Academy of Sciences, BIOCEV, Vestec, Czech Republic
[4] Department of Pathology, Hospital Clínic, Barcelona, Spain
[5] Faculty of Medicine, University of Vic – Central University of Catalonia (UVic-UCC), Barcelona, Spain
[6] Department of Urology, IDIBAPS, Hospital Clínic, Barcelona, Spain,
[7] Clinic Institute of Gynaecology, Obstetrics and Neonatology, Hospital Clínic, Barcelona, Spain
[8] Department of Zoology, Faculty of Science, Charles University, Prague, Czech Republic
[†] Current affiliation: Program in Membrane Biology, Nephrology Division, Department of Medicine, Massachusetts General Hospital and Harvard Medical School, Boston, MA, United States
[*] Correspondence: roliva@ub.edu, juditcastillo@ub.edu

Abstract: Male germ cells experience a drastic chromatin remodeling through the nucleo-histone to nucleo-protamine (NH-NP) transition necessary for proper sperm functionality. Post-translational modifications (PTMs) of H4 Lys5, such as acetylation (H4K5ac), play a crucial role in epigenetic control of nucleosome disassembly facilitating protamine incorporation into paternal DNA. It has been shown that butyrylation on the same residue (H4K5bu) participates in temporal regulation of NH-NP transition in mice, delaying the bromodomain testis specific protein (BRDT)-dependent nucleosome disassembly and potentially marking retained nucleosomes. However, no information was available so far on this modification in human sperm. Here we report a dual behavior of H4K5bu and H4K5ac in human normal spermatogenesis, suggesting a specific role of H4K5bu during spermatid elongation, coexisting with H4K5ac although being mostly present in a more advanced stage of the process. This pattern is stable under different testicular pathologies, suggesting a highly conserved function of these modifications. Despite a drastic decrease of both PTMs in condensed spermatids, they are retained in ejaculated sperm, with 30% of non-colocalizing nucleosome clusters, which could reflect differential paternal genome retention. Whereas no apparent effect of these PTMs was observed associated with sperm quality, their presence in mature sperm would entail a potential role in the zygote.

Keywords: butyrylation, acetylation, H4K5, spermatogenesis, sperm, sperm chromatin, epigenetic regulation.

Citation: Lastname, F.; Lastname, F.; Lastname, F. Title. *Int. J. Mol. Sci.* **2022**, *23*, x. https://doi.org/10.3390/xxxxx

Academic Editor: Firstname Lastname

Received: date
Accepted: date
Published: date

Publisher's Note: MDPI stays neutral with regard to jurisdictional claims in published maps and institutional affiliations.

Copyright: © 2022 by the authors. Submitted for possible open access publication under the terms and conditions of the Creative Commons Attribution (CC BY) license (https://creativecommons.org/licenses/by/4.0/).

1. Introduction

Histone post-translational modifications (PTMs) play an essential role in epigenetic regulation of spermiogenesis, the last phase of spermatogenesis, marked by a unique process of chromatin remodeling of male germ cell's nucleus that is necessary for proper sperm function [1–8]. In mammals, a histone hyperacetylation wave concomitant to nucleosome disassembly is necessary for gradual protamine incorporation into paternal genome through the process of nucleo-histone to nucleo-protamine (NH-NP) transition [9–

14]. Acetylation of histone tails contribute to loosen both histone-DNA and nucleosome-nucleosome interactions [12,15], allowing the incorporation of histone variants and transition proteins, that also contribute to chromatin relaxation for protamine recruitment and processing [13,16–21]. The residues Lys5 and Lys8 of histone H4 (H4K5 and H4K8) are of special importance in the regulation of NH-NP transition since acetylation on these amino acids (H4K5ac and H4K8ac, respectively) is recognized by the first bromodomain of the bromodomain-containing testis specific protein BRDT, which entails the first step for nucleosome instability and genome-wide histone eviction [22–28].

Acetylation of H4 has been widely studied in normal and pathogenic testes within the context of NH-NP transition and has been recently found altered in testis of patients affected by testicular tumors [29–32]. Of note, the presence of additional H4 PTMs also belonging to the group of histone acylations, with similar physicochemical properties as acetylation, have also been identified in the testis. However, their potential role during human spermatogenesis is not well characterized yet [33–35]. Among them, histone butyrylation arises as an interesting epigenetic regulator of NH-NP transition. Contrary to what could be expected from the general role of histone acylations stimulating transcription and, therefore, inducing open chromatin states, BRDT seems to be blind to butyrylated H4K5 (H4K5bu), making H4K5bu-bearing nucleosomes able to escape histone eviction at the time of the hyperacetylation wave in mice [36]. Besides, this behavior takes place regardless the presence of butyrylation or acetylation in H4K8, which points out H4K5 as the main specific residue of this mechanism. Therefore, it has been suggested a temporal regulation of delayed histone replacement of nucleosomes marked by H4K5bu, which could also underlie a specific mechanism of nucleosome retention in mature sperm [36]. During mouse spermatogenesis, H4K5 acetylation and butyrylation also coexist in different spermatogenic stages, being enriched at regions surrounding transcription start sites of active genes in a transcription-dependent manner [36].

The importance of histone PTMs in male germ cells is not limited to their regulatory role during chromatin remodeling. Sperm cells contain many layers of epigenetic information, with modified histones contributing to the non-random distribution of the nucleohistone genomic domain along specific regions of the paternal genome, and marking differential sperm DNA accessibility [2,5,37–40]. In addition, infertile men evidence alterations of histone PTM profile and impaired nucleosome retention in mature sperm [2,4,41]. Sperm epigenetic marks are susceptible to be transmitted to the zygote during fecundation, potentially contributing to early stages of embryo development and future offspring health [42–45].

One of the current challenges of assisted reproduction techniques (ART) relies on selecting the best spermatozoa for intracytoplasmic sperm injection (ICSI), overcoming the intrinsic high heterogeneity of the human sperm sample. Current methods for sperm selection are based on multilayer density gradient centrifugation, often followed by swim-up. However, these techniques mainly rely on the quality of sperm motility and morphology not accounting on the rest of sperm molecular features that could affect the ART success rate (around 30-35% per cycle in Europe) [46]. In terms of sperm chromatin, sperm populations selected through density gradient centrifugation seem to show different retention of histone PTMs and histone variants compared to the corresponding neat sample [47]. However, the effect of density gradient centrifugation on other sperm quality parameters, such as DNA integrity as direct indicator of sperm chromatin maturity, is unclear, with some articles reporting subgroups of patients with increased DNA damage after sperm preparation [48–50]. Therefore, there is unmet need for markers of sperm quality.

Despite the relevance of the H4K5 residue in the regulation of mouse NH-NP transition, there is a lack of information about the significance and distribution of acetylated

and butyrylated forms in normal human spermatogenesis and testicular pathologies, as well as about their possible retention in the mature human spermatozoon. Therefore, the aim of our work was to increase the current knowledge about these specific-residue PTMs in human male germ cells, as well as to try to decipher whether they could be markers of human sperm quality. We report a different behavior of H4K5bu and H4K5ac during human spermatogenesis, which would indicate a highly specific role of H4K5bu during round spermatid (rSPD) elongation, coexisting with H4K5ac during spermiogenesis. Results in patients with testicular cancer evidence that H4K5ac and H4K5bu remain stable under pathological conditions, supporting the important role of these residue-specific modifications towards spermatogenic development. Of note, both H4K5bu and H4K5ac are retained in ejaculated sperm showing differential location in the 30% of nucleosome clusters. Their role as sperm chromatin maturity markers after sperm selection through density gradient centrifugation has also been explored.

2. Results

2.1. H4K5 butyrylation show different spermatogenic pattern to acetylation on the same residue in patients with normal spermatogenesis

After strict anatomopathological evaluation of the testicular biopsies, testicular sections from patients displaying normal spermatogenesis (control group, N) were subjected to immunohistochemistry (IHC) analysis to detect H4K5 butyrylation and acetylation (Table 1, Figure 1). The H4K5ac H-Score (expressed as mean value ± SD), which combines number of positive cells and signal intensity, evidenced mild levels in spermatogonia (SPG, H-Score = 245.3 ± 59.8) that significantly decreased in spermatocytes (SPC, H-Score = 46.8 ± 29.1, $p < 0.001$), to finally recover intermediate levels as spermiogenesis started. Specifically, early-stages (I to V) round spermatids (rSPD I-V) restored the H-Score to 282.7 ± 66.2 ($p < 0.0001$), which increased to 415.8 ± 80.8 ($p < 0.05$) in late-stages rSPD (rSPD VI-VIII) maintaining similar levels in elongated spermatids (eSPD). H4K5ac levels finally decrease to the minimum in condensed spermatids (cSPD, H-Score = 0.9 ± 2.1, $p < 0.0001$). Somatic Sertoli-cells (SC) displayed low levels of H4K5ac (Table 1, Figure 1). In turn, H4K5bu evidenced minimum H-Scores during initial stages of spermatogenesis up to rSPD VI-VIII (33 ± 35.4 in SPG, 0.0 ± 0.0 in SPC, and 30.8 ± 46.9 in rSPD I-V). A striking rise of the H4K5bu H-Score was observed in rSPD VI-VIII (319.1 ± 128.0, $p < 0.01$), reaching maximum levels in eSPD (478.4 ± 40.7, $p < 0.05$). Finally, H4K5bu levels decreased in cSPD (0.9 ± 2.1, $p < 0.0001$). SC showed H4K5bu H-Score close to zero (2.5 ± 6.1) (Table 1, Figure 1). Individual H4K5ac and H4K5bu H-Scores per patient are shown in Table S1 and Table S2, respectively. Representative IHC images in testicular sections corresponding to patients with normal spermatogenesis are shown in Figure 1B (H4K5bu) and 1C (H4K5ac).

Table 1. IHC H-Scores detected in the different cells from the seminiferous tubules according to the group of patients. H-Scores (mean ± SD) correspond to H4K5ac and H4K5bu in control and testicular cancer patients, and H4K5bu in patients with altered spermatogenesis.

		H-Scores (mean ± SD)						
		SC	**SPG**	**SPC**	**rSPD (I-V)**	**rSPD (VI-VIII)**	**eSPD**	**cSPD**
H4K5bu								
Infertile patients with normal spermatogenesis	**N (n=6)**	**2.5 ± 6.1**	**33 ± 35.4#**	**0.0 ± 0.0**	**30.8 ± 46.9**	**319.1 ± 128.0#**	**478.4 ± 40.7#**	**0.9 ± 2.1#**
Infertile patients with altered spermatogenesis	**SCOS (n=3)**	8.9 ± 15.4	-	-	-	-	-	-
	HP (n=2)	0.0 ± 0.0	41.3 ± 58.4	0.0 ± 0.0	10.0 ± 14.14	358.9 ± 118.7	455.6 ± 110.0	0.0 ± 0.0
	SA (n=3)	0.0 ± 0.0	12.8 ± 13.2	1.7 ± 3.3	192.3 ± 0.0	460.0 ± 242.5	439.4 ± 27.4	225.0 ± 0.0
Testicular cancer patients	**SEM (n=4)**	0.0 ± 0.0	51.2 ± 46.3	0.0 ± 0.0	0.0 ± 0.0	219.0 ± 22.9	330.1 ± 69.9*	0.0 ± 0.0
	TER (n=3)	18.7 ± 23.8	135.9 ± 64.3*	0.0 ± 0.0	106.2 ± 57.3*	411.1 ± 120.6	480.2 ± 98.7	0.0 ± 0.0
H4K5ac								
Infertile patients with normal spermatogenesis	**N (n=6)**	**101.1 ± 59.5**	**245.3 ± 59.8**	**46.8 ± 29.1#**	**282.7 ± 66.2#**	**415.8 ± 80.8#**	**494.9 ± 59.4**	**0.9 ± 2.1#**
Testicular cancer patients	**SEM (n=4)**	228.5 ± 74.8*	259.2 ± 108.2	149.4 ± 107.9	320.7 ± 88.4	396.5 ± 135.9	473.4 ± 102.8	5.7 ± 7.86
	TER (n=3)	282.5 ± 39.2*	304.3 ± 40.2	165.5 ± 60.4*	342.9 ± 51.5	447.2 ± 93.7	513.1 ± 81.7	0.0 ± 0.0

#: $p < 0.05$ after comparison of H-Scores between consecutive spermatogenic cell types in normal patients (N). *: $p < 0.05$ after comparison of each testicular cell type between H-Scores of patients with testicular pathologies and the control group. Note that HP was not considered for statistical analysis due to the limited sample availability. The same applies to SA from the spermatogenic stage of rSPD (I-V) on, due to low number of replicates. Abbreviations: cSPD, condensed spermatids; eSPD, elongating spermatids; rSPD I-V, early-stages (I-V) round spermatids; rSPD VI–VIII, late-stages (VI–VIII) round spermatids; SC, Sertoli cells; SPC, spermatocytes; SPG, spermatogonia; N, Normal spermatogenesis; SCOS, Sertoli-cell only syndrome; HP, Hypospermatogenesis; SA, Spermatogenic arrest; SEM, Seminoma; TER, Teratoma.

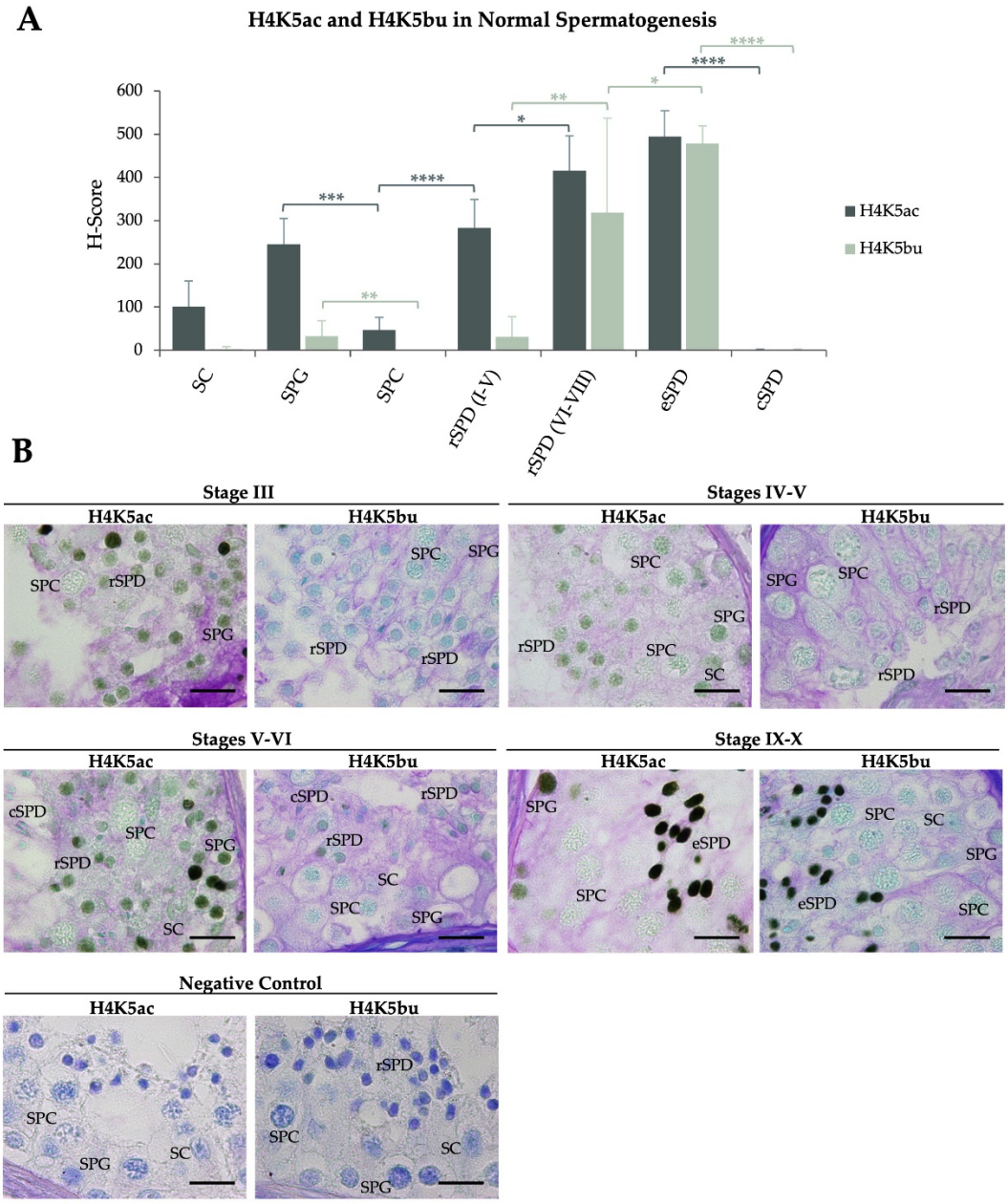


Figure 1. Spermatogenic patterns of H4K5 acetylation and butyrylation during normal spermatogenesis. (**A**) H4K5ac and H4K5bu H-scores represented as mean value ± SD per testicular cell type. *: $p < 0.05$, **: $p < 0.01$, ***: $p < 0.001$, ****: $p < 0.0001$. Results for H4K5ac represented in dark grey and for H4K5bu in green. (**B**) IHC images of H4K5ac and H4K5bu detection (brown-green color) in patients with normal spermatogenesis. Tissues were counterstained with PAS-haematoxylin. Scale bars = 10 μm. SPG: spermatogonia; SPC: spermatocytes; rSPD I–V: early-stages (I–V) round spermatids; rSPD VI–VIII: late-stages (VI–VIII) round spermatids; eSPD: elongating spermatids; cSPD: condensed spermatids; SC: Sertoli cells.

2.2. H4K5 butyrylation spermatogenic levels are not impaired under different testicular defects

After observing the predominant detection of H4K5bu in the late stages of spermatogenesis, we explored the characteristic behavior of this modification in patients displaying different primary testicular failures, such as hypospermatogenesis (HP), spermatogenic

arrest (SA), and Sertoli-cell only syndrome (SCOS), aiming to indentify potential atypical H4K5bu signals in meiotic or mitotic phases, or in supporting somatic SC. H4K5bu H-Scores were analyzed and are shown in Figure 2 and gathered in Table 1 (see Table S2 for detailed information per individual patient). No significant changes in the normal H4K5bu spermatogenic pattern were detected associated with spermatogenic alterations. Notably, a decrease in H4K5bu in rSPD I-V of patients with hypospermatogenesis and an increase in rSPD I-V and cSPD in patients with SA seems to occur. However, due to the limited number of samples in these two groups, we could not perform statistical analyses. Interestingly, the altered levels observed in the SA group are due to the contribution of a single patient with partial rSPD arrest (Table S2).

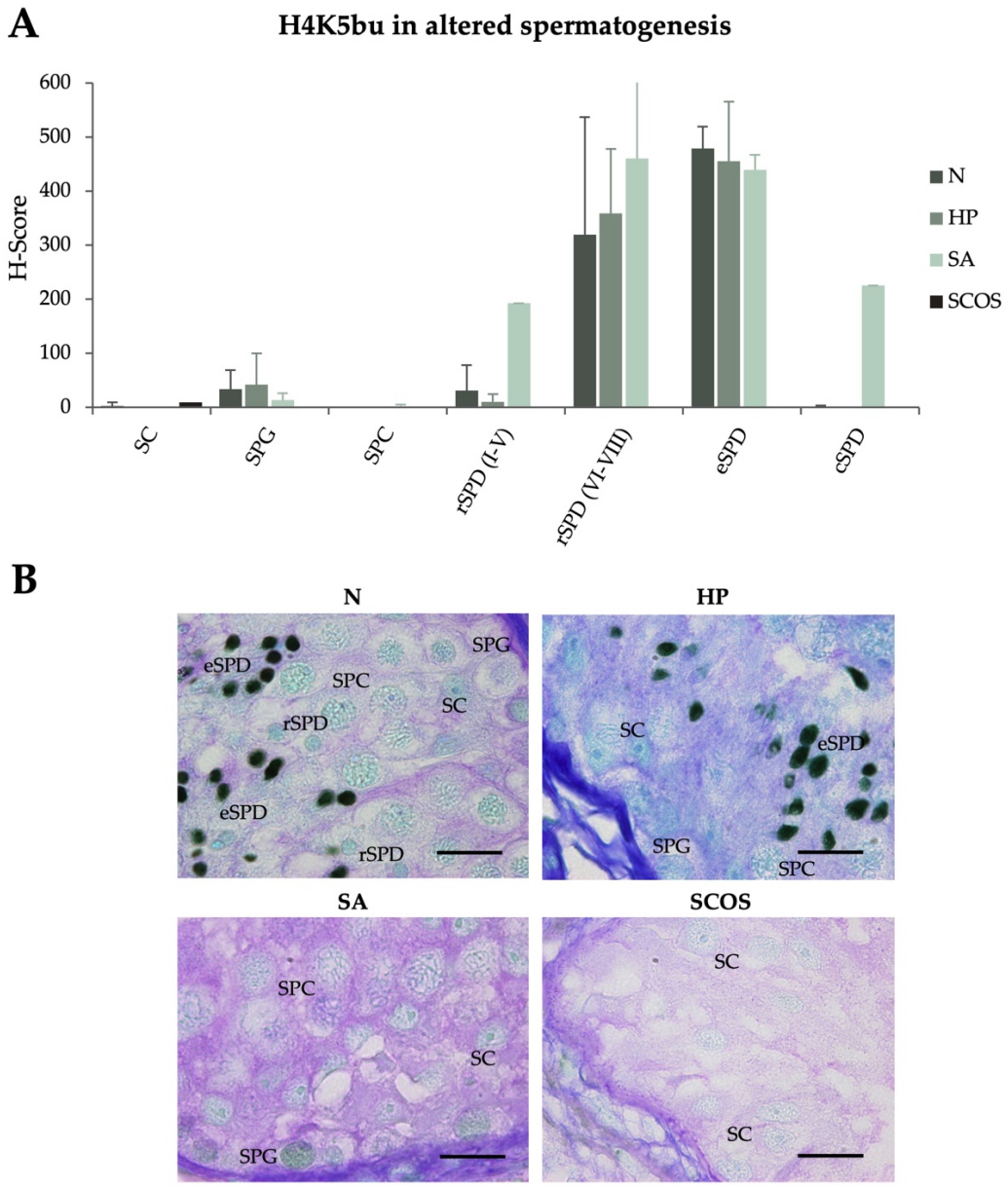


Figure 2. Detection of H4K5 butyrylation levels in testicular biopsies of patients with altered spermatogenesis. (**A**) H4K5bu H-scores of the normal spermatogenesis group (N), hypospermatogenesis (HP), spermatogenic arrest (SA), and Sertoli-cell only syndrome (SCOS), represented as mean value ± SD per testicular cell type. (**B**) Microscopy images showing H4K5bu detection in testicular section of patients affected with different spermatogenic alterations, compared to normal spermatogenesis. Tissues were counterstained with PAS-haematoxylin. Scale bars = 10 μm. SPG: spermatogonia; SPC: spermatocytes; rSPD: round spermatids; eSPD: elongating spermatids; SC: Sertoli cells.

2.3. Testicular cancers do not affect the spermatogenic pattern of butyrylation on H4K5, but neither acetylation on the same residue, in healthy seminiferous tubules with complete spermatogenesis

H4K5bu spermatogenic pattern was also evaluated in patients affected by testicular cancers, such as seminoma (SEM) and teratoma (TER), to identify potential epigenetic alterations. TER patients showed a slight increase of the H4K5bu H-score in SPG (133.4 ± 52.8, $p < 0.05$) and rSPD I-V (142.1 ± 85.8, $p < 0.05$) (Table I, Figure 3A). In turn, SEM patients did not evidence significant changes in the H4K5bu spermatogenic pattern apart from a decrease in rSPD (330.1 ± 69.9, $p<0.05$) (Table I, Figure 3A). Despite these significant changes, the behavior of the H4K5bu spermatogenic pattern found in males with normal spermatogenesis, consisting in low levels at the beginning of the process, an increase from rSPD to eSPD and a decrease in cSPD, is maintained in the testicular cancer patients included in this study (Figure 3A). Data corresponding to each individual patient and the IHC representative images are shown in Table S2 and Figure 3B, respectively.

Considering the relevance of global spermatogenic H4 acetylation in testicular cancer patients, which is completely disturbed in the seminiferous tubules adjacent to the tumor, we proceeded to evaluate specific acetylation of H4K5 in SEM and TER patients. Of note, significant changes to the normal pattern were only identified in SPC from TER patients, evidencing a discreet increase of H4K5ac H-score (165.5 ± 60.4, $p < 0.05$) (Table I, Figure 4A). Despite SEM patients displayed similar H4K5ac spermatocytic levels, the increase was not significant. Besides, the H4K5ac normal spermatogenic pattern in which mild SPG levels decrease to SPC, to rise up to a maximum level in late round/early condensing spermatids followed by a final decrease in cSPD, is maintained in testicular sections of SEM and TER patients (Figure 4A). Somatic Sertoli cells showed higher H4K5ac levels in both groups (SEM: 228.5 ± 74.8, $p < 0.05$; TER: 282.5 ± 39.2, $p < 0.05$) Representative IHC images are shown in Figure 4B, and data corresponding to each individual patient are included in Table S2.

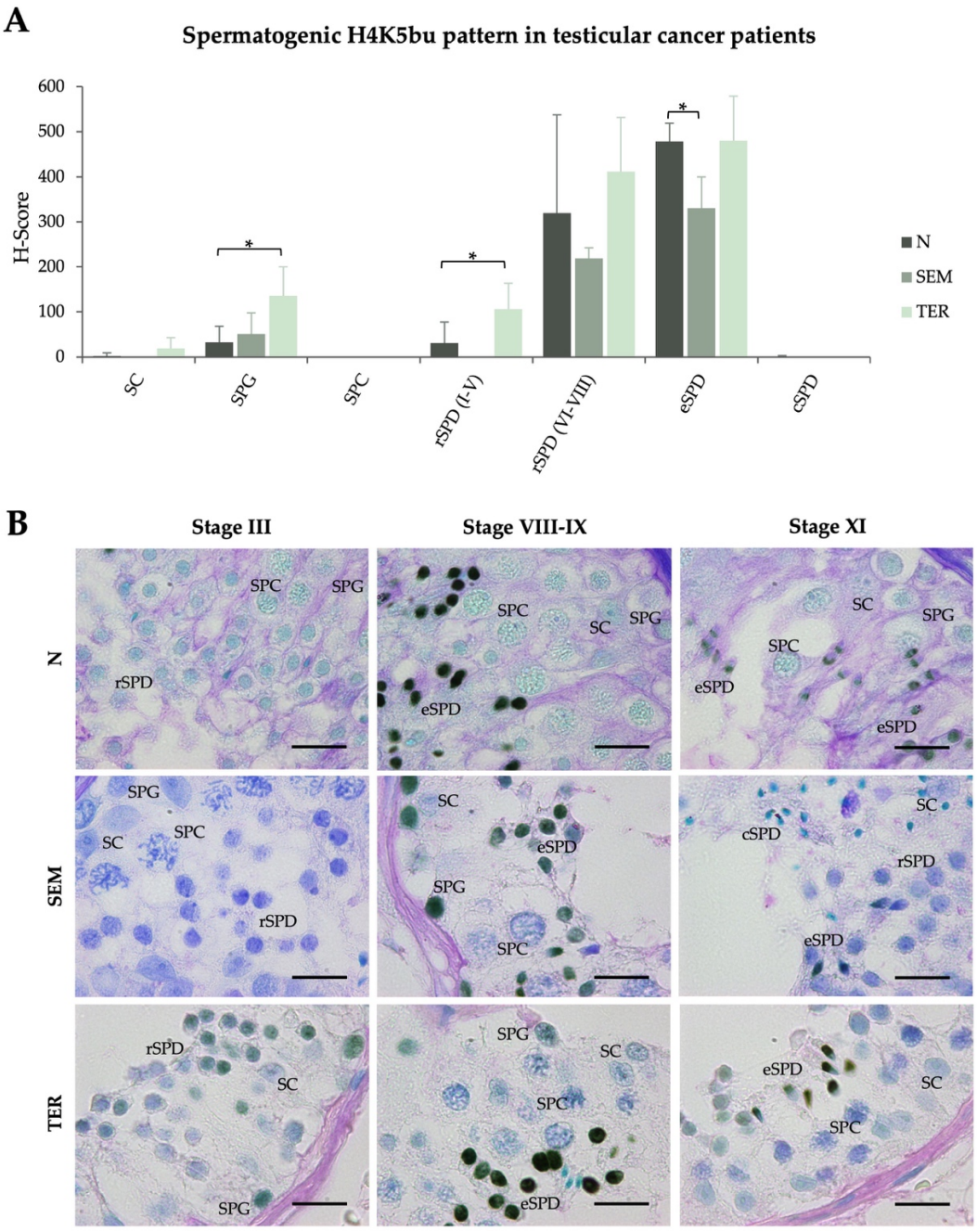


Figure 3. Spermatogenic pattern of H4K5 butyrylation in seminiferous tubules of testicular cancer patients. (**A**) H4K5bu H-scores (mean value ± SD) per testicular cell type corresponding to the normal spermatogenesis group (N), and patients with complete spermatogenesis but affected by seminoma (SEM) or teratoma (TER). (**B**) Microscopy images showing H4K5bu detection in testicular sections of SEM and TER patients, compared to healthy controls with normal spermatogenesis (N). Tissues were counterstained with PAS-hematoxylin. Scale bars = 10 µm. SPG: spermatogonia; SPC: spermatocytes; rSPD: round spermatids; eSPD: elongating spermatids; SC: Sertoli cells.

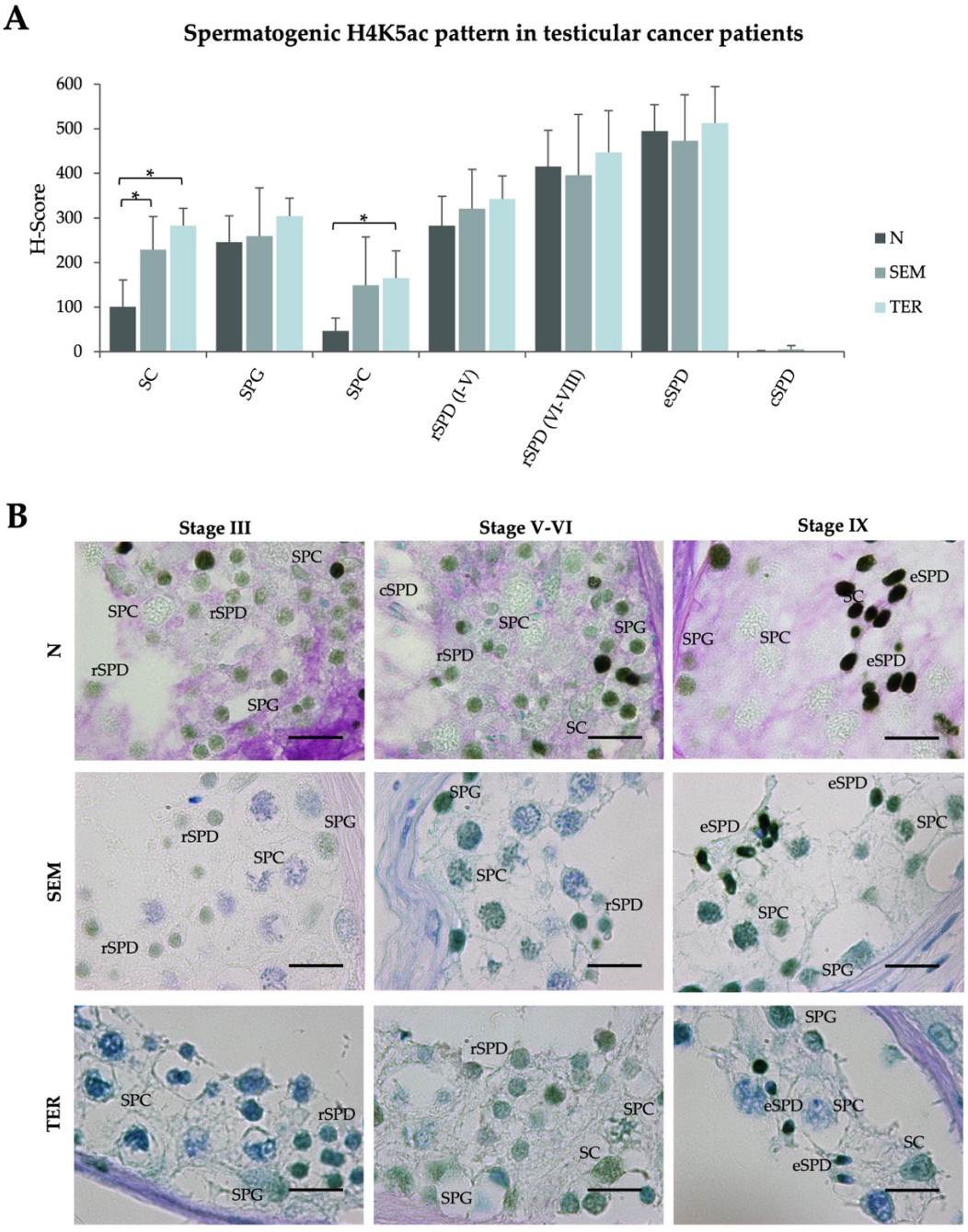


Figure 4. Spermatogenic H4K5 acetylation levels in seminiferous tubules of testicular cancer patients. (**A**) H4K5ac H-scores (mean value ± SD) per testicular cell type corresponding to the normal spermatogenesis group (N), and patients with complete spermatogenesis but affected by seminoma (SEM) or teratoma (TER). (**B**) IHC images corresponding to H4K5bu detection in testicular sections of SEM and TER patients, compared to healthy controls with normal spermatogenesis (N). Tissues were counterstained with PAS-hematoxylin. Scale bars = 10 μm. SPG: spermatogonia; SPC: spermatocytes; rSPD: round spermatids; eSPD: elongating spermatids; SC: Sertoli cells.

2.4. Butyrylation and acetylation on H4K5 are retained in ejaculated human sperm from normozoospermic patients

To further investigate H4K5 butyrylation in male germ cells, we examined its presence and that of the acetylation on the same residue in mature human sperm from patients with normal semen parameters. Both H4K5bu and H4K5ac were detected in all ejaculated sperm cells evaluated from the patients included in the analysis (Figure 5A). To deepen into the interplay among the two PTMs, nucleosome clusters marked by either H4K5bu or H4K5ac were colocalized using confocal imaging (Figure 5B). Mander's colocalization coefficient M1, representing detection of H4K5bu (red staining) over H4K5ac (green staining), corresponded to 0.74 ± 0.18, while M2 coefficient (H4K5ac over H4K5bu) was 0.65 ± 0.17 (mean value ± SD, Figure 4B). These results evidenced that around 70% of the nucleosome clusters marked by H4K5bu colocalized with those containing H4K5ac in the mature sperm head. The remaining 30% of the nucleosome clusters were exclusively marked by one of the epigenetic marks. Pearson coefficient was 0.78 ± 0.12, indicating a high direct correlation between the intensities of both PTMs.

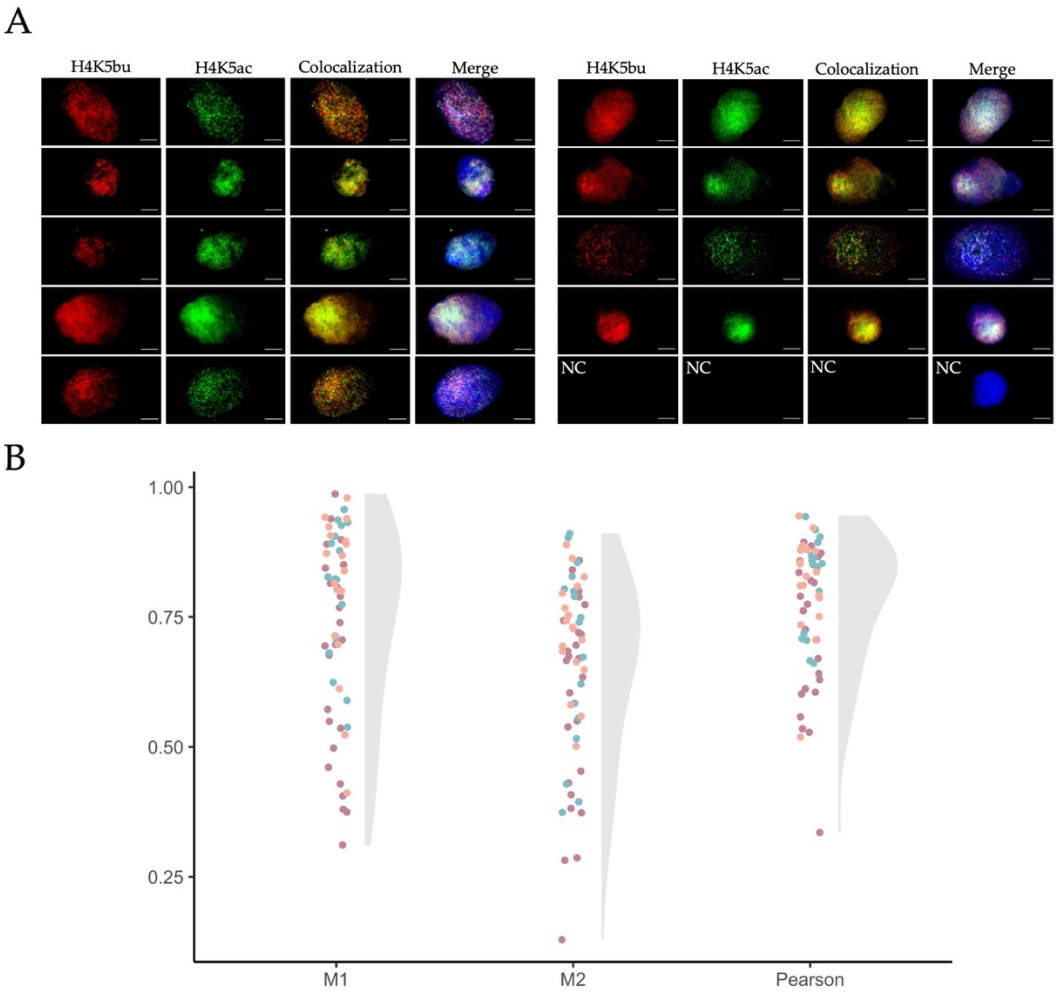


Figure 5. Detection and colocalization of H4K5bu and H4K5ac in human mature sperm by immunofluorescence. (**A**) Representative confocal microscopy images of H4K5bu (Alexa Fluor 633, red channel) and H4K5ac (Alexa Fluor 488, green channel) of the analyzed mature sperm nuclei under decondensed chromatin conditions. Scale bars = 5 μm. Sperm DNA is marked with DAPI (blue) and shown in Merge. NC indicates negative control. (**B**) Raincloud plot of the different colocalization coefficient parameters ("M1" and "M2" correspond to Mander's colocalization coefficients M1 and M2, respectively, and "Pearson" to Pearson's coefficient). Dots indicate individual sperm cells, and colors differentiates between biological replicates (n=3).

2.5. The proportion of H4K5bu over H4K5ac remains constant within different sperm populations selected according to sperm quality.

A 50% density gradient centrifugation, which allows obtaining purified sperm representing total sperm population of a semen sample without the presence of non-sperm contaminating cells (G50), was performed in order to define the relative abundance of both marks in normozoospermic samples (represented as H4K5bu/H4K5ac ratio). Besides, a 3-layered (50%-70%-90%) density gradient centrifugation was performed to compare cell populations according to sperm quality (P50, P70, and P90, respectively). The presence of H4K5bu and H4K5ac was detected in all cell populations evaluated in our experimental set up. When considering the whole semen sample (G50), the relation H4K5bu/H4K5ac was established as 1.02 ± 0.1 (Figure 6). This ratio seems to increase in selected sperm populations, being 1.18 ± 0.32 in P50, 1.36 ± 0.36 in P70, and 1.27 ± 0.37 in P90. However, these differences were not significant among groups ($p > 0.05$), which might be due to the high dispersion of the results observed after the multi-layer gradient preparation, compared to the 50% gradients.

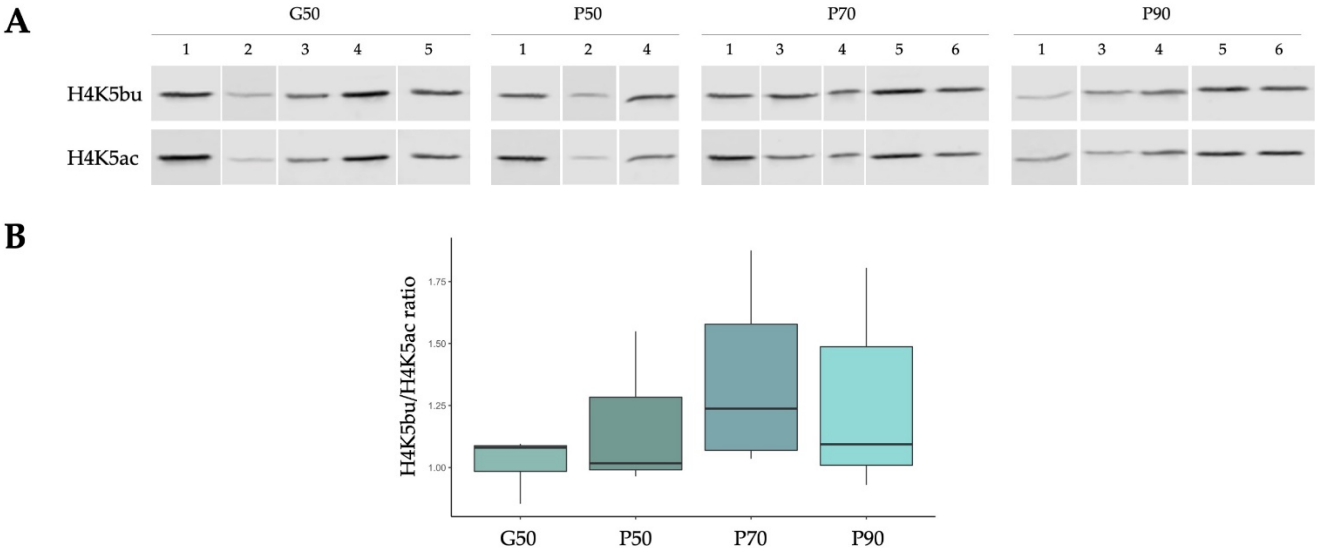


Figure 6. **H4K5bu/H4K5ac ratios based on signal intensity from fluorescent WB analysis.** (**A**) WB images. Sperm populations are indicated on top of the figure, and sample number is shown below to identify the different patients analyzed. Cell populations positive for leukocyte contamination (*PTPRC* cDNA, Ct < 35) or not fitting linearity threshold in both antibodies were discarded from the analysis. (**B**) Boxplot of the ratios according to the sperm population after density gradient separation.

3. Discussion

Despite H4 acetylation has been largely described during mammalian spermatogenesis and shown directly involved in chromatin remodeling during spermiogenesis [9,10,13,29,31,32], similar description of other H4 acylations, such as butyrylation, is still scarce, especially in humans. The present study provides the first characterization of H4K5 butyrylation during human spermatogenesis and in mature sperm, in comparison with the functionally close-related acetylation of the same residue (H4K5ac). We report a different behavior among both PTMs suggesting a highly specific role of H4K5bu in spermatid elongation, temporarily coexisting with the process of histone to protamine transition, that is not altered in patients with testicular conditions. Strikingly, while global H4ac

levels are fully disturbed in the presence of testicular cancer [32], neither H4K5bu nor H4K5ac were found altered in seminiferous tubules adjacent to the tumoral tissue in this study. Therefore, this residue may be somehow resistant against testicular perturbations, compatible with a proper NH-NP transition. Furthermore, both H4K5 PTMs are retained in normal human mature spermatozoa, which open a window to study the potential of this residue as an epigenetic mark delivered into the zygote.

The spermatogenic pattern of H4K5ac found in this study was consistent to that of global H4ac previously described [29–32]. SPG displayed intermediate levels of H4K5ac, which decrease in SPC and are restored in rSPD I-V. During rSPD development, H4K5ac levels gradually increase to reach a maximum value in eSPD. Strikingly, the H4K5bu spermatogenic pattern showed a different behavior, with basal butyrylation levels during the first phases of spermatogenesis and initial stages of round spermatid. Additionally, the drastic increase in H4K5bu levels starts in a more advanced stage of rSPD than H4K5ac does, temporarily coexisting with spermatid elongation when NH-NP transition occurs. Thus, H4K5bu seems to show a highly specific role during the latest steps of human spermatogenesis, coherent with previous reports in mouse models suggesting a temporal regulation of nucleosome disassembly and histone retention based on histone butyrylation [36]. Despite the low immunohistochemical levels of H4K5bu in early spermatogenesis (null in SPC) reported herein, we do not discard that H4K5bu in SPC could be better characterized using more sensitive techniques, as previously reported through western blot and mass spectrometry in sorted mouse spermatogenic germ cells [36].

Due to the apparent highly specific role of H4K5bu during spermiogenesis, we explored whether butyrylation levels were altered under different primary testicular failures. No relevant changes were observed in patients with hypospermatogenesis, SCOS, or spermatogenic arrest, as previously reported for H4ac [32]. Despite that, a patient with partial rSPD arrest displayed increased H4K5bu levels in rSPD I-V and cSPD. This could suggest that even though H4K5bu is not altered nor have a role in meiotic arrest, its alteration could either be involved in the spermatid arrest or be its consequence, which would be coherent with the potential specific role of this PTM observed in normal spermiogenesis. The lack of statistical analysis due to sample number availability limits the interpretation of this finding, but the spermatogenic arrest in post meiotic stages seems to be an interesting phenotype to study H4K5 PTMs in subsequent studies. We were interested in exploring H4K5 PTMs in cancer patients since a drastic dysregulation of the H4ac levels has been recently reported in patients with different types of testicular tumors [32]. However, H4K5bu does not seems to undergo such drastic global increase in patients with testicular cancer, since only TER patients evidence a discrete increase of H4K5bu H-scores in SPG and rSPD I-V. Nevertheless, in the present work, only butyrylation in a single residue of H4 has been studied, which does not discard different results when analyzing global H4bu or lysine butyrylation, as observed for H4ac [32]. It is interesting to remark that spermatogenic H4K5ac levels were not found altered in cancer patients, except from a slight increase in SPC from TER patients. These results contrast with the globally altered H4ac levels in testicular cancer patients reported elsewhere [32], which might be due to altered acetylation on other H4 residues. The stable levels regardless of testicular alterations point out a highly conserved role of H4K5bu and H4K5ac towards a proper regulation of spermiogenesis, and could explain why testicular cancer patients, although having global H4ac disruption, display complete spermatogenesis.

Growing evidence highlights the impact of sperm chromatin state in sperm functionality, fertilization events, and beyond, including sperm modified histones as epigenetic marks inducing differential DNA accessibilities [2,4,5,37–45]. Despite the observed drastic drop of the IHC H4K5bu and H4K5ac levels in cSPD, both were found retained in mature

sperm from normozoospermic patients, colocalizing in around 70% of nucleosome clusters. This high colocalization percentage might be due to the rapid acetylation and butyrylation turnover taking place on H4K5 during spermatogenesis [36], resulting in such "photo-finish" in the transcriptionally and translationally silent sperm cell. Since two H4 are present in the histone octamer conferring the nucleosome, two different scenarios arise from this co-localization: 1) the presence of single nucleosomes containing one H4 marked by butyrylation in K5 and the other by acetylation in the same residue, or 2) nucleosomes with both H4 marked by either butyrylation or acetylation in K5, that are spatially close to nucleosomes with the alternative mark, making the signals coexist. Since single nucleosomes are not resolved at this confocal imaging resolution, both possibilities are equally feasible, again supported by the rapid H4K5ac and H4K5bu turnover in the testis. Interestingly, the remaining proportion of non-colocalizing pixels detected in this study also suggest the presence of a group of nucleosome clusters exclusively marked by either H4K5bu or H4K5ac. This data might point to a functional involvement of the differential wrapping of paternal DNA into H4K5ac or H4K5bu nucleosomes.

While colocalization results might suggest a role of H4K5ac and H4K5bu in sperm function, no variations were observed associated with sperm quality. The study of different sperm populations isolated from neat sample following procedures routinely used in the reproductive clinics to select the best spermatozoon for ICSI sheds light on the molecular cargo of the fertile sperm giving rise to a new individual. In that case, the observed results would discard an impact of H4K5bu and H4K5ac relative levels in sperm fertilizing ability. Further work should focus on determine quantitative H4K5bu and H4K5ac levels in selected sperm populations by complementary techniques, which would help disentangle their individual potential as an indicator of chromatin maturity. Due to the known role of sperm histone marks as epigenetic regulators in early embryo, it will be worthy to know whether they could have an impact beyond fertilization, such as in the formation of preimplantation embryo and transmission of epigenetic information.

4. Materials and Methods

4.1. Biological material

Testicular biopsies

Testicular biopsies (n=23, mean age 37 ± 7, ranging from 21 to 52 years old) were provided by the Departments of Pathology from the Hospital Clínic de Barcelona (Barcelona, Spain) and the Hospital Universitari de Vic (Vic, Spain). The samples were grouped into three main groups: control group, spermatogenic alterations, and testicular cancer. The control group (N; n=7) included infertile patients corresponding to male partners of couples undergoing assisted reproduction studies, displaying normal spermatogenesis at the histological level and showing all germ cell types and spermatogenic stages (1 post-vasectomy individual, 1 patient with obstructive azoospermia due to CFTR genotypes, and 5 azoospermic patients). The group of infertile patients with spermatogenic alterations (n=8) included patients stratified according to the type of spermatogenic impairment into patients with Sertoli-cell only syndrome (SCOS; n=3), hypospermatogenesis (HP; n=2), and spermatogenic arrest (SA; n=3). Among the SA patients, two of them presented spermatocyte arrest (one complete arrest and other partial arrest), and the third one evidenced a partial arrest at round spermatid level. The last group of patients with testicular cancer (n=8), included patients affected by seminoma (SEM; n=4) and teratoma (TER; n=3). In addition to the groups above, one sample corresponding to a patient with normal spermatogenesis was used as technical internal control in all evaluations.

Semen samples

Human normozoospermic semen samples (n = 9) from patients undergoing routine semen analysis were obtained at the Assisted Reproduction Unit from the Clinic Institute of Gynecology, Obstetrics and Neonatology, at the Hospital Clínic de Barcelona, Spain. The ejaculates were collected by masturbation into sterile containers after 3–5 days of sexual abstinence. Evaluation of the seminal parameters was performed using the automatic semen analysis system CASA (Proiser, Paterna, Spain) and samples were classified according to the World Health Organization guidelines [51]. Sperm cells were purified through density gradient centrifugation, depending on the purpose of the analysis. A 50% Puresperm density gradient separation (NidaCon International AB, Gothenburg, Sweden), following manufacturer's instructions, was used to analyze purified sperm representing the heterogeneity of the native sample and avoiding contamination by cells other than sperm. Three-layered 50%-70%-90% Puresperm density gradient separation (NidaCon), was used to separate different sperm populations according to sperm quality for subsequent comparative studies. To discard the presence of somatic contamination that could alter the results, RNA expression analysis of the leukocyte marker receptor-type tyrosin-protein phosphatase C (PTPRC) through RT-PCR was performed to verify the absence of leukocytes according to Jodar *et al*., 2012 [52] (forward primer: CCTTGAACCCGAACATGAGT, reverse primer: ATCTTTGAGGGGGATTCCAG, corresponding to exons 12-13 of *PTPRC*).

4.2. Processing and paraffin-embedding of the testicular material

According to hospital's routine procedures, samples were fixed prior to paraffin-embedding in either Bouin's fixative for 3-4h or 4 % Formol for 24-48h, depending on sample size (biopsies or orchiectomy specimens, respectively), for histopathologic evaluation or other procedures. Samples from infertile patients, either from control or spermatogenic alteration groups, were biopsied. Orchiectomy specimens were obtained from testicular cancer patients. After fixation, the specimens were processed in a fluid-transfer advanced automatic tissue processor and paraffin-embedded to make the blocks. The tissue was covered in molten paraffin in a mold and paraffin cooled down until solidifying. The block was cut through microtome into 4 μm-sections.

4.3. Testicular histopathological evaluation

An experienced anatomopathologist exhaustively performed the histopathological evaluation of the hematoxylin-eosin-stained testicular sections from each patient to identify spermatogenic defects [53] and/or testicular tumors, following the World Health Organization (WHO) guidelines [54,55]. Tumor diagnosis was confirmed in case of need by checking expression of appropriate biomarkers. Ultrasound evaluation was monitored to discard the presence of testicular microlithiasis [56]. In the group of testicular cancer patients, the presence of either complete or partial spermatogenic activity in seminiferous tubules adjacent to the neoplastic area was a strict inclusion criterion. After histopathological confirmation, additional testicular sections from each patient were used for further immunohistochemical analyses.

4.4. Immunohistochemistry

Immunohistochemistry (IHC) was performed on paraffin-embedded testicular sections, as described previously [32]. Testicular tissue samples were randomly grouped in different runs, and an internal positive control was included in each of them to check the different runs' overall intensity. Due to the use of different fixation methods, effect of the fixative was discarded by checking that no changes in the spermatogenic pattern with the

antibodies of interest were detected between an orchiectomy specimen fixed with 4% Formol and a biopsy fixed with Bouin, both showing normal spermatogenesis and no presence of testicular tumor (Figure S1).

Sections were dewaxed in toluene and rehydrated through graded series of ethanol to water with 0.3 % hydrogen peroxide incubation. Subsequently, antigen retrieval was performed with 10 mM sodium citrate (pH 6.0) at 99.5 ºC for 20 min. Slides were then blocked with PBS-5 % skim milk for 30 min at room temperature (RT) and incubated with Avidin/Biotin Blocking Kit (Vector Laboratories, Burlingame, CA, USA). Sections were incubated overnight at 4 ºC with primary antibodies (dil 1:100, Table 2). Negative controls without primary antibody were included. Sections were incubated with biotinylated secondary antibody (Table 2) and an avidin-biotin-peroxidase detection kit (Vectastain ABC Elite Kit, Vector Laboratories). Signal color developed by reaction with diaminobenzidine (DAB, 3,3'-diaminobenzidine tetrahydrochloride) and sections were counterstained with hematoxylin and Periodic Acid-Schiff's (PAS) reagent (Sigma-Aldrich, St. Louis, MO, USA). Sections were dehydrated in ethanol, cleared in toluene, and mounted in Eukitt Mounting Medium (Sigma-Aldrich) to be analyzed in a transmission light microscope (Olympus BX50, Olympus, Tokyo, Japan).

4.4. Spermatogenic stage classification and IHC evaluation

Classification of testicular cells and spermatogenic stages of the seminiferous tubules sections was based on current classification of human spermatogenesis described by Muciaccia et al., 2013 [57]. For each patient, at least 30 seminiferous tubule sections at different spermatogenic stages were analyzed. IHC was assessed by two independent operators using PAS–Haematoxylin staining, blinded to the experimental procedures. H-score was selected as scoring system [32]. Specifically, the H-score was determined by adding the proportion of cells presenting each level of intensity (expressed in percentage) multiplied by the intensity (expressed in ordinal values), as follows: H-score = ($\%_{intensity\ 0} \times 0$) + ($\%_{intensity\ 1} \times 1$) + ($\%_{intensity\ 2} \times 2$) + […], presenting a dynamic range from 0 to 600. Since the intensity of the signal within cells belonging to the same specific cell type per spermatogenic stage was homogeneous along the seminiferous tubule section, the mean intensity of each cell type was considered. Thus, H-score for each testicular cell type analyzed per seminiferous tubule section was provided for each individual patient.

4.5. Immunofluorescence on mature sperm cells

Extensions consisting in 1 million sperm (Mz) per slide were incubated in decondensing solution (2,5 mM DTT, 0,2% Triton X-100, 100 UI/mL heparine in PBS) to facilitate antibody accessibility, monitoring decondensation in optic microscope. Sperm cells were fixed 10 min in 2 % paraformaldehyde and washed with PBS and H_2O before permeabilization for 20 min in 0.05% Triton X-100 in PBS. After washings in PBS, slides were incubated 1h RT in blocking solution (5 % bovine serum albumin in PBS). Primary antibody incubation (Table 2, dil 1:100) was performed overnight (O/N) at 4ºC. After washes, slides were incubated with secondary antibody (Table 2) at dil 1:500 for 2h at RT. After washings, slides were incubated with DAPI 1:10000 5 min protected from light, and mounted with ProLong™ Gold (#P36930, Invitrogen, Waltham, MA, USA). Images were acquired by confocal microscopy (LSMA880 ZEISS) at the Advanced Optical Microscopy Unit (Campus Clínic) from Scientific and Technological Centers from University of Barcelona.

4.6. Colocalization analyses

Colocalization was quantified using ImageJ software distribution FIJI [58]. A custom macro was developed to automatize colocalization analysis with JACOP [59] for every set of images. Briefly, Red and Green Channel Images were background-subtracted with Rolling Ball Radius of 50 and colocalization was quantified from a region of interest delimiting

the cell contour, considering a colocalized point if its respective intensities are strictly higher than the threshold determined for its channels (autothreshold method). Pearson Correlation and Manders Coefficients were analyzed from each image using JACOP plugin.

4.7. Odyssey® Western Blot

Sperm soluble protein extraction was conducted incubating purified sperm cells in lysis buffer (2 % SDS, 1 mM PMSF in PBS, ratio 40Mz:100µL) 15 min on ice followed by centrifugation 17000 *g* 10 min at 4 ºC. Quantification was done using Pierce™ BCA Protein Assay Kit (Thermo Fisher Scientific, Rockford, IL), following manufacturers' recommendation. Replicates with Ct < 35 for the leukocyte marker PTPRC were discarded. A total of 10µg of soluble protein lysate were run into 16% acrylamide gels by SDS-PAGE [5]. Proteins were transferred to PVDF 0.2µm pore size membranes (BioRad, Hercules, CA, USA), activated with methanol, in transference buffer (200 mM glycine, 25 mM Tris, 15 % methanol). Membranes were shortly washed with 100% ethanol prior blocking with Intercept® (TBS) blocking buffer (LI-COR Inc., Lincoln, Nebraska) 1h at RT to incubate O/N with primary antibodies at 4ºC (1:1000, Table 2). After washes with TBT (0.242% Tris, 0.8% NaCl, 0.1% Tween-20), membranes were incubated with secondary antibodies (Table 2) at 1:12.000 dilution, 1h RT. Subsequent washes with TBT and TBS (20 mM Tris, 150 mM NaCl, pH 7.6) and fixation with pure methanol were done and the membrane air-dried. Imaging was performed using Odyssey® infrared analysis system, with laser intensities 700 = 2.0, 800 = 3.0 according to the best fit for antibodies linearity ($R^2 > 0.98$). Signal intensities were determined on the raw scanned data using Image Studio Lite v5.2 software (LI-COR Inc.). Intensities below the minimum linear cutoff were discarded from the analysis. Therefore, after exclusion criteria, from the 6 patients analyzed, n=5 in G50, P70, and P90, and n=3 in P70, were considered for subsequent statistical analysis.

Table 2. Antibodies used in the study.

Antibodies	Company	Reference
Primary antibodies		
Rabbit monoclonal anti-H4K5bu	PTM BIO LLC, Chicago, IL, USA	#PTM-313
Mouse monoclonal anti-H4K5ac	PTM BIO LLC, Chicago, IL, USA	#PTM-163
Secondary antibodies (IHC)		
Goat Anti-Rabbit IgG Antibody (H+L), Biotinylated	Vector Laboratories, Burlingame, CA, USA	BA-1000
Goat Anti-Mouse IgG Antibody (H+L), Biotinylated	Vector Laboratories, Burlingame, CA, USA	BA-9200
Secondary antibodies (IF)		
Goat anti-mouse IgG Alexa Fluor 488	Invitrogen, Waltham, MA, USA	A28175
Goat anti-rabbit IgG Alexa Fluor 633	Invitrogen, Waltham, MA, USA	A21070
Secondary antibodies (Odyssey® Fluorescent WB)		
Anti-Mouse IgG (IRDye-700)	LI-COR, Inc., Lincoln, NE, USA	P/N 925-68070
Anti-Rabbit IgG (IRDye-800)	LI-COR, Inc., Lincoln, NE, USA	P/N 925-32211

4.8. Statistical analysis

Data analysis was conducted in RStudio software version 2022.02.2 [60][60] and the *car* package [61], and using GraphPad Prism version 7.0 for Windows (GraphPad Software, La Jolla, California, USA, www.graphpad.com). Normal distribution was assessed by Shapiro-Wilk normality test followed by Levene's homoscedasticity test. According to the distribution, either Student t-test or Mann-Whitney-U was performed for the analysis

of H-Score levels. Only groups formed by at least three patients were included in the statistical analysis. Paired Student t-test was applied for the analysis of H4K5bu/ac ratios. P-values <0.05 were considered statistically significant.

Supplementary Materials: The following supporting information can be found: **Table S1**: Individual H4K5ac H-Scores in testicular sections from control patients with normal spermatogenesis; **Table S2**: H4K5bu H-Scores in testicular sections per individual patient; **Figure S1**: H4K5 acetylation and butyrylation in an orchiectomy specimen with normal spermatogenesis fixed in 4% Formol.

Author Contributions: Conceptualization, A.I., J.C., and R.O.; methodology, A.I., P.J., M.J., F.B., L.D., C.M., L.R-C., J.C., and R.O.; formal analysis, A.I., M.J., J.C., and R.O.; investigation, A.I., P.J., M.J., F.B., J.C., and R.O.; resources, C.M., L.R-C., J.M.C., J.L.B, and R.O..; writing—original draft preparation, A.I., J.C., and R.O.; writing—review and editing, A.I., P.J., M.J., F.B., L.D., C.M., L.R-C., J.M.C., J.L.B., K.K., J.C., and R.O; supervision, J.C. and R.O.; funding acquisition, R.O. All authors have read and agreed to the published version of the manuscript.

Funding: This research was funded by grants PI16/00346 and PI20/00936 to R.O. from the 'Ministerio de Economía y Competividad' (Spain, 'fondos FEDER, una manera de hacer Europa'). J.C. was supported by the Sara Borrell Postdoctoral Fellowship, 'Acción Estratégica en Salud', CD17/00109. J.C. is a Serra Húnter fellow (Universitat de Barcelona, Generalitat de Catalunya). A.I. is supported by a fellowship from the 'Ministerio de Economía, Industria y Competitividad' (Spain), 'Acción Estratégica en Salud, contrato Predoctoral de Formación en Investigación en Salud' (PFIS, FI17/00224). F.B. received a grant from the Ministerio de Educación, Cultura y Deporte para la Formación de Profesorado Universitario (Spain) (FPU15/02306). M.J. was supported by the Government of Catalonia (Generalitat de Catalunya, pla estratègic de recerca i innovació en salut, PERIS 2016-2020, SLT002/16/00337). L.D. and K.K. were supported by Czech Science Foundation (GACR No. GJ20-17403Y) to L.D. and project BIOCEV (CZ.1.05/1.1.00/02/0109) from the ERDF and the Institute of Biotechnology RVO:86652036 to L.D. and K.K.

Institutional Review Board Statement: The study was conducted in accordance with the Declaration of Helsinki Samples were used following the appropriate ethical guidelines and Internal Review Board, and the Clinical Research Ethics Committee of the corresponding hospitals approved the biological material storing and processing.

Informed Consent Statement: Informed consent was obtained from all subjects involved in the study.

Data Availability Statement: Not applicable.

Acknowledgments: We thank Dr. Maria Calvo, Dr. Gemma Martín, and Elisenda Coll from the Advanced Optical Microscopy Unit (Campus Clínic) from Scientific and Technological Centers from University of Barcelona for their support and advice with confocal microscopy and image analysis.

Conflicts of Interest: The authors declare no competing interests.

References

1. de Mateo, S.; Castillo, J.; Estanyol, J.M.; Ballescà, J.L.; Oliva, R. Proteomic Characterization of the Human Sperm Nucleus. *Proteomics* **2011**, *11*, 2714–2726, doi:10.1002/pmic.201000799.
2. Hammoud, S.; Nix, D.A.; Hammoud, A.O.; Gibson, M.; Cairns, B.R.; Carrell, D. Genome-Wide Analysis Identifies Changes in Histone Retention and Epigenetic Modifications at Developmental and Imprinted Gene Loci in the Sperm of Infertile Men. *Human Reproduction* **2011**, *26*, 2558–2569, doi:10.1093/humrep/der192.
3. Oliva, R.; Luís Ballescà, J. Altered Histone Retention and Epigenetic Modifications in the Sperm of Infertile Men. *Asian J Androl* **2012**, *14*, 239–240, doi:10.1038/aja.2011.159.
4. Azpiazu, R.; Amaral, A.; Castillo, J.; Estanyol, J.M.; Guimerà, M.; Ballescà, J.L.; Balasch, J.; Oliva, R. High-Throughput Sperm Differential Proteomics Suggests That Epigenetic Alterations Contribute to Failed Assisted Reproduction. *Human Reproduction* **2014**, *29*, 1225–1237, doi:10.1093/humrep/deu073.
5. Castillo, J.; Amaral, A.; Azpiazu, R.; Vavouri, T.; Estanyol, J.M.; Ballesca, J.L.; Oliva, R. Genomic and Proteomic Dissection and Characterization of the Human Sperm Chromatin. *Mol Hum Reprod* **2014**, *20*, 1041–1053, doi:10.1093/molehr/gau079.

6. Castillo, J.; Estanyol, J.; Ballescà, J.; Oliva, R. Human Sperm Chromatin Epigenetic Potential: Genomics, Proteomics, and Male Infertility. *Asian J Androl* **2015**, *17*, 601, doi:10.4103/1008-682X.153302.
7. Barrachina, F.; Soler-Ventura, A.; Oliva, R.; Jodar, M. Sperm Nucleoproteins (Histones and Protamines). In *A Clinician's Guide to Sperm DNA and Chromatin Damage*.; Zini, A., Agarwal, A., Eds.; Springer International Publishing: Cham, 2018; pp. 31–51.
8. Oliva, R.; Dixon, G.H. Vertebrate Protamine Genes and the Histone-to-Protamine Replacement Reaction. *Prog Nucleic Acid Res Mol Biol* **1991**, *40*, 25–94, doi:10.1016/S0079-6603(08)60839-9.
9. Christensen, M.E.; Dixon, G.H. Hyperacetylation of Histone H4 Correlates with the Terminal, Transcriptionally Inactive Stages of Spermatogenesis in Rainbow Trout. *Dev Biol* **1982**, *93*, 404–415, doi:10.1016/0012-1606(82)90127-0.
10. Oliva, R.; Mezquita, C. Histone H4 Hyperacetylation and Rapid Turnover of Its Acetyl Groups in Transcriptionally Inactive Rooster Testis Spermatids. *Nucleic Acids Res* **1982**, *10*, 8049–8059, doi:10.1093/nar/10.24.8049.
11. Grimes, S.R.; Henderson, N. Hyperacetylation of Histone H4 in Rat Testis Spermatids. *Exp Cell Res* **1984**, *152*, 91–97, doi:10.1016/0014-4827(84)90232-5.
12. Oliva, R.; Bazett-Jones, D.; Mezquita, C.; Dixon, G.H. Factors Affecting Nucleosome Disassembly by Protamines in Vitro. Histone Hyperacetylation and Chromatin Structure, Time Dependence, and the Size of the Sperm Nuclear Proteins. *J Biol Chem* **1987**, *262*, 17016–17025.
13. Hazzouri, M.; Pivot-Pajot, C.; Faure, A.-K.; Usson, Y.; Pelletier, R.; Sèle, B.; Khochbin, S.; Rousseaux, S. Regulated Hyperacetylation of Core Histones during Mouse Spermatogenesis: Involvement of Histone-Deacetylases. *Eur J Cell Biol* **2000**, *79*, 950–960, doi:10.1078/0171-9335-00123.
14. Oliva, R.; Castillo, J. Proteomics and the Genetics of Sperm Chromatin Condensation. *Asian J Androl* **2011**, *13*, 24–30, doi:10.1038/aja.2010.65.
15. Oliva, R.; Bazett-Jones, D.P.; Locklear, L.; Dixon, G.H. Histone Hyperacetylation Can Induce Unfolding of the Nucleosome Core Particle. *Nucleic Acids Res* **1990**, *18*, 2739–2747, doi:10.1093/nar/18.9.2739.
16. Singh, I.; Parte, P. Heterogeneity in the Epigenetic Landscape of Murine Testis-Specific Histone Variants TH2A and TH2B Sharing the Same Bi-Directional Promoter. *Front Cell Dev Biol* **2021**, *9*, doi:10.3389/fcell.2021.755751.
17. Pentakota, S.K.; Sandhya, S.; P. Sikarwar, A.; Chandra, N.; Satyanarayana Rao, M.R. Mapping Post-Translational Modifications of Mammalian Testicular Specific Histone Variant TH2B in Tetraploid and Haploid Germ Cells and Their Implications on the Dynamics of Nucleosome Structure. *J Proteome Res* **2014**, *13*, 5603–5617, doi:10.1021/pr500597a.
18. Ding, D.; Nguyen, T.T.; Pang, M.Y.H.; Ishibashi, T. Primate-Specific Histone Variants. *Genome* **2021**, *64*, 337–346, doi:10.1139/gen-2020-0094.
19. Hoghoughi, N.; Barral, S.; Vargas, A.; Rousseaux, S.; Khochbin, S. Histone Variants: Essential Actors in Male Genome Programming. *The Journal of Biochemistry* **2018**, *163*, 97–103, doi:10.1093/jb/mvx079.
20. Barral, S.; Morozumi, Y.; Tanaka, H.; Montellier, E.; Govin, J.; de Dieuleveult, M.; Charbonnier, G.; Couté, Y.; Puthier, D.; Buchou, T.; et al. Histone Variant H2A.L.2 Guides Transition Protein-Dependent Protamine Assembly in Male Germ Cells. *Mol Cell* **2017**, *66*, 89-101.e8, doi:10.1016/j.molcel.2017.02.025.
21. Rezaei-Gazik, M.; Vargas, A.; Amiri-Yekta, A.; Vitte, A.-L.; Akbari, A.; Barral, S.; Esmaeili, V.; Chuffart, F.; Sadighi-Gilani, M.A.; Couté, Y.; et al. Direct Visualization of Pre-Protamine 2 Detects Protamine Assembly Failures and Predicts ICSI Success. *Mol Hum Reprod* **2022**, *28*, doi:10.1093/molehr/gaac004.
22. Dhar, S.; Thota, A.; Rao, M.R.S. Insights into Role of Bromodomain, Testis-Specific (Brdt) in Acetylated Histone H4-Dependent Chromatin Remodeling in Mammalian Spermiogenesis. *J Biol Chem* **2012**, *287*, 6387–6405, doi:10.1074/jbc.M111.288167.
23. Goudarzi, A.; Shiota, H.; Rousseaux, S.; Khochbin, S. Genome-Scale Acetylation-Dependent Histone Eviction during Spermatogenesis. *J Mol Biol* **2014**, *426*, 3342–3349, doi:10.1016/j.jmb.2014.02.023.
24. Her, Y.R.; Wang, L.; Chepelev, I.; Manterola, M.; Berkovits, B.; Cui, K.; Zhao, K.; Wolgemuth, D.J. Genome-Wide Chromatin Occupancy of BRDT and Gene Expression Analysis Suggest Transcriptional Partners and Specific Epigenetic Landscapes That Regulate Gene Expression during Spermatogenesis. *Mol Reprod Dev* **2021**, *88*, 141–157, doi:10.1002/mrd.23449.
25. Manterola, M.; Brown, T.M.; Oh, M.Y.; Garyn, C.; Gonzalez, B.J.; Wolgemuth, D.J. BRDT Is an Essential Epigenetic Regulator for Proper Chromatin Organization, Silencing of Sex Chromosomes and Crossover Formation in Male Meiosis. *PLoS Genet* **2018**, *14*, e1007209, doi:10.1371/journal.pgen.1007209.
26. Morinière, J.; Rousseaux, S.; Steuerwald, U.; Soler-López, M.; Curtet, S.; Vitte, A.-L.; Govin, J.; Gaucher, J.; Sadoul, K.; Hart, D.J.; et al. Cooperative Binding of Two Acetylation Marks on a Histone Tail by a Single Bromodomain. *Nature* **2009**, *461*, 664–668, doi:10.1038/nature08397.
27. Pivot-Pajot, C.; Caron, C.; Govin, J.; Vion, A.; Rousseaux, S.; Khochbin, S. Acetylation-Dependent Chromatin Reorganization by BRDT, a Testis-Specific Bromodomain-Containing Protein. *Mol Cell Biol* **2003**, *23*, 5354–5365, doi:10.1128/MCB.23.15.5354-5365.2003.
28. Shang, E.; Nickerson, H.D.; Wen, D.; Wang, X.; Wolgemuth, D.J. The First Bromodomain of Brdt, a Testis-Specific Member of the BET Sub-Family of Double-Bromodomain-Containing Proteins, Is Essential for Male Germ Cell Differentiation. *Development* **2007**, *134*, 3507–3515, doi:10.1242/dev.004481.
29. Sonnack, V.; Failing, K.; Bergmann, M.; Steger, K. Expression of Hyperacetylated Histone H4 during Normal and Impaired Human Spermatogenesis. *Andrologia* **2002**, *34*, 384–390, doi:10.1046/j.1439-0272.2002.00524.x.

30. Faure, A.K.; Pivot-Pajot, C.; Kerjean, A.; Hazzouri, M.; Pelletier, R.; Péoc'h, M.; Sèle, B.; Khochbin, S.; Rousseaux, S. Misregulation of Histone Acetylation in Sertoli Cell-only Syndrome and Testicular Cancer. *Mol Hum Reprod* **2003**, *9*, 757–763, doi:10.1093/molehr/gag101.
31. Kleiman, S.E.; Bar-Shira Maymon, B.; Hauser, R.; Botchan, A.; Paz, G.; Yavetz, H.; Yogev, L. Histone H4 Acetylation and AZFc Involvement in Germ Cells of Specimens of Impaired Spermatogenesis. *Fertil Steril* **2008**, *89*, 1728–1736, doi:10.1016/j.fertnstert.2007.05.068.
32. Barrachina, F.; de la Iglesia, A.; Jodar, M.; Soler-Ventura, A.; Mallofré, C.; Rodriguez-Carunchio, L.; Goudarzi, A.; Corral, J.M.; Ballescà, J.L.; Castillo, J.; et al. Histone H4 Acetylation Is Dysregulated in Active Seminiferous Tubules Adjacent to Testicular Tumours. *Human Reproduction* **2022**, *30*, 1712–1726, doi:10.1093/humrep/deac130.
33. Crespo, M.; Damont, A.; Blanco, M.; Lastrucci, E.; Kennani, S. el; Ialy-Radio, C.; Khattabi, L. el; Terrier, S.; Louwagie, M.; Kieffer-Jaquinod, S.; et al. Multi-Omic Analysis of Gametogenesis Reveals a Novel Signature at the Promoters and Distal Enhancers of Active Genes. *Nucleic Acids Res* **2020**, *48*, 4115–4138, doi:10.1093/nar/gkaa163.
34. Sabari, B.R.; Zhang, D.; Allis, C.D.; Zhao, Y. Metabolic Regulation of Gene Expression through Histone Acylations. *Nat Rev Mol Cell Biol* **2017**, *18*, 90–101, doi:10.1038/nrm.2016.140.
35. Tan, M.; Luo, H.; Lee, S.; Jin, F.; Yang, J.S.; Montellier, E.; Buchou, T.; Cheng, Z.; Rousseaux, S.; Rajagopal, N.; et al. Identification of 67 Histone Marks and Histone Lysine Crotonylation as a New Type of Histone Modification. *Cell* **2011**, *146*, 1016–1028, doi:10.1016/j.cell.2011.08.008.
36. Goudarzi, A.; Zhang, D.; Huang, H.; Barral, S.; Kwon, O.K.; Qi, S.; Tang, Z.; Buchou, T.; Vitte, A.-L.; He, T.; et al. Dynamic Competing Histone H4 K5K8 Acetylation and Butyrylation Are Hallmarks of Highly Active Gene Promoters. *Mol Cell* **2016**, *62*, 169–180, doi:10.1016/j.molcel.2016.03.014.
37. Brykczynska, U.; Hisano, M.; Erkek, S.; Ramos, L.; Oakeley, E.J.; Roloff, T.C.; Beisel, C.; Schübeler, D.; Stadler, M.B.; Peters, A.H.F.M. Repressive and Active Histone Methylation Mark Distinct Promoters in Human and Mouse Spermatozoa. *Nat Struct Mol Biol* **2010**, *17*, 679–687, doi:10.1038/nsmb.1821.
38. Erkek, S.; Hisano, M.; Liang, C.-Y.; Gill, M.; Murr, R.; Dieker, J.; Schübeler, D.; van der Vlag, J.; Stadler, M.B.; Peters, A.H.F.M. Molecular Determinants of Nucleosome Retention at CpG-Rich Sequences in Mouse Spermatozoa. *Nat Struct Mol Biol* **2013**, *20*, 868–875, doi:10.1038/nsmb.2599.
39. Saida, M.; Iles, D.; Elnefati, A.; Brinkworth, M.; Miller, D. Key Gene Regulatory Sequences with Distinctive Ontological Signatures Associate with Differentially Endonuclease-Accessible Mouse Sperm Chromatin. *Reproduction* **2011**, *142*, 73–86, doi:10.1530/REP-10-0536.
40. Vavouri, T.; Lehner, B. Chromatin Organization in Sperm May Be the Major Functional Consequence of Base Composition Variation in the Human Genome. *PLoS Genet* **2011**, *7*, e1002036, doi:10.1371/journal.pgen.1002036.
41. Ihara, M.; Meyer-Ficca, M.L.; Leu, N.A.; Rao, S.; Li, F.; Gregory, B.D.; Zalenskaya, I.A.; Schultz, R.M.; Meyer, R.G. Paternal Poly (ADP-Ribose) Metabolism Modulates Retention of Inheritable Sperm Histones and Early Embryonic Gene Expression. *PLoS Genet* **2014**, *10*, e1004317, doi:10.1371/journal.pgen.1004317.
42. Castillo, J.; Jodar, M.; Oliva, R. The Contribution of Human Sperm Proteins to the Development and Epigenome of the Preimplantation Embryo. *Hum Reprod Update* **2018**, *24*, 535–555, doi:10.1093/humupd/dmy017.
43. Teperek, M.; Simeone, A.; Gaggioli, V.; Miyamoto, K.; Allen, G.E.; Erkek, S.; Kwon, T.; Marcotte, E.M.; Zegerman, P.; Bradshaw, C.R.; et al. Sperm Is Epigenetically Programmed to Regulate Gene Transcription in Embryos. *Genome Res* **2016**, *26*, 1034–1046, doi:10.1101/gr.201541.115.
44. Kaneshiro, K.R.; Rechtsteiner, A.; Strome, S. Sperm-Inherited H3K27me3 Impacts Offspring Transcription and Development in C. Elegans. *Nat Commun* **2019**, *10*, 1271, doi:10.1038/s41467-019-09141-w.
45. Kaufman, P.D.; Rando, O.J. Chromatin as a Potential Carrier of Heritable Information. *Curr Opin Cell Biol* **2010**, *22*, 284–290, doi:10.1016/j.ceb.2010.02.002.
46. de Geyter, C.; Calhaz-Jorge, C.; Kupka, M.S.; Wyns, C.; Mocanu, E.; Motrenko, T.; Scaravelli, G.; Smeenk, J.; Vidakovic, S.; Goossens, V.; et al. ART in Europe, 2014: Results Generated from European Registries by ESHRE: The European IVF-Monitoring Consortium (EIM) for the European Society of Human Reproduction and Embryology (ESHRE). *Hum Reprod* **2018**, *33*, 1586–1601, doi:10.1093/humrep/dey242.
47. de Mateo, S.; Ramos, L.; van der Vlag, J.; de Boer, P.; Oliva, R. Improvement in Chromatin Maturity of Human Spermatozoa Selected through Density Gradient Centrifugation. *Int J Androl* **2011**, *34*, 256–267, doi:10.1111/j.1365-2605.2010.01080.x.
48. Castillo, J.; Simon, L.; de Mateo, S.; Lewis, S.; Oliva, R. Protamine/DNA Ratios and DNA Damage in Native and Density Gradient Centrifuged Sperm From Infertile Patients. *J Androl* **2011**, *32*, 324–332, doi:10.2164/jandrol.110.011015.
49. Chiamchanya, C.; Kaewnoonual, N.; Visutakul, P.; Manochantr, S.; Chaiya, J. Comparative Study of the Effects of Three Semen Preparation Media on Semen Analysis, DNA Damage and Protamine Deficiency, and the Correlation between DNA Integrity and Sperm Parameters. *Asian J Androl* **2010**, *12*, 271–277, doi:10.1038/aja.2009.60.
50. Muratori, M.; Tarozzi, N.; Carpentiero, F.; Danti, S.; Perrone, F.M.; Cambi, M.; Casini, A.; Azzari, C.; Boni, L.; Maggi, M.; et al. Sperm Selection with Density Gradient Centrifugation and Swim up: Effect on DNA Fragmentation in Viable Spermatozoa. *Sci Rep* **2019**, *9*, 7492, doi:10.1038/s41598-019-43981-2.
51. World Health Organization WHO Laboratory Manual for the Examination and Processing of Human Semen, Sixth Edition. In; World Health Organization; 2021. License: CC BY-NC-SA 3.0 IGO.: Geneva (Switzerland), 2021.

52. Jodar, M.; Kalko, S.; Castillo, J.; Ballescà, J.L.; Oliva, R. Differential RNAs in the Sperm Cells of Asthenozoospermic Patients. *Human Reproduction* **2012**, *27*, 1431–1438, doi:10.1093/humrep/des021.
53. Cerilli, L.A.; Kuang, W.; Roger, D. A Practical Approach to Testicular Biopsy Interpretation for Male Infertility. *Archive of Pathology & Laboratory Medicine* **2010**, *134*, 1197–1204.
54. Moch, H.; Cubilla, A.L.; Humphrey, P.A.; Reuter, V.E.; Ulbright, T.M. The 2016 WHO Classification of Tumours of the Urinary System and Male Genital Organs—Part A: Renal, Penile, and Testicular Tumours. *Eur Urol* **2016**, *70*, 93–105, doi:10.1016/j.eururo.2016.02.029.
55. Salonia, A.; Bettocchi, C.; Boeri, L.; Capogrosso, P.; Carvalho, J.; Cilesiz, N.C.; Cocci, A.; Corona, G.; Dimitropoulos, K.; Gül, M.; et al. European Association of Urology Guidelines on Sexual and Reproductive Health—2021 Update: Male Sexual Dysfunction. *Eur Urol* **2021**, *80*, 333–357, doi:10.1016/j.eururo.2021.06.007.
56. Leblanc, L.; Lagrange, F.; Lecoanet, P.; Marçon, B.; Eschwege, P.; Hubert, J. Testicular Microlithiasis and Testicular Tumor: A Review of the Literature. *Basic Clin Androl* **2018**, *28*, 8, doi:10.1186/s12610-018-0073-3.
57. Muciaccia, B.; Boitani, C.; Berloco, B.P.; Nudo, F.; Spadetta, G.; Stefanini, M.; de Rooij, D.G.; Vicini, E. Novel Stage Classification of Human Spermatogenesis Based on Acrosome Development1. *Biol Reprod* **2013**, *89*, 60, doi:10.1095/biolreprod.113.111682.
58. Schindelin, J.; Arganda-Carreras, I.; Frise, E.; Kaynig, V.; Longair, M.; Pietzsch, T.; Preibisch, S.; Rueden, C.; Saalfeld, S.; Schmid, B.; et al. Fiji: An Open-Source Platform for Biological-Image Analysis. *Nat Methods* **2012**, *9*, 676–682, doi:10.1038/nmeth.2019.
59. Bolte, S.; Cordelières, F.P. A Guided Tour into Subcellular Colocalization Analysis in Light Microscopy. *J Microsc* **2006**, *224*, 213–232, doi:10.1111/j.1365-2818.2006.01706.x.
60. RStudio Team *RStudio: Integrated Development Environment for R*; RStudio, Inc., Ed.; RStudio, Inc.: Boston, MA, 2020;
61. Fox, J.; Weisberg, S. *An R Companion to Applied Regression*; Third.; Sage: Thousand Oaks CA, 2019;

Table S1. Individual H4K5ac H-Scores in testicular sections from patients with normal spermatogenesis and testicular cancer. Results are expressed according to the testicular cell type analyzed. H-score is expressed per patient, and summarized at the bottom of the table as mean ± SD. The number of evaluated tubular sections presenting each of the analyzed cell types is indicated in brackets. Data corresponding to the IHC internal control is included.

Group	Patient ID	SC	SPG	SPC	rSPD (I-V)	rSPD (VI-VIII)	eSPD	cSPD
Normal spermatogenesis	**Controls (N)**							
	N1	95.7 (23)	284.0 (25)	33.3 (24)	323.5 (17)	462.5 (8)	553.8 (13)	0.0 (14)
	N2	152.6 (19)	253.8 (26)	53.6 (28)	344.4 (9)	500.0 (7)	559.1 (22)	0.0 (11)
	N3	104.3 (23)	292.0 (25)	72.4 (29)	321.4 (14)	477.8 (9)	415.8 (19)	0.0 (20)
	N5	38.9 (18)	165.5 (29)	20.7 (29)	161.5 (13)	420.0 (5)	505.9 (17)	5.3 (19)
	N6	181.8 (22)	300.0 (29)	86.7 (30)	270.0 (20)	320.0 (10)	500.0 (10)	0.0 (13)
	N7	33.3 (12)	176.2 (21)	13.8 (29)	275.0 (8)	314.3 (7)	434.8 (23)	0.0 (13)
	Internal Control	*200 (29)*	*224.1 (29)*	*46.7 (30)*	*228.6 (14)*	*425.0 (4)*	*466.7 (15)*	*0.0 (14)*
	Mean ± SD	**101.1 ± 59.5**	**245.3 ± 59.8**	**46.8 ± 29.1**	**282.7 ± 66.2**	**415.8 ± 80.8**	**494.9 ± 59.4**	**0.9 ± 2.1**
Testicular cancer	**Seminoma (SEM)**							
	SEM1	304.3 (23)	300.0 (30)	232.0 (25)	341.7 (12)	511.1 (9)	473.3 (15)	16.7 (6)
	SEM2	133.3 (18)	164.0 (25)	100.0 (26)	347.1 (17)	425 (4)	510.0 (10)	0.0 (11)
	SEM3	208.3 (24)	179.3 (29)	20.7 (29)	194.1 (17)	200.0 (2)	333.3 (12)	6.3 (16)
	SEM4	268.2 (22)	393.3 (30)	244.8 (29)	400.0 (17)	450.0 (6)	576.9 (13)	0.0 (21)
	Mean ± SD	**228.5 ± 74.8 ***	**259.2 ± 108.2**	**149.4 ± 107.9**	**320.7 ± 88.4**	**396.5 ± 135.9**	**473.4 ± 102.8**	**5.7 ± 7.86**
	Teratoma (TER)							
	TER1	240.0 (25)	263.0 (27)	96.2 (26)	300.0 (14)	366.7 (6)	420.0 (15)	0.0 (9)
	TER2	317.4 (23)	343.3 (30)	193.1 (29)	400.0 (19)	550.0 (2)	572.7 (11)	0.0 (8)
	TER3	290.0 (20)	306.7 (30)	207.1 (28)	328.6 (14)	425 (4)	546.7 (15)	0.0 (11)
	Mean ± SD	**282.5 ± 39.2 ***	**304.3 ± 40.2**	**165.5 ± 60.4 ***	**342.9 ± 51.5**	**447.2 ± 93.7**	**513.1 ± 81.7**	**0.0 ± 0.0**

* $p < 0.05$, after comparison of H4K5ac H-Scores of infertile patients with altered spermatogenesis and testicular cancer patients with the control group.

Table S2. H4K5bu H-Scores in testicular sections per individual patient. Immunohistochemical results of H4K5bu in testicular sections from control patients (Normal spermatogenesis), patients with altered spermatogenesis (Sertoli cell-only syndrome, hypospermatogenesis, and spermatogenic arrest) and patients with testicular cancer (seminoma and teratoma). Results are expressed according to the testicular cell type analyzed. H-score is expressed per patient, and summarized at the bottom of the table as mean ± SD. The number of evaluated tubular sections presenting each of the analyzed cell types is indicated in brackets. Data corresponding to the IHC internal control is included in the normal spermatogenesis group.

Group	Patient ID	SC	SPG	SPC	rSPD (I-V)	rSPD (VI-VIII)	eSPD	cSPD
Normal spermatogenesis	**Controls (N)**							
	N1	0.0 (29)	48.3 (29)	0.0 (26)	22.2 (9)	300.0 (7)	504.8 (21)	0.0 (17)
	N2	0.0 (24)	4.0 (25)	0.0 (28)	112.5 (8)	390.9 (11)	473.9 (23)	0.0 (17)
	N3	0.0 (20)	59.3 (27)	0.0 (29)	0.0 (9)	288.9 (7)	513.3 (15)	0.0 (16)
	N4	14.8 (27)	83.3 (24)	0.0 (30)	NA	521.4 (14)	451.9 (27)	0.0 (11)
	N5	0.0 (17)	0.0 (28)	0.0 (30)	0.0 (16)	275.0 (4)	514.3 (14)	0.0 (11)
	N6	0.0 (16)	3.3 (30)	0.0 (30)	19.0 (21)	138.5 (13)	412.5 (8)	5.3 (19)
	Internal Control	*0.0 (48)*	*0.0 (49)*	*0.0 (46)*	*22.2 (27)*	*210.0 (10)*	*368.4 (19)*	*6.7 (15)*
	Mean ± SD	**2.5 ± 6.1**	**33 ± 35.4**	**0.0 ± 0.0**	**30.8 ± 46.9**	**319.1 ± 128.0**	**478.4 ± 40.7**	**0.9 ± 2.1**
Altered Spermatogenesis	**Sertoli-Cell Only (SCO)**							
	SCO1	0.0 (30)	NA	NA	NA	NA	NA	NA
	SCO2	26.7 (30)	NA	NA	NA	NA	NA	NA
	SCO3	0.0 (30)	NA	NA		NA	NA	NA
	Mean ± SD	**8.9 ± 15.4**	**NA**	**NA**	**NA**	**NA**	**NA**	**NA**
	Hipospermatogenesis (HP)							
	HP1	0.0 (27)	82.6 (23)	0.0 (25)	20.0 (5)	442.9 (7)	533.3 (18)	0.0 (5)
	HP2	0.0 (17)	0.0 (18)	0.0 (18)	0.0 (6)	275.0 (4)	377.8 (9)	0.0 (5)
	Mean ± SD	**0.0 ± 0.0**	**41.3 ± 58.4**	**0.0 ± 0.0**	**10.0 ± 14.14**	**358.9 ± 118.7**	**455.6 ± 110.0**	**0.0 ± 0.0**
	Spermatogenic Arrest (SA)							
	SA1 (partial rSPD arrest)	0.0 (24)	27.6 (29)	6.7 (30)	192.3 (13)	180.0 (5)	460.0 (10)	225.0 (4)
	SA2 (partial SPC arrest)	0.0 (30)	3.6 (28)	0.0 (13)	NA	600.0 (2)	450.0 (10)	NA
	SA3 (total SPC arrest)	0.0 (29)	20.0 (30)	0.0 (27)	NA	NA	NA	NA
	Mean ± SD	**0.0 ± 0.0**	**12.8 ± 13.2**	**1.7 ± 3.3**	**192.3 ± 0.0**	**460.0 ± 242.5**	**439.4 ± 27.4**	**225.0 ± 0.0**
Testicular cancer	**Seminoma (SEM)**							
	SEM1	0.0 (25)	95.7 (23)	0.0 (29)	0.0 (1)	200.0 (8)	265.4 (26)	0.0 (6)
	SEM2	0.0 (25)	3.4 (29)	0.0 (23)	0.0 (10)	244.4 (9)	429.4 (17)	0.0 (8)
	SEM3	0.0 (30)	20.0 (30)	0.0 (28)	0.0 (14)	NA	312.5 (16)	0.0 (5)
	SEM4	0.0 (20)	85.7 (28)	0.0 (27)	0.0 (8)	212.5 (8)	313.0 (23)	0.0 (9)
	Mean ± SD	**0.0 ± 0.0**	**51.2 ± 46.3**	**0.0 ± 0.0**	**0.0 ± 0.0**	**219.0 ± 22.9**	**330.1 ± 69.9 ***	**0.0 ± 0.0**
	Teratoma (TER)							
	TER1	0.0 (24)	119.2 (26)	0.0 (6)	47.1 (17)	333.3 (3)	578.6 (14)	0.0 (12)
	TER2	45.5 (22)	206.9 (29)	0.0 (24)	161.5 (13)	550.0 (6)	381.3 (16)	0.0 (5)
	TER3	10.7 (28)	81.5 (27)	0.0 (30)	110.0 (10)	350.0 (4)	481.0 (21)	0.0 (8)
	Mean ± SD	**21.9 ± 20.4**	**133.4 ± 52.8 ***	**0.0 ± 0.0**	**142.1 ± 85.8 ***	**408.3 ± 98.6**	**455.2 ± 94.9**	**0.0 ± 0.0**

* $p < 0.05$, after comparison of H4K5bu H-Scores of infertile patients with altered spermatogenesis and testicular cancer patients with the control group. Note that HP was not considered for statistical analysis due to the limited sample availability. The same applies to SA from rSPD (I-V) on, due to number of replicates.

5.2 CHAPTER 2: Layers of epigenetic information contained in the protein fraction of the nucleo-protamine domain

Comprising the following scientific works

Arauz-Garofalo G, Jodar M, Vilanova M, **de la Iglesia A**, Castillo J, Soler-Ventura A, Oliva R, Vilaseca M, Gay M. Protamine Characterization by Top-Down Proteomics: Boosting Proteoform Identification with DBSCAN. *Proteomes*. 2021 Apr 30;9(2):21. doi: 10.3390/proteomes9020021.

Fourth author, IF *N/A* (indexed in JCR), Q2 (Biochemistry, SJR)

Castillo J*, Gay M*, **de la Iglesia A***, Arauz-Garofalo G, Vilanova M, Corral JM, Guimerà M, Vilaseca M, Jodar M, Oliva R. Alterations in the abundance of specific protamine proteoforms related to sperm chromatin packaging, obesity status, and age in men with unexplained infertility. *Manuscript in preparation*.

***First author**

de la Iglesia A, Blanco M, Jodar M, Cocquet J, Castillo J, Oliva R. Protein-protein interaction analysis suggest additional regulatory roles for SRPK1 and PP1γ in male germ cell chromatin remodeling during mouse spermiogenesis. *Manuscript in preparation*.

First author

5.2.1 Work 3: Protamine Characterization by Top-Down Proteomics: Boosting Proteoform Identification with DBSCAN

Published as:

Arauz-Garofalo G[1], Jodar M[2,3], Vilanova M[1], **de la Iglesia Rodriguez A**[2], Castillo J[2], Soler-Ventura A[2], Oliva R[2,3], Vilaseca M[1], Gay M[1]. Protamine Characterization by Top-Down Proteomics: Boosting Proteoform Identification with DBSCAN. *Proteomes*. 2021 Apr 30;9(2):21.

[1] Institute for Research in Biomedicine (IRB Barcelona), The Barcelona Institute of Science and Technology, Baldiri Reixac, 10, 08028 Barcelona, Spain

[2] Molecular Biology of Reproduction and Development Research Group, Institut d'Investigacions Biomèdiques August Pi i Sunyer (IDIBAPS), Fundació Clínic per a la Recerca Biomèdica (FCRB), Faculty of Medicine and Health Sciences, University of Barcelona, 08036 Barcelona, Spain

[3] Biochemistry and Molecular Genetics Service, Hospital Clínic de Barcelona, 08036 Barcelona, Spain

* Corresponding authors

PMID: 33946530 DOI: 10.3390/proteomes9020021

proteomes

MDPI

Article

Protamine Characterization by Top-Down Proteomics: Boosting Proteoform Identification with DBSCAN

Gianluca Arauz-Garofalo [1], Meritxell Jodar [2,3], Mar Vilanova [1], Alberto de la Iglesia Rodriguez [2], Judit Castillo [2], Ada Soler-Ventura [2], Rafael Oliva [2,3,*], Marta Vilaseca [1,*] and Marina Gay [1,*]

1 Institute for Research in Biomedicine (IRB Barcelona), The Barcelona Institute of Science and Technology, Baldiri Reixac, 10, 08028 Barcelona, Spain; gianluca.arauz@irbbarcelona.org (G.A.-G.); mar.vilanova@irbbarcelona.org (M.V.)

2 Molecular Biology of Reproduction and Development Research Group, Institut d'Investigacions Biomèdiques August Pi i Sunyer (IDIBAPS), Fundació Clínic per a la Recerca Biomèdica (FCRB), Faculty of Medicine and Health Sciences, University of Barcelona, 08036 Barcelona, Spain; meritxell.jodar@ub.edu (M.J.); adelaiglesia@ub.edu (A.d.l.I.R.); juditcastillo@ub.edu (J.C.); ada.soler.ventura@gmail.com (A.S.-V.)

3 Biochemistry and Molecular Genetics Service, Hospital Clínic de Barcelona, 08036 Barcelona, Spain

* Correspondence: roliva@ub.edu (R.O.); marta.vilaseca@irbbarcelona.org (M.V.); marina.gay@irbbarcelona.org (M.G.)

Abstract: Protamines replace histones as the main nuclear protein in the sperm cells of many species and play a crucial role in compacting the paternal genome. Human spermatozoa contain protamine 1 (P1) and the family of protamine 2 (P2) proteins. Alterations in protamine PTMs or the P1/P2 ratio may be associated with male infertility. Top-down proteomics enables large-scale analysis of intact proteoforms derived from alternative splicing, missense or nonsense genetic variants or PTMs. In contrast to current gold standard techniques, top-down proteomics permits a more in-depth analysis of protamine PTMs and proteoforms, thereby opening up new perspectives to unravel their impact on male fertility. We report on the analysis of two normozoospermic semen samples by top-down proteomics. We discuss the difficulties encountered with the data analysis and propose solutions as this step is one of the current bottlenecks in top-down proteomics with the bioinformatics tools currently available. Our strategy for the data analysis combines two software packages, ProSight PD (PS) and TopPIC suite (TP), with a clustering algorithm to decipher protamine proteoforms. We identified up to 32 protamine proteoforms at different levels of characterization. This in-depth analysis of the protamine proteoform landscape of normozoospermic individuals represents the first step towards the future study of sperm pathological conditions opening up the potential personalized diagnosis of male infertility.

Keywords: male infertility; sperm; protamine; LC-MS/MS; top-down proteomics; proteoform; post-translational modifications; Bioinformatics; DBSCAN

check for updates

Citation: Arauz-Garofalo, G.; Jodar, M.; Vilanova, M.; de la Iglesia Rodriguez, A.; Castillo, J.; Soler-Ventura, A.; Oliva, R.; Vilaseca, M.; Gay, M. Protamine Characterization by Top-Down Proteomics: Boosting Proteoform Identification with DBSCAN. *Proteomes* **2021**, *9*, 21. https://doi.org/10.3390/proteomes9020021

Academic Editors: Delphine Pflieger and Simone Sidoli

Received: 5 March 2021
Accepted: 27 April 2021
Published: 30 April 2021

Publisher's Note: MDPI stays neutral with regard to jurisdictional claims in published maps and institutional affiliations.

Copyright: © 2021 by the authors. Licensee MDPI, Basel, Switzerland. This article is an open access article distributed under the terms and conditions of the Creative Commons Attribution (CC BY) license (https://creativecommons.org/licenses/by/4.0/).

1. Introduction

Protamines are the main nuclear proteins in the sperm cells of many species, and they play a crucial role in the correct packaging of the paternal DNA [1–3]. During the final stage of spermatogenesis (called spermiogenesis), the chromatin of immature germ cells undergoes marked remodeling, in which histones are sequentially replaced by specific histone variants, transition proteins and, finally, protamines [1,4–7]. Both the small size of protamines (20 to 55 amino acids) and their extremely rich sequence in positively charged arginine residues allow the formation of highly condensed toroidal complexes, together with the negatively charged paternal DNA [8,9]. In addition, the high number of cysteine residues in mammalian protamines promotes the generation of multiple intra- and inter-molecular disulfide bonds and zinc bridges between protamines, thereby stabilizing the compact toroidal nucleoprotamine complex [10,11]. Several functions have been proposed for the nucleoprotamine domain, including the protection of the paternal

genome during transit from the male to the oocyte and contribution to obtaining the required hydrodynamic shape for mature sperm functionality [3,4,12–17]. Of note, the replacement of histones by protamines during spermatogenesis is not complete, resulting in 85–95% of sperm DNA packed by protamines and the remaining 5–15% attached to histones [18]. Several studies have reported that the distribution of the nucleohistone and nucleoprotamine complexes along sperm chromatin is not random. This distinctive chromatin structure has been proposed as a specific epigenetic mark of sperm that could regulate gene expression once the oocyte has been fertilized [19–21].

The crucial role of protamines in the compaction of the paternal genome has given rise to considerable interest in the analysis of protamine alterations in the andrology field. Mammalian spermatozoa contain two types of protamines: protamine 1 (P1) and the family of protamine 2 (P2) proteins. P1 is expressed in all species of protamine-containing vertebrates, while the P2 family is present only in some mammalian species, including the human and mouse. P2 is formed by the proteolysis of the P2 precursor (pre-P2), resulting in the HP2, HP3 and HP4 components, of which HP2 is the most abundant [4] (Figure 1).

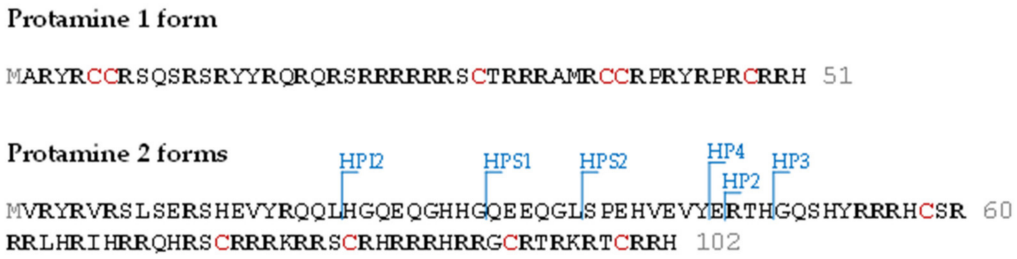


Figure 1. Human protamine amino acid sequences. Protamine 1 is translated as a mature form containing 51 residues (P1). In contrast, protamine 2 is translated as a precursor protein containing 102 residues (pre-P2), which is processed by proteolysis in multiple intermediate forms (HPI2 (22–102), HPS1 (34–102) and HPS2 (37–102)) and mature forms (HP2 (46–102), HP3 (49–102) and HP4 (45–102)).

Several groups have established similar protein levels of P1 and P2 in normal spermatozoa, with an approximate 1:1 proportion, and alterations of the P1/P2 ratio have been associated with male infertility and poor reproductive outcomes [22–24]. However, controversial results have been reported in the literature and the P1/P2 ratio shows a wide range in fertile men [25]. The P1/P2 ratio has been commonly assessed by polyacrylamide gel electrophoresis (PAGE) and protein staining [26–29]. However, this common approach does not provide information on whether a specific alteration of the P1/P2 ratio is due to the deregulation of P1, the P2 family, specific P2 components, or all of three. In addition, the emerging hypothesis that alterations in both histone variants and histone post-translational modifications (PTMs) might lead to male infertility [30] suggests that, in a similar way, alterations in protamine PTMs are also associated with male infertility. Recently, we suggested that the presence of human sperm protamine proteoforms, including truncations or proteoforms containing PTMs, explain the variability observed in the P1/P2 ratio assessed by conventional PAGE [30,31]. Therefore, we propose that more sophisticated methodologies such as mass spectrometry (MS) could help decipher the different protamine proteoforms present in mature sperm cells and their impact on male fertility [31]. However, the peculiar physicochemical properties of protamines (high arginine content with P1 containing 24 Arg residues out of 51 and HP2 32 Arg residues out of 54) and the high similarity between P2 components make them unsuitable for characterization by bottom-up proteomic strategies. The main reason is that conventional trypsin digestion results in extremely small protamine peptides that are lost during their processing. Additionally, the intra- and inter-protamine disulfide bonds and zinc bridges that form due to the high number of cysteine residues in the protamine sequences (6 Cys in P1 and 5 Cys in HP2) require methods for reduction and alkylation to avoid multiple cysteine oxidations. Of note, the low molecular weight

of protamines (P1: 6687 Da and P2: 12,912 Da) is a big advantage for analyzing these molecules by top-down proteomics.

Top-down proteomics is a powerful MS-based technology that allows direct analysis of all proteoforms, whether derived from alternative splicing, missense or nonsense genetic variants or PTMs. This approach offers unique and precise information on proteoforms that is complementary to that achieved using bottom-up proteomics. The top-down analysis of MS-derived data is challenging both due to the deconvolution of the spectra and subsequent searches in databases for correct proteoform assignment. Unlike bottom-up proteomics, where robust solutions are found for the identification, characterization and quantification of peptides and proteins, data analysis in top-down proteomics is not yet fully established. In this regard, it is still one of the bottlenecks for top-down proteomic strategies. One of the main pitfalls is the lack of automated validation of the final IDs, which requires manual inspection of the assignments.

There are two main approaches for top-down data analysis and proteoform identification: (a) analysis based on a search in annotated databases, where all the possible proteoforms with defined PTMs are included in a certain position, like in ProSight PD (PS) [32], and (b) analysis based on spectral alignment algorithms [33], which matches the tandem mass spectra of the proteins with the unannotated database, without prior knowledge of the type of PTMs or their location, like in TopPIC suite (TP) [34,35].

The data analysis workflow that we describe herein combines two distinct software packages (referred to herein as nodes), namely PS and TP. To avoid redundant identifications on the same precursor, our pipeline is based on MS1 clustering and harmonization of the two datasets obtained. This new strategy allowed us to identify 13 proteoforms of P1 and 19 proteoforms of P2 in human semen samples. We envisioned that this strategy could be applied to other highly modified proteins such as histones.

2. Materials and Methods

2.1. Sample Collection

Human semen samples (n = 2) were obtained from patients undergoing routine semen analysis at the Assisted Reproduction Unit at the Clinic Institute of Gynecology, Obstetrics and Neonatology, at the Hospital Clínic of Barcelona, Spain. All patients gave signed informed consent in accordance with the Declaration of Helsinki. The ejaculates were collected by masturbation into sterile containers after 3–5 days of sexual abstinence. Seminal parameters were evaluated using the automatic semen analysis system CASA (Proiser, Paterna, Spain). After seminal analysis, all samples were classified as normozoospermic according to World Health Organization guidelines [36]. Subsequently, sperm was purified through 50% Puresperm® density gradient separation (NidaCon International AB, Gothenburg, Sweden), following the manufacturer's instructions.

2.2. Purification of Human Sperm Protamine

The protamine-enriched fraction of spermatozoa was purified as described in [27]. except that histones and other basic proteins weakly associated with DNA were removed from the sperm by 0.5 M HCl, vortexing and incubation for 10 min at 37 °C and centrifugation at 2000× g for 20 min at 4 °C (three times) prior to suspending the sperm pellet with 0.5% Triton X-100, 20 mM (pH8) Trizma® base HCl, and 2 mM $MgCl_2$. Samples were then processed as described in [27]. For the top-down MS approach, protamine-enriched fractions (equivalent to 15 million spermatozoa) were dried at room temperature overnight under a fume hood and kept at 20 °C. Before liquid chromatography MS analysis (LC-MS/MS), samples were reconstituted in 50 mM NH_4HCO_3, reduced with 10 mM dithiothreitol (DTT) for 45 min at 56 °C, alkylated for 30 min in the dark with 50 mM iodoacetamide (IAA) and further desalted using PolyLC C18 filter tips (PolyLC INC., Columbia, MD, USA).

2.3. Protamine Quantification

Purified extracts of protamines were quantified as described in [27]. Briefly, an aliquot of protamines for each sample was separated in an acid-urea PAGE together with increasing amounts of a protamine standard obtained as described elsewhere [37]. Approximate amounts of P1 and P2 were calculated from protamine optical density measurements and the quantification obtained with the protamine standard, using Quantity One 1-D Analysis Software (Bio-rad, Hercules, CA, USA).

2.4. Top-Down Proteomics

2.4.1. LC-MS

We analyzed two biological replicates, each with two technical replicates. Samples were reconstituted in an aqueous solution of 3% acetonitrile (ACN) and 1% formic acid (FA) and injected to the LC-MS/MS system.

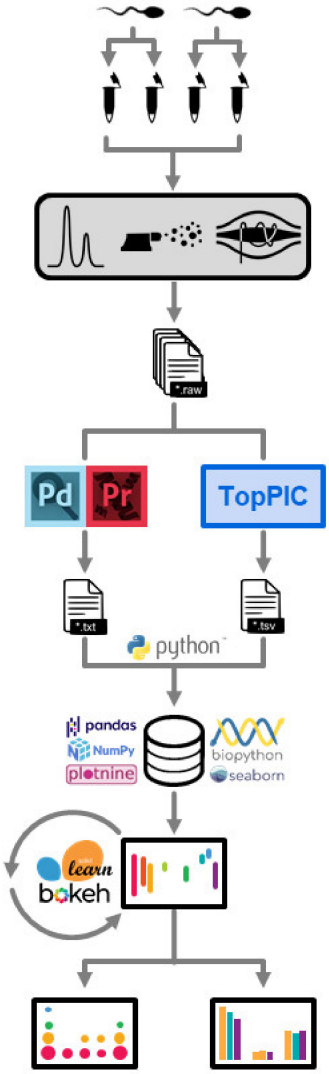
LC-MS/MS analysis of intact protamines was conducted on a Dionex Ultimate 3000 coupled to an Orbitrap Fusion Lumos mass spectrometer (both from Thermo Scientific, San Jose, CA, USA). Samples were loaded onto C18 trap columns (100 µm × 2 cm Acclaim PepMap100, 5 µm, 100 Å (Thermo Scientific) at a flow rate of 15 µL/min. Protein content was separated using C18 analytical columns (Acclaim PepMap® RSLC 75 µm × 50 cm, nanoViper, C18, 2 µm, 100Å (Thermo Scientific) and a linear gradient from 3 to 15% B in 30 min at a flow rate of 250 nl/min (A = 0.1% FA in water, B = 0.1% FA in ACN). The Advion TriVersa NanoMate (Advion Ltd., Harlow, United Kingdom) was used as the nanospray interface with the direct on-line coupling mode with a spray voltage of 1.60 kV. The mass spectrometer was operated in data-dependent acquisition (DDA) mode. Survey MS scans were acquired in the orbitrap with the resolution (defined at 200 m/z) set at 120k. The top N (most intense) ions per scan were fragmented by electron transfer dissociation (ETD) and detected in the orbitrap at 120k. The ion count target value was 400,000 for the survey scan and 1,000,000 for the ETD-fragmented MS/MS scan. Target ions already selected for MS/MS were dynamically excluded for 30 s. RF lens was tuned to 30%. The minimal signal required to trigger the MS to MS/MS switch was set at 500,000.

2.4.2. Proteoform Search

We devised a twin search approach for our top-down proteomics workflow (Figure 2). This strategy encompasses the bioinformatic stools TP and PS.

The first node used for top-down searches was TP v1.4.2, including its tool TopFD to deconvolute the spectra. This node can identify proteoforms of an entire proteome with remarkable speed by searching against a FASTA database without prior knowledge of possible modifications or existing PTMs. Therefore, TP is particularly suitable when dealing with highly modified proteins such as histones or protamines.

We included the following PTMs in the parameters of the TP search: oxidation (in M), phosphorylation (in STY), acetylation (in KS), methylation, dimethylation (both in KR) and trimethylation (in K) for being the major PTMs found in histones and therefore also expected in protamines. We included the following N-terminal forms: none, N-terminal methionine excision (NME), NME_Acetylation and M_Acetylation, which referred to proteoforms with or without the initial methionine non-acetylated or acetylated. We also defined precursor and fragment mass tolerances of 15 ppm, and maximum mass shifts of 500 Da. We only considered Proteoform Spectrum Matches (PrSMs) with FDR < 1% for downstream data integration. We used a FASTA file containing P1 and P2 sequences as a database.



SAMPLES
Two biological replicates (A, B) with two technical replicates each (R01, R02, R03, R04).

SAMPLE PREPARATION
Protamine purification.

LC-MS
- **Dionex Ultimate 3000 nano RSLC**

Column: Acclaim PepMap, 75 µm x 50 cm, C18 2 µm
Gradient: 3 to 15% of B in 30 min.
Flow: 250 nL / min.
- **Advion source**

Spray voltage: 1.6 kV.
Coupling mode: Online.
- **Orbitrap Fusion Lumos™ Tribrid**

8 mbar, RF: 30%
MS1: full Orbitrap MS scan (120k res).
MS2: Orbitrap ETD 10 ms (120k res)

MS DECONVOLUTION AND PROTEOFORM SEARCH
- ProSight PD.
- TopPIC Suite.

DATA ANALYSIS
- **Data integration**

Custom Python code leveraging popular packages (Pandas, NumPy, Biopython, Plotnine, Seaborn…).

- **Proteoform clustering**

DBSCAN algorithm (Scikit-learn), plus interactive data visualization (Bokeh) to optimize ε and n_{min}.

- **Proteform annotation and PTM localization**

Curated proteoform annotation by an expert operator.
Check TP and PS PTM-site localization agreement.

Figure 2. Protamine characterization workflow. We purified the protamine content of two biological replicates (A, B) and injected four technical replicates (R01, R02, R03, R04) into the LC-MS instrument. We then used two bioinformatic tools (ProSight PD (Thermo Scientific, San Jose, CA, USA) and TopPIC Suite (Indianapolis, IN, USA)) to identify proteoform spectrum matches. The whole data analysis pipeline downstream was implemented entirely using Python as a programming language.

The second search was done with Proteome Discoverer v2.5.0.400 (Thermo Fisher Scientific) and its PS v4.0.0.228 node. In contrast with TP, PS requires a database with all theoretical proteoforms explicitly listed. The Protein Annotation option from the PS Database Manager allows such a database to be built from a typical *.xml file available in SwissProt.

It is crucial to mention here the existing bioinformatic bottleneck despite current computing power. As the number of PTMs for a given protein sequence increases, the number of entries in the database rapidly explodes. We can compute the number of theoretical proteoforms for a given database, N, using the following expression:

$$N = \sum_{j=1}^{P} \left[\prod_{i=1}^{n} (m_i + 1)_j \right] \quad (1)$$

where P is the number of protein sequences in the database, n the number of amino acids for each sequence, and m the number of possible modifications for each amino acid on each sequence [38]. Given the PTMs typically found in protamines that we previously

mentioned, this equation returns around $N_{P1} \approx 4.4 \times 10^{15}$ and $N_{P2} \approx 3.9 \times 10^{22}$ theoretical proteoforms for P1 and P2, respectively, which gives $N \approx N_{P2} \approx 10^{22}$ in total. These values would imply an extremely long computational search time. To overcome this issue, we launched a preliminary PS search excluding those PTMs on consecutively repeated arginine residues, but keeping PTMs in selected arginines from the N-terminal, C-terminal and from the middle of the sequence. As a result, the number of theoretical proteoforms in this first search was reduced by 15 orders of magnitude. Since this preliminary search did not find any acetylations, methylations, dimethylations or trimethylations, we launched a second three-tier search (Annotated Proteoform, Subsequent Search and Annotated Proteoform) using a database with only phosphorylations (in STY), oxidations (in M) and acetylation in N-terminal in all the nodes. Using this strategy, we further reduced the number of theoretical proteoforms by 2 orders of magnitude, adding up a total of 17 orders of magnitude and thereby giving a much more reasonable search time. Precursor mass tolerances were 2.2 Da/10 ppm/500 Da for Annotated Proteoform, Subsequent Search and Annotated Proteoformrespectively, and fragment mass tolerances 10 ppm in all cases. The mass spectrometry proteomics data have been deposited to the ProteomeXchange Consortium via the PRIDE [39]. partner repository with the dataset identifier PXD024405.

2.4.3. Data Analysis

The PrSM output format used by PS and TP is highly heterogeneous. The column name used by each node to designate the same concept usually varies (for example: "Spectrum File" in PS and "Data file name" in TP). Even the unit used to express the same magnitude differs (for example: TP expresses retention time in minutes while PS uses seconds). We computationally addressed this issue with a custom Python code [40]. (available on the GitHub repository: https://github.com/MSPCF/2021_Proteomes, accessed on 27 April 2021). To this end, we leveraged some of Python's most popular packages such as Pandas [41], NumPy [42], Biopython [43], Plotnine [44], and Seaborn [45].

Once this harmonized dataset with all PrSMs was ready, we filtered out those identifications with retention times beyond 42 min for being associated with the column wash. We did not apply any PrSMs pre-filter based on PrSM quality (such as the MS1 intensity or the E-value), but this might be convenient depending on the overall PrSM dataset quality. After pre-filtering, we performed the PrSM clustering by means of a density-based spatial clustering algorithm of applications with noise (DBSCAN) [46,47]. implemented within the Scikit-learn Python package [48]. This clustering algorithm is particularly suitable in our scenario because it does not require pre-definition of the number of clusters expected (a priori, we do not know the number of proteoforms within a sample). In addition, DBSCAN has just two main hyperparameters to work with: maximum distance between two samples to accept both as belonging to the same neighborhood (ε), and minimum number of samples in a neighborhood to be accepted as an independent cluster (n_{min}). In our scenario, "samples" and "independent clusters" would correspond to PrSMs and proteoforms, respectively. Regarding the "distance", it is important to mention that we simply passed the standard score (commonly called z-score) of the deconvoluted PrSM masses to the clustering algorithm. Finally, we optimized the DBSCAN hyperparameters ε and n_{min} by interactive exploratory data analysis with a custom Python code leveraging the Bokeh Python package [49], getting $\varepsilon = 1.2 \times 10^{-3}$ (which in our filtered harmonized dataset corresponds to 1.28 Da) and $n_{min} = 10$.

2.4.4. Proteoform Annotation

Once clustering was done, proteoforms were annotated in a semi-automatic manner comprising two major steps. For a given cluster, we first checked to see if most of its PrSMs pointed to a particular protein, usually any full-length or truncated mature or immature protamine form or other sperm-related protein. In this case, we pre-assigned what we call a

"cluster-protein" to this cluster and then computed its corresponding cluster-protein mass shift as follows:

$$\Delta m_{CT} = m_C - m_T, \quad (2)$$

where m_T is the theoretical mass of the fully carbamidomethylated cluster-protein, and m_C the mean mass of all PrSMs within this cluster. When a predominant cluster-protein was not found, we manually attempted to assign a suitable protein consistent with the particular m_C value. Secondly, and depending on the precise Δm_{CT} we manually assigned a suitable PTM set. The proteoform annotation table is provided in the supplementary material (Table S1), as well as the associated harmonized PrSMs dataset, including the clustering outcome and the proteform annotation (Table S2).

3. Results and Discussion

We analyzed two biological replicates (A and B), with two technical replicates each (R01 and R02 for A, R03 and R04 for B). The results presented here are all the data combined with the final aim of characterizing the protamine proteoforms in the samples.

In the following sections we will use the five-level classification system for proteoform identifications proposed by Smith et al. [50]. We will refer to levels 1, 2A, 2B and 3. Level 1 describes proteoforms identified with full knowledge of their gene origin, amino acid sequence and, when present, the identification and localization of their PTMs. Level 2A refers to those proteoforms with a defined amino acid sequence from a known gene with all the PTMs identified but with incomplete localization. In level 2B, the PTMs are not fully characterized but their localization is complete. Level 3 refers to those proteoforms that are certain for two of the four ambiguity classes: gene, sequence, PTM identification and PTM localization. In this manuscript we refer to level 3 as proteoforms with a gene and sequence defined but with an unknown modification and localization.

3.1. Overview of the DBSCAN Approach

The goal of our DBSCAN approach was to integrate and harmonize the PS and TP datasets by PrSM deconvoluted experimental masses. We assumed that a proteoform at level 1 without PTMs, or level 2A or level 3 with an equivalent mass shift, always had the same mass and therefore could be annotated as the same proteoform. In this first step, we were not able to localize modification sites and reach level 1 for proteoforms with PTMs, but we localized PTMs in a second step considering only those PrSMs identified with a high confidence level (Section 3.4). The power of our workflow for top-down proteomic data analysis lies in combining multiple nodes to achieve high-quality PrSMs and a single harmonized dataset.

From the PS and TP searches, a total of 2838 PrSMs passed our filters (56.6% for PS and 43.4% for TP) and were further submitted for clustering. The DBSCAN algorithm successfully clustered 2578 of the PrSMs (55.9% for PS and 44.1% for TP) into 27 well differentiated mass clusters, leaving 260 unclustered PrSMs (63.8% for PS and 36.2% for TP).

We identified the following four main protamine groups: P1 proteoforms, comprising clusters from P|000 to P|008 (7029 Da to 7311 Da); mature P2 forms (HP2, 3 and 4) from P|009 to P|013 (7538 Da to 8123 Da); intermediate P2 forms (HPS1, 2 and HPI2) from P|014 to P|020 (9002 Da to 10,654 Da); and pre-P2 forms from P|021 to P|025 (13,195 Da to 13,516 Da) (Table 1). Cluster P|026 remained unidentified and could presumably be ascribed to a sperm-related protein other than protamines. In addition to several phosphorylated proteoforms (up to +80 Da × 4), we also identified some presenting an unrecognized +61 Da mass shift modification (up to +61 Da × 3), usually in combination with other P1 phosphorylated proteoforms. We found this +61 Da mass shift in P1, HP2, HP3, HP4, HPS1 and HPS2. We had already identified this +61 Da mass shift in previous studies [31]. We cannot explain this +61 Da mass shift yet but propose that these protamines exhibit some metal ion-binding sites for Zn2+ or Cu+ [51,52]. Further verification is required using other MS-based techniques such as inductively coupled plasma MS. Finally, we also observed

the formation of the cyclic pyroglutamyl residue (pyro-Glu) from the N-terminal glutamine of HPS1 [53].

Table 1. Cluster annotation summary. We provide the cluster-to-proteoform correspondence in columns "Cluster" and "Proteoform". Column "m_T (Da)" gives the theoretical mass of the fully carbamidomethylated cluster-protein (for HP4 the mass is 8062.32 Da). Columns "m_C (Da) (mean)" and "m_C (Da) (std)" give the mean mass and the mass standard deviation of all PrSMs comprising each cluster. Column "Δm_{CT} (Da)" gives the cluster-protein mass shift returned by Equation (2). We also report proteoform and PrSM counts according to PS and TP nodes in columns "PF count" and "PrSM count", respectively (ph = phosphorylation, Q = glutamine, pyroGlu = pyroglutamic acid, PF = proteoform, PrSMs = proteoform spectrum matches, ProSight = PS, TopPIC = TP).

Cluster	Proteoform	m_T (Da)	m_C (Da)(mean)	m_C (Da)(std)	Δm_{CT} (Da)	PF Count		PrSM Count	
						PS	TP	PS	TP
P|000	P1	7029.6	7029.45	1.39	−0.14	2	5	247	206
P|001	P1 + 1(61)	-	7090.92	1.92	61.32	5	4	156	97
P|002	P1 + 1ph	-	7108.86	1.58	79.27	3	5	71	74
P|003	P1 + 2(61)	-	7151.59	1.56	122	6	3	71	46
P|004	P1 + 1ph + 1(61)	-	7170.39	1.67	140.79	2	3	51	32
P|005	P1 + 3(61)	-	7212.91	1.85	183.32	4	3	64	41
P|006	P1 + 1ph + 2(61)	-	7231.82	1.66	202.23	6	2	29	20
P|007	P1 + 1ph + 3(61)	-	7293.52	2.73	263.92	4	5	42	29
P|008	P1 + 2ph + 2(61)	-	7310.92	1.43	281.32	3	2	7	5
P|009	HP3	7539.07	7538.54	1.26	−0.53	2	2	72	53
P|010	HP3 + 1(61)	-	7599.63	1.20	60.56	1	2	17	13
P|011	HP2	7933.28	7932.73	1.08	−0.55	1	4	142	119
P|012	HP2 + 1(61)	-	7994.03	1.35	60.75	1	1	64	51
P|013	HP4 + 1(61)	-	8122.66	0.49	60.34	2		16	
P|014	HPS2	9002.75	9002.09	1.10	−0.66	2	3	69	54
P|015	HPS2 + 1(61)	-	9063.4	1.99	60.66	2	3	31	10
P|016	HPS1 − 1Q	-	9172.08	1.09	−128.83	3	1	23	19
P|017	HPS1 +1Pyroglu	-	9283.32	1.27	−17.59	9	3	26	21
P|018	HPS1	9300.91	9301.17	1.07	0.25	1	3	79	70
P|019	HPS1 + 1(61)	-	9363.59	1.51	62.67	3	2	23	18
P|020	HPI2	10,654.46	10,653.97	1.01	−0.49	1	1	6	6
P|021	pre-P2	13,196.82	13,195.97	1.67	−0.85	1	4	58	51
P|022	pre-P2 + 1ph	-	13,275.94	1.80	79.12	3	4	27	22
P|023	pre-P2 + 2ph	-	13,355.92	1.54	159.1	1	5	28	29
P|024	pre-P2 + 3ph	-	13,435.64	1.59	238.82	3	3	14	17
P|025	pre-P2 + 4ph	-	13,515.5	1.19	318.68	2	2	8	6
P|026	Unknown	-	13,873.22	0.78	-		2		28
Unclustered	Unknown	-	-	-	-	57	89	166	94

We used different projections to visualize the clustering outcome and better optimize its ε and $n_{\min}$ parameters with our Bokeh-based web application. In particular, we inspected the following three projections: retention time vs. deconvoluted experimental mass (Figure 3a, Figure S1), $\log_2$ intensity vs. deconvoluted experimental mass (Figure S2a), and retention time vs. $\log_2$ intensity (Figure S2b). This strategy was crucial for gaining greater insight into how the DBSCAN algorithm worked, as well as the differences between the PS and TP nodes.

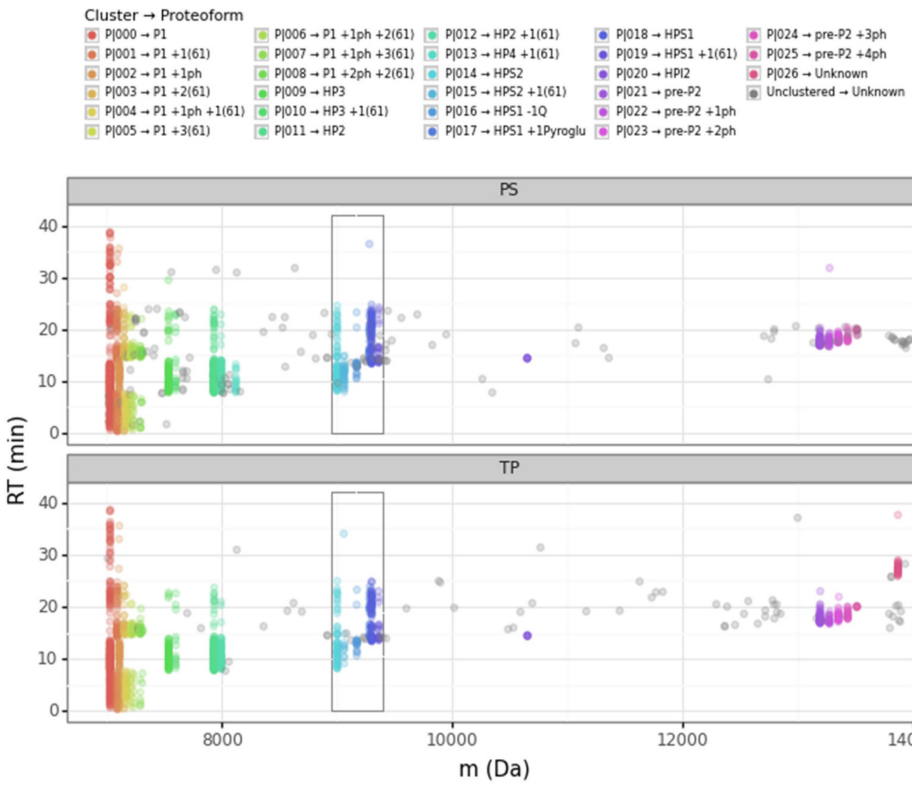
The scatterplot of the retention time vs. the deconvoluted experimental masses was particularly useful. We used colors to differentiate clusters. In this plot, it is easy to see proteoforms with the same mass clustered or to localize PrSMs that did not cluster. The four main protamine groups mentioned above per mass region can be visualized in the same plot, grouped in mass regions: (a) P1: 7000 to 7500 Da; (b) mature P2: 7500 to 8200 Da; (c) Intermediate P2: from 9000 to 11,000 Da; and (c) pre-P2: from 13,000 to 13,600 Da. Each region had the canonical sequences and the subsequent proteoforms with different modifications.

Using the DBSCAN approach, we identified proteoforms at levels 1, 2A and 3 of the classification system [51]. We reached level 1 in proteoforms without PTMs (truncated and non-truncated forms) and in the case of HPS1 +PyroGlu, level 2A in proteoforms with known modifications (phosphorylations), and level 3 with proteoforms with the +61 mass shift.

3.2. Advantages of the DBSCAN Approach vs. PS and TP

When handling PS and TP outputs, we encountered some common difficulties and issues, such as the different output tables generated or incorrectly assigned proteoforms. With the DBSCAN approach, we overcame some of these issues and integrated, simplified and corrected the PS and TP outputs.

We first examined the results at the amino acid sequence level without considering known or unknown modifications. TP identified 65 sequences, of which 41 were truncated at the N-terminal, 5 at the C-terminal and 4 in both the N and C-terminal regions. PS found 14 sequences, of which 9 were truncated at the N-terminus (Table S2). These numbers, based only on the amino acid sequence level, already highlighted the high dispersion between the nodes. When we introduced modifications, the dispersion between results was even higher, thereby hindering comparison of the two datasets. However, after the cluster analysis using the PS and TP data, most of these sequences fell into the 8 sequences previously described in Uniprot (Figure 1).



(**a**)

Figure 3. *Cont.*

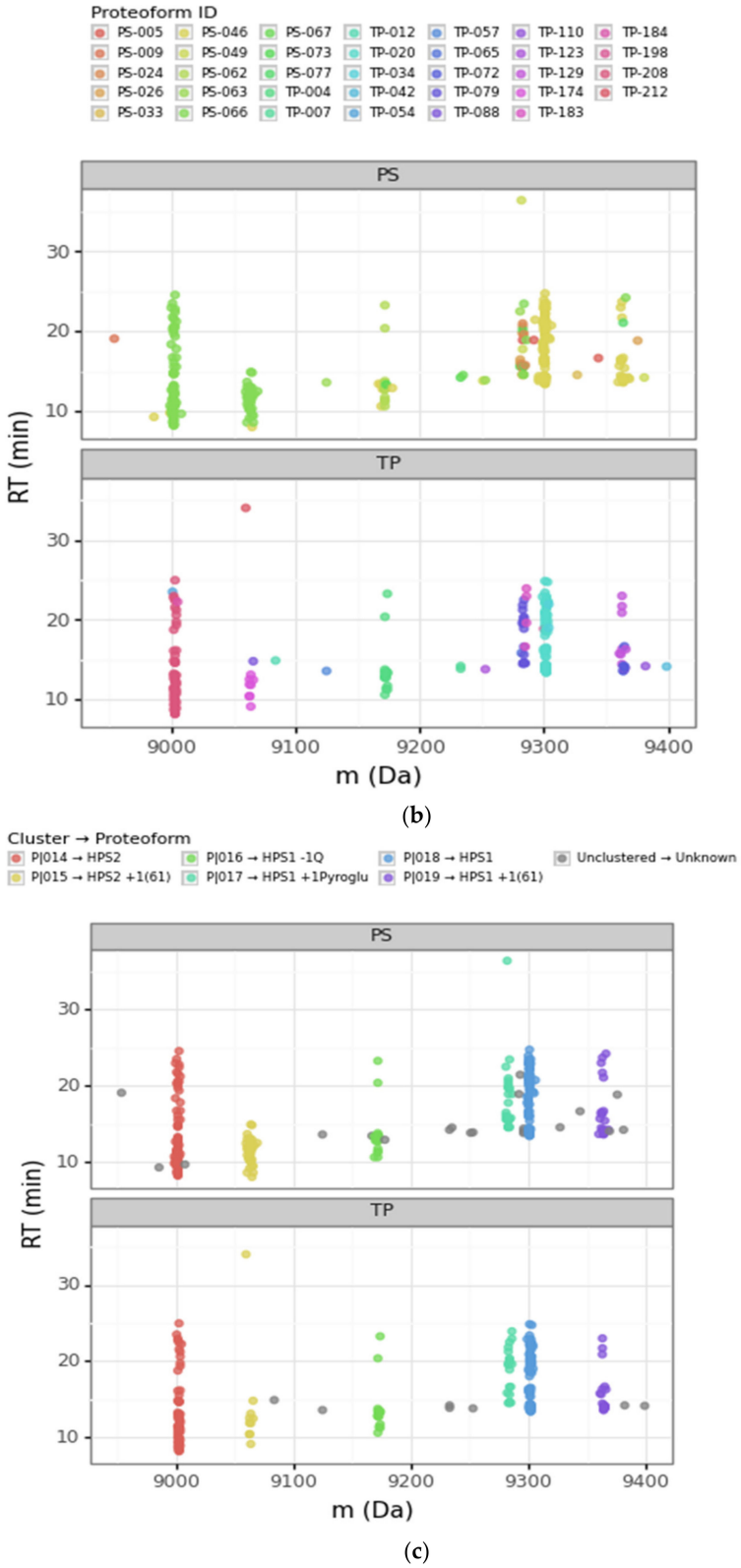


Figure 3. Scatterplots of the retention time (RT) vs. the deconvoluted experimental mass (m) for PS (Prosight PD) and TP (TopPIC Suite). (**a**) Deconvoluted masses from 6000 Da to 14,000 Da. The sequential color scale highlights the clusters obtained sorted by increasing experimental mass, while unclustered PrSMs appear in grey. (**b**,**c**) Deconvoluted masses from 8900 Da to 9400 Da corresponding to clusters that we associated with HPS1 and HPS2 proteoforms (the region highlighted with a rectangle in panel (**a**)). The color scale in panel (**b**) denotes each proteoform according to PS and TP, while the color scale in panel (**c**) denotes each proteoform according to our clustering approach. (ph = phosphorylation, Q = glutamine, pyroGlu = pyroglutamic acid).

144

Going deeper into the data analysis, we observed that PS and TP sometimes failed to assign a proteoform from a given PrSM. We identified two main common cases of incorrect PrSM assignment: (a) PrSMs with very different deconvoluted masses recognized as the same proteoform (which should not be possible for any classification level), and (b) PrSMs with a very similar deconvoluted mass recognized as different proteoforms. The first misassignment case (from now on "converging") was usually found in PS while the second one (from now on "diverging") was found in both PS and TP. Figure 3 illustrates these two misassignment scenarios by zooming in to highlight the mass region where HPS1 and HPS2 are located (Figure 3b). For example, PS considers those PrSMs around 9000 Da and 9060 Da to be the same proteoform (Figure 3b, green data points). Another example, TP does not report those PrSMs clustered around 9283 Da as the same proteoform (Figure 3b, purple and magenta data points). Note how our DBSCAN approach nicely groups those PrSMs with similar masses into well-defined clusters (proteoforms), in striking contrast to how PS and TP perform (Figure 3c).

3.2.1. Converging and Diverging Misassignment of PrSMs

We considered converging misassignment to be those cases in which PrSMs with very different experimental deconvoluted masses (i.e., belonging to different proteoforms according to our clustering approach) are identified by the node as the same proteoform. In general, for a given TP proteoform ID we found just one proteoform according to our clustering approach, meaning that TP did not mix proteoforms with different deconvoluted masses under the same proteoform ID. On the contrary, we observed that PS "converges" into the same proteoform ID PrSMs belonging to different proteoforms according to our clustering approach. In fact, PS classified under the same proteoform ID PrSMs with deconvoluted experimental mass differences up to 980 Da. This PS issue usually occurred when there were no identified modifications, as in the +61 mass shift case.

A clear example of this situation can be observed in Figure 3b. Note how PS converged as HPS2 (theoretical mass 9002.75 Da) PrSMs with quite different deconvoluted masses (9002 Da and 9064 Da). We consider that PrSMs around 9003 Da (cluster P|015) are correctly associated with HPS2, but those around 9064 Da (cluster P|016) should be linked to a new HPS2 +61 Da proteoform because they are clustered apart (Table 2a). We manually validated this hypothesis with the help of ProSight Lite [54], by precisely localizing such +61 Da mass shifts in the same spectrum identified as HPS2 by PS (Table 2b). Note how both the P-Score and the number of matching fragments improved once we assigned this + 61 Da mass shift to the C-46 residue in HPS2 (the first decreases from 1.1×10^{-91} to 7.6×10^{-155} and the second increases from 62 to 95) (Table 2a,b). Similarly, PS also "converged" as HPS1 (9300.91 Da), PrSMs with clearly different deconvoluted masses (this time with values around 9301 Da and 9362 Da). Again, since those PrSMs were clustered apart (P|019 and P|020, respectively), we assumed that PrSMs around 9362 Da correspond to a new HPS1 +61 Da proteoform (Figure 3b).

Table 2. Converging and diverging missassigments examples. Row (a) show an example of converging missassigment and row (b) its corresponding manual reassignation after cluster inspection: HPS2 +1(61) proteoform is more likely than HPS2. Rows (c) and (d) along with (e) and (f) provide two examples of diverging missassigments and their associated corrections. For both examples, HPS1 +1pyroGlu is more likely than HPS2 +2ph or HPS1 +1AcNterm, respectively. Check ProSight Lite fragmentation pattern, mass shift and remaining scoring columns for details (ph = phosphorylation, pyroGlu = pyroglutamic acid). Columns "m_e" and "m_t" give the experimental and theoretical masses, respectively. "Δm" gives the difference between m_e and m_t. "P-Score" is the score as provided by ProSight Lite. "%Res. Cleav. is the percentage of inter-residues observed. "Match. Frag." are the number of assigned matching fragments.

ProSight Lite Fragmentation Pattern	Form	Mod.	m_e (Da)	m_t (Da)	Δm (Da)	P-Score	%Res. Cleav.	Match Frag.
(**a**) Originally assigned by PS *BioRep A—TechRep 02—Scan 349*	HPS2	-	9063.83	9002.75	61.084	1.10×10^{-91}	74	62
(**b**) Manual reassignation *BioRep A—TechRep R02—Scan 349*	HPS2	+1(61)	9063.83	9063.76	0.076	$7.60 \cdot \times 10^{-155}$	82	95
(**c**) Originally assigned by PS *BioRep A—TechRep R02—Scan 539*	HPS2	+2ph	9282.89	9162.68	120.213	$7.90 \cdot \times 10^{-38}$	52	35
(**d**) Manual reassignation *BioRep A—TechRep R02—Scan 539*	HPS1	+1pyroGlu	9282.89	9283.89	−0.992	$2.80 \cdot \times 10^{-103}$	74	75
(**e**) Originally assigned by PS *BioRep B—TechRep R04—Scan 545*	HPS1	+1ph +1AcNterm	9283.87	9422.89	−139.022	$9.70 \cdot \times 10^{-45}$	59	40
(**f**) Manual reassignation *BioRep B—TechRep R04—Scan 545*	HPS1	+1pyroGlu	9283.87	9283.89	−0.019	$1.18 \cdot \times 10^{-118}$	79	84

We considered diverging misassignment to be those cases in which PrSMs with very similar experimental deconvoluted masses (i.e., belonging to the same proteoform according to our clustering approach) were identified as different proteoforms. Both PS and TP tended to make this kind of mistake. Diverging misassignment translated into the identification of multiple proteoforms (according PS or TP) within one of our mass clusters. In particular, the average number of proteoforms per cluster according to PS and TP was 2.81 and 2.96, with extreme cases in which we found up to 9 and 5 proteoforms per cluster, respectively.

A clear example of this situation can be seen in Figure 3b (for PS and TP nodes) and Table 1. Note how the PS and TP nodes "diverged" those PrSMs with deconvoluted experimental mass around 9283 Da (cluster P|018) in up to nine and three distinct proteoforms, respectively. We consider that all these PrSMs should be assigned to an HPS1 proteoform with a pyroglutamic acid at the glutamine located in its N-terminus (−18.010565 Da). Similarly, as in the previous Section 3.2.1, we manually validated our hypothesis using ProSight Lite by including and localizing this pyroglutamic acid (Table 2d–f). Note how for two particular PrSMs, which PS originally assigned to HPS1 + 2 phosphorylations (Table 2c) and HPS2 + 1 phosphorylation + 1 N-term acetylation (Table 2e), both the P-Score and the number of matching fragments improved once we localized the pyroglutamic acid

at HPS1 N-terminus (Table 2d,f) (the first decreases from 7.9×10^{-38} to 2.8×10^{-103} and from 9.7×10^{-45} to 1.8×10^{-118}, respectively, and the second increases from 35 to 75 and from 40 to 85, respectively).

3.2.2. DBSCAN Approach Limitations

The DBSCAN approach was able to merge, harmonize and correct the PS and TP results but had some limitations. The three main limitations were (a) the requirement for previous knowledge of the sample to perform the final semi-manual annotation; (b) the assumption that the same mass meant the same proteoform when two amino acid sequences (with or without PTMs) may in fact have the same mass; and (c) some of the identified PrSMs remained unclustered and were discarded.

At the present stage of development, proteoform assignment to each cluster is semi-automatic and requires a minimum degree of manual validation and previous knowledge of the sample. We therefore believe that this approach can easily be applied to simple samples even when they have a large number of modifications, such as protamines or histones. However, we still have to check its viability in complex samples.

One of the strengths of the DBSCAN approach was also a limitation. We assumed that one mass corresponded to one proteoform without the modification localized. This assumption corrected and simplified the data, but could also lead to incorrect assignments. It is possible for two different proteoforms to have the same mass even if they have different amino acid sequences. To address this limitation and try to distinguish this kind of situation, we intend to add the retention time as a new parameter in the DBSCAN algorithm in a future version of the workflow. This modification would better differentiate and monitor proteforms of the same mass.

As stated in Section 3.1, the DBSCAN algorithm successfully clustered 2838 of the PrSMs, leaving 260 unclustered. Moreover, only one (P|026)—comprising an additional 28 PrSMs—out of 27 clusters was unknown. As a result, our approach left a total of 288 (10.1%) unclassified PrSMs (unclustered/unidentified). However, we observed that unclassified PrSMs showed overall poorer quality than classified ones (clustered/identified).

In particular, unclassified PrSMs had a lower mean E-value and intensity than classified PrSMs for both PS and TP (Figure S3). The mean of the -$\log_{10}$ of the E-value was 73.4 (PS) and 26.6 (TP) for the classified PrSMs and 32.3 (PS) and 11.1 (TP) for the unclassified ones. The mean of z-score normalized $\log_2$ intensities was 0.10 (PS) and 0.18 (TP) for the clustered PrSMs and -0.77 (PS) and -1.91 (TP) for the unclustered ones. The loss of 10.1% of all PrSMs is therefore not particularly concerning since it implies that low confidence matches are discarded.

The DBSCAN approach combines the strengths of the PS and TP nodes, in particular the high spectra identification rate of PS and the ability to identify proteoforms with an arbitrary mass shift of TP. The clustering approach also overcomes the weaknesses of the two nodes, like the two kinds of proteoform misassignment highlighted in Section 3.2.1.

3.3. Protamine Proteoform Landscape and Protamine Ratios

Our DBSCAN-based approach allowed us to identify a total of 26 protamine proteoforms. The protamine forms involved in this proteoform landscape were P1, pre-P2, HPI2, HPS1, HPS2, HP2, HP3 and HP4. Among the PTMs contributing to the landscape, we found phosphorylation, N-terminal cyclic pyroglutamyl, N-terminal glutamine loss and the +61 Da modification, which was discussed in Section 3.1.

To gain greater insight into this rich protamine proteoform landscape, we performed scatterplots for the cluster-protein mass shift associated with each protamine proteoform cluster (Δm_{CT} in Equation (2)) vs. the corresponding protamine forms so that each data point represents a different 1, 2A- or 3-level proteoform (Figure 4). We generated this scatterplot at three levels: global, by technical replicate, and by biological replicate (Figure 4, panels a, b and c, respectively).

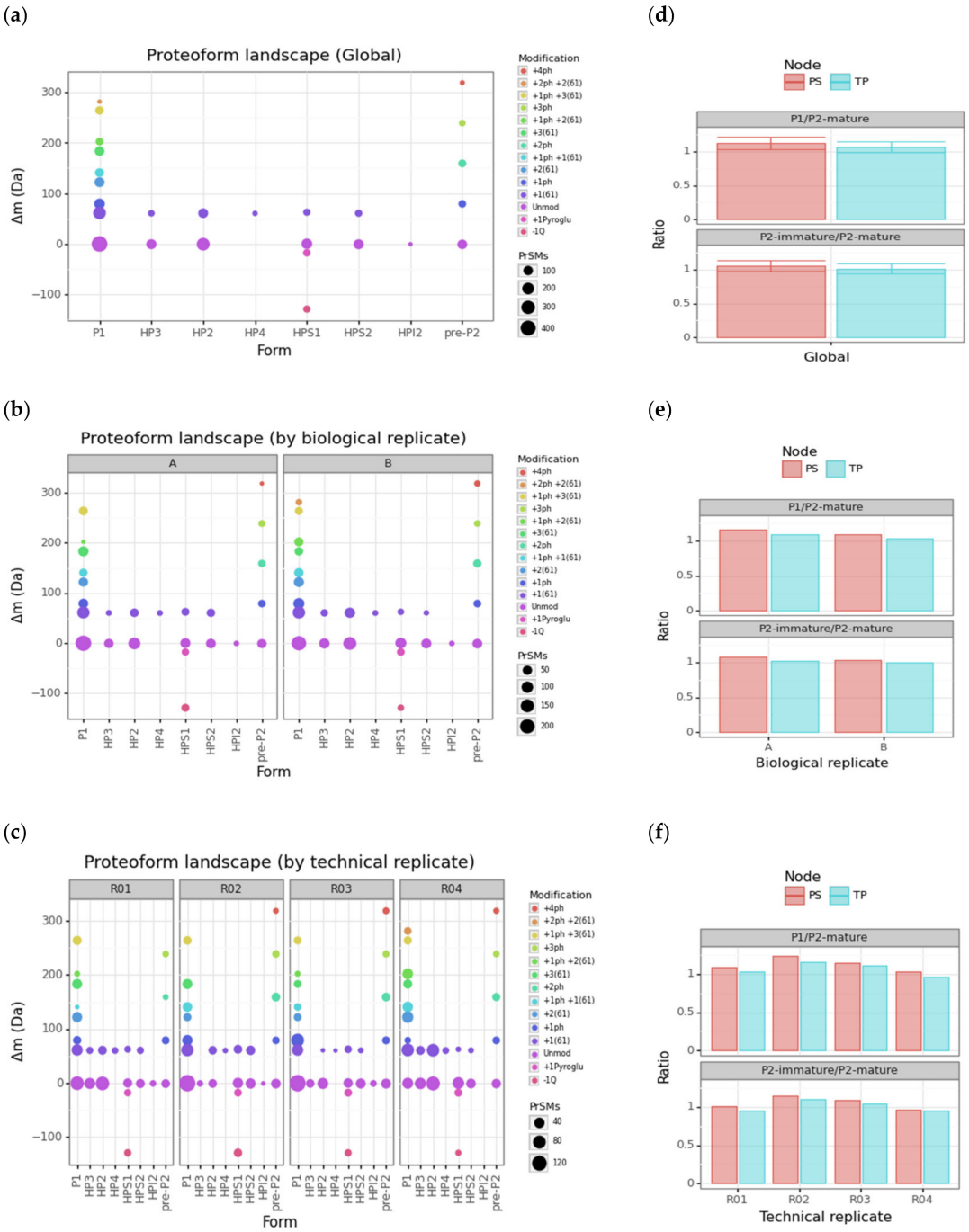


Figure 4. Protamine proteoform landscapes and ratios. (**a**–**c**) Scatterplot of the mass shift vs. the protamine form at global, biological replicate and technical replicate levels, respectively. The sequential color scale in these three scatterplots highlights the particular set of PTMs. The data point size is proportional to the number of PrSMs hitting the corresponding protamine proteoform. (**d**–**f**) Barplots with P1/P2-mature and P2-immature/P2-mature protamine ratios according to each node at global, biological replicate and technical replicate levels, respectively. Error bars correspond to standard deviations of associated technical replicates (ph = phosphorylation, Q = glutamine, pyroGlu = pyroglutamic acid).

Note how 22 out of 25 proteoforms appearing in biological replicate A are found within its two technical replicates R01 and R02 (exceptions are P1 +1ph +2(61), pre-P2 +4ph and HP3 +1(61)). Similarly, 24 out of 26 proteoforms appearing in biological replicate B are found within its two technical replicates R03 and R04 (exceptions are P1 +2ph +2(61) and HP3 +1(61)). The only proteoform not found in the two biological replicates was P1 +2ph +2(61). By revisiting Table 1, we checked that all these exceptions corresponded to clusters

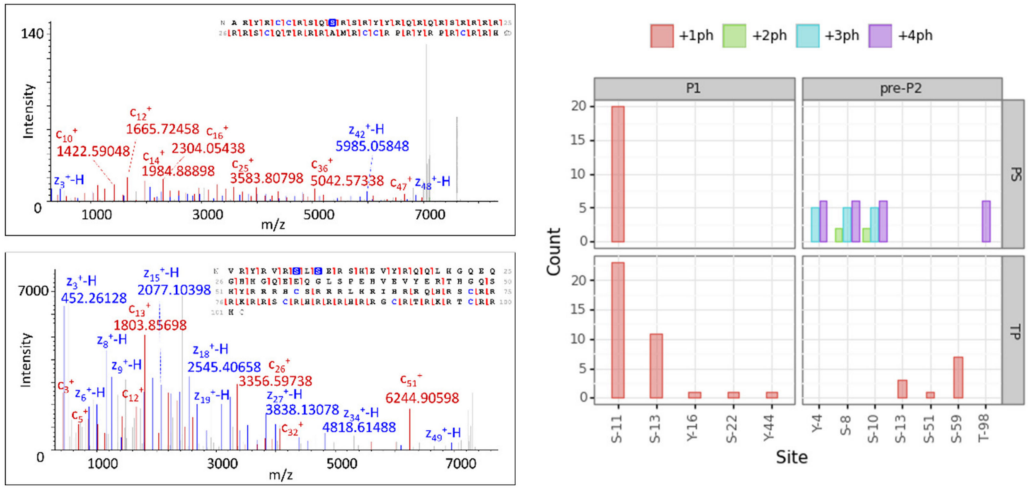
with limited PrSM counts. In particular: P1 +1ph +2(61) with 20 + 29 (TP + PS) counts; pre-P2 +4ph with 6 + 8; HP3 +1(61) with 13 + 17; and P1 +2ph +2(61) with 5 + 7. After inspecting the protamine proteoform landscapes at all levels, we saw that the performance of our characterization was acceptable for intertechnical replicate variability.

As an advantage over classical protamine ratio assessment through gel-staining approaches, our strategy enables computation of the abundance ratio between any protamine proteoforms. The ratio between P1 and P2 mature proteoforms (HP2, HP3, and HP4) is the ratio most widely used for the study of male infertility [3]. Alterations of the P2 family seem to be more frequent than those of P1, and the incomplete processing of the pre-P2 has also been linked to male infertility [55–57]. Therefore, the ratio of the different protamine proteoforms between immature proteoforms of P2, including pre-P2 and intermediate proteoforms (HPI2, HPS1, HPS2) and mature forms of P2, is highly relevant in the context of understanding the chromatin maturity state. We provided barplots for these two ratios (P1/P2-mature and P2-immature/P2-mature) at three levels: global, by technical replicate, and by biological replicate (Figure 4, panels d, e and f, respectively). To better monitor the contribution of each node in each ratio computation, we split them using a color scale. The P1/P2-mature and P2-immature/P2-mature ratios fall around 1 for our two biological replicates and their corresponding technical replicates. Note how PS gives slightly greater ratios than TP. However, this systematic discrepancy is smaller than associated standard deviations.

3.4. Modification Site Assignment

The DBSCAN cluster approach allowed us to identify modified proteoforms at level 2A or 3. We reached level 2A with phosphorylated proteoforms, but we did not localize the p-site. We reached level 2B classification for HPS2 +61 Da shown in Table 2c. However, this localization was done manually. Undertaking this task for all PrSMs would have been time-consuming, so we accepted that proteoforms modified with +61 Da were identified at level 3.

To reach level 1 of proteoform identification for phosphorylated proteoforms, we analyzed those modified PrSMs according to PS and TP. We took into account PrSMs with a 2A classification level that matched our cluster assignment and filtered those with a high localization confidence level (PTM localization probability > 75% in TP and C-Score > 40 in PS [58].). A total of 111 p-sites passed the filter (33% of the total), 63 for PS and 48 for TP. We manually checked two spectra for P1 +ph and P2 +2ph and their localization sites to be confident of the automatic assignment by the softwares (Figure 5, panel a). Both nodes found P1 and pre-P2 phosphorylated (P1 monophosphorylated and pre-P2 with one, two, three and four p-sites). PS and TP mainly localized the phosphorylation of P1 in site S-11 with 20 and 23 PrSMs, respectively. TP also found PrSMs with the phosphorylation site in S-13, Y-16, S-22 and Y-44. While S-13 was identified with 11 PrSMs, the other three sites were identified with only one PrSM each. However, PS and TP showed a distinct behavior when localizing p-sites in pre-P2. TP found pre-P2 monophosphorylated in S-59, S-13 and S-51 and PS found pre-P2 bi-phosphorylated in S-8 and S-10, tri-phosphorylated in Y-4, S-8 and S-10 and tetra-phosphorylated in Y-4, S-8, S-10 and T-98 (Figure 5, panel b). Given the above observations, we concluded that TP tends to localize mono-phosphorylations while PS performs better at localizing multiple sites.



(**a**) (**b**)

Figure 5. Protamine proteoform phosphosite localization analysis. (**a**) MS2 deconvoluted spectra and their fragment map of P1 +ph (up) and P2 +2ph (down) showing all detected c and z ions and p-site localizations (phosphorylated amino acids are marked in blue). (**b**) Barplots report the number of PrSMs hitting the corresponding localization site. The faceting grid breaks down the phosphosite count for P1 and pre-P2 protamine forms (left and right), as well as for each node (up and down). Color scale denotes the number of phosphorylations coexisting in the same sequence (ph = phosphorylation).

Protamine phosphorylation sites have been studied in humans and other mammalian species through conventional approaches [15,59–62]. For instance, protamine 1 phosphorylation at S11 has been described in humans and is conserved among other species, as well as at S9 and S29 residues [24,63–65]. Regarding pre-P2, phosphorylation sites have been identified at S8, S10, S37, T47, S51, S59 and S73 [24,63–65]. Our results not only are consistent with these previous evidences, but also have allowed the identification of novel proteoforms in the human sperm [31]. These results support this new DBSCAN-based strategy combining PS and TP as a robust approach for identifying site-specific mono- and poly-phosphorylated human protamines.

4. Conclusions

Our clustering approach combined the strengths, and overcame the weaknesses, of two popular top-down proteomics bioinformatics tools: ProSight PD (PS) and TopPIC Suite (TP). We showed the usefulness of the DBSCAN algorithm to solve some of the misassignments found when analyzing top-down database searches provided by these two nodes. From a qualitative viewpoint, and despite the limited number of biological replicates available (n = 2), our proteoform characterization showed good reproducibility across individuals since only a level 3 proteoform was not identified in both biological replicates, namely, P1 +2ph +2(61). With this strategy, we identified 13 proteoforms of P1 and 19 proteoforms of P2, 11 of them with the p-site localized. Our results highlighted the capacity of our clustering approach to characterize purified small proteins with a high number of truncated forms or PTMs. The possibility of examining alterations through studying individual protamine proteoforms, including the assessment of specific modified proteoforms, is a first step towards a personalized diagnosis.

Supplementary Materials: The following are available online at https://www.mdpi.com/article/10.3390/proteomes9020021/s1, Figure S1: Scatterplots of the intensity vs. the deconvoluted experimental mass and the retention time for PS and TP by cluster, Figure S2: Scatterplots of the retention time vs. the deconvoluted experimental mass by proteoform ID. Figure S3: Boxplot of -$\log_{10}$ E-value and z-score of $\log_2$ intensity vs. Node by outcome. Table S1: Protamine proteform cluster annotation table. Table S2: Harmonized PrSMs dataset including clustering outcome and proteform annotation. The Python code we implemented to perform the data analysis and to

generate some figures (Figures 3–5; Supplementary Figures S1–S3) and tables appearing on this paper (Table 1; Supplementary Table S1 and S2) is available on the following GitHub repository: https://github.com/MSPCF/2021_Proteomes.

Author Contributions: Conceptualization, G.A.-G., R.O., M.V. (Marta Vilaseca), and M.G.; methodology, A.S.-V., J.C., A.d.l.I.R., M.J., and M.V. (Mar Vilanova); software, G.A.-G. and M.G.; validation, G.A.-G. and M.G.; formal analysis, G.A.-G. and M.G.; investigation, A.S.-V., J.C., A.d.l.I.R., M.J., and M.V. (Mar Vilanova); resources, R.O. and M.V. (Marta Vilaseca); data curation, G.A.-G. and M.G.; writing—original draft preparation, G.A.-G. and M.G.; writing—review and editing, G.A.-G., M.J., M.V. (Mar Vilanova), A.d.l.I.R., J.C., A.S.-V., R.O., M.V. (Marta Vilaseca), and M.G.; visualization, G.A.-G. and M.G.; supervision, M.J., M.G.; project administration, R.O. and M.V. (Marta Vilaseca); funding acquisition, R.O. and M.V. (Marta Vilaseca). All authors have read and agreed to the published version of the manuscript.

Funding: IRB Barcelona Mass Spectrometry and Proteomics Core Facility is a principal unit of Proteored, PRB3-ISCIII, supported by grant PRB3 (IPT17/0019 - ISCIII-SGEFI/ERDF. GA was cofinanced from 01/01/2018-31/12/2021 with grant reference: PT17/0019/0022 (Plataforma de Proteómica, Genotipado y Líneas celulares, PRB3) in the frame of the "Plataforma de apoyo a la Investigación en Ciencias y Tecnología de la Salud de la convocatoria de 2017 de la Acción Estratégica en Salud 2013-2016 of Instituto de Salud Carlos III (ISCIII)". The Proteomics unit is granted for the set up and development of the Biomedical Proteomics Platform (IRB Barcelona's Unit) for biomedical and translational Research. Co-financed by the European Regional Development Fund (ERDF), in the framework of the 2014–2020 ERDF Operational Programme in Catalonia, with EUR 519,500. Reference: IU16-015983. Supported by the Spanish Ministerio de Ciencia e Innovación; fondos FEDER 'una manera de hacer Europa', Proyectos de Investigación en Salud (ISCIII), PI16/00346 and PI20/00936 to R.O, and by Sara Borrell Postdoctoral Fellowship, Acción Estratégica en Salud, CD17/00109 to J.C.

Institutional Review Board Statement: The study was conducted according to the guidelines of the Declaration of Helsinki, and approved by the Clinical Research Ethics Committee of the Hospital Clínic de Barcelona (Barcelona, Spain, protocol approval code 2012/7942).

Informed Consent Statement: Informed consent was obtained from all subjects involved in the study.

Data Availability Statement: The mass spectrometry proteomics data have been deposited to the ProteomeXchange Consortium via the PRIDE [39] partner repository with the dataset identifier PXD024405.

Acknowledgments: We would like to thank the whole developing team behind TopPIC Suite. We are particularly grateful to Xiaowen Liu and In Kwon Choi for their extremely efficient support. We thank Mick Greer, Joseph Greer and Neil Kelleher for their support with ProSight PD. Thanks to Tanya Yates from the IRB Editorial support. Finally, we are grateful to the whole IRB Mass Spec & Proteomics team for their professionality and effort.

Conflicts of Interest: The authors declare no conflict of interest.

References

1. Oliva, R.; Dixon, G.H. Vertebrate protamine genes and the histone-to-protamine replacement reaction. *Prog. Nucleic Acid Res. Mol. Biol.* **1991**, *40*, 25–94. [CrossRef] [PubMed]
2. Balhorn, R. The protamine family of sperm nuclear proteins. *Genome Biol.* **2007**, *8*, 227. [CrossRef]
3. Castillo, J.; Simon, L.; de Mateo, S.; Lewis, S.; Oliva, R. Protamine/DNA ratios and DNA damage in native and density gradient centrifuged sperm from infertile patients. *J. Androl.* **2011**, *32*, 324–332. [CrossRef]
4. Oliva, R. Protamines and male infertility. *Hum. Reprod. Update* **2006**, *12*, 417–435. [CrossRef]
5. Mezquita, C. Chromatin composition, structure and function in spermatogenesis. *Revis. Biol. Celular* **1985**, *5*, 1–124.
6. Kimmins, S.; Sassone-Corsi, P. Chromatin remodelling and epigenetic features of germ cells. *Nature* **2005**, *434*, 583–589. [CrossRef]
7. Oliva, R.; Krawetz, S.A.; GHD Consortium. Gordon Henry Dixon. 25 March 1930–24 July 2016. *Biogr. Mems Fell. R. Soc.* **2020**. [CrossRef]
8. Hud, N.V.; Downing, K.H.; Balhorn, R. A constant radius of curvature model for the organization of DNA in toroidal condensates. *Proc. Natl. Acad. Sci. USA* **1995**, *92*, 3581–3585. [CrossRef]
9. Ward, W.S. Function of sperm chromatin structural elements in fertilization and development. *Mol. Hum. Reprod.* **2010**, *16*, 30–36. [CrossRef]
10. Balhorn, R.; Corzett, M.; Mazrimas, J.A. Formation of intraprotamine disulfides in vitro. *Arch. Biochem. Biophys.* **1992**, *296*, 384–393. [CrossRef]

11. Björndahl, L.; Kvist, U. Human sperm chromatin stabilization: A proposed model including zinc bridges. *Mol. Hum. Reprod.* **2010**, *16*, 23–29. [CrossRef]
12. Oliva, R.; Castillo, J. Proteomics and the genetics of sperm chromatin condensation. *Asian J. Androl.* **2011**, *13*, 24–30. [CrossRef]
13. Zini, A.; Agarwal, A. *Sperm Chromatin: Biological and Clinical Applications in Male Infertility and Assisted Reproduction*; Springer Science & Business Media: Berlin/Heidelberg, Germany, 2011; ISBN 9781441968579.
14. Lüke, L.; Tourmente, M.; Roldan, E.R.S. Sexual Selection of Protamine 1 in Mammals. *Mol. Biol. Evol.* **2016**, *33*, 174–184. [CrossRef]
15. Kasinsky, H.E.; Eirín-López, J.M.; Ausió, J. Protamines: Structural complexity, evolution and chromatin patterning. *Protein Pept. Lett.* **2011**, *18*, 755–771. [CrossRef] [PubMed]
16. Castillo, J.; Estanyol, J.M.; Ballescá, J.L.; Oliva, R. Human sperm chromatin epigenetic potential: Genomics, proteomics, and male infertility. *Asian J. Androl.* **2015**, *17*, 601–609. [CrossRef] [PubMed]
17. Castillo, J.; Jodar, M.; Oliva, R. The contribution of human sperm proteins to the development and epigenome of the preimplantation embryo. *Hum. Reprod. Update* **2018**, *24*, 535–555. [CrossRef]
18. Gatewood, J.M.; Cook, G.R.; Balhorn, R.; Bradbury, E.M.; Schmid, C.W. Sequence-specific packaging of DNA in human sperm chromatin. *Science* **1987**, *236*, 962–964. [CrossRef] [PubMed]
19. Arpanahi, A.; Brinkworth, M.; Iles, D.; Krawetz, S.A.; Paradowska, A.; Platts, A.E.; Saida, M.; Steger, K.; Tedder, P.; Miller, D. Endonuclease-sensitive regions of human spermatozoal chromatin are highly enriched in promoter and CTCF binding sequences. *Genome Res.* **2009**, *19*, 1338–1349. [CrossRef]
20. Hammoud, S.S.; Nix, D.A.; Zhang, H.; Purwar, J.; Carrell, D.T.; Cairns, B.R. Distinctive chromatin in human sperm packages genes for embryo development. *Nature* **2009**, *460*, 473–478. [CrossRef]
21. Castillo, J.; Amaral, A.; Azpiazu, R.; Vavouri, T.; Estanyol, J.M.; Ballescà, J.L.; Oliva, R. Genomic and proteomic dissection and characterization of the human sperm chromatin. *Mol. Hum. Reprod.* **2014**, *20*, 1041–1053. [CrossRef]
22. Jodar, M.; Oliva, R. Protamine alterations in human spermatozoa. *Adv. Exp. Med. Biol.* **2014**, *791*, 83–102. [CrossRef] [PubMed]
23. Ni, K.; Spiess, A.-N.; Schuppe, H.-C.; Steger, K. The impact of sperm protamine deficiency and sperm DNA damage on human male fertility: A systematic review and meta-analysis. *Andrology* **2016**, *4*, 789–799. [CrossRef]
24. Barrachina, F.; Soler-Ventura, A.; Oliva, R.; Jodar, M. Sperm Nucleoproteins (Histones and Protamines). In *A Clinician's Guide to Sperm DNA and Chromatin Damage*; Springer: Cham, Switzerland, 2018; pp. 31–51.
25. Nanassy, L.; Liu, L.; Griffin, J.; Carrell, D.T. The clinical utility of the protamine 1/protamine 2 ratio in sperm. *Protein Pept. Lett.* **2011**, *18*, 772–777. [CrossRef]
26. De Yebra, L.; Oliva, R. Rapid analysis of mammalian sperm nuclear proteins. *Anal. Biochem.* **1993**, *209*, 201–203. [CrossRef]
27. Soler-Ventura, A.; Castillo, J.; de la Iglesia, A.; Jodar, M.; Barrachina, F.; Ballesca, J.L.; Oliva, R. Mammalian Sperm Protamine Extraction and Analysis: A Step-By-Step Detailed Protocol and Brief Review of Protamine Alterations. *Protein Pept. Lett.* **2018**, *25*, 424–433. [CrossRef]
28. Bogle, O.A.; Kumar, K.; Attardo-Parrinello, C.; Lewis, S.E.M.; Estanyol, J.M.; Ballescà, J.L.; Oliva, R. Identification of protein changes in human spermatozoa throughout the cryopreservation process. *Andrology* **2017**, *5*, 10–22. [CrossRef] [PubMed]
29. De Mateo, S.; Ramos, L.; van der Vlag, J.; de Boer, P.; Oliva, R. Improvement in chromatin maturity of human spermatozoa selected through density gradient centrifugation. *Int. J. Androl.* **2011**, *34*, 256–267. [CrossRef]
30. Wang, T.; Gao, H.; Li, W.; Liu, C. Essential Role of Histone Replacement and Modifications in Male Fertility. *Front. Genet.* **2019**, *10*, 962. [CrossRef]
31. Soler-Ventura, A.; Gay, M.; Jodar, M.; Vilanova, M.; Castillo, J.; Arauz-Garofalo, G.; Villarreal, L.; Ballescà, J.L.; Vilaseca, M.; Oliva, R. Characterization of Human Sperm Protamine Proteoforms through a Combination of Top-Down and Bottom-Up Mass Spectrometry Approaches. *J. Proteome Res.* **2020**, *19*, 221–237. [CrossRef]
32. LeDuc, R.D.; Taylor, G.K.; Kim, Y.-B.; Januszyk, T.E.; Bynum, L.H.; Sola, J.V.; Garavelli, J.S.; Kelleher, N.L. ProSight PTM: An integrated environment for protein identification and characterization by top-down mass spectrometry. *Nucleic Acids Res.* **2004**, *32*, W340–W345. [CrossRef] [PubMed]
33. Frank, A.M.; Pesavento, J.J.; Mizzen, C.A.; Kelleher, N.L.; Pevzner, P.A. Interpreting top-down mass spectra using spectral alignment. *Anal. Chem.* **2008**, *80*, 2499–2505. [CrossRef] [PubMed]
34. Kou, Q.; Xun, L.; Liu, X. TopPIC: A software tool for top-down mass spectrometry-based proteoform identification and characterization. *Bioinformatics* **2016**, *32*, 3495–3497. [CrossRef] [PubMed]
35. Kou, Q.; Wu, S.; Tolic, N.; Paša-Tolic, L.; Liu, Y.; Liu, X. A mass graph-based approach for the identification of modified proteoforms using top-down tandem mass spectra. *Bioinformatics* **2017**, *33*, 1309–1316. [CrossRef]
36. Cooper, T.G.; Noonan, E.; von Eckardstein, S.; Auger, J.; Baker, H.W.G.; Behre, H.M.; Haugen, T.B.; Kruger, T.; Wang, C.; Mbizvo, M.T.; et al. World Health Organization reference values for human semen characteristics. *Hum. Reprod. Update* **2010**, *16*, 231–245. [CrossRef] [PubMed]
37. Mengual, L.; Ballescá, J.L.; Ascaso, C.; Oliva, R. Marked differences in protamine content and P1/P2 ratios in sperm cells from percoll fractions between patients and controls. *J. Androl.* **2003**, *24*, 438–447. [CrossRef]
38. Aebersold, R.; Agar, J.N.; Jonathan Amster, I.; Baker, M.S.; Bertozzi, C.R.; Boja, E.S.; Costello, C.E.; Cravatt, B.F.; Fenselau, C.; Garcia, B.A.; et al. How many human proteoforms are there? *Nat. Chem. Biol.* **2018**, *14*, 206–214. [CrossRef]

39. Perez-Riverol, Y.; Csordas, A.; Bai, J.; Bernal-Llinares, M.; Hewapathirana, S.; Kundu, D.J.; Inuganti, A.; Griss, J.; Mayer, G.; Eisenacher, M.; et al. The PRIDE database and related tools and resources in 2019: Improving support for quantification data. *Nucleic Acids Res.* **2019**, *47*, D442–D450. [CrossRef]
40. 3.9.1 Documentation. Available online: https://docs.python.org/3/ (accessed on 30 December 2020).
41. McKinney, W. Data Structures for Statistical Computing in Python. In Proceedings of the 9th Python in Science Conference, Austin, TX, USA, 3–8 July 2010; pp. 56–61.
42. Harris, C.R.; Millman, K.J.; van der Walt, S.J.; Gommers, R.; Virtanen, P.; Cournapeau, D.; Wieser, E.; Taylor, J.; Berg, S.; Smith, N.J.; et al. Array programming with NumPy. *Nature* **2020**, *585*, 357–362. [CrossRef]
43. Cock, P.J.A.; Antao, T.; Chang, J.T.; Chapman, B.A.; Cox, C.J.; Dalke, A.; Friedberg, I.; Hamelryck, T.; Kauff, F.; Wilczynski, B.; et al. Biopython: Freely available Python tools for computational molecular biology and bioinformatics. *Bioinformatics* **2009**, *25*, 1422–1423. [CrossRef]
44. Kibirige, H.; Lamp, G.; Katins, J.; Gdowding; Austin, O.; Matthias, K.; Funnell, T.; Finkernagel, F.; Arnfred, J.; Blanchard, D.; et al. *has2k1/Plotnine; v0.7.1*; Zenodo: Genève, Switzerland, 2020. [CrossRef]
45. Waskom, M.; Gelbart, M.; Botvinnik, O.; Ostblom, J.; Hobson, P.; Lukauskas, S.; Gemperline, D.C.; Augspurger, T.; Halchenko, Y.; Warmenhoven, J.; et al. *Mwaskom/Seaborn*; v0.11.1; Zenodo: Genève, Switzerland, 2020. [CrossRef]
46. Schubert, E.; Sander, J.; Ester, M.; Kriegel, H.P.; Xu, X. DBSCAN Revisited, Revisited. *ACM Trans. Database Syst.* **2017**, *42*, 1–21. [CrossRef]
47. Ester, M.; Kriegel, H.-P.; Sander, J.; Xu, X. *A Density-Based Algorithm for Discovering Clusters in Large Spatial Databases with Noise*; Association for the Advancement of Artificial Intelligence: Palo Alto, CA, USA, 1996.
48. Pedregosa, F.; Varoquaux, G.; Gramfort, A.; Michel, V.; Thirion, B.; Grisel, O.; Blondel, M.; Prettenhofer, P.; Weiss, R.; Dubourg, V.; et al. Scikit-learn: Machine Learning in Python. *J. Mach. Learn. Res.* **2011**, *12*, 2825–2830.
49. Van de Ven, B. Bokeh. Available online: https://bokeh.org/ (accessed on 29 January 2021).
50. Smith, L.M.; Thomas, P.M.; Shortreed, M.R.; Schaffer, L.V.; Fellers, R.T.; LeDuc, R.D.; Tucholski, T.; Ge, Y.; Agar, J.N.; Anderson, L.C.; et al. A five-level classification system for proteoform identifications. *Nat. Methods* **2019**, *16*, 939–940. [CrossRef] [PubMed]
51. Bianchi, F.; Rousseaux-Prevost, R.; Sautiere, P.; Rousseaux, J. P2 protamines from human sperm are zinc -finger proteins with one CYS2/HIS2 motif. *Biochem. Biophys. Res. Commun.* **1992**, *182*, 540–547. [CrossRef]
52. Roskamp, K.W.; Azim, S.; Kassier, G.; Norton-Baker, B.; Sprague-Piercy, M.A.; Miller, R.J.D.; Martin, R.W. Human γS-Crystallin-Copper Binding Helps Buffer against Aggregation Caused by Oxidative Damage. *Biochemistry* **2020**, *59*, 2371–2385. [CrossRef]
53. Liu, H.; Ponniah, G.; Zhang, H.-M.; Nowak, C.; Neill, A.; Gonzalez-Lopez, N.; Patel, R.; Cheng, G.; Kita, A.Z.; Andrien, B. In vitro and in vivo modifications of recombinant and human IgG antibodies. *MAbs* **2014**, *6*, 1145–1154. [CrossRef]
54. Fellers, R.T.; Greer, J.B.; Early, B.P.; Yu, X.; LeDuc, R.D.; Kelleher, N.L.; Thomas, P.M. ProSight Lite: Graphical software to analyze top-down mass spectrometry data. *Proteomics* **2015**, *15*, 1235–1238. [CrossRef] [PubMed]
55. De Yebra, L.; Ballescà, J.L.; Vanrell, J.A.; Bassas, L.; Oliva, R. Complete selective absence of protamine P2 in humans. *J. Biol. Chem.* **1993**, *268*, 10553–10557. [CrossRef]
56. Torregrosa, N.; Domínguez-Fandos, D.; Camejo, M.I.; Shirley, C.R.; Meistrich, M.L.; Ballescà, J.L.; Oliva, R. Protamine 2 precursors, protamine 1/protamine 2 ratio, DNA integrity and other sperm parameters in infertile patients. *Hum. Reprod.* **2006**, *21*, 2084–2089. [CrossRef] [PubMed]
57. De Mateo, S.; Gázquez, C.; Guimerà, M.; Balasch, J.; Meistrich, M.L.; Ballescà, J.L.; Oliva, R. Protamine 2 precursors (Pre-P2), protamine 1 to protamine 2 ratio (P1/P2), and assisted reproduction outcome. *Fertil. Steril.* **2009**, *91*, 715–722. [CrossRef]
58. LeDuc, R.D.; Fellers, R.T.; Early, B.P.; Greer, J.B.; Thomas, P.M.; Kelleher, N.L. The C-score: A Bayesian framework to sharply improve proteoform scoring in high-throughput top down proteomics. *J. Proteome Res.* **2014**, *13*, 3231–3240. [CrossRef]
59. Gusse, M.; Sautière, P.; Bélaiche, D.; Martinage, A.; Roux, C.; Dadoune, J.P.; Chevaillier, P. Purification and characterization of nuclear basic proteins of human sperm. *Biochim. Biophys. Acta* **1986**, *884*, 124–134. [CrossRef]
60. Pruslin, F.H.; Imesch, E.; Winston, R.; Rodman, T.C. Phosphorylation state of protamines 1 and 2 in human spermatids and spermatozoa. *Gamete Res.* **1987**, *18*, 179–190. [CrossRef]
61. Arkhis, A.; Martinage, A.; Sautiere, P.; Chevaillier, P. Molecular structure of human protamine P4 (HP4), a minor basic protein of human sperm nuclei. *Eur. J. Biochem.* **1991**, *200*, 387–392. [CrossRef] [PubMed]
62. Papoutsopoulou, S.; Nikolakaki, E.; Chalepakis, G.; Kruft, V.; Chevaillier, P.; Giannakouros, T. SR protein-specific kinase 1 is highly expressed in testis and phosphorylates protamine 1. *Nucleic Acids Res.* **1999**, *27*, 2972–2980. [CrossRef]
63. Chirat, F.; Arkhis, A.; Martinage, A.; Jaquinod, M.; Chevaillier, P.; Sautière, P. Phosphorylation of human sperm protamines HP1 and HP2: Identification of phosphorylation sites. *Biochim. Biophys. Acta* **1993**, *1203*, 109–114. [CrossRef]
64. Pirhonen, A.; Linnala-Kankkunen, A.; Mäenpää, P.H. Identification of phosphoseryl residues in protamines from mature mammalian spermatozoa. *Biol. Reprod.* **1994**, *50*, 981–986. [CrossRef] [PubMed]
65. Hornbeck, P.V.; Zhang, B.; Murray, B.; Kornhauser, J.M.; Latham, V.; Skrzypek, E. PhosphoSitePlus, 2014: Mutations, PTMs and recalibrations. *Nucleic Acids Res.* **2015**, *43*, D512–D520. [CrossRef] [PubMed]

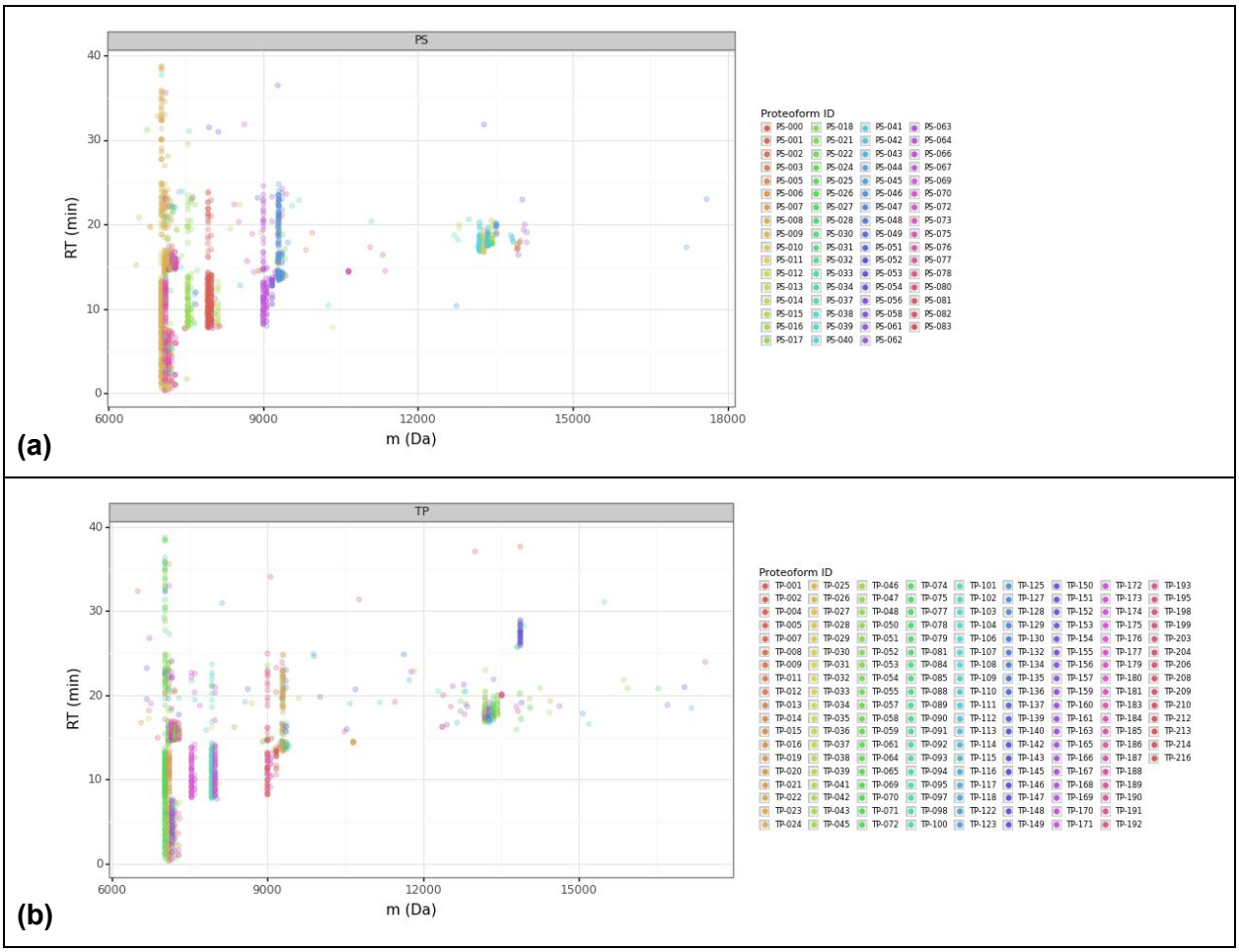


Figure S1. Scatterplots of the retention time (*RT*) vs. the deconvoluted experimental mass (*m*) by proteoform ID. The sequential color scale highlights the proteoform IDs assigned to each PrSM according to a) PS or b) TP.

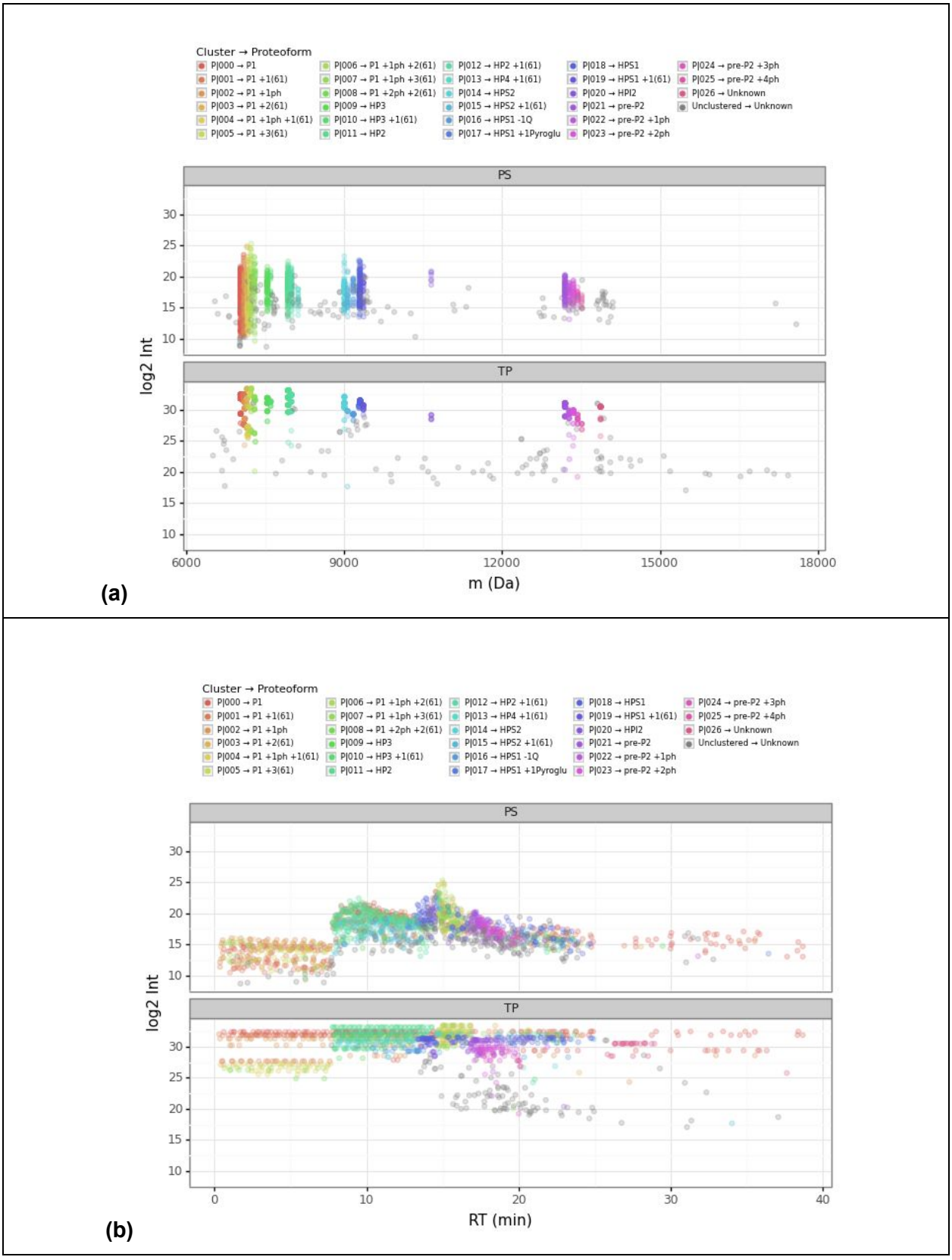


Figure S2. Scatterplots of the intensity (*log2 Int*) vs. the deconvoluted experimental mass (*m*) and the retention time (*RT*) for PS and TP by cluster. The sequential color scale highlights the clusters obtained sorted by increasing experimental mass, while unclustered PrSMs appear in grey. a) *log2 Int* vs. *m* projection. b) *log2 Int* vs. *RT* projection. (ph = phosphorylation, Q = glutamine, pyroGlu = pyroglutamic acid).

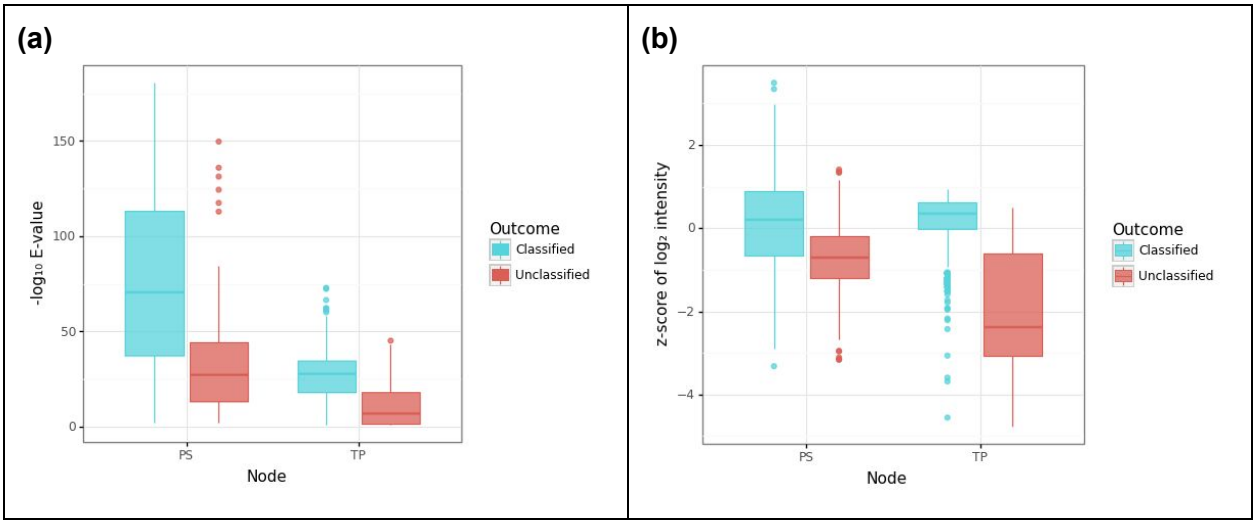


Figure S3. Boxplot of -$\log_{10}$ E-value and z-score of $\log_2$ intensity vs. Node by outcome (classified and unclassified PrSMs).

To download Supplementary Tables from the work “Protamine Characterization by Top-Down Proteomics: Boosting Proteoform Identification with DBSCAN” (https://doi.org/10.3390/proteomes9020021), please visit this link: https://www.mdpi.com/2227-7382/9/2/21#supplementary

Or scan the following QR code:

5.2.2 Work 4: Alterations in the abundance of specific protamine proteoforms related to sperm chromatin packaging, obesity status, and age in men with unexplained infertility

To be submitted as:

Castillo J[1,#,*], Gay M[2,#], **de la Iglesia A[1,#]**, Arauz-Garofalo G[2], Vilanova M[2], Corral JM[3,4], Guimerà M[4], Vilaseca M[2,*], Jodar M[1,5,*], Oliva R[1,5,*]. Alterations in the abundance of specific protamine proteoforms related to sperm chromatin packaging, obesity status, and age in men with unexplained infertility.

1 Molecular Biology of Reproduction and Development Research Group, Department of Biomedical Sciences, Faculty of Medicine and Health Sciences, Institut d'Investigacions Biomèdiques August Pi i Sunyer (IDIBAPS), Fundació Clínic per a la Recerca Biomèdica, Universitat de Barcelona, Barcelona, Spain.

2 Institute for Research in Biomedicine (IRB Barcelona), The Barcelona Institute of Science and Technology (BIST), Barcelona, Spain.

3 Urology Service, Andrology Unit, Nephrology and Urology Clinical Institute (ICNU), Hospital Clínic de Barcelona, Barcelona, Spain.

4 Gynecology, Obstetrics and Neonatology Clinical Institute (ICGON), Hospital Clínic de Barcelona, Barcelona, Spain.

5 Biochemistry and Molecular Genetics Service, Hospital Clínic de Barcelona, Barcelona, Spain.

# The authors contributed equally to this work

* Corresponding authors

Manuscript in preparation

Alterations in the abundance of specific protamine proteoforms related to sperm chromatin packaging, obesity status, and age in men with unexplained infertility

Judit Castillo[1,#,*], Marina Gay[2,#], Alberto de la Iglesia[1,#], Gianluca Arauz-Garofalo[2], Mar Vilanova[2], Juan Manuel Corral[3], Marta Guimerà[4], Marta Vilaseca[2,*], Meritxell Jodar[1,5,*], Rafael Oliva[1,5,*]

[1] Molecular Biology of Reproduction and Development Research Group, Institut d'Investigacions Biomèdiques August Pi i Sunyer (IDIBAPS), Fundació Clínic per a la Recerca Biomèdica (FCRB), Facultat de Medicina i Ciències de la Salut, Universitat de Barcelona (UB), Barcelona, Spain.
[2] Institute for Research in Biomedicine (IRB Barcelona), The Barcelona Institute of Science and Technology (BIST), Barcelona, Spain.
[3] Urology Service, Andrology Unit, Nephrology and Urology Clinical Institute (ICNU), Hospital Clínic de Barcelona, Barcelona, Spain.
[4] Gynecology, Obstetrics and Neonatology Clinical Institute (ICGON), Hospital Clínic de Barcelona, Barcelona, Spain.
[5] Biochemistry and Molecular Genetics Service, Hospital Clínic de Barcelona, Barcelona, Spain.
[#] The authors contributed equally to this work
[*] Corresponding authors: Judit Castillo (juditcastillo@ub.edu), Rafael Oliva (roliva@ub.edu), and Meritxell Jodar (meritxell.jodar@ub.edu)

Abstract

Among the more than 6,000 proteins described in the human sperm, protamines are considered the most relevant nuclear proteins because of their functional implications. Protamines compact most of the paternal genome, resulting in a semi-crystalline chromatin structure needed to achieve proper sperm functionality and DNA protection. Human and mouse sperm contain a complex population of protamine proteoforms, including intact, truncated, and modified forms for protamine 1 (P1), and mature and immature components of protamine 2 family (P2). This complex proteoform scenario raises the interest on deciphering whether it responds to the need of protein redundancy to ensure proper chromatin compaction, or whether there is any still unknown functional implication of specific protamine proteoforms. Furthermore, while altered P1 and P2 relative protein levels have been associated with male infertility, specific proteoform alterations implicated in such deregulation are yet unknown. In this study, we apply Top-Down Mass Spectrometry to identify quantitative alterations in the protamine proteoform profile of normozoospermic men with unexplained infertility relying on main three factors, abnormal P1/P2 ratio, obesity, and age. Accumulation of the P2 immature forms HPS1 and HPI2 was associated to higher P1/P2 ratios, suggesting an impaired processing of P2 in these patients. When considering weight and age as factors, alterations on P1 modified proteoforms were identified. While men with body mass index over 30 revealed alterations in proteoforms with mass shift(s) of +61 Da, either phosphorylated or not, a specific loss of diphosphorylated P1 has been detected in

advanced age men. These results point to alterations on protamine modifying mechanisms, as proteolysis and phosphorylation, rather than on protamine synthesis, as critical factors for proper sperm chromatin maturity with impact on male fertility.

Keywords: protamine, sperm chromatin, proteoform, top-down proteomics, male infertility, phosphorylation, DBSCAN

INTRODUCTION

Protamines are considered the most relevant mature sperm nuclear proteins due to their highly specific function of chromatin compaction into semi crystalline structures, that enable paternal genome protection from external damage and nuclear streamlining for a proper sperm functionality (Barrachina et al., 2018; Oliva, 2006; Oliva & Castillo, 2011). Their short and characteristic aminoacidic sequence, which is arginine-rich and contains cysteine residues, result in highly basic proteins with potential to form inter- and intra-molecular disulfide bonds. These unique physicochemical properties lead to extremely tight genome packaging into structural units that can wrap ~250-fold more DNA than nucleosomes (Balhorn, 2007; Castillo et al., 2014; Oliva, 2006).

Protamines' specific function, conserved among mammals, might lead to think of high stability in terms of protein sequence and low isoform variability. However, the actual scenario is that a complex protamine proteoforms landscape has been identified in human and mouse sperm (Arauz-Garofalo et al., 2021; Brunner et al., 2014; Castillo et al., 2015; Soler-Ventura et al., 2020). Human sperm contain two types of protamines: protamine 1 (P1), translated as mature protein from a single gene (*PRM1*), and protamine 2 family (P2), translated from *PRM2* gene as a precursor (pre-P2) that is then proteolyzed into three mature components: HP2, HP3, and HP4, being HP2 the most abundant. Apart from mature protamines, truncated forms of P1, pre-P2, and additional P2 immature proteoforms (HPI1, HPI2, HPS1, HPS2), with still unknown function, have been identified (Arauz-Garofalo et al., 2021; de Mateo et al., 2011; Soler-Ventura et al., 2020). This highly diverse profile of protamine proteoforms in the normal and mature male gamete raise the question of whether it respond to redundancy ensuring chromatin compaction, or there is some proteoform-specific functional implication the deregulation of which would impact male fertility.

An additional level of complexity is added considering that protamine proteoforms of different mammalian species bear post-translational modifications (PTMs) (Arauz-Garofalo et al., 2021; Brunner et al., 2014; Castillo et al., 2015; Chirat et al., 1993; Pirhonen et al., 1994; Pruslin et al., 1987; Soler-Ventura et al., 2020). Adapting mass spectrometry (MS) approaches and proteoform identification algorithms to the challenging characteristics of protamines, our group has described

the most complete protamine phosphorylation profile in human sperm. Addition of 1, 2, or 3 phosphate groups in P1 molecules, 1 or 2 in P2 mature forms, and up to 4 phosphorylated residues in pre-P2 was described (Soler-Ventura et al., 2020). Besides the role of protamine phosphorylation in testicular protamine incorporation during spermiogenesis (Gou et al., 2020; Papoutsopoulou et al., 1999; Willmitzer et al., 1977b, 1977a; Wu et al., 2000), their presence in mature sperm suggest implications towards sperm function, oocyte fertilization and beyond. Indeed, protamine phosphorylation is involved in paternal nuclear reprogramming in the zygote (Gou et al., 2020). Residue-specific identification of protamine phosphorylation is challenging, but several have been characterized in different studies, such as S9 and S11 in P1, and S37 and S59 in P2 (Chirat et al., 1993; Hornbeck et al., 2015; Soler-Ventura et al., 2020). P1S9 and P2S59 have been also identified in mouse homolog sequences, which rises the interest on deciphering a functional role in male gamete (Brunner et al., 2014).

Relative protein amounts of P1 and P2, expressed as P1/P2 ratio calculated from in-gel quantification by acid-urea polyacrylamide gel electrophoresis (AU-PAGE), have been traditionally used as marker of chromatin maturity and related with several cases of male infertility. While similar abundance of P1 and P2 at protein level (P1/P2 ~1) are related to fertility, altered P1/P2 ratio and individual abundance of P1 and P2 have been associated with impaired sperm count, motility, and morphology, as well as compromised chromatin integrity and lower assisted reproduction technologies success rate (Balhorn et al., 1988; de Yebra et al., 1993; Mengual et al., 2003; Nanassy et al., 2011). Detailed implications of protamine content and human male fertility have been reviewed elsewhere (Jodar & Oliva, 2014; Soler-Ventura et al., 2018). However, in-gel approaches rely just on main P1 and P2 bands, partially excluding protamine proteoforms with different electrophoretic behavior, which could explain variability among protamine ratios reported among different studies (Ni et al., 2016). Apart from chromatin maturity defects, other potential underlying causes of unexplained male infertility are under investigation, such as sociodemographic factors, including increased obesity rates measured through the body mass index (BMI), or advanced paternal age at the time of conception (Agarwal et al., 2021; Mascarenhas et al., 2012; Tiegs et al., 2018). Obesity has been described to affect spermatogenesis at many levels, with impact in sperm epigenome that can be transmitted to subsequent generations and affect newborn's health (Craig et al., 2017; Fullston et al., 2012, 2013; McPherson et al., 2014; Pepin et al., 2022; Soubry et al., 2013, 2016). Despite presenting normal seminal parameters, sperm from obese men carry altered DNA methylation and small-noncoding RNAs (Donkin et al., 2016; Soubry et al., 2016), and obese mice show impaired histone marks, histone-modifying enzymes, and histone positioning within the genome (Deshpande et al., 2021; Palmer et al., 2011; Terashima et al., 2015). In turn, advanced paternal age is associated with rise in *de novo* mutations, telomeric elongation, increased DNA fragmentation, and altered methylation pattern (Jenkins et al., 2014, 2018; Laurentino et al., 2020; Pohl

et al., 2021). Transgenerational effect of age-associated DNA methylation impairments has been also described in mouse (Milekic et al., 2015).

Due to the current lack of information about high-throughput comparative studies on protamine proteoforms levels in males with unexplained infertility, in this study, we apply Top-Down Mass Spectrometry to identify quantitative alterations in the protamine proteoform profile of normozoospermic men with infertility of unknown origin. Strict inclusion criteria were applied to overcome potential bias from associated co-morbidities, stablishing highly homogeneous groups of men differing in a) P1/P2 ratio, b) BMI, and c) age, from the control group. We therefore report altered levels of different protamine proteoforms that are essentially attributed to impaired chromatin status, obesity, and advanced paternal age, opening a new window to sperm protamine proteoforms as epigenetic alterations underlying different cases of unexplained male infertility.

MATERIALS AND METHODS

Biological Material

Human semen samples (n = 15) from men undergoing routine semen analysis were obtained at the Assisted Reproduction Unit from the Clinic Institute of Gynecology, Obstetrics and Neonatology, at the Hospital Clínic of Barcelona, Spain. The ejaculates were collected by masturbation into sterile containers after 3–5 days of sexual abstinence. After seminal parameters evaluation using the automatic semen analysis system CASA (Proiser, Paterna, Spain), samples were classified as normozoospermic according to the latest update of World Health Organization guidelines (World Health Organization, 2021). Patients reporting associated diseases or toxic habits, such as smoking, were excluded from the study. Samples were classified according to body mass index (BMI), age, and chromatin quality (in terms of P1/P2 ratio calculated by AU-PAGE), therefore establishing four groups of study: Control group (BMI < 25, age < 45 y.o., normal P1/P2 ratio 0.8-1.2; n = 5), Obesity (BMI > 30, age < 45 y.o., normal P1/P2 ratio 0.8-1.2; n = 3), Advanced age (BMI < 25, age > 45 y.o., normal P1/P2 ratio 0.8-1.2; n = 4), and Altered P1/P2 (BMI < 25, under 45 y.o., P1/P2 ratio > 1.2; n = 3). Sperm samples were purified from contaminating cells through 50% density gradient using Puresperm® (NidaCon International AB, Gothenburg, Sweden), according to manufacturer's recommendations. All patients signed informed consent in accordance with the Declaration of Helsinki. Samples were used following the appropriate ethical guidelines and Internal Review Board, and the Clinical Research Ethics Committee of the Hospital Clínic de Barcelona approved the biological material storing and processing.

Protamine purification from human semen samples

Protamine-rich fraction of sperm nuclear proteins was extracted as previously described by our group (Soler-Ventura et al., 2018, 2020). Briefly, histones and other basic proteins loosely attached to DNA were removed from sperm nuclei incubating the cells in 0.5 M HCl for 10 min at 37 ºC after vortexing, and centrifuging at 2000 *g* 20 min at 4 ºC, three times. Resulting pellet was resuspended in 0.5 % Triton X-100, 20 mM Tris-HCl (pH 8), and 2 mM $MgCl_2$ to permeabilize cells. After centrifugation at 8940 *g* 5 min at 4 ºC, cells were lysed by osmotic shock by adding miliQ H_2O with 1 mM PMSF, centrifuging again at the same conditions. Chromatin was then denaturated by resuspending the pellets in 575 mM DTT in 6 M GuHCl and precipitated with a minimum of 10 min incubation with cold ethanol at -20 ºC, followed by centrifugation 12880 *g* for 15 min at 4 ºC. Basic nuclear proteins were extracted from DNA incubating with 0.5 M HCl at 37 ºC (5 min followed by vortex and additional 2 min), recovered in the supernatant after centrifugation 17530 *g* 10 min at 4 ºC. At this point, total protamine content was split before precipitation to separate a small aliquot for subsequent protamine quantification, keeping the rest for top-down proteomics analyses. Precipitation was carried out with 20 % TCA on ice. Protamines were washed twice with 1 % β-mercaptoethanol in acetone and dried out at room temperature.

Protamine quantification

Protamine extracts were quantified according to published procedures (Soler-Ventura et al., 2018). Dried purified extracts were resuspended in sample buffer consisting of 5.5 M urea, 20% β-mercaptoethanol, 5% acetic acid and separated using AU-PAGE together with increasing amounts of protamine standard (Mengual et al., 2003). Gels were stained with EZBlue™ Gel Staining Reagent (Sigma-Aldrich) and intensity of the two main bands, corresponding to P1 and P2, was quantified using Quantity One 1-D analysis software (BioRad, Hercules, CA, USA). Regression curve obtained from protein standard intensity determination allowed calculating the quantity of P1 and P2 for each sample and the derived P1/P2 ratio.

Protamine proteoforms characterization by top-down mass spectrometry-based proteomics

Protamine-enriched fractions extracted from 15 million spermatozoa were reconstituted in 50 mM NH_4HCO_3, reduced with 2 mM DTT for 1h at RT and carbamidomethylated for 30 min in the dark at RT with 5 mM iodoacetamide. DTT was added to a final concentration of 2mM to consume any unreacted iodoacetamide. Protamines were further desalted using PolyLC C18 filter tips (PolyLC Inc., Columbia, MD, USA), eluted with 80% acetonitrile and 1% trifluoroacetic acid, evaporated to dryness, and reconstituted in aqueous solution of 3 % acetonitrile and 1 % formic acid

for LC-MS/MS system injection. Samples were loaded to a 300 µm × 5 mm PepMap100, 5 µm, 100 Å, C18 µ-precolumn (Thermo Scientific) at a flow rate of 15 µl/min using a Thermo Scientific Dionex Ultimate 3000 chromatographic system (Thermo Scientific). Proteins were separated using a C18 analytical column Acclaim PepMap® RSLC (75 µm × 50 cm, nanoViper, C18, 2µm, 100 Å) (Thermo Scientific) with a 60 min run, comprising two consecutive steps with linear gradients from 3 to 15% B in 30 min and from 15 to 85% B in 5 min, followed by isocratic elution at 85% B in 5 min and stabilization to initial conditions (A = 0.1% FA in water, B = 0.1% FA in CH3CN). The column outlet was directly connected to an Advion TriVersa NanoMate (Advion) fitted on an Orbitrap Fusion Lumos™ Tribrid (Thermo Scientific). The mass spectrometer was operated in a data-dependent acquisition (DDA) mode. Survey MS scans were acquired in the Orbitrap with the resolution (defined at 200 m/z) set to 120,000. The lock mass was user-defined at 445.12 m/z in each Orbitrap scan. The top speed (most intense) ions per scan were fragmented by ETD and detected in the orbitrap. The ion count target value was 400,000 and 1,000,000 for the survey scan and for the MS/MS scan respectively. Target ions already selected for MS/MS were dynamically excluded for 30s. Spray voltage in the NanoMate source was set to 1.60 kV. RF Lens were tuned to 30%. Minimal signal required to trigger MS to MS/MS switch was set to 50,000. The spectrometer was working in positive polarity mode and singly charge state precursors were rejected for fragmentation.

Protamine proteoform search, data analysis and proteoform annotation

Top-down proteomics workflow was based on a twin search strategy, encompassing the bioinformatics tools TopPIC suite (Kou et al., 2016) (TP; Indianapolis, IN, USA) and ProSight PD (LeDuc et al., 2004) (PS; Thermo Scientific, San Jose, CA, USA) to identify spectrum matches, classified according to the density-based spatial clustering of applications with noise (DBSCAN) algorithm implemented using Python as described in (Arauz-Garofalo et al., 2021). Proteome Discoverer v2.5.0.400 (Thermo Fisher Scientific) with PS v4.0 and TP v1.4.8 were used for protamine identification and PTM assignment. Database searches in PS were performed using an xml-annotated database from SwissProt, containing P1 and P2 entries. The annotated database was modified to include phosphorylation modification to all STY residues, and oxidation in M. A 3-tier search (Absolute, Biomarker and Absolute) was performed with precursor mass tolerances of 2.2 Da / 10 ppm / 500 Da, respectively, and fragment mass tolerances of 10 ppm. Searches in TP were done using TopFD tool for top-down spectral deconvolution and a FASTA format database, which contained P1 and P2 sequences. Common modifications were included (oxidations in M, phosphorylation in STY, acetylation in K, methylation in KR, dimethylation in KR and trimethylation in K). Precursor and fragment mass tolerances were set to 15 ppm and maximum mass shift to 500 Da. Proteoform spectrum matches with FDR < 1% were considered for further data integration and clustering analysis. PS and TP top-down search outputs were combined into a single harmonized dataset using a custom

Python script previously developed by our group (Arauz-Garofalo et al., 2021). Identified proteoform spectrum masses (PrSMs) were filtered according to the following criteria: retention time window (minutes) = (0, 48), mass window (Da) = (0, +∞) and intensity window (Da) = (0, +∞). Filtered PrSMs were subsequently processed by standardizing deconvoluted masses values via the z-xcore. PrSMs were classified using DBSCAN algorithm with ε = 0.0005 and nmin = 49 as hyperparameters.

Ratio computation and comparative statistical analysis of protamine proteoform abundance

Proteoforms were grouped according to the native protein (P1, mature P2 and immature P2) and the type of modification (unmodified, phosphorylated and +61Da) to evaluate the relative abundance of proteoforms groups. Ratios were computed with linear intensity values of the involved PrSMs at the Node pair level and compared among groups with pairwise t-test using R statistical software R 4.0.1 with rstatix library (R Core Team, 2020). Differential analysis of protamine proteoforms abundance was conducted with limma using R 4.01 and the packages lme4, lmerTest, tidyverse, tidyr, ggplot2, plotly. PS and TP intensities were $\log_2$-transformed and fitted to a linear model according to lmer function from lme4 package or lm from stats. Advanced age, Obesity and Altered P1/P2 groups were compared with Control group, and multiple comparisons were corrected by Benjamini & Hochberg. Significant protein stablished threshold was |FC| > 1.5 and $p < 0.05$.

RESULTS

Protamine relative levels calculated by AU-PAGE and classification of the different study groups

Seminal characteristics, as well as BMI, age and P1/P2 values of the samples included in this study are indicated in Table 1 (mean value ± standard deviation per group). Samples with P1/P2 above 1.2, determined from quantification of the main P1 and P2 bands detected by AU-PAGE, were classified as “Altered P1/P2” ratio (Figure 1).

Table 1. Patient groups included in the analysis. Relevant seminal parameters, age, BMI, and P1/P2 ratio are shown as mean value ± standard deviation.

Sample group	Conc. (Mz/mL)	A +B (%)	Vol. (mL)	NF (%)	Age	BMI	P1/P2 ratio
Control (n=5)	155.4 ± 117.6	59.3 ± 16.8	2.4 ± 1.2	16.8 ± 4.3	35.2 ± 0.4	24.2 ± 1.8	0.99 ± 0.16
Altered P1/P2 (> 1.2) (n=3)	74.8 ± 5.7	48.3 ± 6.9	2.6 ± 1.2	15.0 ± 5.3	33.7 ± 2.1	26.0 ± 1.7	**1.4 ± 0.12**
Obesity (BMI > 30) (n=3)	144.3 ± 40.8	55.1 ± 24.1	2.6 ± 1.0	23.7 ± 12.7	39.3 ± 0.6	**35.4 ± 1.3**	0.95 ± 0.06
Advanced age (> 45 y.o.) (n=4)	129.3 ± 38.3	51.4 ± 18.9	2.2 ± 1.1	16.3 ± 10.6	**50.3 ± 3.2**	25.0 ± 1.1	0.94 ± 0.19

Conc. (Mz/mL): sperm concentration; A + B (%): sperm with progressive motility; Vol.: semen volume; NF: sperm with normal forms; BMI: Body Mass Index; P1/P2 ratio: protamine 1/protamine 2 protein ratio calculated by AU-PAGE. Values used to classify the samples among groups are highlighted in bold.

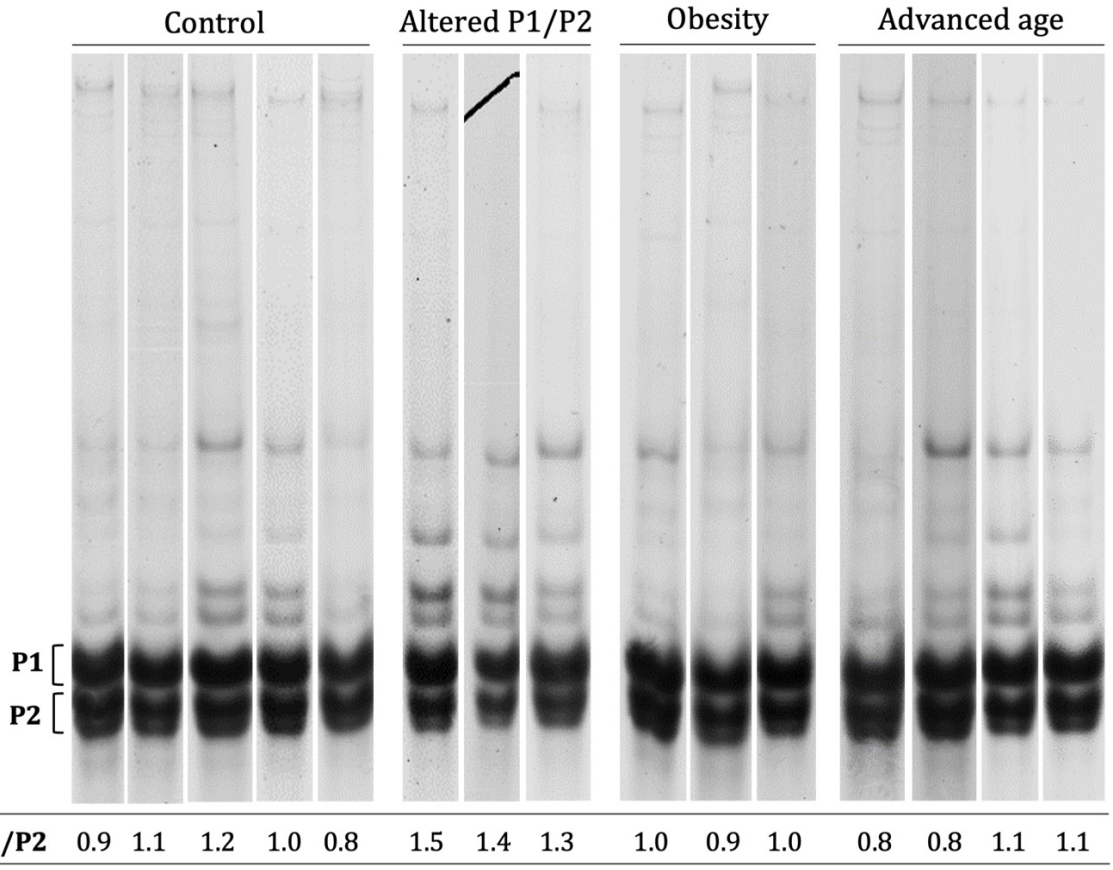


Figure 1. P1/P2 ratio calculated with AU-PAGE. Ratios per individual patients were calculated by determination of optical densities of the main bands corresponding to P1 and P2 in comparison with a protein standard with known concentration. Individual samples are sorted per group of study.

Global protamine proteoform profiles among study groups

Protamine proteoform identification was launched using our recently developed DBSCAN-based approach and two identifying nodes: ProSight (PS) and TopPIC (TP). Both software evidenced good Pearson correlation (R = 0.91) and results from both were considered for further analyses (Figure 2A). From the total 36,554 PrSMs identified, 95% passed quality filters, 88% were successfully clustered, and 84% were successfully classified (Table 2). The resulting 30,689 classified PrSMs yielded 28 protamine proteoforms after collapsing artifact PTMs (carbamidomethylation, oxidation, mesityloxidation, and pyroglutamic acid from glutamine). From those, 13 proteoforms were identified for P1, 6 for P2 mature forms (HP2, HP3 and HP4) and 9 for P2 immature forms (Pre-P2, HPS1, HPS2 and HPI2) (Figure 2B). Truncated forms P1[8-51] and P2 [8-102] were not identified with this approach. Identified proteoforms included molecules with no modifications as well as forms bearing phosphate groups in combination or not with a +61Da modification, the correspondence of which could not be assigned (Figure 2B). P1 proteoforms were globally detected with higher intensity than P2 proteoforms due to their more favorable ionization, as shown in Figure S1.

Table 2: Proteoform spectrum masses (PrSMs) identified by Top-Down proteomics of purified protamine extracts. Total number of PrSMs identified (before and after filtering) are reported for each node (PS = ProSight, TP = TopPIC). The number of PrSMs successfully clustered and classified is shown.

Node	PrSMs (before filters)	PrSMs (after filters)	PrSMs Clustered	PrSMs Classified
PS	19235	18358	17965	17461
PS (%)	100.0	95.4	93.4	90.8
TP	17319	16505	14268	13228
TP (%)	100.0	95.3	82.4	76.4
Total	36554	34863	32233	30689
Total (%)	100.0	95.4	88.2	84.0

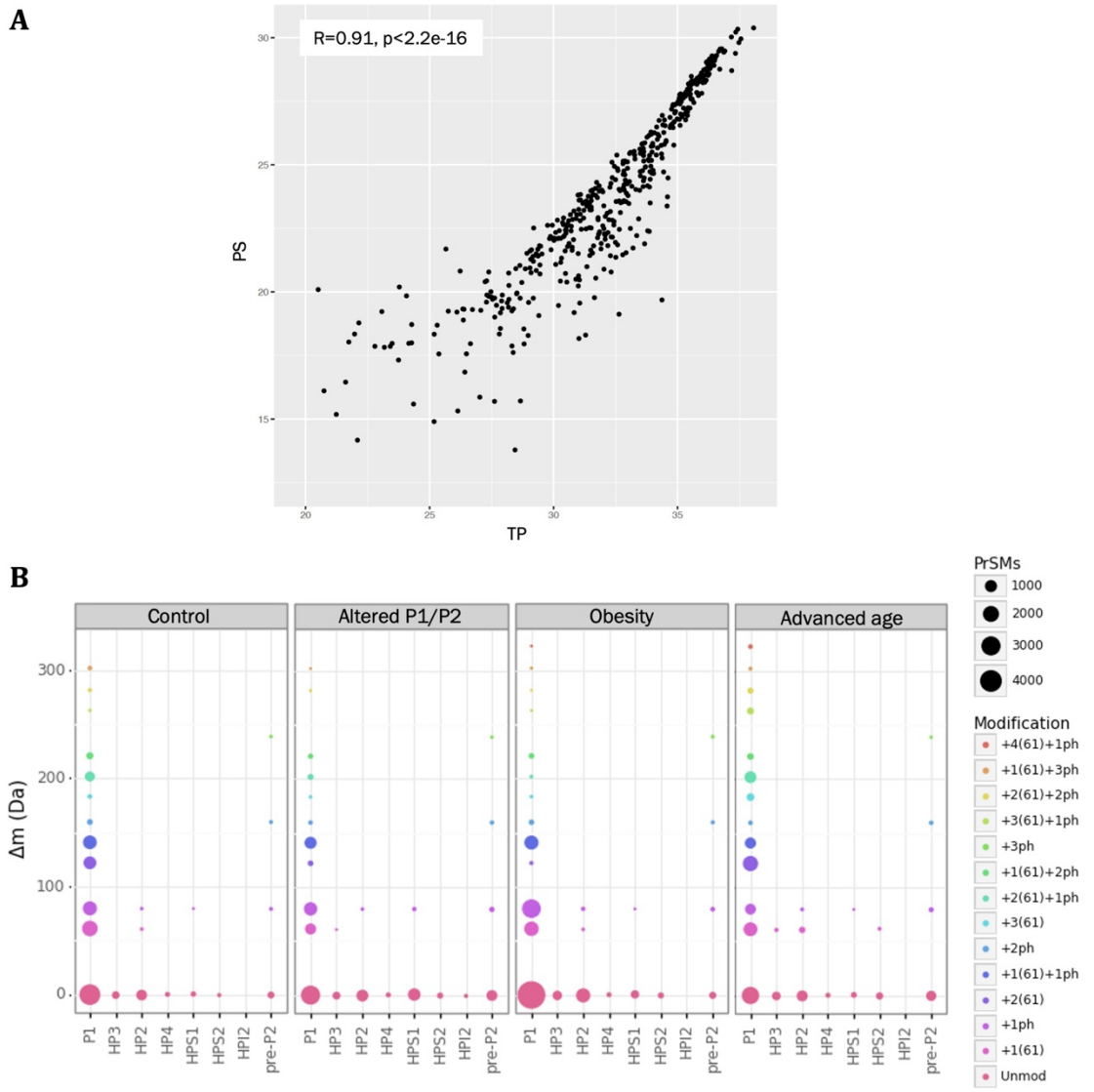


Figure 2. Human protamine proteoform identification by Top-Down proteomics using DBSCAN algorithm. (**A**) Scatter plot showing the correlation between proteoform log_2 Intensity according to the nodes ProSight (y-axis) and TopPIC (x-axis) (PS = ProSight, TP = TopPIC). Each datapoint represents a protamine proteoform identification at the technical replicate level. Missing values were imputed at 10 only for visualization purposes. Pearson correlation coefficient without considering missing values was R = 0.91. (**B**) Proteoform landscape of the different groups of study after collapsing artifact PTMs. "ph" stands for Phosphorylation, "(61)" represents a not assigned +61 Da mass shift, "PrSMs" are proteoform spectrum masses.

The relative abundance of protamine proteoforms groups is stable among patients with unexplained infertility except for the relation between unmodified P1 and P2.

To detect global deregulations of the protamine proteoform profile according to native protein and modification status, the relative abundance of proteoform groups was evaluated. Intensities for all proteoforms identified for P1 and mature components of P2 (HP2, HP3 and HP4) were used to establish the MS-based P1/P2 ratio (P1-P2 mature; Figure 3), which resulted stable among study groups. MS-based P1/P2 ratio values contrasts with P1/P2 ratio obtained by conventional

electrophoretic approaches (Figure 1), indicating that the main bands observed and quantified in AU-PAGE do not include the totality of protamine proteoforms contained in the sperm. Of note, when considering only unmodified forms of P1 and P2 (P1-unmod/P2-mature-umod; Figure 3), significant differences were found in Obesity and Advanced age groups compared with the control group ($p < 0.05$).

The order of magnitude of the MS-based ratios that relate the levels of P1 and P2 proteoforms show large differences in their respective abundance, with P1 being detected in greater quantity. However, this result is likely derived from technical bias due to the favorable ionization of P1 resulting in higher intensities (Figure S1). This technical issue is discarded when comparing relative abundance of proteoforms groups within same native protein, as observed for P1-ph/P1 and P2-mature-ph/P2 mature ratios, which relate the amounts of P1 and P2 phosphorylated forms with their respective total amount of proteoforms (Figure 3). Stable levels of global protamine phosphorylation were detected in Obesity, Advanced age, and Altered P1/P2 groups in comparison with the control group (Figure 3). Furthermore, no significant differences were found on the relative levels of all P2 immature forms over P2 mature forms (P2-immature/P2-mature) among groups (Figure 3).

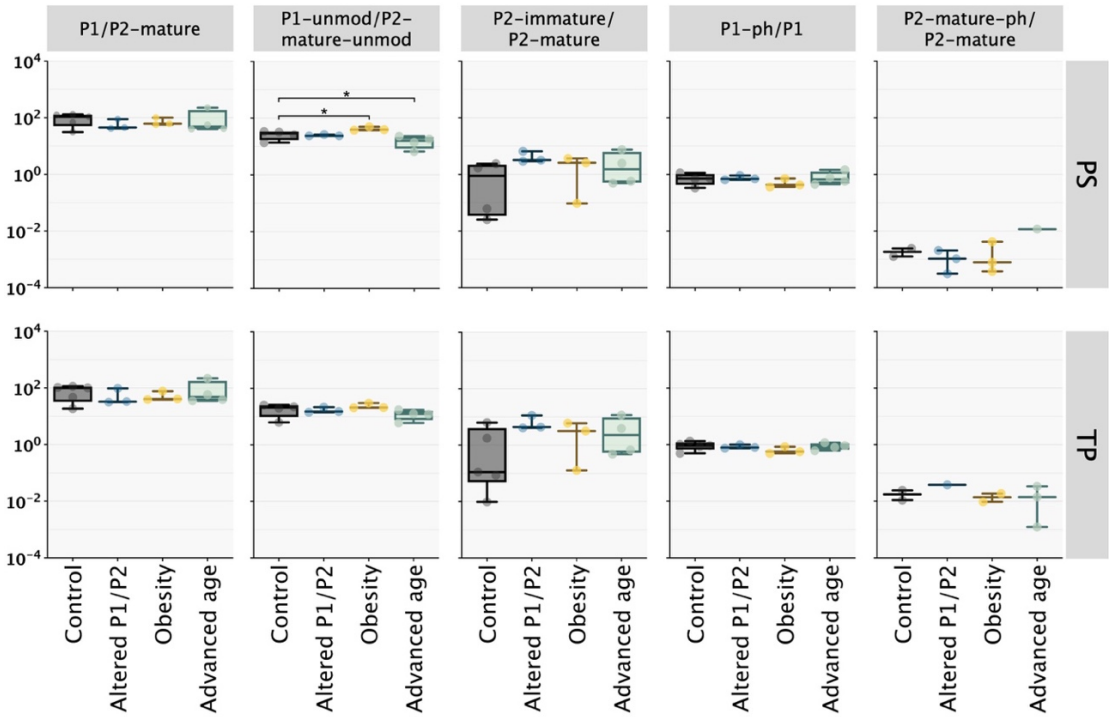


Figure 3. Box plot showing the protamine ratios (y-axis) versus the experimental groups (x-axis and hue color). The facet grid breaks down the five ratios defined (columns) and the searching nodes (rows). The asterisks (*) denote those ratios significantly different from each other after statistical testing ($p < 0.05$). P1: all P1 proteoforms; P2-mature: all proteoforms corresponding to the P2 mature forms HP2, HP3 and HP4; P1-unmod: unmodified P1 proteoforms; P2-mature-unmod: unmodified proteoforms corresponding to the P2 mature forms HP2, HP3 and HP4; P2-immature: all proteoforms corresponding to the P2 immature forms Pre-P2, HPS1, HPS2 and HPI2; P1-ph: phosphorylated P1 proteoforms; P2-mature-ph: phosphorylated proteoforms corresponding to the P2 mature forms HP2, HP3 and HP4.

Infertile men with high P1/P2 ratio calculated by AU-PAGE accumulate P2 immature forms

Quantitative proteoform analysis revealed increased levels of the P2 immature form HPS1 in Altered P1/P2 samples compared to Control Group (FC_{PS} = 82.69, *p*-$value_{PS}$ = 0.008; FC_{TP} = 434.93, *p*-$value_{TP}$ = 0.022) (Figure 4). Besides, another P2 immature form, HPI2, was exclusively identified in Altered P1/P2 patients and not present in any other group of study (Figure 2 and 4). These results suggest an accumulation of P2 immature forms in patients with high P1/P2 ratio calculated by conventional approaches. The proteoform P1+2(61)+2ph was found significantly less abundant in the Altered P1/P2 group only with PS node (Figure 4).

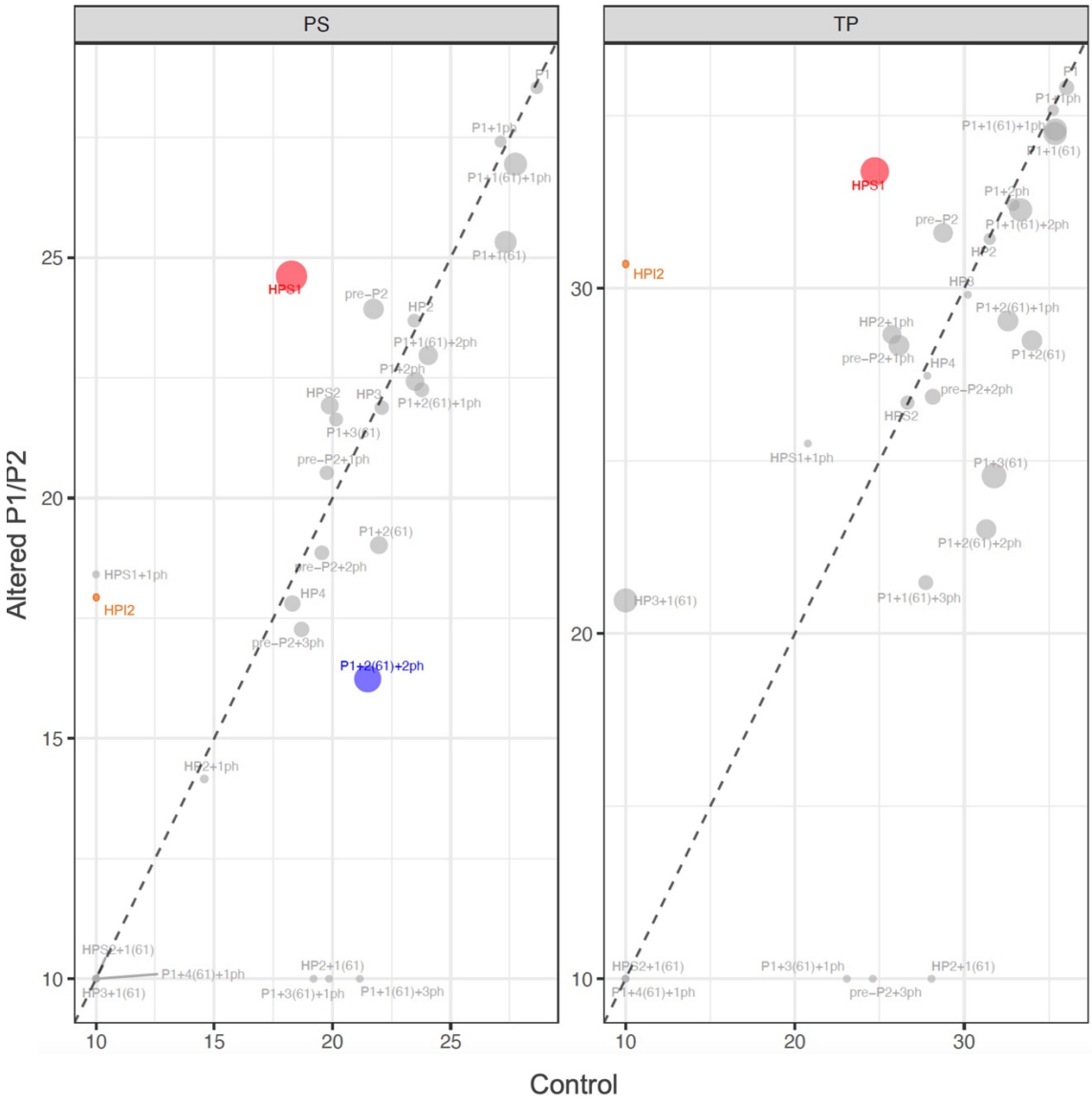


Figure 4. Proteoforms with differential abundance in Altered P1/P2 patients. Boxplot showing the log_2 Fold Change (FC) (y-axis) for Altered P1/P2 vs Control group comparison (x-axis) for ProSight (PS, left) and TopPIC (TP, right). Red and blue dots indicate proteoforms with higher and lower abundance, respectively (|FC| > 1.5, $p < 0.05$), and b/w identifications are shown in orange.

Obesity and advance age are associated with reduced abundance of modified P1 proteoforms

Obesity group revealed a characteristic reduction of P1 proteoforms bearing the not assigned modification corresponding to +61 Da mass shift (61), either coupled or not to a monophosphorylation (Figure 5). P1+1(61)+1ph levels were lower compared to controls (FC_{PS} = 0.35, p-$value_{PS}$ = 0.021; FC_{TP} = 0.40, p-$value_{TP}$ = 0.033), and P1 with 3(61) was also reduced according to TopPIC (P1+3(61); FC_{TP} = 0.003, p-$value_{TP}$ = 0.024).

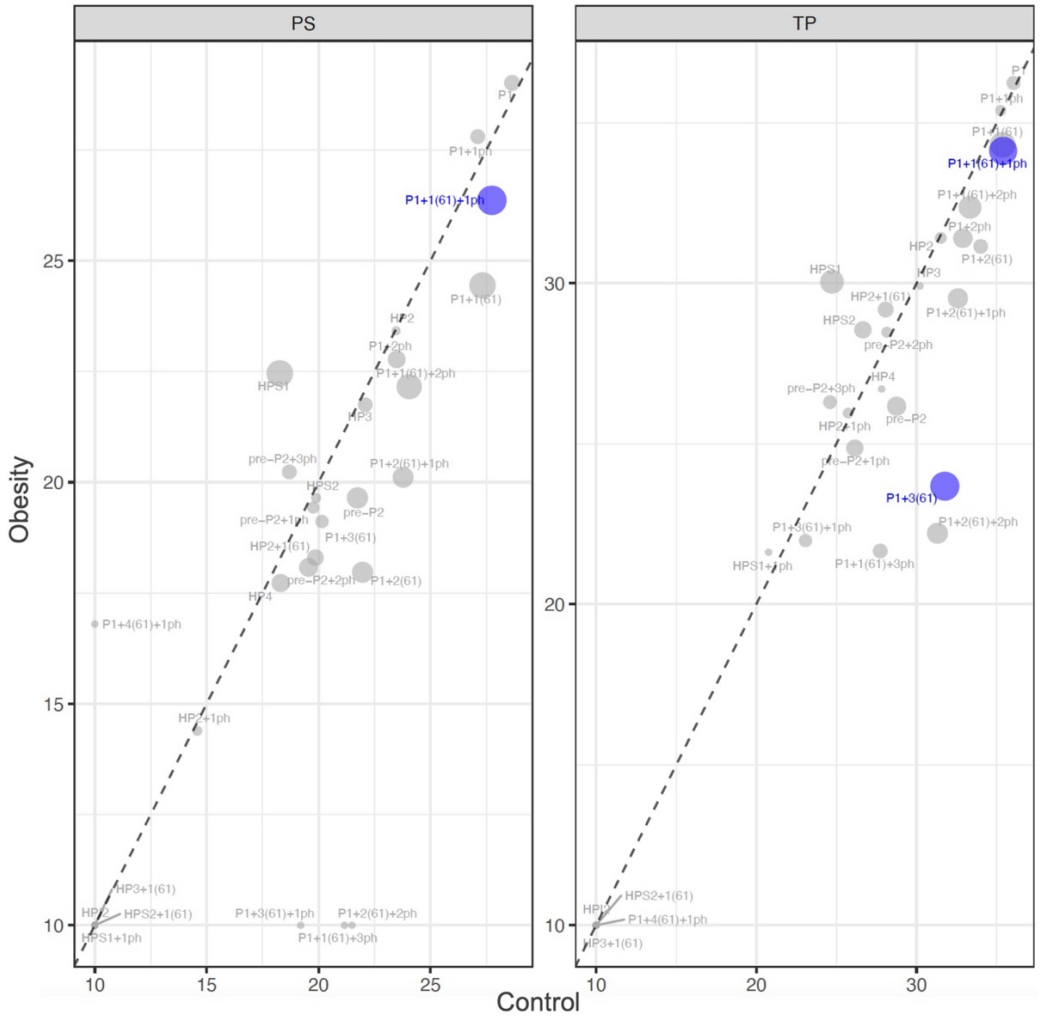


Figure 5. Differential protamine proteoforms abundance in patients with obesity. Plots showing the log_2 Fold Change (FC) for Obesity vs Control groups comparison for ProSight (PS, left) and TopPIC (TP, right). Blue dots indicate proteoforms with lower abundance (|FC| > 1.5, p < 0.05).

In turn, diphosphorylated P1, was found with significant lower abundance in Advanced age group, compared to controls, according to TP (P1+2ph; FC_{TP} = 0.01, p-$value_{TP}$ = 0.012) (Figure 6A). The alteration on this P1 proteoform not bearing any other modification but phosphorylation, lead us to look for the potential residues contributing to the reduced P1+2ph abundance. From all possible combinations, Ser 11 and 22 evidenced the most pronounced phosphorylation loss (13 counts in

Controls vs 3 counts in Advanced age), being likely responsible to the alteration observed (Figure 6B). Diphosphorylations in Ser 11 and 29 were reduced to half counts in the Advance age group (4 vs 2 counts in Control vs Advanced age) which, despite not being a relevant decrease, highlights Ser 11 as the main contributor of this change (17 vs 5 counts in Control and Advanced age groups, respectively).

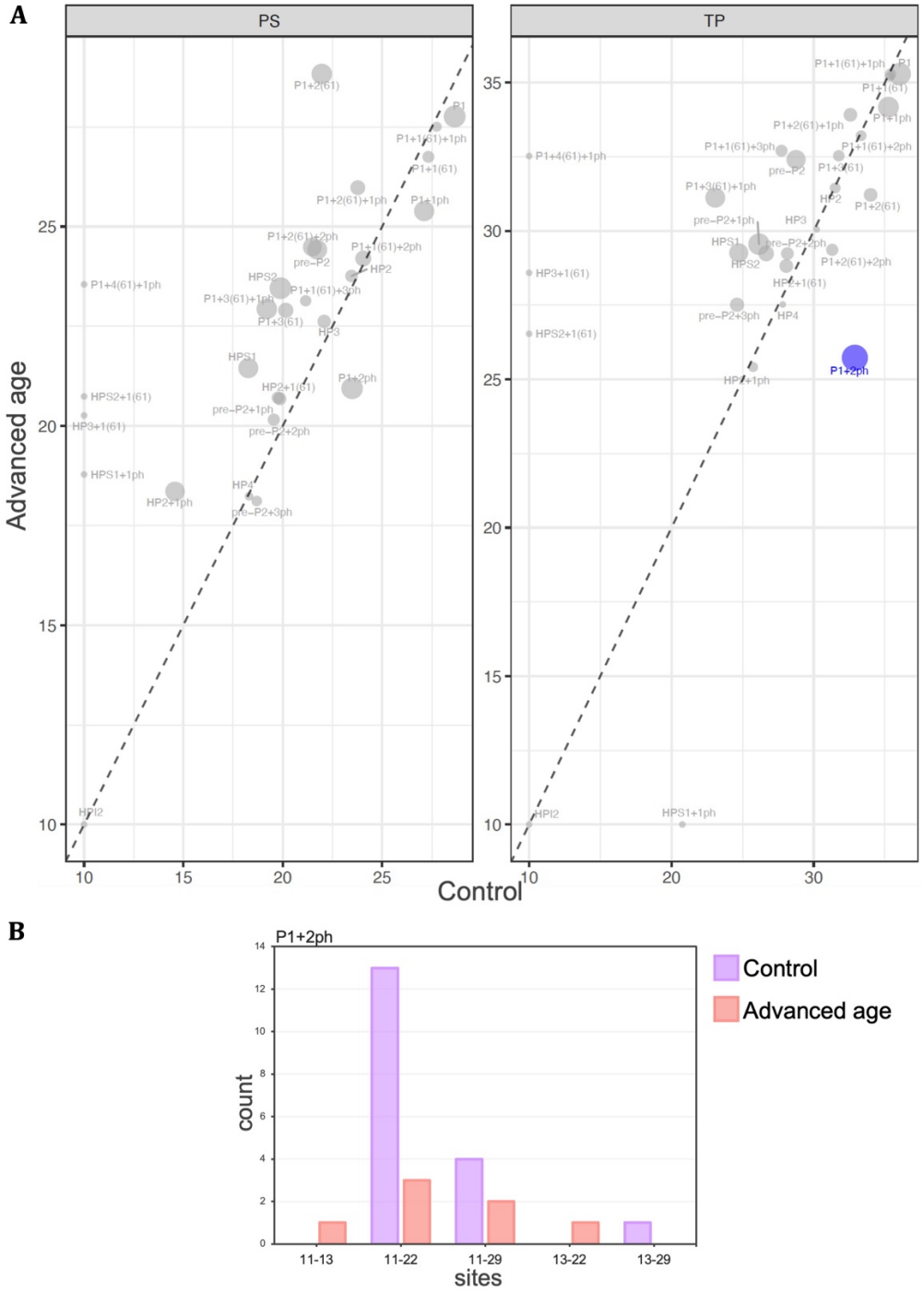


Figure 6. Differential protamine proteoforms abundance in patients with advanced age. (**A**) Plots showing the log_2 Fold Change (FC) for Advanced age vs Control groups comparison for ProSight (PS, left) and TopPIC (TP, right). Blue dots indicate lower abundance ($|FC| > 1.5$, $p < 0.05$). (**B**) Comparative site counts of simultaneously phosphorylated residues in P1 to identify the residues most likely contributing to the differential reduced abundance.

DISCUSSION

The present work discloses protamine proteoform alterations in the male gamete of men with unexplained infertility under different biological or lifestyle-associated conditions related with impaired chromatin epigenetic status, such as elevated P1/P2 ratio, obesity, and advanced age. The approach developed by our team comprising top-down proteomics followed by data analysis strategy combining ProSight (PS) and TopPIC (TP), as search nodes, with DBSCAN, as clustering algorithm (Arauz-Garofalo et al., 2021), allowed the detection of protamine proteoforms presenting differential abundance among the different study groups, adding one layer of epigenetic alteration associated to these phenotypes not described up to date.

Our clustering algorithm has highly refined protamine proteoform search to achieve a reliable identification of changes in proteoform abundance. Therefore, the protamine proteoform profile described by the control group and the phenotypes of interest include a smaller number of proteoforms than previous reports in normal human sperm (Soler-Ventura et al., 2020).

P1 and P2 relative levels determined by the quantification of main P1 and P2 electrophoretic bands obtained by AU-PAGE, allowed sorting out patients with normal seminal parameters, BMI under 30, and younger than 45 years old, that displayed an increased P1/P2 ratio. In-gel observations suggest reduced P2 as underlying cause of the alteration, which could indicate a bad processing of pre-P2 leading to lower abundance of P2 mature forms. In fact, top-down proteomics analysis revealed an accumulation of the P2 immature forms HPS1 and HPI2 compared to controls. Interestingly, HPI2 was not detected in Control, Obesity and Advance age groups, evidencing a highly specific presence of this immature form in patients with altered protamination. Recent findings have shown that mice with impaired pre-P2 processing were infertile and evidenced switched P1/P2 ratio and pre-P2 accumulation (Arévalo et al., 2022; Schneider et al., 2016, 2020). However, the protamine proteoform profile of Altered P1/P2 patients did not evidence any significant alteration in pre-P2 nor P2 mature forms, and despite the relative proportion of immature P2 forms over P2-mature forms seems to be slightly higher than controls, according to top-down MS-derived ratios, no significant differences were detected. All this suggests that the accumulation of HPS1 and HPI2 might be the result of an increased expression and processing of pre-P2 to reach normal P2 levels in these patients, generating an excess of immature forms as subproducts. Next step should focus on evaluating pre-P2 gene expression levels in sperm from patients with increased P1/P2 ratio to find the origin of the accumulation of P2 immature forms. Additionally, since altered P1/P2 ratio have been related with higher DNA oxidative damage and impaired chromatin integrity (Ni et al., 2016; Soler-Ventura et al., 2018), it could be interesting to check DNA oxidation marks, as well as simple and double strand DNA breaks, for a global understanding of the phenotype.

Interestingly, while this protamine-related impaired chromatin status, which potentially arise during male germ cells development, evidenced P2-associated defects, non-molecular parameters, such as age and weight, seem to be preferentially related with alterations in P1 posttranslational modifications. Despite it was not possible to assign the detected +61 mass shift to a specific modification, it was surprising to find it in all P1 proteoforms with reduced abundance described in obese patients, either alone or coupled to monophosphorylation. Our initial supposition for this modification was that it may correspond to a Zn^{2+} molecule, which is known to be crucial to stabilize the nucleo protamine structure (Björndahl & Kvist, 2011; Soler-Ventura et al., 2020). However, the PrSM pattern of the +61 Da modification detected herein does not match with that of Zn^{2+}. In contrast, it might coincide the mass of a N-(2-propenal)-lysine modification derived from the lipid peroxidation product malondialdehyde (MDA; ~60 Da). This hypothesis arises an interesting field of research, since MDA has been associated with male reproductive problems (Collodel et al., 2015; Uchida et al., 1997). Despite there is no evidence of altered MDA levels in patients with unexplained infertility, high fat dietary patterns have been related with increased sperm membrane lipid peroxidation, which indeed is one major consequence of intracellular ROS production, also observed increased in sperm of obese men (Akbarian et al., 2021; McPherson et al., 2014; McPherson & Lane, 2015). Therefore, the study of membrane lipid peroxidation and ROS intracellular levels in obese patients with altered P1 proteoforms bearing the +61 Da mass shift would provide more hints on the origin of this modification.

Of note, the only alteration found in patients with advanced age was the reduction of diphosphorylated forms of P1, likely happening due to loss of phosphate groups in Ser11 in combination mainly with Ser22. Previous results in mouse models evidence that, while loss of a single protamine phosphorylation site has no effect on fertilization potential, likely due to a redundancy of monophosphorylated protamine proteoforms in the sperm cell the simultaneous depletion of two phosphorylation sites in P1 ends up in drastically impaired fertility (Gou et al., 2020). This evidence increases the relevance of the decrease of this specific proteoform in men with advance age. Besides, protamine phosphorylation status may have a role on zygotic male pronuclear reprogramming, since protamine phosphorylation is an essential mechanism to unwrap paternal DNA after fertilization (Gou et al., 2020). Studies in patients alongside ageing would be useful to unravel whether alterations on protamine proteoforms increase with time. Nevertheless, when evaluating global levels of phosphorylated P1 proteoforms, no significant differences have been found compared to control group. Therefore, further research is needed to determine whether reduced P1-diphosphorylation levels have an impact on sperm functionality, or whether the unaltered global P1-phosphorylation levels show a trade-off between phosphorylated forms to maintain correct sperm function.

Altogether, the evaluation of the protamine proteoform profile in males with unexplained infertility has suggested alterations on protein modifying mechanisms,

rather than on protein expression, as critical factors for the proper maturity of the sperm chromatin with impact on male infertility, and highlights sperm protamine proteoforms as an additional layer of epigenetic information in the male gamete.

ACKNOWLEDGMENTS

We thank the Andrology lab of the Assisted Reproduction Unit from the Clinic Institute of Gynecology, Obstetrics and Neonatology, at the Hospital Clínic of Barcelona, Spain, for semen analysis. Mass spectrometry/Proteomics was performed at the IRB Barcelona Mass Spectrometry and Proteomics Core Facility, which is a member of ProteoRed, PRB3-ISCIII, supported by grant PRB3 (IPT17/0019 - ISCIII-SGEFI / ERDF) and is granted in the framework of the 2014-2020 ERDF Operational Programme in Catalonia, co-financed by the European Regional Development Fund (ERDF). Reference: IU16-015983.

FUNDING

This work has been funded by grants from the “Plataforma en Red de Proteómica Carlos III (PROTEORED)” to R.O., and “Ministerio de Ciencia e Innovación” PI20/00936 to R.O., CD17/00109 to J.C., and FI17/00224 to A.I. J.C. is a Serra Húnter fellow (Universitat de Barcelona, Generalitat de Catalunya).

REFERENCES

Agarwal, A., Baskaran, S., Parekh, N., Cho, C.-L., Henkel, R., Vij, S., Arafa, M., Panner Selvam, M. K., & Shah, R. (2021). Male infertility. *Lancet (London, England)*, *397*(10271), 319–333. https://doi.org/10.1016/S0140-6736(20)32667-2

Akbarian, F., Rahmani, M., Tavalaee, M., Abedpoor, N., Taki, M., Ghaedi, K., & Nasr-Esfahani, M. H. (2021). Effect of Different High-Fat and Advanced Glycation End-Products Diets in Obesity and Diabetes-Prone C57BL/6 Mice on Sperm Function. *International Journal of Fertility & Sterility*, *15*(3), 226–233. https://doi.org/10.22074/IJFS.2021.137231.1022

Arauz-Garofalo, G., Jodar, M., Vilanova, M., de la Iglesia Rodriguez, A., Castillo, J., Soler-Ventura, A., Oliva, R., Vilaseca, M., & Gay, M. (2021). Protamine Characterization by Top-Down Proteomics: Boosting Proteoform Identification with DBSCAN. *Proteomes*, *9*(2). https://doi.org/10.3390/proteomes9020021

Arévalo, L., Merges, G. E., Schneider, S., Oben, F. E., Neumann, I. S., & Schorle, H. (2022). Loss of the cleaved-protamine 2 domain leads to incomplete histone-to-protamine exchange and infertility in mice. *PLOS Genetics*, *18*(6), e1010272. https://doi.org/10.1371/journal.pgen.1010272

Balhorn, R. (2007). The protamine family of sperm nuclear proteins. *Genome Biology*, *8*(9), 227. https://doi.org/10.1186/gb-2007-8-9-227

Balhorn, R., Reed, S., & Tanphaichitr, N. (1988). Aberrant protamine 1/protamine 2 ratios in sperm of infertile human males. *Experientia*, *44*(1), 52–55. https://doi.org/10.1007/BF01960243

Barrachina, F., Soler-Ventura, A., Oliva, R., & Jodar, M. (2018). Sperm Nucleoproteins (Histones and Protamines). In A. Zini & A. Agarwal (Eds.), *A Clinician's Guide to Sperm DNA and Chromatin Damage.* (pp. 31–51). Springer International Publishing. https://doi.org/10.1007/978-3-319-71815-6_2

Björndahl, L., & Kvist, U. (2011). A model for the importance of zinc in the dynamics of human sperm chromatin stabilization after ejaculation in relation to sperm DNA vulnerability. *Systems Biology in Reproductive Medicine*, *57*(1–2), 86–92. https://doi.org/10.3109/19396368.2010.516306

Brunner, A. M., Nanni, P., & Mansuy, I. M. (2014). Epigenetic marking of sperm by post-translational modification of histones and protamines. *Epigenetics & Chromatin*, *7*(1), 2. https://doi.org/10.1186/1756-8935-7-2

Castillo, J., Amaral, A., & Oliva, R. (2014). Sperm nuclear proteome and its epigenetic potential. *Andrology*, *2*(3), 326–338. https://doi.org/10.1111/j.2047-2927.2013.00170.x

Castillo, J., Estanyol, J., Ballescà, J., & Oliva, R. (2015). Human sperm chromatin epigenetic potential: genomics, proteomics, and male infertility. *Asian Journal of Andrology*, *17*(4), 601. https://doi.org/10.4103/1008-682X.153302

Chirat, F., Arkhis, A., Martinage, A., Jaquinod, M., Chevaillier, P., & Sautière, P. (1993). Phosphorylation of human sperm protamines HP1 and HP2: identification of phosphorylation sites. *Biochimica et Biophysica Acta*, *1203*(1), 109–114. https://doi.org/10.1016/0167-4838(93)90043-q

Collodel, G., Moretti, E., Micheli, L., Menchiari, A., Moltoni, L., & Cerretani, D. (2015). Semen characteristics and malondialdehyde levels in men with different reproductive problems. *Andrology*, *3*(2), 280–286. https://doi.org/10.1111/andr.297

Craig, J. R., Jenkins, T. G., Carrell, D. T., & Hotaling, J. M. (2017). Obesity, male infertility, and the sperm epigenome. *Fertility and Sterility*, *107*(4), 848–859. https://doi.org/10.1016/j.fertnstert.2017.02.115

de Mateo, S., Ramos, L., de Boer, P., Meistrich, M., & Oliva, R. (2011). Protamine 2 Precursors and Processing. *Protein & Peptide Letters*, *18*(8), 778–785. https://doi.org/10.2174/092986611795713998

de Yebra, L., Ballescà, J. L., Vanrell, J. A., Bassas, L., & Oliva, R. (1993). Complete selective absence of protamine P2 in humans. *The Journal of Biological Chemistry*, *268*(14), 10553–10557.

Deshpande, S. S. S., Nemani, H., & Balasinor, N. H. (2021). Diet-induced- and genetic-obesity differentially alters male germline histones. *Reproduction*, *162*(6), 411–425. https://doi.org/10.1530/REP-21-0034

Donkin, I., Versteyhe, S., Ingerslev, L. R., Qian, K., Mechta, M., Nordkap, L., Mortensen, B., Appel, E. V. R., Jørgensen, N., Kristiansen, V. B., Hansen, T., Workman, C. T., Zierath, J. R., & Barrès, R. (2016). Obesity and Bariatric Surgery Drive Epigenetic Variation of Spermatozoa in Humans. *Cell Metabolism*, *23*(2), 369–378. https://doi.org/10.1016/j.cmet.2015.11.004

Fullston, T., Ohlsson Teague, E. M. C., Palmer, N. O., DeBlasio, M. J., Mitchell, M., Corbett, M., Print, C. G., Owens, J. A., & Lane, M. (2013). Paternal obesity initiates metabolic disturbances in two generations of mice with incomplete penetrance to the F2 generation and alters the transcriptional profile of testis and sperm microRNA content. *FASEB Journal : Official Publication of the Federation of American Societies for Experimental Biology*, *27*(10), 4226–4243. https://doi.org/10.1096/fj.12-224048

Fullston, T., Palmer, N. O., Owens, J. A., Mitchell, M., Bakos, H. W., & Lane, M. (2012). Diet-induced paternal obesity in the absence of diabetes diminishes the reproductive health of two subsequent generations of mice. *Human Reproduction*, *27*(5), 1391–1400. https://doi.org/10.1093/humrep/des030

Gou, L.-T., Lim, D.-H., Ma, W., Aubol, B. E., Hao, Y., Wang, X., Zhao, J., Liang, Z., Shao, C., Zhang, X., Meng, F., Li, H., Zhang, X., Xu, R., Li, D., Rosenfeld, M. G., Mellon, P. L., Adams, J. A., Liu, M.-F., &

Fu, X.-D. (2020). Initiation of Parental Genome Reprogramming in Fertilized Oocyte by Splicing Kinase SRPK1-Catalyzed Protamine Phosphorylation. *Cell*, *180*(6), 1212-1227.e14. https://doi.org/10.1016/j.cell.2020.02.020

Hornbeck, P. v, Zhang, B., Murray, B., Kornhauser, J. M., Latham, V., & Skrzypek, E. (2015). PhosphoSitePlus, 2014: mutations, PTMs and recalibrations. *Nucleic Acids Research*, *43*(Database issue), D512-20. https://doi.org/10.1093/nar/gku1267

Jenkins, T. G., Aston, K. I., & Carrell, D. T. (2018). Sperm epigenetics and aging. *Translational Andrology and Urology*, *7*(S3), S328–S335. https://doi.org/10.21037/tau.2018.06.10

Jenkins, T. G., Aston, K. I., Pflueger, C., Cairns, B. R., & Carrell, D. T. (2014). Age-associated sperm DNA methylation alterations: possible implications in offspring disease susceptibility. *PLoS Genetics*, *10*(7), e1004458. https://doi.org/10.1371/journal.pgen.1004458

Jodar, M., & Oliva, R. (2014). Protamine alterations in human spermatozoa. *Advances in Experimental Medicine and Biology*, *791*, 83–102. https://doi.org/10.1007/978-1-4614-7783-9_6

Kou, Q., Xun, L., & Liu, X. (2016). TopPIC: a software tool for top-down mass spectrometry-based proteoform identification and characterization. *Bioinformatics*, btw398. https://doi.org/10.1093/bioinformatics/btw398

Laurentino, S., Cremers, J., Horsthemke, B., Tüttelmann, F., Czeloth, K., Zitzmann, M., Pohl, E., Rahmann, S., Schröder, C., Berres, S., Redmann, K., Krallmann, C., Schlatt, S., Kliesch, S., & Gromoll, J. (2020). A germ cell-specific ageing pattern in otherwise healthy men. *Aging Cell*, *19*(10). https://doi.org/10.1111/acel.13242

LeDuc, R. D., Taylor, G. K., Kim, Y.-B., Januszyk, T. E., Bynum, L. H., Sola, J. v., Garavelli, J. S., & Kelleher, N. L. (2004). ProSight PTM: an integrated environment for protein identification and characterization by top-down mass spectrometry. *Nucleic Acids Research*, *32*(Web Server), W340–W345. https://doi.org/10.1093/nar/gkh447

Mascarenhas, M. N., Flaxman, S. R., Boerma, T., Vanderpoel, S., & Stevens, G. A. (2012). National, Regional, and Global Trends in Infertility Prevalence Since 1990: A Systematic Analysis of 277 Health Surveys. *PLoS Medicine*, *9*(12), e1001356. https://doi.org/10.1371/journal.pmed.1001356

McPherson, N. O., Fullston, T., Bakos, H. W., Setchell, B. P., & Lane, M. (2014). Obese father's metabolic state, adiposity, and reproductive capacity indicate son's reproductive health. *Fertility and Sterility*, *101*(3), 865–873. https://doi.org/10.1016/j.fertnstert.2013.12.007

McPherson, N. O., & Lane, M. (2015). Male obesity and subfertility, is it really about increased adiposity? *Asian Journal of Andrology*, *17*(3), 450–458. https://doi.org/10.4103/1008-682X.148076

Mengual, L., Ballescá, J. L., Ascaso, C., & Oliva, R. (2003). Marked differences in protamine content and P1/P2 ratios in sperm cells from percoll fractions between patients and controls. *Journal of Andrology*, *24*(3), 438–447. https://doi.org/10.1002/j.1939-4640.2003.tb02692.x

Milekic, M. H., Xin, Y., O'Donnell, A., Kumar, K. K., Bradley-Moore, M., Malaspina, D., Moore, H., Brunner, D., Ge, Y., Edwards, J., Paul, S., Haghighi, F. G., & Gingrich, J. A. (2015). Age-related sperm DNA methylation changes are transmitted to offspring and associated with abnormal behavior and dysregulated gene expression. *Molecular Psychiatry*, *20*(8), 995–1001. https://doi.org/10.1038/mp.2014.84

Nanassy, L., Liu, L., Griffin, J., & Carrell, D. (2011). The clinical utility of the protamine 1/protamine 2 ratio in sperm. *Protein and Peptide Letters*, *18*(8), 772–777. https://doi.org/10.2174/092986611795713934

Ni, K., Spiess, A.-N., Schuppe, H.-C., & Steger, K. (2016). The impact of sperm protamine deficiency and sperm DNA damage on human male fertility: a systematic review and meta-analysis. *Andrology*, *4*(5), 789–799. https://doi.org/10.1111/andr.12216

Oliva, R. (2006). Protamines and male infertility. *Human Reproduction Update*, *12*(4), 417–435. https://doi.org/10.1093/humupd/dml009

Oliva, R., & Castillo, J. (2011). Proteomics and the genetics of sperm chromatin condensation. *Asian Journal of Andrology*, *13*(1), 24–30. https://doi.org/10.1038/aja.2010.65

Palmer, N. O., Fullston, T., Mitchell, M., Setchell, B. P., & Lane, M. (2011). SIRT6 in mouse spermatogenesis is modulated by diet-induced obesity. *Reproduction, Fertility, and Development*, *23*(7), 929–939. https://doi.org/10.1071/RD10326

Papoutsopoulou, S., Nikolakaki, E., Chalepakis, G., Kruft, V., Chevaillier, P., & Giannakouros, T. (1999). SR protein-specific kinase 1 is highly expressed in testis and phosphorylates protamine 1. *Nucleic Acids Research*, *27*(14), 2972–2980. https://doi.org/10.1093/nar/27.14.2972

Pepin, A.-S., Lafleur, C., Lambrot, R., Dumeaux, V., & Kimmins, S. (2022). Sperm histone H3 lysine 4 tri-methylation serves as a metabolic sensor of paternal obesity and is associated with the inheritance of metabolic dysfunction. *Molecular Metabolism*, *59*, 101463. https://doi.org/10.1016/j.molmet.2022.101463

Pirhonen, A., Linnala-Kankkunen, A., & Mäenpää, P. H. (1994). Identification of phosphoseryl residues in protamines from mature mammalian spermatozoa. *Biology of Reproduction*, *50*(5), 981–986. https://doi.org/10.1095/biolreprod50.5.981

Pohl, E., Gromoll, J., Wistuba, J., & Laurentino, S. (2021). Healthy ageing and spermatogenesis. *Reproduction*, *161*(4), R89–R101. https://doi.org/10.1530/REP-20-0633

Pruslin, F. H., Imesch, E., Winston, R., & Rodman, T. C. (1987). Phosphorylation state of protamines 1 and 2 in human spermatids and spermatozoa. *Gamete Research*, *18*(2), 179–190. https://doi.org/10.1002/mrd.1120180208

R Core Team. (2020). *R: A Language and Environment for Statistical Computing*. R Foundation for Statistical Computing. https://www.R-project.org

Schneider, S., Balbach, M., Jan F Jikeli, Fietz, D., Nettersheim, D., Jostes, S., Schmidt, R., Kressin, M., Bergmann, M., Wachten, D., Steger, K., & Schorle, H. (2016). Re-visiting the Protamine-2 locus: deletion, but not haploinsufficiency, renders male mice infertile. *Scientific Reports*, *6*, 36764. https://doi.org/10.1038/srep36764

Schneider, S., Shakeri, F., Trötschel, C., Arévalo, L., Kruse, A., Buness, A., Poetsch, A., Steger, K., & Schorle, H. (2020). Protamine-2 Deficiency Initiates a Reactive Oxygen Species (ROS)-Mediated Destruction Cascade during Epididymal Sperm Maturation in Mice. *Cells*, *9*(8). https://doi.org/10.3390/cells9081789

Soler-Ventura, A., Castillo, J., de la Iglesia, A., Jodar, M., Barrachina, F., Ballesca, J. L., & Oliva, R. (2018). Mammalian Sperm Protamine Extraction and Analysis: A Step-By-Step Detailed Protocol and Brief Review of Protamine Alterations. *Protein and Peptide Letters*, *25*(5), 424–433. https://doi.org/10.2174/0929866525666180412155205

Soler-Ventura, A., Gay, M., Jodar, M., Vilanova, M., Castillo, J., Arauz-Garofalo, G., Villarreal, L., Ballescà, J. L., Vilaseca, M., & Oliva, R. (2020). Characterization of Human Sperm Protamine Proteoforms through a Combination of Top-Down and Bottom-Up Mass Spectrometry Approaches. *Journal of Proteome Research*, *19*(1), 221–237. https://doi.org/10.1021/acs.jproteome.9b00499

Soubry, A., Guo, L., Huang, Z., Hoyo, C., Romanus, S., Price, T., & Murphy, S. K. (2016). Obesity-related DNA methylation at imprinted genes in human sperm: Results from the TIEGER study. *Clinical Epigenetics*, *8*(1), 51. https://doi.org/10.1186/s13148-016-0217-2

Soubry, A., Schildkraut, J. M., Murtha, A., Wang, F., Huang, Z., Bernal, A., Kurtzberg, J., Jirtle, R. L., Murphy, S. K., & Hoyo, C. (2013). Paternal obesity is associated with IGF2 hypomethylation in newborns: results from a Newborn Epigenetics Study (NEST) cohort. *BMC Medicine*, *11*, 29. https://doi.org/10.1186/1741-7015-11-29

Terashima, M., Barbour, S., Ren, J., Yu, W., Han, Y., & Muegge, K. (2015). Effect of high fat diet on paternal sperm histone distribution and male offspring liver gene expression. *Epigenetics*, *10*(9), 861–871. https://doi.org/10.1080/15592294.2015.1075691

Tiegs, A. W., Landis, J., Garrido, N., Scott, R., & Hotaling, J. (2018). Total motile sperm count trend over time across two continents: evaluation of semen analyses from 119,972 infertile men. *Fertility and Sterility*, *110*(4), e27. https://doi.org/10.1016/j.fertnstert.2018.07.093

Uchida, K., Sakai, K., Itakura, K., Osawa, T., & Toyokuni, S. (1997). Protein Modification by Lipid Peroxidation Products: Formation of Malondialdehyde-DerivedNϵ-(2-Propenal)lysine in

Proteins. *Archives of Biochemistry and Biophysics*, *346*(1), 45–52. https://doi.org/10.1006/abbi.1997.0266

Willmitzer, L., Bode, J., & Wagner, K. G. (1977a). Phosphorylated protamines. I. Binding stoichiometry and thermal stability of complexes in DNA. *Nucleic Acids Research*, *4*(1), 149–162. https://doi.org/10.1093/nar/4.1.149

Willmitzer, L., Bode, J., & Wagner, K. G. (1977b). Phosphorylated protamines. II. Circular dichroism of complexes with DNA, dependency on ionic strength. *Nucleic Acids Research*, *4*(1), 163–176. https://doi.org/10.1093/nar/4.1.163

World Health Organization. (2021). *WHO laboratory manual for the examination and processing of human semen, sixth edition*. World Health Organization; 2021. License: CC BY-NC-SA 3.0 IGO.

Wu, J. Y., Ribar, T. J., Cummings, D. E., Burton, K. A., McKnight, G. S., & Means, A. R. (2000). Spermiogenesis and exchange of basic nuclear proteins are impaired in male germ cells lacking Camk4. *Nature Genetics*, *25*(4), 448–452. https://doi.org/10.1038/78153

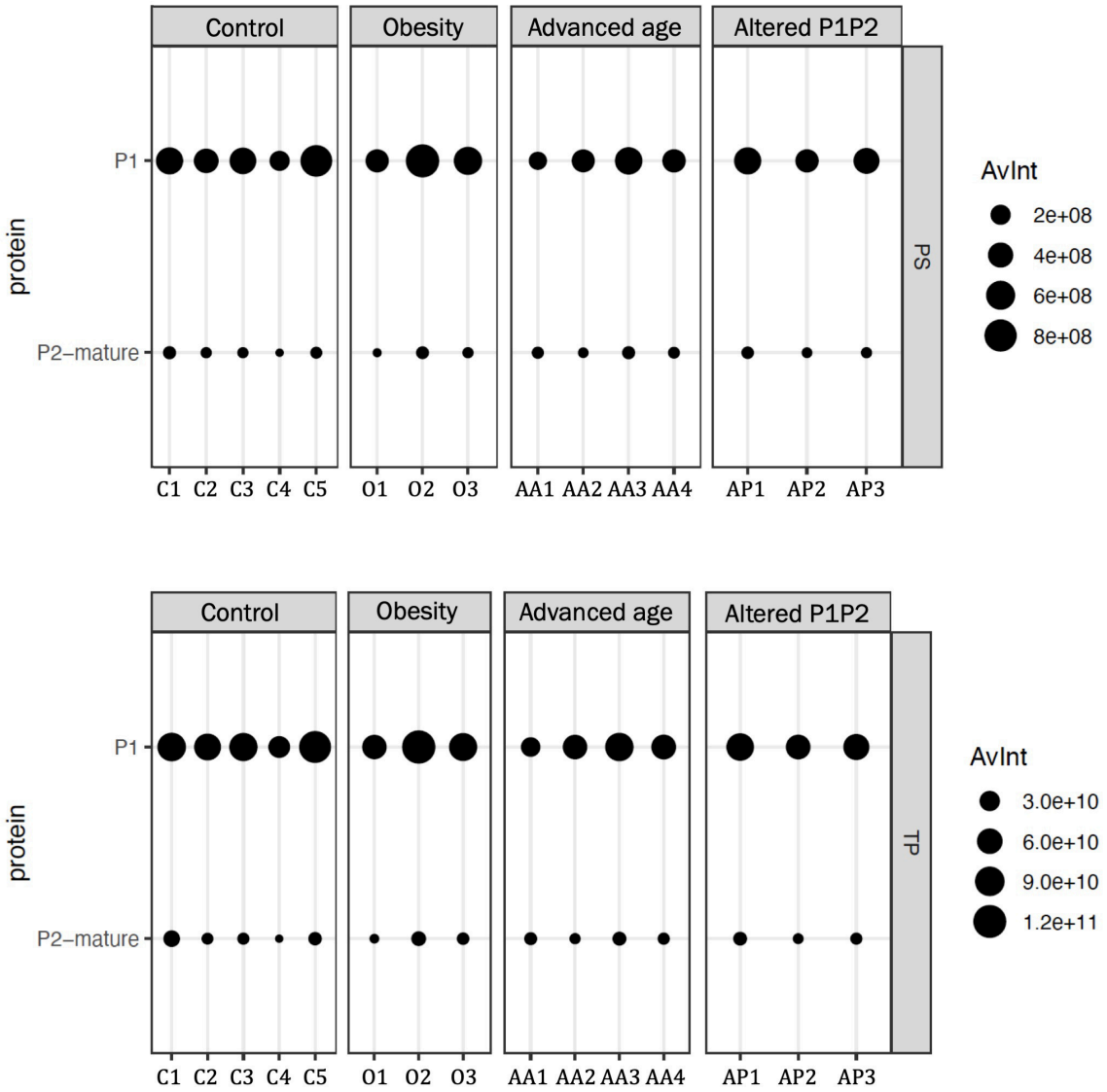


Figure S1. P1 and mature P2 detection in the different groups of study. Average intensity is shown as dots, whose size indicates level of intensity. Each replicate is shown in the X-axis.

5.2.3 Work 5: Protein-protein interaction analysis suggest additional regulatory roles for SRPK1 and PP1γ in male germ cell chromatin remodeling during mouse spermiogenesis

To be submitted as:

de la Iglesia A[1], Blanco M[2], Jodar M[1,3], Cocquet J[2,*], Castillo J[1,*], Oliva R[1,3,*]. Alterations in the abundance of specific protamine proteoforms related to sperm chromatin packaging, obesity status, and age in men with unexplained infertility.

[1] Molecular Biology of Reproduction and Development Research Group, Department of Biomedical Sciences, Faculty of Medicine and Health Sciences, Institut d'Investigacions Biomèdiques August Pi i Sunyer (IDIBAPS), Fundació Clínic per a la Recerca Biomèdica, Universitat de Barcelona, Barcelona, Spain.

[2] Institut Cochin-Inserm U1016-CNRS UMR8104-Université de Paris, Paris, France

[3] Biochemistry and Molecular Genetics Service, Hospital Clínic de Barcelona, Barcelona, Spain.

* Corresponding authors

Manuscript in preparation

Protein-protein interaction analysis suggest additional regulatory roles for SRPK1 and PP1γ in male germ cell chromatin remodeling during mouse spermiogenesis

Alberto de la Iglesia[1], Mélina Blanco[2], Meritxell Jodar[1,3], Julie Cocquet[2,*], Judit Castillo[1,*], Rafael Oliva[1,3,*]

[1] Molecular Biology of Reproduction and Development Research Group, Institut d'Investigacions Biomèdiques August Pi i Sunyer (IDIBAPS), Fundació Clínic per a la Recerca Biomèdica, Departament de Biomedicina, Facultat de Medicina i Ciències de la Salut, Universitat de Barcelona (UB), Barcelona, Spain

[2] Institut Cochin-Inserm U1016-CNRS UMR8104-Université de Paris, Paris, France

[3] Biochemistry and Molecular Genetics Service, Hospital Clínic, Barcelona, Spain

[*] Corresponding authors: roliva@ub.edu, juditcastillo@ub.edu, julie.cocquet@inserm.fr

Abstract

A proper balance of protamine phosphorylation is essential for nucleohistone–nucleoprotamine (NH-NP) transition during spermiogenesis and generation of functional spermatozoa. Serine/arginine protein kinase 1 (SRPK1) and isoform 2 of Serine/threonine-protein phosphatase PP1-gamma catalytic subunit (PP1γ) are key proteins regulating this process. In the testes, SRPK1 phosphorylates protamine 1 (P1), and isoform 2 of PP1γ dephosphorylates protamine 2 (P2). Their deregulation has previously been linked to defective chromatin structure and male infertility. The aim of this study is to decipher whether SRPK1 and PP1γ interact with other proteins involved in sperm chromatin remodeling, towards a better characterization of this complex epigenetic process. With this aim, we performed immunoprecipitation against SRPK1 and PP1γ in testicular protein lysates, followed by mass spectrometry protein identification. The most expressed candidates in post-meiotic cells were identified by analyzing single-cell gene expression data from the Repro Genomics Viewer (https://rgv.genouest.org/). Protein and functional networks and enriched molecular pathways were evaluated, as well as phosphorylation status from available datasets. We report yet undescribed SRPK1- and PP1γ-interacting proteins in the mouse testis, which are implicated in the regulation of gene expression in post meiotic cells and/or have a potential direct impact on chromatin remodeling. These results show additional regulatory functions for both proteins during spermiogenesis and highlight potential molecular targets that could contribute to solve idiopathic male reproductive health problems.

Keywords: SRPK1, PP1γ2, immunoprecipitation, LC-MS/MS, spermatogenesis, testis, protamine phosphorylation, epigenetic regulation, male reproduction

INTRODUCTION

Male germ cells undergo marked chromatin remodeling as part of the process of generating functional spermatozoa (Castillo et al., 2015; Oliva, 2006; Oliva et al., 1987; Oliva & Dixon, 1991). During spermiogenesis, the last stage of spermatogenesis, histones are gradually replaced by transition proteins and, ultimately, by protamines, small proteins with a high positive charge due to a large proportion of arginine residues in their sequence (50-70%). This chromatin remodeling process is known as the nucleohistone to nucleoprotamine (NH-NP) transition, and results in 85%-95% of sperm DNA being tightly packaged by protamines and 5-15% less compacted by histones (Balhorn, 2007; Castillo et al., 2015; Oliva, 2006).

Posttranslational modifications (PTMs) of male germ cell chromatin-associated proteins play an essential role in the orchestrated regulation of the NH-NP process (Bao & Bedford, 2016; Hazzouri et al., 2000; Oliva, 2006). Among them, phosphorylation has been identified as the main PTM in protamines (Arauz-Garofalo et al., 2021; Brunner et al., 2014; Soler-Ventura et al., 2020), and its dynamics is known to be essential for adequate protamination of the DNA. In fact, protamine-phosphorylated proteoforms show lower DNA affinity than unmodified proteoforms (Willmitzer et al., 1977b, 1977a), which would regulate protamine loading on paternal DNA in early spermiogenesis. After incorporation of phosphorylated protamines into DNA, a subsequent dephosphorylation wave takes place, which would lead to a chromatin conformation with higher compaction (Carrell et al., 2007; Oliva, 2006; Oliva & Dixon, 1991; Soler-Ventura et al., 2020).

Proteins acting as writers, readers, and erasers of PTMs arise as an additional layer of epigenetic regulation during spermatogenesis. Kinases and phosphatases (which incorporate and remove phosphate groups, respectively), are known to have a relevant function in phosphorylation and dephosphorylation dynamics of protamines. In the testis, the most well-characterized protamine kinase is serine/arginine protein kinase 1 (SRPK1), responsible for phosphorylating protamine 1 (P1) (Gou et al., 2020; Papoutsopoulou et al., 1999), and its dysregulation has been linked to male infertility (Azpiazu et al., 2014). While no P1-specific phosphatases have been described yet, germ cell-specific isoform 2 of Serine/threonine-protein phosphatase PP1-gamma catalytic subunit (PP1γ) is involved in removing phosphate groups from protamine 2 (P2) (Itoh et al., 2019). Interestingly, although the depletion of the chaperone needed for recruiting isoform 2 of PP1γ to sperm chromatin in mice (Heat shock 70 kDa protein 4L, HS74L) leads to infertility due to altered sperm head morphology, normal phenotype is rescued when the P2 phosphorylation site is substituted by a non-phosphorylatable residue. This suggests that P2 dephosphorylation mediated by PP1γ isoform 2 is essential to achieve mouse fertility, avoiding abnormal P2 phosphorylation levels in epididymal sperm (Itoh et al., 2019).

Besides epigenetic regulation of the NH-NP transition through PTMs, a tight spermiogenic gene expression program contributes to coordinate key proteins

governing the process (Blanco & Cocquet, 2019; Moritz & Hammoud, 2022; Wang et al., 2019). Regulation at posttranscriptional level by ribonucleoproteins associated to mRNAs corresponding to transition proteins and P2 has been identified in the mouse testis, mediating the temporal gene expression regulation of the process (Phillips et al., 2019; Xu et al., 2014).

Considering the very complex regulation of chromatin remodeling that takes place during spermatogenesis, in this work we explored whether the dialogue between proteins modulating protamine phosphorylation and other proteins regulating male germ cells' differentiation could be orchestrating the process, with a special focus on those involved in chromatin remodeling. Therefore, the aim of our study was to define the testicular interactive protein network of SRPK1 and PP1γ in mouse to identify candidates with potential to be developed as biomarkers or useful molecular targets for solving male reproductive health problems.

MATERIALS AND METHODS

Biological Material

The six adult mice used in the present study were of C57BL/6 background and processed at adult age (2-3 months old). All procedures were subjected to local ethical review (*Comité d'Ethique pour l'Experimentation Animale, Université Paris Descartes*, registration number CEEA34.JC.114.12, APAFIS 14214-2017072510448522v26).

Testicular soluble proteins extraction

Mouse testes were freshly dissected and washed in DMEM (Gibco BRL, Grand Island, NY, USA). Tunica albuginea was removed to minimize somatic contamination and the resulting testicular mass was subjected to mechanical cleavage and homogenization in lysis solution (150 mM NaCl, 20 mM Tris-HCl pH 8.0, 0.5% NP40, 5 mM EDTA) containing protease inhibitor cocktail (#P8340, Sigma-Aldrich), 1 mM PMSF, 1 mM Sodium butyrate, 1X phosphatase inhibitors (10 mM sodium fluoride, 3 mM tetrasodium pyrophosphate, 1 mM trisodium vanadate). Lysis was carried out by incubating for 1 hour at 4°C in rotation. Soluble proteins were recovered in the supernatant after centrifugation at 10,000 g for 10 minutes at 4°C. The protein extract was used immediately for immunoprecipitation experiments.

Protein immunoprecipitation

Three biological replicates were performed per immunoprecipitation (IP). IP was performed as described in (Moretti et al., 2017), with minor modifications. Briefly, for each experiment, 5 µg of primary antibody against the candidate protein (Table 1) was crosslinked with 50 µl of protein A/G-coated magnetic beads (#4630, Ademtech, Pessac, France). IP against the corresponding IgG was performed in

parallel as negative control. For crosslinking, magnetic beads were washed three times with 0.65% Tween-20 in PBS prior primary antibody incubation 30 min at room temperature (RT) in rotation. Then, bead-antibody complexes were incubated for 30 min with dimethyl-pimelimidate 200 mM at pH 9.0 at RT. The crosslinking reaction was stopped with 50 mM Tris-HCl at pH 7.5. Crosslinked beads were incubated with the testis lysate overnight at 4 °C. Elution of retained proteins was done with PAG Elution Buffer (#10701, Ademtech) incubating for 5 minutes at RT. The pH was neutralized with triethylammonium bicarbonate (TEAB) pH 8.4. Eluted material was used for the identification by bottom-up proteomics of the candidate proteins, and for IP validation by western blot.

Table 1. Antibodies used in the study.

Primary Antibody	Reference	Company
Anti-rabbit SRPK1 polyclonal antibody	#14073-1-AP	ProteinTech Group (Chicago, IL, USA)
Anti-mouse PP1γ monoclonal antibody	#sc-515943	Santa Cruz Biotechnology (Dallas, TX, USA)
Mouse IgG Isotype Control	#02-6502	Invitrogen (Waltham, MA, USA)
Rabbit IgG Isotype Control	#02-6102	Invitrogen

Sample preparation for mass spectrometry

Proteins were denatured in 200mM TEAB pH8.5 and 2% SDS while disulfide bonds were reduced using 10mM TCEP (tris 2-carboxyethyl phosphine) and subsequent free thiols groups were protected using 50 mM chloroacetamide for 5 min at 95°C. Proteins were trypsin digested overnight using the suspension trapping (S-Trap) method to collect peptides as previously described (Ludwig et al., 2018). Eluted peptides were vacuum-dried in a Speed Vac (Eppendorf, Hamburg, Germany).

C18 Liquid nanochromatography–Tandem Mass Spectrometry (LC-MS/MS)

NanoflowHPLC and MS analyses were performed at the 3P5 proteom'IC facility (University of Paris) using an U3000 RSLC system hyphenated to an Orbitrap fusion MS (all from ThermoFisher, Watham, MA, USA). All mobile phases are made with milliQ-grade H_2O produced with a milliQ integral-3 (Millipore, Burlington, MA, USA). Peptides were solubilized in 10 µl of 0.1% trifluoroacetic acid (TFA) and 10% acetonitrile (ACN). 1 µl was loaded, concentrated, and washed for 3 min on a C18 reverse-phase precolumn (3-µm particle size, 100 Å pore size, 75-µm inner diameter, 2-cm length; Thermo Fischer) with loading solvent containing 0.1% TFA and 2% ACN. Peptides were separated on a C18 reverse phase resin (2-µm particle size, 100 Å pore size, 75-µm inner diameter, 25-cm length; ThermoFisher) with a 35-min binary gradient starting from 99% of solvent A containing 0.1% formic acid and ending in 40% of solvent B containing 80% ACN, 0.085% formic acid. The mass spectrometer acquired data throughout the elution process and operated in a data-dependent scheme with full MS scans acquired with the Orbitrap, followed by as many MS/MS ion trap HCD spectra 5 seconds can fit (data-dependent acquisition with top speed

mode: 5-s cycle) using the following settings for full MS: automatic gain control (AGC) target value: 2.10e5, maximum ion injection time (MIIT): 60 ms, resolution: 6.10e4, m/z range 350–1500. For HCD MS/MS: Quadrupole filtering, Normalized Collision Energy: 30. Ion trap rapid detection: isolation width: 1.6 Th, minimum signal threshold: 5000, AGC: 2.10e4, MIIT: 100 ms, resolution: 3.10e4. Peptides with undefined charge state or charge state of 1 or over 7 were excluded from fragmentation, a dynamic exclusion time was set at 30 s.

MS data analysis of IP samples

Identifications (protein hits) and quantifications were performed by comparison of experimental peak lists with a database of theoretical sequences using MaxQuant version 1.6.17.0 (Cox et al., 2014). The databases used were the Mus musculus sequences from the NCBI nr database (release February 2021) and a list of in-house frequent contaminant sequences. The cleavage specificity was trypsin's with maximum 2 missed cleavages. Carbamidomethylation of cysteines was set as constant modification, whereas acetylation of the protein N terminus and oxidation of methionines were set as variable modifications. For LFQ analysis data were imported into the Perseus software version 1.6.2.3 (Tyanova et al., 2016). The list of proteins and peptide numbers were extracted from myProMS software (Poullet et al., 2007). False discovery rate (FDR) was kept below 1% on both peptides and proteins. Proteins showing more than 2 significant and distinct peptides with mascot scores >25 in at least one of the conditions were considered unambiguously present.

Western Blot

For IP validation, 50% of the total eluted material was denatured with 4X NuPage LDS sample buffer (Life Technologies, Carlsbad, CA, USA) supplemented with 10% β-mercaptoethanol, incubating for 5 min at 95ºC. Denatured proteins were loaded on a 12% SDS-polyacrylamide gel for electrophoresis (SDS-PAGE) and subsequently transferred to a nitrocellulose membrane at 80V during 1.5 h. Blocking was performed incubating 1h at RT with 5% skimmed milk in PBST. Primary antibodies were diluted in blocking solution (1:750 anti-SRPK1, 1:2000 anti-PP1γ) incubated overnight at 4 ºC. Corresponding secondary antibodies were diluted 1:3000 in blocking solution and incubated 2h at RT. Imaging was performed with Immobilon ECL Ultra Western HRP substrate (Millipore) on ImageQuant™ LAS 4000 imager (GE Healthcare, Chicaco, IL, USA).

Data analysis

To identify immunoprecipitated proteins, proteins with at least three valid proteomic values in the immunoprecipitated products against the candidate protein and its respective IgG negative control were compared using t-student statistical test. Only proteins with *p*-value < 0.01 and fold-change (FC) > 1.5 were considered as enriched in the IP and, then, associated with the candidate protein. Venn diagrams were imaged using InteractiVenn (Heberle et al., 2015). The list of identified proteins

was analyzed with the Gene Ontology (GO) tool (http://www.geneontology.org/) to determine enriched biological processes, molecular functions, and cellular components (Ashburner et al., 2000; The Gene Ontology Consortium, 2017). Gene lists associated to GO terms were retrieved from the Gene Ontology Consortium Database (release date September 4th, 2022), and the significance of the enrichment analyses was calculated by Fisher Exact Test (p-value < 0.05 after multiple-comparisons adjustment with Bonferroni correction). Enriched metabolic pathways were determined using Reactome (https://reactome.org), with p-value < 0.05 after hypergeometric distribution test corrected for false discovery rate using the Benjamani-Hochberg method. The STRING 11.5 database (https://string-db.org/) was used to identify protein networks and connections between the identified proteins (Szklarczyk et al., 2021). Only those interactions with highest confidence interaction score (score ≥ 0.9 according to STRING 11.5 indications) were included in the analysis. In addition, data from the ReproGenomics Viewer (https://rgv.genouest.org/) (Darde et al., 2019) extracted from the article by (Green et al., 2018) were used to analyze single-cell gene expression data (scRNA- Seq) corresponding to the different adult mouse testicular cell types, expressed as ln-transformation of normalized transcripts-per-10K. This analysis allowed us to discard proteins exclusively expressed in somatic Sertoli cells and to identify those ones expressed in post meiotic cells in at least a relative 30% from the total gene expression during the whole process of spermatogenesis. Biological function was retrieved from available information at the Uniprot Knowledgebase (UniProtKB/Swiss-Prot) website (http://www.uniprot.org). Protein phosphorylation status was checked by comparing the different datasets with available data from (Y. Li et al., 2019; Qi et al., 2014) on mouse whole testis and spermatid phosphoproteomics, respectively, and using PhosphositePlus (http://www.phosphosite.org/) (Hornbeck et al., 2015).

RESULTS

SRPK1 mainly associates with proteins that interact with mRNA or single-strand DNA

Immunoprecipitation (IP) against SRPK1 was validated by western blot before proteomic identification, which revealed a protein interactive network of 39 proteins associated with SRPK1 (Fig 1A and B, Table S1). The presence of SRPK1 among the immunoprecipitated material (40 identified proteins in total) reinforces the good quality of the IP. Among the interacting proteins, 17 were exclusively found in SRPK1 IP, and 22 were significantly enriched in SRPK1-IP compared to negative control (p < 0.01, fold-change enrichment > 1.5; Figure 1C, Table S1). STRING analysis evidenced that only Serine/arginine-rich splicing factor 1 (ASF/SF2) was known to interact

SRPK1. Additional interactions between immunoprecipitated proteins, not including SRPK1, were also detected (Figure 1D).

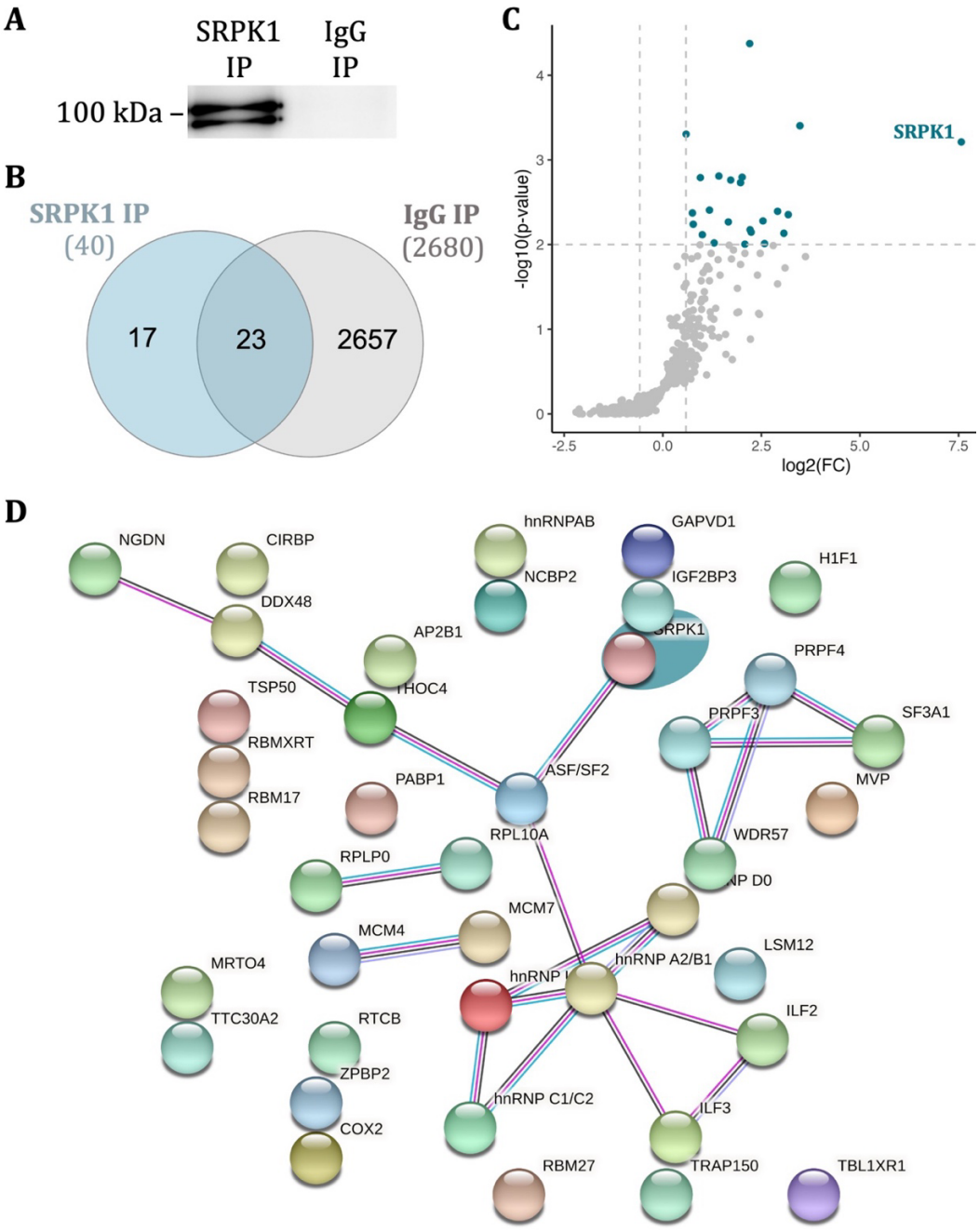


Figure 1. SRPK1-associated proteins. (**A**) Validation of SRPK immunoprecipitation (IP) compared with negative control (IgG). SRPK1 band (100 kDa) is indicated. (**B**) Comparison between proteins identified in SRPK1-IP and IgG-IP. (**C**) Proteins significantly enriched in SRPK1-IP (blue dots) compared with IgG-IP. Proteins only identified in SRPK1-IP are not shown. *P*-value and fold-change enrichment thresholds are indicated as dashed lines (horizontal, p<0.01; vertical, FC: |1.5|). (**D**) Highest-confidence (interaction score ≥ 0.9) STRING interactive network of SRPK1-associated proteins. SRPK1 is identified with a blue background. Other proteins found to interact with SRPK1 are shown in different colors arbitrarily assigned. Interactions are represented by

lines: blue, curated databases (known); pink, known interactions (experiments); black, co-expression (predicted); lilac, protein homology (predicted).

Gene ontology (GO) enrichment analyses showed that SRPK1-associated proteins are mainly involved in biological processes related with mRNA (stabilization, regulation of catabolic process, splicing, and transport) and assembly of ribonucleoprotein complexes (Table S2). Molecular functions evidenced that they mainly bind to RNA, mRNA, or single-stranded DNA, and they are part of different complexes (exon-exon junction, nuclear protein-containing complex, spliceosomal complex, ribonucleoprotein complexes) located in cytoplasmic ribonucleoprotein granules or nuclear speck (Table S2). Reactome analysis reinforced GO findings, identifying mRNA splicing and processing as the two unique pathways enriched (p < 0.05 after FDR correction) (Table S2).

Gene expression data (sc-RNA seq) in adult mice testis extracted from the ReproGenomics Viewer evidenced no proteins exclusively expressed in somatic cells (Table S3). From these data, proteins with at least a 30% of gene expression in spermiogenesis with respect to the total gene expression levels during the three spermatogenic phases were sorted to search for interesting candidates with a potential role in sperm chromatin remodeling in post meiotic cells (Figure 2). Following this criterion, 13 candidate proteins were identified as potentially involved in spermiogenesis (Figure 2, Table 2).

Surprisingly, DNA replication licensing factor MCM7 (MCM7) with a known role in DNA replication, was expressed during spermiogenesis. Observing that MCM4, also immunoprecipitated against SRPK1, was barely expressed in post meiotic cells (Figure 2, Table S3), we explored the different minichromosome maintenance (MCM) protein family members (Table S4). Among them, MCM7 is the only one with reasonable gene expression levels beyond meiosis, reinforcing its potential role during spermatid elongation.

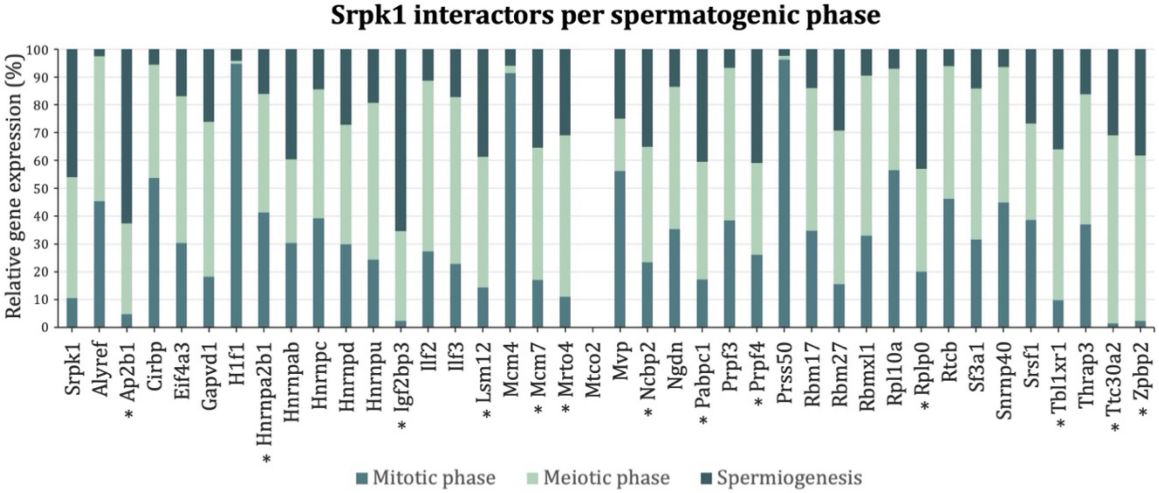


Figure 2. Relative gene expression levels (%) corresponding to SRPK1 interacting proteins sorted by spermatogenic phase. Relative gene expression levels with respect to total spermatogenic gene expression levels, extracted from (Green et al., 2018) using the

Table 2. SRPK1-associated proteins with potential role during spermiogenesis. Based on gene expression levels in post meiotic cells retrieved from the ReproGenomics Viewer (Green et al., 2018).

Protein symbol	Accession number	Biological role according to UniProt Database
AP2B1	Q9DBG3	Vesicle-mediated transport, intracellular protein transport
hnRNP A/B	Q99020	Regulation of transcription, mRNA metabolic process
IGF2BP3	Q9CPN8	Regulation of translation, regulation of gene expression, mRNA stabilization
LSM12	Q9D0R8	Nicotinic acid adenine dinucleotide phosphate (NAADP) binding protein
MCM7	Q61881	Replicative helicase essential for DNA replication
MRTO4	Q9D0I8	mRNA metabolic process, ribosome biogenesis
NCBP2	Q9CQ49	Regulation of transcription, mRNA metabolic process
PABP1	P29341	RNA splicing, mRNA processing, RNA decay
PRPF4	Q9DAW6	mRNA metabolic process
RPLP0	P14869	Ribosome biogenesis
TBL1XR1	Q8BHJ5	Transcription activation mediated by nuclear receptors
T30A2	A2AKQ8	Cilium organization, microtubule-based movement
ZPBP2	Q6X786	Reproductive process, lipid metabolic process

ReproGenomics Viewer tool, are indicated in %. * genes with >30% gene expression levels in spermiogenesis. X axis indicate gene names.

PP1γ mainly associates with proteins regulating protein dephosphorylation and assembly of small nucleolar ribonucleoproteins

IP against PP1γ was validated by western blot before proteomic identification (Fig 3A). A total of 54 PP1γ-associated proteins were identified as PP1γ protein interactive network (Fig 3B). PP1γ was also found among the immunoprecipitated material (55 identified proteins in total), reinforcing the good quality of the IP. According to the same criteria used for SRPK1 ($p < 0.01$, fold-change enrichment > 1.5), 8 proteins were significantly enriched in PP1γ-IP compared to negative control (Figure 3C, Table S5) and 46 proteins were exclusively found associated with PP1γ. Among the protein network, one interaction was previously described for PP1γ (Serine/threonine-protein phosphatase 1 regulatory subunit 10, PNUTS) according to STRING analysis, and additional interactions among proteins, not including PP1γ, were observed (Figure 3D). Interestingly, ILF2 and TBLX1R1, identified in SRPK1 interactome, were also identified associated with PP1γ.

GO enrichment analyses showed that proteins associated with PP1γ mainly participate in protein dephosphorylation regulation and assembly of small nucleolar ribonucleoprotein (snoRNP) complex (Table S6). Enriched molecular function terms

included protein phosphatase inhibitor activity (either general or in serine/threonine phosphatases) and binding to protein phosphatase 1 or other enzymes.

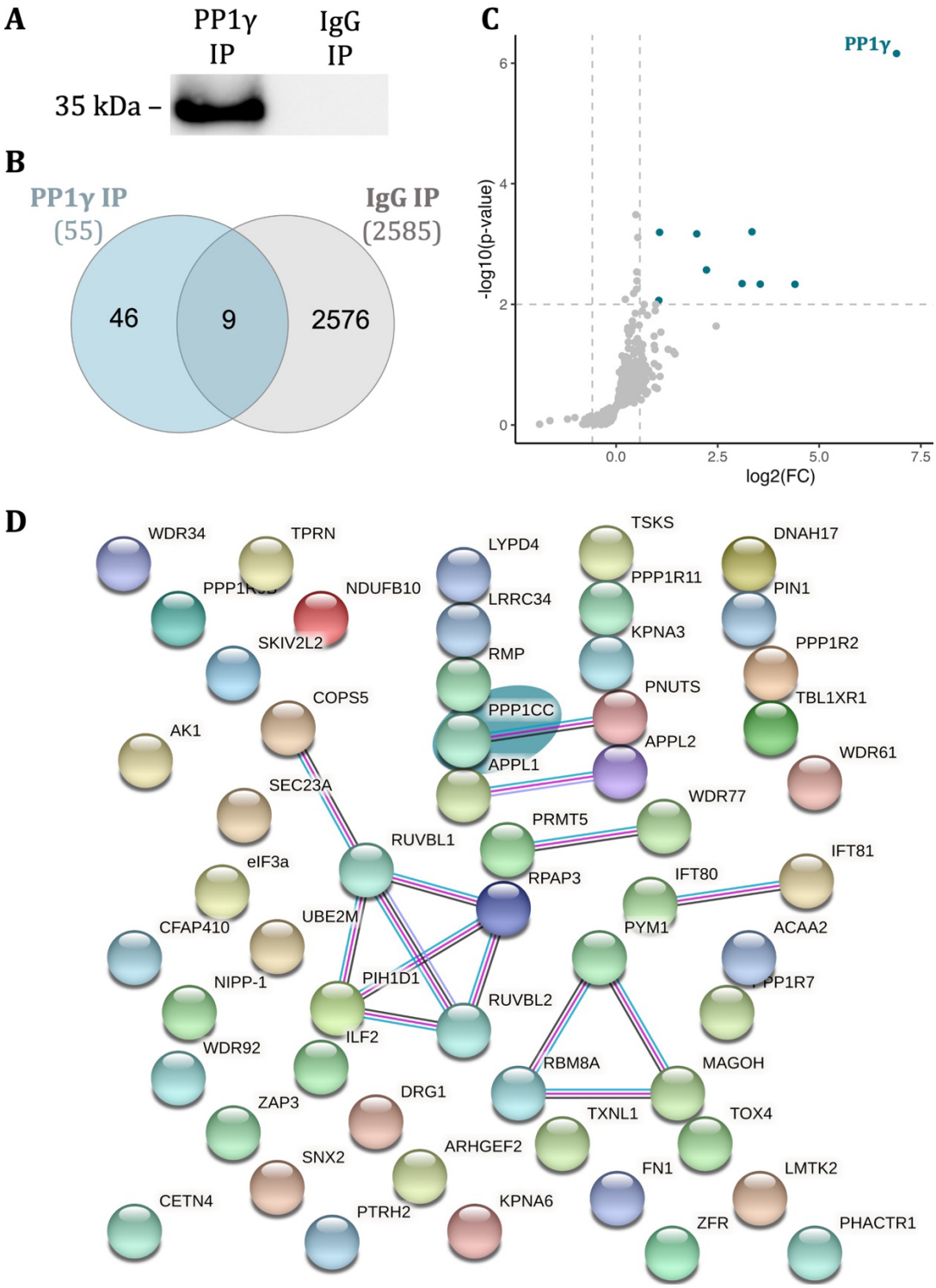


Figure 3. Identification of protein network associated with PP1γ. (**A**) Western blot validation of the immunoprecipitation against PP1γ compared with the negative control (IgG). PP1γ band at 35 kDa is indicated. (**B**) Comparison between proteins identified in PP1γ-IP and IgG-IP. (**C**) Volcano plot identifying proteins significantly enriched in PP1γ-IP (blue dots) compared with negative control. Proteins exclusively identified in PP1γ-IP are not shown in this plot. Grey dashed lines indicate threshold of p-value (horizontal, $p<0.01$) and fold-change enrichment (vertical, FC:

|1.5|). (**D**) STRING interactive network of PP1γ associated proteins. PP1γ is indicated with a blue background. Interconnecting lines: blue, known interactions from curated databases; pink, experimentally determined known interactions; black, predicted interaction by co-expression; lilac, predicted interaction by protein homology. Interactions with highest confidence (interaction score ≥ 0.9) are shown.

The enrichment analysis of cellular components evidenced proteins belonging to specific complexes, such as a) R2TP complex (including RVB1-RVB2-RPAP3-PIHD1), b) RPAP3/R2TP/prefolding-like complex (comprised of a R2TP module, a prefoldin-like module containing both prefoldin-like proteins and canonical prefoldins such as RMP, WD40 repeat protein Monad/WDR92 and DNA-dependent RNA polymerase subunit RPB5, and c) PTW/PP1 phosphatase complex, a protein serine/threonine phosphatase complex that contains a catalytic subunit (PPP1CA, PPP1CB or PPP1CC) and the regulatory subunit PPP1R10 (PNUTS), TOX4 and WDR82 (Table S6). No Reactome enriched pathways were found (p > 0.05 after FDR correction; Table S6).

In silico analysis of gene expression data (sc-RNA seq) in adult mice testis extracted from the ReproGenomics Viewer evidenced that 3-ketoacyl-CoA thiolase, mitochondrial (THIM) and DCC-interacting protein 13-beta (DP13B) were mostly exclusively expressed in somatic cells (Table S7), and they were therefore excluded from subsequent analyses.

Proteins with at least a 30% of gene expression in spermiogenesis with respect to the total gene expression levels during the three spermatogenic phases were sorted out (Figure 4). Following this criteria, PP1γ interactive network evidenced a high proportion of proteins with potential impact during spermiogenesis (28 proteins) (Figure 4, Table 3). Among the 28 proteins, we searched for interesting candidates with a potential role in sperm chromatin remodeling during spermiogenesis, and found proteins involved in post meiotic gene expression regulation or nucleosome exchange.

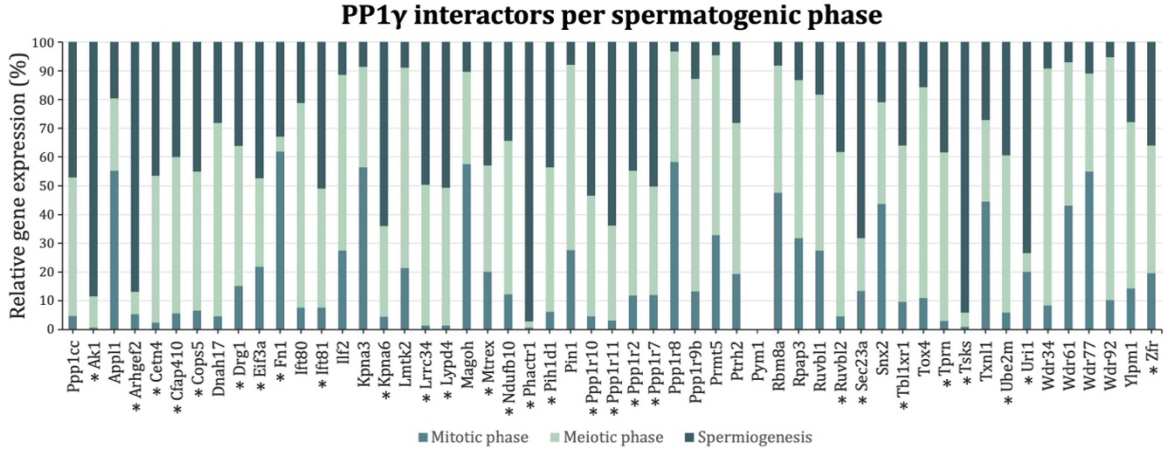


Figure 4. Relative gene expression levels of PP1γ interacting proteins sorted by spermatogenic phase, with respect to the total spermatogenic gene expression levels, extracted from (Green et al., 2018) using the ReproGenomics Viewer tool. * genes with >30% expression levels in spermiogenesis.

Table 3. PP1γ-associated proteins with potential role during spermiogenesis. Based on gene expression levels in post meiotic cells retrieved from the ReproGenomics Viewer (Green et al., 2018).

Protein symbol	Accession number	Biological role
AK1	Q9R0Y5	Adenine nucleotide metabolism, sperm motility
ARHGEF2	Q60875	Activates Rho-GTPases by promoting the exchange of GDP for GTP.
CETN4	Q8K4K1	Basal body assembly or subsequent step of ciliogenesis
CFAP410	Q8C6G1	Cilia formation and/or maintenance
COPS5	O35864	Part of complex regulating the ubiquitin conjugation pathway
DRG1	P32233	Catalyzes the conversion of GTP to GDP
eIF3a	P23116	RNA-binding component of translation initiation factor 3 complex
FN1	P11276	Establishment or maintenance of cell polarity, signaling
IFT81	O35594	Modulates assembly and elongation of the sperm flagella
KPNA6	O35345	Protein transport
LRRC34	Q9DAM1	Gene expression regulator
LYPD4	Q8BVP6	Synthesis of Glycosylphosphatidylinositol (GPI)-anchored proteins
SKIV2L2	Q9CZU3	mRNA metabolic process, ribosome biogenesis
NDUFB10	Q9DCS9	Functional assembly of mitochondrial respiratory chain complex I
PHACTR1	Q2M3X8	Binds actin monomers (G actin)
PIH1D1	Q9CQJ2	R2TP complex subunit, co-chaperone activity
PNUTS	Q80W00	Mediates the formation of the PTW/PP1 phosphatase complex
PPP1R11	Q8K1L5	Atypical E3 ubiquitin-protein ligase
PPP1R2	Q9DCL8	Protein phosphatase 1 inhibitor
PPP1R7	Q3UM45	Regulatory subunit of protein phosphatase 1
RMP	Q3TLD5	Mediates inhibition of PPP1CC phosphatase activity in mitochondria
RUVBL2	Q9WTM5	Component of the NuA4 histone acetyltransferase complex
SEC23A	Q01405	Intracellular and vesicle-mediated protein transport
TBL1XR1	Q8BHJ5	Transcription activation mediated by nuclear receptors
TPRN	A2AI08	Sterocilium maintenance
TSKS	O54887	Kinase, testis specific, testicular physiology
UBE2M	P61082	Covalent attachment of uniquitin-like NEDD8 to other proteins
ZFR	O88532	DNA/RNA binding, gene expression regulation

Protein phosphorylation analyses revealed candidate proteins susceptible to bear phosphorylated residues

To better characterize the phosphorylation profile of the different candidates, SRPK1-IP and PP1γ-IP proteins were matched with whole mouse testis phosphoproteins reported by Qi et al., 2014, and mouse spermatids phosphoproteins from Li et al., 2019. Proteins bearing phosphorylation sites, then susceptible to be phosphorylated by SRPK1 or dephosphorylated by PP1γ, were identified (Table S7,

Table S8, Figure 5). According to information from PhosphositePlus, most phosphorylated SRPK1- or PP1γ-associated proteins presented phosphorylation in Ser, Thr, and Tyr (Table S7, Table S8).

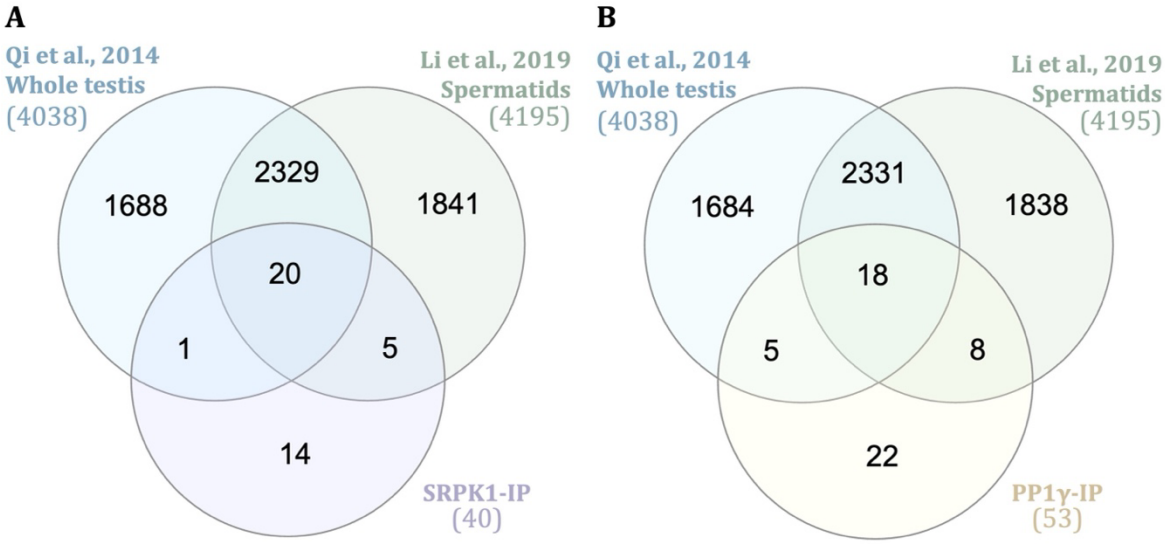


Figure 5. Venn diagrams of the protein networks identified for SRPK1 and PP1γ and available data from mouse whole testis and spermatids phosphoproteome. (**A**) The list of proteins identified in SRPK-IP and (**B**) PP1γ-IP were compared with the phosphoproteins reported in Qi et al., 2014 and Li et al., 2019 for mouse whole testis and spermatids, respectively. Proteins found enriched in somatic cells were removed from the analysis.

Since SRPK1 is a SR-protein kinase phosphorylating Ser residues within RS domains, 'SR' or 'RS' motifs were searched in the SRPK1-interacting proteins presenting at least 30% of the total spermatogenic gene expression levels in post meiotic cells. Only proteins reported as mouse phosphoproteins in previous reports were considered (Y. Li et al., 2019; Qi et al., 2014). Polyadenylate-binding protein 1 (PABP1), DNA replication licensing factor MCM7 (MCM7), Insulin-like growth factor 2 mRNA-binding protein 3 (IGF2BP3), and 60S acidic ribosomal protein P0 (RPLP0), contained phosphorylated Ser residues either in SR/RS motifs or closely placed in the amino acid sequence.

DISCUSSION

The present study discloses the interactive protein networks of SRPK1, a kinase phosphorylating protamine 1, and PP1γ, a phosphatase whose testis-specific isoform 2 is involved in dephosphorylating protamine 2, in mouse testis. We provide evidence of protein-protein associations not described up to date for both proteins that shed light on their participation in additional levels of regulation during spermiogenesis. This is in line with the essential role of phosphorylation events in maintaining a proper testicular activity (Castillo et al., 2019; Qi et al., 2014), and coherent with the

already described role of SRPK1 and PP1γ in phosphorylation-dependent testicular male germ cell chromatin remodeling (Gou et al., 2020; Itoh et al., 2019).

SRPK1 is a widely described moonlight protein known to be involved in mRNA splicing among many other cellular processes (Bullock & Oltean, 2017; Gui et al., 1994; Patel et al., 2019). Accordingly, we found that testicular SRPK1 interacts with RNA in ribonucleoprotein complexes to regulate mRNAs at different levels, including splicing. Serine/arginine-rich splicing factor 1 (ASF/SF2) interacts with SRPK1 in mouse testis, and it was interesting to observe that it presents already known interactions with other proteins from the IP network. It leads to think that the presence of the proteins interacting with ASF/SF2 in the SRPK1 network may be due because their interaction with ASF/SF2 rather than with SRPK1. No other members of the Serine/arginine-rich splicing factor (SRSF) protein family, well-known targets of SRPK1 in different cell types, were identified. This indicates there might be a wider set of proteins implicated in gene expression regulation during spermatogenesis, either regulated by SRPK1 or acting in synergy with it as part of a complex. Indeed, we identified proteins involved in deadenylation-dependent mRNA decay, which coupled to alternative splicing is an efficient strategy to regulate gene expression (Lewis et al., 2003; Song et al., 2020). Also, proteins binding to N^6-methyladenosine m^6A, a posttranscriptional mRNA modification playing a pivotal role in alternative splicing and RNA degradation were identified as interacting with testicular SRPK1 (Cao et al., 2016; Song et al., 2020). Therefore, potential new candidates associated with SRPK1 during mouse spermatogenesis and modulating gene expression are reported.

Among SRPK1-interacting proteins with an expected role in post-meiotic cells according to gene expression levels, Insulin-like growth factor 2 mRNA-binding protein 3 (IGF2BP3) and Polyadenylate-binding protein 1 (PABP1) arise as interesting candidates because they have been found phosphorylated in mouse spermatids (Y. Li et al., 2019; Qi et al., 2014). Of note, these proteins contain SR/RS motifs within their amino acid sequence, so they are susceptible to Ser phosphorylation by SRPK1, which reinforces a functional association. Besides, a role in gene expression regulation of key proteins involved in the process of NH-NP transition has been proposed for both. PABP1 binds sperm-specific mRNAs that are translated during elongating stages in spermatids, localizing in the chromatoid body and participating at different steps of spermatogenic mRNA metabolism (Xu et al., 2014). It interacts with transition protein 1 and 2 (*Tnp1* and *Tnp2*, respectively) and protamine 2 (*Prm2*) transcripts, and participates in an interesting process of kinase-dependent spatiotemporal regulation of protein translation by protein kinase A (PKA) during mouse spermiogenesis, inducing protein translation (Xu et al., 2014). Likewise, we hypothesize that a similar role of SRPK1 could contribute to protein translation initiation of nascent mRNAs during spermiogenesis. In turn, IGF2BP3 locates in messenger ribonucleoprotein (mRNP) granules, which contain non-translating mRNAs bound to regulating proteins (Phillips et al., 2019). Among other mRNAs, they

have been associated with one or both *Tnp1* and *Tnp2* transcripts in round spermatids. The relatively low MS spectral counts of IGF2BP3 in our study agrees with the low signal reported for IGF2BP3 in round spermatids (Phillips et al., 2019), which does not discard their functional role in temporal regulation of transition proteins translation, which has been shown essential for fertility (Tseden et al., 2007). Among proteins regulating sperm-specific RNAs participating in chromatin remodeling, heterogeneous nuclear ribonucleoprotein A/B (hnRNP A/B) was also found. hnRNP A/B is involved in temporal regulation of *Prm2* translation, playing an important role in stage-specific translation of spermiogenic mRNAs (Fukuda et al., 2013). From the identified hnRNP family members, hnRNP A/B is the only one keeping gene expression levels in post meiotic cells, reinforcing its role during spermatid elongation. However, it was not characterized as phosphoprotein in the testis, suggesting that it might act together with SRPK1 as part of a bigger protein complex rather than being directly phosphorylated by SRPK1.

It was surprising to find DNA replication licensing factor MCM7 (MCM7), involved in DNA replication, among the proteins with a potential role in spermiogenesis, since at this stage haploid male germ cells undergo differentiation without replicating. Interestingly, from the MCM family proteins, MCM7 was the one maintaining transcriptional levels in meiotic and post meiotic cells. MCM7 transcripts have been found enriched in testis compared to other organs, and two additional transcripts originated from alternative splicing are present in meiotic and post-meiotic germ cells (Com et al., 2006). Therefore, a specialized specific function in post meiotic cells for MCM7 could be hypothesized. Its single-strand DNA binding ability and helicase activity would be coherent with the transition DNA breaks appearing in spermiogenesis to release tensional stress in DNA helixes, therefore inducing a relaxed state to accommodate nucleosome removal (Marcon & Boissonneault, 2004; Risley et al., 1986). Besides, MCM7 was found as mouse spermatid phosphoprotein, containing Ser residues susceptible to be phosphorylated by SRPK1. Therefore, SRPK1 might be involved in regulating or exerting the role of MCM7 towards spermiogenic chromatin remodeling.

Despite consisting of a higher number of proteins, PP1γ interacting network revealed reduced number of enriched biological processes than that of SRPK1, since several members of the same protein complexes were found among the immunoprecipitated proteins. It is worth mentioning that due to antibody availability, PP1γ-IP was performed against PP1γ (recognizing both isoforms 1 and 2) instead of PP1γ2. However, whereas PP1γ1 is ubiquitous, PP1γ2 is a testis-specific isoform enriched in male germ cells (Dudiki et al., 2019; Okano et al., 1997). Therefore, after discarding potential somatic contaminants from Sertoli cells, all identified proteins are likely associated with the specific testicular enriched isoform PP1γ2. In fact, proteins already reported to interact with PP1γ2 in the testis were present in our dataset, such as protein phosphatase 1 regulatory subunits 7 (PPP1R7) and 11 (PPP1R11) (Cheng et al., 2009).

Mouse testicular PP1γ was found associated with the four members of R2TP complex (regulatory factors RPAP3-PIH1D1 as heterodimer bound to the catalytic ATPases RUVBL1 and RUVBL2), a co-chaperone with unusual function specialized in quaternary protein folding. Among the substrates of R2TP complex, spliceosomal small nucleolar RNAs and RNA polymerases have been described, pointing out a role in spermatogenic gene expression program (Kakihara & Houry, 2012). The catalytic dimer RUVBL1 and RUVBL2 are also part of chromatin remodeling complexes such as SRCAP and hINO80 complexes, by mediating their association with nucleosomes, playing a role in histone variant exchange, nucleosome eviction, and nucleosome remodeling (Gerhold & Gasser, 2014). Concretely, RUVBL1 and RUVBL2 ATPase activity promote the exchange between H2A-H2B canonical dimer and H2A.Z-H2B dimers, which may be coupled to histone PTMs as acetylation by NuA4 histone acetyltransferase complex (Choi et al., 2009; Gerhold & Gasser, 2014; Papamichos-Chronakis et al., 2011). Thus, it may be interesting to explore whether R2TP in association with PP1γ mediate the loading of RUVBL1 and 2 into chromatin remodeling complexes. An RMP-mediated stabilization of R2TP complex by RMP has been reported, depending on RMP phosphorylation status (Burén et al., 2016; Lynham & Houry, 2018). Among other proteins identified, RMP has been described as interactor of PP1γ in other cell types and is suggested to recruit proteins to R2TP (Kakihara & Houry, 2012). When interacting with WDR92 through RPAP3, RPAP3/R2TP/prefoldin-like complex is involved in axoneme structure, and loss of some of the R2TP complex have been linked with impaired sperm motility (Djouder et al., 2007; Kakihara & Houry, 2012). Further studies would be needed to decipher whether R2TP complex is acting as co-chaperone for quaternary folding of macromolecules involving PP1γ, or whether PP1γ plays a role in dephosphorylation of some R2TP complex regulating its activity.

TBLX1R1 was the only common protein found in SRPK1 and PP1γ interactomes with a potential role during spermiogenesis. This protein is part of the SMRT/N-CoR complex, that interacts with nuclear hormone receptors, transcription factors, and chromatin modifying enzymes such as histone deacetylases, suggested to participated in SLY-mediated gene expression control (J. Li et al., 2000; Perissi et al., 2008; Yoon et al., 2003). Despite it was not found among spermatid phosphoproteins, TBLX1R1 function and specificity depends on phosphorylation (Perissi et al., 2008), which may suggest an interplay between SRPK1 and PP1γ in the control of its phosphorylation status.

A list of proteins associated with the kinase SRPK1 and the phosphatase PP1γ in adult mouse testis is provided, pointing out additional roles of both proteins during chromatin remodeling and other essential processes for a proper development of spermatogenesis. These candidates arise as potential new targets to be scaled up and validated as biomarkers and molecular targets helping to disentangle idiopathic male infertility health problems derived from spermiogenesis regulation defects.

ACKNOWLEDGMENTS

We thank the proteomic platform 3P5 from the *Université de Paris* for mass-spectrometry technical support and statistical analyses, and the staff from Institut Cochin animal house.

FUNDING

This work has been funded by grants from "Ministerio de Ciencia e Innovación" PI20/00936 to R.O., FI17/00224 and MV20/00026 to A.I.; and from the "Agence Nationale de la Recherche" ANR-17-CE12-816 0004-01 to J.Co. J.Ca. is a Serra Húnter fellow (Universitat de Barcelona, Generalitat de Catalunya).

REFERENCES

Arauz-Garofalo, G., Jodar, M., Vilanova, M., de la Iglesia Rodriguez, A., Castillo, J., Soler-Ventura, A., Oliva, R., Vilaseca, M., & Gay, M. (2021). Protamine Characterization by Top-Down Proteomics: Boosting Proteoform Identification with DBSCAN. *Proteomes*, *9*(2). https://doi.org/10.3390/proteomes9020021

Ashburner, M., Ball, C. A., Blake, J. A., Botstein, D., Butler, H., Cherry, J. M., Davis, A. P., Dolinski, K., Dwight, S. S., Eppig, J. T., Harris, M. A., Hill, D. P., Issel-Tarver, L., Kasarskis, A., Lewis, S., Matese, J. C., Richardson, J. E., Ringwald, M., Rubin, G. M., & Sherlock, G. (2000). Gene Ontology: tool for the unification of biology. *Nature Genetics*, *25*(1), 25–29. https://doi.org/10.1038/75556

Azpiazu, R., Amaral, A., Castillo, J., Estanyol, J. M., Guimerà, M., Ballescà, J. L., Balasch, J., & Oliva, R. (2014). High-throughput sperm differential proteomics suggests that epigenetic alterations contribute to failed assisted reproduction. *Human Reproduction*, *29*(6), 1225–1237. https://doi.org/10.1093/humrep/deu073

Balhorn, R. (2007). The protamine family of sperm nuclear proteins. *Genome Biology*, *8*(9), 227. https://doi.org/10.1186/gb-2007-8-9-227

Bao, J., & Bedford, M. T. (2016). Epigenetic regulation of the histone-to-protamine transition during spermiogenesis. *Reproduction*, *151*(5), R55–R70. https://doi.org/10.1530/REP-15-0562

Blanco, M., & Cocquet, J. (2019). Genetic Factors Affecting Sperm Chromatin Structure. *Advances in Experimental Medicine and Biology*, *1166*, 1–28. https://doi.org/10.1007/978-3-030-21664-1_1

Brunner, A. M., Nanni, P., & Mansuy, I. M. (2014). Epigenetic marking of sperm by post-translational modification of histones and protamines. *Epigenetics & Chromatin*, *7*(1), 2. https://doi.org/10.1186/1756-8935-7-2

Bullock, N., & Oltean, S. (2017). The many faces of SRPK1. *The Journal of Pathology*, *241*(4), 437–440. https://doi.org/10.1002/path.4846

Burén, S., Gomes, A. L., Teijeiro, A., Fawal, M.-A., Yilmaz, M., Tummala, K. S., Perez, M., Rodriguez-Justo, M., Campos-Olivas, R., Megías, D., & Djouder, N. (2016). Regulation of OGT by URI in

Response to Glucose Confers c-MYC-Dependent Survival Mechanisms. *Cancer Cell*, *30*(2), 290–307. https://doi.org/10.1016/j.ccell.2016.06.023

Cao, G., Li, H.-B., Yin, Z., & Flavell, R. A. (2016). Recent advances in dynamic m ^{6} A RNA modification. *Open Biology*, *6*(4), 160003. https://doi.org/10.1098/rsob.160003

Carrell, D., Emery, B. R., & Hammoud, S. (2007). Altered protamine expression and diminished spermatogenesis: what is the link? *Human Reproduction Update*, *13*(3), 313–327. https://doi.org/10.1093/humupd/dml057

Castillo, J., Estanyol, J., Ballescà, J., & Oliva, R. (2015). Human sperm chromatin epigenetic potential: genomics, proteomics, and male infertility. *Asian Journal of Andrology*, *17*(4), 601. https://doi.org/10.4103/1008-682X.153302

Castillo, J., Knol, J. C., Korver, C. M., Piersma, S. R., Pham, T. v., de Goeij-de Haas, R. R., van Pelt, A. M. M., Jimenez, C. R., & Jansen, B. J. H. (2019). Human Testis Phosphoproteome Reveals Kinases as Potential Targets in Spermatogenesis and Testicular Cancer. *Molecular & Cellular Proteomics*, *18*, S132–S144. https://doi.org/10.1074/mcp.RA118.001278

Cheng, L., Pilder, S., Nairn, A. C., Ramdas, S., & Vijayaraghavan, S. (2009). PP1γ2 and PPP1R11 Are Parts of a Multimeric Complex in Developing Testicular Germ Cells in which their Steady State Levels Are Reciprocally Related. *PLoS ONE*, *4*(3), e4861. https://doi.org/10.1371/journal.pone.0004861

Choi, J., Heo, K., & An, W. (2009). Cooperative action of TIP48 and TIP49 in H2A.Z exchange catalyzed by acetylation of nucleosomal H2A. *Nucleic Acids Research*, *37*(18), 5993–6007. https://doi.org/10.1093/nar/gkp660

Com, E., Rolland, A. D., Guerrois, M., Aubry, F., Jégou, B., Vallet-Erdtmann, V., & Pineau, C. (2006). Identification, molecular cloning, and cellular distribution of the rat homolog of minichromosome maintenance protein 7 (MCM7) in the rat testis. *Molecular Reproduction and Development*, *73*(7), 866–877. https://doi.org/10.1002/mrd.20453

Cox, J., Hein, M. Y., Luber, C. A., Paron, I., Nagaraj, N., & Mann, M. (2014). Accurate proteome-wide label-free quantification by delayed normalization and maximal peptide ratio extraction, termed MaxLFQ. *Molecular & Cellular Proteomics : MCP*, *13*(9), 2513–2526. https://doi.org/10.1074/mcp.M113.031591

Darde, T. A., Lecluze, E., Lardenois, A., Stévant, I., Alary, N., Tüttelmann, F., Collin, O., Nef, S., Jégou, B., Rolland, A. D., & Chalmel, F. (2019). The ReproGenomics Viewer: a multi-omics and cross-species resource compatible with single-cell studies for the reproductive science community. *Bioinformatics (Oxford, England)*, *35*(17), 3133–3139. https://doi.org/10.1093/bioinformatics/btz047

Djouder, N., Metzler, S. C., Schmidt, A., Wirbelauer, C., Gstaiger, M., Aebersold, R., Hess, D., & Krek, W. (2007). S6K1-Mediated Disassembly of Mitochondrial URI/PP1γ Complexes Activates a Negative Feedback Program that Counters S6K1 Survival Signaling. *Molecular Cell*, *28*(1), 28–40. https://doi.org/10.1016/j.molcel.2007.08.010

Dudiki, T., Joudeh, N., Sinha, N., Goswami, S., Eisa, A., Kline, D., & Vijayaraghavan, S. (2019). The protein phosphatase isoform PP1γ1 substitutes for PP1γ2 to support spermatogenesis but not normal sperm function and fertility†. *Biology of Reproduction*, *100*(3), 721–736. https://doi.org/10.1093/biolre/ioy225

Fukuda, N., Fukuda, T., Sinnamon, J., Hernandez-Hernandez, A., Izadi, M., Raju, C. S., Czaplinski, K., & Percipalle, P. (2013). The Transacting Factor CBF-A/Hnrnpab Binds to the A2RE/RTS Element of Protamine 2 mRNA and Contributes to Its Translational Regulation during Mouse Spermatogenesis. *PLoS Genetics*, *9*(10), e1003858. https://doi.org/10.1371/journal.pgen.1003858

Gerhold, C. B., & Gasser, S. M. (2014). INO80 and SWR complexes: relating structure to function in chromatin remodeling. *Trends in Cell Biology*, *24*(11), 619–631. https://doi.org/10.1016/j.tcb.2014.06.004

Gou, L.-T., Lim, D.-H., Ma, W., Aubol, B. E., Hao, Y., Wang, X., Zhao, J., Liang, Z., Shao, C., Zhang, X., Meng, F., Li, H., Zhang, X., Xu, R., Li, D., Rosenfeld, M. G., Mellon, P. L., Adams, J. A., Liu, M.-F., & Fu, X.-D. (2020). Initiation of Parental Genome Reprogramming in Fertilized Oocyte by

Splicing Kinase SRPK1-Catalyzed Protamine Phosphorylation. *Cell*, *180*(6), 1212-1227.e14. https://doi.org/10.1016/j.cell.2020.02.020

Green, C. D., Ma, Q., Manske, G. L., Shami, A. N., Zheng, X., Marini, S., Moritz, L., Sultan, C., Gurczynski, S. J., Moore, B. B., Tallquist, M. D., Li, J. Z., & Hammoud, S. (2018). A Comprehensive Roadmap of Murine Spermatogenesis Defined by Single-Cell RNA-Seq. *Developmental Cell*, *46*(5), 651-667.e10. https://doi.org/10.1016/j.devcel.2018.07.025

Gui, J. F., Tronchère, H., Chandler, S. D., & Fu, X. D. (1994). Purification and characterization of a kinase specific for the serine- and arginine-rich pre-mRNA splicing factors. *Proceedings of the National Academy of Sciences*, *91*(23), 10824–10828. https://doi.org/10.1073/pnas.91.23.10824

Hazzouri, M., Pivot-Pajot, C., Faure, A.-K., Usson, Y., Pelletier, R., Sèle, B., Khochbin, S., & Rousseaux, S. (2000). Regulated hyperacetylation of core histones during mouse spermatogenesis: involvement of histone-deacetylases. *European Journal of Cell Biology*, *79*(12), 950–960. https://doi.org/10.1078/0171-9335-00123

Heberle, H., Meirelles, G. V., da Silva, F. R., Telles, G. P., & Minghim, R. (2015). InteractiVenn: a web-based tool for the analysis of sets through Venn diagrams. *BMC Bioinformatics*, *16*(1), 169. https://doi.org/10.1186/s12859-015-0611-3

Hornbeck, P. v, Zhang, B., Murray, B., Kornhauser, J. M., Latham, V., & Skrzypek, E. (2015). PhosphoSitePlus, 2014: mutations, PTMs and recalibrations. *Nucleic Acids Research*, *43*(Database issue), D512-20. https://doi.org/10.1093/nar/gku1267

Itoh, K., Kondoh, G., Miyachi, H., Sugai, M., Kaneko, Y., Kitano, S., Watanabe, H., Maeda, R., Imura, A., Liu, Y., Ito, C., Itohara, S., Toshimori, K., & Fujita, J. (2019). Dephosphorylation of protamine 2 at serine 56 is crucial for murine sperm maturation in vivo. *Science Signaling*, *12*(574). https://doi.org/10.1126/scisignal.aao7232

Kakihara, Y., & Houry, W. A. (2012). The R2TP complex: Discovery and functions. *Biochimica et Biophysica Acta (BBA) - Molecular Cell Research*, *1823*(1), 101–107. https://doi.org/10.1016/j.bbamcr.2011.08.016

Lewis, B. P., Green, R. E., & Brenner, S. E. (2003). Evidence for the widespread coupling of alternative splicing and nonsense-mediated mRNA decay in humans. *Proceedings of the National Academy of Sciences*, *100*(1), 189–192. https://doi.org/10.1073/pnas.0136770100

Li, J., Wang, J., Wang, J., Nawaz, Z., Liu, J. M., Qin, J., & Wong, J. (2000). Both corepressor proteins SMRT and N-CoR exist in large protein complexes containing HDAC3. *The EMBO Journal*, *19*(16), 4342–4350. https://doi.org/10.1093/emboj/19.16.4342

Li, Y., Cheng, Y., Zhu, T., Zhang, H., Li, W., Guo, Y., Qi, Y., Chen, X., Zhang, J., Sha, J., Zhou, Z., Zhu, H., & Guo, X. (2019). The Protein Phosphorylation Landscape of Mouse Spermatids during Spermiogenesis. *Proteomics*, *19*(11), e1900055. https://doi.org/10.1002/pmic.201900055

Ludwig, K. R., Schroll, M. M., & Hummon, A. B. (2018). Comparison of In-Solution, FASP, and S-Trap Based Digestion Methods for Bottom-Up Proteomic Studies. *Journal of Proteome Research*, *17*(7), 2480–2490. https://doi.org/10.1021/acs.jproteome.8b00235

Lynham, J., & Houry, W. A. (2018). The Multiple Functions of the PAQosome: An R2TP- and URI1 Prefoldin-Based Chaperone Complex. In *Prefoldins: the new chaperones. Advances in Experimental Medicine and Biology* (Vol. 1106, pp. 37–72). https://doi.org/10.1007/978-3-030-00737-9_4

Marcon, L., & Boissonneault, G. (2004). Transient DNA Strand Breaks During Mouse and Human Spermiogenesis:New Insights in Stage Specificity and Link to Chromatin Remodeling1. *Biology of Reproduction*, *70*(4), 910–918. https://doi.org/10.1095/biolreprod.103.022541

Moretti, C., Serrentino, M.-E., Ialy-Radio, C., Delessard, M., Soboleva, T. A., Tores, F., Leduc, M., Nitschké, P., Drevet, J. R., Tremethick, D. J., Vaiman, D., Kocer, A., & Cocquet, J. (2017). SLY regulates genes involved in chromatin remodeling and interacts with TBL1XR1 during sperm differentiation. *Cell Death & Differentiation*, *24*(6), 1029–1044. https://doi.org/10.1038/cdd.2017.32

Moritz, L., & Hammoud, S. S. (2022). The Art of Packaging the Sperm Genome: Molecular and Structural Basis of the Histone-To-Protamine Exchange. *Frontiers in Endocrinology*, *13*. https://doi.org/10.3389/fendo.2022.895502

Okano, K., Heng, H., Trevisanato, S., Tyers, M., & Varmuza, S. (1997). Genomic Organization and Functional Analysis of the Murine Protein Phosphatase 1c γ (Ppp1cc) Gene. *Genomics*, *45*(1), 211–215. https://doi.org/10.1006/geno.1997.4907

Oliva, R. (2006). Protamines and male infertility. *Human Reproduction Update*, *12*(4), 417–435. https://doi.org/10.1093/humupd/dml009

Oliva, R., Bazett-Jones, D., Mezquita, C., & Dixon, G. H. (1987). Factors affecting nucleosome disassembly by protamines in vitro. Histone hyperacetylation and chromatin structure, time dependence, and the size of the sperm nuclear proteins. *The Journal of Biological Chemistry*, *262*(35), 17016–17025.

Oliva, R., & Dixon, G. H. (1991). Vertebrate Protamine Genes and the Histone-to-Protamine Replacement Reaction. *Progress in Nucleic Acid Research and Molecular Biology*, *40*(C), 25–94. https://doi.org/10.1016/S0079-6603(08)60839-9

Papamichos-Chronakis, M., Watanabe, S., Rando, O. J., & Peterson, C. L. (2011). Global regulation of H2A.Z localization by the INO80 chromatin-remodeling enzyme is essential for genome integrity. *Cell*, *144*(2), 200–213. https://doi.org/10.1016/j.cell.2010.12.021

Papoutsopoulou, S., Nikolakaki, E., Chalepakis, G., Kruft, V., Chevaillier, P., & Giannakouros, T. (1999). SR protein-specific kinase 1 is highly expressed in testis and phosphorylates protamine 1. *Nucleic Acids Research*, *27*(14), 2972–2980. https://doi.org/10.1093/nar/27.14.2972

Patel, M., Sachidanandan, M., & Adnan, M. (2019). Serine arginine protein kinase 1 (SRPK1): a moonlighting protein with theranostic ability in cancer prevention. *Molecular Biology Reports*, *46*(1), 1487–1497. https://doi.org/10.1007/s11033-018-4545-5

Perissi, V., Scafoglio, C., Zhang, J., Ohgi, K. A., Rose, D. W., Glass, C. K., & Rosenfeld, M. G. (2008). TBL1 and TBLR1 phosphorylation on regulated gene promoters overcomes dual CtBP and NCoR/SMRT transcriptional repression checkpoints. *Molecular Cell*, *29*(6), 755–766. https://doi.org/10.1016/j.molcel.2008.01.020

Phillips, B. T., Williams, J. G., Atchley, D. T., Xu, X., Li, J.-L., Adams, A. L., Johnson, K. L., & Hall, T. M. T. (2019). Mass spectrometric identification of candidate RNA-binding proteins associated with Transition Nuclear Protein mRNA in the mouse testis. *Scientific Reports*, *9*(1), 13618. https://doi.org/10.1038/s41598-019-50052-z

Poullet, P., Carpentier, S., & Barillot, E. (2007). myProMS, a web server for management and validation of mass spectrometry-based proteomic data. *Proteomics*, *7*(15), 2553–2556. https://doi.org/10.1002/pmic.200600784

Qi, L., Liu, Z., Wang, J., Cui, Y., Guo, Y., Zhou, T., Zhou, Z., Guo, X., Xue, Y., & Sha, J. (2014). Systematic Analysis of the Phosphoproteome and Kinase-substrate Networks in the Mouse Testis. *Molecular & Cellular Proteomics*, *13*(12), 3626–3638. https://doi.org/10.1074/mcp.M114.039073

Risley, M. S., Einheber, S., & Bumcrot, D. A. (1986). Changes in DNA topology during spermatogenesis. *Chromosoma*, *94*(3), 217–227. https://doi.org/10.1007/BF00288496

Soler-Ventura, A., Gay, M., Jodar, M., Vilanova, M., Castillo, J., Arauz-Garofalo, G., Villarreal, L., Ballescà, J. L., Vilaseca, M., & Oliva, R. (2020). Characterization of Human Sperm Protamine Proteoforms through a Combination of Top-Down and Bottom-Up Mass Spectrometry Approaches. *Journal of Proteome Research*, *19*(1), 221–237. https://doi.org/10.1021/acs.jproteome.9b00499

Song, H., Wang, L., Chen, D., & Li, F. (2020). The Function of Pre-mRNA Alternative Splicing in Mammal Spermatogenesis. *International Journal of Biological Sciences*, *16*(1), 38–48. https://doi.org/10.7150/ijbs.34422

Szklarczyk, D., Gable, A. L., Nastou, K. C., Lyon, D., Kirsch, R., Pyysalo, S., Doncheva, N. T., Legeay, M., Fang, T., Bork, P., Jensen, L. J., & von Mering, C. (2021). The STRING database in 2021: customizable protein–protein networks, and functional characterization of user-uploaded

gene/measurement sets. *Nucleic Acids Research*, *49*(D1), D605–D612. https://doi.org/10.1093/nar/gkaa1074

The Gene Ontology Consortium. (2017). Expansion of the Gene Ontology knowledgebase and resources. *Nucleic Acids Research*, *45*(D1), D331–D338. https://doi.org/10.1093/nar/gkw1108

Tseden, K., Topaloglu, Ö., Meinhardt, A., Dev, A., Adham, I., Müller, C., Wolf, S., Böhm, D., Schlüter, G., Engel, W., & Nayernia, K. (2007). Premature translation of transition protein 2 mRNA causes sperm abnormalities and male infertility. *Molecular Reproduction and Development*, *74*(3), 273–279. https://doi.org/10.1002/mrd.20570

Tyanova, S., Temu, T., Sinitcyn, P., Carlson, A., Hein, M. Y., Geiger, T., Mann, M., & Cox, J. (2016). The Perseus computational platform for comprehensive analysis of (prote)omics data. *Nature Methods*, *13*(9), 731–740. https://doi.org/10.1038/nmeth.3901

Wang, T., Gao, H., Li, W., & Liu, C. (2019). Essential Role of Histone Replacement and Modifications in Male Fertility. *Frontiers in Genetics*, *10*. https://doi.org/10.3389/fgene.2019.00962

Willmitzer, L., Bode, J., & Wagner, K. G. (1977a). Phosphorylated protamines. I. Binding stoichiometry and thermal stability of complexes in DNA. *Nucleic Acids Research*, *4*(1), 149–162. https://doi.org/10.1093/nar/4.1.149

Willmitzer, L., Bode, J., & Wagner, K. G. (1977b). Phosphorylated protamines. II. Circular dichroism of complexes with DNA, dependency on ionic strength. *Nucleic Acids Research*, *4*(1), 163–176. https://doi.org/10.1093/nar/4.1.163

Xu, K., Yang, L., Zhao, D., Wu, Y., & Qi, H. (2014). AKAP3 Synthesis Is Mediated by RNA Binding Proteins and PKA Signaling During Mouse Spermiogenesis1. *Biology of Reproduction*, *90*(6). https://doi.org/10.1095/biolreprod.113.116111

Yoon, H.-G., Chan, D. W., Huang, Z.-Q., Li, J., Fondell, J. D., Qin, J., & Wong, J. (2003). Purification and functional characterization of the human N-CoR complex: the roles of HDAC3, TBL1 and TBLR1. *The EMBO Journal*, *22*(6), 1336–1346. https://doi.org/10.1093/emboj/cdg120

Table S1. SRPK1-associated proteins identified by LC-MS/MS. Data corresponding to spectral count (MS/MS count), total peptides identified, unique peptides identified, and sequence coverage expressed in % are shown for SRPK1 and IgG (negative control) immunoprecipitations.

Gene names	Protein symbol	Protein names (Abbreviation)	Accesion number	P-value SRPK1_IgG	log2(FC)	MS/MS count SRPK1	MS/MS count IgG	Total peptides SRPK1	Total peptides IgG	Unique peptides SRPK1	Unique peptides IgG	Sequence coverage SRPK1 [%]	Sequence coverage IgG [%]
Pabpc1	**PABP1**	Polyadenylate-binding protein 1	P29341	1.55E-03	1.42	53	24	32	19	32	19	57.5	41.2
Srpk1	**SRPK1**	SRSF protein kinase 1	O70551	6.14E-04	7.57	47	2	28	2	24	1	51.7	4.5
Hnrnpa2b1	**hnRNP A2/B1**	Heterogeneous nuclear ribonucleoproteins A2/B1	O88569	7.15E-03	2.24	28	11	17	9	16	8	45.7	32.9
Ilf3	**ILF3**	Interleukin enhancer-binding factor 3	Q9Z1X4	4.43E-03	3.18	24	8	22	7	20	6	33.9	9.9
Ap2b1	**AP2B1**	AP-2 complex subunit beta	Q9DBG3	1.62E-03	0.95	21	14	19	14	10	7	25.6	20.1
Rtcb	**RTCB**	tRNA-splicing ligase RtcB homolog	Q99LF4	9.58E-03	1.30	20	14	16	12	16	12	38.7	33.8
Rpl10a	**RPL10A**	60S ribosomal protein L10a	P53026	1.60E-03	2.01	20	8	11	7	11	7	38.9	28.3
Mvp	**MVP**	Major vault protein	Q9EQK5	Apparition in SRPK1		19	1	17	1	17	1	28.0	1.3
Hnrnpu	**hnRNP U**	Heterogeneous nuclear ribonucleoprotein U	Q8VEK3	3.92E-03	1.18	19	13	16	12	16	12	20.6	19.2
Rplp0	**RPLP0**	60S acidic ribosomal protein P0	P14869	6.69E-03	2.21	17	8	12	6	12	6	49.1	35.4
Ilf2	**ILF2**	Interleukin enhancer-binding factor 2	Q9CXY6	5.26E-03	2.54	16	6	12	5	12	5	45.3	21.3
Mcm7	**MCM7**	DNA replication licensing factor MCM7	Q61881	Apparition in SRPK1		16	0	14	0	14	0	25.4	0.8
Mcm4	**MCM4**	DNA replication licensing factor MCM4	P49717	Apparition in SRPK1		15	0	13	0	13	0	20.3	0.0
Sf3a1	**SF3A1**	Splicing factor 3A subunit 1	Q8K4Z5	7.66E-03	1.00	15	8	12	7	12	7	20.5	12.2
Thrap3	**TRAP150**	Thyroid hormone receptor-associated protein 3	Q569Z6	1.86E-03	1.97	14	6	13	6	13	6	15.7	8.8
Snrnp40	**WDR57**	U5 small nuclear ribonucleoprotein 40 kDa protein	Q6PE01	1.73E-03	1.72	13	5	11	5	11	5	46.7	18.5
Alyref	**THOC4**	THO complex subunit 4	O08583	7.37E-03	3.07	13	4	8	4	8	4	39.0	16.2
Srsf1	**ASF/SF2**	Serine/arginine-rich splicing factor 1	Q6PDM2	9.91E-03	2.08	13	5	10	5	10	5	39.0	23.1
Hist1h1a	**H1F1**	Histone H1.1	P43275	5.41E-03	1.66	12	6	5	4	5	4	33.7	28.2
Hnrnpab	**hnRNP A/B**	Heterogeneous nuclear ribonucleoprotein A/B	Q99020	3.94E-04	3.48	12	3	10	3	10	3	32.6	16.0
Hnrnpd	**hnRNP D0**	Heterogeneous nuclear ribonucleoprotein D0	Q60668	4.05E-03	2.91	12	4	9	4	9	4	28.6	13.3
Eif4a3	**DDX48**	Eukaryotic initiation factor 4A-III	Q91VC3	4.95E-04	0.59	11	9	11	9	9	7	32.0	27.6
Prpf4	**PRPF4**	U4/U6 small nuclear ribonucleoprotein Prp4	Q9DAW6	Apparition in SRPK1		9	0	9	0	9	0	25.3	0.9
Gapvd1	**GAPVD1**	GTPase-activating protein and VPS9 domain-containing protein 1	Q6PAR5	Apparition in SRPK1		9	0	8	0	8	0	9.2	0.5
Hnrnpc	**hnRNP C1/C2**	Heterogeneous nuclear ribonucleoproteins C1/C2	Q9Z204	9.74E-03	2.58	9	5	7	5	7	5	24.3	17.9
Ttc30a2	**TTC30A2**	Tetratricopeptide repeat protein 30A2	A2AKQ8	Apparition in SRPK1		6	1	6	1	2	1	12.0	1.5
Rbmxl1	**RBMXRT**	RNA binding motif protein, X-linked-like-1	Q91VM5	Apparition in SRPK1		6	1	6	1	1	0	16.8	2.7
Rbm17	**RBM17**	Splicing factor 45	Q8JZX4	5.76E-03	0.77	6	4	6	4	6	4	19.7	11.2
Cirbp	**CIRBP**	Cold-inducible RNA-binding protein	P60824	Apparition in SRPK1		6	1	5	1	5	1	29.6	10.7
Rbm27	**RBM27**	RNA-binding protein 27	Q5SFM8	Apparition in SRPK1		6	0	6	0	5	0	6.6	0.0
Prpf3	**PRPF3**	U4/U6 small nuclear ribonucleoprotein Prp3	Q922U1	Apparition in SRPK1		6	0	5	0	5	0	10.8	0.6
Mrto4	**MRTO4**	mRNA turnover protein 4 homolog	Q9D0I8	Apparition in SRPK1		6	1	5	1	5	1	22.7	4.2
Lsm12	**LSM12**	Protein LSM12 homolog	Q9D0R8	4.24E-03	0.75	5	3	5	3	5	3	36.8	20.0
Mtco2	**COX2**	Cytochrome c oxidase subunit 2	P00405	4.22E-05	2.20	5	4	3	2	3	2	16.0	17.4
Zpbp2	**ZPBP2**	Zona pellucida-binding protein 2	Q6X786	Apparition in SRPK1		5	0	4	0	4	0	13.9	0.0
Tbl1xr1	**TBL1XR1**	F-box-like/WD repeat-containing protein TBL1XR1	Q8BHJ5	Apparition in SRPK1		5	1	5	1	5	1	16.4	2.6
Ncbp2	**NCBP2**	Nuclear cap-binding protein subunit 2	Q9CQ49	Apparition in SRPK1		5	1	4	1	4	1	32.9	6.0
Igf2bp3	**IGF2BP3**	Insulin-like growth factor 2 mRNA-binding protein 3	Q9CPN8	Apparition in SRPK1		3	1	3	1	3	1	8.7	2.2
Prss50	**TSP50**	Probable threonine protease PRSS50	Q8BLH5	Apparition in SRPK1		3	1	3	1	3	1	7.9	3.7
Ngdn	**NGDN**	Neuroguidin	Q9DB96	Apparition in SRPK1		2	1	2	1	2	1	8.9	6.7

Proteins with at least 1 unique peptide identified after 1%FDR correction are shown. Proteins exclusively identified in SRPK1 IP, or with p value < 0.01 and fold-change enrichment (FC) > 1.5 (corresponding to log2FC = 0.58) after comparison with the negative control (IgG) were considered as SRPK1 interactors. Proteins exclusively identified in SRPK1 IP are expressed as "Apparition in SRPK1".

Table S2. Gene ontology (GO) and Reactome pathway enrichment analyses of SRPK1-IP protein dataset. A representation of GO enriched terms for biological processes, molecular functions, and cellular components are listed.

GO biological processes	count	*p* -value	Gene names
CRD-mediated mRNA stabilization (GO:0070934)	4	2.74E-04	Pabpc1, Hnrnpu, Hnrnpd, Igf2bp3
mRNA stabilization (GO:0048255)	7	2.74E-07	Pabpc1, Hnrnpu, Hnrnpd, Igf2bp3, Srsf1, Cirbp, Thrap3
negative regulation of mRNA catabolic process (GO:1902373)	8	1.51E-08	Pabpc1, Hnrnpab, Hnrnpu, Hnrnpd, Igf2bp3, Srsf1, Cirbp, Thrap3
RNA stabilization (GO:0043489)	7	7.31E-07	Pabpc1, Hnrnpu, Hnrnpd, Igf2bp3, Srsf1, Cirbp, Thrap3
post-transcriptional regulation of gene expression (GO:0010608)	11	1.10E-05	Ngdn, Pabpc1, Hnrnpu, Ncbp2, Hnrnpd, Srsf1, Cirbp, Ilf3, Igf2bp3, Eif4a3, Thrap3,
negative regulation of nuclear-transcribed mRNA catabolic process, deadenylation-dependent decay (GO:1900152)	3	4.32E-02	Pabpc1, Hnrnpu, Hnrnpd
regulation of translation (GO:0006417)	9	3.60E-04	Ngdn, Pabpc1, Hnrnpu, Ncbp2, Hnrnpd, Cirbp, Ilf3, Igf2bp3, Eif4a3
regulation of cellular macromolecule biosynthetic process (GO:2000112)	9	2.14E-03	Ngdn, Pabpc1, Hnrnpu, Ncbp2, Hnrnpd, Cirbp, Ilf3, Igf2bp3, Eif4a3
positive regulation of mRNA splicing, via spliceosome (GO:0048026)	4	1.13E-02	Cirbp, Rbmxl1, Eif4a3, Thrap3
positive regulation of mRNA processing (GO:0050685)	5	5.57E-04	Ncbp2, Cirbp, Rbmxl1, Eif4a3, Thrap3
mRNA export from nucleus (GO:0006406)	4	2.13E-03	Ncbp2, Alyref, Hnrnpa2b1, Eif4a3
RNA transport (GO:0050658)	6	1.58E-04	Ncbp2, Alyref, Srsf1, Ig2bp3, Hnrnpa2b1, Eif4a3
establishment of RNA localization (GO:0051236)	7	1.73E-04	Ncbp2, Alyref, Srsf1, Ig2bp3, Hnrnpa2b1, Eif4a3
nuclear-transcribed mRNA catabolic process (GO:0000956)	5	1.51E-02	Pabpc1, Ncbp2, Mrto4, Eif4a3, Thrap3
mRNA splicing, via spliceosome (GO:0000398)	9	3.70E-06	Ncbp2, Prpf4, Srsf1, Prpf3, Hnrnpa2b1, Eif4a3, Srpk1, Rbm17, Sf3a1
RNA splicing, via transesterification reactions (GO:0000375)	9	3.70E-06	Ncbp2, Prpf4, Srsf1, Prpf3, Hnrnpa2b1, Eif4a3, Srpk1, Rbm17, Sf3a1
ribonucleoprotein complex assembly (GO:0022618)	6	9.29E-03	Mrto4, Srsf1, Rplp0, Prpf3, Srpk1, Sf3a1
ribonucleoprotein complex subunit organization (GO:0071826)	6	1.21E-02	Mrto4, Srsf1, Rplp0, Prpf3, Srpk1, Sf3a1
ribonucleoprotein complex biogenesis (GO:0022613)	8	1.03E-02	Ngdn, Mrto4, Srsf1, Rplp0, Prpf3, Rpl10a, Srpk1, Sf3a1

GO molecular functions	count	*p* -value	Gene names
N6-methyladenosine-containing RNA binding (GO:1990247)	3	5.73E-03	Hnrnpc, Igf2bp3, Hnrnpa2b1
RNA binding (GO:0003723)	21	3.74E-14	Pabpc1, Hnrnpc, Hnrnpu, Ncbp2, Alyref, Rbm27, Hnrnpd, Prpf4, Srsf1, Ilf3, Rplp0, Cirbp, Rbmxl1, Ilf2, Igf2bp3, Hnrnpa2b1, Eif4a3, Rpl10a, Rbm17, Alyref, Sf3a1
poly-pyrimidine tract binding (GO:0008187)	4	1.85E-03	Pabpc1, Hnrnpc, Hnrnpu, Cirbp
single-stranded RNA binding (GO:0003727)	6	1.40E-04	Pabpc1, Hnrnpc, Hnrnpu, Cirbp, Ilf3, Eif4a3
mRNA 3'-UTR binding (GO:0003730)	8	1.02E-07	Pabpc1, Hnrnpc, Hnrnpu, Hnrnpd, Hnrnpa2b1, Cirbp, Ilf3, Igf2bp3
mRNA binding (GO:0003729)	12	2.13E-10	Pabpc1, Hnrnpc, Hnrnpu, Hnrnpd, Hnrnpa2b1, Cirbp, Ilf3, Igf2bp3, Ncbp2, Alyref, Srsf1, Eif4a3
single-stranded DNA binding (GO:0003697)	5	5.36E-04	Mcm4, Hnrnpu, Alyref, Hnrnpa2b1, Mcm7

GO cellular components	count	*p* -value	Gene names
exon-exon junction complex (GO:0035145)	4	2.71E-06	Alyref, Srsf1, Eif4a3, Thrap3
nuclear protein-containing complex (GO:0140513)	20	6.97E-12	Hnrnpab, Pabpc1, Hnrnpc, Hnrnpu, Alyref, Prpf4, Tbl1x, Srsf1, Cirbp, Rbmxl1, Prpf3, Tbl1xr1, Hnrnpa2b1, Snrnp40, Eif4a3, Mcm7, Rbm17, Thrap3, Sf3a1
catalytic step 2 spliceosome (GO:0071013)	9	1.24E-11	Pabpc1, Hnrnpc, Hnrnpu, Alyref, Srsf1, Hnrnpa2b1, Snrnp40, Eif4a3, Sf3a1
spliceosomal complex (GO:0005681)	14	1.56E-16	Pabpc1, Hnrnpc, Hnrnpu, Alyref, Prpf4, Prpf3, Srsf1, Cirbp, Rbmxl1, Hnrnpa2b1, Snrnp40, Rbm17, Eif4a3, Sf3a1
U2-type spliceosomal complex (GO:0005684)	5	2.28E-03	Prpf4, Prpf3, Snrnp40, Eif4a3, Sf3a1
ribonucleoprotein complex (GO:1990904)	22	6.52E-20	Hnrnpab, Pabpc1, Hnrnpc, Hnrnpu, Mrto4, Alyref, Hnrnpd, Prpf4, Srsf1, Ilf3, Rplp0, Cirbp, Rbmxl1, Prpf3, Ilf2, Hnrnpa2b1, Snrnp40, Eif4a3, Rpl10a, Rbm17, Sf3a1
cytoplasmic ribonucleoprotein granule (GO:0036464)	6	1.06E-02	Pabpc1, Hnrnpu, Rplp0, Cirbp, Igf2bp3, Hnrnpa2b1
nuclear speck (GO:0016607)	8	5.68E-04	Hnrnpu, Prpf4, Srsf1, Prpf3, Snrnp40, Srpk1, Thrap3, Sf3a1

Reactome overrepresented pathways	*Found reactions*	FDR	Gene names
mRNA Splicing - Major Pathway	8/9	0.003	Alyref, Eif4a3, Hnrnpa2b1, Hnrnpc, Hnrnpd, Hnrnpu, Ncbp2, Prpf3, Prpf4, Rbm17, Sf3a1, Snrnp40, Srsf1
mRNA Splicing	13/14	0.003	
Processing of Capped Intron-Containing pre-mRNA	31/32	0.025	

Table S3. Gene expression data of SRPK1-associated proteins extracted from Green et al., 2018, expressed as ln(transcripts-per-10K+1)

		Mitotic phase	Meiotic phase	Spermiogenesis	
Gene name	*Somatic cells*	*Spermatogonia*	*Spermatocytes*	*Round spermatids*	*Elongating spermatids*
Srpk1	**0.353**	**0.615**	**2.552**	**1.938**	**0.763**
Alyref	0.04	0.209	0.24	0.007	0.004
Ap2b1	0.206	0.165	1.17	1.29	0.935
Cirbp	0.24	0.799	0.608	0.054	0.027
Eif4a3	0.224	0.602	1.046	0.292	0.042
Gapvd1	0.158	0.129	0.392	0.132	0.052
H1f1	0.002	0.091	0.001	0.003	0.001
Hnrnpa2b1	1.383	1.892	1.953	0.584	0.147
Hnrnpab	0.628	0.881	0.876	1.003	0.15
Hnrnpc	0.615	1.012	1.2	0.321	0.049
Hnrnpd	0.404	0.58	0.834	0.462	0.067
Hnrnpu	0.263	0.29	0.671	0.2	0.029
Igf2bp3	0.059	0.057	0.797	0.776	0.84
Ilf2	0.248	0.463	1.036	0.167	0.024
Ilf3	0.207	0.46	1.21	0.295	0.052
Lsm12	0.173	0.323	1.054	0.585	0.285
Mcm4	0.037	0.202	0.006	0.011	0.002
Mcm7	0.068	0.336	0.937	0.639	0.061
Mrto4	0.077	0.195	1.042	0.53	0.025
Mtco2	NA	NA	NA	NA	NA
Mvp	0.081	0.009	0.003	0.003	0.001
Ncbp2	0.228	0.476	0.842	0.66	0.052
Ngdn	0.147	0.258	0.372	0.089	0.009
Pabpc1	1.828	2.441	6.015	4.809	0.957
Prpf3	0.052	0.245	0.35	0.034	0.008
Prpf4	0.074	0.146	0.185	0.199	0.03
Prss50	0.005	0.374	0.005	0.004	0.005
Rbm17	0.348	0.468	0.69	0.159	0.028
Rbm27	0.208	0.457	1.616	0.805	0.051
Rbmxl1	0.13	0.111	0.193	0.028	0.004
Rpl10a	0.589	0.608	0.393	0.042	0.032
Rplp0	1.287	1.634	3.015	2.239	1.271
Rtcb	0.137	0.214	0.221	0.022	0.006
Sf3a1	0.086	0.176	0.301	0.073	0.005
Snrnp40	0.083	0.422	0.457	0.05	0.01
Srsf1	0.231	0.344	0.308	0.175	0.063
Tbl1xr1	0.103	0.068	0.382	0.209	0.044
Thrap3	0.507	0.685	0.87	0.267	0.032
Ttc30a2	0.021	0.026	1.263	0.551	0.027
Zpbp2	0.065	0.107	2.698	1.68	0.056

Color legend
0
0.2
0.4
0.6
0.8
1
1.2
1.4
1.6
1.8
2
2.2
2.4
2.6
2.8
3
3.2
3.4
3.6
3.8
4
4.2
4.4
4.6
4.8
5
5.2
5.4
5.6
5.8
6
6.2

Table S4. Testicular gene expression levels of the different Minichromosome (MCM) protein family members.

		Mitotic phase	Meiotic phase	Spermiogenesis	
Gene name	*Somatic cells*	*Spermatogonia*	*Spermatocytes*	*Round spermatids*	*Elongating spermatids*
Mcm2	0.02	0.292	0.003	0.002	0.002
Mcm3	0.05	0.314	0.031	0.005	0.003
Mcm4	0.037	0.202	0.006	0.011	0.002
Mcm5	0.013	0.209	0.015	0.018	0.002
Mcm6	0.033	0.256	0.055	0.012	0.004
Mcm7	0.068	0.336	0.937	0.639	0.061
Mcm8	0.019	0.144	0.018	0.053	0.003
Mcm9	0.024	0.029	0.127	0.032	0.007
Mcm10	0.005	0.07	0.055	0.005	0.002

Color legend
0
0.2
0.4
0.6
0.8
1

Table S5. PP1γ-associated proteins identified by LC-MS/MS. Data corresponding to spectral count (MS/MS count), total peptides identified, unique peptides identified, and sequence coverage expressed in % are shown for PP1γ and IgG (negative control) immunoprecipitations.

Gene names	Protein symbol	Protein names	Accession number	p-value PP1γ_IgG	log2(ratio PP1γ/IgG)	MS/MS count PP1γ	MS/MS count IgG	Total peptides PP1γ	Total peptides IgG	Unique peptides PP1γ	Unique peptides IgG	Sequence coverage PP1γ [%]	Sequence coverage IgG [%]
Ppp1cc	**PPP1CC**	Serine/threonine-protein phosphatase PP1-gamma catalytic subunit (PP1γ)	P63087	6.9E-07	6.90281	45	5	20	5	8	1	69.3	19.7
Ppp1r2	**PPP1R2**	Protein phosphatase inhibitor 2	Q9DCL8	Apparition in PP1γ		38	0	13	0	13	0	83.3	0.0
Ppp1r7	**PPP1R7**	Protein phosphatase 1 regulatory subunit 7	Q3UM45	Apparition in PP1γ		32	1	18	1	18	1	58.7	2.8
Ppp1r9b	**PPP1R9B**	Neurabin-2	Q6R891	Apparition in PP1γ		25	0	19	0	19	0	29.3	0.0
Ylpm1	**ZAP3**	YLP motif-containing protein 1	Q9R0I7	Apparition in PP1γ		24	0	18	0	18	0	17.4	0.0
Ilf2	**ILF2**	Interleukin enhancer-binding factor 2	Q9CXY6	0.00068	1.98471	22	9	15	8	15	8	48.0	28.8
Zfr	**ZFR**	Zinc finger RNA-binding protein	O88532	Apparition in PP1γ		19	1	16	1	16	1	24.7	1.1
Ruvbl2	**RUVBL2**	RuvB-like 2	Q9WTM5	0.00269	2.22331	19	6	15	6	15	6	36.8	17.0
Rpap3	**RPAP3**	RNA polymerase II-associated protein 3	Q9D706	Apparition in PP1γ		18	0	16	0	16	0	38.5	0.9
Appl2	**APPL2**	DCC-interacting protein 13-beta	Q8K3G9	Apparition in PP1γ		18	0	15	0	15	0	37.4	0.0
Ppp1r8	**NIPP-1**	Nuclear inhibitor of protein phosphatase 1	Q8R3G1	Apparition in PP1γ		17	0	11	0	11	0	50.8	2.0
Ruvbl1	**RUVBL1**	RuvB-like 1	P60122	0.00453	3.10159	16	4	13	4	13	4	44.1	15.7
Ppp1r10	**PNUTS**	Serine/threonine-protein phosphatase 1 regulatory subunit 10	Q80W00	Apparition in PP1γ		16	0	15	0	15	0	21.4	0.0
Prmt5	**PRMT5**	Protein arginine N-methyltransferase 5	Q8CIG8	0.00063	3.34549	12	3	10	3	10	3	21.2	6.3
Ppp1r11	**PPP1R11**	Protein phosphatase 1 regulatory subunit 11	Q8K1L5	Apparition in PP1γ		12	0	4	0	4	0	34.4	0.0
Wdr77	**WDR77**	Methylosome protein 50	Q99J09	0.00463	3.5476	12	2	7	2	7	2	36.9	8.6
Wdr92	**WDR92**	WD repeat-containing protein 92	Q8BGF3	Apparition in PP1γ		11	0	9	0	9	0	38.8	0.0
Uri1	**RMP**	Unconventional prefoldin RPB5 interactor	Q3TLD5	Apparition in PP1γ		11	0	10	0	10	0	30.9	0.0
Pym1	**PYM1**	Partner of Y14 and mago	Q8CHP5	Apparition in PP1γ		10	0	6	0	6	0	55.5	0.0
Appl1	**APPL1**	DCC-interacting protein 13-alpha	Q8K3H0	Apparition in PP1γ		10	0	9	0	9	0	22.3	0.0
Eif3a	**eIF3a**	Eukaryotic translation initiation factor 3 subunit A	P23116	Apparition in PP1γ		8	1	8	1	8	1	7.2	0.6
Tox4	**TOX4**	TOX high mobility group box family member 4	Q8BU11	Apparition in PP1γ		8	0	6	0	6	0	15.0	0.0
Snx2	**SNX2**	Sorting nexin-2	Q9CWK8	Apparition in PP1γ		8	0	8	0	6	0	20.7	0.7
Fn1	**FN1**	Fibronectin;Anastellin	P11276	Apparition in PP1γ		8	0	8	0	8	0	5.3	0.0
Rbm8a	**RBM8A**	RNA-binding protein 8A	Q9CWZ3	0.00465	4.40475	7	2	5	2	5	2	48.7	13.0
Dnah17	**DNAH17**	Dynein heavy chain 17, axonemal	Q69Z23	Apparition in PP1γ		6	0	6	0	6	0	2.2	0.0
Pih1d1	**PIH1D1**	PIH1 domain-containing protein 1	Q9CQJ2	Apparition in PP1γ		6	0	5	0	5	0	28.4	0.0
Tsks	**TSKS**	Testis-specific serine kinase substrate	O54887	Apparition in PP1γ		6	0	6	0	6	0	14.9	0.8
Lmtk2	**LMTK2**	Serine/threonine-protein kinase LMTK2	Q3TYD6	Apparition in PP1γ		6	0	6	0	6	0	6.9	0.0
Ift81	**IFT81**	Intraflagellar transport protein 81 homolog	O35594	Apparition in PP1γ		5	0	5	0	5	0	11.0	0.0
Drg1	**DRG1**	Developmentally-regulated GTP-binding protein 1	P32233	0.00064	1.06975	5	3	5	3	5	3	17.9	12.9
Tprn	**TPRN**	Taperin	A2AI08	Apparition in PP1γ		5	0	4	0	4	0	10.6	0.0
Arhgef2	**ARHGEF2**	Rho guanine nucleotide exchange factor 2	Q60875	Apparition in PP1γ		4	0	4	0	4	0	7.4	0.0
Wdr34	**WDR34**	WD repeat-containing protein 34	Q5U4F6	Apparition in PP1γ		4	1	4	1	4	1	14.1	4.7
Mtrex	**SKIV2L2**	Exosome RNA helicase MTR4	Q9CZU3	Apparition in PP1γ		4	1	3	1	3	1	5.0	1.2
Kpna6	**KPNA6**	Importin subunit alpha-7	O35345	Apparition in PP1γ		3	1	3	1	2	1	9.4	3.9
Acaa2	**ACAA2**	3-ketoacyl-CoA thiolase, mitochondrial	Q8BWT1	Apparition in PP1γ		3	1	3	1	3	1	12.3	6.1
Cfap410	**CFAP410**	Protein C21orf2 homolog	Q8C6G1	0.0086	1.04965	3	2	3	2	3	2	17.9	11.5
Cops5	**COPS5**	COP9 signalosome complex subunit 5	O35864	Apparition in PP1γ		3	1	3	1	3	1	14.9	2.9
Wdr61	**WDR61**	WD repeat-containing protein 61	Q9ERF3	Apparition in PP1γ		3	0	3	0	3	0	18.6	0.0
Sec23a	**SEC23A**	Protein transport protein Sec23A	Q01405	Apparition in PP1γ		3	1	3	1	3	1	5.2	2.2
Magoh	**MAGOH**	Protein mago nashi homolog 2;Protein mago nashi homolog	P61327	Apparition in PP1γ		3	0	3	0	3	0	25.3	2.3
Ift80	**IFT80**	Intraflagellar transport protein 80 homolog	Q8K057	Apparition in PP1γ		3	0	3	0	3	0	5.5	0.0
Cetn4	**CETN4**	Centrin-4	Q8K4K1	Apparition in PP1γ		3	0	3	0	3	0	27.4	2.6
Lrrc34	**LRRC34**	Leucine-rich repeat-containing protein 34	Q9DAM1	Apparition in PP1γ		3	0	3	0	3	0	8.3	0.9
Ndufb10	**NDUFB10**	NADH dehydrogenase [ubiquinone] 1 beta subcomplex subunit 10	Q9DCS9	Apparition in PP1γ		3	1	3	1	3	1	18.6	5.3
Ube2m	**UBE2M**	NEDD8-conjugating enzyme Ubc12	P61082	Apparition in PP1γ		2	0	2	0	2	0	16.8	2.9
Kpna3	**KPNA3**	Importin subunit alpha-4	O35344	Apparition in PP1γ		2	0	2	0	2	0	6.9	1.2
Phactr1	**PHACTR1**	Phosphatase and actin regulator 1	Q2M3X8	Apparition in PP1γ		2	0	2	0	2	0	5.8	0.0
Tbl1xr1	**TBL1XR1**	F-box-like/WD repeat-containing protein TBL1XR1	Q8BHJ5	Apparition in PP1γ		2	0	2	0	1	0	7.8	0.8
Lypd4	**LYPD4**	Ly6/PLAUR domain-containing protein 4	Q8BVP6	Apparition in PP1γ		2	1	2	1	2	1	17.4	6.5
Txnl1	**TXNL1**	Thioredoxin-like protein 1	Q8CDN6	Apparition in PP1γ		2	1	2	1	2	1	15.0	6.0
Ak1	**AK1**	Adenylate kinase isoenzyme 1	Q9R0Y5	Apparition in PP1γ		2	1	2	1	2	1	17.0	4.5
Ptrh2	**PTRH2**	Peptidyl-tRNA hydrolase 2, mitochondrial	Q8R2Y8	Apparition in PP1γ		2	1	2	1	2	1	17.5	8.8
Pin1	**PIN1**	Peptidyl-prolyl cis-trans isomerase NIMA-interacting 1	Q9QUR7	Apparition in PP1γ		2	1	2	1	2	1	23.6	8.1

Proteins with at least 1 unique peptide identified after 1% FDR correction are shown. Proteins exclusively identified in PP1γ IP, or with p value < 0.01 and fold-change enrichment (FC) > 1.5 (corresponding to log2FC = 0.58) after comparison with the negative control (IgG) were considered as SRPK1 interactors. Proteins exclusively identified in PP1γ IP are expressed as "Apparition in PP1γ".

Table S6. Gene ontology (GO) and Reactome pathway enrichment analyses of PP1γ-associated proteins. A representation of GO enriched terms for biological processes, molecular functions, and cellular components are listed.

GO biological processes	count	*p* -value	Gene names
box C/D snoRNP assembly (GO:0000492)	3	3.86E-02	Ruvbl1, Ruvbl2, Pih1d1
ribonucleoprotein complex assembly (GO:0022618)	6	4.08E-02	Ruvbl1, Ruvbl2, Pih1d1, Eif3a, Wdr77, Prmt5
regulation of protein dephosphorylation (GO:0035304)	6	1.91E-03	Pin1, Ppp1r2, Ppp1r8, Ppp1r11, Ppp1r7, Ppp1r9b

GO molecular functions	count	*p* -value	Gene names
protein serine/threonine phosphatase inhibitor activity (GO:0004865)	3	3.43E-02	Ppp1r8, Ppp1r11, Ppp1r7
phosphatase inhibitor activity (GO:0019212)	9	4.53E-11	Ppp1r10, Lmtk2, Uri1, Phactr1, Ppp1r2, Ppp1r8, Ppp1r11, Ppp1r7, Ppp1r9b
protein phosphatase 1 binding (GO:0008157)	5	1.27E-04	Ppp1r10, Ppp1cc, Phactr1, Ppp1r11, Ppp1r9b
enzyme binding (GO:0019899)	18	2.43E-02	Cops5, Ppp1r10, Ppp1cc, Uri1, Pin1, Appl1, Fn1, Arhgef2, Tprn, Ruvbl1, Eif3a, Ruvbl2, Appl2, Tsks, Phactr1, Ppp1r11, Ppp1r9b, Pih1d1

GO cellular components	count	*p* -value	Gene names
R2TP complex (GO:0097255)	4	6.75E-06	Rpap3, Ruvbl1, Ruvbl2, Pih1d1
RPAP3/R2TP/prefoldin-like complex (GO:1990062)	6	3.44E-09	Rpap3, Ruvbl1, Ruvbl2, Pih1d1, Uri1, Wdr92
PTW/PP1 phosphatase complex (GO:0072357)	3	2.72E-03	Ppp1r10, Ppp1cc, Tox4
protein serine/threonine phosphatase complex (GO:0008287)	4	2.54E-02	Ppp1r10, Ppp1cc, Ppp1r7, Tox4
ciliary basal body (GO:0036064)	6	9.72E-03	Pin1, Cfap410, Ift81, Cetn4, Wdr34, Ift80
ribonucleoprotein complex (GO:1990904)	10	1.64E-02	Mtrex, Magoh, Drg1, Ruvbl1, Eif3a, Ruvbl2, Rbm8a, Ppp1r8, Ilf2, Pih1d1
cytosol (GO:0005829)	26	6.95E-04	Cops5, Magoh, Rpap3, Ak1, Wdr61, Uri1, Pin1, Appl1, Cfap410, Tprn, Kpna3, Drg1, Ruvbl1, Eif3a, Ptrh2, Ruvbl2, Phactr1, Kpna6, Sec23a, Rbm8a, Pym1, Txnl1, Wdr34, Wdr77, Prmt5, Ylpm1
nucleus (GO:0005634)	34	2.61E-02	Mtrex, Cops5, Ppp1r10, Magoh, Ppp1cc, Wdr61, Uri1, Lrrc34, Pin1, Appl1, Kpna3, Drg1, Ruvbl1, Eif3a, Ruvbl2, Appl2, Phactr1, Kpna6, Rbm8a, Pym1, Ppp1r8, Txnl1, Ilf2, Ppp1r11, Tbl1xr1, Ube2m, Ppp1r7, Tox4, Zfr, Wdr77
integral component of membrane (GO:0016021)	2	1.68E-02	Lmtk2, Ndufb10

Reactome overrepresented pathways	*Found reactions*	FDR	Gene names
No overrepresented pathways	-	-	-

Table S7. Gene expression data of PP1γ-associated proteins extracted from Green et al., 2018, expressed as ln(transcripts-per-10K+1)

		Mitotic phase	Meiotic phase	Spermiogenesis	
Gene name	*Somatic cells*	*Spermatogonia*	*Spermatocytes*	*Round spermatids*	*Elongating spermatids*
Ppp1cc	**0.158**	**0.124**	**1.277**	**0.928**	**0.318**
Acaa2	0.498	0.013	0.017	0.012	0.013
Ak1	0.095	0.012	0.218	0.775	0.985
Appl1	0.272	0.309	0.14	0.085	0.025
Appl2	0.429	0.063	0.074	0.016	0.013
Arhgef2	0.113	0.061	0.089	0.709	0.28
Cetn4	0.165	0.131	2.851	2.073	0.528
Cfap410	0.049	0.03	0.293	0.166	0.05
Cops5	0.196	0.201	1.468	1.041	0.328
Dnah17	0.02	0.04	0.585	0.212	0.033
Drg1	0.128	0.256	0.823	0.492	0.117
Eif3a	1.021	1.067	1.503	1.647	0.665
Fn1	0.016	0.107	0.009	0.056	0.001
Ift80	0.04	0.088	0.827	0.224	0.023
Ift81	0.091	0.218	1.18	1.33	0.123
Ilf2	0.248	0.463	1.036	0.167	0.024
Kpna3	0.088	0.26	0.161	0.032	0.008
Kpna6	0.077	0.055	0.389	0.709	0.081
Lmtk2	0.024	0.036	0.118	0.012	0.003
Lrrc34	0.065	0.054	1.894	1.889	0.04
Lypd4	0.093	0.07	2.407	2.286	0.258
Magoh	0.169	0.556	0.31	0.09	0.01
Mtrex	0.153	0.408	0.753	0.835	0.035
Ndufb10	0.443	0.385	1.683	0.943	0.143
Phactr1	0.134	0.011	0.032	0.614	0.83
Pih1d1	0.119	0.188	1.55	1.08	0.262
Pin1	0.183	0.296	0.69	0.063	0.022
Ppp1r10	0.105	0.105	0.969	1.02	0.216
Ppp1r11	0.303	0.201	2.131	2.281	1.835
Ppp1r2	0.324	0.363	1.34	1.058	0.325
Ppp1r7	0.176	0.315	0.988	1.048	0.27
Ppp1r8	0.055	0.162	0.107	0.006	0.003
Ppp1r9b	0.046	0.029	0.162	0.02	0.008
Prmt5	0.105	0.243	0.463	0.026	0.008
Ptrh2	0.082	0.144	0.391	0.197	0.013
Pym1	NA	NA	NA	NA	NA
Rbm8a	0.396	0.888	0.827	0.127	0.026
Rpap3	0.118	0.101	0.175	0.033	0.009
Ruvbl1	0.103	0.185	0.366	0.116	0.007
Ruvbl2	0.032	0.035	0.433	0.28	0.01
Sec23a	0.081	0.103	0.142	0.141	0.386
Snx2	0.141	0.15	0.122	0.063	0.009
Tbl1xr1	0.103	0.068	0.382	0.209	0.044
Tox4	0.175	0.158	1.055	0.2	0.026
Tprn	0.047	0.087	1.712	0.985	0.135
Tsks	0.134	0.03	0.161	1.513	1.538
Txnl1	0.263	0.567	0.361	0.317	0.028
Ube2m	0.092	0.057	0.537	0.321	0.065
Uri1	0.307	0.47	0.15	1.587	0.129
Wdr34	0.047	0.041	0.403	0.038	0.007
Wdr61	0.165	0.39	0.452	0.054	0.009
Wdr77	0.059	0.251	0.156	0.047	0.003
Wdr92	0.056	0.052	0.427	0.022	0.005
Ylpm1	0.201	0.271	1.094	0.48	0.048
Zfr	0.457	0.604	1.363	0.899	0.207

Color legend
0
0.2
0.4
0.6
0.8
1
1.2
1.4
1.6
1.8
2
2.2
2.4
2.6

Table S8. Phosphorylation status of SRPK1-associated proteins. Data from whole testis phosphoproteomics (Qi et al., 2014), spermatids phosphoproteomics (Li et al., 2019), and PhosphositePlus are included. Phosphorylated Serine residues in SR-motifs were searched on PhosphositePlus in those proteins expressed in post meiotic cells with at least a relative 30% from total gene expression during the whole process of spermatogenesis (highlighted in blue) and described as phosphoproteins in whole testis and spermatids.

Gene name	Protein symbol	Accession number	Mouse testis phosphoproteome (Qi et al., 2014)	Mouse spermatids phosphoproteome (Li et al., 2019)	Phosphorylation sites (PhosphositePlus)	ph-Ser in SR-motifs
Alyref	THOC4	O08583	No	Yes	S-p, T-p, Y-p	
Ap2b1	AP2B1	Q9DBG3	No	Yes	S-p, T-p, Y-p	
Cirbp	CIRBP	P60824	No	No	-	
Eif4a3	DDX48	Q91VC3	No	Yes	S-p, T-p, Y-p	
Gapvd1	GAPVD1	Q6PAR5	Yes	Yes	S-p, T-p, Y-p	
H1f1	H1F1	P43275	Yes	Yes	S-p, T-p, Y-p	
Hnrnpa2b1	hnRNP A2/B1	O88569	Yes	Yes	S-p, T-p, Y-p	
Hnrnpab	hnRNP A/B	Q99020	No	No	-	
Hnrnpc	hnRNP C1/C2	Q9Z204	Yes	Yes	S-p, T-p, Y-p	
Hnrnpd	hnRNP D0	Q60668	Yes	Yes	S-p, T-p, Y-p	
Hnrnpu	hnRNP U	Q8VEK3	Yes	Yes	S-p, T-p, Y-p	
Igf2bp3	IGF2BP3	Q9CPN8	Yes	Yes	S-p, T-p, Y-p	S180, S184, S187, S438, S576
Ilf2	ILF2	Q9CXY6	Yes	No	S-p, T-p, Y-p	
Ilf3	ILF3	Q9Z1X4	Yes	Yes	S-p, T-p, Y-p	
Lsm12	LSM12	Q9D0R8	Yes	Yes	S-p, T-p, Y-p	-
Mcm4	MCM4	P49717	No	No	-	
Mcm7	MCM7	Q61881	Yes	Yes	S-p, T-p, Y-p	S500, S674, S678
Mrto4	MRTO4	Q9D0I8	Yes	Yes	S-p, T-p, Y-p	-
mt-Co2	COX2	P00405	No	No	-	
Mvp	MVP	Q9EQK5	No	No	-	
Ncbp2	NCBP2	Q9CQ49	No	No	-	
Ngdn	NGDN	Q9DB96	No	No	-	
Pabpc1	PABP1	P29341	Yes	Yes	S-p, T-p, Y-p	S51, S599
Prpf3	PRPF3	Q922U1	Yes	Yes	S-p, T-p, Y-p	
Prpf4	PRPF4	Q9DAW6	No	No	-	
Prss50	TSP50	Q8BLH5	No	No	-	
Rbm17	RBM17	Q8JZX4	Yes	Yes	S-p, T-p, Y-p	
Rbm27	RBM27	Q5SFM8	Yes	Yes	S-p, T-p, Y-p	
Rbmxl1	RBMXRT	Q91VM5	Yes	Yes	S-p, T-p, Y-p	
Rpl10a	RPL10A	P53026	No	No	-	
Rplp0	RPLP0	P14869	Yes	Yes	S-p, T-p, Y-p	(S148 in humans)
Rtcb	RTCB	Q99LF4	No	Yes	S-p, T-p, Y-p	
Sf3a1	SF3A1	Q8K4Z5	Yes	Yes	S-p, T-p, Y-p	
Snrnp40	WDR57	Q6PE01	No	No	-	
Srpk1	SRPK1	O70551	Yes	Yes	S-p, T-p, Y-p	
Srsf1	ASF/SF2	Q6PDM2	No	Yes	S-p, T-p, Y-p	
Tbl1xr1	TBL1XR1	Q8BHJ5	No	No	-	
Thrap3	TRAP150	Q569Z6	Yes	Yes	S-p, T-p, Y-p	
Ttc30a2	TTC30A2	A2AKQ8	No	No	-	
Zpbp2	ZPBP2	Q6X786	No	No	-	

Table S8. Phosphorylation status of PP1γ-associated proteins. Data from whole testis phosphoproteomics (Qi et al., 2014), spermatids phosphoproteomics (Li et al., 2019), and PhosphositePlus are included. Proteins expressed in post meiotic cells with at least a relative 30% from total gene expression during the whole process of spermatogenesis are highlighted in blue.

Gene name	Protein symbol	Accession number	Mouse testis phosphoproteome (Qi et al., 2014)	Mouse spermatids phosphoproteome (Li et al., 2019)	Phosphorylation sites (PhosphositePlus)
Ak1	AK1	Q9R0Y5	Yes	Yes	S-p, T-p
Appl1	APPL1	Q8K3H0	Yes	Yes	S-p, T-p, Y-p
Arhgef2	ARHGEF2	Q60875	Yes	Yes	S-p, T-p, Y-p
Cetn4	CETN4	Q8K4K1	No	No	-
Cfap410	CFAP410	Q8C6G1	No	No	-
Cops5	COPS5	O35864	No	Yes	S-p, Y-p
Dnah17	DNAH17	Q69Z23	No	No	-
Drg1	DRG1	P32233	No	No	-
Eif3a	eIF3a	P23116	No	No	-
Fn1	FN1	P11276	Yes	No	S-p, T-p, Y-p
Ift80	IFT80	Q8K057	No	No	-
Ift81	IFT81	O35594	Yes	No	S-p, T-p, Y-p
Ilf2	ILF2	Q9CXY6	Yes	No	S-p, T-p, Y-p
Kpna3	KPNA3	O35344	Yes	Yes	S-p, T-p, Y-p
Kpna6	KPNA6	O35345	No	Yes	S-p, T-p, Y-p
Lmtk2	LMTK2	Q3TYD6	Yes	Yes	S-p, T-p, Y-p
Lrrc34	LRRC34	Q9DAM1	No	No	-
Lypd4	LYPD4	Q8BVP6	No	No	-
Magoh	MAGOH	P61327	Yes	No	S-p, Y-p
Mtrex	SKIV2L2	Q9CZU3	No	No	-
Ndufb10	NDUFB10	Q9DCS9	No	No	-
Phactr1	PHACTR1	Q2M3X8	No	No	-
Pih1d1	PIH1D1	Q9CQJ2	Yes	Yes	S-p, T-p, Y-p
Pin1	PIN1	Q9QUR7	No	No	-
Ppp1cc	PPP1CC	P63087	No	Yes	S-p, T-p, Y-p
Ppp1r10	PNUTS	Q80W00	Yes	Yes	S-p, T-p, Y-p
Ppp1r11	PPP1R11	Q8K1L5	No	Yes	S-p, T-p, Y-p
Ppp1r2	PPP1R2	Q9DCL8	Yes	Yes	S-p, T-p, Y-p
Ppp1r7	PPP1R7	Q3UM45	Yes	Yes	S-p, T-p, Y-p
Ppp1r8	NIPP-1	Q8R3G1	No	No	-
Ppp1r9b	PPP1R9B	Q6R891	Yes	No	S-p, T-p, Y-p
Prmt5	PRMT5	Q8CIG8	No	No	-
Ptrh2	PTRH2	Q8R2Y8	No	Yes	S-p, T-p, Y-p
Pym1	PYM1	Q8CHP5	No	No	-
Rbm8a	RBM8A	Q9CWZ3	Yes	Yes	S-p, T-p, Y-p
Uri1	RMP	Q3TLD5	Yes	Yes	S-p, T-p, Y-p
Rpap3	RPAP3	Q9D706	Yes	Yes	S-p, T-p, Y-p
Ruvbl1	RUVBL1	P60122	No	No	-
Ruvbl2	RUVBL2	Q9WTM5	No	No	-
Sec23a	SEC23A	Q01405	No	No	-
Snx2	SNX2	Q9CWK8	Yes	Yes	S-p, T-p, Y-p
Tbl1xr1	TBL1XR1	Q8BHJ5	No	No	-
Tox4	TOX4	Q8BU11	Yes	Yes	S-p, T-p, Y-p
Tprn	TPRN	A2AI08	Yes	Yes	S-p, T-p, Y-p
Tsks	TSKS	O54887	Yes	Yes	S-p, T-p
Txnl1	TXNL1	Q8CDN6	Yes	Yes	S-p, T-p, Y-p
Ube2m	UBE2M	P61082	No	No	-
Wdr34	WDR34	Q5U4F6	No	Yes	S-p, T-p
Wdr61	WDR61	Q9ERF3	No	No	-
Wdr77	WDR77	Q99J09	Yes	Yes	S-p, T-p
Wdr92	WDR92	Q8BGF3	No	No	-
Ylpm1	ZAP3	Q9R0I7	No	Yes	S-p, T-p, Y-p
Zfr	ZFR	O88532	No	Yes	S-p, T-p, Y-p

5.3 CHAPTER 3: Nanoscale insights into mature sperm chromatin reveals a fractal supramolecular structure which is altered in patients with double strand DNA breaks

de la Iglesia A, Huck-Iriart C, Malfois M, Leiva M, Jodar M, Guimerà M, Peralta S, Corral JM, Oliva R, Castillo J. Nanoscale insights into human sperm chromatin through synchrotron light small-angle X-ray scattering (SAXS): fine-tuning the current model of paternal genome packaging in vivo. *Manuscript in preparation*.

First author

5.3.1 Work 6: Nanoscale insights into human sperm chromatin through synchrotron light small-angle X-ray scattering (SAXS): fine-tuning the current model of paternal genome packaging *in vivo*

To be submitted as:

de la Iglesia A[1], Huck-Iriart C[2], Malfois M[2], Leiva M[1], Jodar M[1,3], Guimerà M[4], Peralta S[4], Corral JM[4,5], Oliva R[1,3]*, Castillo J[1,*]. Nanoscale insights into human sperm chromatin through synchrotron light small-angle X-ray scattering (SAXS): fine-tuning the current model of paternal genome packaging in vivo.

[1] Molecular Biology of Reproduction and Development Research Group, Department of Biomedical Sciences, Faculty of Medicine and Health Sciences, Institut d'Investigacions Biomèdiques August Pi i Sunyer (IDIBAPS), Fundació Clínic per a la Recerca Biomèdica, Universitat de Barcelona, Barcelona, Spain.

[2] ALBA Synchrotron, BL11 NCD-SWEET Beamline, Cerdanyola del Vallès, Spain

[3] Biochemistry and Molecular Genetics Service, Hospital Clinic, Barcelona, Spain

[4] Institute of Gynaecology, Obstetrics and Neonatology, Hospital Clínic, Barcelona, Spain

[5] Department of Urology, IDIBAPS, Hospital Clínic, Barcelona, Spain

* Corresponding authors

Manuscript in preparation

Nanoscale insights into human sperm chromatin through synchrotron light small-angle X-ray scattering (SAXS): fine-tuning the current model of paternal genome packaging *in vivo*

de la Iglesia A[1], Huck-Iriart C[2], Malfois M[2], Leiva M[1], Jodar M[1,3], Guimerà M[4], Peralta S[4], Corral JM[4,5], Oliva R[1,3]*, Castillo J[1,*]

[1] Molecular Biology of Reproduction and Development Research Group, Department of Biomedical Sciences, Faculty of Medicine and Health Sciences, Institut d'Investigacions Biomèdiques August Pi I Sunyer (IDIBAPS), Fundació Clínic per a la Recerca Biomèdica, Universitat de Barcelona (UB), Barcelona, Spain
[2] ALBA Synchrotron, BL11 NCD-SWEET Beamline, Cerdanyola del Vallès, Spain
[3] Biochemistry and Molecular Genetics Service, Hospital Clinic, Barcelona, Spain
[4] Institute of Gynaecology, Obstetrics and Neonatology, Hospital Clínic, Barcelona, Spain
[5] Department of Urology, IDIBAPS, Hospital Clínic, Barcelona, Spain
* Corresponding authors: Judit Castillo, contact email juditcastillo@ub.edu, and Rafael Oliva, contact email roliva@ub.edu

Abstract

Spermatozoa acquire a unique chromatin structure after protamine incorporation during spermiogenesis, essential for their proper functionality. The exceptional properties conferred by these small and highly basic proteins have attracted interest over the years, and the application of a wide range of methodologies allowed establishing the current model of sperm chromatin packaging in toroidal and rod-like structures. However, there is not enough evidence about how the human sperm chromatin structure behaves in solution and in the context of the whole sperm nucleus. The present work applies Small-Angle X-ray Scattering (SAXS) from synchrotron light (BL11 NCD-SWEET beamline from the ALBA Synchrotron Light source, Spain) to describe the human sperm chromatin fiber in solution. Furthermore, different impaired chromatin states were analyzed to unravel their impact at the nanoscale, including patients with unbalanced protamine ratio and pathological levels of double-strand DNA. Overall, we provide information not reported up to date about the nanoscale organization of the chromatin fiber in intact human sperm nuclei, identifying a hierarchical 2-level organization in which supramolecular structures (R_g ~67 nm) arise from the aggregation of small subunits with smooth surface that are highly compacted (R_{eq} ~7.7 nm). The small subunits are highly stable among patients with impaired chromatin quality, and remarkable changes are observed in the supramolecular aggregates in patients with pathological levels of DNA damage, reinforcing the close relationship between chromatin and DNA integrities.

Keywords: chromatin structure, human sperm, SAXS, synchrotron light, nanoscale, male infertility, nucleoprotamine

INTRODUCTION

The sperm cell has a unique, tightly compacted and transcriptionally silent, chromatin thanks to the expression of the small and extremely basic protamines. This exceptional nuclear compaction occurs during the spermiogenesis through the synchronized and epigenetically regulated process of nucleo-histone to nucleo-protamine transition, essential for proper sperm functionality (Arpanahi et al., 2009; Barrachina et al., 2022; Gaucher et al., 2010; Hazzouri et al., 2000; Oliva, 2006; Rathke et al., 2014). Indeed, alterations on either the process of chromatin compaction or the mature sperm chromatin structure have been related with male infertility, such as altered morphology, increased DNA damage, or worse outcome after assisted reproductive techniques (Balhorn et al., 1988; Castillo et al., 2015; Oliva, 2006; Soler-Ventura et al., 2018).

The uniqueness of sperm chromatin structure has attracted interest over the years, and the application of a wide range of methodologies has led to the current model of chromatin compaction. The information and models available so far about the nucleo-protamine (NP) structure are based on the combination of microscopy techniques and X-ray diffraction in NP extracted from sperm cells or in protamine-DNA complexes reconstituted *in vitro* (Allen et al., 1993, 1997; Ausió et al., 2014; Balhorn, 2007; Conwell et al., 2003; Conwell & Hud, 2004; DeRouchey & Rau, 2011; Hud et al., 1993, 1995; Vilfan et al., 2004, 2006). Microscopy methods evidence a highly condensed structure of the sperm nucleus that suggest strong electrostatical interactions between DNA and protamines. In fact, protamines are 45-80% arginine rich and contain cysteines in their sequence that can accommodate intra/inter-molecular disulphide bonds to stabilize the NP structure (Balhorn, 1982; Oliva, 2006). X-ray diffraction on *in vitro* reconstituted NP in solution contributed to propose the alignment of protamines along the major groove of DNA(Balhorn, 2007). Furthermore, the application of Small-Angle X-ray Scattering (SAXS) and infrared spectroscopy concluded that protamines promote a tight hexagonal DNA packing stabilized by hydrogen bonds (Hutchison et al., 2017).

By electron microscopy and/or atomic force microscopy, it was described a supramolecular rearrangement of protamines and DNA in toroidal structures of 50-160 nm diameter and 40-55 nm width (Ausió et al., 2014; Balhorn, 2007). Interestingly, longer rod-like structures (160-350 nm) with thickness of 40-55 nm were also observed applying the same techniques, which evidenced two differential ways of supramolecular organization in the male gamete nucleus (Ausió et al., 2014; Balhorn, 2007). These techniques based on the extension of samples over a surface, and despite providing very useful information about size, some technical artifacts could appear, differing from what it would be detected in solution. Protamine-DNA complexes formed *in vitro* with linear DNA from calf thymus and salmon protamines were found to form fractal-like structures, that is supramolecular structures (with a

radius of gyration of 100 nm) originated from the repetition of small subunits (radius of 2,5 nm) (Motta et al., 2013).

Despite the availability of studies analyzing the NP in sperm from model species and the different approaches of *in* vitro reconstitution, there is still no evidence at the nanoscale on the human sperm chromatin structure *in vivo* and in solution. In the present work, we apply SAXS through synchrotron light to provide information not reported so far about how the human sperm chromatin is compacted. Besides, we studied how different naturally altered chromatin status could affect chromatin structure, including patients with altered protamine 1/Protamine 2 (P1/P2) ratio and patients with pathological levels of double-strand DNA (dsDNA) breaks.

MATERIALS AND METHODS

Biological Material

Human normozoospermic semen samples (n=30) from males undergoing routine semen analysis were obtained at the Assisted Reproduction Unit from the Clinic Institute of Gynecology, Obstetrics and Neonatology, at the Hospital Clínic de Barcelona, Spain. Patients with body mass index above 30, age above 45 years old and reporting known diseases or noxious habits, such as smoking, were discarded from the study. Informed consents were obtained, and the study was conducted in accordance with the Declaration of Helsinki. Samples were used following the appropriate ethical guidelines and Internal Review Board, and the Clinical Research Ethics Committee of the Hospital Clínic de Barcelona approved the biological material storing and processing. Informed consent was obtained from all subjects involved in the study.

Ejaculates were collected by masturbation into sterile containers respecting 3–5 days of sexual abstinence. Automatic semen analysis system CASA (Proiser, Paterna, Spain) was performed to evaluate seminal parameters and samples were classified as normozoospermic according to the World Health Organization guidelines (World Health Organization, 2021). Sperm cells were purified from other cells from the semen through 50% Puresperm density gradient centrifugation (NidaCon International AB, Gothenburg, Sweden), following manufacturer's instructions. Chromatin integrity status, in terms of presence of cells with dsDNA damage determined by neutral comet assay and the balance on protamine abundance determined by P1/P2 ratio, was evaluated to stratified samples into three groups: a) controls, corresponding to normozoospermic patients with no dsDNA damage and normal P1/P2 ratio (n=19); b) P1P2, comprising normozoospermic patients with no dsDNA damage and altered P1/P2 ratio (n=4); and c) dsDNA, including patients with

dsDNA damage and normal P1/P2 ratio (n=7). An additional group with similar characteristics as the control group was established according to sample processing: control-NP (n=9), in which histones and other basic proteins with low affinity to the DNA were removed.

Determination of DNA integrity towards patient classification

DNA damage was evaluated by neutral comet based on protocols described in (Ribas-Maynou et al., 2012; Simon & Carrell, 2013). Briefly, 10K sperm from cryopreserved neat sample were submerged in 1% low melting agarose and, once gelified, sperm were lysed in 3 sequential phases of 60, 30, and 90 min, respectively. After lysis, 22V electrophoresis was run 15 min, keeping <280 mA, into neutral electrophoresis sample buffer (0.05 M Trizma Base, 0.15 M sodium acetate, pH 9.0). After electrophoresis, gels are fixed in 1 mM ammonium acetate in ethanol and washed, prior staining with Sybr Gold. Percentage of fragmented cells was calculated after counting 60-120 cells.

P1/P2 protamine ratio was analyzed following procedures of protamine-rich fraction of sperm nuclear proteins extraction and analysis previously described by our group (Soler-Ventura et al., 2018). For in-gel quantification, dried purified extracts were resuspended in sample buffer consisting of 5.5 M urea, 20% β-mercaptoethanol, 5% acetic acid and separated using acetic-acid urea gel electrophoresis (AU-PAGE) including increasing amounts of human protamine standard as described in (Mengual et al., 2003). Band intensity was quantified using Quantity One 1-D analysis software (BioRad, Hercules, CA, USA). Regression curve obtained from protein standard intensity determination allowed calculating the quantity of P1 and P2 for each sample and the derived P1/P2 ratio.

Sperm nuclei preparation

Sperm tails were removed to decrease sample structural dispersity according to (Hutchison et al., 2017), with some modifications. Aliquots of approximately 100 million sperm per sample were prepared. After centrifugation at 700 *g*, 15 min, room temperature (RT), pellets were gently resuspended in washing solution (150mM NaCl, 20 mM Tris-HCl pH 7.5, 2 mM EDTA, 0.25 M sucrose, 1 mM PMSF) using a 25-gauge needle. Samples were centrifuged at 2000 *g,* 5 min, 5 ºC. Washing step was repeated before resuspending in sonication solution (75 mM NaCl, 10 mM Tris, 1 mM EDTA, PureSperm 100 (Nidacon, Mölndal, Sweden), 1 mM PMSF). Sonication was performed on ice at 35% amplitude, 10 pulses of 10 seg considering 2 min waiting time between pulses, using a Branson Sonifier B-12. Sonicated material was centrifuged at 14,000 *g*, 20 min, 5 ºC, and supernatant was carefully removed. Pellet was resuspended in solubilization solution (100 mM Tris-HCl pH 7.5, 10 mM CHAPS, 20 % Glycerol, 0.25 M Sucrose) and incubated 30 min at 37 ºC. Tubes were ice-cold few seconds and centrifuged at 5000 *g*, 5 min, 5 ºC. Supernatant was discarded and

sonication and solubilization steps were repeated. Pellets were resuspended in a solution of 150 mM NaCl, 10 mM Tris-HCl pH 7.5, 0.02 % NP-40, 0.25 M sucrose and nuclei were counted. Samples belonging to control-NP group (n=9) were kept in the same solution to be further processed to deplete histones from the DNA. Samples belonging to control (n=10), P1/P2 (n=4), and dsDNA (n=7) groups, were centrifuged at 5000 *g*, 5 min, 5 ºC, resuspended in 150 mM NaCl, 10 mM Tris-HCl pH 7.5 at a concentration of 300 million nuclei/mL, and stored at -80 ºC days before SAXS measurements. Nuclei monodispersity and purity was monitored by optical microscopy.

Histone depletion

Histones and other loosely attached chromatin basic proteins were removed using 0.65 M NaCl as performed elsewhere (Castillo, Amaral, Azpiazu, et al., 2014). Samples were centrifuged at 5000 *g*, 5 min, 5 ºC and pellets were subsequently resuspended in extraction solution (0.65 M NaCl, 10 mM Tris-HCl pH 7.5, 1 mM EDTA, 0.05 % p/v digitonin) and incubated 15 min in ice, shaking manually often. After centrifugation at 3000 *g*, 2 min, 5 ºC, supernatant (containing histones and other proteins loosely attached to DNA) was discarded and pellet (containing histone-depleted nuclei) was resuspended again at 3000 *g*, 2 min, 5 ºC. Pellets were washed with 150 mM NaCl, 10 mM Tris-HCl pH 7.5, resuspended in the same solution at a concentration of 300 million $nuclei_i$/mL, and stored at -80 ºC days before SAXS measurements.

SAXS measurements

Small Angle X-ray Scattering (SAXS) measurements were performed in the BL11 NCD-SWEET beamline from the ALBA Synchrotron Light source, Barcelona, Spain (project IDs 2020094502 and 2021095294). Experiments were done using 2 mm glass capillaries. The incoming beam energy was set at 12.4 keV, with spot size 100 x 100 Micrometers x Micrometers (FWHM) Horizontal x Vertical. Detector distance of 6700 mm. *q*-range was established from 0.03 to 2.5 nm^{-1}. 2D patterns were recorded in a Pilatus 1M (Dectris, Switzerland) detector. 60 frames of 0.5 seconds were recorded for each sample to analyze possible radiation damage. A blank consisting on the medio in which the cells were resuspended was measured to substract the background. Three technical replicates were measured per sample.

SAXS model

The Pattern features were characterized by well-defined small particles which formed larger supramolecular aggregates. To obtain average structural information from each system, the analysis was simplified to a mass fractal structure:

$$I(q) = Sc \cdot S(q)P(q) + back(q)$$

Where Sc is a scale factor and S(q) was the mass fractal structure factor proposed by Texeira (Teixeira, 1988):

$$S(q) = 1 + \frac{D\,\Gamma(1-D)}{(qr)^D[1+1/(q\xi^2)]^{(D-1)/2}}\sin[(D-1)\tan^{-1}(q\xi)]$$

Here, D and ξ are the fractal dimension and fractal correlation length (or fractal cutoff), respectively. This structure factor was modeled in terms of the aggregation of small spherical subunits of radius "r". Here, the form factor "P(q)" was replaced by a cylindrical model (Pedersen, 1997) of radius R and length L with an aspect ratio close to 1 ($0.75 < 2R/L < 1.5$). Where "R_{eq}" was calculated by the radius of an equivalent sphere with same radius of gyration of the proposed cylindrical object (Craievich, 2016):

$$R_{eq} = \sqrt{\frac{5}{3}\left(\frac{R^2}{2} + \frac{H^2}{12}\right)}$$

Moreover, to compare between samples, the radius of gyration (R_g) of the larger aggregates was be computed with the following relationship (Craievich, 2016):

$$R_{eq} = \left[\frac{D(D+1)}{2}\right]^{1/2} \xi$$

Finally, the background was composed by a Gaussian chain form factor (Pedersen, 1997) to consider the flexible parts of the proteins/DNA plus a constant parameter. SAXS data was modeled using Python 3.8 scripts and lmfit library (Newville et al., 2014) for nonlinear least squares procedure.

SAXS parameters were compared among groups using ANOVA followed by Tukey analysis as pos-hoc test, considering significant changes those with *p*-value < 0.05. After outlier analysis, 1 patient was removed from the dsDNA group and another one from the control-NP group.

RESULTS

SAXS analysis of normal human sperm chromatin structure evidenced a hierarchical two-level supramolecular organization at the nanoscale

The analysis of human sperm nuclei from 10 normozoospermic samples included in the control group disclosed a hierarchical model of chromatin organization in two different levels, reflected by the linear region observed in the SAXS profile (Figure 1). Therefore, large macromolecular structures observed at low dispersion angles ($q < 0.2$ nm^{-1}) arise from the aggregation of small subunits that are described at higher angles ($q > 0.2$ nm^{-1}). The small subunits evidence best fit adjustments to a cylinder model with an aspect ratio close to 1 ($0.75 < 2R/L < 1.5$), with radius (R) = 7.42 ± 0.07 nm (mean ± SD) and length (L) = 9.56 ± 0.18 nm. It all resulted in an equivalent radius (i.e., radius of gyration resulting from the cylindrical subunit) of 7.66 ± 0.08 nm (Table 1). The characteristic oscillations observed at high ranges (q around 1) indicate that the small subunits are highly compact and non-rugous, with a smooth surface, suggesting a small geometric anisotropy (Figure 1). The small cylindrical subunits are spatially organized until a maximum distance (fractal cutoff, ξ) of 31.89 ± 2.67 nm, without a specific order, to generate supramolecular aggregates with radius of gyration (R_g) corresponding to 66.46 ± 5.66 nm and fractal dimension (D) of 2.50 ± 0.15, indicative of a highly compacted aggregates (Table 2). The shape of the macromolecular structure resulting from the aggregation of small subunits is still unknown, because it failed to adjust to the already proposed model of sperm NP structure of toroidal organization. Results per individual samples are shown in Table S1.

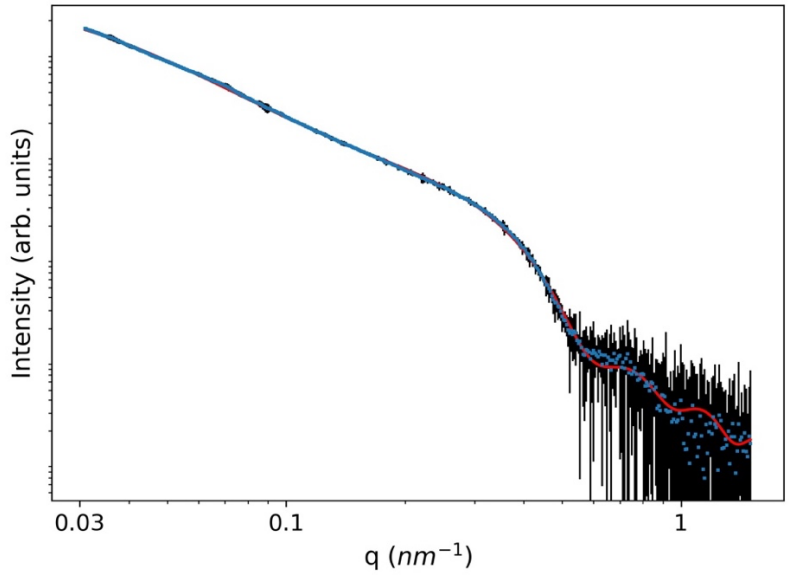


Figure 1. SAXS profile of chromatin structure in normal human sperm nuclei. Averaged scattering intensity is plotted as function of scattering vector q (nm^{-1}). Low angles ($q < 0.2$ nm^{-1}) give information about larges aggregates formed from the aggregation of small subunits ($q > 0.2$ nm^{-1}).

SAXS profiles revealed alterations at the supramolecular level of aggregation associated with dsDNA damage

Comparative analysis among the different biological groups of study with impaired chromatin integrity (P1P2 group, comprising patients with altered protamine P1/P2 protein ratio, and dsDNA group, including patients with pathological levels of dsDNA breaks) displayed interesting features of sperm nuclear structure (Figure 2, Table 1). Small cylindrical subunits were highly stable between the three groups of study. SAXS profiles of P1P2 and dsDNA groups showed the characteristic high angles (q around 1) oscillations observed in the control group meaning that the small cylindrical subunits were also highly compact aggregates with smooth surface (Figure 2A). Cylinder dimensions were maintained compared to controls, corresponding to R = 7.47 ± 0.18 nm and L = 9.53 ± 0.15 nm in P1P2 group, and R = 7.40 ± 0.15 nm and L = 9.61 ± 0.30 nm in dsDNA group (expressed as mean ± SD, Table 1, Figure 2B), evidencing no significant differences compared with the control group (p > 0.05 after Tukey correction). The resulting R_{eq} neither changed from the reported control values (R_{eq} = 7.69 ± 0.15 nm in P1P2, R_{eq} = 7.65 ± 0.12 nm in P1P2, p > 0.05 after Tukey correction, Figure 2B, Table 1). They arrange into a higher level of aggregation like control group, with fractal cutoff ξ = 31.42 ± 5.53 nm, p > 0.05 after Tukey correction (Table 2, Figure 2B). Despite dsDNA displayed slightly higher fractal cutoff (35.64 ± 2.27 nm) compared to control values, the difference was also unsignificant (p > 0.05 after Tukey correction, Table 1, Figure 2B). Parameters per individual sample analyzed are gathered in Table S1.

Table 1. SAXS parameters reported in the study of sperm chromatin under biologically impaired conditions. Results are expressed as mean value ± standard deviation.

Group	R (nm)	L (nm)	R_{eq} (nm)	ξ (nm)	D	R_g (nm)
Control	7.42 ± 0.07	9.56 ± 0.18	7.66 ± 0.08	31.89 ± 2.67	2.50 ± 0.15	66.46 ± 5.66
P1P2	7.47 ± 0.18	9.53 ± 0.15	7.69 ± 0.15	31.42 ± 5.53	2.62 ± 0.22	67.89 ± 7.62
dsDNA	7.40 ± 0.15	9.61 ± 0.30	7.65 ± 0.12	35.64 ± 2.27	2.51 ± 0.21	**74.58 ± 4.90 ***

R: radius (small subunit), L: length (small subunit), ξ: fractal cutoff, D: fractal dimension, R_{eq}: equivalent radius (small subunit), R_g: radius of gyration (large aggregation), * p < 0.05 after Tukey correction.

At the supramolecular level of aggregation, SAXS profiles revealed striking findings (Figure 2). Whereas the supramolecular structures originated from the aggregation of small subunits in P1P2 group did not show different R_g with respect to controls (67.89 ± 7.62 nm, p > 0.05), the group of dsDNA breaks evidenced increased R_g (74.58 ± 4.90 nm, p < 0.05, Table 1, Figure 2B). No differences were neither found in the fractal dimension (2.62 ± 0.22 in P1P2 group, 2.51 ± 0.21 nm in dsDNA group), indicating that the high level of compaction was not altered. See Table S1 for parameters obtained per individual sample analyzed.

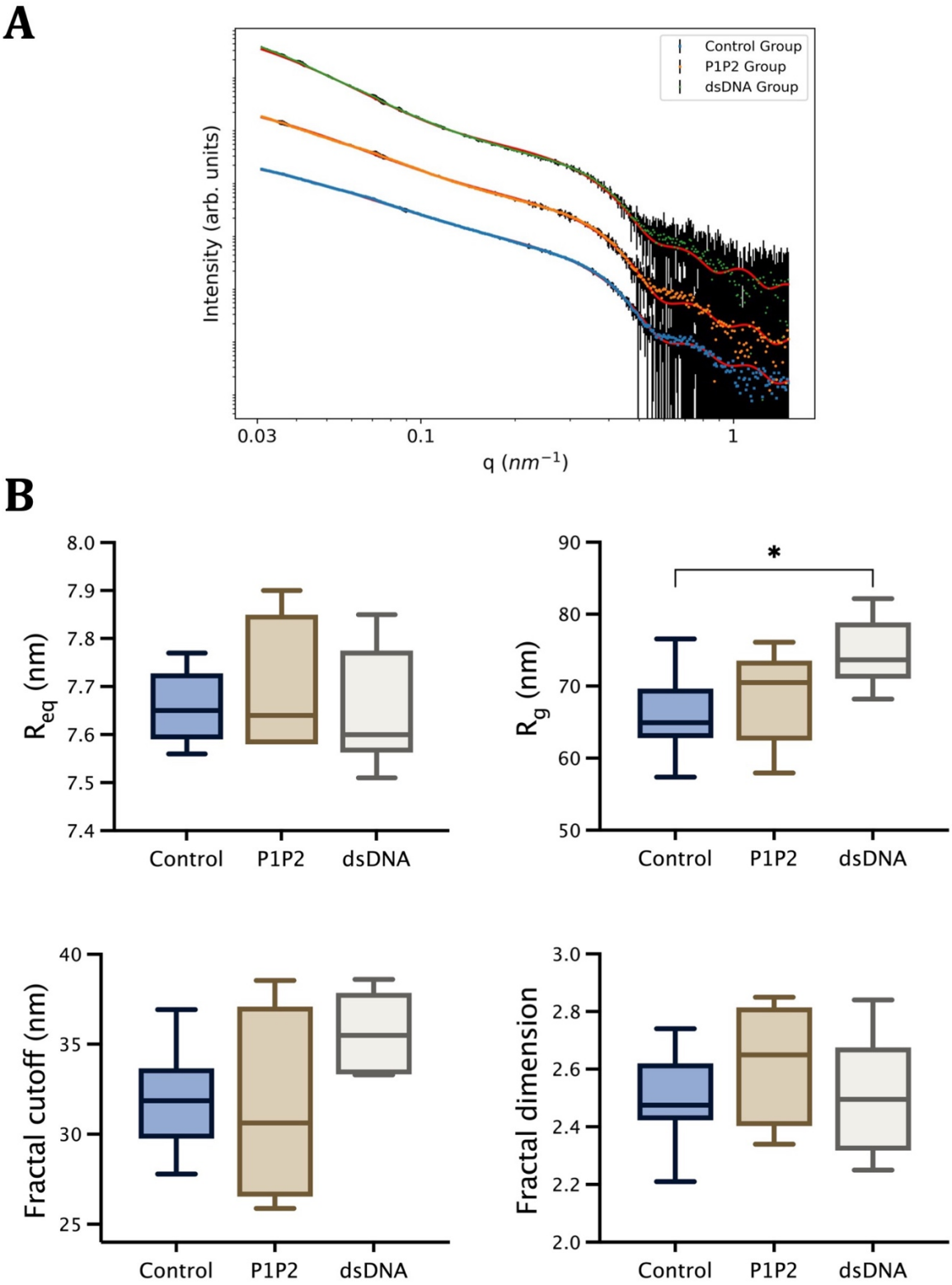


Figure 2. SAXS profile of human sperm nuclei in comparison to patients with impaired chromatin structure. Averaged scattering intensity is plotted as function of scattering vector q (nm^{-1}). Low angles ($q < 0.2$ nm^{-1}) give information about larges aggregates formed from the aggregation of small subunits ($q > 0.2$ nm^{-1}). 'P1P2 Group' refers to the group of patients with altered P1/P2 protamine ratio, and 'dsDNA Group' to the group of patients with pathological levels of double strand (dsDNA) breaks.

Sperm chromatin after histone removal displayed different SAXS profile than the observed in native conditions

Aiming to reduce the complexity inside the sperm nucleus, histones and other loosely attached sperm chromatin proteins were removed. The resulting structure maintained the hierarchical 2-level of organization, organized from small and highly compacted subunits with smooth surface as observed in the SAXS profile (Figure 3A). Small subunits adjusted to a cylindrical model of dimensions R = 7.70 ± 0.23 nm and L = 9.41 ± 0.14 nm (mean ± SD), not presenting differences compared to the one observed in control groups (p > 0.05 after Tukey correction, Figure 3B, Table 2). However, the resulting R_{eq} was higher than that observed in native chromatin (7.85 ± 0.19 nm, p < 0.05 after Tukey correction, Figure 3B, Table 2).

The way in which small subunits dispose in space is altered, reflected by a reduced fractal cutoff compared with the control group (26.95 ± 3.36, p < 0.05 after Tukey correction), resulting in supramolecular structures of smaller R_g (58.86 ± 4.20 nm, p < 0.05 after Tukey correction) but keeping similar grade of compaction (D = 2.65 ± 0.17, p > 0.05 after Tukey correction) (Table 2, Figure 3B).

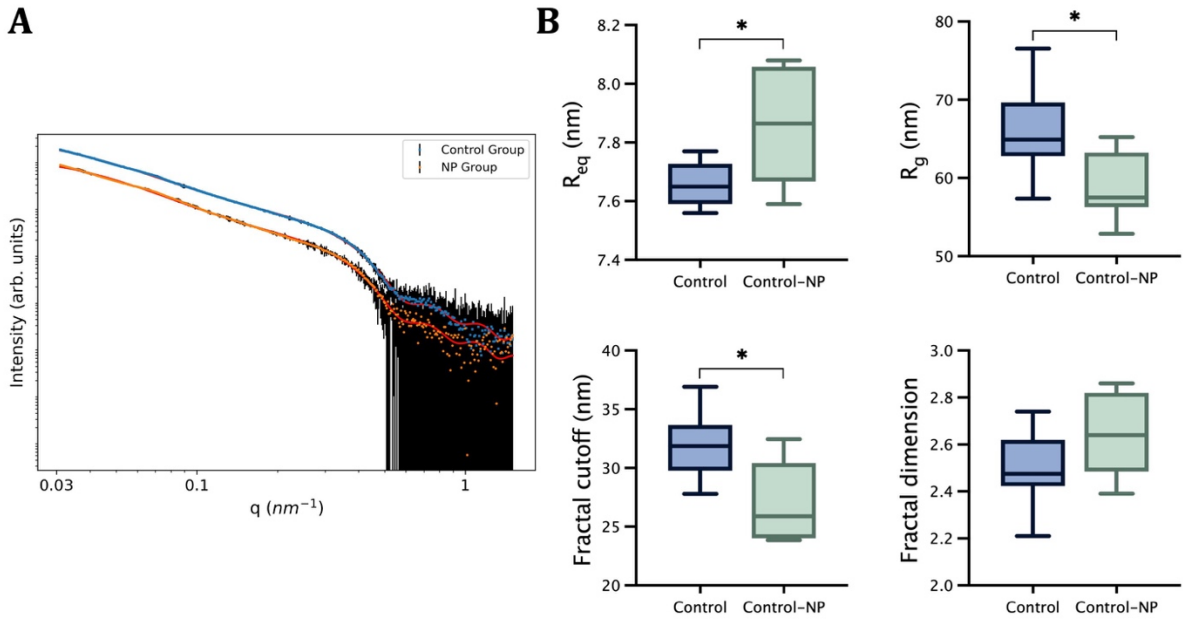


Figure 3. SAXS profile of human sperm nuclei after removal of histones and other basic proteins with low affinity to DNA. Averaged scattering intensity is plotted as function of scattering vector q (nm^{-1}). Low angles (q < 0.2 nm^{-1}) give information about larges aggregates formed from the aggregation of small subunits (q > 0.2 nm^{-1}). 'P1P2 Group' refers to the group of patients with altered P1/P2 protamine ratio, and 'dsDNA Group' to the group of patients with pathological levels of double strand (dsDNA) breaks.

Table 2. SAXS parameters comparing chromatin structure in whole and histone-depleted nuclei. Results are expressed as mean value ± standard deviation.

Group	R (nm)	L (nm)	R_{eq} (nm)	ξ (nm)	D	R_g (nm)
Control	7.42 ± 0.07	9.56 ± 0.18	7.66 ± 0.08	31.89 ± 2.67	2.50 ± 0.15	66.46 ± 5.66
NP	7.70 ± 0.23	9.41 ± 0.14	**7.85 ± 0.19 ***	**26.95 ± 3.36 ***	2.65 ± 0.17	**58.86 ± 4.20 ***

R: radius (small subunit), L: length (small subunit), ξ: fractal cutoff, D: fractal dimension, R_{eq}: equivalent radius (small subunit), R_g: radius of gyration (large aggregation), * $p < 0.05$ after Tukey correction. "Control" refers to Control group, "NP" refers to Control-NP group.

DISCUSSION

In the present work, we report for the very first time the existence of hierarchical organization in human sperm chromatin at the nanoscale, identifying supramolecular structures resulting from the aggregation of small particles. Small-angle X-ray Scattering (SAXS) provided the advantage of studying intact whole sperm nuclei in solution, becoming closer to decipher what really happens inside the sperm nucleus. Apart from the description of the chromatin structure in normal sperm nuclei, this approach allowed the identification of alterations at the supramolecular level in nucleus from patients with impaired chromatin integrity. While patients with altered protamine 1/protamine 2 (P1/P2) ratio did not display alterations at any level of nanoscale chromatin organization, patients with pathological levels of double strand DNA (dsDNA) breaks revealed alterations at the supramolecular level.

The SAXS profile of human sperm chromatin evidenced an overall high level of compaction at the nanometer level, describing primary particles of R_{eq} ~7.7 nm that aggregate without a specific order into a bigger structure, which is in consonance with a two-level organization identified by applying SAXS in NP particles generated *in vitro* (Motta et al., 2013). SAXS study of in vitro DNA-protamine complexes reported small subunits with smaller R_{eq}, of approximate 2.5 nm. Differences in size could derive from the use of salmon protamine to originate the complexes *in vitro*, which has an arginine-rich amino acid sequence but does not contain cysteine residues to accommodate disulfide bonds (Ausió et al., 2014; Oliva, 2006; Oliva & Dixon, 1991). Also, the presence of a complex protamine proteoform population conferring the human NP particle containing mature and immature forms bearing posttranslational modifications, which is further stabilized by cysteine bonds and Zn^{2+} molecules, could contribute to the generation of a more complex *in vivo* conformation of the chromatin fiber (Arauz-Garofalo et al., 2021; Björndahl & Kvist, 2011; Oliva, 2006; Soler-Ventura et al., 2020). In human sperm chromatin, primary particles identified through SAXS consisted of well-characterized highly compacted small subunits that adjusted to a

cylindrical model with a smooth surface, indicating the absence of free molecules outside the edges. The unspecific aggregation of small particles resulted in a higher level of supramolecular organization of R_g ~67 nm that did not adjust to toroidal or rod-like structure models of sperm chromatin compaction described up to date (Allen et al., 1993, 1997; Ausió et al., 2014; Balhorn, 2007; Hud et al., 1993, 1995; Vilfan et al., 2006). Nonetheless, the expected R_g of a toroidal particle with the experimentally reported size in vertebrates would be around 40 nm, which is in the same order of magnitude as the one obtained from the larger aggregates in the control group.

The lack of adjustment to toroidal models could be derived from a) the supramolecular aggregates detected herein correspond to a different structure, b) phase contrast between the medium and the aggregates may be hiding toroids, or c) the small particles do not organize into toroidal structures, indicating that 'perfect toroids' may not exist or are not the most abundant structure in solution. The possibility of confounding chromatin structures with other sperm nuclear structures (*i.e.*, membrane, envelopes) is unlikely due to their size (which is of microns and identifications are made at the nanoscale) and subsequent low surface/volume ratio, which would not give that much scattering intensity. Despite we cannot fully discard inferences in scattering intensity, our findings point out that toroids may not be the most abundant chromatin organization in the human sperm. Techniques applied up to date describing toroids are based on scanning probes attached to a surface (Allen et al., 1993, 1997; Ausió et al., 2014; Balhorn, 2007; Hud et al., 1993, 1995; Vilfan et al., 2006). However, dropping and drying over the substrate to take the micrograph could induce the formation of toroidal supramolecular structures which may not completely correspond to the *in vivo* organization of the NP particles inside the sperm nucleus. Moreover, transmission electron microscopy images obtained from *in vivo* samples showed elongated non-specific shapes named as rod-like structures (Ausió et al., 2014). Despite toroidal constructions have also been described using similar techniques upon condensation of DNA with purified protamines *in vitro* (Conwell et al., 2003; Conwell & Hud, 2004; DeRouchey & Rau, 2011), application of SAXS to the description of *in vitro* reconstituted DNA-protamine complexes described supramolecular aggregates that neither matched toroidal nor rod-like structures (Motta et al., 2013), which reinforces that protamines could not mainly arrange into toroidal supramolecular structures in solution. Supramolecular aggregations of higher R_g (101 nm) were reported in SAXS *in vitro* NP studies (Motta et al., 2013), likely due to the same reasons described above for differences between *in vivo* and *in vitro* description of small particles.

Deep diving into the functional relevance of the identified human sperm chromatin structures, we explored the chromatin status of patients with biologically impaired chromatin integrity, such as patients with altered P1/P2 ratio and patients with pathological levels of dsDNA breaks. Strikingly, the small particles were highly stable among the groups of study, reinforcing that the identified subunits could in fact

correspond to the canonical 'building block' originating the resulting supramolecular chromatin structures. No changes from the reported normal sperm values in terms of the way they arrange into space, size, or level of compaction, were found in patients with altered P1/P2 ratio. Despite the clinical implications of altered P1/P2 associated with sperm function, chromatin integrity, and outcome of assisted reproduction techniques (Ni et al., 2016; Soler-Ventura et al., 2018), it seems they do not underlie chromatin structural changes in patients with impaired P1/P2 ratio and unexplained infertility. In fact, our results interestingly reinforce the already suggested redundant function of sperm protamines in DNA packaging (Oliva, 2006; Soler-Ventura et al., 2020). The main difference was found in patients with pathological dsDNA damage, observed at low angles ($q < 0.2$ nm^{-1}), revealing a higher R_g of the supramolecular aggregates. The slight (but non-significative) increase in the fractal cutoff contribute, at least partially, to the higher R_g due to the direct relationship between these two values. Indeed, the fractal cutoff gives an idea about the largest distance separating two points inside the fractal, setting the range in which the self-similarity among structures can be observed. Therefore, a higher spatial correlation between the small cylindrical subunits may result in higher supramolecular structures. Despite this increase in dimensionality, no changes were observed in the level of compaction of the supramolecular aggregates. Overall, although it should be deciphered whether the dsDNA breaks are cause or consequence of this alteration, our findings reinforce the idea that genomic and chromatin integrities are closely related.

Human sperm DNA is packaged in >85% per protamines and still presents histone-associated regions and other basic DNA-associated proteins (Amaral et al., 2014; Castillo, Amaral, & Oliva, 2014; Castillo, Amaral, Azpiazu, et al., 2014; Oliva, 2006). Despite nucleosomes are minoritarian in sperm chromatin with respect to NP particles, we considered relevant to explore the presence of potential inferences in the signal scattering coming from non-protamine chromatin-related elements. Therefore, complexity inside the sperm nucleus was reduced by removing histones and other basic-associated proteins loosely attached to the DNA, generating normal sperm nuclei containing nearly pure NP particles (control-NP group). The originated structures were different from the ones described in controls, differing even in the small subunits. These higher primary particles correlated in space in a different way than in controls, evidenced by the reduced fractal cutoff and the resulting decreased R_g of the supramolecular aggregates. With these results, we face two different scenarios: a) pure NP particles have different size and we are not observing them in when analyzing intact nuclei, or b) the electrostatic forces originated by histones and other proteins contribute to the spatial arrangement of the sperm NP in whole nuclei, and therefore the changes observed are due to technical artifacts induced by the treatment. At this point, any option is feasible, but the higher dispersion observed in R_{eq} of the small particles detected in histone-depleted samples would contradict the idea of being evaluating "pure protamine" primary particles, which besides are higher in size than those of control native chromatin. Smaller spatial correlation (fractal

cutoff) translated into decreased R_g of the supramolecular structures in nuclei with no histones nor other less attached proteins, which was coupled to a non-significative trend of increased fractal dimension (higher compaction) than native chromatin. All mention above points out to changes induced by the experimental treatment rather than observation of a real situation, but further validation is needed to confirm whether the chromatin structures detected exclusively correspond to NP particles.

Summing up, our work entails the first nanoscale approach to describe the human sperm chromatin in solution. Further work is needed to decipher whether the scatter intensity comes primarily from NP particles, or we are detecting contribution of different structures. Nonetheless, the identification of a hierarchical level of organization constituting the human sperm chromatin provides useful knowledge towards finding the origin of alterations in cases of unexplained male infertility.

ACKNOWLEDGMENTS

We thank the Andrology lab of the Assisted Reproduction Unit from the Clinic Institute of Gynecology, Obstetrics and Neonatology, at the Hospital Clínic of Barcelona, Spain, for semen analysis.

FUNDING

Work funded by ALBA Synchrotron (project IDs 2020094502 and 2021095294) to J.C., "Ministerio de Economía y competitividad" PI16/00346 to R.O. and FI17/00224 to A.I., and "Ministerio de Ciencia e Innovación" PI20/00936 to R.O. J.C. is a Serra Húnter fellow (Universitat de Barcelona, Generalitat de Catalunya).

REFERENCES

Allen, M. J., Bradbury, E. M., & Balhorn, R. (1997). AFM analysis of DNA-protamine complexes bound to mica. *Nucleic Acids Research*, *25*(11), 2221–2226. https://doi.org/10.1093/nar/25.11.2221

Allen, M. J., Lee, C., Lee, J. D., Pogany, G. C., Balooch, M., Siekhaus, W. J., & Balhorn, R. (1993). Atomic force microscopy of mammalian sperm chromatin. *Chromosoma*, *102*(9), 623–630. https://doi.org/10.1007/BF00352310

Amaral, A., Castillo, J., Ramalho-Santos, J., & Oliva, R. (2014). The combined human sperm proteome: cellular pathways and implications for basic and clinical science. *Human Reproduction Update*, *20*(1), 40–62. https://doi.org/10.1093/humupd/dmt046

Arauz-Garofalo, G., Jodar, M., Vilanova, M., de la Iglesia Rodriguez, A., Castillo, J., Soler-Ventura, A., Oliva, R., Vilaseca, M., & Gay, M. (2021). Protamine Characterization by Top-Down Proteomics: Boosting Proteoform Identification with DBSCAN. *Proteomes*, *9*(2). https://doi.org/10.3390/proteomes9020021

Arpanahi, A., Brinkworth, M., Iles, D., Krawetz, S. A., Paradowska, A., Platts, A. E., Saida, M., Steger, K., Tedder, P., & Miller, D. (2009). Endonuclease-sensitive regions of human spermatozoal

chromatin are highly enriched in promoter and CTCF binding sequences. *Genome Research*, *19*(8), 1338–1349. https://doi.org/10.1101/gr.094953.109

Ausió, J., González-Romero, R., & Woodcock, C. L. (2014). Comparative structure of vertebrate sperm chromatin. *Journal of Structural Biology*, *188*(2), 142–155. https://doi.org/10.1016/j.jsb.2014.09.004

Balhorn, R. (1982). A model for the structure of chromatin in mammalian sperm. *The Journal of Cell Biology*, *93*(2), 298–305. https://doi.org/10.1083/jcb.93.2.298

Balhorn, R. (2007). The protamine family of sperm nuclear proteins. *Genome Biology*, *8*(9), 227. https://doi.org/10.1186/gb-2007-8-9-227

Balhorn, R., Reed, S., & Tanphaichitr, N. (1988). Aberrant protamine 1/protamine 2 ratios in sperm of infertile human males. *Experientia*, *44*(1), 52–55. https://doi.org/10.1007/BF01960243

Barrachina, F., de la Iglesia, A., Jodar, M., Soler-Ventura, A., Mallofré, C., Rodriguez-Carunchio, L., Goudarzi, A., Corral, J. M., Ballescà, J. L., Castillo, J., & Oliva, R. (2022). Histone H4 acetylation is dysregulated in active seminiferous tubules adjacent to testicular tumours. *Human Reproduction*, *30*(8), 1712–1726. https://doi.org/10.1093/humrep/deac130

Björndahl, L., & Kvist, U. (2011). A model for the importance of zinc in the dynamics of human sperm chromatin stabilization after ejaculation in relation to sperm DNA vulnerability. *Systems Biology in Reproductive Medicine*, *57*(1–2), 86–92. https://doi.org/10.3109/19396368.2010.516306

Castillo, J., Amaral, A., Azpiazu, R., Vavouri, T., Estanyol, J. M., Ballesca, J. L., & Oliva, R. (2014). Genomic and proteomic dissection and characterization of the human sperm chromatin. *Molecular Human Reproduction*, *20*(11), 1041–1053. https://doi.org/10.1093/molehr/gau079

Castillo, J., Amaral, A., & Oliva, R. (2014). Sperm nuclear proteome and its epigenetic potential. *Andrology*, *2*(3), 326–338. https://doi.org/10.1111/j.2047-2927.2013.00170.x

Castillo, J., Estanyol, J., Ballescà, J., & Oliva, R. (2015). Human sperm chromatin epigenetic potential: genomics, proteomics, and male infertility. *Asian Journal of Andrology*, *17*(4), 601. https://doi.org/10.4103/1008-682X.153302

Conwell, C. C., & Hud, N. v. (2004). Evidence that both kinetic and thermodynamic factors govern DNA toroid dimensions: effects of magnesium(II) on DNA condensation by hexammine cobalt(III). *Biochemistry*, *43*(18), 5380–5387. https://doi.org/10.1021/bi049872u

Conwell, C. C., Vilfan, I. D., & Hud, N. v. (2003). Controlling the size of nanoscale toroidal DNA condensates with static curvature and ionic strength. *Proceedings of the National Academy of Sciences of the United States of America*, *100*(16), 9296–9301. https://doi.org/10.1073/pnas.1533135100

Craievich, A. F. (2016). Small-Angle X-ray Scattering by Nanostructured Materials. In *Handbook of Sol-Gel Science and Technology* (pp. 1–46). Springer International Publishing. https://doi.org/10.1007/978-3-319-19454-7_37-1

DeRouchey, J. E., & Rau, D. C. (2011). Salt effects on condensed protamine-DNA assemblies: anion binding and weakening of attraction. *The Journal of Physical Chemistry. B*, *115*(41), 11888–11894. https://doi.org/10.1021/jp203834z

Gaucher, J., Reynoird, N., Montellier, E., Boussouar, F., Rousseaux, S., & Khochbin, S. (2010). From meiosis to postmeiotic events: the secrets of histone disappearance. *The FEBS Journal*, *277*(3), 599–604. https://doi.org/10.1111/j.1742-4658.2009.07504.x

Hazzouri, M., Pivot-Pajot, C., Faure, A.-K., Usson, Y., Pelletier, R., Sèle, B., Khochbin, S., & Rousseaux, S. (2000). Regulated hyperacetylation of core histones during mouse spermatogenesis: involvement of histone-deacetylases. *European Journal of Cell Biology*, *79*(12), 950–960. https://doi.org/10.1078/0171-9335-00123

Hud, N. v, Allen, M. J., Downing, K. H., Lee, J., & Balhorn, R. (1993). Identification of the Elemental Packing Unit of DNA in Mammalian Sperm Cells by Atomic Force Microscopy. *Biochemical and Biophysical Research Communications*, *193*(3), 1347–1354. https://doi.org/10.1006/bbrc.1993.1773

Hud, N. v, Downing, K. H., & Balhorn, R. (1995). A constant radius of curvature model for the organization of DNA in toroidal condensates. *Proceedings of the National Academy of Sciences*, *92*(8), 3581–3585. https://doi.org/10.1073/pnas.92.8.3581

Hutchison, J. M., Rau, D. C., & DeRouchey, J. E. (2017). Role of Disulfide Bonds on DNA Packaging Forces in Bull Sperm Chromatin. *Biophysical Journal*, *113*(9), 1925–1933. https://doi.org/10.1016/j.bpj.2017.08.050

Mengual, L., Ballescá, J. L., Ascaso, C., & Oliva, R. (2003). Marked differences in protamine content and P1/P2 ratios in sperm cells from percoll fractions between patients and controls. *Journal of Andrology*, *24*(3), 438–447. https://doi.org/10.1002/j.1939-4640.2003.tb02692.x

Motta, S., Brocca, P., del Favero, E., Rondelli, V., Cantù, L., Amici, A., Pozzi, D., & Caracciolo, G. (2013). Nanoscale structure of protamine/DNA complexes for gene delivery. *Applied Physics Letters*, *102*(5), 053703. https://doi.org/10.1063/1.4790588

Newville, M., Stensitzki, T., Allen, D. B., & Ingargiola, A. (2014). LMFIT: Non-Linear Least-Square Minimization and Curve-Fitting for Python. *Zenodo*. https://doi.org/10.5281/ZENODO.11813

Ni, K., Spiess, A.-N., Schuppe, H.-C., & Steger, K. (2016). The impact of sperm protamine deficiency and sperm DNA damage on human male fertility: a systematic review and meta-analysis. *Andrology*, *4*(5), 789–799. https://doi.org/10.1111/andr.12216

Oliva, R. (2006). Protamines and male infertility. *Human Reproduction Update*, *12*(4), 417–435. https://doi.org/10.1093/humupd/dml009

Oliva, R., & Dixon, G. H. (1991). Vertebrate Protamine Genes and the Histone-to-Protamine Replacement Reaction. *Progress in Nucleic Acid Research and Molecular Biology*, *40*(C), 25–94. https://doi.org/10.1016/S0079-6603(08)60839-9

Pedersen, J. S. (1997). Analysis of small-angle scattering data from colloids and polymer solutions: modeling and least-squares fitting. *Advances in Colloid and Interface Science*, *70*, 171–210. https://doi.org/10.1016/S0001-8686(97)00312-6

Rathke, C., Baarends, W. M., Awe, S., & Renkawitz-Pohl, R. (2014). Chromatin dynamics during spermiogenesis. *Biochimica et Biophysica Acta (BBA) - Gene Regulatory Mechanisms*, *1839*(3), 155–168. https://doi.org/10.1016/j.bbagrm.2013.08.004

Ribas-Maynou, J., Garcia-Peiro, A., Abad, C., Amengual, M. J., Navarro, J., & Benet, J. (2012). Alkaline and neutral Comet assay profiles of sperm DNA damage in clinical groups. *Human Reproduction*, *27*(3), 652–658. https://doi.org/10.1093/humrep/der461

Simon, L., & Carrell, D. T. (2013). *Sperm DNA Damage Measured by Comet Assay* (pp. 137–146). https://doi.org/10.1007/978-1-62703-038-0_13

Soler-Ventura, A., Castillo, J., de la Iglesia, A., Jodar, M., Barrachina, F., Ballesca, J. L., & Oliva, R. (2018). Mammalian Sperm Protamine Extraction and Analysis: A Step-By-Step Detailed Protocol and Brief Review of Protamine Alterations. *Protein and Peptide Letters*, *25*(5), 424–433. https://doi.org/10.2174/0929866525666180412155205

Soler-Ventura, A., Gay, M., Jodar, M., Vilanova, M., Castillo, J., Arauz-Garofalo, G., Villarreal, L., Ballescà, J. L., Vilaseca, M., & Oliva, R. (2020). Characterization of Human Sperm Protamine Proteoforms through a Combination of Top-Down and Bottom-Up Mass Spectrometry Approaches. *Journal of Proteome Research*, *19*(1), 221–237. https://doi.org/10.1021/acs.jproteome.9b00499

Teixeira, J. (1988). Small-angle scattering by fractal systems. *Journal of Applied Crystallography*, *21*(6), 781–785. https://doi.org/10.1107/S0021889888000263

Vilfan, I. D., Conwell, C. C., & Hud, N. v. (2004). Formation of Native-like Mammalian Sperm Cell Chromatin with Folded Bull Protamine. *Journal of Biological Chemistry*, *279*(19), 20088–20095. https://doi.org/10.1074/jbc.M312777200

Vilfan, I. D., Conwell, C. C., Sarkar, T., & Hud, N. v. (2006). Time Study of DNA Condensate Morphology: Implications Regarding the Nucleation, Growth, and Equilibrium Populations of Toroids and Rods. *Biochemistry*, *45*(26), 8174–8183. https://doi.org/10.1021/bi060396c

World Health Organization. (2021). *WHO laboratory manual for the examination and processing of human semen, sixth edition*. World Health Organization; 2021. License: CC BY-NC-SA 3.0 IGO.

6.

DISCUSSION

6. DISCUSSION

Opposed to the traditional idea of the male gamete being a simple carrier of the paternal DNA, evidence in the last decades revealed that the sperm cell provides the embryo with different layers of epigenetic information, not only limited to DNA methylation and non-coding RNAs but also involving the protein fraction of the sperm chromatin. Posttranslational modifications (PTMs) of chromatin-associated proteins, and the complex population of sperm nuclear proteins with gene regulatory roles would also have an impact in fertilization and pre-implantation embryo development (Castillo, Amaral, Azpiazu, et al., 2014; Castillo et al., 2018; Jodar et al., 2013; Laurentino et al., 2016; Oliva, 2006). Furthermore, the sperm chromatin, understood as the association between DNA and two different types of proteins, histones and protamines, bearing PTMs and resulting in two distinct genome compaction states, arises as a new concept of epigenetic mark that is exclusive for the male gamete (Blanco & Cocquet, 2019; Castillo, Amaral, & Oliva, 2014; Castillo et al., 2015; Y. Wang et al., 2019). The relevance and peculiarities of sperm chromatin have attracted interest over the years, and many efforts have been made to disentangle it, not only in mature sperm but also during spermatid differentiation. However, the chromatin of male germ cells is as attractive as challenging, requiring adaptation of conventional techniques or application of new ones for its study. Despite that, many important factors are being related with the regulation and formation of the sperm chromatin, as well as with the correct transmission of epigenetic information from the father to the zygote. Thus, protamines, histones and their PTMs, both during male gamete development and once matured, as well as the peculiarly compacted chromatin structure of mature sperm, emerge as interesting features to be further studied and increase the current knowledge on the epigenetic content of the protein fraction of sperm chromatin, and its potential involvement in cases of unexplained male infertility.

The findings disclosed in the present doctoral thesis shed new light into the chromatin of human male germ cells and its epigenetic potential, both during sperm testicular formation and in the mature sperm cell. **Chapter 1** describes PTMs on histone H4 and the specific residue of Lys5 (H4K5), key regulator of the chromatin remodeling process taking place during spermiogenesis, showing a characteristic testicular pattern supporting their involvement in human spermiogenic regulation similar to that described in mouse models. The behaviour of the well-characterized H4 and H4K5 acetylation along spermatogenesis present some similarities and remarkable differences to that of the recently described butyrylation on H4K5, which could impact the temporal regulation of the human nucleo-histone to nucleo-protamine (NH-NP) transition. Whereas global H4 acetylation was altered in patients with testicular pathologies, H4K5 seems to be somehow protected to external perturbations, remaining stable. Besides, the way in which H4K5 butyrylation and acetylation are retained in human mature sperm point out a potential differential distribution alongside the paternal genome with potential effects in post-fertilization events.

Of note, not only sperm histones bear PTMs, but also protamines. In **Chapter 2**, the data analysis pipeline for top-down proteomics set up by our team allowed the reliable description of protamine proteoforms in human sperm, evidencing altered abundance of some proteoforms in patients with biologically impaired chromatin and patients influenced by their lifestyle or demographic characteristics. Age- and weight-associated changes affected posttranslationally modified protamine 1 (P1) proteoforms, mainly with phosphorylations. The study in the mouse testis of the protamine modulating proteins SRPK1 and PP1γ revealed potential role of both proteins not characterized so far in regulatory mechanisms during spermiogenesis, through their association with proteins participating in transcriptional and translational regulation, as well as in chromatin remodeling. When focusing on molecular characteristics of sperm chromatin maturity such as relative protamine levels, protamine 2 (P2) proteoforms alterations (accumulation of P2 immature forms) are revealed, suggesting potential P2 processing errors. However, as disclosed in **Chapter 3**, this alteration does not induce ultrastructural nanoscale changes in sperm chromatin. By applying Small-Angle X-ray Scattering (SAXS) using synchrotron light for the study of normal human sperm nuclei in solution, we described the presence of a 2-level chromatin organization in which supramolecular arrangements of ~67 nm radius arise from the aggregation of highly compacted, smooth, and very stable small subunits with ~7.7 nm radius. Strikingly, supramolecular aggregates were altered in patients with pathological levels of double strand DNA breaks, pointing out to strong interconnection between genomic stability and chromatin architecture.

6.1 Acetylation and butyrylation marks on histone H4 as potential regulators of human male germ cells' chromatin remodeling

A global H4 hyperacetylation wave is widely described in nucleosome instability for subsequent chromatin remodeling during spermatogenesis, event that is highly conserved among mammals (Christensen & Dixon, 1982; Grimes & Henderson, 1984; Hazzouri et al., 2000; Oliva & Mezquita, 1982). **Work 1** described in detail the H4ac pattern in human testicular tissue using the spermatogenic classification method into twelve different stages reported elsewhere (Muciaccia et al., 2013). This approach allowed the identification of mild H4ac levels in spermatogonia that were reduced in spermatocytes, followed by a gradual increase of H4ac levels from post meiotic cells, and reaching a maximum in elongated spermatids to finally drop in condensed spermatids. Alterations in H4ac levels were previously reported in men with different spermatogenic impairments (Faure et al., 2003; Sonnack et al., 2002), but nothing was known regarding seminiferous tubule cells with active spermatogenesis adjacent to testicular tumors. Strikingly, we observed a general increase in H4ac levels among patients affected by different tumors, whose orchiectomies were performed before starting any gonadotoxic treatment. Germ

cells from active seminiferous tubules in testes affected by tumors displayed increased H4ac levels mainly in early stages of spermatogenesis, while more developed spermatogenic cell types displayed lower H4ac levels compared with the normal spermatogenic pattern. The most remarkable finding was the total disruption of the characteristic gradual increase in H4ac in post meiotic cells. All these changes might lead to a premature nucleosome destabilization and histone displacement, coupled to an early loss of H4 hyperacetylation in later stages of spermatogenesis (Christensen & Dixon, 1982; Grimes & Henderson, 1984; Hazzouri et al., 2000; Oliva et al., 1987, 1990; Oliva & Mezquita, 1982). Chromatin epigenetic impairments during spermatogenesis are linked to decreased H4ac levels in later stages of the spermiogenesis and, consequently, to defective histone retention and chromatin remodelling (Moretti et al., 2017).

The disruption of H4ac spermatogenic pattern was observed in seminiferous tubules of patients affected by testicular tumors with different origin and pathogenicity, including patients affected by germ cell tumors derived from germ cell neoplasia *in situ* (GCNIS) such as seminoma, teratoma, and embryonal carcinoma, germ cell tumors unrelated with CGNIS such as spermatocytic tumor, and a sex-cord stromal tumor (Leydig cell tumor). Despite their different pathogenesis, the alteration was comparable among the different groups of study and regardless the intratubuluar detection of pre-invasive GCNIS, which was only observed in some patients with seminoma an embryonal carcinoma. Therefore, the potential effect of intratubular neoplasia on the observed alteration was discarded and, in theory, no direct effect of a tumor without germ cell-related origin, such as Leydig cell tumor, should be expected. The affectation by germ cell tumors was then associated with H4ac dysregulation regardless a) germ cell tumor type and b) presence or not of tubular pre-invasive GCNIS. These striking observations point to the tumor environment as responsible for the epigenetic alteration found within the seminiferous tubules.

Derived from our results, we suggested a paracrine effect of the testicular tumor on the adjacent seminiferous tubules as potential underlying cause of the global dysregulation observed in spermatogenic H4ac levels, in which the simple presence of a neoplasia could impair the homeostasis in the testicular stroma. Stemming from it, dysregulation of interstitial protein levels would lead to an impaired cell signaling. We hypothesize that the tumor secretes small proteins or paracrine signals that could impair the intercellular communication causing an altered signal transduction, therefore producing a dysregulation of intracellular signaling cascades and altering nuclear gene expression in the intratubular cells. Infiltration of immune cells is indeed a common event of testicular tumors and contributes to tumor microenvironment composition. In that case, some cytokines and chemokines with normal protective roles could exert a negative impact on testicular function and physiology (Loveland et al., 2017). Furthermore, immune cell infiltration is associated with disrupted blood-testis barrier in affected seminiferous tubules, allowing the permeabilization of small molecules (Pérez et al., 2013). Impaired

intracellular phosphorylation cascades involved in male germ cell development could carry out changes in gene activity coupled to changes on H4ac levels. Our *in silico* approach would support this hypothesis, identifying potentially secreted proteins highly expressed in tumor cells that were undetectable or underexpressed in the healthy testicular tissue, supporting the existence of a potential paracrine disruption of cell signaling. Indeed, overrepresented pathways would support paracrine communication between tumor and seminiferous tubule cells, identifying ligand–receptor pathways, including cytokine signaling and growth factors, as well as phosphorylation-mediated signal transduction. However, the interpretation of this *in silico* prediction is limited by the scarce availability of gene expression data in testicular tumors sorted by tumor subtypes and it requires further experimental confirmation. Indeed, this common global increase of H4ac levels found in all types of tumors might rely on mechanisms that could vary according to different cellularity and secretory patterns.

Fertility preservation is routinely considered in men affected by testicular tumors, since its diagnostic is commonly made during reproductive age, including semen cryopreservation when possible, and testicular tissue or spermatogenic cells cryopreservation in cases associated with male subfertility (Fraietta et al., 2010; Laguna et al., 2022; Oktay et al., 2018; Picton et al., 2015; Saltzman & Cost, 2018). Thus, the alteration identified in our work is an additional epigenetic disruption to be considered apart from the already described alterations in the male gamete of patients affected by testicular tumors, that are associated to sperm function, sperm protein profile, and DNA methylation (Åsenius et al., 2020; Bruno et al., 2018; T. Dias et al., 2020; Suzuki et al., 2015; Xavier et al., 2021). Indeed, this is the only one reported in immature germ cells, which would be a potential risk when considering fertility preservation using testicular tissue. Besides, the observed H4ac alteration during the spermatogenesis in testicular tumor patients could be related to a subsequent defective retention of histone epigenetic marks in mature sperm, potentially leading to the transmission of altered epigenetic modifications and affecting events beyond fertilization.

As acetylation, other recently described histone acylations, some of them still with unknown role during spermatogenic development, arise as potential candidates regulating chromatin remodeling in post meiotic cells. Among them, histone butyrylation in H4K5 has been related with delayed nucleosome removal and sperm histone retention in mice (Goudarzi et al., 2016). Due to the especially relevant role of H4K5 residue controlling proper NH–NP transition, (Dhar et al., 2012; Goudarzi et al., 2014, 2016; Her et al., 2021; Manterola et al., 2018; Morinière et al., 2009; Pivot-Pajot et al., 2003; Shang et al., 2007), in **Work 2** we studied the specific acetylation and butyrylation on H4K5 (H4K5ac and H4K5bu, respectively) during human spermatogenesis, which were yet unexplored. Interestingly, whereas H4K5ac

displayed a spermatogenic pattern consistent with the one described in **Work 1** for global H4ac, H4K5bu revealed a different behavior pointing out a highly specific role during the latest steps of human spermatogenesis. Basal butyrylation levels were detected during mitotic phase, meiotic phase, and initial stages of spermiogenesis, and a drastic increase in H4K5bu levels started in a more advanced stage of round spermatids compared to H4K5ac profile. Furthermore, both H4K5ac and H4K5bu evidenced a drastic drop in condensing spermatids. Therefore, we found that H4K5 PTMs temporarily coexist during spermatid elongation, when NH-NP transition occurs, coherent with previous reports in mouse models suggesting a temporal regulation of nucleosome disassembly and histone retention based on competing H4K5 butyrylation and acetylation (Goudarzi et al., 2016).

The analysises of H4K5bu during spermiogenesis under different primary testicular failure, did not report any relevant change associated with hypospermatogenesis, Sertoli cell-only syndrome, and spermatogenic arrest. Despite we could not perform statistical analysis due to the limited number of samples, higher H4K5bu levels than in normal spermatogenesis pattern were found in post meiotic cells from a patient with partial spermatid arrest, which is coherent with the highly specialized known function of H4K5bu after meiosis. It is also interesting to highlight that while results from Work 1 revealed a drastic dysregulation of global H4ac levels in testicular cancer patients, neither specific H4K5bu nor H4K5ac levels were altered in patients with seminoma and teratoma. These contrasting results suggest a highly conserved role of both PTMs in H4K5 residue towards a correct spermiogenic development and could explain why testicular cancer patients studied in Work 1 displayed complete spermatogenesis and spermatid elongation despite the global H4ac disruption, which in turn would derive from the contribution of other acetylated residues in H4.

The relationship between sperm chromatin status and its impact on sperm functionality and events beyond fertilization is becoming more and more evident (Azpiazu et al., 2014; Brykczynska et al., 2010; Castillo, Amaral, Azpiazu, et al., 2014; Castillo et al., 2018; Erkek et al., 2013; S. Hammoud et al., 2011; Ihara et al., 2014; Kaneshiro et al., 2019; Kaufman & Rando, 2010; Saida et al., 2011; Teperek et al., 2016; Vavouri & Lehner, 2011). Therefore, we investigated the presence and potential role of both H4K5bu and H4K5ac in mature sperm cells. Despite their drastic drop observed in condensing spermatids, both PTMs were retained in mature sperm from normozoospermic patients, colocalizing in approximately 70% of nucleosome clusters. This high level of colocalization, supported by the high correlation reported by Pearson coefficient, is coherent with the rapid PTM turnover on H4K5 during spermatogenesis, in which acetylated and butyrylated H4K5 co-occur in the same genomic regions (Goudarzi et al., 2016). Since two H4 are present in a single nucleosome, two different scenarios arise from this co-localization: 1) the presence of single nucleosomes containing one H4 marked by butyrylation in K5 and the other by acetylation in the same residue, or 2) nucleosomes with both H4 marked by either butyrylation or acetylation in K5, that are spatially close to

nucleosomes bearing the alternative mark. At this point, both options are equally feasible because we were not able to resolve single nucleosomes with the imaging resolution of the approach applied. Interestingly, the remaining proportion of non-colocalizing marks also suggest the presence of a minor group of nucleosome clusters exclusively marked by either H4K5bu or H4K5ac, pointing to a potential functional involvement of the differential wrapping of paternal DNA into H4K5ac or H4K5bu nucleosomes.

While colocalization results would suggest a role of H4K5ac and H4K5bu in sperm function, they did not relate with sperm quality. The study of sperm populations isolated from neat sample, following procedures routinely used in the reproductive clinics to select the best spermatozoon for ICSI, discarded an impact of H4K5bu and H4K5ac relative levels in sperm fertilizing ability. Complementary molecular approaches to further characterize both PTMs in sperm chromatin will help to decipher their potential as indicators of chromatin maturity. Due to the known role of sperm histone marks as epigenetic regulators in early embryo, it will be worthy to know whether they can have an impact beyond fertilization, such as in the formation of preimplantation embryo and transmission of epigenetic information.

6.2 Epigenetic information contained in the less accessible fraction of the sperm chromatin: the role of protamine proteoforms and associated proteins

Histones have traditionally attracted the most interest regarding sperm epigenetic cargo among chromatin-associated sperm proteins. Despite of that, in the last years, the epigenetic potential of protamines has been suggested and reinforced after the characterization of protamine PTMs alongside a complex population of protamine proteoforms, both in human and mice (Brunner et al., 2014; Soler-Ventura et al., 2020). One of the main reasons of this delayed discovery was basically the technical challenges that protamines study entailed, and our group did a great work overcoming them, providing the first description of the human sperm protamine proteoforms profile through different proteomics approaches (Soler-Ventura et al., 2020). However, the complexity of protamine proteoforms study is not only reduced to the experimental set-up, but also requires a carefully designed analysis pipeline for their identification.

In **Work 3**, our team developed a strategy to identify with high fidelity human protamine proteoforms from top-down proteomics data, combining the software packages ProSight PD and TopPIC Suite with the clustering algorithm DBSCAN (Arauz-Garofalo et al., 2021). In that work, we proved the usefulness of the DBSCAN algorithm to solve some of the misassignments found when analyzing top-down database searches provided by these two nodes. The application of this clustering algorithm highly refined protamine proteoform search to achieve a reliable

identification of changes in proteoform abundance in comparative analyses. The improvements made brought the possibility of studying sperm protamine proteoform content under pathological conditions towards personalized diagnosis of male infertility.

Thus, in **Work 4**, we searched for alterations in the protamine proteoform profile in patients potentially bearing sperm chromatin alterations. We selected patients with unexplained infertility with biologically impaired chromatin status according to P1/P2 ratio, whose levels outside the fertile range [0.8–1.2] have been traditionally associated with altered seminal parameters (sperm count, motility, and morphology), increased DNA damage, and lower success rates of assisted reproduction technologies (Jodar & Oliva, 2014; Soler-Ventura et al., 2018). Also, patients with specific demographic characteristics or lifestyle were considered, *i.e.*, seeking for a child at advanced age, or considered obese according to their body mass index (BMI), since sperm chromatin epigenetic alterations have been reported in both phenotypes (Deshpande et al., 2021; Donkin et al., 2016; Laurentino et al., 2020; Pohl et al., 2021; Soubry et al., 2016; Terashima et al., 2015).

We provided additional evidence of the improvements after applying the pipeline analysis described in Work 3, with a reduction of a considerable number of artifacts before collapsing them. The group of patients with high P1/P2 ratio (>1.2) revealed an accumulation of P2 immature forms (HPS1 and HPI2), with intact phosphorylation levels compared to controls. It was coherent with In-gel observations, suggesting reduced P2 as underlying cause of the altered P1/P2 ratio, which could indicate a bad processing of P2 precursor leading to lower abundance of mature P2 forms. The recent application of CRISPR/Cas9 technology to design mouse models with impaired P2 precursor processing revealed that proper P2 processing is essential for fertility and to maintain stable P1/P2 ratio. Furthermore, P2-depleted models showed that the total loss of P2 induced upregulation of P1 as compensating mechanism, apart from resulting in fertility problems as well (Arévalo et al., 2022; Schneider et al., 2016, 2020). However, the protamine proteoform landscape of altered P1/P2 patients did not significant alterations in the total abundance of P2 precursor nor P2 mature forms, suggesting that accumulation of HPS1 and HPI2 may result from compensating increased expression and processing of P2 precursor to reach normal P2 levels, generating an excess of immature forms as subproducts. To further understand the phenotype, the evaluation of P2 precursor gene expression levels would give hints on the origin of the accumulation of P2 immature forms. As it will be further discussed in **Section 4.3**, patients with high P1/P2 ratio, despite accumulating P2 immature forms, did not evidence alterations in their chromatin structure at the nanoscale, reinforcing the theory of a redundant function of the different protamine proteoforms in compacting paternal genome for sperm streamlining. However, despite this redundant function of protamines in chromatin compaction, it is still unknown whether there is a specific placement of each proteoform or whether different protamine proteoform incorporation undergo a temporal regulation, so the epigenetic effect towards paternal nuclear reprogramming in the zygote should not be discarded.

While biologically impaired chromatin status evidenced P2 family-associated defects, alterations reported in patients according to age and weight were related with posttranslational modifications of P1. Obese patients displayed reduced abundance of P1-associated proteoforms bearing a still unknown +61 mass shift, either alone or coupled to monophosphorylation. Although our previous hypothesis pointed to Zn^{2+} molecule incorporation as responsible of this mass shift, the PrSM profile obtained in our study does not match that of Zn^{2+} (Soler-Ventura et al., 2020). Current work focuses on figuring out whether the unknown +61 Da incorporation could be related with altered membrane lipid peroxidation, which is increased in patients with high fat dietary patterns, also coupled to (and derived from) a rise of intracellular ROS levels (Akbarian et al., 2021; McPherson et al., 2014; McPherson & Lane, 2015). N^{ε}-(2-propenal)-lysine, deriving from the lipid peroxidation subproduct malondialdehyde (MDA) of ~60 Da, emerges as an interesting candidate due to its more favorable fitting with the PrSM pattern, as well as to the fact that altered levels of MDA have been related with male reproductive problems (Collodel et al., 2015; Uchida et al., 1997).

In turn, the single alteration found in patients with advanced age consisted of reduced abundance of diphosphorylated forms of P1, likely due to loss of phosphorylation in Ser11 mainly in combination with Ser22, but also with Ser29 in less extent. The biological relevance of this finding on the reproductive outcome of advance age men could be high based on previous results in mouse models evidencing a drastic reduction of fertility when two phosphorylation sites were simultaneously depleted on P1 (Gou et al., 2020). Despite P1 Ser 11 and 22 phosphorylation sites are not conserved in mouse (Brunner et al., 2014), our results reinforce the functional role of these two P1 residues. Besides, protamine phosphorylation status may have a role on zygotic male pronuclear reprogramming, since protamine phosphorylation is an essential mechanism to unwrap paternal DNA after fertilization (Gou et al., 2020). It will be interesting to check whether the extent of the reduction of diphosphorylated P1 is directly proportional to male age, or whether additional proteoforms show altered abundance, in time-course studies.

Thus, our results derived from **Work 4** highlight the relevance of not only mature, but also inmature and phosphorylated, protamine proteoforms towards sperm functionality and male fertility status, and point to alterations on protamine modifying mechanisms, rather thatn on protamine synthesis, as critical factors for proper sperm chromatin maturity. Opposed, but not incompatible, to their suggested redundant function of paternal genome packaging, the potential involvement of sperm protamine proteoforms as a new level of sperm epigenetic alteration is reinforced, either induced by lifestyle or consequence of biological errors in protamine processing.

Apart from their presence in mature sperm and its epigenetic potential, protamine phosphorylation plays an essential role in chromatin remodeling during sperm formation (Bao & Bedford, 2016; Hazzouri et al., 2000; Oliva, 2006). Phosphorylation dynamics is known to be essential for adequate protamination of

the DNA, where protamine-phosphorylated proteoforms, showing lower DNA affinity than unmodified proteoforms, would assist protamine loading on paternal DNA in early spermiogenesis (Willmitzer et al., 1977b, 1977a). After incorporation of phosphorylated protamines into DNA, a subsequent dephosphorylation wave takes place inducing a higher sperm chromatin conformation (Carrell et al., 2007a; Oliva, 2006; Oliva & Dixon, 1991; Soler-Ventura et al., 2020). SRPK1 is the most well-characterized protamine kinase in the testis, responsible for phosphorylating P1 (Gou et al., 2020; Papoutsopoulou et al., 1999), and its dysregulation has been linked to male infertility (Azpiazu et al., 2014). While no P1-specific phosphatases have been described yet, germ cell-specific isoform 2 of PP1γ is involved in removing phosphate groups from P2, essential to achieve fertility in mouse maintaining P2 phosphorylation levels (Itoh et al., 2019). Since a highly orchestrated regulation happens during spermiogenesis, and in line with the essential role of phosphorylation events in maintaining a proper testicular activity (Castillo, Knol, et al., 2019; Qi et al., 2014), **Work 5** focused on identifying the protein-protein associations of SRPK1 and PP1γ in the mouse testis, to seek for additional roles of these phosphorylation-modulating proteins during post meiotic regulation.

Identified interactions were coherent with molecular roles already described for both proteins. SRPK1 is a widely described moonlight protein known to be involved in mRNA splicing among many other cellular processes (Bullock & Oltean, 2017; Gui et al., 1994; Patel et al., 2019). Accordingly, SRPK1 interacts with RNA in ribonucleoprotein complexes in the testis to regulate mRNAs at different levels, including splicing. Serine/arginine-rich splicing factor 1 (ASF/SF2), identified as SRPK1-associated protein, interacted with proteins from the IP protein network. Therefore, the presence of ASF/SF2 interacting proteins in the SRPK1 network may derive from their interaction with ASF/SF2 rather than with SRPK1. Despite the Serine/arginine-rich splicing factor (SRSF) protein family are well-known targets of SRPK1 in different cell types, no other family members were identified in our study, suggesting that SRPK1 is associated with a wider set of proteins implicated in gene expression regulation during spermatogenesis, either regulated by SRPK1 or acting in synergy with it as part of a complex. Indeed, we identified proteins involved in deadenylation-dependent mRNA decay, which coupled to alternative splicing is an efficient strategy to regulate gene expression (B. P. Lewis et al., 2003; Song et al., 2020). Also, proteins binding to N6-methyladenosine m6A, a posttranscriptional mRNA modification playing a pivotal role in alternative splicing and RNA degradation were identified as interacting with testicular SRPK1 (Cao et al., 2016; Song et al., 2020). Therefore, we report potential new candidates associated with SRPK1 during mouse spermatogenesis and modulating gene expression. Among the proteins with expected role in post meiotic cells, IGF2BP3 and PABP1 are interesting candidates because they have been found as phosphoproteins in mouse spermatids (Y. Li et al., 2019; Qi et al., 2014), so SRPK1 may mediate their phosphorylation, and are involved in temporal translation of proteins essential to achieve a proper NH-NP transition, such as TP1, TP2, and P2. Additionally, PABP1 is implicated in kinase-dependent spatiotemporal regulation of protein translation mediated by protein kinase A (PKA) during mouse spermiogenesis, promoting translation (Xu et al.,

2014). Likewise, a similar role of SRPK1 would be feasible, contributing to protein translation initiation of nascent sperm-specific mRNAs during spermiogenesis. Apart from proteins involved in protein mRNA-related processes, it was surprising to find MCM7, involved in DNA replication, among the proteins with a potential role in spermiogenesis, since at this stage haploid male germ cells undergo differentiation without replicating. Interestingly, MCM7 was the only MCM-family member maintaining transcriptional levels from meiosis on, and two additional MCM7 transcripts originated from alternative splicing are present in meiotic and post-meiotic germ cells (Com et al., 2006). Therefore, a specialized specific function in post meiotic cells for MCM7 could be hypothesized. Its single-strand DNA binding ability and helicase activity would be coherent with the transition DNA breaks appearing in spermiogenesis to release torsional stress in DNA helixes, therefore inducing a relaxed state to accommodate nucleosome removal (Marcon & Boissonneault, 2004b; Risley et al., 1986). Besides, MCM7 is a mouse spermatid phosphoprotein, susceptible to be phosphorylated by SRPK1. Therefore, SRPK1 might be involved in regulating or MCM7 towards spermiogenic chromatin remodeling.

Due to antibody availability, PP1γ-IP was performed against PP1γ (recognizing both isoforms 1 and 2) instead of PP1γ2. However, whereas PP1γ1 is ubiquitous, PP1γ2 is a testis-specific isoform enriched in male germ cells (Dudiki et al., 2019; Okano et al., 1997). Therefore, after discarding potential somatic contaminants from Sertoli cells, all identified proteins are likely associated with the specific testicular enriched isoform PP1γ2. Indeed, proteins already reported to interact with PP1γ2 in the testis were present in our dataset, such as protein phosphatase 1 regulatory subunits 7 (PPP1R7) and 11 (PPP1R11) (L. Cheng et al., 2009).

In turn, PP1γ interacting network revealed several protein complexes. So, despite comprising a higher number of proteins, a low number of enriched biological processes were found. The four members of R2TP complex (regulatory heterodimer RPAP3-PIH1D1 bound to the catalytic ATPases RUVBL1 and RUVBL2), a co-chaperone with unusual function specialized in quaternary protein folding, were identified. RNA polymerases and spliceosomal small nucleolar RNAs have been described as substrates of R2TP complex, pointing out a role of this complex in regulating spermatogenic gene expression program (Kakihara & Houry, 2012). The catalytic dimer RUVBL1 and RUVBL2 is also part of chromatin remodeling complexes such as SRCAP and hINO80 complexes mediating their association with nucleosomes, playing a role in histone variant exchange, nucleosome eviction, and nucleosome remodeling (Gerhold & Gasser, 2014). RUVBL1 and RUVBL2 ATPase activity promote the exchange between H2A-H2B canonical dimer and H2A.Z-H2B dimers, which may be coupled to histone PTMs as acetylation by NuA4 histone acetyltransferase complex (Choi et al., 2009; Gerhold & Gasser, 2014; Papamichos-Chronakis et al., 2011). Thus, it may be interesting to explore whether R2TP in association with PP1γ mediate the loading of RUVBL1 and 2 into chromatin remodeling complexes. An RMP-mediated stabilization of R2TP complex has been reported, depending on RMP phosphorylation status (Burén et al., 2016; Lynham & Houry, 2018). Among other proteins identified, RMP has been described as

interactor of PP1γ in other cell types and is suggested to recruit proteins to R2TP (Kakihara & Houry, 2012). When interacting with WDR92 through RPAP3, RPAP3/R2TP/prefoldin-like complex is involved in axoneme structure, and loss of some of the R2TP complex have been linked with impaired sperm motility (Djouder et al., 2007; Kakihara & Houry, 2012). Further studies would be needed to decipher whether R2TP complex is acting as co-chaperone for quaternary folding of macromolecules involving PP1γ, or whether PP1γ plays a role in dephosphorylation of some R2TP complex regulating its activity.

TBLX1R1 was the only common protein found in SRPK1 and PP1γ interactomes with a potential role during spermiogenesis. This protein is part of the SMRT/N-CoR complex, that interacts with nuclear hormone receptors, transcription factors, and chromatin modifying enzymes such as histone deacetylases, suggested to participated in SLY-mediated gene expression control (J. Li et al., 2000; Perissi et al., 2008; Yoon et al., 2003). Despite it was not found among spermatid phosphoproteins, TBLX1R1 function and specificity depends on phosphorylation (Perissi et al., 2008), which may suggest an interplay between SRPK1 and PP1γ in the control of its phosphorylation status.

Therefore, a list of proteins associated with the kinase SRPK1 and the phosphatase PP1γ in adult mouse testis is provided, pointing out additional roles of both proteins during chromatin remodeling and other essential processes for a proper development of spermatogenesis. These candidates arise as potential new targets to be scaled up and validated as biomarkers and molecular targets helping to disentangle idiopathic male infertility health problems derived from spermiogenesis regulation defects.

6.3 Nanoscale features of human sperm chromatin organization

After having identified molecular changes associated with altered chromatin states in previous works, we wanted to explore whether these alterations translate into errors in the way chromatin is compacted in mature sperm. In **Work 6**, the application of Small-angle X-ray scattering (SAXS) provides advantages over other techniques, making possible the study of sperm chromatin in intact nuclei in solution, and becoming close to the real scenario inside the sperm *in vivo*.

The application of this technique using synchrotron light allowed the identification of nanoscale chromatin features not reported up to date in normal human sperm. SAXS profiles in human normal sperm chromatin evidenced an overall high level of compaction at the nanometer level, describing primary particles of radius ~7.7 nm that aggregate without a specific order into a second level of higher-order structures of radius of gyration ~67 nm, coherent with a two-level organization identified by applying SAXS in nucleo-protamine particles generated *in vitro* (Motta et al., 2013). SAXS study of *in vitro* DNA-protamine complexes reported small subunits with smaller radius, of approximate 2.5 nm. Differences in

size could derive from the use of salmon protamine to originate the complexes *in vitro*, which is arginine-rich but does not contain cysteine residues to accommodate disulfide bonds (Ausió et al., 2014; Oliva & Dixon, 1991). Also, the presence of a complex protamine proteoform population conferring the human nucleo-protamine particle, containing mature and immature forms bearing posttranslational modifications and further stabilized by cysteine bonds and Zn^{2+} molecules, could contribute to the generation of a more complex *in vivo* conformation of the chromatin fiber (Arauz-Garofalo et al., 2021; Björndahl & Kvist, 2011; Oliva, 2006; Soler-Ventura et al., 2020). In human sperm chromatin, primary particles identified through SAXS consisted of well-characterized highly compacted small subunits that adjusted to a cylindrical model with a smooth surface, indicating the absence of free molecules outside the edges. The unspecific aggregation of small particles resulted in a higher level of supramolecular organization that did not adjust to the toroidal and rod-like structure models of sperm chromatin compaction described up to date (Allen et al., 1993, 1997; Ausió et al., 2014; Balhorn, 2007; Hud et al., 1993, 1995; Vilfan et al., 2006). Nonetheless, the expected Rg of a toroidal particle with the experimentally reported size in vertebrates would be around 40 nm, which is in the same order of magnitude as the one obtained in our study from the larger aggregates in the control group.

The lack of adjustment to toroidal models could be derived from a) the supramolecular aggregates detected herein correspond to a different structure, b) phase contrast between the medium and the aggregates may be hiding toroids in SAXS determinations, or c) the small particles do not organize into toroidal structures, indicating that 'perfect toroids' may not exist in the sperm or are not the most abundant structure in solution. The possibility of confounding chromatin structures with other sperm nuclear structures (i.e., membrane, envelopes) is unlikely due to their size (which is of microns and SAXS identifications are made at the nanoscale) and subsequent low surface/volume ratio (which would not give that much scattering intensity). Despite we cannot fully discard interferences in scattering intensity, our findings point out that toroids may not be the most abundant chromatin organization in the human sperm. Techniques applied up to date describing toroids are based on scanning probes attached to a surface (Allen et al., 1993, 1997; Ausió et al., 2014; Balhorn, 2007; Hud et al., 1993, 1995; Vilfan et al., 2006). However, dropping and drying over the substrate to take the micrograph could induce the formation of toroidal supramolecular structures which may not completely correspond to the *in vivo* organization of the nucleo-protamine particles inside the sperm nucleus. Moreover, transmission electron microscopy images obtained from *in vivo* rooster and mice sperm showed elongated non-specific shapes named as rod-like structures (Ausió et al., 2014). Using similar techniques, toroidal constructions have also been described upon *in vitro* condensation of DNA with purified protamines (Conwell et al., 2003; Conwell & Hud, 2004; DeRouchey & Rau, 2011). However, application of SAXS to the description of *in vitro* reconstituted DNA-protamine complexes described supramolecular aggregates with Rg of about 101 nm that neither matched toroidal nor rod-like

structures (Motta et al., 2013), which reinforces that protamines could not mainly arrange into toroidal supramolecular structures in solution.

Deep diving into the functional relevance of the identified human sperm chromatin structures, we explored the chromatin status of patients with biologically impaired chromatin integrity, such as patients with altered P1/P2 ratio and patients with pathological levels of dsDNA breaks. Strikingly, the small particles were highly stable among the groups of study, reinforcing that the identified subunits could in fact correspond to the canonical 'building block' originating the resulting supramolecular chromatin structures. Although in **Work 4** we identified accumulation of P2 immature proteoforms, patients with altered P1/P2 ratio did no show changes in the way sperm chromatin arrange into space, size, or level of compaction. Therefore, despite the clinical implications of altered P1/P2 associated with sperm function, chromatin integrity, and outcome of assisted reproduction techniques (Ni et al., 2016; Soler-Ventura et al., 2018), it seems they do not underlie chromatin structural changes in patients with impaired P1/P2 ratio and unexplained infertility. In fact, our results interestingly reinforce the already suggested redundant function of sperm protamines in DNA packaging (Oliva, 2006; Soler-Ventura et al., 2020). The main difference in sperm chromatin structure at the nanoscale was found at low angles ($q < 0.2$ nm^{-1}) in patients with pathological dsDNA damage, revealing a higher Rg of the supramolecular aggregates. The slight (but non-significative) increase in the fractal cutoff contributes, at least partially, to the higher Rg due to the direct relationship between these two values. Indeed, fractal cutoff gives an idea about the largest distance separating two points inside the fractal, setting the range in which the self-similarity among structures can be observed. Therefore, a higher spatial correlation between the small cylindrical subunits may result in higher supramolecular structures. Despite this increase in dimensionality, no changes were observed in the level of compaction of the supramolecular aggregates. Overall, although it should be deciphered whether the dsDNA breaks are cause or consequence of this alteration, our findings reinforce the idea that genomic and chromatin integrities are closely related.

Human sperm DNA is packaged in >85% by protamines and still presents histone-associated regions and other basic DNA-associated proteins (Amaral et al., 2014; Castillo, Amaral, & Oliva, 2014; Castillo, Amaral, Azpiazu, et al., 2014; Oliva, 2006). Despite nucleosomes are minoritarian in sperm chromatin with respect to nucleo-protamine particles, we considered relevant to explore the presence of potential interferences in the signal scattering coming from non-protamine chromatin-related elements. Therefore, complexity inside the sperm nucleus was reduced by removing histones and other basic-associated proteins loosely attached to the DNA, generating normal sperm nuclei containing nearly pure nucleo-protamine particles. The originated structures were different from the ones described in native chromatin, differing even in the small subunits. These higher primary particles correlated in space differently in histone-depleted nuclei, evidenced by the reduced fractal cutoff and the resulting decreased Rg of the supramolecular aggregates. With these results, we face two different scenarios: a)

pure nucleo-protamine particles have different size and are not revealed when analyzing native chromatin, or b) the electrostatic forces originated by histones and other proteins contribute to the spatial arrangement of the sperm nucleo-protamine in intact nuclei, and therefore the changes observed are due to technical artifacts induced by the histone-depletion treatment. At this point, any option is feasible, but the higher dispersion observed in Req of the small particles detected in histone-depleted samples would contradict the idea of being evaluating "pure nucleo protamine" primary particles, which besides are higher in size than those of control native chromatin. Smaller spatial correlation (fractal cutoff) translated into decreased Rg of the supramolecular structures in nuclei with no histones nor other less attached proteins, which was coupled to a non-significative trend of increased fractal dimension (higher compaction) than native chromatin. All mentioned above points out to changes induced by the experimental treatment rather than observation of a real situation, but further validation is needed to confirm whether the chromatin structures detected correspond exclusively to nucleo-protamine particles.

Summing up, our work entails the first nanoscale approach to describe the human sperm chromatin in solution. Further work is needed to decipher whether the scatter intensity comes primarily from nucleo-protamine particles, or we are detecting contribution of different structures. Nonetheless, the identification of a hierarchical level of organization constituting the human sperm chromatin provides useful knowledge towards finding the origin of alterations in cases of unexplained male infertility.

7.

CONCLUSIONS

7. CONCLUSIONS

Conclusions derived from the results obtained in the present doctoral thesis are the following:

1. Spermatogenic global H4ac pattern during normal human spermatogenesis experiences a marked hyperacetylation after meiosis in agreement with previously reported results, also coherent with that described in other species. In addition, H4ac levels among different subtypes of post meiotic cells (Stages I to XI) were further characterized, detecting the highest H4ac levels in eSPD, preceded by a gradual increase starting from early-stages rSPD, concomitant with the NH-NP transition observed in post meiotic cells during spermiogenesis.

2. Normal H4 acetylation spermatogenic pattern is disrupted in the presence of testicular tumors of different origins before gonadotoxic treatment, resulting in adjacent markedly increased H4 acetylation levels in early spermatogenesis and beyond, suggesting a paracrine effect of the testicular tumors on surrounding active seminiferous tubules.

3. Residue-specific acetylation on H4K5 shows similar patterns than global H4 acetylation during human spermatogenesis and coexists with butyrylation on the same residue. Increase in H4K5 butyrylation levels during human spermatid elongation takes place later than acetylation, arising as an interesting epigenetic mark potentially involved in the process of human nucleo-histone to nucleo-protamine transition.

4. Normal H4K5 butyrylation and acetylation spermatogenic patterns are not impaired under testicular pathologies, suggesting a specific protection of the H4K5 epigenetic status for a proper spermatid differentiation.

5. H4K5 butyrylation and acetylation are retained in mature human sperm, and their relative levels are stable in independent sperm cell populations differing in quality. The presence of a fraction of non-colocalizing nucleosome clusters suggests specific paternal genomic retention of these residue-specific histone marks with potential effects after fertilization.

6. Human protamine proteoforms are identified with high confidence by a strategy for top-down proteomics data analysis combining the software packages ProSight PD and TopPIC Suite with the clustering algorithm DBSCAN. This brings the possibility of studying the sperm protamine proteoform content under pathological conditions towards personalized diagnosis of male infertility.

7. Increased abundance of protamine 2 immature proteoforms HPS1 and HPI2 have been detected in men with unexplained infertility and altered protamine 1/protamine 2 ratio, which could be related with errors in protamine 2 precursor processing.

8. Protamine 1 proteoform profile is altered in unexplained infertile men with obesity and advance age. Obese men showed reduced abundance of proteoforms with a still unknown origin corresponding to +61 Da mass shift, coupled or not to phosphorylation. Advanced age was associated with a specific loss of diphosphorylated protamine 1, potentially at Ser11 and Ser22, which could impact postfertilization events.

9. Interactomes of SRPK1 (kinase phosphorylating protamine 1) and PP1g (phosphatase dephosphorylating protamine 2) revealed protein–protein associations not described up to date that point out additional roles for both proteins in spermiogenic regulation. While SRPK1 interacts with proteins involved in the temporal regulation of gene expression in post meiotic cells, PP1g associates with protein complexes participating in quaternary folding of macromolecular structures which are involved in gene expression control and nucleosome exchange.

10. Identification of protein–protein interactions in testicular post meiotic cells is a useful tool to scale up and validate molecular targets towards deciphering idiopathic male infertility health problems derived from defects in spermiogenesis regulation.

11. Nanoscale approach to the study of human sperm chromatin structure in solution through Small Angle X-ray Scattering identified for the very first time a hierarchical level of organization into supramolecular compacted aggregates (radius of gyration ~67 nm) arising from highly stable small subunits (equivalent radius of ~7.7 nm) working as construction bricks.

12. The presence of an altered protamine 1/protamine 2 ratio does not modify supramolecular organization of the sperm chromatin, supporting a redundant function of protamines compacting the paternal genome. In turn, pathological levels of double strand DNA damage disrupts the supramolecular arrangement of small aggregates, indicating that genome and chromatin integrities are closely related.

8.

REFERENCES

Agarwal, A., Baskaran, S., Parekh, N., Cho, C.-L., Henkel, R., Vij, S., Arafa, M., Panner Selvam, M. K., & Shah, R. (2021). Male infertility. *Lancet (London, England)*, *397*(10271), 319–333. https://doi.org/10.1016/S0140-6736(20)32667-2

Agarwal, A., Majzoub, A., Baskaran, S., Panner Selvam, M. K., Cho, C. L., Henkel, R., Finelli, R., Leisegang, K., Sengupta, P., Barbarosie, C., Parekh, N., Alves, M. G., Ko, E., Arafa, M., Tadros, N., Ramasamy, R., Kavoussi, P., Ambar, R., Kuchakulla, M., … Shah, R. (2020). Sperm DNA Fragmentation: A New Guideline for Clinicians. *The World Journal of Men's Health*, *38*(4), 412. https://doi.org/10.5534/wjmh.200128

Agarwal, A., Makker, K., & Sharma, R. (2008). Clinical relevance of oxidative stress in male factor infertility: an update. *American Journal of Reproductive Immunology (New York, N.Y.: 1989)*, *59*(1), 2–11. https://doi.org/10.1111/j.1600-0897.2007.00559.x

Aitken, R. J., de Iuliis, G. N., Finnie, J. M., Hedges, A., & McLachlan, R. I. (2010). Analysis of the relationships between oxidative stress, DNA damage and sperm vitality in a patient population: development of diagnostic criteria. *Human Reproduction*, *25*(10), 2415–2426. https://doi.org/10.1093/humrep/deq214

Akama, K., Kondo, M., Sato, H., & Nakano, M. (1999). Transition protein 4 from boar late spermatid nuclei is a topological factor that stimulates DNA-relaxing activity of topoisomerase I. *FEBS Letters*, *442*(2–3), 189–192. https://doi.org/10.1016/s0014-5793(98)01649-4

Akbarian, F., Rahmani, M., Tavalaee, M., Abedpoor, N., Taki, M., Ghaedi, K., & Nasr-Esfahani, M. H. (2021). Effect of Different High-Fat and Advanced Glycation End-Products Diets in Obesity and Diabetes-Prone C57BL/6 Mice on Sperm Function. *International Journal of Fertility & Sterility*, *15*(3), 226–233. https://doi.org/10.22074/IJFS.2021.137231.1022

Akinloye, O., Gromoll, J., Callies, C., Nieschlag, E., & Simoni, M. (2007). Mutation analysis of the X-chromosome linked, testis-specific TAF7L gene in spermatogenic failure. *Andrologia*, *39*(5), 190–195. https://doi.org/10.1111/j.1439-0272.2007.00789.x

Alami-Ouahabi, N., Veilleux, S., Meistrich, M. L., & Boissonneault, G. (1996). The testis-specific high-mobility-group protein, a phosphorylation-dependent DNA-packaging factor of elongating and condensing spermatids. *Molecular and Cellular Biology*, *16*(7), 3720–3729. https://doi.org/10.1128/MCB.16.7.3720

Allen, M. J., Bradbury, E. M., & Balhorn, R. (1997). AFM analysis of DNA-protamine complexes bound to mica. *Nucleic Acids Research*, *25*(11), 2221–2226. https://doi.org/10.1093/nar/25.11.2221

Allen, M. J., Lee, C., Lee, J. D., Pogany, G. C., Balooch, M., Siekhaus, W. J., & Balhorn, R. (1993). Atomic force microscopy of mammalian sperm chromatin. *Chromosoma*, *102*(9), 623–630. https://doi.org/10.1007/BF00352310

Alshahrani, S., Ahmed, A.-F., Gabr, A. H., Abalhassan, M., & Ahmad, G. (2016). The impact of body mass index on semen parameters in infertile men. *Andrologia*, *48*(10), 1125–1129. https://doi.org/10.1111/and.12549

Amaral, A., Castillo, J., Ramalho-Santos, J., & Oliva, R. (2014). The combined human sperm proteome: cellular pathways and implications for basic and clinical science. *Human Reproduction Update*, *20*(1), 40–62. https://doi.org/10.1093/humupd/dmt046

Anbazhagan, R., Kavarthapu, R., Coon, S. L., & Dufau, M. L. (2020). Role of Phosphorylated Gonadotropin-Regulated Testicular RNA Helicase (GRTH/DDX25) in the Regulation of Germ Cell Specific mRNAs in Chromatoid Bodies During Spermatogenesis. *Frontiers in Cell and Developmental Biology*, *8*. https://doi.org/10.3389/fcell.2020.580019

Andersen, E., Juhl, C. R., Kjøller, E. T., Lundgren, J. R., Janus, C., Dehestani, Y., Saupstad, M., Ingerslev, L. R., Duun, O. M., Jensen, S. B. K., Holst, J. J., Stallknecht, B. M., Madsbad, S., Torekov, S. S., & Barrès, R. (2022). Sperm count is increased by diet-induced weight loss and maintained by exercise or GLP-1 analogue treatment: a randomized controlled trial. *Human Reproduction*, *37*(7), 1414–1422. https://doi.org/10.1093/humrep/deac096

Aoshima, K., Inoue, E., Sawa, H., & Okada, Y. (2015). Paternal H3K4 methylation is required for minor zygotic gene activation and early mouse embryonic development. *EMBO Reports*, *16*(7), 803–812. https://doi.org/10.15252/embr.201439700

Arauz-Garofalo, G., Jodar, M., Vilanova, M., de la Iglesia Rodriguez, A., Castillo, J., Soler-Ventura, A., Oliva, R., Vilaseca, M., & Gay, M. (2021). Protamine Characterization by Top-Down Proteomics: Boosting Proteoform Identification with DBSCAN. *Proteomes*, *9*(2). https://doi.org/10.3390/proteomes9020021

Arévalo, L., Merges, G. E., Schneider, S., Oben, F. E., Neumann, I. S., & Schorle, H. (2022). Loss of the cleaved-protamine 2 domain leads to incomplete histone-to-protamine exchange and infertility in mice. *PLOS Genetics*, *18*(6), e1010272. https://doi.org/10.1371/journal.pgen.1010272

Arpanahi, A., Brinkworth, M., Iles, D., Krawetz, S. A., Paradowska, A., Platts, A. E., Saida, M., Steger, K., Tedder, P., & Miller, D. (2009). Endonuclease-sensitive regions of human spermatozoal chromatin are highly enriched in promoter and CTCF binding sequences. *Genome Research*, *19*(8), 1338–1349. https://doi.org/10.1101/gr.094953.109

Åsenius, F., Danson, A. F., & Marzi, S. J. (2020). DNA methylation in human sperm: a systematic review. *Human Reproduction Update*, *26*(6), 841–873. https://doi.org/10.1093/humupd/dmaa025

Ausió, J., González-Romero, R., & Woodcock, C. L. (2014). Comparative structure of vertebrate sperm chromatin. *Journal of Structural Biology*, *188*(2), 142–155. https://doi.org/10.1016/j.jsb.2014.09.004

Azorin, F., Martínez, A. B., & Subirana, J. A. (1980). Organization of nucleosomes and spacer DNA in chromatin fibres. *International Journal of Biological Macromolecules*, *2*(2), 81–92. https://doi.org/10.1016/0141-8130(80)90033-1

Azpiazu, R., Amaral, A., Castillo, J., Estanyol, J. M., Guimerà, M., Ballescà, J. L., Balasch, J., & Oliva, R. (2014). High-throughput sperm differential proteomics suggests that epigenetic alterations contribute to failed assisted reproduction. *Human Reproduction*, *29*(6), 1225–1237. https://doi.org/10.1093/humrep/deu073

Baarends, W. M., Hoogerbrugge, J. W., Roest, H. P., Ooms, M., Vreeburg, J., Hoeijmakers, J. H. J., & Grootegoed, J. A. (1999). Histone Ubiquitination and Chromatin Remodeling in Mouse Spermatogenesis. *Developmental Biology*, *207*(2), 322–333. https://doi.org/10.1006/dbio.1998.9155

Bai, S., Fu, K., Yin, H., Cui, Y., Yue, Q., Li, W., Cheng, L., Tan, H., Liu, X., Guo, Y., Zhang, Y., Xie, J., He, W., Wang, Y., Feng, H., Xin, C., Zhang, J., Lin, M., Shen, B., … Ye, L. (2018). Sox30 initiates transcription of haploid genes during late meiosis and spermiogenesis in mouse testes. *Development (Cambridge, England)*, *145*(13). https://doi.org/10.1242/dev.164855

Balawender, K., & Orkisz, S. (2020). The impact of selected modifiable lifestyle factors on male fertility in the modern world. *Central European Journal of Urology*, *73*(4), 563–568. https://doi.org/10.5173/ceju.2020.1975

Balhorn, R. (1982). A model for the structure of chromatin in mammalian sperm. *The Journal of Cell Biology*, *93*(2), 298–305. https://doi.org/10.1083/jcb.93.2.298

Balhorn, R. (2007). The protamine family of sperm nuclear proteins. *Genome Biology*, *8*(9), 227. https://doi.org/10.1186/gb-2007-8-9-227

Balhorn, R., Reed, S., & Tanphaichitr, N. (1988). Aberrant protamine 1/protamine 2 ratios in sperm of infertile human males. *Experientia*, *44*(1), 52–55. https://doi.org/10.1007/BF01960243

Bao, J., & Bedford, M. T. (2016). Epigenetic regulation of the histone-to-protamine transition during spermiogenesis. *Reproduction*, *151*(5), R55–R70. https://doi.org/10.1530/REP-15-0562

Barrachina, F., Battistone, M. A., Castillo, J., Mallofré, C., Jodar, M., Breton, S., & Oliva, R. (2022). Sperm acquire epididymis-derived proteins through epididymosomes. *Human Reproduction*, *37*(4), 651–668. https://doi.org/10.1093/humrep/deac015

Barrachina, F., de la Iglesia, A., Jodar, M., Soler-Ventura, A., Mallofré, C., Rodriguez-Carunchio, L., Goudarzi, A., Corral, J. M., Ballescà, J. L., Castillo, J., & Oliva, R. (2022). Histone H4 acetylation is dysregulated in active seminiferous tubules adjacent to testicular tumours. *Human Reproduction*, *30*(8), 1712–1726. https://doi.org/10.1093/humrep/deac130

Barrachina, F., Jodar, M., Delgado-Dueñas, D., Soler-Ventura, A., Estanyol, J. M., Mallofré, C., Ballescà, J. L., & Oliva, R. (2019). Stable-protein Pair Analysis as A Novel Strategy to Identify Proteomic Signatures: Application To Seminal Plasma From Infertile Patients. *Molecular & Cellular Proteomics*, *18*(Supplement 1), S77–S90. https://doi.org/10.1074/mcp.RA118.001248

Barrachina, F., Soler-Ventura, A., Oliva, R., & Jodar, M. (2018). Sperm Nucleoproteins (Histones and Protamines). In A. Zini & A. Agarwal (Eds.), *A Clinician's Guide to Sperm DNA and Chromatin Damage.* (pp. 31–51). Springer International Publishing. https://doi.org/10.1007/978-3-319-71815-6_2

Barral, S., Morozumi, Y., Tanaka, H., Montellier, E., Govin, J., de Dieuleveult, M., Charbonnier, G., Couté, Y., Puthier, D., Buchou, T., Boussouar, F., Urahama, T., Fenaille, F., Curtet, S., Héry, P., Fernandez-Nunez, N., Shiota, H., Gérard, M., Rousseaux, S., … Khochbin, S. (2017). Histone Variant H2A.L.2 Guides Transition Protein-Dependent Protamine Assembly in Male Germ Cells. *Molecular Cell*, *66*(1), 89–101.e8. https://doi.org/10.1016/j.molcel.2017.02.025

Battulin, N., Fishman, V. S., Mazur, A. M., Pomaznoy, M., Khabarova, A. A., Afonnikov, D. A., Prokhortchouk, E. B., & Serov, O. L. (2015). Comparison of the three-dimensional organization of sperm and fibroblast genomes using the Hi-C approach. *Genome Biology*, *16*(1), 77. https://doi.org/10.1186/s13059-015-0642-0

Bell, E. L., Nagamori, I., Williams, E. O., Del Rosario, A. M., Bryson, B. D., Watson, N., White, F. M., Sassone-Corsi, P., & Guarente, L. (2014). SirT1 is required in the male germ cell for differentiation and fecundity in mice. *Development*, *141*(18), 3495–3504. https://doi.org/10.1242/dev.110627

Berger, S. L., & Sassone-Corsi, P. (2016). Metabolic Signaling to Chromatin. *Cold Spring Harbor Perspectives in Biology*, *8*(11), a019463. https://doi.org/10.1101/cshperspect.a019463

Bianchi, F., Rousseaux-Prevost, R., Sautiere, P., & Rousseaux, J. (1992). P2 protamines from human sperm are zinc -finger proteins with one CYS2/HIS2 motif. *Biochemical and Biophysical Research Communications*, *182*(2), 540–547. https://doi.org/10.1016/0006-291x(92)91766-j

Björndahl, L., & Kvist, U. (2011). A model for the importance of zinc in the dynamics of human sperm chromatin stabilization after ejaculation in relation to sperm DNA vulnerability. *Systems Biology in Reproductive Medicine*, *57*(1–2), 86–92. https://doi.org/10.3109/19396368.2010.516306

Blanco, M., & Cocquet, J. (2019). Genetic Factors Affecting Sperm Chromatin Structure. *Advances in Experimental Medicine and Biology*, *1166*, 1–28. https://doi.org/10.1007/978-3-030-21664-1_1

Bloch, D. P. (1969). A catalog of sperm histones. *Genetics*, *61*(1), Suppl:93–111.

Boissonneault, G., & Lau, Y. F. (1993). A testis-specific gene encoding a nuclear high-mobility-group box protein located in elongating spermatids. *Molecular and Cellular Biology*, *13*(7), 4323–4330. https://doi.org/10.1128/mcb.13.7.4323-4330.1993

Bolcun-Filas, E., & Handel, M. A. (2018). Meiosis: the chromosomal foundation of reproduction. *Biology of Reproduction*, *99*(1), 112–126. https://doi.org/10.1093/biolre/ioy021

Bonisch, C., & Hake, S. B. (2012). Histone H2A variants in nucleosomes and chromatin: more or less stable? *Nucleic Acids Research*, *40*(21), 10719–10741. https://doi.org/10.1093/nar/gks865

Boulard, M., Gautier, T., Mbele, G. O., Gerson, V., Hamiche, A., Angelov, D., Bouvet, P., & Dimitrov, S. (2006). The NH $_2$ Tail of the Novel Histone Variant H2BFWT Exhibits Properties Distinct from Conventional H2B with Respect to the Assembly of Mitotic Chromosomes. *Molecular and Cellular Biology*, *26*(4), 1518–1526. https://doi.org/10.1128/MCB.26.4.1518-1526.2006

Boussouar, F., Rousseaux, S., & Khochbin, S. (2008). A new insight into male genome reprogramming by histone variants and histone code. *Cell Cycle*, *7*(22), 3499–3502. https://doi.org/10.4161/cc.7.22.6975

Braun, R. E. (2000). Temporal control of protein synthesis during spermatogenesis. *International Journal of Andrology*, *23*(S2), 92–94. https://doi.org/10.1046/j.1365-2605.2000.00027.x

Brunner, A. M., Nanni, P., & Mansuy, I. M. (2014). Epigenetic marking of sperm by post-translational modification of histones and protamines. *Epigenetics & Chromatin*, *7*(1), 2. https://doi.org/10.1186/1756-8935-7-2

Bruno, C., Blagoskonov, O., Barberet, J., Guilleman, M., Daniel, S., Tournier, B., Binquet, C., Choux, C., & Fauque, P. (2018). Sperm imprinting integrity in seminoma patients? *Clinical Epigenetics*, *10*(1), 125. https://doi.org/10.1186/s13148-018-0559-z

Bryant, J. M., Donahue, G., Wang, X., Meyer-Ficca, M., Luense, L. J., Weller, A. H., Bartolomei, M. S., Blobel, G. A., Meyer, R. G., Garcia, B. A., & Berger, S. L. (2015). Characterization of BRD4 during mammalian postmeiotic sperm development. *Molecular and Cellular Biology*, *35*(8), 1433–1448. https://doi.org/10.1128/MCB.01328-14

Brykczynska, U., Hisano, M., Erkek, S., Ramos, L., Oakeley, E. J., Roloff, T. C., Beisel, C., Schübeler, D., Stadler, M. B., & Peters, A. H. F. M. (2010). Repressive and active histone methylation mark distinct promoters in human and mouse spermatozoa. *Nature Structural & Molecular Biology*, *17*(6), 679–687. https://doi.org/10.1038/nsmb.1821

Buenrostro, J. D., Giresi, P. G., Zaba, L. C., Chang, H. Y., & Greenleaf, W. J. (2013). Transposition of native chromatin for fast and sensitive epigenomic profiling of open chromatin, DNA-binding proteins and nucleosome position. *Nature Methods*, *10*(12), 1213–1218. https://doi.org/10.1038/nmeth.2688

Bullock, N., & Oltean, S. (2017). The many faces of SRPK1. *The Journal of Pathology*, *241*(4), 437–440. https://doi.org/10.1002/path.4846

Burén, S., Gomes, A. L., Teijeiro, A., Fawal, M.-A., Yilmaz, M., Tummala, K. S., Perez, M., Rodriguez-Justo, M., Campos-Olivas, R., Megías, D., & Djouder, N. (2016). Regulation of OGT by URI in Response to Glucose Confers c-MYC-Dependent Survival Mechanisms. *Cancer Cell*, *30*(2), 290–307. https://doi.org/10.1016/j.ccell.2016.06.023

Cao, G., Li, H.-B., Yin, Z., & Flavell, R. A. (2016). Recent advances in dynamic m ^{6} A RNA modification. *Open Biology*, *6*(4), 160003. https://doi.org/10.1098/rsob.160003

Carone, B. R., Hung, J.-H., Hainer, S. J., Chou, M.-T., Carone, D. M., Weng, Z., Fazzio, T. G., & Rando, O. J. (2014). High-resolution mapping of chromatin packaging in mouse embryonic stem cells and sperm. *Developmental Cell*, *30*(1), 11–22. https://doi.org/10.1016/j.devcel.2014.05.024

Carrell, D., Emery, B. R., & Hammoud, S. (2007a). Altered protamine expression and diminished spermatogenesis: what is the link? *Human Reproduction Update*, *13*(3), 313–327. https://doi.org/10.1093/humupd/dml057

Carrell, D., Emery, B. R., & Hammoud, S. (2007b). Altered protamine expression and diminished spermatogenesis: what is the link? *Human Reproduction Update*, *13*(3), 313–327. https://doi.org/10.1093/humupd/dml057

Carrell, D., Emery, B. R., & Hammoud, S. (2008). The aetiology of sperm protamine abnormalities and their potential impact on the sperm epigenome. *International Journal of Andrology*, *31*(6), 537–545. https://doi.org/10.1111/j.1365-2605.2008.00872.x

Carrell, D., & Liu, L. (2001). Altered protamine 2 expression is uncommon in donors of known fertility, but common among men with poor fertilizing capacity, and may reflect other abnormalities of spermiogenesis. *Journal of Andrology*, *22*(4), 604–610.

Carrell, D., Liu, L., Peterson, C. M., Jones, K. P., Hatasaka, H. H., Erickson, L., & Campbell, B. (2003). Sperm DNA fragmentation is increased in couples with unexplained recurrent pregnancy loss. *Archives of Andrology*, *49*(1), 49–55. https://doi.org/10.1080/01485010290099390

Casadio, F., Lu, X., Pollock, S. B., LeRoy, G., Garcia, B. A., Muir, T. W., Roeder, R. G., & Allis, C. D. (2013). H3R42me2a is a histone modification with positive transcriptional effects. *Proceedings of the National Academy of Sciences*, *110*(37), 14894–14899. https://doi.org/10.1073/pnas.1312925110

Castaneda, J. M., Shimada, K., Satouh, Y., Yu, Z., Devlin, D. J., Ikawa, M., & Matzuk, M. M. (2021). FAM209 associates with DPY19L2, and is required for sperm acrosome biogenesis and fertility in mice. *Journal of Cell Science*, *134*(21). https://doi.org/10.1242/jcs.259206

Castillo, J., Amaral, A., Azpiazu, R., Vavouri, T., Estanyol, J. M., Ballesca, J. L., & Oliva, R. (2014). Genomic and proteomic dissection and characterization of the human sperm chromatin. *Molecular Human Reproduction*, *20*(11), 1041–1053. https://doi.org/10.1093/molehr/gau079

Castillo, J., Amaral, A., & Oliva, R. (2014). Sperm nuclear proteome and its epigenetic potential. *Andrology*, *2*(3), 326–338. https://doi.org/10.1111/j.2047-2927.2013.00170.x

Castillo, J., Bogle, O. A., Jodar, M., Torabi, F., Delgado-Dueñas, D., Estanyol, J. M., Ballescà, J. L., Miller, D., & Oliva, R. (2019). Proteomic Changes in Human Sperm During Sequential in vitro Capacitation and Acrosome Reaction. *Frontiers in Cell and Developmental Biology*, *7*. https://doi.org/10.3389/fcell.2019.00295

Castillo, J., de Mateo, S., Estanyol, J. M., Ballescà, J. L., & Oliva, R. (2011). Anàlisi del proteoma de nuclis d'espermatozoides humans per cromatografia líquida i espectrometria de masses (LC-MS/MS). In Enric Ribes (Ed.), *Biologia de la Reproducció* (Vol. 12, pp. 57–60). Ediciones Gráficas Rey, S.L.

Castillo, J., Estanyol, J., Ballescà, J., & Oliva, R. (2015). Human sperm chromatin epigenetic potential: genomics, proteomics, and male infertility. *Asian Journal of Andrology*, *17*(4), 601. https://doi.org/10.4103/1008-682X.153302

Castillo, J., Jodar, M., & Oliva, R. (2018). The contribution of human sperm proteins to the development and epigenome of the preimplantation embryo. *Human Reproduction Update*, *24*(5), 535–555. https://doi.org/10.1093/humupd/dmy017

Castillo, J., Knol, J. C., Korver, C. M., Piersma, S. R., Pham, T. v., de Goeij-de Haas, R. R., van Pelt, A. M. M., Jimenez, C. R., & Jansen, B. J. H. (2019). Human Testis Phosphoproteome Reveals Kinases as Potential Targets in Spermatogenesis and Testicular Cancer. *Molecular & Cellular Proteomics*, *18*, S132–S144. https://doi.org/10.1074/mcp.RA118.001278

Castillo, J., Simon, L., de Mateo, S., Lewis, S., & Oliva, R. (2011). Protamine/DNA Ratios and DNA Damage in Native and Density Gradient Centrifuged Sperm From Infertile Patients. *Journal of Andrology*, *32*(3), 324–332. https://doi.org/10.2164/jandrol.110.011015

Cerilli, L. A., Kuang, W., & Roger, D. (2010). A practical approach to testicular biopsy interpretation for male infertility. *Archive of Pathology & Laboratory Medicine*, *134*(8), 1197–1204.

Chalmel, F., Com, E., Lavigne, R., Hernio, N., Teixeira-Gomes, A.-P., Dacheux, J.-L., & Pineau, C. (2014). An Integrative Omics Strategy to Assess the Germ Cell Secretome and to Decipher Sertoli-Germ Cell Crosstalk in the Mammalian Testis. *PLoS ONE*, *9*(8), e104418. https://doi.org/10.1371/journal.pone.0104418

Cheng, L., Pilder, S., Nairn, A. C., Ramdas, S., & Vijayaraghavan, S. (2009). PP1γ2 and PPP1R11 Are Parts of a Multimeric Complex in Developing Testicular Germ Cells in which their Steady State Levels Are Reciprocally Related. *PLoS ONE*, *4*(3), e4861. https://doi.org/10.1371/journal.pone.0004861

Cheng, Y., Buffone, M. G., Kouadio, M., Goodheart, M., Page, D. C., Gerton, G. L., Davidson, I., & Wang, P. J. (2007). Abnormal sperm in mice lacking the Taf7l gene. *Molecular and Cellular Biology*, *27*(7), 2582–2589. https://doi.org/10.1128/MCB.01722-06

Chiamchanya, C., Kaewnoonual, N., Visutakul, P., Manochantr, S., & Chaiya, J. (2010). Comparative study of the effects of three semen preparation media on semen analysis, DNA damage and protamine deficiency, and the correlation between DNA integrity and sperm parameters. *Asian Journal of Andrology*, *12*(2), 271–277. https://doi.org/10.1038/aja.2009.60

Chioccarelli, T., Cacciola, G., Altucci, L., Lewis, S. E. M., Simon, L., Ricci, G., Ledent, C., Meccariello, R., Fasano, S., Pierantoni, R., & Cobellis, G. (2010). Cannabinoid Receptor 1 Influences Chromatin Remodeling in Mouse Spermatids by Affecting Content of Transition Protein 2 mRNA and Histone Displacement. *Endocrinology*, *151*(10), 5017–5029. https://doi.org/10.1210/en.2010-0133

Chioccarelli, T., Manfrevola, F., Porreca, V., Fasano, S., Altucci, L., Pierantoni, R., & Cobellis, G. (2020). The Cannabinoid Receptor CB1 Stabilizes Sperm Chromatin Condensation Status During Epididymal Transit by Promoting Disulphide Bond Formation. *International Journal of Molecular Sciences*, *21*(9), 3117. https://doi.org/10.3390/ijms21093117

Chirat, F., Arkhis, A., Martinage, A., Jaquinod, M., Chevaillier, P., & Sautière, P. (1993). Phosphorylation of human sperm protamines HP1 and HP2: identification of phosphorylation sites. *Biochimica et Biophysica Acta*, *1203*(1), 109–114. https://doi.org/10.1016/0167-4838(93)90043-q

Cho, C., Jung-Ha, H., Willis, W. D., Goulding, E. H., Stein, P., Xu, Z., Schultz, R. M., Hecht, N. B., & Eddy, E. M. (2003). Protamine 2 deficiency leads to sperm DNA damage and embryo death in mice. *Biology of Reproduction*, *69*(1), 211–217. https://doi.org/10.1095/biolreprod.102.015115

Cho, C., Willis, W. D., Goulding, E. H., Jung-Ha, H., Choi, Y. C., Hecht, N. B., & Eddy, E. M. (2001). Haploinsufficiency of protamine-1 or -2 causes infertility in mice. *Nature Genetics*, *28*(1), 82–86. https://doi.org/10.1038/ng0501-82

Choi, J., Heo, K., & An, W. (2009). Cooperative action of TIP48 and TIP49 in H2A.Z exchange catalyzed by acetylation of nucleosomal H2A. *Nucleic Acids Research*, *37*(18), 5993–6007. https://doi.org/10.1093/nar/gkp660

Christensen, M. E., & Dixon, G. H. (1982). Hyperacetylation of histone H4 correlates with the terminal, transcriptionally inactive stages of spermatogenesis in rainbow trout. *Developmental Biology*, *93*(2), 404–415. https://doi.org/10.1016/0012-1606(82)90127-0

Cissen, M., Wely, M. van, Scholten, I., Mansell, S., Bruin, J. P. de, Mol, B. W., Braat, D., Repping, S., & Hamer, G. (2016). Measuring Sperm DNA Fragmentation and Clinical Outcomes of Medically Assisted Reproduction: A Systematic Review and Meta-Analysis. *PLOS ONE*, *11*(11), e0165125. https://doi.org/10.1371/journal.pone.0165125

Collas, P., & Poccia, D. (1998). Remodeling the sperm nucleus into a male pronucleus at fertilization. *Theriogenology*, *49*(1), 67–81. https://doi.org/10.1016/S0093-691X(97)00403-2

Collodel, G., Moretti, E., Micheli, L., Menchiari, A., Moltoni, L., & Cerretani, D. (2015). Semen characteristics and malondialdehyde levels in men with different reproductive problems. *Andrology*, *3*(2), 280–286. https://doi.org/10.1111/andr.297

Com, E., Rolland, A. D., Guerrois, M., Aubry, F., Jégou, B., Vallet-Erdtmann, V., & Pineau, C. (2006). Identification, molecular cloning, and cellular distribution of the rat homolog of minichromosome maintenance protein 7 (MCM7) in the rat testis. *Molecular Reproduction and Development*, *73*(7), 866–877. https://doi.org/10.1002/mrd.20453

Conwell, C. C., & Hud, N. v. (2004). Evidence that both kinetic and thermodynamic factors govern DNA toroid dimensions: effects of magnesium(II) on DNA condensation by

hexammine cobalt(III). *Biochemistry*, *43*(18), 5380–5387. https://doi.org/10.1021/bi049872u

Conwell, C. C., Vilfan, I. D., & Hud, N. v. (2003). Controlling the size of nanoscale toroidal DNA condensates with static curvature and ionic strength. *Proceedings of the National Academy of Sciences of the United States of America*, *100*(16), 9296–9301. https://doi.org/10.1073/pnas.1533135100

Cortés-Gutiérrez, E. I., López-Fernández, C., Fernández, J. L., Dávila-Rodríguez, M. I., Johnston, S. D., & Gosálvez, J. (2014). Interpreting sperm DNA damage in a diverse range of mammalian sperm by means of the two-tailed comet assay. *Frontiers in Genetics*, *5*, 404. https://doi.org/10.3389/fgene.2014.00404

Craig, J. R., Jenkins, T. G., Carrell, D. T., & Hotaling, J. M. (2017). Obesity, male infertility, and the sperm epigenome. *Fertility and Sterility*, *107*(4), 848–859. https://doi.org/10.1016/j.fertnstert.2017.02.115

Crespo, M., Damont, A., Blanco, M., Lastrucci, E., Kennani, S. el, Ialy-Radio, C., Khattabi, L. el, Terrier, S., Louwagie, M., Kieffer-Jaquinod, S., Hesse, A.-M., Bruley, C., Chantalat, S., Govin, J., Fenaille, F., Battail, C., Cocquet, J., & Pflieger, D. (2020). Multi-omic analysis of gametogenesis reveals a novel signature at the promoters and distal enhancers of active genes. *Nucleic Acids Research*, *48*(8), 4115–4138. https://doi.org/10.1093/nar/gkaa163

Dacheux, J.-L., & Dacheux, F. (2014). New insights into epididymal function in relation to sperm maturation. *Reproduction (Cambridge, England)*, *147*(2), R27–42. https://doi.org/10.1530/REP-13-0420

Dahm, R. (2005a). Friedrich Miescher and the discovery of DNA. *Developmental Biology*, *278*(2), 274–288. https://doi.org/10.1016/j.ydbio.2004.11.028

Dahm, R. (2005b). Friedrich Miescher and the discovery of DNA. *Developmental Biology*, *278*(2), 274–288. https://doi.org/10.1016/j.ydbio.2004.11.028

de Geyter, C., Calhaz-Jorge, C., Kupka, M. S., Wyns, C., Mocanu, E., Motrenko, T., Scaravelli, G., Smeenk, J., Vidakovic, S., Goossens, V., & European IVF-monitoring Consortium (EIM) for the European Society of Human Reproduction and Embryology (ESHRE). (2018). ART in Europe, 2014: results generated from European registries by ESHRE: The European IVF-monitoring Consortium (EIM) for the European Society of Human Reproduction and Embryology (ESHRE). *Human Reproduction (Oxford, England)*, *33*(9), 1586–1601. https://doi.org/10.1093/humrep/dey242

de Mateo, S., Castillo, J., Estanyol, J. M., Ballescà, J. L., & Oliva, R. (2011). Proteomic characterization of the human sperm nucleus. *PROTEOMICS*, *11*(13), 2714–2726. https://doi.org/10.1002/pmic.201000799

de Mateo, S., Gázquez, C., Guimerà, M., Balasch, J., Meistrich, M. L., Ballescà, J. L., & Oliva, R. (2009). Protamine 2 precursors (Pre-P2), protamine 1 to protamine 2 ratio (P1/P2), and assisted reproduction outcome. *Fertility and Sterility*, *91*(3), 715–722. https://doi.org/10.1016/j.fertnstert.2007.12.047

de Mateo, S., Ramos, L., de Boer, P., Meistrich, M., & Oliva, R. (2011). Protamine 2 Precursors and Processing. *Protein & Peptide Letters*, *18*(8), 778–785. https://doi.org/10.2174/092986611795713998

de Mateo, S., Ramos, L., van der Vlag, J., de Boer, P., & Oliva, R. (2011). Improvement in chromatin maturity of human spermatozoa selected through density gradient centrifugation. *International Journal of Andrology*, *34*(3), 256–267. https://doi.org/10.1111/j.1365-2605.2010.01080.x

de Yebra, L., Ballescà, J. L., Vanrell, J. A., Bassas, L., & Oliva, R. (1993). Complete selective absence of protamine P2 in humans. *The Journal of Biological Chemistry*, *268*(14), 10553–10557.

DeRouchey, J. E., & Rau, D. C. (2011). Salt effects on condensed protamine-DNA assemblies: anion binding and weakening of attraction. *The Journal of Physical Chemistry. B*, *115*(41), 11888–11894. https://doi.org/10.1021/jp203834z

Deshpande, S. S. S., Nemani, H., & Balasinor, N. H. (2021). Diet-induced- and genetic-obesity differentially alters male germline histones. *Reproduction*, *162*(6), 411–425. https://doi.org/10.1530/REP-21-0034

Dhar, S., Thota, A., & Rao, M. R. S. (2012). Insights into role of bromodomain, testis-specific (Brdt) in acetylated histone H4-dependent chromatin remodeling in mammalian spermiogenesis. *The Journal of Biological Chemistry*, *287*(9), 6387–6405. https://doi.org/10.1074/jbc.M111.288167

Dias, G. M., Retamal, C. A., Tobella, L., Arnholdt, A. C. v, & López, M. L. (2006). Nuclear status of immature and mature stallion spermatozoa. *Theriogenology*, *66*(2), 354–365. https://doi.org/10.1016/j.theriogenology.2005.10.024

Dias, T., Agarwal, A., Pushparaj, P., Ahmad, G., & Sharma, R. (2020). Reduced semen quality in patients with testicular cancer seminoma is associated with alterations in the expression of sperm proteins. *Asian Journal of Andrology*, *22*(1), 88. https://doi.org/10.4103/aja.aja_17_19

Dieterich, K., Soto Rifo, R., Faure, A. K., Hennebicq, S., Ben Amar, B., Zahi, M., Perrin, J., Martinez, D., Sèle, B., Jouk, P.-S., Ohlmann, T., Rousseaux, S., Lunardi, J., & Ray, P. F. (2007). Homozygous mutation of AURKC yields large-headed polyploid spermatozoa and causes male infertility. *Nature Genetics*, *39*(5), 661–665. https://doi.org/10.1038/ng2027

Ding, D., Nguyen, T. T., Pang, M. Y. H., & Ishibashi, T. (2021). Primate-specific histone variants. *Genome*, *64*(4), 337–346. https://doi.org/10.1139/gen-2020-0094

Dixon, G. H. (1972). THE BASIC PROTEINS OF TROUT TESTIS CHROMATIN: ASPECTS OF THEIR SYNTHESIS, POST-SYNTHETIC MODIFICATIONS AND BINDING TO DNA. *Acta Endocrinologica*, *71*(2_Suppla), S130–S154. https://doi.org/10.1530/acta.0.071S130

Djouder, N., Metzler, S. C., Schmidt, A., Wirbelauer, C., Gstaiger, M., Aebersold, R., Hess, D., & Krek, W. (2007). S6K1-Mediated Disassembly of Mitochondrial URI/PP1γ Complexes Activates a Negative Feedback Program that Counters S6K1 Survival Signaling. *Molecular Cell*, *28*(1), 28–40. https://doi.org/10.1016/j.molcel.2007.08.010

Dong, Y., Isono, K., Ohbo, K., Endo, T. A., Ohara, O., Maekawa, M., Toyama, Y., Ito, C., Toshimori, K., Helin, K., Ogonuki, N., Inoue, K., Ogura, A., Yamagata, K., Kitabayashi, I., & Koseki, H. (2017). EPC1/TIP60-Mediated Histone Acetylation Facilitates Spermiogenesis in Mice. *Molecular and Cellular Biology*, *37*(19). https://doi.org/10.1128/MCB.00082-17

Donkin, I., Versteyhe, S., Ingerslev, L. R., Qian, K., Mechta, M., Nordkap, L., Mortensen, B., Appel, E. V. R., Jørgensen, N., Kristiansen, V. B., Hansen, T., Workman, C. T., Zierath, J. R., & Barrès, R. (2016). Obesity and Bariatric Surgery Drive Epigenetic Variation of Spermatozoa in Humans. *Cell Metabolism*, *23*(2), 369–378. https://doi.org/10.1016/j.cmet.2015.11.004

Dottermusch-Heidel, C., Klaus, E. S., Gonzalez, N. H., Bhushan, S., Meinhardt, A., Bergmann, M., Renkawitz-Pohl, R., Rathke, C., & Steger, K. (2014). H3K79 methylation directly precedes the histone-to-protamine transition in mammalian spermatids and is sensitive to bacterial infections. *Andrology*, *2*(5), 655–665. https://doi.org/10.1111/j.2047-2927.2014.00248.x

du Fossé, N. A., van der Hoorn, M.-L. P., van Lith, J. M. M., le Cessie, S., & Lashley, E. E. L. O. (2020). Advanced paternal age is associated with an increased risk of spontaneous miscarriage: a systematic review and meta-analysis. *Human Reproduction Update*, *26*(5), 650–669. https://doi.org/10.1093/humupd/dmaa010

Dudiki, T., Joudeh, N., Sinha, N., Goswami, S., Eisa, A., Kline, D., & Vijayaraghavan, S. (2019). The protein phosphatase isoform PP1γ1 substitutes for PP1γ2 to support spermatogenesis but not normal sperm function and fertility†. *Biology of Reproduction*, *100*(3), 721–736. https://doi.org/10.1093/biolre/ioy225

Eelaminejad, Z., Favaedi, R., Sodeifi, N., Sadighi Gilani, M. A., & Shahhoseini, M. (2017). Deficient expression of JMJD1A histone demethylase in patients with round spermatid

maturation arrest. *Reproductive BioMedicine Online*, *34*(1), 82–89. https://doi.org/10.1016/j.rbmo.2016.09.005

El Kennani, S., Adrait, A., Permiakova, O., Hesse, A.-M., Ialy-Radio, C., Ferro, M., Brun, V., Cocquet, J., Govin, J., & Pflieger, D. (2018). Systematic quantitative analysis of H2A and H2B variants by targeted proteomics. *Epigenetics & Chromatin*, *11*(1), 2. https://doi.org/10.1186/s13072-017-0172-y

Erkek, S., Hisano, M., Liang, C.-Y., Gill, M., Murr, R., Dieker, J., Schübeler, D., van der Vlag, J., Stadler, M. B., & Peters, A. H. F. M. (2013). Molecular determinants of nucleosome retention at CpG-rich sequences in mouse spermatozoa. *Nature Structural & Molecular Biology*, *20*(7), 868–875. https://doi.org/10.1038/nsmb.2599

Faure, A. K., Pivot-Pajot, C., Kerjean, A., Hazzouri, M., Pelletier, R., Péoc'h, M., Sèle, B., Khochbin, S., & Rousseaux, S. (2003). Misregulation of histone acetylation in Sertoli cell-only syndrome and testicular cancer. *Molecular Human Reproduction*, *9*(12), 757–763. https://doi.org/10.1093/molehr/gag101

Feng, C.-W. A., Spiller, C., Merriner, D. J., O'Bryan, M. K., Bowles, J., & Koopman, P. (2017). SOX30 is required for male fertility in mice. *Scientific Reports*, *7*(1), 17619. https://doi.org/10.1038/s41598-017-17854-5

Fita, I., Campos, J. L., Puigjaner, L. C., & Subirana, J. A. (1983). X-ray diffraction study of DNA complexes with arginine peptides and their relation to nucleoprotamine structure. *Journal of Molecular Biology*, *167*(1), 157–177. https://doi.org/10.1016/s0022-2836(83)80039-4

Fraietta, R., Spaine, D. M., Bertolla, R. P., Ortiz, V., & Cedenho, A. P. (2010). Individual and seminal characteristics of patients with testicular germ cell tumors. *Fertility and Sterility*, *94*(6), 2107–2112. https://doi.org/10.1016/j.fertnstert.2009.12.021

Fullston, T., Ohlsson Teague, E. M. C., Palmer, N. O., DeBlasio, M. J., Mitchell, M., Corbett, M., Print, C. G., Owens, J. A., & Lane, M. (2013). Paternal obesity initiates metabolic disturbances in two generations of mice with incomplete penetrance to the F2 generation and alters the transcriptional profile of testis and sperm microRNA content. *FASEB Journal: Official Publication of the Federation of American Societies for Experimental Biology*, *27*(10), 4226–4243. https://doi.org/10.1096/fj.12-224048

Fullston, T., Palmer, N. O., Owens, J. A., Mitchell, M., Bakos, H. W., & Lane, M. (2012). Diet-induced paternal obesity in the absence of diabetes diminishes the reproductive health of two subsequent generations of mice. *Human Reproduction*, *27*(5), 1391–1400. https://doi.org/10.1093/humrep/des030

Fulton, M. D., Dang, T., Brown, T., & Zheng, Y. G. (2022). Effects of substrate modifications on the arginine dimethylation activities of PRMT1 and PRMT5. *Epigenetics*, *17*(1), 1–18. https://doi.org/10.1080/15592294.2020.1864170

Gatewood, J., Cook, G. R., Balhorn, R., Bradbury, E. M., & Schmid, C. W. (1987). Sequence-Specific Packaging of DNA in Human Sperm Chromatin. *Science*, *236*(4804), 962–964. https://doi.org/10.1126/science.3576213

Gaucher, J., Boussouar, F., Montellier, E., Curtet, S., Buchou, T., Bertrand, S., Hery, P., Jounier, S., Depaux, A., Vitte, A.-L., Guardiola, P., Pernet, K., Debernardi, A., Lopez, F., Holota, H., Imbert, J., Wolgemuth, D. J., Gérard, M., Rousseaux, S., & Khochbin, S. (2012). Bromodomain-dependent stage-specific male genome programming by Brdt. *The EMBO Journal*, *31*(19), 3809–3820. https://doi.org/10.1038/emboj.2012.233

Ge, S.-Q., Grifin, J., Liu, L.-H., Aston, K. I., Simon, L., Jenkins, T. G., Emery, B. R., & Carrell, D. (2015). Associations of single nucleotide polymorphisms in the Pygo2 coding sequence with idiopathic oligospermia and azoospermia. *Genetics and Molecular Research*, *14*(3), 9053–9061. https://doi.org/10.4238/2015.August.7.14

Gerhold, C. B., & Gasser, S. M. (2014). INO80 and SWR complexes: relating structure to function in chromatin remodeling. *Trends in Cell Biology*, *24*(11), 619–631. https://doi.org/10.1016/j.tcb.2014.06.004

Gervasi, M. G., & Visconti, P. E. (2017). Molecular changes and signaling events occurring in spermatozoa during epididymal maturation. *Andrology*, *5*(2), 204–218. https://doi.org/10.1111/andr.12320

Gibcus, J. H., Samejima, K., Goloborodko, A., Samejima, I., Naumova, N., Nuebler, J., Kanemaki, M. T., Xie, L., Paulson, J. R., Earnshaw, W. C., Mirny, L. A., & Dekker, J. (2018). A pathway for mitotic chromosome formation. *Science*, *359*(6376). https://doi.org/10.1126/science.aao6135

Gode, F., Gürbüz, A. S., Tamer, B., Pala, I., & Isik, A. Z. (2020). The Effects of Microfluidic Sperm Sorting, Density Gradient and Swim-up Methods on Semen Oxidation Reduction Potential. *Urology Journal*, *17*(4), 397–401. https://doi.org/10.22037/uj.v0i0.5639

Gómez-H, L., Felipe-Medina, N., Condezo, Y. B., Garcia-Valiente, R., Ramos, I., Suja, J. A., Barbero, J. L., Roig, I., Sánchez-Martín, M., de Rooij, D. G., Llano, E., & Pendas, A. M. (2019). The PSMA8 subunit of the spermatoproteasome is essential for proper meiotic exit and mouse fertility. *PLOS Genetics*, *15*(8), e1008316. https://doi.org/10.1371/journal.pgen.1008316

Goossens, E., & Tournaye, H. (2013). Adult Stem Cells in the Human Testis. *Seminars in Reproductive Medicine*, *31*(01), 039–048. https://doi.org/10.1055/s-0032-1331796

Gou, L.-T., Kang, J.-Y., Dai, P., Wang, X., Li, F., Zhao, S., Zhang, M., Hua, M.-M., Lu, Y., Zhu, Y., Li, Z., Chen, H., Wu, L.-G., Li, D., Fu, X.-D., Li, J., Shi, H.-J., & Liu, M.-F. (2017). Ubiquitination-Deficient Mutations in Human Piwi Cause Male Infertility by Impairing Histone-to-Protamine Exchange During Spermiogenesis. *Obstetrical & Gynecological Survey*, *72*(9), 540–541. https://doi.org/10.1097/OGX.0000000000000482

Gou, L.-T., Lim, D.-H., Ma, W., Aubol, B. E., Hao, Y., Wang, X., Zhao, J., Liang, Z., Shao, C., Zhang, X., Meng, F., Li, H., Zhang, X., Xu, R., Li, D., Rosenfeld, M. G., Mellon, P. L., Adams, J. A., Liu, M.-F., & Fu, X.-D. (2020). Initiation of Parental Genome Reprogramming in Fertilized Oocyte by Splicing Kinase SRPK1-Catalyzed Protamine Phosphorylation. *Cell*, *180*(6), 1212–1227.e14. https://doi.org/10.1016/j.cell.2020.02.020

Goudarzi, A., Shiota, H., Rousseaux, S., & Khochbin, S. (2014). Genome-Scale Acetylation-Dependent Histone Eviction during Spermatogenesis. *Journal of Molecular Biology*, *426*(20), 3342–3349. https://doi.org/10.1016/j.jmb.2014.02.023

Goudarzi, A., Zhang, D., Huang, H., Barral, S., Kwon, O. K., Qi, S., Tang, Z., Buchou, T., Vitte, A.-L., He, T., Cheng, Z., Montellier, E., Gaucher, J., Curtet, S., Debernardi, A., Charbonnier, G., Puthier, D., Petosa, C., Panne, D., … Khochbin, S. (2016). Dynamic Competing Histone H4 K5K8 Acetylation and Butyrylation Are Hallmarks of Highly Active Gene Promoters. *Molecular Cell*, *62*(2), 169–180. https://doi.org/10.1016/j.molcel.2016.03.014

Grimes, S. R., & Henderson, N. (1984). Hyperacetylation of histone H4 in rat testis spermatids. *Experimental Cell Research*, *152*(1), 91–97. https://doi.org/10.1016/0014-4827(84)90232-5

Griswold, M. D. (2016). Spermatogenesis: The Commitment to Meiosis. *Physiological Reviews*, *96*(1), 1–17. https://doi.org/10.1152/physrev.00013.2015

Gui, J. F., Tronchère, H., Chandler, S. D., & Fu, X. D. (1994). Purification and characterization of a kinase specific for the serine- and arginine-rich pre-mRNA splicing factors. *Proceedings of the National Academy of Sciences*, *91*(23), 10824–10828. https://doi.org/10.1073/pnas.91.23.10824

Guo, Y., Song, Y., Guo, Z., Hu, M., Liu, B., Duan, H., Wang, L., Yuan, T., & Wang, D. (2018). Function of RAD6B and RNF8 in spermatogenesis. *Cell Cycle*, *17*(2), 162–173. https://doi.org/10.1080/15384101.2017.1361066

Gupta, N., Madapura, M. P., Bhat, U. A., & Rao, M. R. S. (2015). Mapping of Post-translational Modifications of Transition Proteins, TP1 and TP2, and Identification of Protein Arginine Methyltransferase 4 and Lysine Methyltransferase 7 as Methyltransferase for TP2. *Journal of Biological Chemistry*, *290*(19), 12101–12122. https://doi.org/10.1074/jbc.M114.620443

Gupta, N., Pentakota, S., Mishra, L. N., Jones, R., & Rao, M. R. S. (2017). *Identification of Posttranslational Modifications of Endogenous Chromatin Proteins From Testicular Cells by Mass Spectrometry* (pp. 115–142). https://doi.org/10.1016/bs.mie.2016.09.031

Gustafson, E. A., Seymour, K. A., Sigrist, K., Rooij, D. G. D. E., & Freiman, R. N. (2020). ZFP628 Is a TAF4b-Interacting Transcription Factor Required for Mouse Spermiogenesis. *Molecular and Cellular Biology*, *40*(7). https://doi.org/10.1128/MCB.00228-19

Hamilton, T. R. dos S., & Assumpção, M. E. O. D. (2020). Sperm DNA fragmentation: causes and identification. *Zygote*, *28*(1), 1–8. https://doi.org/10.1017/S0967199419000595

Hammoud, A. O., Wilde, N., Gibson, M., Parks, A., Carrell, D., & Meikle, A. W. (2008). Male obesity and alteration in sperm parameters. *Fertility and Sterility*, *90*(6), 2222–2225. https://doi.org/10.1016/j.fertnstert.2007.10.011

Hammoud, S., Nix, D. A., Hammoud, A. O., Gibson, M., Cairns, B. R., & Carrell, D. (2011). Genome-wide analysis identifies changes in histone retention and epigenetic modifications at developmental and imprinted gene loci in the sperm of infertile men. *Human Reproduction*, *26*(9), 2558–2569. https://doi.org/10.1093/humrep/der192

Hammoud, S., Nix, D. A., Zhang, H., Purwar, J., Carrell, D., & Cairns, B. R. (2009). Distinctive chromatin in human sperm packages genes for embryo development. *Nature*, *460*(7254), 473–478. https://doi.org/10.1038/nature08162

Hammoud, S., Purwar, J., Pflueger, C., Cairns, B. R., & Carrell, D. (2010). Alterations in sperm DNA methylation patterns at imprinted loci in two classes of infertility. *Fertility and Sterility*, *94*(5), 1728–1733. https://doi.org/10.1016/j.fertnstert.2009.09.010

Harbuz, R., Zouari, R., Pierre, V., Ben Khelifa, M., Kharouf, M., Coutton, C., Merdassi, G., Abada, F., Escoffier, J., Nikas, Y., Vialard, F., Koscinski, I., Triki, C., Sermondade, N., Schweitzer, T., Zhioua, A., Zhioua, F., Latrous, H., Halouani, L., … Ray, P. F. (2011). A Recurrent Deletion of DPY19L2 Causes Infertility in Man by Blocking Sperm Head Elongation and Acrosome Formation. *The American Journal of Human Genetics*, *88*(3), 351–361. https://doi.org/10.1016/j.ajhg.2011.02.007

Hatanaka, Y., Tsusaka, T., Shimizu, N., Morita, K., Suzuki, T., Machida, S., Satoh, M., Honda, A., Hirose, M., Kamimura, S., Ogonuki, N., Nakamura, T., Inoue, K., Hosoi, Y., Dohmae, N., Nakano, T., Kurumizaka, H., Matsumoto, K., Shinkai, Y., & Ogura, A. (2017). Histone H3 Methylated at Arginine 17 Is Essential for Reprogramming the Paternal Genome in Zygotes. *Cell Reports*, *20*(12), 2756–2765. https://doi.org/10.1016/j.celrep.2017.08.088

Hayakawa, T., Ohtani, Y., Hayakawa, N., Shinmyozu, K., Saito, M., Ishikawa, F., & Nakayama, J. (2007). RBP2 is an MRG15 complex component and down-regulates intragenic histone H3 lysine 4 methylation. *Genes to Cells*, *0*(0), 070606122915002–??? https://doi.org/10.1111/j.1365-2443.2007.01089.x

Hazzouri, M., Pivot-Pajot, C., Faure, A.-K., Usson, Y., Pelletier, R., Sèle, B., Khochbin, S., & Rousseaux, S. (2000). Regulated hyperacetylation of core histones during mouse spermatogenesis: involvement of histone-deacetylases. *European Journal of Cell Biology*, *79*(12), 950–960. https://doi.org/10.1078/0171-9335-00123

Hecht, N. B. (1998). Molecular mechanisms of male germ cell differentiation. *BioEssays: News and Reviews in Molecular, Cellular and Developmental Biology*, *20*(7), 555–561. https://doi.org/10.1002/(SICI)1521-1878(199807)20:7<555::AID-BIES6>3.0.CO;2-J

Heller, C. G., & Clermont, Y. (1963). Spermatogenesis in Man: An Estimate of Its Duration. *Science*, *140*(3563), 184–186. https://doi.org/10.1126/science.140.3563.184

Her, Y. R., Wang, L., Chepelev, I., Manterola, M., Berkovits, B., Cui, K., Zhao, K., & Wolgemuth, D. J. (2021). Genome-wide chromatin occupancy of BRDT and gene expression analysis suggest transcriptional partners and specific epigenetic landscapes that regulate gene expression during spermatogenesis. *Molecular Reproduction and Development*, *88*(2), 141–157. https://doi.org/10.1002/mrd.23449

Hernández-Hernández, A., Lilienthal, I., Fukuda, N., Galjart, N., & Höög, C. (2016). CTCF contributes in a critical way to spermatogenesis and male fertility. *Scientific Reports*, *6*(1), 28355. https://doi.org/10.1038/srep28355

Hoghoughi, N., Barral, S., Vargas, A., Rousseaux, S., & Khochbin, S. (2018). Histone variants: essential actors in male genome programming. *The Journal of Biochemistry*, *163*(2), 97–103. https://doi.org/10.1093/jb/mvx079

Holstein, A.-F., Schulze, W., & Davidoff, M. (2003). Understanding spermatogenesis is a prerequisite for treatment. *Reproductive Biology and Endocrinology*, *1*(1), 107. https://doi.org/10.1186/1477-7827-1-107

Horard, B., Sapey-Triomphe, L., Bonnefoy, E., & Loppin, B. (2018). ASF1 is required to load histones on the HIRA complex in preparation of paternal chromatin assembly at fertilization. *Epigenetics & Chromatin*, *11*(1), 19. https://doi.org/10.1186/s13072-018-0189-x

Hornbeck, P. v, Zhang, B., Murray, B., Kornhauser, J. M., Latham, V., & Skrzypek, E. (2015). PhosphoSitePlus, 2014: mutations, PTMs and recalibrations. *Nucleic Acids Research*, *43*(Database issue), D512–20. https://doi.org/10.1093/nar/gku1267

Hud, N. v, Allen, M. J., Downing, K. H., Lee, J., & Balhorn, R. (1993). Identification of the Elemental Packing Unit of DNA in Mammalian Sperm Cells by Atomic Force Microscopy. *Biochemical and Biophysical Research Communications*, *193*(3), 1347–1354. https://doi.org/10.1006/bbrc.1993.1773

Hud, N. V, & Downing, K. H. (2001). Cryoelectron microscopy of λ phage DNA condensates in vitreous ice: The fine structure of DNA toroids. *Proceedings of the National Academy of Sciences*, *98*(26), 14925–14930. https://doi.org/10.1073/pnas.261560398

Hud, N. v, Downing, K. H., & Balhorn, R. (1995). A constant radius of curvature model for the organization of DNA in toroidal condensates. *Proceedings of the National Academy of Sciences*, *92*(8), 3581–3585. https://doi.org/10.1073/pnas.92.8.3581

Hud, N. V, & Vilfan, I. D. (2005). Toroidal DNA Condensates: Unraveling the Fine Structure and the Role of Nucleation in Determining Size. *Annual Review of Biophysics and Biomolecular Structure*, *34*(1), 295–318. https://doi.org/10.1146/annurev.biophys.34.040204.144500

Hutchison, J. M., Rau, D. C., & DeRouchey, J. E. (2017). Role of Disulfide Bonds on DNA Packaging Forces in Bull Sperm Chromatin. *Biophysical Journal*, *113*(9), 1925–1933. https://doi.org/10.1016/j.bpj.2017.08.050

Ihara, M., Meyer-Ficca, M. L., Leu, N. A., Rao, S., Li, F., Gregory, B. D., Zalenskaya, I. A., Schultz, R. M., & Meyer, R. G. (2014). Paternal poly (ADP-ribose) metabolism modulates retention of inheritable sperm histones and early embryonic gene expression. *PLoS Genetics*, *10*(5), e1004317. https://doi.org/10.1371/journal.pgen.1004317

Inoue, A., & Zhang, Y. (2014). Nucleosome assembly is required for nuclear pore complex assembly in mouse zygotes. *Nature Structural & Molecular Biology*, *21*(7), 609–616. https://doi.org/10.1038/nsmb.2839

Itoh, K., Kondoh, G., Miyachi, H., Sugai, M., Kaneko, Y., Kitano, S., Watanabe, H., Maeda, R., Imura, A., Liu, Y., Ito, C., Itohara, S., Toshimori, K., & Fujita, J. (2019). Dephosphorylation of protamine 2 at serine 56 is crucial for murine sperm maturation in vivo. *Science Signaling*, *12*(574). https://doi.org/10.1126/scisignal.aao7232

Iuso, D., Czernik, M., Toschi, P., Fidanza, A., Zacchini, F., Feil, R., Curtet, S., Buchou, T., Shiota, H., Khochbin, S., Ptak, G. E., & Loi, P. (2015). Exogenous Expression of Human Protamine 1 (hPrm1) Remodels Fibroblast Nuclei into Spermatid-like Structures. *Cell Reports*, *13*(9), 1765–1771. https://doi.org/10.1016/j.celrep.2015.10.066

Iwamori, N., Tominaga, K., Sato, T., Riehle, K., Iwamori, T., Ohkawa, Y., Coarfa, C., Ono, E., & Matzuk, M. M. (2016). MRG15 is required for pre-mRNA splicing and spermatogenesis. *Proceedings of the National Academy of Sciences*, *113*(37). https://doi.org/10.1073/pnas.1611995113

Jang, S., Kang, C., Yang, H.-S., Jung, T., Hebert, H., Chung, K. Y., Kim, S. J., Hohng, S., & Song, J.-J. (2019). Structural basis of recognition and destabilization of the histone H2B ubiquitinated nucleosome by the DOT1L histone H3 Lys79 methyltransferase. *Genes & Development*, *33*(11–12), 620–625. https://doi.org/10.1101/gad.323790.118

Jenkins, T. G., Aston, K. I., & Carrell, D. T. (2018). Sperm epigenetics and aging. *Translational Andrology and Urology*, *7*(S3), S328–S335. https://doi.org/10.21037/tau.2018.06.10

Jenkins, T. G., Aston, K. I., Pflueger, C., Cairns, B. R., & Carrell, D. T. (2014). Age-associated sperm DNA methylation alterations: possible implications in offspring disease susceptibility. *PLoS Genetics*, *10*(7), e1004458. https://doi.org/10.1371/journal.pgen.1004458

Jenuwein, T., & Allis, C. D. (2001). Translating the Histone Code. *Science*, *293*(5532), 1074–1080. https://doi.org/10.1126/science.1063127

Jha, K. N., Tripurani, S. K., & Johnson, G. R. (2017). TSSK6 is required for γH2AX formation and the histone-to-protamine transition during spermiogenesis. *Journal of Cell Science*. https://doi.org/10.1242/jcs.202721

Ji, X., Dadon, D. B., Abraham, B. J., Lee, T. I., Jaenisch, R., Bradner, J. E., & Young, R. A. (2015). Chromatin proteomic profiling reveals novel proteins associated with histone-marked genomic regions. *Proceedings of the National Academy of Sciences*, *112*(12), 3841–3846. https://doi.org/10.1073/pnas.1502971112

Jodar, M., & Oliva, R. (2014). Protamine alterations in human spermatozoa. *Advances in Experimental Medicine and Biology*, *791*, 83–102. https://doi.org/10.1007/978-1-4614-7783-9_6

Jodar, M., Selvaraju, S., Sendler, E., Diamond, M. P., Krawetz, S. A., & Reproductive Medicine Network. (2013). The presence, role and clinical use of spermatozoal RNAs. *Human Reproduction Update*, *19*(6), 604–624. https://doi.org/10.1093/humupd/dmt031

Jodar, M., Sendler, E., Moskovtsev, S. I., Librach, C. L., Goodrich, R., Swanson, S., Hauser, R., Diamond, M. P., & Krawetz, S. A. (2015). Absence of sperm RNA elements correlates with idiopathic male infertility. *Science Translational Medicine*, *7*(295), 295re6. https://doi.org/10.1126/scitranslmed.aab1287

Jodar, M., Soler-Ventura, A., Oliva, R., & Molecular Biology of Reproduction and Development Research Group. (2017). Semen proteomics and male infertility. *Journal of Proteomics*, *162*, 125–134. https://doi.org/10.1016/j.jprot.2016.08.018

Jung, J. H., & Seo, J. T. (2014). Empirical medical therapy in idiopathic male infertility: Promise or panacea? *Clinical and Experimental Reproductive Medicine*, *41*(3), 108–114. https://doi.org/10.5653/cerm.2014.41.3.108

Jung, Y. H., Sauria, M. E. G., Lyu, X., Cheema, M. S., Ausió, J., Taylor, J., & Corces, V. G. (2017). Chromatin States in Mouse Sperm Correlate with Embryonic and Adult Regulatory Landscapes. *Cell Reports*, *18*(6), 1366–1382. https://doi.org/10.1016/j.celrep.2017.01.034

Jungwirth, A., Diemer, T., Kopa, Z., Krausz, C., Minhas, S., & Tournaye, H. (2019). EAU Guidelines on Male Infertility. In *EAU Guidelines. Edn. presented at the EAU Annual Congress Barcelona 2019.* . EAU Guidelines Office.

Kakihara, Y., & Houry, W. A. (2012). The R2TP complex: Discovery and functions. *Biochimica et Biophysica Acta (BBA) - Molecular Cell Research*, *1823*(1), 101–107. https://doi.org/10.1016/j.bbamcr.2011.08.016

Kaneshiro, K. R., Rechtsteiner, A., & Strome, S. (2019). Sperm-inherited H3K27me3 impacts offspring transcription and development in C. elegans. *Nature Communications*, *10*(1), 1271. https://doi.org/10.1038/s41467-019-09141-w

Kasinsky, H. E., Mann, M., Huang, S. Y., Fabre, L., Coyle, B., & Byrd, E. W. (1987). On the diversity of sperm basic proteins in the vertebrates: V. Cytochemical and amino acid analysis in Squamata, Testudines, and Crocodylia. *The Journal of Experimental Zoology*, *243*(1), 137–151. https://doi.org/10.1002/jez.1402430116

Kasinsky, H. E., Maria Eirin-Lopez, J., & Ausió, J. (2011). Protamines: Structural Complexity, Evolution and Chromatin Patterning. *Protein & Peptide Letters*, *18*(8), 755–771. https://doi.org/10.2174/092986611795713989

Kaufman, P. D., & Rando, O. J. (2010). Chromatin as a potential carrier of heritable information. *Current Opinion in Cell Biology*, *22*(3), 284–290. https://doi.org/10.1016/j.ceb.2010.02.002

Kavarthapu, R., Anbazhagan, R., Raju, M., Morris, C.-H. T., Pickel, J., & Dufau, M. L. (2019). Targeted knock-in mice with a human mutation in GRTH/DDX25 reveals the essential role of phosphorylated GRTH in spermatid development during spermatogenesis. *Human Molecular Genetics*, *28*(15), 2561–2572. https://doi.org/10.1093/hmg/ddz079

Ke, Y., Xu, Y., Chen, X., Feng, S., Liu, Z., Sun, Y., Yao, X., Li, F., Zhu, W., Gao, L., Chen, H., Du, Z., Xie, W., Xu, X., Huang, X., & Liu, J. (2017). 3D Chromatin Structures of Mature Gametes and Structural Reprogramming during Mammalian Embryogenesis. *Cell*, *170*(2), 367–381.e20. https://doi.org/10.1016/j.cell.2017.06.029

Khor, B., Bredemeyer, A. L., Huang, C.-Y., Turnbull, I. R., Evans, R., Maggi, L. B., White, J. M., Walker, L. M., Carnes, K., Hess, R. A., & Sleckman, B. P. (2006). Proteasome Activator PA200 Is Required for Normal Spermatogenesis. *Molecular and Cellular Biology*, *26*(8), 2999–3007. https://doi.org/10.1128/MCB.26.8.2999-3007.2006

Kim, C. R., Noda, T., Kim, H., Kim, G., Park, S., Na, Y., Oura, S., Shimada, K., Bang, I., Ahn, J.-Y., Kim, Y. R., Oh, S. K., Choi, H.-J., Kim, J.-S., Jung, I., Lee, H., Okada, Y., Ikawa, M., & Baek, S. H. (2020). PHF7 Modulates BRDT Stability and Histone-to-Protamine Exchange during Spermiogenesis. *Cell Reports*, *32*(4), 107950. https://doi.org/10.1016/j.celrep.2020.107950

Kimmins, S., Crosio, C., Kotaja, N., Hirayama, J., Monaco, L., Höög, C., van Duin, M., Gossen, J. A., & Sassone-Corsi, P. (2007). Differential functions of the Aurora-B and Aurora-C kinases in mammalian spermatogenesis. *Molecular Endocrinology (Baltimore, Md.)*, *21*(3), 726–739. https://doi.org/10.1210/me.2006-0332

Kimmins, S., & Sassone-Corsi, P. (2005). Chromatin remodelling and epigenetic features of germ cells. *Nature*, *434*(7033), 583–589. https://doi.org/10.1038/nature03368

Kimura, T., Ito, C., Watanabe, S., Takahashi, T., Ikawa, M., Yomogida, K., Fujita, Y., Ikeuchi, M., Asada, N., Matsumiya, K., Okuyama, A., Okabe, M., Toshimori, K., & Nakano, T. (2003). Mouse germ cell-less as an essential component for nuclear integrity. *Molecular and Cellular Biology*, *23*(4), 1304–1315. https://doi.org/10.1128/MCB.23.4.1304-1315.2003

Kistler, W. S., Baas, D., Lemeille, S., Paschaki, M., Seguin-Estevez, Q., Barras, E., Ma, W., Duteyrat, J.-L., Morlé, L., Durand, B., & Reith, W. (2015). RFX2 Is a Major Transcriptional Regulator of Spermiogenesis. *PLOS Genetics*, *11*(7), e1005368. https://doi.org/10.1371/journal.pgen.1005368

Kobayashi, Y., Tomizawa, S., Ono, M., Kuroha, K., Minamizawa, K., Natsume, K., Dizdarević, S., Dočkal, I., Tanaka, H., Kawagoe, T., Seki, M., Suzuki, Y., Ogonuki, N., Inoue, K., Matoba, S., Anastassiadis, K., Mizuki, N., Ogura, A., & Ohbo, K. (2021). *Tsga8* is required for spermatid morphogenesis and male fertility in mice. *Development*, *148*(8). https://doi.org/10.1242/dev.196212

Kong, A., Frigge, M. L., Masson, G., Besenbacher, S., Sulem, P., Magnusson, G., Gudjonsson, S. A., Sigurdsson, A., Jonasdottir, A., Jonasdottir, A., Wong, W. S. W., Sigurdsson, G., Walters, G. B., Steinberg, S., Helgason, H., Thorleifsson, G., Gudbjartsson, D. F., Helgason, A., Magnusson, O. Th., … Stefansson, K. (2012). Rate of de novo mutations and the importance of father's age to disease risk. *Nature*, *488*(7412), 471–475. https://doi.org/10.1038/nature11396

Korhonen, H. M., Meikar, O., Yadav, R. P., Papaioannou, M. D., Romero, Y., Da Ros, M., Herrera, P. L., Toppari, J., Nef, S., & Kotaja, N. (2011). Dicer is required for haploid male germ cell differentiation in mice. *PloS One*, *6*(9), e24821. https://doi.org/10.1371/journal.pone.0024821

Kotaja, N., De Cesare, D., Macho, B., Monaco, L., Brancorsini, S., Goossens, E., Tournaye, H., Gansmuller, A., & Sassone-Corsi, P. (2004). Abnormal sperm in mice with targeted deletion of the act (activator of cAMP-responsive element modulator in testis) gene. *Proceedings of the National Academy of Sciences of the United States of America*, *101*(29), 10620–10625. https://doi.org/10.1073/pnas.0401947101

Krishnamoorthy, T., Chen, X., Govin, J., Cheung, W. L., Dorsey, J., Schindler, K., Winter, E., Allis, C. D., Guacci, V., Khochbin, S., Fuller, M. T., & Berger, S. L. (2006). Phosphorylation of histone H4 Ser1 regulates sporulation in yeast and is conserved in fly and mouse spermatogenesis. *Genes & Development*, *20*(18), 2580–2592. https://doi.org/10.1101/gad.1457006

Kumar, N., & Singh, A. K. (2021). The anatomy, movement, and functions of human sperm tail: an evolving mystery. *Biology of Reproduction*, *104*(3), 508–520. https://doi.org/10.1093/biolre/ioaa213

Kwak, H.-G., & Dohmae, N. (2016). Proteomic characterization of histone variants in the mouse testis by mass spectrometry-based top-down analysis. *BioScience Trends*, *10*(5), 357–364. https://doi.org/10.5582/bst.2016.01090

Laguna, M., Albers, P., Algaba, F., Bokemeyer, C., Boormans, J., di Nardo, D., Fischer, S., Fizazi, K., Gremmels, H., Leão, R., Nicol, D., Nicolai, N., Oldenburg, J., & Tandstad, T. (2022). *EAU Guidelines on Testicular Cancer*. EAU Guidelines Office.

Laurentino, S., Borgmann, J., & Gromoll, J. (2016). On the origin of sperm epigenetic heterogeneity. *Reproduction*, *151*(5), R71–R78. https://doi.org/10.1530/REP-15-0436

Laurentino, S., Cremers, J., Horsthemke, B., Tüttelmann, F., Czeloth, K., Zitzmann, M., Pohl, E., Rahmann, S., Schröder, C., Berres, S., Redmann, K., Krallmann, C., Schlatt, S., Kliesch, S., & Gromoll, J. (2020). A germ cell-specific ageing pattern in otherwise healthy men. *Aging Cell*, *19*(10). https://doi.org/10.1111/acel.13242

Leduc, F., Maquennehan, V., Nkoma, G. B., & Boissonneault, G. (2008). DNA damage response during chromatin remodeling in elongating spermatids of mice. *Biology of Reproduction*, *78*(2), 324–332. https://doi.org/10.1095/biolreprod.107.064162

Lee, K., Fajardo, M. A., & Braun, R. E. (1996). A testis cytoplasmic RNA-binding protein that has the properties of a translational repressor. *Molecular and Cellular Biology*, *16*(6), 3023–3034. https://doi.org/10.1128/MCB.16.6.3023

Leitão, E., di Persio, S., Laurentino, S., Wöste, M., Dugas, M., Kliesch, S., Neuhaus, N., & Horsthemke, B. (2020). The sperm epigenome does not display recurrent epimutations in patients with severely impaired spermatogenesis. *Clinical Epigenetics*, *12*(1), 61. https://doi.org/10.1186/s13148-020-00854-0

Lévesque, D., Veilleux, S., Caron, N., & Boissonneault, G. (1998). Architectural DNA-binding properties of the spermatidal transition proteins 1 and 2. *Biochemical and Biophysical Research Communications*, *252*(3), 602–609. https://doi.org/10.1006/bbrc.1998.9687

Levine, H., Jørgensen, N., Martino-Andrade, A., Mendiola, J., Weksler-Derri, D., Mindlis, I., Pinotti, R., & Swan, S. H. (2017). Temporal trends in sperm count: a systematic review and meta-regression analysis. *Human Reproduction Update*, *23*(6), 646–659. https://doi.org/10.1093/humupd/dmx022

Lewis, B. P., Green, R. E., & Brenner, S. E. (2003). Evidence for the widespread coupling of alternative splicing and nonsense-mediated mRNA decay in humans. *Proceedings of the National Academy of Sciences*, *100*(1), 189–192. https://doi.org/10.1073/pnas.0136770100

Lewis, J. D., Abbott, D. W., & Ausió, J. (2003). A haploid affair: core histone transitions during spermatogenesis. *Biochemistry and Cell Biology = Biochimie et Biologie Cellulaire*, *81*(3), 131–140. https://doi.org/10.1139/o03-045

Lewis, S. E. M., & Simon, L. (2010). Clinical implications of sperm DNA damage. *Human Fertility*, *13*(4), 201–207. https://doi.org/10.3109/14647273.2010.528823

Li, A., Maffey, A. H., Abbott, W. D., Conde e Silva, N., Prunell, A., Siino, J., Churikov, D., Zalensky, A. O., & Ausió, J. (2005). Characterization of Nucleosomes Consisting of the Human Testis/Sperm-Specific Histone H2B Variant (hTSH2B). *Biochemistry*, *44*(7), 2529–2535. https://doi.org/10.1021/bi048061n

Li, J., Liu, Y.-F., Xu, H.-Y., Zhang, J.-Y., Lv, P.-P., Liu, M.-E., Ying, Y.-Y., Qian, Y.-Q., Li, K., Li, C., Huang, Y., Xu, G.-F., Ding, G.-L., Mao, Y.-C., Xu, C.-M., Liu, X.-M., Sheng, J.-Z., Zhang, D., & Huang, H.-F. (2020). Basonuclin 1 deficiency causes testicular premature aging: BNC1 cooperates with TAF7L to regulate spermatogenesis. *Journal of Molecular Cell Biology*, *12*(1), 71–83. https://doi.org/10.1093/jmcb/mjz035

Li, J., Wang, J., Wang, J., Nawaz, Z., Liu, J. M., Qin, J., & Wong, J. (2000). Both corepressor proteins SMRT and N-CoR exist in large protein complexes containing HDAC3. *The EMBO Journal*, *19*(16), 4342–4350. https://doi.org/10.1093/emboj/19.16.4342

Li, W., Wu, J., Kim, S.-Y., Zhao, M., Hearn, S. A., Zhang, M. Q., Meistrich, M. L., & Mills, A. A. (2014). Chd5 orchestrates chromatin remodelling during sperm development. *Nature Communications*, *5*, 3812. https://doi.org/10.1038/ncomms4812

Li, Y., Cheng, Y., Zhu, T., Zhang, H., Li, W., Guo, Y., Qi, Y., Chen, X., Zhang, J., Sha, J., Zhou, Z., Zhu, H., & Guo, X. (2019). The Protein Phosphorylation Landscape of Mouse Spermatids during Spermiogenesis. *Proteomics*, *19*(11), e1900055. https://doi.org/10.1002/pmic.201900055

Li, Z., Zhang, X., Xie, S., Liu, X., Fei, C., Huang, X., Tang, Y., & Zhou, L.-Q. (2022). H3K36me2 methyltransferase NSD2 orchestrates epigenetic reprogramming during spermatogenesis. *Nucleic Acids Research*. https://doi.org/10.1093/nar/gkac533

Lin, C.-J., Koh, F. M., Wong, P., Conti, M., & Ramalho-Santos, M. (2014). Hira-Mediated H3.3 Incorporation Is Required for DNA Replication and Ribosomal RNA Transcription in the Mouse Zygote. *Developmental Cell*, *30*(3), 268–279. https://doi.org/10.1016/j.devcel.2014.06.022

Ling, L., Li, F., Yang, P., Oates, R. D., Silber, S., Kurischko, C., Luca, F. C., Leu, N. A., Zhang, J., Yue, Q., Skaletsky, H., Brown, L. G., Rozen, S., Page, D. C., Wang, P. J., & Zheng, K. (2022). Genetic characterization of a missense mutation in the X-linked *TAF7L* gene identified in an oligozoospermic man. *Biology of Reproduction*. https://doi.org/10.1093/biolre/ioac093

Liu, D. Y., Liu, M. L., Clarke, G. N., & Baker, H. W. G. (2007). Hyperactivation of capacitated human sperm correlates with the zona pellucida-induced acrosome reaction of zona pellucida-bound sperm. *Human Reproduction*, *22*(10), 2632–2638. https://doi.org/10.1093/humrep/dem245

Liu, N., Qadri, F., Busch, H., Huegel, S., Sihn, G., Chuykin, I., Hartmann, E., Bader, M., & Rother, F. (2021). Kpna6 deficiency causes infertility in male mice by disrupting spermatogenesis. *Development*, *148*(19). https://doi.org/10.1242/dev.198374

Liu, S., Yu, H., Liu, Y., Liu, X., Zhang, Y., Bu, C., Yuan, S., Chen, Z., Xie, G., Li, W., Xu, B., Yang, J., He, L., Jin, T., Xiong, Y., Sun, L., Liu, X., Han, C., Cheng, Z., … Shang, Y. (2017). Chromodomain Protein CDYL Acts as a Crotonyl-CoA Hydratase to Regulate Histone Crotonylation and Spermatogenesis. *Molecular Cell*, *67*(5), 853–866.e5. https://doi.org/10.1016/j.molcel.2017.07.011

Liu, Z., Zhou, S., Liao, L., Chen, X., Meistrich, M., & Xu, J. (2010). Jmjd1a Demethylase-regulated Histone Modification Is Essential for cAMP-response Element Modulator-regulated Gene Expression and Spermatogenesis. *Journal of Biological Chemistry*, *285*(4), 2758–2770. https://doi.org/10.1074/jbc.M109.066845

Loveland, K. L., Klein, B., Pueschl, D., Indumathy, S., Bergmann, M., Loveland, B. E., Hedger, M. P., & Schuppe, H.-C. (2017). Cytokines in Male Fertility and Reproductive Pathologies: Immunoregulation and Beyond. *Frontiers in Endocrinology*, *8*, 307. https://doi.org/10.3389/fendo.2017.00307

Luense, L. J., Donahue, G., Lin-Shiao, E., Rangel, R., Weller, A. H., Bartolomei, M. S., & Berger, S. L. (2019). Gcn5-Mediated Histone Acetylation Governs Nucleosome Dynamics in

Spermiogenesis. *Developmental Cell*, *51*(6), 745–758.e6. https://doi.org/10.1016/j.devcel.2019.10.024

Luo, Z., Wang, X., Jiang, H., Wang, R., Chen, J., Chen, Y., Xu, Q., Cao, J., Gong, X., Wu, J., Yang, Y., Li, W., Han, C., Cheng, C. Y., Rosenfeld, M. G., Sun, F., & Song, X. (2020). Reorganized 3D Genome Structures Support Transcriptional Regulation in Mouse Spermatogenesis. *IScience*, *23*(4), 101034. https://doi.org/10.1016/j.isci.2020.101034

Lv, M.-Q., Ge, P., Zhang, J., Yang, Y.-Q., Zhou, L., & Zhou, D.-X. (2021). Temporal trends in semen concentration and count among 327 373 Chinese healthy men from 1981 to 2019: a systematic review. *Human Reproduction (Oxford, England)*, *36*(7), 1751–1775. https://doi.org/10.1093/humrep/deab124

Lynham, J., & Houry, W. A. (2018). The Multiple Functions of the PAQosome: An R2TP- and URI1 Prefoldin-Based Chaperone Complex. In *Prefoldins: the new chaperones. Advances in Experimental Medicine and Biology* (Vol. 1106, pp. 37–72). https://doi.org/10.1007/978-3-030-00737-9_4

Maione, B., Pittoggi, C., Achene, L., Lorenzini, R., & Spadafora, C. (1997). Activation of endogenous nucleases in mature sperm cells upon interaction with exogenous DNA. *DNA and Cell Biology*, *16*(9), 1087–1097. https://doi.org/10.1089/dna.1997.16.1087

Makita, N., Yoshikawa, Y., Takenaka, Y., Sakaue, T., Suzuki, M., Watanabe, C., Kanai, T., Kanbe, T., Imanaka, T., & Yoshikawa, K. (2011). Salt Has a Biphasic Effect on the Higher-Order Structure of a DNA−Protamine Complex. *The Journal of Physical Chemistry B*, *115*(15), 4453–4459. https://doi.org/10.1021/jp111331q

Makker, K., Agarwal, A., & Sharma, R. (2009). Oxidative stress & male infertility. *The Indian Journal of Medical Research*, *129*(4), 357–367.

Male Infertility Best Practice Policy Committee of the American Urological Association, & Practice Committee of the American Society for Reproductive Medicine. (2006). Report on optimal evaluation of the infertile male. *Fertility and Sterility*, *86*(5 Suppl 1), S202–9. https://doi.org/10.1016/j.fertnstert.2006.08.029

Manterola, M., Brown, T. M., Oh, M. Y., Garyn, C., Gonzalez, B. J., & Wolgemuth, D. J. (2018). BRDT is an essential epigenetic regulator for proper chromatin organization, silencing of sex chromosomes and crossover formation in male meiosis. *PLoS Genetics*, *14*(3), e1007209. https://doi.org/10.1371/journal.pgen.1007209

Marcon, L., & Boissonneault, G. (2004a). Transient DNA Strand Breaks During Mouse and Human Spermiogenesis:New Insights in Stage Specificity and Link to Chromatin Remodeling1. *Biology of Reproduction*, *70*(4), 910–918. https://doi.org/10.1095/biolreprod.103.022541

Marcon, L., & Boissonneault, G. (2004b). Transient DNA Strand Breaks During Mouse and Human Spermiogenesis:New Insights in Stage Specificity and Link to Chromatin Remodeling1. *Biology of Reproduction*, *70*(4), 910–918. https://doi.org/10.1095/biolreprod.103.022541

Maruyama, R., & Singson, A. (2006). Taking care of Dad's DNA. *Genome Biology*, *7*(12), 244. https://doi.org/10.1186/gb-2006-7-12-244

Mascarenhas, M. N., Flaxman, S. R., Boerma, T., Vanderpoel, S., & Stevens, G. A. (2012). National, Regional, and Global Trends in Infertility Prevalence Since 1990: A Systematic Analysis of 277 Health Surveys. *PLoS Medicine*, *9*(12), e1001356. https://doi.org/10.1371/journal.pmed.1001356

Mazur, D. J., & Lipshultz, L. I. (2018). Infertility in the Aging Male. *Current Urology Reports*, *19*(7), 54. https://doi.org/10.1007/s11934-018-0802-3

McLachlan, R. I., Rajpert-De Meyts, E., Hoei-Hansen, C. E., de Kretser, D. M., & Skakkebaek, N. E. (2007). Histological evaluation of the human testis--approaches to optimizing the clinical value of the assessment: mini review. *Human Reproduction (Oxford, England)*, *22*(1), 2–16. https://doi.org/10.1093/humrep/del279

McPherson, N. O., Fullston, T., Bakos, H. W., Setchell, B. P., & Lane, M. (2014). Obese father's metabolic state, adiposity, and reproductive capacity indicate son's reproductive health.

Fertility and Sterility, *101*(3), 865–873. https://doi.org/10.1016/j.fertnstert.2013.12.007

McPherson, N. O., & Lane, M. (2015). Male obesity and subfertility, is it really about increased adiposity? *Asian Journal of Andrology*, *17*(3), 450–458. https://doi.org/10.4103/1008-682X.148076

McQueen, D. B., Zhang, J., & Robins, J. C. (2019). Sperm DNA fragmentation and recurrent pregnancy loss: a systematic review and meta-analysis. *Fertility and Sterility*, *112*(1), 54–60.e3. https://doi.org/10.1016/j.fertnstert.2019.03.003

Meistrich, M. L., Mohapatra, B., Shirley, C. R., & Zhao, M. (2003). Roles of transition nuclear proteins in spermiogenesis. *Chromosoma*, *111*(8), 483–488. https://doi.org/10.1007/s00412-002-0227-z

Meng, C., Liao, J., Zhao, D., Huang, H., Qin, J., Lee, T.-L., Chen, D., Chan, W.-Y., & Xia, Y. (2019). L3MBTL2 regulates chromatin remodeling during spermatogenesis. *Cell Death & Differentiation*, *26*(11), 2194–2207. https://doi.org/10.1038/s41418-019-0283-z

Mengual, L., Ballescá, J. L., Ascaso, C., & Oliva, R. (2003). Marked differences in protamine content and P1/P2 ratios in sperm cells from percoll fractions between patients and controls. *Journal of Andrology*, *24*(3), 438–447. https://doi.org/10.1002/j.1939-4640.2003.tb02692.x

Merges, G. E., Meier, J., Schneider, S., Kruse, A., Fröbius, A. C., Kirfel, G., Steger, K., Arévalo, L., & Schorle, H. (2022). Loss of *Prm1* leads to defective chromatin protamination, impaired PRM2 processing, reduced sperm motility and subfertility in male mice. *Development*. https://doi.org/10.1242/dev.200330

Mezquita, C. (1985). Chromatin composition, structure and function in spermatogenesis. *Revisiones Sobre Biologia Celular: RBC*, *5*, V–XIV, 1–124.

Miescher, F. (1874). Das Protamin, eine neue organische Base aus den Samenfäden des Rheinlachses. *Berichte Der Deutschen Chemischen Gesellschaft*, *7*(1), 376–379. https://doi.org/10.1002/cber.187400701119

Milekic, M. H., Xin, Y., O'Donnell, A., Kumar, K. K., Bradley-Moore, M., Malaspina, D., Moore, H., Brunner, D., Ge, Y., Edwards, J., Paul, S., Haghighi, F. G., & Gingrich, J. A. (2015). Age-related sperm DNA methylation changes are transmitted to offspring and associated with abnormal behavior and dysregulated gene expression. *Molecular Psychiatry*, *20*(8), 995–1001. https://doi.org/10.1038/mp.2014.84

Minhas, S., Bettocchi, C., Boeri, L., Capogrosso, P., Carvalho, J., Cilesiz, N. C., Cocci, A., Corona, G., Dimitropoulos, K., Gül, M., Hatzichristodoulou, G., Jones, T. H., Kadioglu, A., Martínez Salamanca, J. I., Milenkovic, U., Modgil, V., Russo, G. I., Serefoglu, E. C., Tharakan, T., … Salonia, A. (2021). European Association of Urology Guidelines on Male Sexual and Reproductive Health: 2021 Update on Male Infertility. *European Urology*, *80*(5), 603–620. https://doi.org/10.1016/j.eururo.2021.08.014

Misell, L. M., Holochwost, D., Boban, D., Santi, N., Shefi, S., Hellerstein, M. K., & Turek, P. J. (2006). A Stable Isotope-Mass Spectrometric Method for Measuring Human Spermatogenesis Kinetics In Vivo. *Journal of Urology*, *175*(1), 242–246. https://doi.org/10.1016/S0022-5347(05)00053-4

Mishra, L. N., Gupta, N., & Rao, S. M. R. (2015). Mapping of post-translational modifications of spermatid-specific linker histone H1-like protein, HILS1. *Journal of Proteomics*, *128*, 218–230. https://doi.org/10.1016/j.jprot.2015.08.001

Moch, H., Cubilla, A. L., Humphrey, P. A., Reuter, V. E., & Ulbright, T. M. (2016). The 2016 WHO Classification of Tumours of the Urinary System and Male Genital Organs—Part A: Renal, Penile, and Testicular Tumours. *European Urology*, *70*(1), 93–105. https://doi.org/10.1016/j.eururo.2016.02.029

Montellier, E., Boussouar, F., Rousseaux, S., Zhang, K., Buchou, T., Fenaille, F., Shiota, H., Debernardi, A., Héry, P., Curtet, S., Jamshidikia, M., Barral, S., Holota, H., Bergon, A., Lopez, F., Guardiola, P., Pernet, K., Imbert, J., Petosa, C., … Khochbin, S. (2013). Chromatin-to-nucleoprotamine transition is controlled by the histone H2B variant

TH2B. *Genes & Development*, *27*(15), 1680–1692. https://doi.org/10.1101/gad.220095.113

Moretti, C., Serrentino, M.-E., Ialy-Radio, C., Delessard, M., Soboleva, T. A., Tores, F., Leduc, M., Nitschké, P., Drevet, J. R., Tremethick, D. J., Vaiman, D., Kocer, A., & Cocquet, J. (2017). SLY regulates genes involved in chromatin remodeling and interacts with TBL1XR1 during sperm differentiation. *Cell Death & Differentiation*, *24*(6), 1029–1044. https://doi.org/10.1038/cdd.2017.32

Morinière, J., Rousseaux, S., Steuerwald, U., Soler-López, M., Curtet, S., Vitte, A.-L., Govin, J., Gaucher, J., Sadoul, K., Hart, D. J., Krijgsveld, J., Khochbin, S., Müller, C. W., & Petosa, C. (2009). Cooperative binding of two acetylation marks on a histone tail by a single bromodomain. *Nature*, *461*(7264), 664–668. https://doi.org/10.1038/nature08397

Moritz, L., & Hammoud, S. S. (2022). The Art of Packaging the Sperm Genome: Molecular and Structural Basis of the Histone-To-Protamine Exchange. *Frontiers in Endocrinology*, *13*. https://doi.org/10.3389/fendo.2022.895502

Motta, S., Brocca, P., del Favero, E., Rondelli, V., Cantù, L., Amici, A., Pozzi, D., & Caracciolo, G. (2013). Nanoscale structure of protamine/DNA complexes for gene delivery. *Applied Physics Letters*, *102*(5), 053703. https://doi.org/10.1063/1.4790588

Muciaccia, B., Boitani, C., Berloco, B. P., Nudo, F., Spadetta, G., Stefanini, M., de Rooij, D. G., & Vicini, E. (2013). Novel Stage Classification of Human Spermatogenesis Based on Acrosome Development1. *Biology of Reproduction*, *89*(3), 60. https://doi.org/10.1095/biolreprod.113.111682

Mukherjee, A., Saurabh, S., Olive, E., Jang, Y. H., & Lansac, Y. (2021). Protamine Binding Site on DNA: Molecular Dynamics Simulations and Free Energy Calculations with Full Atomistic Details. *The Journal of Physical Chemistry B*, *125*(12), 3032–3044. https://doi.org/10.1021/acs.jpcb.0c09166

Muratori, M., & de Geyter, C. (2019). Chromatin condensation, fragmentation of DNA and differences in the epigenetic signature of infertile men. *Best Practice & Research Clinical Endocrinology & Metabolism*, *33*(1), 117–126. https://doi.org/10.1016/j.beem.2018.10.004

Muratori, M., Marchiani, S., Tamburrino, L., Cambi, M., Lotti, F., Natali, I., Filimberti, E., Noci, I., Forti, G., Maggi, M., & Baldi, E. (2015). DNA fragmentation in brighter sperm predicts male fertility independently from age and semen parameters. *Fertility and Sterility*, *104*(3), 582–590.e4. https://doi.org/10.1016/j.fertnstert.2015.06.005

Muratori, M., Tarozzi, N., Cambi, M., Boni, L., Iorio, A. L., Passaro, C., Luppino, B., Nadalini, M., Marchiani, S., Tamburrino, L., Forti, G., Maggi, M., Baldi, E., & Borini, A. (2016). Variation of DNA Fragmentation Levels During Density Gradient Sperm Selection for Assisted Reproduction Techniques. *Medicine*, *95*(20), e3624. https://doi.org/10.1097/MD.0000000000003624

Muratori, M., Tarozzi, N., Carpentiero, F., Danti, S., Perrone, F. M., Cambi, M., Casini, A., Azzari, C., Boni, L., Maggi, M., Borini, A., & Baldi, E. (2019). Sperm selection with density gradient centrifugation and swim up: effect on DNA fragmentation in viable spermatozoa. *Scientific Reports*, *9*(1), 7492. https://doi.org/10.1038/s41598-019-43981-2

Murray, C. J. L., Callender, C. S. K. H., Kulikoff, X. R., Srinivasan, V., Abate, D., Abate, K. H., Abay, S. M., Abbasi, N., Abbastabar, H., Abdela, J., Abdelalim, A., Abdel-Rahman, O., Abdi, A., Abdoli, N., Abdollahpour, I., Abdulkader, R. S., Abebe, H. T., Abebe, M., Abebe, Z., … Lim, S. S. (2018). Population and fertility by age and sex for 195 countries and territories, 1950–2017: a systematic analysis for the Global Burden of Disease Study 2017. *The Lancet*, *392*(10159), 1995–2051. https://doi.org/10.1016/S0140-6736(18)32278-5

Nagamori, I., Yomogida, K., Adams, P. D., Sassone-Corsi, P., & Nojima, H. (2006). Transcription Factors, cAMP-responsive Element Modulator (CREM) and Tisp40, Act in Concert in Postmeiotic Transcriptional Regulation. *Journal of Biological Chemistry*, *281*(22), 15073–15081. https://doi.org/10.1074/jbc.M602051200

Nair, M., Nagamori, I., Sun, P., Mishra, D. P., Rhéaume, C., Li, B., Sassone-Corsi, P., & Dai, X. (2008). Nuclear regulator Pygo2 controls spermiogenesis and histone H3 acetylation. *Developmental Biology*, *320*(2), 446–455. https://doi.org/10.1016/j.ydbio.2008.05.553

Nanassy, L., Liu, L., Griffin, J., & Carrell, D. (2011). The clinical utility of the protamine 1/protamine 2 ratio in sperm. *Protein and Peptide Letters*, *18*(8), 772–777. https://doi.org/10.2174/092986611795713934

Nantel, F., Monaco, L., Foulkes, N. S., Masquilier, D., LeMeur, M., Henriksén, K., Dierich, A., Parvinen, M., & Sassone-Corsi, P. (1996). Spermiogenesis deficiency and germ-cell apoptosis in CREM-mutant mice. *Nature*, *380*(6570), 159–162. https://doi.org/10.1038/380159a0

Nashun, B., Yukawa, M., Liu, H., Akiyama, T., & Aoki, F. (2010). Changes in the nuclear deposition of histone H2A variants during pre-implantation development in mice. *Development*, *137*(22), 3785–3794. https://doi.org/10.1242/dev.051805

Nayernia, K., Vauti, F., Meinhardt, A., Cadenas, C., Schweyer, S., Meyer, B. I., Schwandt, I., Chowdhury, K., Engel, W., & Arnold, H.-H. (2003). Inactivation of a testis-specific Lis1 transcript in mice prevents spermatid differentiation and causes male infertility. *The Journal of Biological Chemistry*, *278*(48), 48377–48385. https://doi.org/10.1074/jbc.M309583200

Neto, F. T. L., Bach, P. V., Najari, B. B., Li, P. S., & Goldstein, M. (2016). Spermatogenesis in humans and its affecting factors. *Seminars in Cell & Developmental Biology*, *59*, 10–26. https://doi.org/10.1016/j.semcdb.2016.04.009

Ni, K., Spiess, A.-N., Schuppe, H.-C., & Steger, K. (2016). The impact of sperm protamine deficiency and sperm DNA damage on human male fertility: a systematic review and meta-analysis. *Andrology*, *4*(5), 789–799. https://doi.org/10.1111/andr.12216

Nicopoullos, J., Vicens-Morton, A., Lewis, S. E. M., Lee, K., Larsen, P., Ramsay, J., Yap, T., & Minhas, S. (2019). Novel use of COMET parameters of sperm DNA damage may increase its utility to diagnose male infertility and predict live births following both IVF and ICSI. *Human Reproduction*, *34*(10), 1915–1923. https://doi.org/10.1093/humrep/dez151

Nosrati, R., Graham, P. J., Zhang, B., Riordon, J., Lagunov, A., Hannam, T. G., Escobedo, C., Jarvi, K., & Sinton, D. (2017). Microfluidics for sperm analysis and selection. *Nature Reviews Urology*, *14*(12), 707–730. https://doi.org/10.1038/nrurol.2017.175

Okada, Y., Scott, G., Ray, M. K., Mishina, Y., & Zhang, Y. (2007). Histone demethylase JHDM2A is critical for Tnp1 and Prm1 transcription and spermatogenesis. *Nature*, *450*(7166), 119–123. https://doi.org/10.1038/nature06236

Okada, Y., Tateishi, K., & Zhang, Y. (2010). Histone Demethylase JHDM2A Is Involved in Male Infertility and Obesity. *Journal of Andrology*, *31*(1), 75–78. https://doi.org/10.2164/jandrol.109.008052

Okada, Y., & Yamaguchi, K. (2017). Epigenetic modifications and reprogramming in paternal pronucleus: sperm, preimplantation embryo, and beyond. *Cellular and Molecular Life Sciences*, *74*(11), 1957–1967. https://doi.org/10.1007/s00018-016-2447-z

Okano, K., Heng, H., Trevisanato, S., Tyers, M., & Varmuza, S. (1997). Genomic Organization and Functional Analysis of the Murine Protein Phosphatase 1c γ (Ppp1cc) Gene. *Genomics*, *45*(1), 211–215. https://doi.org/10.1006/geno.1997.4907

Oktay, K., Harvey, B. E., Partridge, A. H., Quinn, G. P., Reinecke, J., Taylor, H. S., Wallace, W. H., Wang, E. T., & Loren, A. W. (2018). Fertility Preservation in Patients With Cancer: ASCO Clinical Practice Guideline Update. *Journal of Clinical Oncology*, *36*(19), 1994–2001. https://doi.org/10.1200/JCO.2018.78.1914

Oliva, R. (2006). Protamines and male infertility. *Human Reproduction Update*, *12*(4), 417–435. https://doi.org/10.1093/humupd/dml009

Oliva, R., Bazett-Jones, D., Mezquita, C., & Dixon, G. H. (1987). Factors affecting nucleosome disassembly by protamines in vitro. Histone hyperacetylation and chromatin structure, time dependence, and the size of the sperm nuclear proteins. *Journal of Biological*

Chemistry, *262*(35), 17016–17025. http://www.jbc.org/content/262/35/17016.abstract

Oliva, R., Bazett-Jones, D. P., Locklear, L., & Dixon, G. H. (1990). Histone hyperacetylation can induce unfolding of the nucleosome core particle. *Nucleic Acids Research*, *18*(9), 2739–2747. https://doi.org/10.1093/nar/18.9.2739

Oliva, R., & Castillo, J. (2011). Proteomics and the genetics of sperm chromatin condensation. *Asian Journal of Andrology*, *13*(1), 24–30. https://doi.org/10.1038/aja.2010.65

Oliva, R., & Dixon, G. H. (1991). Vertebrate Protamine Genes and the Histone-to-Protamine Replacement Reaction. *Progress in Nucleic Acid Research and Molecular Biology*, *40*(C), 25–94. https://doi.org/10.1016/S0079-6603(08)60839-9

Oliva, R., & Mezquita, C. (1982). Histone H4 hyperacetylation and rapid turnover of its acetyl groups in transcriptionally inactive rooster testis spermatids. *Nucleic Acids Research*, *10*(24), 8049–8059. https://doi.org/10.1093/nar/10.24.8049

Oliva, R., & Mezquita, C. (1986). Marked differences in the ability of distinct protamines to disassemble nucleosomal core particles in vitro. *Biochemistry*, *25*(21), 6508–6511. https://doi.org/10.1021/bi00369a025

Orgebin-Crist, M. C. (1969). Studies on the function of the epididymis. *Biology of Reproduction*, *1*, Suppl 1:155–75. https://doi.org/10.1095/biolreprod1.supplement_1.155

Ozturk, N., Dansranjavin, T., Gies, S., Calay, D., Shiplu, S., Creppe, C., Hendrickx, J., & Schagdarsurengin, U. (2021). H4K20me3 marks distal intergenic and repetitive regions in human mature spermatozoa. *Development (Cambridge, England)*, *148*(15). https://doi.org/10.1242/dev.196477

Padavattan, S., Thiruselvam, V., Shinagawa, T., Hasegawa, K., Kumasaka, T., Ishii, S., & Kumarevel, T. (2017). Structural analyses of the nucleosome complexes with human testis-specific histone variants, hTh2a and hTh2b. *Biophysical Chemistry*, *221*, 41–48. https://doi.org/10.1016/j.bpc.2016.11.013

Palmer, N. O., Fullston, T., Mitchell, M., Setchell, B. P., & Lane, M. (2011). SIRT6 in mouse spermatogenesis is modulated by diet-induced obesity. *Reproduction, Fertility, and Development*, *23*(7), 929–939. https://doi.org/10.1071/RD10326

Papamichos-Chronakis, M., Watanabe, S., Rando, O. J., & Peterson, C. L. (2011). Global regulation of H2A.Z localization by the INO80 chromatin-remodeling enzyme is essential for genome integrity. *Cell*, *144*(2), 200–213. https://doi.org/10.1016/j.cell.2010.12.021

Papoutsopoulou, S., Nikolakaki, E., Chalepakis, G., Kruft, V., Chevaillier, P., & Giannakouros, T. (1999). SR protein-specific kinase 1 is highly expressed in testis and phosphorylates protamine 1. *Nucleic Acids Research*, *27*(14), 2972–2980. https://doi.org/10.1093/nar/27.14.2972

Patel, M., Sachidanandan, M., & Adnan, M. (2019). Serine arginine protein kinase 1 (SRPK1): a moonlighting protein with theranostic ability in cancer prevention. *Molecular Biology Reports*, *46*(1), 1487–1497. https://doi.org/10.1007/s11033-018-4545-5

Pattabiraman, S., Baumann, C., Guisado, D., Eppig, J. J., Schimenti, J. C., & De La Fuente, R. (2015). Mouse BRWD1 is critical for spermatid postmeiotic transcription and female meiotic chromosome stability. *The Journal of Cell Biology*, *208*(1), 53–69. https://doi.org/10.1083/jcb.201404109

Pentakota, S. K., Sandhya, S., P. Sikarwar, A., Chandra, N., & Satyanarayana Rao, M. R. (2014). Mapping Post-translational Modifications of Mammalian Testicular Specific Histone Variant TH2B in Tetraploid and Haploid Germ Cells and Their Implications on the Dynamics of Nucleosome Structure. *Journal of Proteome Research*, *13*(12), 5603–5617. https://doi.org/10.1021/pr500597a

Pepin, A.-S., Lafleur, C., Lambrot, R., Dumeaux, V., & Kimmins, S. (2022). Sperm histone H3 lysine 4 tri-methylation serves as a metabolic sensor of paternal obesity and is

associated with the inheritance of metabolic dysfunction. *Molecular Metabolism*, *59*, 101463. https://doi.org/10.1016/j.molmet.2022.101463

Pérez, C. v., Theas, M. S., Jacobo, P. v., Jarazo-Dietrich, S., Guazzone, V. A., & Lustig, L. (2013). Dual role of immune cells in the testis. *Spermatogenesis*, *3*(1), e23870. https://doi.org/10.4161/spmg.23870

Perissi, V., Scafoglio, C., Zhang, J., Ohgi, K. A., Rose, D. W., Glass, C. K., & Rosenfeld, M. G. (2008). TBL1 and TBLR1 phosphorylation on regulated gene promoters overcomes dual CtBP and NCoR/SMRT transcriptional repression checkpoints. *Molecular Cell*, *29*(6), 755–766. https://doi.org/10.1016/j.molcel.2008.01.020

Philipps, D. L., Wigglesworth, K., Hartford, S. A., Sun, F., Pattabiraman, S., Schimenti, K., Handel, M., Eppig, J. J., & Schimenti, J. C. (2008). The dual bromodomain and WD repeat-containing mouse protein BRWD1 is required for normal spermiogenesis and the oocyte-embryo transition. *Developmental Biology*, *317*(1), 72–82. https://doi.org/10.1016/j.ydbio.2008.02.018

Phillips, B. T., Williams, J. G., Atchley, D. T., Xu, X., Li, J.-L., Adams, A. L., Johnson, K. L., & Hall, T. M. T. (2019). Mass spectrometric identification of candidate RNA-binding proteins associated with Transition Nuclear Protein mRNA in the mouse testis. *Scientific Reports*, *9*(1), 13618. https://doi.org/10.1038/s41598-019-50052-z

Philpott, A., & Leno, G. H. (1992). Nucleoplasmin remodels sperm chromatin in Xenopus egg extracts. *Cell*, *69*(5), 759–767. https://doi.org/10.1016/0092-8674(92)90288-N

Picton, H. M., Wyns, C., Anderson, R. A., Goossens, E., Jahnukainen, K., Kliesch, S., Mitchell, R. T., Pennings, G., Rives, N., Tournaye, H., van Pelt, A. M. M., Eichenlaub-Ritter, U., & Schlatt, S. (2015). A European perspective on testicular tissue cryopreservation for fertility preservation in prepubertal and adolescent boys. *Human Reproduction*, *30*(11), 2463–2475. https://doi.org/10.1093/humrep/dev190

Pirhonen, A., Linnala-Kankkunen, A., & Mäenpää, P. H. (1994). Identification of phosphoseryl residues in protamines from mature mammalian spermatozoa. *Biology of Reproduction*, *50*(5), 981–986. https://doi.org/10.1095/biolreprod50.5.981

Pirhonen, A., Linnala-Kankkunen, A., & Mënpää, P. H. (1994). P2 protamines are phosphorylated in vitro by protein kinase C, whereas P1 protamines prefer cAMP-dependent protein kinase. A comparative study of five mammalian species. *European Journal of Biochemistry*, *223*(1), 165–169. https://doi.org/10.1111/j.1432-1033.1994.tb18979.x

Pivot-Pajot, C., Caron, C., Govin, J., Vion, A., Rousseaux, S., & Khochbin, S. (2003). Acetylation-Dependent Chromatin Reorganization by BRDT, a Testis-Specific Bromodomain-Containing Protein. *Molecular and Cellular Biology*, *23*(15), 5354–5365. https://doi.org/10.1128/MCB.23.15.5354-5365.2003

Pohl, E., Gromoll, J., Wistuba, J., & Laurentino, S. (2021). Healthy ageing and spermatogenesis. *Reproduction*, *161*(4), R89–R101. https://doi.org/10.1530/REP-20-0633

Pradeepa, M. M., Nikhil, G., Hari Kishore, A., Bharath, G. N., Kundu, T. K., & Rao, M. R. S. (2009). Acetylation of transition protein 2 (TP2) by KAT3B (p300) alters its DNA condensation property and interaction with putative histone chaperone NPM3. *The Journal of Biological Chemistry*, *284*(43), 29956–29967. https://doi.org/10.1074/jbc.M109.052043

Pruslin, F. H., Imesch, E., Winston, R., & Rodman, T. C. (1987). Phosphorylation state of protamines 1 and 2 in human spermatids and spermatozoa. *Gamete Research*, *18*(2), 179–190. https://doi.org/10.1002/mrd.1120180208

Puga Molina, L. C., Luque, G. M., Balestrini, P. A., Marín-Briggiler, C. I., Romarowski, A., & Buffone, M. G. (2018). Molecular Basis of Human Sperm Capacitation. *Frontiers in Cell and Developmental Biology*, *6*. https://doi.org/10.3389/fcell.2018.00072

Qi, L., Liu, Z., Wang, J., Cui, Y., Guo, Y., Zhou, T., Zhou, Z., Guo, X., Xue, Y., & Sha, J. (2014). Systematic Analysis of the Phosphoproteome and Kinase-substrate Networks in the

Mouse Testis. *Molecular & Cellular Proteomics*, *13*(12), 3626–3638. https://doi.org/10.1074/mcp.M114.039073

Qian, M.-X., Pang, Y., Liu, C. H., Haratake, K., Du, B.-Y., Ji, D.-Y., Wang, G.-F., Zhu, Q.-Q., Song, W., Yu, Y., Zhang, X.-X., Huang, H.-T., Miao, S., Chen, L.-B., Zhang, Z.-H., Liang, Y.-N., Liu, S., Cha, H., Yang, D., … Qiu, X.-B. (2013). Acetylation-Mediated Proteasomal Degradation of Core Histones during DNA Repair and Spermatogenesis. *Cell*, *153*(5), 1012–1024. https://doi.org/10.1016/j.cell.2013.04.032

Quinn, M. M., Jalalian, L., Ribeiro, S., Ona, K., Demirci, U., Cedars, M. I., & Rosen, M. P. (2018). Microfluidic sorting selects sperm for clinical use with reduced DNA damage compared to density gradient centrifugation with swim-up in split semen samples. *Human Reproduction (Oxford, England)*, *33*(8), 1388–1393. https://doi.org/10.1093/humrep/dey239

Rajabi, H., Mohseni-kouchesfehani, H., Eslami-Arshaghi, T., & Salehi, M. (2018). Sperm DNA fragmentation affects epigenetic feature in human male pronucleus. *Andrologia*, *50*(1), e12800. https://doi.org/10.1111/and.12800

Rajpert-De Meyts, E., McGlynn, K. A., Okamoto, K., Jewett, M. A. S., & Bokemeyer, C. (2016). Testicular germ cell tumours. *The Lancet*, *387*(10029), 1762–1774. https://doi.org/10.1016/S0140-6736(15)00991-5

Raman, P., Rominger, M. C., Young, J. M., Molaro, A., Tsukiyama, T., & Malik, H. S. (2022). Novel Classes and Evolutionary Turnover of Histone H2B Variants in the Mammalian Germline. *Molecular Biology and Evolution*, *39*(2). https://doi.org/10.1093/molbev/msac019

Rashki Ghaleno, L., Alizadeh, A., Drevet, J. R., Shahverdi, A., & Valojerdi, M. R. (2021). Oxidation of Sperm DNA and Male Infertility. *Antioxidants (Basel, Switzerland)*, *10*(1). https://doi.org/10.3390/antiox10010097

Rathke, C., Baarends, W. M., Awe, S., & Renkawitz-Pohl, R. (2014). Chromatin dynamics during spermiogenesis. *Biochimica et Biophysica Acta (BBA) - Gene Regulatory Mechanisms*, *1839*(3), 155–168. https://doi.org/10.1016/j.bbagrm.2013.08.004

Ray-Gallet, D., Quivy, J.-P., Scamps, C., Martini, E. M.-D., Lipinski, M., & Almouzni, G. (2002). HIRA is critical for a nucleosome assembly pathway independent of DNA synthesis. *Molecular Cell*, *9*(5), 1091–1100. https://doi.org/10.1016/s1097-2765(02)00526-9

Reynoird, N., Schwartz, B. E., Delvecchio, M., Sadoul, K., Meyers, D., Mukherjee, C., Caron, C., Kimura, H., Rousseaux, S., Cole, P. A., Panne, D., French, C. A., & Khochbin, S. (2010). Oncogenesis by sequestration of CBP/p300 in transcriptionally inactive hyperacetylated chromatin domains. *The EMBO Journal*, *29*(17), 2943–2952. https://doi.org/10.1038/emboj.2010.176

Rezaei-Gazik, M., Vargas, A., Amiri-Yekta, A., Vitte, A.-L., Akbari, A., Barral, S., Esmaeili, V., Chuffart, F., Sadighi-Gilani, M. A., Couté, Y., Eftekhari-Yazdi, P., Khochbin, S., Rousseaux, S., & Totonchi, M. (2022). Direct visualization of pre-protamine 2 detects protamine assembly failures and predicts ICSI success. *Molecular Human Reproduction*, *28*(2). https://doi.org/10.1093/molehr/gaac004

Riel, J. M., Yamauchi, Y., Sugawara, A., Li, H. Y. J., Ruthig, V., Stoytcheva, Z., Ellis, P. J. I., Cocquet, J., & Ward, M. A. (2012). Deficiency of the multi-copy mouse Y gene *Sly* causes sperm DNA damage and abnormal chromatin packaging. *Journal of Cell Science*. https://doi.org/10.1242/jcs.114488

Risley, M. S., Einheber, S., & Bumcrot, D. A. (1986). Changes in DNA topology during spermatogenesis. *Chromosoma*, *94*(3), 217–227. https://doi.org/10.1007/BF00288496

Rivero-Hinojosa, S., Pugacheva, E. M., Kang, S., Méndez-Catalá, C. F., Kovalchuk, A. L., Strunnikov, A. V., Loukinov, D., Lee, J. T., & Lobanenkov, V. V. (2021). The combined action of CTCF and its testis-specific paralog BORIS is essential for spermatogenesis. *Nature Communications*, *12*(1), 3846. https://doi.org/10.1038/s41467-021-24140-6

Roque, A., Ponte, I., & Suau, P. (2011). Secondary structure of protamine in sperm nuclei: an infrared spectroscopy study. *BMC Structural Biology*, *11*, 14. https://doi.org/10.1186/1472-6807-11-14

Rousseaux, S., Reynoird, N., & Khochbin, S. (2022). NUT Is a Driver of p300-Mediated Histone Hyperacetylation: From Spermatogenesis to Cancer. *Cancers*, *14*(9), 2234. https://doi.org/10.3390/cancers14092234

Ruthenburg, A. J., Allis, C. D., & Wysocka, J. (2007). Methylation of lysine 4 on histone H3: intricacy of writing and reading a single epigenetic mark. *Molecular Cell*, *25*(1), 15–30. https://doi.org/10.1016/j.molcel.2006.12.014

Sabari, B. R., Zhang, D., Allis, C. D., & Zhao, Y. (2017). Metabolic regulation of gene expression through histone acylations. *Nature Reviews. Molecular Cell Biology*, *18*(2), 90–101. https://doi.org/10.1038/nrm.2016.140

Saida, M., Iles, D., Elnefati, A., Brinkworth, M., & Miller, D. (2011). Key gene regulatory sequences with distinctive ontological signatures associate with differentially endonuclease-accessible mouse sperm chromatin. *Reproduction (Cambridge, England)*, *142*(1), 73–86. https://doi.org/10.1530/REP-10-0536

Sakkas, D., & Alvarez, J. G. (2010). Sperm DNA fragmentation: mechanisms of origin, impact on reproductive outcome, and analysis. *Fertility and Sterility*, *93*(4), 1027–1036. https://doi.org/10.1016/j.fertnstert.2009.10.046

Salonia, A., Bettocchi, C., Boeri, L., Capogrosso, P., Carvalho, J., Cilesiz, N. C., Cocci, A., Corona, G., Dimitropoulos, K., Gül, M., Hatzichristodoulou, G., Jones, T. H., Kadioglu, A., Martínez Salamanca, J. I., Milenkovic, U., Modgil, V., Russo, G. I., Serefoglu, E. C., Tharakan, T., … Minhas, S. (2021). European Association of Urology Guidelines on Sexual and Reproductive Health—2021 Update: Male Sexual Dysfunction. *European Urology*, *80*(3), 333–357. https://doi.org/10.1016/j.eururo.2021.06.007

Saltzman, A. F., & Cost, N. G. (2018). Adolescent and Young Adult Testicular Germ Cell Tumors: Special Considerations. *Advances in Urology*, *2018*, 1–8. https://doi.org/10.1155/2018/2375176

Samans, B., Yang, Y., Krebs, S., Sarode, G. V., Blum, H., Reichenbach, M., Wolf, E., Steger, K., Dansranjavin, T., & Schagdarsurengin, U. (2014). Uniformity of nucleosome preservation pattern in Mammalian sperm and its connection to repetitive DNA elements. *Developmental Cell*, *30*(1), 23–35. https://doi.org/10.1016/j.devcel.2014.05.023

Sansone, A., di Dato, C., de Angelis, C., Menafra, D., Pozza, C., Pivonello, R., Isidori, A., & Gianfrilli, D. (2018). Smoke, alcohol and drug addiction and male fertility. *Reproductive Biology and Endocrinology: RB&E*, *16*(1), 3. https://doi.org/10.1186/s12958-018-0320-7

Sartori Blanc, N., Senn, A., Leforestier, A., Livolant, F., & Dubochet, J. (2001). DNA in Human and Stallion Spermatozoa Forms Local Hexagonal Packing with Twist and Many Defects. *Journal of Structural Biology*, *134*(1), 76–81. https://doi.org/10.1006/jsbi.2001.4365

Schneider, S., Balbach, M., Jan F Jikeli, Fietz, D., Nettersheim, D., Jostes, S., Schmidt, R., Kressin, M., Bergmann, M., Wachten, D., Steger, K., & Schorle, H. (2016). Re-visiting the Protamine-2 locus: deletion, but not haploinsufficiency, renders male mice infertile. *Scientific Reports*, *6*, 36764. https://doi.org/10.1038/srep36764

Schneider, S., Shakeri, F., Trötschel, C., Arévalo, L., Kruse, A., Buness, A., Poetsch, A., Steger, K., & Schorle, H. (2020). Protamine-2 Deficiency Initiates a Reactive Oxygen Species (ROS)-Mediated Destruction Cascade during Epididymal Sperm Maturation in Mice. *Cells*, *9*(8). https://doi.org/10.3390/cells9081789

Schoysman, R. J., & Bedford, J. M. (1986). The role of the human epididymis in sperm maturation and sperm storage as reflected in the consequences of epididymovasostomy. *Fertility and Sterility*, *46*(2), 293–299. https://doi.org/10.1016/s0015-0282(16)49528-2

Schulze, W., & Rehder, U. (1984). Organization and morphogenesis of the human seminiferous epithelium. *Cell and Tissue Research*, *237*(3). https://doi.org/10.1007/BF00228424

Seet, B. T., Dikic, I., Zhou, M.-M., & Pawson, T. (2006). Reading protein modifications with interaction domains. *Nature Reviews Molecular Cell Biology*, *7*(7), 473–483. https://doi.org/10.1038/nrm1960

Shang, E., Nickerson, H. D., Wen, D., Wang, X., & Wolgemuth, D. J. (2007). The first bromodomain of Brdt, a testis-specific member of the BET sub-family of double-bromodomain-containing proteins, is essential for male germ cell differentiation. *Development*, *134*(19), 3507–3515. https://doi.org/10.1242/dev.004481

Sharma, A., Minhas, S., Dhillo, W. S., & Jayasena, C. N. (2021). Male infertility due to testicular disorders. *The Journal of Clinical Endocrinology & Metabolism*, *106*(2), e442–e459. https://doi.org/10.1210/clinem/dgaa781

Sharma, R., & Agarwal, A. (2011). Spermatogenesis: An Overview. In *Sperm Chromatin* (pp. 19–44). Springer New York. https://doi.org/10.1007/978-1-4419-6857-9_2

Sharma, R., Biedenharn, K. R., Fedor, J. M., & Agarwal, A. (2013). Lifestyle factors and reproductive health: taking control of your fertility. *Reproductive Biology and Endocrinology: RB&E*, *11*, 66. https://doi.org/10.1186/1477-7827-11-66

Shinagawa, T., Huynh, L. M., Takagi, T., Tsukamoto, D., Tomaru, C., Kwak, H.-G., Dohmae, N., Noguchi, J., & Ishii, S. (2015). Disruption of *Th2a* and *Th2b* genes causes defects in spermatogenesis. *Development*. https://doi.org/10.1242/dev.121830

Shinagawa, T., Takagi, T., Tsukamoto, D., Tomaru, C., Huynh, L. M., Sivaraman, P., Kumarevel, T., Inoue, K., Nakato, R., Katou, Y., Sado, T., Takahashi, S., Ogura, A., Shirahige, K., & Ishii, S. (2014). Histone Variants Enriched in Oocytes Enhance Reprogramming to Induced Pluripotent Stem Cells. *Cell Stem Cell*, *14*(2), 217–227. https://doi.org/10.1016/j.stem.2013.12.015

Shiota, H., Barral, S., Buchou, T., Tan, M., Couté, Y., Charbonnier, G., Reynoird, N., Boussouar, F., Gérard, M., Zhu, M., Bargier, L., Puthier, D., Chuffart, F., Bourova-Flin, E., Picaud, S., Filippakopoulos, P., Goudarzi, A., Ibrahim, Z., Panne, D., … Khochbin, S. (2018). Nut Directs p300-Dependent, Genome-Wide H4 Hyperacetylation in Male Germ Cells. *Cell Reports*, *24*(13), 3477–3487.e6. https://doi.org/10.1016/j.celrep.2018.08.069

Shirley, C. R., Hayashi, S., Mounsey, S., Yanagimachi, R., & Meistrich, M. L. (2004). Abnormalities and Reduced Reproductive Potential of Sperm from Tnp1- and Tnp2-Null Double Mutant Mice1. *Biology of Reproduction*, *71*(4), 1220–1229. https://doi.org/10.1095/biolreprod.104.029363

Shmueli, M. D., Sheban, D., Eisenberg-Lerner, A., & Merbl, Y. (2021). Histone degradation by the proteasome regulates chromatin and cellular plasticity. *The FEBS Journal*. https://doi.org/10.1111/febs.15903

Siklenka, K., Erkek, S., Godmann, M., Lambrot, R., McGraw, S., Lafleur, C., Cohen, T., Xia, J., Suderman, M., Hallett, M., Trasler, J., Peters, A. H. F. M., & Kimmins, S. (2015). Disruption of histone methylation in developing sperm impairs offspring health transgenerationally. *Science (New York, N.Y.)*, *350*(6261), aab2006. https://doi.org/10.1126/science.aab2006

Simon, L., Aston, K. I., Emery, B. R., Hotaling, J., & Carrell, D. (2017). Sperm DNA damage output parameters measured by the alkaline Comet assay and their importance. *Andrologia*, *49*(2). https://doi.org/10.1111/and.12608

Simon, L., Emery, B., & Carrell, D. T. (2019). *Sperm DNA Fragmentation: Consequences for Reproduction* (pp. 87–105). https://doi.org/10.1007/978-3-030-21664-1_6

Simopoulou, M., Gkoles, L., Bakas, P., Giannelou, P., Kalampokas, T., Pantos, K., & Koutsilieris, M. (2016). Improving ICSI: A review from the spermatozoon perspective. *Systems Biology in Reproductive Medicine*, *62*(6), 359–371. https://doi.org/10.1080/19396368.2016.1229365

Singh, I., & Parte, P. (2021). Heterogeneity in the Epigenetic Landscape of Murine Testis-Specific Histone Variants TH2A and TH2B Sharing the Same Bi-Directional Promoter. *Frontiers in Cell and Developmental Biology*, *9*. https://doi.org/10.3389/fcell.2021.755751

Singh, J., & Rao, M. R. (1988). Interaction of rat testis protein, TP, with nucleosome core particle. *Biochemistry International*, *17*(4), 701–710.

Skakkebaek, N. E., Jørgensen, N., Andersson, A.-M., Juul, A., Main, K. M., Jensen, T. K., & Toppari, J. (2019). Populations, decreasing fertility, and reproductive health. *The Lancet*, *393*(10180), 1500–1501. https://doi.org/10.1016/S0140-6736(19)30690-7

Skakkebaek, N. E., Rajpert-De Meyts, E., Buck Louis, G. M., Toppari, J., Andersson, A.-M., Eisenberg, M. L., Jensen, T. K., Jørgensen, N., Swan, S. H., Sapra, K. J., Ziebe, S., Priskorn, L., & Juul, A. (2016a). Male Reproductive Disorders and Fertility Trends: Influences of Environment and Genetic Susceptibility. *Physiological Reviews*, *96*(1), 55–97. https://doi.org/10.1152/physrev.00017.2015

Skakkebaek, N. E., Rajpert-De Meyts, E., Buck Louis, G. M., Toppari, J., Andersson, A.-M., Eisenberg, M. L., Jensen, T. K., Jørgensen, N., Swan, S. H., Sapra, K. J., Ziebe, S., Priskorn, L., & Juul, A. (2016b). Male Reproductive Disorders and Fertility Trends: Influences of Environment and Genetic Susceptibility. *Physiological Reviews*, *96*(1), 55–97. https://doi.org/10.1152/physrev.00017.2015

Skakkebæk, N. E., Rajpert-De Meyts, E., & Main, K. M. (2001). Testicular dysgenesis syndrome: an increasingly common developmental disorder with environmental aspects: Opinion. *Human Reproduction*, *16*(5), 972–978. https://doi.org/10.1093/humrep/16.5.972

Soler-Ventura, A., Castillo, J., de la Iglesia, A., Jodar, M., Barrachina, F., Ballesca, J. L., & Oliva, R. (2018). Mammalian Sperm Protamine Extraction and Analysis: A Step-By-Step Detailed Protocol and Brief Review of Protamine Alterations. *Protein and Peptide Letters*, *25*(5), 424–433. https://doi.org/10.2174/0929866525666180412155205

Soler-Ventura, A., Gay, M., Jodar, M., Vilanova, M., Castillo, J., Arauz-Garofalo, G., Villarreal, L., Ballescà, J. L., Vilaseca, M., & Oliva, R. (2020). Characterization of Human Sperm Protamine Proteoforms through a Combination of Top-Down and Bottom-Up Mass Spectrometry Approaches. *Journal of Proteome Research*, *19*(1), 221–237. https://doi.org/10.1021/acs.jproteome.9b00499

Song, H., Wang, L., Chen, D., & Li, F. (2020). The Function of Pre-mRNA Alternative Splicing in Mammal Spermatogenesis. *International Journal of Biological Sciences*, *16*(1), 38–48. https://doi.org/10.7150/ijbs.34422

Sonnack, V., Failing, K., Bergmann, M., & Steger, K. (2002). Expression of hyperacetylated histone H4 during normal and impaired human spermatogenesis. *Andrologia*, *34*(6), 384–390. https://doi.org/10.1046/j.1439-0272.2002.00524.x

Soubry, A., Guo, L., Huang, Z., Hoyo, C., Romanus, S., Price, T., & Murphy, S. K. (2016). Obesity-related DNA methylation at imprinted genes in human sperm: Results from the TIEGER study. *Clinical Epigenetics*, *8*(1), 51. https://doi.org/10.1186/s13148-016-0217-2

Soubry, A., Schildkraut, J. M., Murtha, A., Wang, F., Huang, Z., Bernal, A., Kurtzberg, J., Jirtle, R. L., Murphy, S. K., & Hoyo, C. (2013). Paternal obesity is associated with IGF2 hypomethylation in newborns: results from a Newborn Epigenetics Study (NEST) cohort. *BMC Medicine*, *11*, 29. https://doi.org/10.1186/1741-7015-11-29

Soupsana, K., Karanika, E., Kiosse, F., Christogianni, A., Sfikas, Y., Topalis, P., Batistatou, A., Kanaki, Z., Klinakis, A., Politou, A. S., & Georgatos, S. (2021). Distinct roles of haspin in stem cell division and male gametogenesis. *Scientific Reports*, *11*(1), 19901. https://doi.org/10.1038/s41598-021-99307-8

Spiridonov, N. A., Wong, L., Zerfas, P. M., Starost, M. F., Pack, S. D., Paweletz, C. P., & Johnson, G. R. (2005). Identification and Characterization of SSTK, a Serine/Threonine Protein

Kinase Essential for Male Fertility. *Molecular and Cellular Biology*, *25*(10), 4250–4261. https://doi.org/10.1128/MCB.25.10.4250-4261.2005

Steilmann, C., Paradowska, A., Bartkuhn, M., Vieweg, M., Schuppe, H.-C., Bergmann, M., Kliesch, S., Weidner, W., & Steger, K. (2011). Presence of histone H3 acetylated at lysine 9 in male germ cells and its distribution pattern in the genome of human spermatozoa. *Reproduction, Fertility and Development*, *23*(8), 997. https://doi.org/10.1071/RD10197

Strahl, B. D., & Allis, C. D. (2000). The language of covalent histone modifications. *Nature*, *403*(6765), 41–45. https://doi.org/10.1038/47412

Subirana, J. A. (1983). Proceedings of the Fourth International Symposium on Spermatology. In *The sperm cell* (pp. 197–213). Martinus Nijhoff Pub The Hague (The Netherlands).

Subirana, J. A. (1997). A crystallographic approach to DNA bending: prediction of nucleosome formation by DNA triple repeats and other repetitive sequences. *FEBS Letters*, *417*(3), 352–354. https://doi.org/10.1016/S0014-5793(97)01317-3

Subirana, J. A., Muñoz-Guerra, S., Aymamí, J., Radermacher, M., & Frank, J. (1985). The layered organization of nucleosomes in 30 nm chromatin fibers. *Chromosoma*, *91*(5), 377–390. https://doi.org/10.1007/BF00291012

Suzuki, K., Shin, T., Shimomura, Y., Iwahata, T., & Okada, H. (2015). Spermatogenesis in tumor-bearing testes in germ cell testicular cancer patients. *Human Reproduction*, *30*(12), 2853–2858. https://doi.org/10.1093/humrep/dev250

Tachiwana, H., Kagawa, W., Osakabe, A., Kawaguchi, K., Shiga, T., Hayashi-Takanaka, Y., Kimura, H., & Kurumizaka, H. (2010). Structural basis of instability of the nucleosome containing a testis-specific histone variant, human H3T. *Proceedings of the National Academy of Sciences*, *107*(23), 10454–10459. https://doi.org/10.1073/pnas.1003064107

Tagami, H., Ray-Gallet, D., Almouzni, G., & Nakatani, Y. (2004). Histone H3.1 and H3.3 Complexes Mediate Nucleosome Assembly Pathways Dependent or Independent of DNA Synthesis. *Cell*, *116*(1), 51–61. https://doi.org/10.1016/S0092-8674(03)01064-X

Takeda, N., Yoshinaga, K., Furushima, K., Takamune, K., Li, Z., Abe, S., Aizawa, S., & Yamamura, K. (2016). Viable offspring obtained from Prm1-deficient sperm in mice. *Scientific Reports*, *6*(1), 27409. https://doi.org/10.1038/srep27409

Tan, M., Luo, H., Lee, S., Jin, F., Yang, J. S., Montellier, E., Buchou, T., Cheng, Z., Rousseaux, S., Rajagopal, N., Lu, Z., Ye, Z., Zhu, Q., Wysocka, J., Ye, Y., Khochbin, S., Ren, B., & Zhao, Y. (2011). Identification of 67 Histone Marks and Histone Lysine Crotonylation as a New Type of Histone Modification. *Cell*, *146*(6), 1016–1028. https://doi.org/10.1016/j.cell.2011.08.008

Tang, M. C. W., Jacobs, S. A., Mattiske, D. M., Soh, Y. M., Graham, A. N., Tran, A., Lim, S. L., Hudson, D. F., Kalitsis, P., O'Bryan, M. K., Wong, L. H., & Mann, J. R. (2015). Contribution of the Two Genes Encoding Histone Variant H3.3 to Viability and Fertility in Mice. *PLOS Genetics*, *11*(2), e1004964. https://doi.org/10.1371/journal.pgen.1004964

Teperek, M., Simeone, A., Gaggioli, V., Miyamoto, K., Allen, G. E., Erkek, S., Kwon, T., Marcotte, E. M., Zegerman, P., Bradshaw, C. R., Peters, A. H. F. M., Gurdon, J. B., & Jullien, J. (2016). Sperm is epigenetically programmed to regulate gene transcription in embryos. *Genome Research*, *26*(8), 1034–1046. https://doi.org/10.1101/gr.201541.115

Terashima, M., Barbour, S., Ren, J., Yu, W., Han, Y., & Muegge, K. (2015). Effect of high fat diet on paternal sperm histone distribution and male offspring liver gene expression. *Epigenetics*, *10*(9), 861–871. https://doi.org/10.1080/15592294.2015.1075691

Tiegs, A. W., Landis, J., Garrido, N., Scott, R., & Hotaling, J. (2018). Total motile sperm count trend over time across two continents: evaluation of semen analyses from 119,972 infertile men. *Fertility and Sterility*, *110*(4), e27. https://doi.org/10.1016/j.fertnstert.2018.07.093

Toshimori, K., & Ito, C. (2003). Formation and organization of the mammalian sperm head. *Archives of Histology and Cytology*, *66*(5), 383–396. https://doi.org/10.1679/aohc.66.383

Tsai-Morris, C.-H., Sheng, Y., Lee, E., Lei, K.-J., & Dufau, M. L. (2004). Gonadotropin-regulated testicular RNA helicase (GRTH/Ddx25) is essential for spermatid development and completion of spermatogenesis. *Proceedings of the National Academy of Sciences*, *101*(17), 6373–6378. https://doi.org/10.1073/pnas.0401855101

Uchida, K., Sakai, K., Itakura, K., Osawa, T., & Toyokuni, S. (1997). Protein Modification by Lipid Peroxidation Products: Formation of Malondialdehyde-DerivedNε-(2-Propenal)lysine in Proteins. *Archives of Biochemistry and Biophysics*, *346*(1), 45–52. https://doi.org/10.1006/abbi.1997.0266

Ueda, J., Harada, A., Urahama, T., Machida, S., Maehara, K., Hada, M., Makino, Y., Nogami, J., Horikoshi, N., Osakabe, A., Taguchi, H., Tanaka, H., Tachiwana, H., Yao, T., Yamada, M., Iwamoto, T., Isotani, A., Ikawa, M., Tachibana, T., … Yamagata, K. (2017). Testis-Specific Histone Variant H3t Gene Is Essential for Entry into Spermatogenesis. *Cell Reports*, *18*(3), 593–600. https://doi.org/10.1016/j.celrep.2016.12.065

Urahama, T., Harada, A., Maehara, K., Horikoshi, N., Sato, K., Sato, Y., Shiraishi, K., Sugino, N., Osakabe, A., Tachiwana, H., Kagawa, W., Kimura, H., Ohkawa, Y., & Kurumizaka, H. (2016). Histone H3.5 forms an unstable nucleosome and accumulates around transcription start sites in human testis. *Epigenetics & Chromatin*, *9*(1), 2. https://doi.org/10.1186/s13072-016-0051-y

Utley, R. T., Lacoste, N., Jobin-Robitaille, O., Allard, S., & Côté, J. (2005). Regulation of NuA4 Histone Acetyltransferase Activity in Transcription and DNA Repair by Phosphorylation of Histone H4. *Molecular and Cellular Biology*, *25*(18), 8179–8190. https://doi.org/10.1128/MCB.25.18.8179-8190.2005

van der Heijden, G. W., Dieker, J. W., Derijck, A. A. H. A., Muller, S., Berden, J. H. M., Braat, D. D. M., van der Vlag, J., & de Boer, P. (2005). Asymmetry in Histone H3 variants and lysine methylation between paternal and maternal chromatin of the early mouse zygote. *Mechanisms of Development*, *122*(9), 1008–1022. https://doi.org/10.1016/j.mod.2005.04.009

Vara, C., Paytuví-Gallart, A., Cuartero, Y., le Dily, F., Garcia, F., Salvà-Castro, J., Gómez-H, L., Julià, E., Moutinho, C., Aiese Cigliano, R., Sanseverino, W., Fornas, O., Pendás, A. M., Heyn, H., Waters, P. D., Marti-Renom, M. A., & Ruiz-Herrera, A. (2019). Three-Dimensional Genomic Structure and Cohesin Occupancy Correlate with Transcriptional Activity during Spermatogenesis. *Cell Reports*, *28*(2), 352–367.e9. https://doi.org/10.1016/j.celrep.2019.06.037

Vavouri, T., & Lehner, B. (2011). Chromatin organization in sperm may be the major functional consequence of base composition variation in the human genome. *PLoS Genetics*, *7*(4), e1002036. https://doi.org/10.1371/journal.pgen.1002036

Vilfan, I. D., Conwell, C. C., & Hud, N. v. (2004). Formation of Native-like Mammalian Sperm Cell Chromatin with Folded Bull Protamine. *Journal of Biological Chemistry*, *279*(19), 20088–20095. https://doi.org/10.1074/jbc.M312777200

Vilfan, I. D., Conwell, C. C., Sarkar, T., & Hud, N. v. (2006). Time Study of DNA Condensate Morphology: Implications Regarding the Nucleation, Growth, and Equilibrium Populations of Toroids and Rods. *Biochemistry*, *45*(26), 8174–8183. https://doi.org/10.1021/bi060396c

Vollmuth, F., & Geyer, M. (2010). Interaction of Propionylated and Butyrylated Histone H3 Lysine Marks with Brd4 Bromodomains. *Angewandte Chemie International Edition*, *49*(38), 6768–6772. https://doi.org/10.1002/anie.201002724

Wang, H., Huang, Z.-Q., Xia, L., Feng, Q., Erdjument-Bromage, H., Strahl, B. D., Briggs, S. D., Allis, C. D., Wong, J., Tempst, P., & Zhang, Y. (2001). Methylation of Histone H4 at Arginine 3 Facilitating Transcriptional Activation by Nuclear Hormone Receptor. *Science*, *293*(5531), 853–857. https://doi.org/10.1126/science.1060781

Wang, T., Gao, H., Li, W., & Liu, C. (2019). Essential Role of Histone Replacement and Modifications in Male Fertility. *Frontiers in Genetics*, *10*. https://doi.org/10.3389/fgene.2019.00962

Wang, X., Kang, J.-Y., Wei, L., Yang, X., Sun, H., Yang, S., Lu, L., Yan, M., Bai, M., Chen, Y., Long, J., Li, N., Li, D., Huang, J., Lei, M., Shao, Z., Yuan, W., Zuo, E., Lu, K., … Li, J. (2019). PHF7 is a novel histone H2A E3 ligase prior to histone-to-protamine exchange during spermiogenesis. *Development*. https://doi.org/10.1242/dev.175547

Wang, Y., Wang, H., Zhang, Y., Du, Z., Si, W., Fan, S., Qin, D., Wang, M., Duan, Y., Li, L., Jiao, Y., Li, Y., Wang, Q., Shi, Q., Wu, X., & Xie, W. (2019). Reprogramming of Meiotic Chromatin Architecture during Spermatogenesis. *Molecular Cell*, *73*(3), 547-561.e6. https://doi.org/10.1016/j.molcel.2018.11.019

Warrant, R. W., & Kim, S.-H. (1978). α-Helix-double helix interaction shown in the structure of a protamine-transfer RNA complex and a nucleoprotamine model. *Nature*, *271*(5641), 130–135. https://doi.org/10.1038/271130a0

Wike, C. L., Guo, Y., Tan, M., Nakamura, R., Shaw, D. K., Díaz, N., Whittaker-Tademy, A. F., Durand, N. C., Aiden, E. L., Vaquerizas, J. M., Grunwald, D., Takeda, H., & Cairns, B. R. (2021). Chromatin architecture transitions from zebrafish sperm through early embryogenesis. *Genome Research*, *31*(6), 981–994. https://doi.org/10.1101/gr.269860.120

Williamson, S. R., Delahunt, B., Magi-Galluzzi, C., Algaba, F., Egevad, L., Ulbright, T. M., Tickoo, S. K., Srigley, J. R., Epstein, J. I., Berney, D. M., & Members of the ISUP Testicular Tumour Panel. (2017). The World Health Organization 2016 classification of testicular germ cell tumours: a review and update from the International Society of Urological Pathology Testis Consultation Panel. *Histopathology*, *70*(3), 335–346. https://doi.org/10.1111/his.13102

Willmitzer, L., Bode, J., & Wagner, K. G. (1977a). Phosphorylated protamines. I. Binding stoichiometry and thermal stability of complexes in DNA. *Nucleic Acids Research*, *4*(1), 149–162. https://doi.org/10.1093/nar/4.1.149

Willmitzer, L., Bode, J., & Wagner, K. G. (1977b). Phosphorylated protamines. II. Circular dichroism of complexes with DNA, dependency on ionic strength. *Nucleic Acids Research*, *4*(1), 163–176. https://doi.org/10.1093/nar/4.1.163

Wirbelauer, C., Bell, O., & Schübeler, D. (2005). Variant histone H3.3 is deposited at sites of nucleosomal displacement throughout transcribed genes while active histone modifications show a promoter-proximal bias. *Genes & Development*, *19*(15), 1761–1766. https://doi.org/10.1101/gad.347705

World Health Organization. (2021). *WHO laboratory manual for the examination and processing of human semen, sixth edition*. World Health Organization; 2021. License: CC BY-NC-SA 3.0 IGO.

World Health Organization. (2022). *International Classification of Diseases: Mortality and Morbidity Statistics, Eleventh Revision (ICD-11)*. World Health Organization. License: CC BY-ND 3.0 IGO.

Wu, J. Y., Ribar, T. J., Cummings, D. E., Burton, K. A., McKnight, G. S., & Means, A. R. (2000). Spermiogenesis and exchange of basic nuclear proteins are impaired in male germ cells lacking Camk4. *Nature Genetics*, *25*(4), 448–452. https://doi.org/10.1038/78153

Wu, Y., Hu, X., Li, Z., Wang, M., Li, S., Wang, X., Lin, X., Liao, S., Zhang, Z., Feng, X., Wang, S., Cui, X., Wang, Y., Gao, F., Hess, R. A., & Han, C. (2016). Transcription Factor RFX2 Is a Key Regulator of Mouse Spermiogenesis. *Scientific Reports*, *6*(1), 20435. https://doi.org/10.1038/srep20435

Xavier, R., de Carvalho, R. C., & Fraietta, R. (2021). Semen quality from patients affected by seminomatous and non-seminomatous testicular tumor. *International Braz j Urol: Official Journal of the Brazilian Society of Urology*, *47*(3), 495—502. https://doi.org/10.1590/s1677-5538.ibju.2021.99.01

Xia, X., Zhou, X., Quan, Y., Hu, Y., Xing, F., Li, Z., Xu, B., Xu, C., & Zhang, A. (2019). Germline deletion of Cdyl causes teratozoospermia and progressive infertility in male mice. *Cell Death & Disease*, *10*(3), 229. https://doi.org/10.1038/s41419-019-1455-y

Xu, K., Yang, L., Zhao, D., Wu, Y., & Qi, H. (2014). AKAP3 Synthesis Is Mediated by RNA Binding Proteins and PKA Signaling During Mouse Spermiogenesis1. *Biology of Reproduction*, *90*(6). https://doi.org/10.1095/biolreprod.113.116111

Xue, X., Wang, W.-S., Shi, J.-Z., Zhang, S.-L., Zhao, W.-Q., Shi, W.-H., Guo, B.-Z., & Qin, Z. (2014). Efficacy of swim-up versus density gradient centrifugation in improving sperm deformity rate and DNA fragmentation index in semen samples from teratozoospermic patients. *Journal of Assisted Reproduction and Genetics*, *31*(9), 1161–1166. https://doi.org/10.1007/s10815-014-0287-z

Yamaguchi, K., Hada, M., Fukuda, Y., Inoue, E., Makino, Y., Katou, Y., Shirahige, K., & Okada, Y. (2018). Re-evaluating the Localization of Sperm-Retained Histones Revealed the Modification-Dependent Accumulation in Specific Genome Regions. *Cell Reports*, *23*(13), 3920–3932. https://doi.org/10.1016/j.celrep.2018.05.094

Yassine, S., Escoffier, J., Martinez, G., Coutton, C., Karaouzène, T., Zouari, R., Ravanat, J.-L., Metzler-Guillemain, C., Lee, H. C., Fissore, R., Hennebicq, S., Ray, P. F., & Arnoult, C. (2015). Dpy19l2-deficient globozoospermic sperm display altered genome packaging and DNA damage that compromises the initiation of embryo development. *Molecular Human Reproduction*, *21*(2), 169–185. https://doi.org/10.1093/molehr/gau099

Yifu, P., Lei, Y., Shaoming, L., Yujin, G., & Xingwang, Z. (2020). Sperm DNA fragmentation index with unexplained recurrent spontaneous abortion: A systematic review and meta-analysis. *Journal of Gynecology Obstetrics and Human Reproduction*, *49*(10), 101740. https://doi.org/10.1016/j.jogoh.2020.101740

Yin, H., Kang, Z., Zhang, Y., Gong, Y., Liu, M., Xue, Y., He, W., Wang, Y., Zhang, S., Xu, Q., Fu, K., Zheng, B., Xie, J., Zhang, J., Wang, Y., Lin, M., Zhang, Y., Feng, H., Xin, C., … Ye, L. (2021). HDAC3 controls male fertility through enzyme-independent transcriptional regulation at the meiotic exit of spermatogenesis. *Nucleic Acids Research*, *49*(9), 5106–5123. https://doi.org/10.1093/nar/gkab313

Yoon, H.-G., Chan, D. W., Huang, Z.-Q., Li, J., Fondell, J. D., Qin, J., & Wong, J. (2003). Purification and functional characterization of the human N-CoR complex: the roles of HDAC3, TBL1 and TBLR1. *The EMBO Journal*, *22*(6), 1336–1346. https://doi.org/10.1093/emboj/cdg120

Yoshida, K., Muratani, M., Araki, H., Miura, F., Suzuki, T., Dohmae, N., Katou, Y., Shirahige, K., Ito, T., & Ishii, S. (2018). Mapping of histone-binding sites in histone replacement-completed spermatozoa. *Nature Communications*, *9*(1), 3885. https://doi.org/10.1038/s41467-018-06243-9

Yu, Y. E., Zhang, Y., Unni, E., Shirley, C. R., Deng, J. M., Russell, L. D., Weil, M. M., Behringer, R. R., & Meistrich, M. L. (2000). Abnormal spermatogenesis and reduced fertility in transition nuclear protein 1-deficient mice. *Proceedings of the National Academy of Sciences*, *97*(9), 4683–4688. https://doi.org/10.1073/pnas.97.9.4683

Yuen, B. T. K., Bush, K. M., Barrilleaux, B. L., Cotterman, R., & Knoepfler, P. S. (2014). Histone H3.3 regulates dynamic chromatin states during spermatogenesis. *Development*, *141*(18), 3483–3494. https://doi.org/10.1242/dev.106450

Zhang, D., Xie, D., Lin, X., Ma, L., Chen, J., Zhang, D., Wang, Y., Duo, S., Feng, Y., Zheng, C., Jiang, B., Ning, Y., & Han, C. (2018). The transcription factor SOX30 is a key regulator of mouse spermiogenesis. *Development (Cambridge, England)*, *145*(11). https://doi.org/10.1242/dev.164723

Zhao, M., Shirley, C. R., Mounsey, S., & Meistrich, M. L. (2004). Nucleoprotein Transitions During Spermiogenesis in Mice with Transition Nuclear Protein Tnp1 and Tnp2 Mutations1. *Biology of Reproduction*, *71*(3), 1016–1025. https://doi.org/10.1095/biolreprod.104.028191

Zhao, M., Shirley, C. R., Yu, Y. E., Mohapatra, B., Zhang, Y., Unni, E., Deng, J. M., Arango, N. A., Terry, N. H. A., Weil, M. M., Russell, L. D., Behringer, R. R., & Meistrich, M. L. (2001). Targeted Disruption of the Transition Protein 2 Gene Affects Sperm Chromatin Structure and Reduces Fertility in Mice. *Molecular and Cellular Biology*, *21*(21), 7243–7255. https://doi.org/10.1128/MCB.21.21.7243-7255.2001

Zhong, J., Peters, A. H. F. M., Lee, K., & Braun, R. E. (1999). A double-stranded RNA binding protein required for activation of repressed messages in mammalian germ cells. *Nature Genetics*, *22*(2), 171–174. https://doi.org/10.1038/9684

Zhou, H., Grubisic, I., Zheng, K., He, Y., Wang, P. J., Kaplan, T., & Tjian, R. (2013). Taf7l cooperates with Trf2 to regulate spermiogenesis. *Proceedings of the National Academy of Sciences of the United States of America*, *110*(42), 16886–16891. https://doi.org/10.1073/pnas.1317034110

Zhuang, T., Hess, R. A., Kolla, V., Higashi, M., Raabe, T. D., & Brodeur, G. M. (2014). CHD5 is required for spermiogenesis and chromatin condensation. *Mechanisms of Development*, *131*, 35–46. https://doi.org/10.1016/j.mod.2013.10.005

Živković, D., Sanchez Dafun, A., Menneteau, T., Schahl, A., Lise, S., Kervarrec, C., Toste Rêgo, A., da Fonseca, P. C. A., Chavent, M., Pineau, C., Burlet-Schiltz, O., Marcoux, J., & Bousquet, M.-P. (2022). Proteasome complexes experience profound structural and functional rearrangements throughout mammalian spermatogenesis. *Proceedings of the National Academy of Sciences*, *119*(15). https://doi.org/10.1073/pnas.2116826119

Zuo, X., Rong, B., Li, L., Lv, R., Lan, F., & Tong, M.-H. (2018). The histone methyltransferase SETD2 is required for expression of acrosin-binding protein 1 and protamines and essential for spermiogenesis in mice. *Journal of Biological Chemistry*, *293*(24), 9188–9197. https://doi.org/10.1074/jbc.RA118.002851

9.

APPENDIX

9.1 Appendix 1: Insights into the sperm chromatin and implications for male infertility from a protein perspective

Review accepted for publication as:

de la Iglesia A[1], Jodar M[1,3], Castillo J[1,*], Oliva R[1,3,*]. Insights into the sperm chromatin and implications for male infertility from a protein perspective. *WIREs Mech Dis*[†]. 2022. Accepted for publication (September 12th, 2022)

First author

[1] Molecular Biology of Reproduction and Development Research Group, Department of Biomedical Sciences, Faculty of Medicine and Health Sciences, Institut d'Investigacions Biomèdiques August Pi i Sunyer (IDIBAPS), Fundació Clínic per a la Recerca Biomèdica, Universitat de Barcelona, Barcelona, Spain.

[2] Institut Cochin–Inserm U1016–CNRS UMR8104–Université de Paris, Paris, France

[3] Biochemistry and Molecular Genetics Service, Hospital Clínic de Barcelona, Barcelona, Spain.

* Corresponding authors

[†] Previously named Wiley Interdisciplinary Reviews–Systems Biology and Medicine (ISSN 1939–5094, **IF 7.288, Q1 in the category of Medicine, Research & Experimental**)

WIREs
Wiley Interdisciplinary Reviews

Article Title: Insights into the sperm chromatin and implications for male infertility from a protein perspective.

Authors:

First author full name Alberto de la Iglesia Molecular Biology of Reproduction and Development Research Group, Institut d'Investigacions Biomèdiques August Pi i Sunyer (IDIBAPS), Fundació Clínic per a la Recerca Biomèdica, Departament de Biomedicina, Facultat de Medicina i Ciències de la Salut, Universitat de Barcelona (UB), Barcelona, Spain adelaiglesia@ub.edu ORCID iD: 0000-0003-3475-2086
Second author full name Meritxell Jodar Molecular Biology of Reproduction and Development Research Group, Institut d'Investigacions Biomèdiques August Pi i Sunyer (IDIBAPS), Fundació Clínic per a la Recerca Biomèdica, Departament de Biomedicina, Facultat de Medicina i Ciències de la Salut, Universitat de Barcelona (UB), Barcelona, Spain Biochemistry and Molecular Genetics Service, Hospital Clinic, Barcelona, Spain meritxell.jodar@ub.edu ORCID iD: 0000-0002-3272-0163
Third author full name Rafael Oliva * Molecular Biology of Reproduction and Development Research Group, Institut d'Investigacions Biomèdiques August Pi i Sunyer (IDIBAPS), Fundació Clínic per a la Recerca Biomèdica, Departament de Biomedicina, Facultat de Medicina i Ciències de la Salut, Universitat de Barcelona (UB), Barcelona, Spain Biochemistry and Molecular Genetics Service, Hospital Clinic, Barcelona, Spain roliva@ub.edu ORCID iD: 0000-0003-4876-2410
Last author full name Judit Castillo * Molecular Biology of Reproduction and Development Research Group, Institut d'Investigacions Biomèdiques August Pi i Sunyer (IDIBAPS), Fundació Clínic per a la Recerca Biomèdica, Departament de Biomedicina, Facultat de Medicina i Ciències de la Salut, Universitat de Barcelona (UB), Barcelona, Spain juditcastillo@ub.edu ORCID iD: 0000-0002-9407-2675

Conflict of Interest

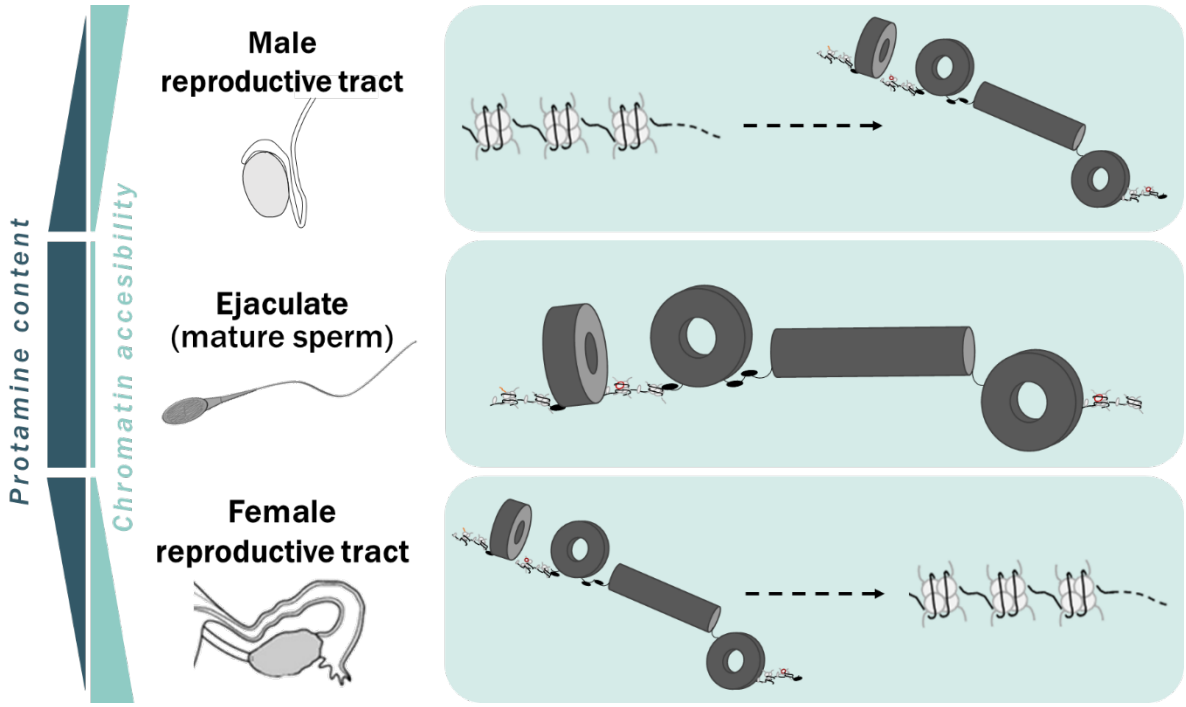
The authors declare no conflict of interest.

Abstract

Male germ cells undergo an extreme but fascinating process of chromatin remodelling that begins in the testis during the last phase of spermatogenesis and continues through epididymal sperm maturation. Most of the histones are replaced by small proteins named protamines, whose high basicity leads to a tight genomic compaction. This process is epigenetically regulated at many levels, not only by posttranslational modifications, but also by readers, writers, and erasers, in a context of a highly coordinated post-meiotic gene expression program. Protamines are key proteins for acquiring this highly specialized chromatin conformation, needed for sperm functionality. Interestingly, and contrary to what could be inferred from its very specific DNA-packaging function across protamine-containing species, human sperm chromatin contains a wide spectrum of protamine proteoforms, including truncated and post-translationally modified proteoforms. The generation of protamine knock-out models revealed not only chromatin compaction defects, but also collateral sperm alterations contributing to infertile phenotypes, evidencing the importance of sperm chromatin protamination towards the generation of a new individual.

The unique features of sperm chromatin have motivated its study, applying from conventional to the most ground-breaking techniques to disentangle its peculiarities and the cellular mechanisms governing its successful conferment, especially relevant from the protein point of view due to the important epigenetic role of sperm nuclear proteins. Gathering and contextualizing the most striking discoveries will provide a global understanding of the importance and complexity of achieving a proper chromatin compaction and exploring its implications on post-fertilization events and beyond.

Graphical/Visual Abstract and Caption



Caption: A synchronized chromatin remodelling process takes place during sperm development in the male reproductive tract, leading to a unique chromatin conformation, needed to protect paternal genome and with potential of transmitting epigenetic information upon fertilization. Paternal pronucleus in the zygote is then restructured for proper embryo development.

1. INTRODUCTION

Haploid paternal genome needs to be tightly wrapped into highly specialized structures for a proper sperm function. Sperm chromatin compaction is part of the complex process of male germ cell development named spermatogenesis. Spermatogenesis comprises three well-defined phases: 1) a mitotic phase, in which type A replicating spermatogonia are in charge of maintaining the germ cell niche, whereas type B spermatogonia commit to meiosis and divide mitotically one more time to generate primary spermatocytes, 2) a meiotic phase, in which primary spermatocytes undergo two consecutive meiotic divisions: the first one to generate two diploid secondary spermatocytes, and the second one without a previous DNA replication step to generate haploid round spermatids, and 3) a phase called spermiogenesis, in which post-meiotic round spermatids elongate through a series of marked nuclear, cytoplasmic, and morphological changes (Bolcun-Filas &

Handel, 2018; de Kretser et al., 1998; Hecht, 1998; Oliva & Castillo, 2011; Oliva & Dixon, 1991).

Sperm nuclear compaction is achieved through the process known as nucleo-histone to nucleo-protamine (NH-NP) transition, that occurs during spermiogenesis (Christensen & Dixon, 1982; Grimes & Henderson, 1984; Hazzouri et al., 2000; Oliva et al., 1987; Oliva & Castillo, 2011; Oliva & Mezquita, 1982). Through this process, small, extremely basic protamines replace most of the histones, leading to highly packaged toroidal and rod-like structures that are able to compact 250 times more DNA than a nucleosome (Ausió et al., 2014; Balhorn, 2007; Bao & Bedford, 2016; Castillo, Amaral, & Oliva, 2014; Castillo et al., 2015; Gaucher et al., 2010; Torres-Flores & Hernández-Hernández, 2020; Vilfan et al., 2006; T. Wang et al., 2019). A complex regulation is needed during NH-NP transition, involving posttranslational modifications (PTMs) and associated modulating proteins, in the context of a fine-tuned post meiotic gene expression program of genes encoding the main proteins taking part in the process (Blanco & Cocquet, 2019; T. Wang et al., 2019).

Despite being hydrodynamically shaped, testicular sperm are still immature and unable to fertilise on their own. Sperm maturation continues outside the testes during transit and storage through the male reproductive tract, where forward progressive motility is acquired, membrane composition and fluidity are modified, and sperm chromatin structure is stabilized. The contact of spermatozoa with fluids secreted by the epididymis and the accessory sex glands gives rise to fully mature and motile ejaculated sperm with fertilizing potential (Dacheux & Dacheux, 2014; Gervasi & Visconti, 2017; Jodar et al., 2017; Orgebin-Crist, 1969; Schoysman & Bedford, 1986; Yoshida et al., 2018).

Opposed to the traditional idea that the spermatozoon is a simple carrier of paternal genetic information, the application of high-throughput techniques has proven that the mature sperm cell contains a wide set of layers of information that are transmitted to the zygote and can impact fertilization and beyond (Castillo,

Amaral, & Oliva, 2014; Castillo, Amaral, Azpiazu, et al., 2014; Castillo et al., 2018; Chen et al., 2016; Hammoud et al., 2009; Krawetz, 2005; Rando, 2012; Siklenka et al., 2015). In addition, alterations in the sperm epigenetic cargo, as well as impairments during the spermiogenic process, are associated with male infertility (Carrell et al., 2008; Castillo et al., 2015; Hammoud et al., 2010, 2011). When referring to the evaluation of the epigenetic potential of sperm chromatin, many studies have focused mainly on DNA methylation and chromatin organization (Hammoud et al., 2010; Laurentino et al., 2016; Leitão et al., 2020; Siklenka et al., 2015). However, advances in the description of the sperm proteome have revealed that the male gamete carries a substantial amount of proteins with epigenetic roles, being involved in gene expression regulation through the modulation of transcription, biogenesis of non-coding RNAs, and establishment of DNA and histone marks (Castillo, Amaral, & Oliva, 2014; Castillo, Amaral, Azpiazu, et al., 2014; Castillo et al., 2015, 2018; de Mateo, Castillo, et al., 2011). Although the presence of some of these proteins in mature sperm could represent simple leftovers of their spermatogenic activity, others may also have an impact during fertilization events or preimplantation embryo development, contributing to the early embryonic epigenome (Castillo et al., 2018). In the present review, we aim to highlight, from a protein point of view, the critical impact of the tightly regulated process of sperm chromatin compaction and its associated epigenetic marks towards the formation of a fully functional male gamete with a role beyond fertilization. To that end, we summarize the process of protamine-dependent histone removal to compile the latest findings on its orchestrated epigenetic regulation, giving rise to the complex final structure of sperm chromatin. In addition, we review the most recent knowledge on the most abundant protein components of mature sperm chromatin, the protamines, which have traditionally been less well characterized than histones in terms of their function, marks, and epigenetic potential. Finally, we propose our model of sperm chromatin structure and gene distribution according to the latest available evidence, based on a wide range of complementary techniques.

2. THE SYNCHRONIZED MOLECULAR PROCESS OF NUCLEO-HISTONE TO NUCLEO-PROTAMINE TRANSITION IN THE MALE REPRODUCTIVE TRACT

2.1. Synergistic, rather than sequential, mechanisms of testicular histone replacement

The NH-NP transition is a unique process of chromatin remodelling taking place in male germ cells during spermiogenesis, which gives rise to tightly compacted nuclei necessary to produce functional sperm (Christensen & Dixon, 1982; Grimes & Henderson, 1984; Hazzouri et al., 2000; Mezquita, 1985; Oliva et al., 1987; Oliva & Castillo, 2011; Oliva & Mezquita, 1982). It comprises a gradual replacement of somatic cell-like core histones by testis-specific histone variants, followed by transition proteins 1 and 2 (TP1 and TP2, respectively) and, finally, by protamines (Balhorn, 2007; Barrachina et al., 2018; Castillo et al., 2011; Gatewood et al., 1987; Kimmins & Sassone-Corsi, 2005; Oliva, 2006; Oliva & Dixon, 1991; Rathke et al., 2014). Two protamines have been described in mammalian sperm, protamine 1 (P1), which is synthetized as mature form, and protamine 2 (P2), which arises from the proteolytic cleavage of a precursor (pre-P2) (Oliva, 2006). This tightly regulated process results in 85-95% of the paternal human genome (92-98% in mouse) being packed with protamines, giving rise to two differential chromatin regions: the nucleo-histone domain, containing the most accessible fraction of the genome; and the nucleo-protamine domain, inaccessible and silenced (Arpanahi et al., 2009; Castillo, Amaral, Azpiazu, et al., 2014; Hammoud et al., 2009).

The incorporation of histone variants contributes to nucleosome conformational changes and the destabilization needed to achieve an open chromatin state. Male germ cells express the largest number of histone variants, including unique testicular variants of H2A, H2B, and H3, as well as almost all

histone variants present in somatic nuclei (Barrachina et al., 2018; Boussouar et al., 2008; Ding et al., 2021; Hoghoughi et al., 2018). Changes in amino acid sequence of testis-specific histone variants, such as TH2A, TH2B and H2BFWT, and other histone variants, such as H3.3 and H3.4, are responsible for low-affinity binding to DNA (Bonisch & Hake, 2012; Boulard et al., 2006; Li et al., 2005; Padavattan et al., 2017; Tachiwana et al., 2010; Ueda et al., 2017; Urahama et al., 2016). Loss of TH2A and TH2B in mice has been related to impaired histone retention and sterility (Shinagawa et al., 2015), and depletion of the two H3.3 encoding genes (*H3f3a* and *H3f3b*) has been related with male subfertility and sterility in mouse, respectively (Tang et al., 2015; Yuen et al., 2014). Furthermore, novel histone variants have recently been discovered in testis, like H2B.K and H2B.N, without a specific function yet, likely redundant but vital for unusual chromatin packing (Raman et al., 2022).

While traditional approaches have shown that the incorporation of histone variants, TPs, and protamines during spermatogenesis, occurs in a purely sequential way (Balhorn, 2007; Bao & Bedford, 2016; Barrachina et al., 2018; Gaucher et al., 2012; Kimmins & Sassone-Corsi, 2005; Lewis et al., 2003; Meistrich et al., 2003; Oliva, 2006; Oliva & Castillo, 2011; Oliva & Dixon, 1991; Rathke et al., 2014), recent findings have pointed to a more synergistic than sequential NH-NP process (Arévalo et al., 2022; Barral et al., 2017; Rezaei-Gazik et al., 2022). It has been found that the synthesis of the spermatid-specific histone variant H2A.L.2, coincides with that of TPs, and that its depletion would lead to an aberrant loading of TPs in the chromatin and an inadequate processing of pre-P2. This suggests that H2A.L.2 creates an open conformation of the nucleosome that allows TP loading into chromatin (Barral et al., 2017). Furthermore, TPs are spatiotemporally co-expressed with pre-P2, which suggest their joint action during NH-NP transition (Rezaei-Gazik et al., 2022), and co-exist with protamines in late spermatids, when histones are still detectable (Meistrich et al., 2003; Zhao et al., 2004). Interestingly, recent evidence has shown that pre-P2 cleaved domain (cP2) mediates the correct interaction between TP1-H2A.L.2 complexes and pre-P2 (Arévalo et al., 2022). Therefore, under normal conditions, TPs are loaded into H2A.L.2-containing nucleosomes, not displacing histones but generating an open chromatin interface

for protamine recruitment and pre-P2 processing, orientating protamines to finally displace histones (Arévalo et al., 2022; Barral et al., 2017). Indeed, the specific depletion of cP2 domain does not allow the correct incorporation of P2 into sperm chromatin, being P2 accumulated in the cytoplasm of spermatids and residual bodies (Arévalo et al., 2022). Besides, the specific loss of TP2 is responsible for the accumulation of pre-P2, which ends up in altered levels of P2 (Zhao et al., 2001). Knockout mouse models of the genes encoding TP1 and TP2 (*Tnp1* or *Tnp2,* respectively) are subfertile, producing sperm with abnormal chromatin condensation. Of note, these mice seem to compensate the lack of one of the TPs by overexpressing the other, so that only the simultaneous depletion of both genes would end in sterility (Shirley et al., 2004; Yu et al., 2000; Zhao et al., 2001). Despite of that, testicular spermatids and few epididymal sperm, whose chromatin compaction is impaired, are generated in the double *Tnp1-Tnp2* knockout. This would support that protamines would be capable to replace histones without the participation of TPs (Shirley et al., 2004).

All this evidence highlights protamines as the main actors of histone displacement during spermiogenesis (Barral et al., 2017; Meistrich et al., 2003; Oliva et al., 1987; Oliva & Mezquita, 1986). In fact, it has been shown that the mere presence of protamines allows DNA to be compacted *in vitro* (Makita et al., 2011; Oliva et al., 1987; Oliva & Mezquita, 1986). For instance, human protamine 1 (P1) can displace nucleosomes from somatic chromatin, leading to a spermatid-like nuclear compaction in non-germ cell types (Iuso et al., 2015). Strikingly, this P1-compacted somatic nucleus can be reversibly loosened by maternal histones after *in vitro* fertilization of an oocyte, producing embryos that progress until blastocyst stage (Iuso et al., 2015). Similarly, P2 condensation ability has been proved in HEK cells, observing fully condensed nuclei after 48h cell culture (Arévalo et al., 2022). Nonetheless, the process of paternal genome compaction is way more complex than simple affinity of protamines to DNA, with a tight epigenetic regulation underlying protamine incorporation.

2.2. The regulation of the nucleo-histone to nucleo-protamine transition through protein modification and implications in male fertility

2.2.1. Posttranslational modification of proteins regulating the NH-NP transition

Global histone H4 hyperacetylation wave is crucial for a proper NH-NP transition, as it neutralizes the positivity of histone tails and destabilizes the histone-DNA and nucleosome-nucleosome interactions (Barrachina et al., 2022; Hazzouri et al., 2000; Oliva & Mezquita, 1982). In fact, acetylation on H4 Lys 5 and 8 (H4K5K8ac) is the first step towards nucleosome instability and histone eviction for large-scale remodelling of the chromatin. H4K5K8ac is recognized by the first bromodomain of the bromodomain testis-specific protein (BRDT), which triggers the NH-NP transition (Dhar et al., 2012; Goudarzi et al., 2014; Her et al., 2021; Manterola et al., 2018; Morinière et al., 2009; Pivot-Pajot et al., 2003; Shang et al., 2007). Together with H4 hyperacetylation, a specific wave of H3 Lys79 trimethylation (H3K79me3) also precedes the NH-NP transition, specifically, before TP1 incorporation, potentially contributing to its regulation (Dottermusch-Heidel et al., 2014; Moretti et al., 2017). Besides, residue-specific lysine acetylation of other histones, as described for H3, contributes to the final global histone hyperacetylation state, destabilizing nucleosomes and favouring their removal (Grimes & Henderson, 1984; Hazzouri et al., 2000; Nair et al., 2008; Steilmann et al., 2011; Tan et al., 2011).

In the last years, other less-known histone PTMs from the group of acylations have been identified in histones (Crespo et al., 2020; Sabari et al., 2017; Tan et al., 2011). Acylations such as propionylation, butyrylation, and crotonylation have similar physicochemical properties to those of histone acetylation, which would also lead to an open conformation of the nucleosome favouring histone eviction (Sabari et al., 2017). Interestingly, butyrylation on H4K5 (together with either acetylation or butyrylation on K8) is not recognized by the first bromodomain of BRDT, thus escaping histone detachment. This could lead either to a temporarily regulated histone replacement in specific nucleosomes during spermiogenesis, or to histone retention of specific gene sequences in mature sperm (Goudarzi et al., 2016). It has been shown that, in addition to the effect on relaxing nucleosomal

conformation, PTMs also mark histones for a subsequent proteasomal degradation needed to achieve a proper histone replacement, as it is the case of histone (poly)ubiquitination of core histones H2A and H2B (Baarends et al., 1999; Gou et al., 2017; Guo et al., 2018; Meng et al., 2019; Shmueli et al., 2021; X. Wang et al., 2019). The spermatoproteasome, a proteasome subunit alpha type-8 (PSMA8)-containing proteasome enriched in haploid cells, also plays a key role degrading histones in an acetylation-dependent manner (Gómez-H et al., 2019; Živković et al., 2022). This evidence on the tight regulation of histone replacement by PTMs highlights the need for further insight into the role during spermiogenesis of less well-characterized histone modifications, such as non-acetyl histone acylations. For instance, crotonylation of H3K27, although not confirmed as direct regulator of the NH-NP transition, has been detected in high abundance in post meiotic cells, concomitant to H4 hyperacetylation and histone removal, as well as retained in sperm, which suggests a comparable function to that of H4K5 and K8 butyrylation (Crespo et al., 2020). Interestingly, crotonylated H3K27 regulates the expression of spermiogenesis-specific genes, such as TP2 and P1, which together with acetylation on the same residue are associated with the highest gene expression levels (Crespo et al., 2020).

Histone variants and TPs also bear PTMs, which affects their binding affinity to DNA (Gupta et al., 2015, 2017; Hazzouri et al., 2000; Kwak & Dohmae, 2016; Mishra et al., 2015; Pentakota et al., 2014; Pradeepa et al., 2009; Singh & Parte, 2021). Of note, TP2 acetylation reduces its ability to condense DNA (Pradeepa et al., 2009), suggesting that modified TPs may contribute to establish the final sperm epigenome.

Epigenetic regulation of spermiogenesis through the modification of specific protein residues has also observed in protamines from different mammalian species, including human, mice, stallion, boar, bull, and ram (Arauz-Garofalo et al., 2021; Brunner et al., 2014; Castillo et al., 2015; Chirat et al., 1993; Pirhonen, Linnala-Kankkunen, & Mäenpää, 1994; Pruslin et al., 1987; Soler-Ventura et al., 2020). The most relevant modification in protamines is phosphorylation, which regulates their binding to DNA. The negative charge of the phosphate group leads

to a weaker affinity of phosphorylated protamines for negatively charged DNA, compared to unmodified protamines (Willmitzer et al., 1977a, 1977b). Thus, while protamine phosphorylation would be necessary to incorporate protamines into DNA, subsequent dephosphorylation is needed for tight sperm chromatin compaction (Itoh et al., 2019; Willmitzer et al., 1977a).

2.2.2. The interplay between PTMs and their modulators during NH-NP transition

Protein modification and its implication on cellular processes are modulated by proteins that incorporate PTMs to specific amino acids (writers), recognize PTMs from specific modified residues (readers), or remove PTMs from already modified amino acids (erasers) (Jenuwein & Allis, 2001; Ruthenburg et al., 2007; Strahl & Allis, 2000). In the context of sperm chromatin compaction, histone acetyltransferases (HATs), which are writers of histone acetylation, develop an important role in the mediation of NH-NP transition. This process is mediated by the recruitment of Histone acetyltransferase p300 (p300 HAT) and CREB-binding protein (CBP) by Nuclear protein in testis (NUTM1, also known as NUT), which enhances H4K5/K8 acetylation (Shiota et al., 2018). Similarly, the components Enhancer of polycomb homolog 1 (EPC1) and Histone acetyltransferase Tip60 (TIP60) of the mammalian nucleosome acetyltransferase of H4 (NuA4) complex, are involved in histone hyperacetylation during spermiogenesis (Dong et al., 2017). It is also notable the role of BRDT as one of the main readers of histone PTMs during this last phase of spermatogenesis, which not only recognizes acetylated H4K5K8 to trigger and amplify the process of histone eviction, but also interacts with transcription factors in round spermatids to regulate gene expression of target genes essential for this developmental stage (Her et al., 2021). Modulators of histone methylation have been also shown to control the expression of TPs and protamine genes (Eelaminejad et al., 2017; Z. Liu et al., 2010; Okada et al., 2007, 2010; Zuo et al., 2018). Details of these proteins and additional examples, the

deregulation of which has been related with male infertility and impaired chromatin compaction, can be found in Table 1.

Additionally, the epigenetic control of the NH-NP transition seems to be also affected by a crosstalk among different histone PTMs and modulators, suggesting a new layer of coordination. For instance, reduced expression of the Sypc3 like Y-linked (*Sly)* gene in mice, which is exclusively expressed in post-meiotic male germ cells, deregulates not only Histone-lysine N-methyltransferase, H3 lysine-79 specific (DOT1L) but also H4ac levels in elongated spermatids, leading to a global alteration of the state of chromatin compaction (Moretti et al., 2017). DOT1L also recognizes ubiquitinated H2B, enhancing a noncatalytic function of this methyltransferase on nucleosome destabilization, suggesting an interplay between H3 methylation and H2B ubiquitination towards nucleosome removal (Jang et al., 2019).

Although protamines and their PTMs have been historically less studied than histones, modulators of protamine phosphorylation have been also identified. SRSF protein kinase 1 (SRPK1) and Calcium/calmodulin-dependent protein kinase type IV (CAMK4) phosphorylate P1 and P2 in the testis, respectively (Papoutsopoulou et al., 1999; Wu et al., 2000). Additional candidates have been found *in vitro*, such as c-AMP-dependent protein kinase A (PKA), which phosphorylates P1, and protein kinase C (PKC), which phosphorylates P2 (Pirhonen, Linnala-Kankkunen, & Mënpää, 1994). In terms of erasers, while no P1-specific phosphatases have been described yet, the germ cell-specific isoform 2 of Serine/threonine-protein phosphatase PP1-gamma catalytic subunit (PP1γ2) has been found to be involved in the removal of phosphate groups from P2 in mice (Itoh et al., 2019). Depletion of the chaperone needed for recruiting *PP1γ2* to the sperm chromatin (Heat shock 70 kDa protein 4L, HS74L) leads to infertility in the knockout mice due to altered sperm head morphology, being normal phenotype rescued when the P2 phosphorylation site is substituted by a non-phosphorylatable residue. These interesting results suggest that PP1γ2-mediated dephosphorylation is essential to achieve mouse fertility avoiding abnormal P2 phosphorylation levels in epididymal sperm (Itoh et al., 2019).

All studies mentioned above reinforce the idea of a highly orchestrated process of epigenetic regulation through a complex interplay between histone PTMs and their writers, readers, and erasers.

Table 1. Writers, readers, and erasers of posttranslational modifications of histone and protamines expected to be involved in the regulation of the NH-NP transition.

Name	Molecular role	Description	References
Effectors of histones and protamines PTMs			
BRD4	Bromodomain-containing protein, reader of histone acetylation	Acetylation reader, with preference for acetylated H4 over H3 *in vivo*. Associated with active genes in round spermatids. Differential gene expression through specific binding to residue-specific (H3K27) histone acetylation but not butyrylation, unlikely to bind crotonylation in the same residue. Potentially involved in nuclear proteins eviction linked to acrosome formation during spermiogenesis	(Bryant et al., 2015; Crespo et al., 2020; Ji et al., 2015; Vollmuth & Geyer, 2010)
BRDT	Bromodomain-containing protein, reader of histone acetylation	Reader of H4 acetylation. First bromodomain recognition of H4K5K8 is essential to trigger NH-NP transition, depletion leads to infertility (post-meiotic arrest). Gene expression regulation of post-meiotic genes	(Dhar et al., 2012; Gaucher et al., 2012; Her et al., 2021; Manterola et al., 2018; Pivot-Pajot et al., 2003; Shang et al., 2007)
CAMK4	Calcium/calmodulin-dependent kinase	Phosphorylates P2, depletion of Camk4 leads to infertility, impaired elongating spermatids with prolonged retention of Tnp2 and specific loss of P2	(Wu et al., 2000)
CDYL	Chromodomain-containing protein, reader of histone methylation	Histone crotonylation regulator facilitating TP1 and PRM2 incorporation. Depletion of CDYL caused changes in histone methylation and acetylation profiles and altered gene expression, giving rise to teratozoospermia and progressive infertility in adulthood	(S. Liu et al., 2017; Xia et al., 2019)
DOT1L	Histone methyltransferase	Methyltransferase in the testis of H3K79, which precedes the NH-NP transition, more precisely prior TP1 incorporation	(Dottermusch-Heidel et al., 2014; Moretti et al., 2017)
EPC1	Component of NuA4 histone acetyltransferase (HAT) complex	Its depletion, together with TIP60, leads to impaired histone H4 hyperacetylation and subsequent histone replacement	(Dong et al., 2017)
HDAC3	Histone deacetylase	Inactivates meiotic program and activates postmeiotic genes during meiotic exit. Depletion of HDAC3 leads to infertility due to meiotic/early-stages round spermatids arrest, and increased H3 acetylation in spermatocytes and round spermatids. Coordinates gene expression program with SOX30	(Yin et al., 2021)
MRG15	Component of the NuA4 HAT complex	Recognizes methylated H3K36 and regulates alternative splicing mediated by polypyrimidine tract binding protein PTB, part of the HAT and HDAC complexes balancing histone acetylation	(Hayakawa et al., 2007; Iwamori et al., 2016)
P300	Histone acetyl-transferase	Involved in histone H4 hyperacetylation and essential for histone-to-protamine exchange. Acetylation of TP2 by p300 leads to significant reduction in its DNA condensation	(Pradeepa et al., 2009; Reynoird et al., 2010; Shiota et al., 2018)
PA200	Component of the proteasome, specifically recognizing acetylatied histones, promoting degradation of core histones	Depletion leads to hypofertility with abnormal sperm, core histone retention in elongating spermatids due to defective acetylation-dependent histone proteasomal degradation. Its level of incorporation to the spermatoproteasome-containing PSMA8 subunit is 10-fold higher in spermatids than early spermatogenesis, key for proteasomal activity during spermiogenesis	(Khor et al., 2006; Qian et al., 2013; Živković et al., 2022)
PHF7	Ubiquitin ligase	E3-ubiquitin ligase for H3K14 in post-meiotic cells, required for histone to protamine transition. Stabilizes BRDT by attenuating BRDT ubiquitination	(Kim et al., 2020; X. Wang et al., 2019)
PP1γ2	Protein phosphatase	Dephosphorylates Ser56 of protamine 2 in mouse. HSPA4L-mediated chromatin localization of PP1γ2 is essential for fertility and maintenance of low oxidative stress levels during epididymal transit	(Itoh et al., 2019)
SIRT1	Histone deacetylase	Loss of Sirt1 causes defects on H4 Lys5, 8, and 12 acetylation, and subsequent histone removal	(Bell et al., 2014)
SRPK1	Serine/Threonine kinase	Phosphorylation of protamine 1 in the testis, which favours protamine incorporation to the DNA	(Gou et al., 2020; Papoutsopoulou et al., 1999; Willmitzer et al., 1977b, 1977a)
TIP60	Catalytic subunit of NuA4 histone acetyltransferase (HAT) complex	Its depletion, together with Epc1, leads to impaired histone H4 hyperacetylation and subsequent histone replacement	(Dong et al., 2017)

2.2.3. Post-testicular events involved in sperm chromatin stabilization

Interestingly, the formation of sperm chromatin does not finish when condensed spermatids (immature sperm) are released from the testis but continues through crucial events taking place in the epididymis (Yoshida et al., 2018). Cannabinoid receptor 1 (CB1) promotes the generation of disulphide bonds during epididymal transit, stabilizing the structure of sperm chromatin (Chioccarelli et al., 2020). Of note, CB1 depletion has been shown to reduce H4 acetylation and increase TP2 in the testis, as well as to induce increasing levels of sperm DNA fragmentation along the epididymis (Chioccarelli et al., 2010), suggesting that disulphide bonds formation is essential for post-testicular chromatin stability and DNA integrity. Other interesting approaches suggest additional mechanisms of chromatin stabilization during epididymal transit, such as protamine dephosphorylation that result in the release of zinc molecules acquired in the testes, mainly by P2, during protamine incorporation to DNA (Bianchi et al., 1992; Björndahl & Kvist, 2011; Dias et al., 2006; Gou et al., 2020; Itoh et al., 2019; Schneider et al., 2020). All this indicates that, even though the focus of the study of NH-NP transition has mostly been set on the testicular processes, attention should also be paid to post-testicular events that would contribute to the acquisition of a proper chromatin structure to protect the paternal genome from external damage.

Sidebar 1: usefulness of deciphering the molecular mechanisms governing the NH-NP transition towards a complete *in vitro* development of human haploid male germ cells

The knowledge obtained from the molecular study of the NH-NP transition could be useful in the future to help developing complete human spermatogenesis *in vitro*. Functional sperm have been successfully generated from mouse testicular tissue culture (Sato, Katagiri, Gohbara, et al., 2011; Sato, Katagiri, Yokonishi, et al., 2011; Yokonishi et al., 2014). However, despite the great advances obtained using different approaches of *in vitro* human spermatogenesis, no elongated spermatids have been achieved yet (Baert et al., 2017; Medrano et al., 2018; Portela et al., 2019; Reda et al., 2016; Richer et al., 2021; Stukenborg et al., 2009). Even though meiosis is one of the most striking points to be overcome in these *in vitro* systems using testicular tissue (Lei et al., 2021), a low number of round spermatid-like haploid cells have been originated

from human induced pluripotent stem cells (Eguizabal et al., 2011). Still, they did not progress through differentiation, evidencing the importance and complexity of the post meiotic phase regulation.

3. THE UNIQUE FEATURES OF THE MATURE SPERM CHROMATIN CONTENT

3.1 Different levels of DNA accessibility and protein affinity in the sperm chromatin with implications in male infertility

The interest on deciphering whether the peculiar chromatin structure remaining in the mature male gamete is predetermined and with a role beyond oocyte fertilization has been present since the 20th century. In fact, in 1987 it was published the first study reporting the presence of sequence-specific nucleo-histone and nucleo-protamine domains in human sperm (Gatewood et al., 1987). Although this was followed by many other studies applying conventional strategies and focusing on specific genes with complementary results (Gardiner-Garden et al., 1998; Nazarov et al., 2008; Wykes & Krawetz, 2003; Zalenskaya et al., 2000), it was not until the application of high-throughput techniques for DNA sequencing that the main advances in this field were obtained. In 2009, it was proposed for the first time, in two independent studies, the specific association of nucleosomal DNA to regulatory regions of developmental genes characterized by high CpG density in both human and mice (Arpanahi et al., 2009; Hammoud et al., 2009). These and subsequent studies applying similar strategies confirmed those previous results suggesting a non-random DNA distribution through sperm chromatin domains and pointing to its role as an epigenetic mark with impact on early embryo development (Brykczynska et al., 2010; Castillo, Amaral, Azpiazu, et al., 2014; Castillo et al., 2015; Erkek et al., 2013; Saida et al., 2011; Vavouri & Lehner, 2011).

Nevertheless, this remarkable enrichment in genic regions with crucial developmental functions contrasts with the fact that the male gamete contains only a small proportion of the whole genetic material associated to histones (approximately 2% and 8% in mouse and human, respectively), which is the most vulnerable and exposed DNA to damaging factors. In this regard, several studies have suggested an

opposing composition of the sperm nucleo-histone domain. While the specific distribution seems to be maintained, some groups suggested that the association of nucleosomal DNA to regulatory gene regions was minimal, while the major part localizes on repetitive sequences and intergenic regions (Carone et al., 2014; Samans et al., 2014). This agreed with previous studies showing the association of histones with telomeric DNA by using methods based on DNA probes and Southern hybridation (Zalenskaya et al., 2000), as well as to centromeric and pericentromeric regions using immunostaining (Govin et al., 2007; van der Heijden et al., 2006). As a potential explanation for these contrary reports regarding the content of the sperm nucleosomal DNA, it has been suggested the presence of technical artefacts at the levels of chromatin dissection and sequencing data analysis (Carone et al., 2014; Royo et al., 2016). DNA digestion by micrococcal nuclease (MNase) has been the preferred method to isolate sperm histone-associated DNA (Arpanahi et al., 2009; Brykczynska et al., 2010; Carone et al., 2014; Castillo, Amaral, Azpiazu, et al., 2014; Erkek et al., 2013; Hammoud et al., 2009; Ozturk et al., 2021; Saida et al., 2011; Samans et al., 2014) (Table 2). Nevertheless, the amount of enzyme used for chromatin dissection has been suggested as a critical source of variability. By comparing light (<10U per 100 million sperm) and longer (>10U per 100 million sperm) MNase digestions in crosslinked sperm chromatin, Carone and collaborators reported the presence of two types of nucleosomes: 1) a minor group with higher stability located around promoters and 2) a predominant group more sensible to the method and associated to gene-poor regions (Carone et al., 2014). According to this, sperm DNA enriched in regulatory regions of developmental genes would represent an infrequent population of highly stable nucleosomes with specific histone modifications and variants. However, it is important to remark that two studies have reported human and mouse sperm nucleosomal enrichment in DNA surrounding transcriptional start sites using light MNase digestions (Arpanahi et al., 2009; Castillo, Amaral, Azpiazu, et al., 2014). This fact leaves the only difference between these studies and Carone's protocol limited to a previous formaldehyde-crosslinking of the sperm in the latter, a technical factor that might be also considered to induce variability on the results (Table 2). Of note, one of these studies applying light MNase digestions with no previous crosslinking showed the presence of two nucleosomal particles, differing on size and located in non-

overlapping sites (Castillo, Amaral, Azpiazu, et al., 2014). In spite of this, both types of nucleosomes showed a preference association to CpG enriched regions and transcriptional start sites (Castillo, Amaral, Azpiazu, et al., 2014). As another technical artefact influencing the results, Royo and colleagues pointed to the approach for DNA sequencing data analyses as a potential source of bias. According to this work, the alignment of the reads to multiple locations in the genome would lead to an overrepresentation of repetitive sequences, while allowing only a single alignment per mapped read would derive on better identification of genic regions (Royo et al., 2016).

Table 2. Type of major genomic sequences associated with histones in sperm, according to the experimental procedure followed for nucleosomal DNA extraction in experiments applying DNA sequencing analyses. MNase: Micrococcal nuclease; NPM: nucleoplasmin

MNase-based digestion				**Alternative strategies**		
Light digestion (<10 U/100 million)		**Longer digestion (>10U/100 million)**		**NPM-protamine depletion**	**0.65 M NaCl-histone depletion**	**ATAC-seq**
No crosslinking	**Crosslinking**	**No crosslinking**	**Crosslinking**			
Regulatory gene regions[1,7]	Gene deserts/ Repetitive DNA[6]	Regulatory gene regions[2,3,4,5] Gene deserts/ Repetitive DNA[8] Dual[12]	Regulatory gene regions[6]	Gene deserts/Repetitive DNA[10]	Regulatory gene regions[1]	Regulatory gene regions[9] Gene deserts/Repetitive DNA [11]

1. (Arpanahi et al., 2009) (human/mouse); 2. (Hammoud et al., 2009) (human); 3. (Brykczynska et al., 2010) (human/mouse); 4. (Saida et al., 2011) (mouse); 5. (Erkek et al., 2013) (mouse); 6. (Carone et al., 2014) (mouse); 7. (Castillo, Amaral, Azpiazu, et al., 2014) (human); 8. (Samans et al., 2014) (human/bovine); 9. (Jung et al., 2017) (mouse); 10. (Yamaguchi et al., 2018) (mouse); 11. (Luense et al., 2019) (mouse); 12. (Ozturk et al., 2021) (human)

All these data obtained by independent groups reveal the complexity of the sperm DNA accessibility and maintain the debate about whether nucleosome-associated DNA is enriched in developmental genes, repetitive sequences, or poor genic regions as the main question to be solved about sperm chromatin function and relevance on male fertility.

To deep into this matter, it is important to review the results obtained using no MNase-based techniques (Table 2). Since DNA compaction might impede the accessibility of the enzymes, some groups have designed smart approaches based on the depletion of either histones (Arpanahi et al., 2009) or protamines (Yamaguchi et

al., 2018) before chromatin immunoprecipitation of specific histone variants or modified histones. Removal of histone-DNA associations by 0.65 M NaCl followed by endonuclease restriction enzyme digestion is a classical method for sperm chromatin dissection that supports the hypothesis of sperm nucleosomal association to promoters, as well as an enrichment in CTCF binding sequences (Arpanahi et al., 2009). Yamaguchi and colleagues, in contrast, decided to address this issue differently by ensuring nucleosome solubility depleting protamines with nucleoplasmin, an oocyte protein responsible for paternal DNA remodelling after fertilization (Philpott & Leno, 1992). Following this protocol, a histone modification-dependent retention was detected, being H4, H3K9me3 and the N-terminal part of the H3 (corresponding to 14 amino acids) preferentially mapped to distal intergenic regions and gene deserts, whereas H3K4me3 and cleaved H3 (with no presence of the N-terminal part) were associated to regulatory regions of developmental genes (Figure 1). Despite this dual behaviour, gene coding regions represented a minority of the nucleosomal DNA (Yamaguchi et al., 2018). More recently, some studies applied ATAC-seq technology based on the use of the Tn5 transposase to reveal accessible and inaccessible regions of the sperm chromatin (Buenrostro et al., 2013). Interestingly, this novel approach showed a distinct association of nucleosome-retained DNA characterized by presence of DNA bound to CTCF and cohesin similarly to round spermatids and embryonic stem cells, and a retention in intergenic regions that seems to not increase along spermatogenesis (Jung et al., 2017; Luense et al., 2019) (Table 2). Nonetheless, as seen with other technical approaches, ATAC-seq studies did not show consensus data regarding the main type of histone-associated genomic sequences in the mature sperm (Table 2).

It is important to remark the detection in mature sperm cells of predetermined enhancers and super-enhancers associated to elements involved in the 3D organization of the chromatin that are functional in embryonic and adult tissues (Jung et al., 2017). Interestingly, sperm genomic 3D organization revealed many similarities to that of somatic cells, such as fibroblasts and embryonic stem cells, in which DNA is distributed in two compartments called A and B and associated to active and repressive chromatin regions, respectively. In addition, topologically associated domains (TADs) are partially conserved (Battulin et al., 2015; Jung et al., 2017; Ke et al., 2017; Y. Wang

et al., 2019). Nonetheless, sperm possess a major number of long-range interactions (> 2Mb), most of them between TADs, that could contribute to either establishing or maintaining the highly compacted state of its chromatin. Indeed, 3D conformation of sperm DNA packaging from non-protamine-containing species lacks TADs, resembling mitotic chromosomes (Gibcus et al., 2018; Wike et al., 2021). This A-B and TADs compartmentalization correlates with retained histones in sperm. Some controversy arises from the use of current 3D-chromatin technologies in such compacted and inaccessible genome, which would potentially bias the results from the real *in vivo* genomic architecture (Moritz & Hammoud, 2022).

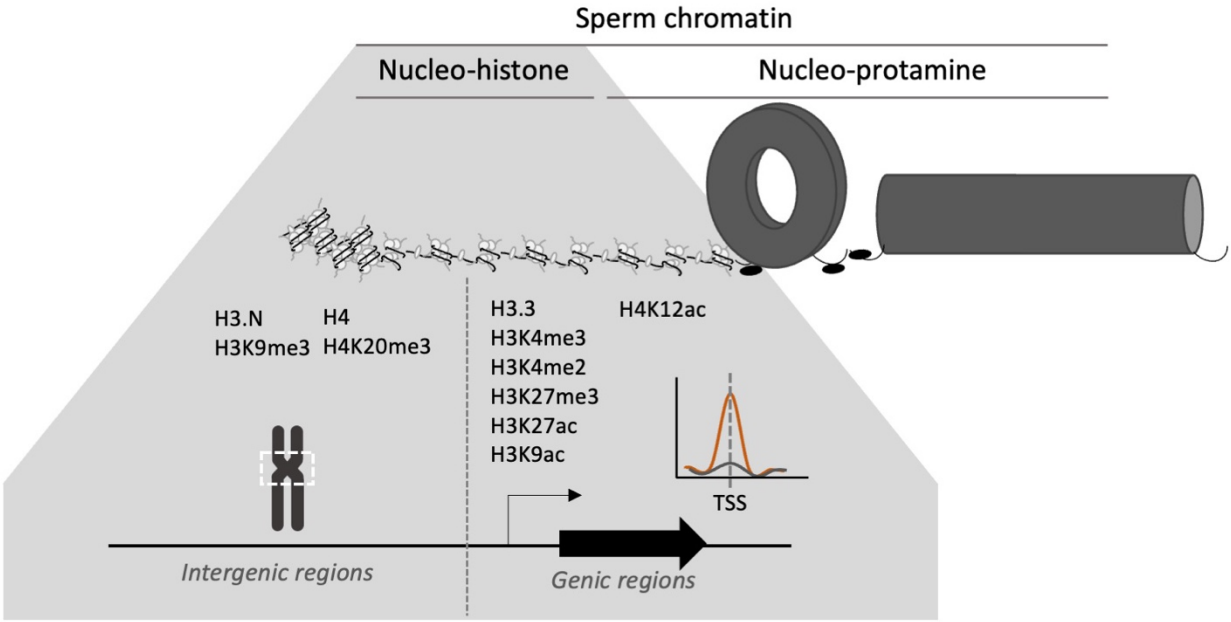


Figure 1. Modification-dependent retention of sperm histones to either intergenic (gene deserts or repetitive DNA) or genic regions (regulatory elements and transcriptional start sites, TSS). ChIP-based studies targeting histone variants and modified histones revealed a modification-dependent preferential association along the nucleosomal DNA (Nucleo-histone domain, highlighted in grey). Histone H4 and the N-terminal part of Histone H3 (H3.N), as well as the modified H3K9me3 and H4K20me3 have been detected associated with intergenic regions and repetitive DNA, as those found on the chromosomal centromeres (highlighted with a white-line box). Histone 3.3 and modified histones H3K4me3, H3K4me2, H3K27me3, H3K27ac, H3K9ac and H4K12ac are preferentially associated with promoters and genic regions characterised by the enrichment of transcriptional start sites (TSS; enrichment represented as an orange line). Based on results derived from (Arpanahi et al., 2009; Carone et al., 2014; Erkek et al., 2013; Hammoud et al., 2009; Jung et al., 2017; Ozturk et al., 2021).

Therefore, when globally evaluated, the results obtained so far lead to the hypothesis of a non-random dual behaviour of the sperm nucleo-histone DNA, with a main enrichment of intergenic regions and repetitive DNA principally associated to

centromeric loci, and the presence of promoters of developmental genes that would represent a minor proportion of the nucleosomal DNA (Castillo et al., 2015; Luense et al., 2019; Ozturk et al., 2021; Vavouri & Lehner, 2011; Yamaguchi et al., 2018) (Figure 1). Of note, when focussing on the protein fraction of the human sperm chromatin, two different sets of chromatin-associated proteins are also detected, according to their affinity to the paternal genome. Protamines and structural proteins are strongly associated to DNA, supporting the most condensed fraction of sperm chromatin. Histones, in contrast, are more easily detached simultaneously with a remarkably rich population of transcription factors and chromatin modifying proteins, which would add another layer of regulatory elements to the complex structure of human sperm chromatin (Castillo, Amaral, Azpiazu, et al., 2014).

The specific distribution of the sperm chromatin, establishing a mark of epigenetic information exclusive for the male gamete, is then robustly supported, as well as its impact on sperm function. In fact, infertile men seem to lose the specificity of the most accessible sperm DNA, showing a random nucleosomal retention and a diminished association of H3K4me or H3K27me at developmental transcription factors (Hammoud et al., 2011). Alterations in sperm histone retention, as well as in the abundance of other proteins involved in the correct packaging of sperm DNA, have also been associated to the inability to achieve a successful pregnancy after application of assisted reproduction technologies (Azpiazu et al., 2014). It has been shown in mouse that an impaired poly (ADP-ribose) metabolism during spermiogenesis give rise to sperm with an altered number of retained histones, which, remarkably, seem to promote differences also on the expression of specific embryonic genes in the offspring (Ihara et al., 2014). In addition, sperm influence on the correct embryo gene expression has been robustly demonstrated in Xenopus, showing how the specific loss of sperm histone marks results in paternally derived embryo transcriptional de-regulation with an effect on its development (Teperek et al., 2016).

Since the relevance of this exceptional epigenetic mark on sperm function and embryo development is clear, further studies should focus on still unsolved questions regarding its effect on male infertility, such as whether differences on DNA accessibility

549 can be detected among individual cells within the ejaculate, or on the possibilities to
550 overcome aberrant histone deposition in infertile patients.

551

552 **3.2. The complexity of the sperm protamines**

553 *3.2.1. The remarkable number of protamine proteoforms in the normal sperm*

554 Protamines represent the vast majority of the protein content of male gamete
555 nucleus, despite more than 6,000 different proteins having been identified (Castillo et
556 al., 2018). This is due to the highly relevant function of protamines, whose main role is
557 to compact DNA in a semi crystalline structure that allows sperm to achieve a
558 hydrodynamic shape needed to reach the oocyte, as well as to protect paternal
559 genome from external damage during this journey (Barrachina et al., 2018; Oliva,
560 2006; Oliva & Castillo, 2011).

561 The packaging capacity of protamines is higher than that of histones. In
562 particular, while a nucleosome is able to compact around 200 bp of DNA, it has been
563 estimated that the structural unit formed by the union of protamines and DNA may
564 contain at least 50,000 bp (Castillo, Amaral, & Oliva, 2014) (check further details on
565 the structure of nucleo-protamine in section 3.3 of this review). This is possible thanks
566 to the extreme physicochemical properties of protamines, which are very small and
567 extremely basic proteins, and are able to form inter- and intramolecular disulfide bonds
568 to stabilize the nucleo-protamine structure (Balhorn, 2007; Oliva, 2006). Protamine
569 function and properties are maintained among mammals, which might point also to a
570 high stability in the amino acid sequence and low isoform variety within the same
571 species. However, the fact is that a notable number of different protamine proteoforms
572 have been identified in human and mouse spermatozoa (Arauz-Garofalo et al., 2021;
573 Brunner et al., 2014; Castillo et al., 2015; Soler-Ventura et al., 2020). Protamines from
574 human sperm, as well as from other mammals, are divided in two main groups:
575 protamine 1 (P1) and protamine 2 family (P2) (Balhorn, 2007; Barrachina et al., 2019;
576 Jodar & Oliva, 2014; Oliva, 2006; Oliva & Castillo, 2011). Human P1 is translated from
577 a unique gene, named *PRM1*, as a mature protein of 6,823 Da, with 51 amino acids
578 and a 47.1% of arginine, which confers an extremely positive charge (pI=12.08;
579 UniProtKB database https://www.uniprot.org/). Human P2, in contrast, is translated
580 from the *PRM2* gene as a precursor (pre-P2) of 102 amino acids that is processed by

proteolysis in the N-terminal part giving rise to three mature components, HP2 (the most abundant one), HP3, and HP4 (Jodar & Oliva, 2014; Oliva, 2006). Interestingly, the human mature sperm not only contains P2 mature forms in its chromatin, but also retain pre-P2 and other immature proteoforms, named HPI1, HPI2, HPS1 and HPS2, the function of which has not been revealed yet (de Mateo, Ramos, et al., 2011). In addition to these P2 immature proteoforms generated by proteolysis and slightly differing between them in the number of amino acids in the N-terminal part, there is evidence at protein level of another isoform generated by alternative splicing (Soler-Ventura et al., 2020). This protein, named P2 isoform 2, contains 140 amino acids and differs from pre-P2 by the incorporation of 50 amino acids between positions 91 and 102 of the canonical sequence (Soler-Ventura et al., 2020). Of note, in the same work it was also identified an RNA corresponding to an additional splice variant, the P2 isoform 3, although it was not detected at protein level (Soler-Ventura et al., 2020). Both P2 isoforms generated by alternative splicing seem to be only conserved among higher primates but not in other mammals such as mice and rats, and no specific function has been suggested for any of them yet (Soler-Ventura et al., 2020). In global, these results reveal a high diversity of protamine amino acid sequences in human sperm, which raises the interest on deciphering whether this is the result of a simple inefficient processing of pre-P2, it responds to the need of redundancy to ensure protamine function, or there is any proteoform-specific functional implication still unknown.

The complexity of protamine proteoform composition in the sperm cell is even higher when considering post-translational modifications. As indicated in section 2.2.1. of this review, protamine phosphorylation is required for a proper deposition of protamines in the sperm chromatin and displacement of histones (Gou et al., 2020; Papoutsopoulou et al., 1999; Willmitzer et al., 1977a, 1977b; Wu et al., 2000). Despite this function during spermatogenesis, it has been shown in different mammalian species that the sperm cell retains phosphorylated protamine proteoforms (Arauz-Garofalo et al., 2021; Brunner et al., 2014; Castillo et al., 2015; Chirat et al., 1993; Pirhonen, Linnala-Kankkunen, & Mäenpää, 1994; Pruslin et al., 1987; Soler-Ventura et al., 2020). Our group has recently determined the most complete profile of phoshorylated protamine proteoforms to date in the normal human spermatozoon, by

adapting mass spectrometry approaches and proteoform identification algorithm to the special properties of protamines (Arauz-Garofalo et al., 2021; Soler-Ventura et al., 2020). In particular, mono-, di- and tri-phosphorylated proteoforms were detected for P1, while P2 was identified with one or two phosphorylations in its sequence. Of note, pre-P2 showed the highest incorporation of phosphate groups, since mono-, di-, tri- and tetra-phosphorylated proteoforms were identified (Soler-Ventura et al., 2020). In an attempt to localize the phosphor groups in the protamine sequences, several target residues have been suggested, being some of them maintained among different studies, such as S9 and S11 in P1, counting the first methionine, and S37 and S59 for P2 (Chirat et al., 1993; Hornbeck et al., 2015; Soler-Ventura et al., 2020). From those, P1 S9 and P2 S59 were also identified in the corresponding homolog protamine sequences in mice, increasing the interest on the functional role of these specific residues and their modification in the male gamete (Brunner et al., 2014). By using mouse sperm as a model, acetylation and methylation groups were also identified in protamine sequences, either as a single modification or in combination, demonstrating that protamines can bear multiple PTMs in a single molecule (Brunner et al., 2014). The relevance of some of these modifications on sperm functionality and its impact on sperm chromatin formation has been achieved using mouse models, as discussed in the following section of this review. This, together with the identification of potential alterations in specific groups of infertile patients, will not only allow increasing the knowledge on sperm chromatin compaction, but also to find novel causes of male infertility.

3.2.2. Protamine-deficient mouse models and implications for fertility status

A substantial proportion of our knowledge about the importance of the role of sperm protamines in male fertility has been obtained from functional studies in transgenic mouse models (Table 3). Early studies on protamine genes disruption in chimeric mice suggested that haploinsufficiency of Prm1 and/or Prm2 genes resulted in male infertility (Cho et al., 2001, 2003; Takeda et al., 2016). Even so, the recent introduction of sophisticated CRISPR/Cas9 technology has clearly demonstrated that while loss of a single Prm2 allele was well tolerated, disruption of both Prm2 alleles resulted in infertile mice (Schneider et al., 2016). The precision and efficiency of

CRISPR/Cas9 technology in gene editing without disturbing gene structure or regulatory DNA sequences could explain these differences. Sperm evaluation of targeted Prm2–/– mice revealed normal epididymal sperm counts but with very drastic morphological alterations in both flagellum and acrosome structures, resulting in immotile sperm (Schneider et al., 2016). However, apparently no morphological changes were observed in testicular sperm, suggesting that sperm defects in Prm2–/– mice are acquired during epididymal transit (Schneider et al., 2020). In fact, Prm2-deficient testicular sperm showed a success rate to develop blastocyst after ICSI as that of wild-type testicular sperm. Upregulation of P1 expression is observed in deficient Prm2–/– mice to compensate for the loss of P2, but even though it seems enough to properly package testicular sperm DNA, it is insufficient to generate functional epididymal spermatozoa. It has been suggested that P2 incorporates zinc into its structure to stabilize sperm chromatin in the testis (Bianchi et al., 1992; Björndahl & Kvist, 2011), but zinc molecules are released during sperm epididymal maturation (Dias et al., 2006). Recent findings have proposed that zinc released by P2 is incorporated into the protein structure of the antioxidant protein SOD1 in the epididymis, conferring stability and ensuring an optimal antioxidant activity inside spermatozoa during sperm maturation (Schneider et al., 2020). Therefore, loss of P2 could result in a low antioxidant capability of epididymal sperm that might promote alterations in sperm DNA, membranes, and morphology.

CRISPR/Cas9 technology has also been used to target *Prm1* gene. Contrary to the observed for *Prm2*+/-, disruption of just one allele of *Prm1* shows a negative impact on male fertility (Mashiko et al., 2013; Merges et al., 2022). In contrast, the phenotype of Prm1–/– mice is very similar to that of Prm2–/– mice, both being infertile with dramatic alterations in epididymal spermatozoa motility and morphology. Interestingly, accumulation of pre-processed P2 is observed when one or both alleles of Prm1 are disrupted, suggesting that P1 is required for proper P2 processing. This fact could explain why Prm1+/–, but not Prm2+/–, are subfertile. Indeed, disruption of the cleaved part of pre-P2 (cP2 domain) in one or both alleles (Prm2+/Δc and Prm2-/Δc, respectively) results in immotile and inviable sperm, similar to Prm2-/- and Prm1-/- spermatozoa (Arévalo et al., 2022). Additionally, testicular sperm from Prm2+/Δc and Prm2-/Δc transgenic mice already show DNA fragmentation that increase throughout

epididymal transit, contrasting with the phenotype observed in Prm2–/– mice. These different results could be explained by a disruption of the synergistic process of NH-NP mediated by H2A.L.2–TP complexes potentially induced by the loss of cP2, which may end with a random incorporation of P2 in the sperm chromatin (Arévalo et al., 2022). Non-specific binding of protamines to DNA lead to strong DNA hypercondensation, which could result in strand breaks in testicular spermatozoa. Moreover, it seems that TPs are retained in sperm chromatin in absence of cP2, therefore avoiding P1 and P2 incorporation. Strong oxidative DNA damage in cauda epididymis and complete epididymal sperm DNA fragmentation were reported in both Prm2+/Δc and Prm2-/Δc mice. Of note, the Prm2-/Δc model displayed a more severe phenotype, showing not only alterations on sperm motility and morphology, but also reduced sperm counts.

Table 3. Sperm evaluation and fertility status of the available protamine-deficient mouse models

	Generation of protamine mice mutants	Sperm concentration	Sperm motility	Sperm morphology	Sperm DNA damage	Fertility	Others	References
Chimeras *Prm1*+/–	Disruption of either *Prm1* or *Prm2* coding sequence of one allele in ES cells by homologous recombination and ES injection into blastocysts	Normal	Reduced	Flagellum tightly wrapped around the head or with elongated heads having a reduced ventral flexure	Altered sperm chromatin integrity, higher sperm DNA fragmentation	No sire produced	Only P1 protein was reduced. Abnormally processed P2	(Cho et al., 2001, 2003)
Chimeras *Prm2*+/–							P1 and mature P2 were reduced. Abnormally processed P2	
Prm1+/–	*Prm1*-deficient female chimeric mice carrying *Prm1*-deficient oocytes	Normal	Reduced	Abnormal morphology mainly in the tail	Altered sperm chromatin integrity, higher sperm DNA fragmentation	No sire produced by natural mating or IVF but by IVF with zona-free oocytes	Enhanced acrosome reaction and reduced mitochondrial membrane potential. Reduced P1 and mature P2. Abnormally processed P2	(Takeda et al., 2016)
Prm1+/–	CRISPR/Cas9 mediated gene-editing in zygotes	Normal	Drastically decreased	Normal (no drastic head defects)	Low but detectable DNA fragmentation	Subfertile (low pregnancy rate, reduced litter size)	Accumulation of P2 precursor. Impaired flagellar structure.	(Merges et al., 2022)
Prm1–/–		Normal	Immotile	Head defects (lose of hooked-shape, smaller, elliptic, thinner), membrane damage, disrupted acrosome	Altered sperm chromatin integrity. Almost all DNA is fragmented, some part remains intact	No sire produced	Accumulation of P2 precursor, increased histone retention, defects on chromatin hypercondensation. Impaired flagellar structure and membrane	
Prm2+/–	CRISPR/Cas9 mediated gene-editing in oocytes	Normal	Normal	Normal	Normal	Fertile	Reduced P2	(Schneider et al., 2016, 2020)
Prm2–/–		Normal	Immotile	No acrosome, midpiece wrapped around sperm head	Altered sperm chromatin integrity, sperm DNA fully fragmented	No sire produced	No P2 and upregulation of P1. Declined viability	
Prm2+/Δc	CRISPR/Cas9 mediated gene-editing in oocytes	Normal	Drastically decreased	a) Slimmer less-hooked nucleus, and b) smaller hookless nucleus	Completely fragmented DNA	Infertile	Drastically decreased viability. Switched P1/P2 ratio, P2 precursor accumulation. Incorrect eviction of P2 from spermatid nucleus.	(Arévalo et al., 2022)
Prm2–/Δc		Reduced	Drastically decreased	Similar but more severe nuclear defects than $Prm2^{+/\Delta c}$	Completely fragmented DNA, even more severe	Infertile	Drastically decreased viability. More pronounced switch of P1/P2 ratio. Additional P2 signal in spermatid cytoplasm and residual bodies.	
P1S9A/+	CRISPR/Cas9 mediated Knock-in Mutations in specific Phosphorylation Sites of P1	Normal	NA	Normal	Normal DNA compaction	Fertile	-	(Gou et al., 2020)
P1S43A/+		Normal	NA	Normal	Normal DNA compaction	Fertile		
P1S9S43A/+		Slightly reduced	NA	Normal	Normal DNA compaction	Drastic Reduced		
P2S56A/A	CRISPR/Cas9 mediated Knock-in Mutations in specific Phosphorylation Sites of P2	NA	NA	NA	NA	Fertile	-	(Itoh et al., 2019)
P2S56D/D		NA	NA	NA	NA	Fertile		

3.2.3. Alterations on human protamines and association to male infertility

It is difficult to establish the phenotypic effects of protamine disruption in humans, since there is too little genetic variation among human protamine genes (Jodar et al., 2011). Among population variation of the harmonized sequencing data of 125,748 exome sequences and 15,708 whole genome sequences provided by gnomAD v2 1.1, we found 24 and 11 alleles with a frameshift or stop gain variant in *PRM1* and *PRM2* genes, respectively. To the best of our knowledge, just one infertile patient has been described to be carrier of the nonsense variant c.248C>T (p.Q50*) in the *PRM2* gene in heterozygosis (Tanaka et al., 2003). Although this infertile patient did not show any sperm in the ejaculate, the pathogenesis of the variant could not be confirmed since no functional or segregation studies were performed in this case. However, according to the results in disrupted *Prm1* and *Prm2* mice described in the section above, this nonsense variant in heterozygosis does not seem to be the cause of the azoospermia observed in this patient.

Additionally, pathogenic missense variants in protamine genes are extremely rare in infertile patients and are always identified in heterozygous state (Jodar et al., 2011). In fact, from the 2,992 and 795 alleles with a missense variant in *PRM1* and *PRM2* genes, respectively, identified in the general population, only 31 and 4 individuals carried a missense variant in homozygosis (Figure 2). Of those, the most frequent genetic variant is c.102G>T (p.Arg34Ser) in *PRM1* gene with an allelic frequency of 0.9% and a total of 30 homozygotes detected in the general population. Although some studies suggested this variant as a potential risk factor for male infertility, due to the replacement of an arginine residue by a serine, which could represent a new potential phosphorylation site on P1, this hypothesis was not supported by the meta-analysis performed by our group (Jodar et al., 2011). This likely silent effect agrees with the fertile phenotypes observed in transgenic mice with knock-in mutations at specific phosphorylated residues of P1 and P2 (Gou et al., 2020; Itoh et al., 2019). Specifically, these knock-in mice were generated to evaluate whether loss of specific sites of phosphorylation on protamines would affect fertility, and no adverse effects were observed for single mutations. These results suggest a redundancy within protamine phosphorylation sites, with no individual direct impact on

fertility. Nevertheless, a minimum level of phosphorylation on P1 must be reached for proper sperm functionality, since drastic reduced fertility was observed in mice when two phosphorylation sites were simultaneously depleted on P1 (Gou et al., 2020). In contrast to the redundancy associated with the protamine phosphorylation sites, protamine dephosphorylation, at least for P2, has been revealed as crucial for fertility. In particular, male infertility together with abnormal sperm morphology has been observed in mice when dephosphorylation of residue 56 of P2 is disrupted, being the phenotype rescued when the same residue is modified to avoid phosphorylation (Itoh et al., 2019). A correct dephosphorylation of the new phosphorylation site created by the variant c.102G>T in P1 mentioned above could explain why it has no impact in fertility. Therefore, the search for alterations in the PTMs of protamines, rather than in the unmodified residues, seems to provide more answers about the impact of protamines on male fertility.

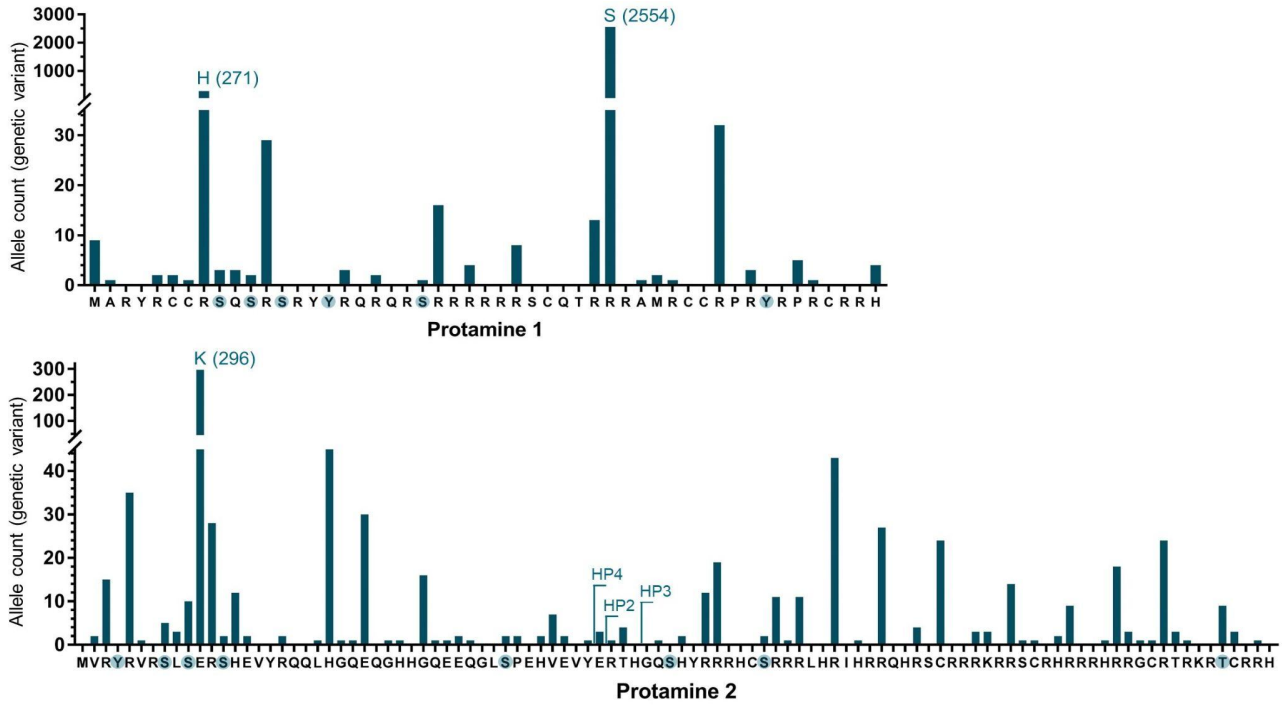


Figure 2. Number of alleles presenting missense variants identified in human protamine genes in the general population. A total of 2,992 alleles have been found with missense variants in protamine 1 (upper plot), being p.Arg8His and p.Arg34Ser the two most abundant changes. Of the 795 alleles with a missense variant in protamine 2 (lower plot), p.Glu11Lys is the most abundant one, found in the catalytic part of the protamine 2 precursor. Most of the variants reported herein are found in heterozygosis. The most frequent amino acid resulting from the missense variant is shown at the top of the bars corresponding to the most abundant alleles (specific count shown in brackets). Amino acid sequence is shown on the X-axis for both protamines, and annotated phosphorylation sites are

highlighted with a blue circle. Cleavage sites for human protamine 2, 3, and 4 (HP2, HP3, and HP4, respectively) are shown on the plot.

Apart from the search of single-nucleotide variants in protamine gene sequences, the relative protein levels of P1 and P2 have traditionally been evaluated as an indicator of sperm chromatin status and male infertility. It has been proposed that mature sperm from fertile men have a P1/P2 ratio around 1, suggesting a similar abundance of P1 and P2 components at the protein level (Balhorn et al., 1988; de Yebra et al., 1993; Mengual et al., 2003; Nanassy et al., 2011). Alterations in the P1/P2 ratio, as well as in the individual abundance of P1 and P2, have been associated with altered seminal parameters (sperm count, motility, and morphology), increased DNA damage, and lower success rates of assisted reproduction technologies (ART), as summarized in (Jodar & Oliva, 2014) and (Soler-Ventura et al., 2018).

Not only protein alterations in mature P1 and P2, but also in pre-P2 seem to compromise male fertility, either due to incomplete processing of pre-P2 or the total absence of mature P2 (Carrell & Liu, 2001; de Mateo et al., 2009; de Mateo, Ramos, et al., 2011; Rezaei-Gazik et al., 2022), with impact on increased DNA damage, lower sperm count, reduced motility, abnormal morphology, and worse ART outcomes (Rezaei-Gazik et al., 2022; Soler-Ventura et al., 2018). It has recently been reported that increased retention of pre-P2 in sperm is associated with fertilization failure, as well as to impaired nucleosome disassembly during spermatogenesis (Rezaei-Gazik et al., 2022), which could explain the origin of the observed sperm defects.

Overall, these findings support a role of protamines in the production of fully functional sperm, ART success, and post-fertilization events, evidencing that alterations in the relative amount between P1 and P2, as well as in pre-P2 processing, have a direct impact on male infertility. It is important to remark that the threshold for the P1/P2 ratio has been defined by conventional techniques based on acid-urea polyacrylamide gel electrophoresis (acid-urea PAGE), which limits quantification to the main bands corresponding to P1 and P2. Therefore, this approach would not encompass the whole amount of protamine proteoforms that have been described by mass spectrometry (Arauz-Garofalo et al., 2021; Soler-Ventura et al., 2020); see previous section 3.2.1. for more information), which could explain the variability in P1/P2 levels detected among studies (Ni et al., 2016).

3.3. The nucleo-protamine structure model: knowledge derived from different complementary methodological approaches

The current model of the human sperm chromatin structure is summarized in Figure 3 and is the result of the application of a wide range of methodologies. The first clues to understand the structure of nucleo-protamine were derived from knowledge of the chemical composition of its constituents (protamines and DNA) together with the extremely condensed structure of the sperm nucleus, as observed by microscopy (Figure 3B). Protamines were one of the first proteins to be isolated more than a century ago by Friedreich Miescher, who extracted a basic component that he called “protamin” coupled to an acidic component that he called “nuclein” (later known as DNA) from salmon sperm (Dahm, 2005; Miescher, 1874). The extreme basic nature of “protamin” and the acidic nature of “nuclein” readily suggested a condensed structure based on strong electrostatic interactions that explained the highly condensed structure of the sperm nucleus observed by microscopy methods (Figure 3B). Despite that, while protamines were one of the first proteins to be isolated, study of the details of the nucleo-protamine structure, composition and function started much later (Bloch, 1969; Dixon, 1972).

When comparing among species, protamines are found to be highly variable proteins, since many vertebrates either have no protamines in their mature spermatozoa or, when present, the amino acid sequences show low homology (Kasinsky et al., 1987, 2011; Mezquita, 1985; Oliva & Dixon, 1991; Soler-Ventura et al., 2018; Subirana, 1983). This diversity contrasts with the extremely well conserved eukaryotic somatic chromatin packaged by nucleosomal particles (Figure 3C). Possibly due to its high conservation, nucleo-histone structure was elucidated much earlier than that of the nucleo-protamine by a combination of electron microscopy techniques. This approach evidenced “beads on a string” images, combined with information derived from partial micrococcal nuclease digestion of chromatin and size determination of the generated DNA ladders, which allowed determining the nucleosomal elementary size (Subirana et al., 1985). Furthermore, nucleosome crystallization allowed determining its high-resolution structure by X-ray diffraction (Azorin et al., 1980; Subirana, 1997). In contrast, no nucleo-protamine crystals have

been obtained so far. Thus, the information and models available on the nucleo-protamine structure, either extracted *in vivo* or reconstituted *in vitro,* are based on the combination of a wide range of microscopic techniques and X-ray diffraction in solution.

Different reports applying electron microscopy and/or atomic force microscopy to the study of human, mouse and rooster sperm chromatin have evidenced a combination of toroidal structures with an external diameter of 50-160 nm and a width of 40-55 nm, and rod-like structures with a thickness of 40-55 nm and a length of 160-350 nm (Figure 3D; (Allen et al., 1993, 1997; Ausió et al., 2014; Balhorn, 2007; Hud et al., 1993, 1995; Vilfan et al., 2006). Of note, similar toroidal structures were obtained *in vitro* upon DNA condensation with purified protamines and other cations (Conwell et al., 2003; Conwell & Hud, 2004; DeRouchey & Rau, 2011).

At its finer structure, one of the initial approximations was based on a tRNA-protamine crystal and X-ray diffraction which led to the proposal of a model where protamine molecules would bind to the narrow groove of double helical portion of tRNA (Warrant & Kim, 1978). Nevertheless, results based on tRNA-protamine complexes are not necessarily extrapolated to infer the DNA-protamine complex structure. In fact, the results derived from X-ray diffraction studies using *in vitro* reconstituted nucleo-protamine in solution or using native sperm chromatin, suggest a model favoured by most studies where protamine molecules would align along of DNA and bind to the major groove (Figure 3E) (Balhorn, 1982; Fita et al., 1983; Vilfan et al., 2004).

Furthermore, molecular dynamics simulations and free energy calculations with full atomistic details have indicated that protamine molecules located in the major groove rather utilize the DNA backbone as a binding site, which represents the best compromise between enthalpy and entropy gains (Mukherjee et al., 2021).

These linear complexes of DNA and protamine have been also proposed to be associated side-by-side in a close-packed hexagonal arrangement (Figure 3F-right; (Allen et al., 1993; Balhorn, 1982; Fita et al., 1983; Hud & Downing, 2001; Hud & Vilfan, 2005; Sartori Blanc et al., 2001). Accurate measurements using small angle x-ray scattering (SAXS) concluded that in this hexagonal lattice, the equilibrium

interaxial spacing (Dint) representing the actual distance between DNA helices is 30.1 A° for bull sperm nuclei and 29.2 A° for salmon sperm nuclei, both in solution under near physiological salt conditions (150 mM NaCl), without added reducing agent and at a temperature of 20ºC (Hutchison et al., 2017) (Figure 3F). A different approach based on an infrared spectroscopy study of salmon and squid protamines complexed with DNA also concluded that DNA-bound protamine in sperm nuclei contains large amounts of defined secondary structure that is stabilized by intramolecular hydrogen bonding and that efficiently promotes tight hexagonal packing of DNA molecules (Roque et al., 2011).

In addition to the strong electrostatic interactions derived from the positively charged arginine residues in protamines, and the negatively charged phosphates of the DNA backbone, an additional layer of stabilization occurring in cysteine-containing protamines is provided by the formation of inter- and intra-molecular disulfide bonds and the formation of zinc bridges (Balhorn, 2007; Björndahl & Kvist, 2011; Hutchison et al., 2017; Vilfan et al., 2004). As discussed in other sections of this review, this tightly packed nucleo-protamine structure condenses most of the sperm DNA, is non-randomly distributed in the genome, and intercalates with regions retaining histones and nucleosomes (Figure 3D), providing an epigenetic richness that is transferred to the oocyte upon fertilization (Castillo, Amaral, Azpiazu, et al., 2014; Castillo et al., 2015; Gatewood et al., 1987; Hammoud et al., 2009; Oliva, 2006).

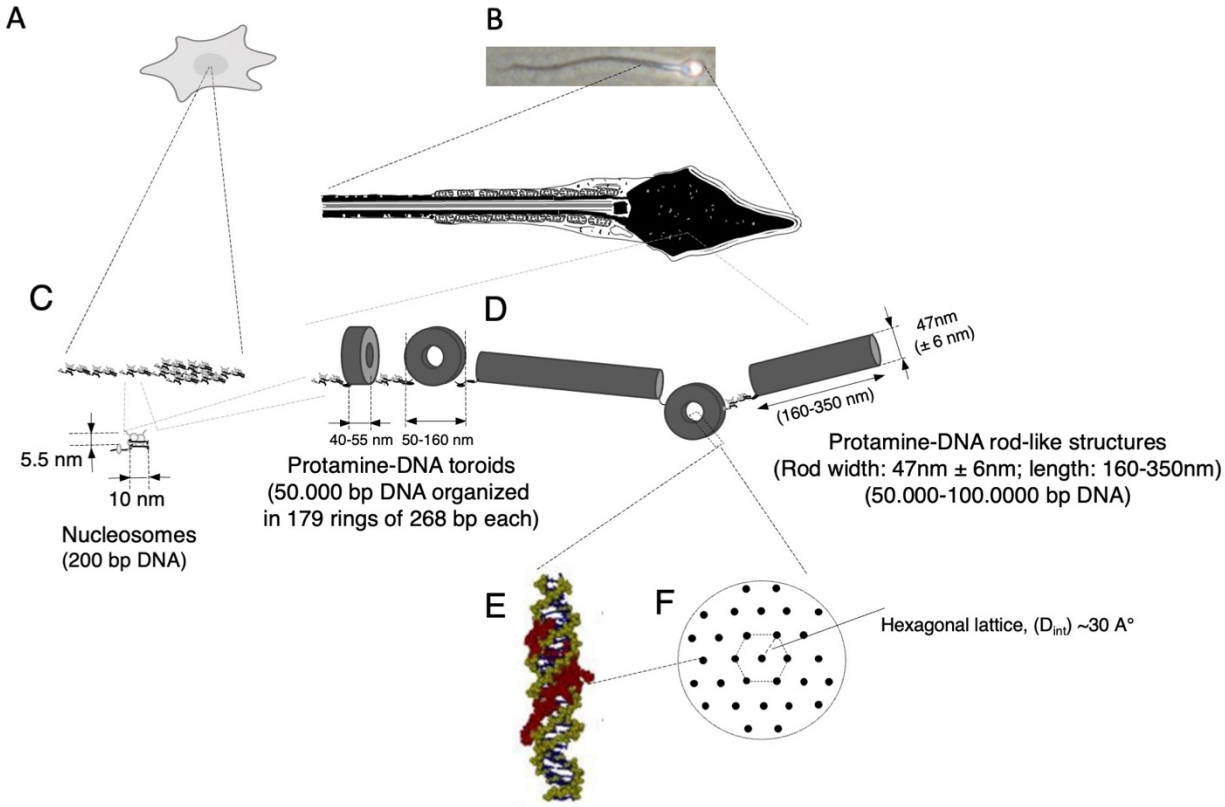


Figure 3. Current model of the mammalian nucleo-protamine structure. At the top of the figure, scale representations of a human somatic cell (A) compared to an optical microscopy image of a human spermatozoa (B) and an enlarged section of the head and midpiece, where it is possible to appreciate a reduction in the size of the sperm head, are shown. C: schematic representation of the nucleo-histone structure of somatic cells where each nucleosome organizes approximately 200bp of DNA. D: Current model of the nucleo-protamine structure formed by toroidal and rod-like structures. E: favoured model where protamines would bind longitudinally located in the major groove of the DNA. F: Evidence indicates that linear complexes of DNA and protamine are associated side-by-side in a close-packed hexagonal arrangement with an interaxial spacing (Dint) representing the actual distance between DNA helices of 30.1 A° (see text for references and more details).

4. PATERNAL CHROMATIN REMODELLING BEYOND FERTILIZATION: THE ZYGOTIC EVENT OF PROTAMINE-TO-HISTONE TRANSITION AS A MODEL TO STUDY THE PROCESS OF CHROMATIN (DE-)COMPACTION

The interplay between histones and protamines is not limited to male germ cell development. As it can be seen in the scheme of male germ cells' chromatin remodelling through DNA (de-)protamination in Figure 4, once the nucleoprotamine structure has been established in mature sperm, the male pronucleus must be de-compacted after fertilization to start activation of the embryonic genome. Nucleoplasmins are a protein family that plays an essential role in male pronuclear decompaction (Philpott & Leno, 1992). Interestingly, some of the key players involved in the NH-NP transition, or in its regulation, have been found to be crucial for the

inverse process of protamine-to-histone transition in the zygote. A very elegant study demonstrated the crucial role of SRPK1-mediated protamine phosphorylation accelerating the process by recruiting nucleoplasmin to H3.3-retained nucleosomes, which would be the starting point of the protamine removal (Gou et al., 2020). Additionally, phosphorylated protamines would allow recruitment of Protein HIRA to deposit H3.3 into newly free DNA regions, which is essential for *de novo* nucleosome assembly and required for proper nuclear envelope formation in the zygote (Gou et al., 2020; Inoue & Zhang, 2014; Lin et al., 2014; van der Heijden et al., 2005). Histone chaperone ASF1 assists in the loading of H3.3-H4 dimers into HIRA, before their incorporation into the paternal chromatin (Horard et al., 2018). Other histone variants such as TH2A, TH2B, and H2A.X (Montellier et al., 2013; Nashun et al., 2010; Shinagawa et al., 2014) and histone PTMs such as H3K4 methylation mediated by the Histone-lysine N-methyltransferase (MLL) complex MLL3/4 (Aoshima et al., 2015) also play a crucial role in paternal genome reprogramming guiding genome-wide chromatin transitions.

These findings also suggest a coordinated epigenetic regulation of the process, that somehow resembles that of the NH-NP transition. Therefore, it could be thought that impairments in the nucleo-protamine structure, derived from a non-efficient process of nuclear compaction, from poor structural stabilization during sperm maturation in the male reproductive tract, or from an altered composition of protamine proteoforms in the sperm chromatin, could also impact de-protaminization rhythms in the zygote and potential effects on paternal nuclear reprogramming and beyond.

The study of this reverse process could be of high interest as a model to find new regulators of the spermiogenic process. For example, H4R3 methylation has been found to play a role in de-protaminization of the male pronucleus (Hatanaka et al., 2017), the potential role of which is still unknown during spermiogenesis. Recent findings have identified arginine methylation of histone H3 prior to phosphorylation of H3T3 by Serine/threonine-protein kinase haspin (Haspin) during spermiogenesis, but with unknown function (Soupsana et al., 2021). Also, H3 arginine dimethylation in the core histone weakens histone affinity to DNA (Casadio et al., 2013). It is known that some arginine methylations on the histone tail are related with transcriptional activation (i.e., open chromatin states), and H4R3me2, in particular, triggers a subsequent acetylation of H4 histone tails by p300 (H. Wang et al., 2001). H4 arginine methylation is indeed regulated by the crosstalk of its modulators with other H4 coil PTMs, such as acetylated or butyrylated K5, or phosphorylated S1 (Fulton et al., 2022), which is involved in histone accessibility and mitotic chromatin compaction and is essential for histone deacetylation after DNA-breaks repair (Krishnamoorthy et al., 2006; Utley et al., 2005). This may lead us to envisage a role for histone arginine methylation on nucleosome destabilization during spermiogenesis coordinated with acetylation, phosphorylation, and their writers, readers, and erasers.

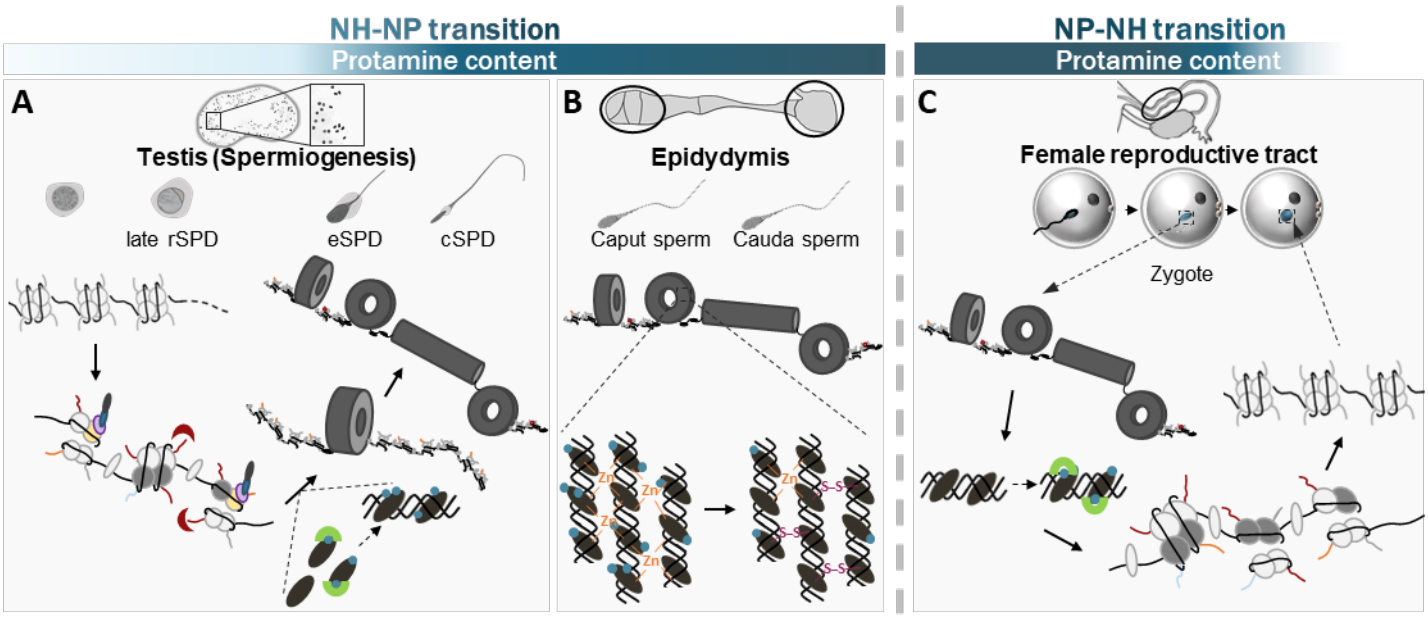


Figure 4. Schematic representation of male germ cell chromatin compaction through the nucleo-histone to nucleo-protamine transition, and the reverse post-fertilization process of male pronuclear decompaction through the nucleo-protamine to nucleo-histone transition in the zygote, based on the current literature. A During spermiogenesis, core histones (light grey) are replaced by H2A.L.2 (in yellow), other histone variants (dark grey), and transition proteins (purple), building the template for the processing of immature protamine 2 (elongated forms in blue and grey). Other histone PTMs (represented as multi-coloured histone tails), and their writers, readers, and erasers (moon-shaped, in red) assist nucleosome removal. Protamine (elongated shape, dark grey) incorporation is facilitated by phosphorylation (blue dots) added by kinases (in green), allowing protamine accommodation to originate higher-order structures (in grey). Some nucleosomes bearing specific histone PTMs are retained. **B** In the epididymis, part of zinc bridges (Zn, in orange) are lost, and the chromatine is stabilized through disulphide bonds (S-S, in magenta), coupled to a potential protamine dephosphorylation wave. **C** The reverse process occurs in the zygote, where some essential proteins to achieve a proper NH-NP transition play a role in reprogramming the male genome.

Conclusion

In this article, we review all advances made, from the use of conventional techniques to the most novel approaches, to deeply explore the formation of sperm chromatin during sperm development and the final nucleo-protamine structure from the protein point of view, with a special focus on the lead actors, the protamines, and the implications in male infertility. We provide evidence on the complexity of the chromatin compaction process, in which orchestrated events involving different levels of protein regulation through histone PTMs and their modulators allow the displacement of canonical nucleosomes from the paternal genome and the incorporation of protamines. Besides the well-known regulators of the NH-NP transition during spermiogenesis, we gather new findings on other histone PTMs, such as the lesser-described non-acetyl histone acylations and the protamine PTMs, and

highlight the importance of their readers, writers, and erasers as a new layer of regulation in post-meiotic sperm development. Even after leaving the testis, the process of nuclear compaction continues to fine-tune the final genome packaging in sperm, stabilizing the structure through inter- and intra-molecular disulphide bonds during epididymal maturation. This exceptionally complex scenario evidences the handicaps that need to be overcome to develop human *in vitro* spermatogenesis models and obtain fully functional male gametes. There is still need to increase the knowledge on the processes of DNA protaminization and de-protaminization, during post meiotic cell development and zygotal male pronuclear reprogramming, respectively, to be able to properly mimick the process of protamine incorporation in humans *in vitro*.

Apart from that, the own aminoacidic nature of the small and arginine-rich protamines is what gives them their intrinsic unique way of compacting sperm DNA. However, top-down proteomic studies on purified protamines have revealed a much more complex population of protamine proteoforms than previously thought, including mature, immature, and truncated forms of P1 and P2, also bearing PTMs. Such diversity raises the question of whether this is the result of a need of functional redundancy to cover protamine demand during the short window of spermatid elongation, or it is revealing the presence of protamine proteoforms with specific roles. In this regard, it is interesting to highlight that although some levels of protamine phosphorylation are needed for proper sperm development, what has been revealed as essential to achieve fertility potential is the dephosphorylation of specific residues at least for P2. Therefore, although many details about the implication of protamine proteoforms remain to be discovered, this complex population points to potential specific roles for some of the candidates, either in protamine deposition on DNA, or in achieving higher-order chromatin structures. Indeed, the nucleo-protamine structure model evidences that the protamine-packaged genome does not result in a unique way of chromatin compaction, but in a combination of toroidal and *rod-like* structures. Investigating whether these two different high-order chromatin organizations arise from a differential composition of protamine proteoforms would suppose a milestone in understanding paternal genome packaging and protection, and subsequent implications for male fertility.

Taking together the role of sperm chromatin-associated and regulatory proteins needed to achieve a successful post meiotic germ cell development and to contribute to the mature sperm epigenome, as well as the implications of their alterations on sperm functionality, we provide evidence on the importance of maintaining a proper chromatin structure and composition to support male fertility. Therefore, we highlight the importance of monitoring sperm chromatin quality, on its many different levels, towards the successful generation of a new individual.

Funding Information

This work was supported by grants to R.O. from the "Ministerio de Economía y Competividad (Spain)" (fondos FEDER 'una manera de hacer Europa', PI20/00936). A.I. is supported by a fellowship of the Ministerio de Economía, Industria y Competitividad (Spain) (PFIS, FI17/00224). J.C. is Serra Húnter fellow (Universitat de Barcelona, Generalitat de Catalunya).

References

Allen, M. J., Bradbury, E. M., & Balhorn, R. (1997). AFM analysis of DNA-protamine complexes bound to mica. *Nucleic Acids Research*, *25*(11), 2221–2226. https://doi.org/10.1093/nar/25.11.2221

Allen, M. J., Lee, C., Lee, J. D., Pogany, G. C., Balooch, M., Siekhaus, W. J., & Balhorn, R. (1993). Atomic force microscopy of mammalian sperm chromatin. *Chromosoma*, *102*(9), 623–630. https://doi.org/10.1007/BF00352310

Aoshima, K., Inoue, E., Sawa, H., & Okada, Y. (2015). Paternal H3K4 methylation is required for minor zygotic gene activation and early mouse embryonic development. *EMBO Reports*, *16*(7), 803–812. https://doi.org/10.15252/embr.201439700

Arauz-Garofalo, G., Jodar, M., Vilanova, M., de la Iglesia Rodriguez, A., Castillo, J., Soler-Ventura, A., Oliva, R., Vilaseca, M., & Gay, M. (2021). Protamine Characterization by Top-Down Proteomics: Boosting Proteoform Identification with DBSCAN. *Proteomes*, *9*(2). https://doi.org/10.3390/proteomes9020021

Arévalo, L., Merges, G. E., Schneider, S., Oben, F. E., Neumann, I. S., & Schorle, H. (2022). Loss of the cleaved-protamine 2 domain leads to incomplete histone-to-protamine exchange and infertility in mice. *PLOS Genetics*, *18*(6), e1010272. https://doi.org/10.1371/journal.pgen.1010272

Arpanahi, A., Brinkworth, M., Iles, D., Krawetz, S. A., Paradowska, A., Platts, A. E., Saida, M., Steger, K., Tedder, P., & Miller, D. (2009). Endonuclease-sensitive regions of human spermatozoal chromatin are highly enriched in promoter and CTCF binding sequences. *Genome Research*, *19*(8), 1338–1349. https://doi.org/10.1101/gr.094953.109

Ausió, J., González-Romero, R., & Woodcock, C. L. (2014). Comparative structure of vertebrate sperm chromatin. *Journal of Structural Biology*, *188*(2), 142–155. https://doi.org/10.1016/j.jsb.2014.09.004

Azorin, F., Martínez, A. B., & Subirana, J. A. (1980). Organization of nucleosomes and spacer DNA in chromatin fibres. *International Journal of Biological Macromolecules*, *2*(2), 81–92. https://doi.org/10.1016/0141-8130(80)90033-1

Azpiazu, R., Amaral, A., Castillo, J., Estanyol, J. M., Guimerà, M., Ballescà, J. L., Balasch, J., & Oliva, R. (2014). High-throughput sperm differential proteomics suggests that epigenetic alterations contribute to failed assisted reproduction. *Human Reproduction*, *29*(6), 1225–1237. https://doi.org/10.1093/humrep/deu073

Baarends, W. M., Hoogerbrugge, J. W., Roest, H. P., Ooms, M., Vreeburg, J., Hoeijmakers, J. H. J., & Grootegoed, J. A. (1999). Histone Ubiquitination and Chromatin Remodeling in Mouse Spermatogenesis. *Developmental Biology*, *207*(2), 322–333. https://doi.org/10.1006/dbio.1998.9155

Baert, Y., De Kock, J., Alves-Lopes, J. P., Söder, O., Stukenborg, J.-B., & Goossens, E. (2017). Primary Human Testicular Cells Self-Organize into Organoids with Testicular Properties. *Stem Cell Reports*, *8*(1), 30–38. https://doi.org/10.1016/j.stemcr.2016.11.012

Balhorn, R. (1982). A model for the structure of chromatin in mammalian sperm. *The Journal of Cell Biology*, *93*(2), 298–305. https://doi.org/10.1083/jcb.93.2.298

Balhorn, R. (2007). The protamine family of sperm nuclear proteins. *Genome Biology*, *8*(9), 227. https://doi.org/10.1186/gb-2007-8-9-227

Balhorn, R., Reed, S., & Tanphaichitr, N. (1988). Aberrant protamine 1/protamine 2 ratios in sperm of infertile human males. *Experientia*, *44*(1), 52–55. https://doi.org/10.1007/BF01960243

Bao, J., & Bedford, M. T. (2016). Epigenetic regulation of the histone-to-protamine transition during spermiogenesis. *Reproduction*, *151*(5), R55–R70. https://doi.org/10.1530/REP-15-0562

Barrachina, F., de la Iglesia, A., Jodar, M., Soler-Ventura, A., Mallofré, C., Rodriguez-Carunchio, L., Goudarzi, A., Corral, J. M., Ballescà, J. L., Castillo, J., & Oliva, R. (2022). Histone H4 acetylation is dysregulated in active seminiferous tubules adjacent to testicular tumours. *Human Reproduction*. https://doi.org/10.1093/humrep/deac130

Barrachina, F., Jodar, M., Delgado-Dueñas, D., Soler-Ventura, A., Estanyol, J. M., Mallofré, C., Ballescà, J. L., & Oliva, R. (2019). Stable-protein Pair Analysis as A Novel Strategy to Identify Proteomic Signatures: Application To Seminal Plasma From Infertile Patients. *Molecular & Cellular Proteomics*, *18*(Supplement 1), S77–S90. https://doi.org/10.1074/mcp.RA118.001248

Barrachina, F., Soler-Ventura, A., Oliva, R., & Jodar, M. (2018). Sperm Nucleoproteins (Histones and Protamines). In A. Zini & A. Agarwal (Eds.), *A Clinician's Guide to Sperm DNA and Chromatin Damage.* (pp. 31–51). Springer International Publishing. https://doi.org/10.1007/978-3-319-71815-6_2

Barral, S., Morozumi, Y., Tanaka, H., Montellier, E., Govin, J., de Dieuleveult, M., Charbonnier, G., Couté, Y., Puthier, D., Buchou, T., Boussouar, F., Urahama, T., Fenaille, F., Curtet, S., Héry, P., Fernandez-Nunez, N., Shiota, H., Gérard, M., Rousseaux, S., … Khochbin, S. (2017). Histone Variant H2A.L.2 Guides Transition Protein-Dependent Protamine Assembly in Male Germ Cells. *Molecular Cell*, *66*(1), 89-101.e8. https://doi.org/10.1016/j.molcel.2017.02.025

Battulin, N., Fishman, V. S., Mazur, A. M., Pomaznoy, M., Khabarova, A. A., Afonnikov, D. A., Prokhortchouk, E. B., & Serov, O. L. (2015). Comparison of the three-dimensional organization of sperm and fibroblast genomes using the Hi-C approach. *Genome Biology*, *16*(1), 77. https://doi.org/10.1186/s13059-015-0642-0

Bell, E. L., Nagamori, I., Williams, E. O., Del Rosario, A. M., Bryson, B. D., Watson, N., White, F. M., Sassone-Corsi, P., & Guarente, L. (2014). SirT1 is required in the male germ cell for differentiation and fecundity in mice. *Development*, *141*(18), 3495–3504. https://doi.org/10.1242/dev.110627

Bianchi, F., Rousseaux-Prevost, R., Sautiere, P., & Rousseaux, J. (1992). P2 protamines from human sperm are zinc -finger proteins with one CYS2/HIS2 motif. *Biochemical and Biophysical Research Communications*, *182*(2), 540–547. https://doi.org/10.1016/0006-291x(92)91766-j

Björndahl, L., & Kvist, U. (2011). A model for the importance of zinc in the dynamics of human sperm chromatin stabilization after ejaculation in relation to sperm DNA vulnerability. *Systems Biology in Reproductive Medicine*, *57*(1–2), 86–92. https://doi.org/10.3109/19396368.2010.516306

Blanco, M., & Cocquet, J. (2019). Genetic Factors Affecting Sperm Chromatin Structure. *Advances in Experimental Medicine and Biology*, *1166*, 1–28. https://doi.org/10.1007/978-3-030-21664-1_1

Bloch, D. P. (1969). A catalog of sperm histones. *Genetics*, *61*(1), Suppl:93-111.

Bolcun-Filas, E., & Handel, M. A. (2018). Meiosis: the chromosomal foundation of reproduction. *Biology of Reproduction*, *99*(1), 112–126. https://doi.org/10.1093/biolre/ioy021

Bonisch, C., & Hake, S. B. (2012). Histone H2A variants in nucleosomes and chromatin: more or less stable? *Nucleic Acids Research*, *40*(21), 10719–10741. https://doi.org/10.1093/nar/gks865

Boulard, M., Gautier, T., Mbele, G. O., Gerson, V., Hamiche, A., Angelov, D., Bouvet, P., & Dimitrov, S. (2006). The NH_2 Tail of the Novel Histone Variant H2BFWT Exhibits Properties Distinct from Conventional H2B with Respect to the Assembly of Mitotic Chromosomes. *Molecular and Cellular Biology*, *26*(4), 1518–1526. https://doi.org/10.1128/MCB.26.4.1518-1526.2006

Boussouar, F., Rousseaux, S., & Khochbin, S. (2008). A new insight into male genome reprogramming by histone variants and histone code. *Cell Cycle*, *7*(22), 3499–3502. https://doi.org/10.4161/cc.7.22.6975

Brunner, A. M., Nanni, P., & Mansuy, I. M. (2014). Epigenetic marking of sperm by post-translational modification of histones and protamines. *Epigenetics & Chromatin*, *7*(1), 2. https://doi.org/10.1186/1756-8935-7-2

Bryant, J. M., Donahue, G., Wang, X., Meyer-Ficca, M., Luense, L. J., Weller, A. H., Bartolomei, M. S., Blobel, G. A., Meyer, R. G., Garcia, B. A., & Berger, S. L. (2015). Characterization of BRD4 during mammalian postmeiotic sperm development. *Molecular and Cellular Biology*, *35*(8), 1433–1448. https://doi.org/10.1128/MCB.01328-14

Brykczynska, U., Hisano, M., Erkek, S., Ramos, L., Oakeley, E. J., Roloff, T. C., Beisel, C., Schübeler, D., Stadler, M. B., & Peters, A. H. F. M. (2010). Repressive and active histone methylation mark distinct promoters in human and mouse spermatozoa. *Nature Structural & Molecular Biology*, *17*(6), 679–687. https://doi.org/10.1038/nsmb.1821

Buenrostro, J. D., Giresi, P. G., Zaba, L. C., Chang, H. Y., & Greenleaf, W. J. (2013). Transposition of native chromatin for fast and sensitive epigenomic profiling of open chromatin, DNA-binding proteins and nucleosome position. *Nature Methods*, *10*(12), 1213–1218. https://doi.org/10.1038/nmeth.2688

Carone, B. R., Hung, J.-H., Hainer, S. J., Chou, M.-T., Carone, D. M., Weng, Z., Fazzio, T. G., & Rando, O. J. (2014). High-resolution mapping of chromatin packaging in mouse embryonic stem cells and sperm. *Developmental Cell*, *30*(1), 11–22. https://doi.org/10.1016/j.devcel.2014.05.024

Carrell, D., Emery, B. R., & Hammoud, S. (2008). The aetiology of sperm protamine abnormalities and their potential impact on the sperm epigenome. *International Journal of Andrology*, *31*(6), 537–545. https://doi.org/10.1111/j.1365-2605.2008.00872.x

Carrell, D., & Liu, L. (2001). Altered protamine 2 expression is uncommon in donors of known fertility, but common among men with poor fertilizing capacity, and may reflect other abnormalities of spermiogenesis. *Journal of Andrology*, *22*(4), 604–610.

Casadio, F., Lu, X., Pollock, S. B., LeRoy, G., Garcia, B. A., Muir, T. W., Roeder, R. G., & Allis, C. D. (2013). H3R42me2a is a histone modification with positive transcriptional effects. *Proceedings of the National Academy of Sciences*, *110*(37), 14894–14899. https://doi.org/10.1073/pnas.1312925110

Castillo, J., Amaral, A., Azpiazu, R., Vavouri, T., Estanyol, J. M., Ballesca, J. L., & Oliva, R. (2014). Genomic and proteomic dissection and characterization of the human sperm chromatin. *Molecular Human Reproduction*, *20*(11), 1041–1053. https://doi.org/10.1093/molehr/gau079

Castillo, J., Amaral, A., & Oliva, R. (2014). Sperm nuclear proteome and its epigenetic potential. *Andrology*, *2*(3), 326–338. https://doi.org/10.1111/j.2047-2927.2013.00170.x

Castillo, J., de Mateo, S., Estanyol, J. M., Ballescà, J. L., & Oliva, R. (2011). Anàlisi del proteoma de nuclis d'espermatozoides humans per cromatografia líquida i espectrometria de masses (LC-MS/MS). In Enric Ribes (Ed.), *Biologia de la Reproducció* (Vol. 12, pp. 57–60). Ediciones Gráficas Rey, S.L.

Castillo, J., Estanyol, J., Ballescà, J., & Oliva, R. (2015). Human sperm chromatin epigenetic potential: genomics, proteomics, and male infertility. *Asian Journal of Andrology*, *17*(4), 601. https://doi.org/10.4103/1008-682X.153302

Castillo, J., Jodar, M., & Oliva, R. (2018). The contribution of human sperm proteins to the development and epigenome of the preimplantation embryo. *Human Reproduction Update*, *24*(5), 535–555. https://doi.org/10.1093/humupd/dmy017

Chen, Q., Yan, W., & Duan, E. (2016). Epigenetic inheritance of acquired traits through sperm RNAs and sperm RNA modifications. *Nature Reviews. Genetics*, *17*(12), 733–743. https://doi.org/10.1038/nrg.2016.106

Chioccarelli, T., Cacciola, G., Altucci, L., Lewis, S. E. M., Simon, L., Ricci, G., Ledent, C., Meccariello, R., Fasano, S., Pierantoni, R., & Cobellis, G. (2010). Cannabinoid Receptor 1 Influences Chromatin Remodeling in Mouse Spermatids by Affecting Content of Transition Protein 2 mRNA and Histone Displacement. *Endocrinology*, *151*(10), 5017–5029. https://doi.org/10.1210/en.2010-0133

Chioccarelli, T., Manfrevola, F., Porreca, V., Fasano, S., Altucci, L., Pierantoni, R., & Cobellis, G. (2020). The Cannabinoid Receptor CB1 Stabilizes Sperm Chromatin Condensation Status During Epididymal Transit by Promoting Disulphide Bond Formation. *International Journal of Molecular Sciences*, *21*(9), 3117. https://doi.org/10.3390/ijms21093117

Chirat, F., Arkhis, A., Martinage, A., Jaquinod, M., Chevaillier, P., & Sautière, P. (1993). Phosphorylation of human sperm protamines HP1 and HP2: identification of phosphorylation sites. *Biochimica et Biophysica Acta*, *1203*(1), 109–114. https://doi.org/10.1016/0167-4838(93)90043-q

Cho, C., Jung-Ha, H., Willis, W. D., Goulding, E. H., Stein, P., Xu, Z., Schultz, R. M., Hecht, N. B., & Eddy, E. M. (2003). Protamine 2 deficiency leads to sperm DNA damage and embryo death in mice. *Biology of Reproduction*, *69*(1), 211–217. https://doi.org/10.1095/biolreprod.102.015115

Cho, C., Willis, W. D., Goulding, E. H., Jung-Ha, H., Choi, Y. C., Hecht, N. B., & Eddy, E. M. (2001). Haploinsufficiency of protamine-1 or -2 causes infertility in mice. *Nature Genetics*, *28*(1), 82–86. https://doi.org/10.1038/ng0501-82

Christensen, M. E., & Dixon, G. H. (1982). Hyperacetylation of histone H4 correlates with the terminal, transcriptionally inactive stages of spermatogenesis in rainbow trout. *Developmental Biology*, *93*(2), 404–415. https://doi.org/10.1016/0012-1606(82)90127-0

Conwell, C. C., & Hud, N. V. (2004). Evidence that both kinetic and thermodynamic factors govern DNA toroid dimensions: effects of magnesium(II) on DNA condensation by hexammine cobalt(III). *Biochemistry*, *43*(18), 5380–5387. https://doi.org/10.1021/bi049872u

Conwell, C. C., Vilfan, I. D., & Hud, N. V. (2003). Controlling the size of nanoscale toroidal DNA condensates with static curvature and ionic strength. *Proceedings of the National Academy of Sciences of the United States of America*, *100*(16), 9296–9301. https://doi.org/10.1073/pnas.1533135100

Crespo, M., Damont, A., Blanco, M., Lastrucci, E., Kennani, S. el, Ialy-Radio, C., Khattabi, L. el, Terrier, S., Louwagie, M., Kieffer-Jaquinod, S., Hesse, A.-M., Bruley, C., Chantalat, S., Govin, J., Fenaille, F., Battail, C., Cocquet, J., & Pflieger, D. (2020). Multi-omic analysis of gametogenesis reveals a novel signature at the promoters and distal enhancers of active genes. *Nucleic Acids Research*, *48*(8), 4115–4138. https://doi.org/10.1093/nar/gkaa163

Dacheux, J.-L., & Dacheux, F. (2014). New insights into epididymal function in relation to sperm maturation. *Reproduction (Cambridge, England)*, *147*(2), R27-42. https://doi.org/10.1530/REP-13-0420

Dahm, R. (2005). Friedrich Miescher and the discovery of DNA. *Developmental Biology*, *278*(2), 274–288. https://doi.org/10.1016/j.ydbio.2004.11.028

de Kretser, D. M., Loveland, K. L., Meinhardt, A., Simorangkir, D., & Wreford, N. (1998). Spermatogenesis. *Human Reproduction*, *13*(suppl 1), 1–8. https://doi.org/10.1093/humrep/13.suppl_1.1

de Mateo, S., Castillo, J., Estanyol, J. M., Ballescà, J. L., & Oliva, R. (2011). Proteomic characterization of the human sperm nucleus. *PROTEOMICS*, *11*(13), 2714–2726. https://doi.org/10.1002/pmic.201000799

de Mateo, S., Gázquez, C., Guimerà, M., Balasch, J., Meistrich, M. L., Ballescà, J. L., & Oliva, R. (2009). Protamine 2 precursors (Pre-P2), protamine 1 to protamine 2 ratio (P1/P2), and assisted reproduction outcome. *Fertility and Sterility*, *91*(3), 715–722. https://doi.org/10.1016/j.fertnstert.2007.12.047

de Mateo, S., Ramos, L., de Boer, P., Meistrich, M., & Oliva, R. (2011). Protamine 2 Precursors and Processing. *Protein & Peptide Letters*, *18*(8), 778–785. https://doi.org/10.2174/092986611795713998

de Yebra, L., Ballescà, J. L., Vanrell, J. A., Bassas, L., & Oliva, R. (1993). Complete selective absence of protamine P2 in humans. *The Journal of Biological Chemistry*, *268*(14), 10553–10557.

DeRouchey, J. E., & Rau, D. C. (2011). Salt effects on condensed protamine-DNA assemblies: anion binding and weakening of attraction. *The Journal of Physical Chemistry. B*, *115*(41), 11888–11894. https://doi.org/10.1021/jp203834z

Dhar, S., Thota, A., & Rao, M. R. S. (2012). Insights into role of bromodomain, testis-specific (Brdt) in acetylated histone H4-dependent chromatin remodeling in mammalian spermiogenesis. *The Journal of Biological Chemistry*, *287*(9), 6387–6405. https://doi.org/10.1074/jbc.M111.288167

Dias, G. M., Retamal, C. A., Tobella, L., Arnholdt, A. C. v, & López, M. L. (2006). Nuclear status of immature and mature stallion spermatozoa. *Theriogenology*, *66*(2), 354–365. https://doi.org/10.1016/j.theriogenology.2005.10.024

Ding, D., Nguyen, T. T., Pang, M. Y. H., & Ishibashi, T. (2021). Primate-specific histone variants. *Genome*, *64*(4), 337–346. https://doi.org/10.1139/gen-2020-0094

Dixon, G. H. (1972). THE BASIC PROTEINS OF TROUT TESTIS CHROMATIN: ASPECTS OF THEIR SYNTHESIS, POST-SYNTHETIC MODIFICATIONS AND BINDING TO DNA. *Acta Endocrinologica*, *71*(2_Suppla), S130–S154. https://doi.org/10.1530/acta.0.071S130

Dong, Y., Isono, K., Ohbo, K., Endo, T. A., Ohara, O., Maekawa, M., Toyama, Y., Ito, C., Toshimori, K., Helin, K., Ogonuki, N., Inoue, K., Ogura, A., Yamagata, K., Kitabayashi, I., & Koseki, H. (2017). EPC1/TIP60-Mediated Histone Acetylation Facilitates Spermiogenesis in Mice. *Molecular and Cellular Biology*, *37*(19). https://doi.org/10.1128/MCB.00082-17

Dottermusch-Heidel, C., Klaus, E. S., Gonzalez, N. H., Bhushan, S., Meinhardt, A., Bergmann, M., Renkawitz-Pohl, R., Rathke, C., & Steger, K. (2014). H3K79 methylation directly precedes the histone-to-protamine transition in mammalian spermatids and is sensitive to bacterial infections. *Andrology*, *2*(5), 655–665. https://doi.org/10.1111/j.2047-2927.2014.00248.x

Eelaminejad, Z., Favaedi, R., Sodeifi, N., Sadighi Gilani, M. A., & Shahhoseini, M. (2017). Deficient expression of JMJD1A histone demethylase in patients with round spermatid maturation arrest. *Reproductive BioMedicine Online*, *34*(1), 82–89. https://doi.org/10.1016/j.rbmo.2016.09.005

Eguizabal, C., Montserrat, N., Vassena, R., Barragan, M., Garreta, E., Garcia-Quevedo, L., Vidal, F., Giorgetti, A., Veiga, A., & Belmonte, J. C. I. (2011). Complete Meiosis from Human Induced Pluripotent Stem Cells. *Stem Cells*, *29*(8), 1186–1195. https://doi.org/10.1002/stem.672

Erkek, S., Hisano, M., Liang, C.-Y., Gill, M., Murr, R., Dieker, J., Schübeler, D., van der Vlag, J., Stadler, M. B., & Peters, A. H. F. M. (2013). Molecular determinants of nucleosome retention at CpG-rich sequences in mouse spermatozoa. *Nature Structural & Molecular Biology*, *20*(7), 868–875. https://doi.org/10.1038/nsmb.2599

Fita, I., Campos, J. L., Puigjaner, L. C., & Subirana, J. A. (1983). X-ray diffraction study of DNA complexes with arginine peptides and their relation to nucleoprotamine structure. *Journal of Molecular Biology*, *167*(1), 157–177. https://doi.org/10.1016/s0022-2836(83)80039-4

Fulton, M. D., Dang, T., Brown, T., & Zheng, Y. G. (2022). Effects of substrate modifications on the arginine dimethylation activities of PRMT1 and PRMT5. *Epigenetics*, *17*(1), 1–18. https://doi.org/10.1080/15592294.2020.1864170

Gardiner-Garden, M., Ballesteros, M., Gordon, M., & Tam, P. P. (1998). Histone- and protamine-DNA association: conservation of different patterns within the beta-globin domain in human sperm. *Molecular and Cellular Biology*, *18*(6), 3350–3356. https://doi.org/10.1128/MCB.18.6.3350

Gatewood, J., Cook, G. R., Balhorn, R., Bradbury, E. M., & Schmid, C. W. (1987). Sequence-Specific Packaging of DNA in Human Sperm Chromatin. *Science*, *236*(4804), 962–964. https://doi.org/10.1126/science.3576213

Gaucher, J., Boussouar, F., Montellier, E., Curtet, S., Buchou, T., Bertrand, S., Hery, P., Jounier, S., Depaux, A., Vitte, A.-L., Guardiola, P., Pernet, K., Debernardi, A., Lopez, F., Holota, H., Imbert, J., Wolgemuth, D. J., Gérard, M., Rousseaux, S., & Khochbin, S. (2012). Bromodomain-dependent stage-specific male genome programming by Brdt. *The EMBO Journal*, *31*(19), 3809–3820. https://doi.org/10.1038/emboj.2012.233

Gaucher, J., Reynoird, N., Montellier, E., Boussouar, F., Rousseaux, S., & Khochbin, S. (2010). From meiosis to postmeiotic events: the secrets of histone disappearance. *The FEBS Journal*, *277*(3), 599–604. https://doi.org/10.1111/j.1742-4658.2009.07504.x

Gervasi, M. G., & Visconti, P. E. (2017). Molecular changes and signaling events occurring in spermatozoa during epididymal maturation. *Andrology*, *5*(2), 204–218. https://doi.org/10.1111/andr.12320

Gibcus, J. H., Samejima, K., Goloborodko, A., Samejima, I., Naumova, N., Nuebler, J., Kanemaki, M. T., Xie, L., Paulson, J. R., Earnshaw, W. C., Mirny, L. A., & Dekker, J. (2018). A pathway for mitotic chromosome formation. *Science*, *359*(6376). https://doi.org/10.1126/science.aao6135

Gómez-H, L., Felipe-Medina, N., Condezo, Y. B., Garcia-Valiente, R., Ramos, I., Suja, J. A., Barbero, J. L., Roig, I., Sánchez-Martín, M., de Rooij, D. G., Llano, E., & Pendas, A. M. (2019). The PSMA8 subunit of the spermatoproteasome is essential for proper meiotic exit and mouse fertility. *PLOS Genetics*, *15*(8), e1008316. https://doi.org/10.1371/journal.pgen.1008316

Gou, L.-T., Kang, J.-Y., Dai, P., Wang, X., Li, F., Zhao, S., Zhang, M., Hua, M.-M., Lu, Y., Zhu, Y., Li, Z., Chen, H., Wu, L.-G., Li, D., Fu, X.-D., Li, J., Shi, H.-J., & Liu, M.-F. (2017). Ubiquitination-Deficient Mutations in Human Piwi Cause Male Infertility by Impairing Histone-to-Protamine Exchange During Spermiogenesis. *Obstetrical & Gynecological Survey*, *72*(9), 540–541. https://doi.org/10.1097/OGX.0000000000000482

Gou, L.-T., Lim, D.-H., Ma, W., Aubol, B. E., Hao, Y., Wang, X., Zhao, J., Liang, Z., Shao, C., Zhang, X., Meng, F., Li, H., Zhang, X., Xu, R., Li, D., Rosenfeld, M. G., Mellon, P. L., Adams, J. A., Liu, M.-F., & Fu, X.-D. (2020). Initiation of Parental Genome Reprogramming in Fertilized Oocyte by Splicing Kinase SRPK1-Catalyzed Protamine Phosphorylation. *Cell*, *180*(6), 1212-1227.e14. https://doi.org/10.1016/j.cell.2020.02.020

Goudarzi, A., Shiota, H., Rousseaux, S., & Khochbin, S. (2014). Genome-Scale Acetylation-Dependent Histone Eviction during Spermatogenesis. *Journal of Molecular Biology*, *426*(20), 3342–3349. https://doi.org/10.1016/j.jmb.2014.02.023

Goudarzi, A., Zhang, D., Huang, H., Barral, S., Kwon, O. K., Qi, S., Tang, Z., Buchou, T., Vitte, A.-L., He, T., Cheng, Z., Montellier, E., Gaucher, J., Curtet, S., Debernardi, A., Charbonnier, G., Puthier, D., Petosa, C., Panne, D., … Khochbin, S. (2016). Dynamic Competing Histone H4 K5K8 Acetylation and Butyrylation Are Hallmarks of Highly Active Gene Promoters. *Molecular Cell*, *62*(2), 169–180. https://doi.org/10.1016/j.molcel.2016.03.014

Govin, J., Escoffier, E., Rousseaux, S., Kuhn, L., Ferro, M., Thévenon, J., Catena, R., Davidson, I., Garin, J., Khochbin, S., & Caron, C. (2007). Pericentric heterochromatin reprogramming by new histone variants during mouse spermiogenesis. *Journal of Cell Biology*, *176*(3), 283–294. https://doi.org/10.1083/jcb.200604141

Grimes, S. R., & Henderson, N. (1984). Hyperacetylation of histone H4 in rat testis spermatids. *Experimental Cell Research*, *152*(1), 91–97. https://doi.org/10.1016/0014-4827(84)90232-5

Guo, Y., Song, Y., Guo, Z., Hu, M., Liu, B., Duan, H., Wang, L., Yuan, T., & Wang, D. (2018). Function of RAD6B and RNF8 in spermatogenesis. *Cell Cycle*, *17*(2), 162–173. https://doi.org/10.1080/15384101.2017.1361066

Gupta, N., Madapura, M. P., Bhat, U. A., & Rao, M. R. S. (2015). Mapping of Post-translational Modifications of Transition Proteins, TP1 and TP2, and Identification of Protein Arginine Methyltransferase 4 and Lysine Methyltransferase 7 as Methyltransferase for TP2. *Journal of Biological Chemistry*, *290*(19), 12101–12122. https://doi.org/10.1074/jbc.M114.620443

Gupta, N., Pentakota, S., Mishra, L. N., Jones, R., & Rao, M. R. S. (2017). *Identification of Posttranslational Modifications of Endogenous Chromatin Proteins From Testicular Cells by Mass Spectrometry* (pp. 115–142). https://doi.org/10.1016/bs.mie.2016.09.031

Hammoud, S., Nix, D. A., Hammoud, A. O., Gibson, M., Cairns, B. R., & Carrell, D. (2011). Genome-wide analysis identifies changes in histone retention and epigenetic modifications at developmental and imprinted gene loci in the sperm of infertile men. *Human Reproduction*, *26*(9), 2558–2569. https://doi.org/10.1093/humrep/der192

Hammoud, S., Nix, D. A., Zhang, H., Purwar, J., Carrell, D., & Cairns, B. R. (2009). Distinctive chromatin in human sperm packages genes for embryo development. *Nature*, *460*(7254), 473–478. https://doi.org/10.1038/nature08162

Hammoud, S., Purwar, J., Pflueger, C., Cairns, B. R., & Carrell, D. (2010). Alterations in sperm DNA methylation patterns at imprinted loci in two classes of infertility. *Fertility and Sterility*, *94*(5), 1728–1733. https://doi.org/10.1016/j.fertnstert.2009.09.010

Hatanaka, Y., Tsusaka, T., Shimizu, N., Morita, K., Suzuki, T., Machida, S., Satoh, M., Honda, A., Hirose, M., Kamimura, S., Ogonuki, N., Nakamura, T., Inoue, K., Hosoi, Y., Dohmae, N., Nakano, T., Kurumizaka, H., Matsumoto, K., Shinkai, Y., & Ogura, A. (2017). Histone H3 Methylated at Arginine 17 Is Essential for Reprogramming the Paternal Genome in Zygotes. *Cell Reports*, *20*(12), 2756–2765. https://doi.org/10.1016/j.celrep.2017.08.088

Hayakawa, T., Ohtani, Y., Hayakawa, N., Shinmyozu, K., Saito, M., Ishikawa, F., & Nakayama, J. (2007). RBP2 is an MRG15 complex component and down-regulates intragenic histone H3 lysine 4 methylation. *Genes to Cells*, *0*(0), 070606122915002-??? https://doi.org/10.1111/j.1365-2443.2007.01089.x

Hazzouri, M., Pivot-Pajot, C., Faure, A.-K., Usson, Y., Pelletier, R., Sèle, B., Khochbin, S., & Rousseaux, S. (2000). Regulated hyperacetylation of core histones during mouse spermatogenesis: involvement of histone-deacetylases. *European Journal of Cell Biology*, *79*(12), 950–960. https://doi.org/10.1078/0171-9335-00123

Hecht, N. B. (1998). Molecular mechanisms of male germ cell differentiation. *BioEssays : News and Reviews in Molecular, Cellular and Developmental Biology*, *20*(7), 555–561. https://doi.org/10.1002/(SICI)1521-1878(199807)20:7<555::AID-BIES6>3.0.CO;2-J

Her, Y. R., Wang, L., Chepelev, I., Manterola, M., Berkovits, B., Cui, K., Zhao, K., & Wolgemuth, D. J. (2021). Genome-wide chromatin occupancy of BRDT and gene expression analysis suggest transcriptional partners

and specific epigenetic landscapes that regulate gene expression during spermatogenesis. *Molecular Reproduction and Development*, *88*(2), 141–157. https://doi.org/10.1002/mrd.23449

Hoghoughi, N., Barral, S., Vargas, A., Rousseaux, S., & Khochbin, S. (2018). Histone variants: essential actors in male genome programming. *The Journal of Biochemistry*, *163*(2), 97–103. https://doi.org/10.1093/jb/mvx079

Horard, B., Sapey-Triomphe, L., Bonnefoy, E., & Loppin, B. (2018). ASF1 is required to load histones on the HIRA complex in preparation of paternal chromatin assembly at fertilization. *Epigenetics & Chromatin*, *11*(1), 19. https://doi.org/10.1186/s13072-018-0189-x

Hornbeck, P. v, Zhang, B., Murray, B., Kornhauser, J. M., Latham, V., & Skrzypek, E. (2015). PhosphoSitePlus, 2014: mutations, PTMs and recalibrations. *Nucleic Acids Research*, *43*(Database issue), D512-20. https://doi.org/10.1093/nar/gku1267

Hud, N. v, Allen, M. J., Downing, K. H., Lee, J., & Balhorn, R. (1993). Identification of the Elemental Packing Unit of DNA in Mammalian Sperm Cells by Atomic Force Microscopy. *Biochemical and Biophysical Research Communications*, *193*(3), 1347–1354. https://doi.org/10.1006/bbrc.1993.1773

Hud, N. V, & Downing, K. H. (2001). Cryoelectron microscopy of λ phage DNA condensates in vitreous ice: The fine structure of DNA toroids. *Proceedings of the National Academy of Sciences*, *98*(26), 14925–14930. https://doi.org/10.1073/pnas.261560398

Hud, N. v, Downing, K. H., & Balhorn, R. (1995). A constant radius of curvature model for the organization of DNA in toroidal condensates. *Proceedings of the National Academy of Sciences*, *92*(8), 3581–3585. https://doi.org/10.1073/pnas.92.8.3581

Hud, N. V, & Vilfan, I. D. (2005). Toroidal DNA Condensates: Unraveling the Fine Structure and the Role of Nucleation in Determining Size. *Annual Review of Biophysics and Biomolecular Structure*, *34*(1), 295–318. https://doi.org/10.1146/annurev.biophys.34.040204.144500

Hutchison, J. M., Rau, D. C., & DeRouchey, J. E. (2017). Role of Disulfide Bonds on DNA Packaging Forces in Bull Sperm Chromatin. *Biophysical Journal*, *113*(9), 1925–1933. https://doi.org/10.1016/j.bpj.2017.08.050

Ihara, M., Meyer-Ficca, M. L., Leu, N. A., Rao, S., Li, F., Gregory, B. D., Zalenskaya, I. A., Schultz, R. M., & Meyer, R. G. (2014). Paternal poly (ADP-ribose) metabolism modulates retention of inheritable sperm histones and early embryonic gene expression. *PLoS Genetics*, *10*(5), e1004317. https://doi.org/10.1371/journal.pgen.1004317

Inoue, A., & Zhang, Y. (2014). Nucleosome assembly is required for nuclear pore complex assembly in mouse zygotes. *Nature Structural & Molecular Biology*, *21*(7), 609–616. https://doi.org/10.1038/nsmb.2839

Itoh, K., Kondoh, G., Miyachi, H., Sugai, M., Kaneko, Y., Kitano, S., Watanabe, H., Maeda, R., Imura, A., Liu, Y., Ito, C., Itohara, S., Toshimori, K., & Fujita, J. (2019). Dephosphorylation of protamine 2 at serine 56 is crucial for murine sperm maturation in vivo. *Science Signaling*, *12*(574). https://doi.org/10.1126/scisignal.aao7232

Iuso, D., Czernik, M., Toschi, P., Fidanza, A., Zacchini, F., Feil, R., Curtet, S., Buchou, T., Shiota, H., Khochbin, S., Ptak, G. E., & Loi, P. (2015). Exogenous Expression of Human Protamine 1 (hPrm1) Remodels Fibroblast Nuclei into Spermatid-like Structures. *Cell Reports*, *13*(9), 1765–1771. https://doi.org/10.1016/j.celrep.2015.10.066

Iwamori, N., Tominaga, K., Sato, T., Riehle, K., Iwamori, T., Ohkawa, Y., Coarfa, C., Ono, E., & Matzuk, M. M. (2016). MRG15 is required for pre-mRNA splicing and spermatogenesis. *Proceedings of the National Academy of Sciences*, *113*(37). https://doi.org/10.1073/pnas.1611995113

Jang, S., Kang, C., Yang, H.-S., Jung, T., Hebert, H., Chung, K. Y., Kim, S. J., Hohng, S., & Song, J.-J. (2019). Structural basis of recognition and destabilization of the histone H2B ubiquitinated nucleosome by the DOT1L histone H3 Lys79 methyltransferase. *Genes & Development*, *33*(11–12), 620–625. https://doi.org/10.1101/gad.323790.118

Jenuwein, T., & Allis, C. D. (2001). Translating the Histone Code. *Science*, *293*(5532), 1074–1080. https://doi.org/10.1126/science.1063127

Ji, X., Dadon, D. B., Abraham, B. J., Lee, T. I., Jaenisch, R., Bradner, J. E., & Young, R. A. (2015). Chromatin proteomic profiling reveals novel proteins associated with histone-marked genomic regions. *Proceedings of the National Academy of Sciences*, *112*(12), 3841–3846. https://doi.org/10.1073/pnas.1502971112

Jodar, M., & Oliva, R. (2014). Protamine alterations in human spermatozoa. *Advances in Experimental Medicine and Biology*, *791*, 83–102. https://doi.org/10.1007/978-1-4614-7783-9_6

Jodar, M., Oriola, J., Mestre, G., Castillo, J., Giwercman, A., Vidal-Taboada, J. M., Ballescà, J. L., & Oliva, R. (2011). Polymorphisms, haplotypes and mutations in the protamine 1 and 2 genes. *International Journal of Andrology*, *34*(5pt1), 470–485. https://doi.org/10.1111/j.1365-2605.2010.01115.x

Jodar, M., Soler-Ventura, A., Oliva, R., & Molecular Biology of Reproduction and Development Research Group. (2017). Semen proteomics and male infertility. *Journal of Proteomics*, *162*, 125–134. https://doi.org/10.1016/j.jprot.2016.08.018

Jung, Y. H., Sauria, M. E. G., Lyu, X., Cheema, M. S., Ausió, J., Taylor, J., & Corces, V. G. (2017). Chromatin States in Mouse Sperm Correlate with Embryonic and Adult Regulatory Landscapes. *Cell Reports*, *18*(6), 1366–1382. https://doi.org/10.1016/j.celrep.2017.01.034

Kasinsky, H. E., Mann, M., Huang, S. Y., Fabre, L., Coyle, B., & Byrd, E. W. (1987). On the diversity of sperm basic proteins in the vertebrates: V. Cytochemical and amino acid analysis in Squamata, Testudines, and Crocodylia. *The Journal of Experimental Zoology*, *243*(1), 137–151. https://doi.org/10.1002/jez.1402430116

Kasinsky, H. E., Maria Eirin-Lopez, J., & Ausió, J. (2011). Protamines: Structural Complexity, Evolution and Chromatin Patterning. *Protein & Peptide Letters*, *18*(8), 755–771. https://doi.org/10.2174/092986611795713989

Ke, Y., Xu, Y., Chen, X., Feng, S., Liu, Z., Sun, Y., Yao, X., Li, F., Zhu, W., Gao, L., Chen, H., Du, Z., Xie, W., Xu, X., Huang, X., & Liu, J. (2017). 3D Chromatin Structures of Mature Gametes and Structural Reprogramming during Mammalian Embryogenesis. *Cell*, *170*(2), 367-381.e20. https://doi.org/10.1016/j.cell.2017.06.029

Khor, B., Bredemeyer, A. L., Huang, C.-Y., Turnbull, I. R., Evans, R., Maggi, L. B., White, J. M., Walker, L. M., Carnes, K., Hess, R. A., & Sleckman, B. P. (2006). Proteasome Activator PA200 Is Required for Normal Spermatogenesis. *Molecular and Cellular Biology*, *26*(8), 2999–3007. https://doi.org/10.1128/MCB.26.8.2999-3007.2006

Kim, C. R., Noda, T., Kim, H., Kim, G., Park, S., Na, Y., Oura, S., Shimada, K., Bang, I., Ahn, J.-Y., Kim, Y. R., Oh, S. K., Choi, H.-J., Kim, J.-S., Jung, I., Lee, H., Okada, Y., Ikawa, M., & Baek, S. H. (2020). PHF7 Modulates BRDT Stability and Histone-to-Protamine Exchange during Spermiogenesis. *Cell Reports*, *32*(4), 107950. https://doi.org/10.1016/j.celrep.2020.107950

Kimmins, S., & Sassone-Corsi, P. (2005). Chromatin remodelling and epigenetic features of germ cells. *Nature*, *434*(7033), 583–589. https://doi.org/10.1038/nature03368

Krawetz, S. A. (2005). Paternal contribution: new insights and future challenges. *Nature Reviews. Genetics*, *6*(8), 633–642. https://doi.org/10.1038/nrg1654

Krishnamoorthy, T., Chen, X., Govin, J., Cheung, W. L., Dorsey, J., Schindler, K., Winter, E., Allis, C. D., Guacci, V., Khochbin, S., Fuller, M. T., & Berger, S. L. (2006). Phosphorylation of histone H4 Ser1 regulates sporulation in yeast and is conserved in fly and mouse spermatogenesis. *Genes & Development*, *20*(18), 2580–2592. https://doi.org/10.1101/gad.1457006

Kwak, H.-G., & Dohmae, N. (2016). Proteomic characterization of histone variants in the mouse testis by mass spectrometry-based top-down analysis. *BioScience Trends*, *10*(5), 357–364. https://doi.org/10.5582/bst.2016.01090

Laurentino, S., Borgmann, J., & Gromoll, J. (2016). On the origin of sperm epigenetic heterogeneity. *Reproduction*, *151*(5), R71–R78. https://doi.org/10.1530/REP-15-0436

Lei, Q., Zhang, E., van Pelt, A. M. M., & Hamer, G. (2021). Meiotic Chromosome Synapsis and XY-Body Formation In Vitro. *Frontiers in Endocrinology*, *12*. https://doi.org/10.3389/fendo.2021.761249

Leitão, E., di Persio, S., Laurentino, S., Wöste, M., Dugas, M., Kliesch, S., Neuhaus, N., & Horsthemke, B. (2020). The sperm epigenome does not display recurrent epimutations in patients with severely impaired spermatogenesis. *Clinical Epigenetics*, *12*(1), 61. https://doi.org/10.1186/s13148-020-00854-0

Lewis, J. D., Abbott, D. W., & Ausió, J. (2003). A haploid affair: core histone transitions during spermatogenesis. *Biochemistry and Cell Biology = Biochimie et Biologie Cellulaire*, *81*(3), 131–140. https://doi.org/10.1139/o03-045

Li, A., Maffey, A. H., Abbott, W. D., Conde e Silva, N., Prunell, A., Siino, J., Churikov, D., Zalensky, A. O., & Ausió, J. (2005). Characterization of Nucleosomes Consisting of the Human Testis/Sperm-Specific Histone H2B Variant (hTSH2B). *Biochemistry*, *44*(7), 2529–2535. https://doi.org/10.1021/bi048061n

Lin, C.-J., Koh, F. M., Wong, P., Conti, M., & Ramalho-Santos, M. (2014). Hira-Mediated H3.3 Incorporation Is Required for DNA Replication and Ribosomal RNA Transcription in the Mouse Zygote. *Developmental Cell*, *30*(3), 268–279. https://doi.org/10.1016/j.devcel.2014.06.022

Liu, S., Yu, H., Liu, Y., Liu, X., Zhang, Y., Bu, C., Yuan, S., Chen, Z., Xie, G., Li, W., Xu, B., Yang, J., He, L., Jin, T., Xiong, Y., Sun, L., Liu, X., Han, C., Cheng, Z., … Shang, Y. (2017). Chromodomain Protein CDYL Acts as a Crotonyl-CoA Hydratase to Regulate Histone Crotonylation and Spermatogenesis. *Molecular Cell*, *67*(5), 853-866.e5. https://doi.org/10.1016/j.molcel.2017.07.011

Liu, Z., Zhou, S., Liao, L., Chen, X., Meistrich, M., & Xu, J. (2010). Jmjd1a Demethylase-regulated Histone Modification Is Essential for cAMP-response Element Modulator-regulated Gene Expression and Spermatogenesis. *Journal of Biological Chemistry*, *285*(4), 2758–2770. https://doi.org/10.1074/jbc.M109.066845

Luense, L. J., Donahue, G., Lin-Shiao, E., Rangel, R., Weller, A. H., Bartolomei, M. S., & Berger, S. L. (2019). Gcn5-Mediated Histone Acetylation Governs Nucleosome Dynamics in Spermiogenesis. *Developmental Cell*, *51*(6), 745-758.e6. https://doi.org/10.1016/j.devcel.2019.10.024

Makita, N., Yoshikawa, Y., Takenaka, Y., Sakaue, T., Suzuki, M., Watanabe, C., Kanai, T., Kanbe, T., Imanaka, T., & Yoshikawa, K. (2011). Salt Has a Biphasic Effect on the Higher-Order Structure of a DNA–Protamine Complex. *The Journal of Physical Chemistry B*, *115*(15), 4453–4459. https://doi.org/10.1021/jp111331q

Manterola, M., Brown, T. M., Oh, M. Y., Garyn, C., Gonzalez, B. J., & Wolgemuth, D. J. (2018). BRDT is an essential epigenetic regulator for proper chromatin organization, silencing of sex chromosomes and crossover formation in male meiosis. *PLoS Genetics*, *14*(3), e1007209. https://doi.org/10.1371/journal.pgen.1007209

Mashiko, D., Fujihara, Y., Satouh, Y., Miyata, H., Isotani, A., & Ikawa, M. (2013). Generation of mutant mice by pronuclear injection of circular plasmid expressing Cas9 and single guided RNA. *Scientific Reports*, *3*(1), 3355. https://doi.org/10.1038/srep03355

Medrano, J. V., Vilanova-Pérez, T., Fornés-Ferrer, V., Navarro-Gomezlechon, A., Martínez-Triguero, M. L., García, S., Gómez-Chacón, J., Povo, I., Pellicer, A., Andrés, M. M., & Novella-Maestre, E. (2018). Influence of temperature, serum, and gonadotropin supplementation in short- and long-term organotypic culture of human

immature testicular tissue. *Fertility and Sterility*, *110*(6), 1045-1057.e3. https://doi.org/10.1016/j.fertnstert.2018.07.018
Meistrich, M. L., Mohapatra, B., Shirley, C. R., & Zhao, M. (2003). Roles of transition nuclear proteins in spermiogenesis. *Chromosoma*, *111*(8), 483–488. https://doi.org/10.1007/s00412-002-0227-z
Meng, C., Liao, J., Zhao, D., Huang, H., Qin, J., Lee, T.-L., Chen, D., Chan, W.-Y., & Xia, Y. (2019). L3MBTL2 regulates chromatin remodeling during spermatogenesis. *Cell Death & Differentiation*, *26*(11), 2194–2207. https://doi.org/10.1038/s41418-019-0283-z
Mengual, L., Ballescá, J. L., Ascaso, C., & Oliva, R. (2003). Marked differences in protamine content and P1/P2 ratios in sperm cells from percoll fractions between patients and controls. *Journal of Andrology*, *24*(3), 438–447. https://doi.org/10.1002/j.1939-4640.2003.tb02692.x
Merges, G. E., Meier, J., Schneider, S., Kruse, A., Fröbius, A. C., Kirfel, G., Steger, K., Arévalo, L., & Schorle, H. (2022). Loss of *Prm1* leads to defective chromatin protamination, impaired PRM2 processing, reduced sperm motility and subfertility in male mice. *Development*. https://doi.org/10.1242/dev.200330
Mezquita, C. (1985). Chromatin composition, structure and function in spermatogenesis. *Revisiones Sobre Biologia Celular : RBC*, *5*, V–XIV, 1–124.
Miescher, F. (1874). Das Protamin, eine neue organische Base aus den Samenfäden des Rheinlachses. *Berichte Der Deutschen Chemischen Gesellschaft*, *7*(1), 376–379. https://doi.org/10.1002/cber.187400701119
Mishra, L. N., Gupta, N., & Rao, S. M. R. (2015). Mapping of post-translational modifications of spermatid-specific linker histone H1-like protein, HILS1. *Journal of Proteomics*, *128*, 218–230. https://doi.org/10.1016/j.jprot.2015.08.001
Montellier, E., Boussouar, F., Rousseaux, S., Zhang, K., Buchou, T., Fenaille, F., Shiota, H., Debernardi, A., Héry, P., Curtet, S., Jamshidikia, M., Barral, S., Holota, H., Bergon, A., Lopez, F., Guardiola, P., Pernet, K., Imbert, J., Petosa, C., … Khochbin, S. (2013). Chromatin-to-nucleoprotamine transition is controlled by the histone H2B variant TH2B. *Genes & Development*, *27*(15), 1680–1692. https://doi.org/10.1101/gad.220095.113
Moretti, C., Serrentino, M.-E., Ialy-Radio, C., Delessard, M., Soboleva, T. A., Tores, F., Leduc, M., Nitschké, P., Drevet, J. R., Tremethick, D. J., Vaiman, D., Kocer, A., & Cocquet, J. (2017). SLY regulates genes involved in chromatin remodeling and interacts with TBL1XR1 during sperm differentiation. *Cell Death & Differentiation*, *24*(6), 1029–1044. https://doi.org/10.1038/cdd.2017.32
Morinière, J., Rousseaux, S., Steuerwald, U., Soler-López, M., Curtet, S., Vitte, A.-L., Govin, J., Gaucher, J., Sadoul, K., Hart, D. J., Krijgsveld, J., Khochbin, S., Müller, C. W., & Petosa, C. (2009). Cooperative binding of two acetylation marks on a histone tail by a single bromodomain. *Nature*, *461*(7264), 664–668. https://doi.org/10.1038/nature08397
Moritz, L., & Hammoud, S. S. (2022). The Art of Packaging the Sperm Genome: Molecular and Structural Basis of the Histone-To-Protamine Exchange. *Frontiers in Endocrinology*, *13*. https://doi.org/10.3389/fendo.2022.895502
Mukherjee, A., Saurabh, S., Olive, E., Jang, Y. H., & Lansac, Y. (2021). Protamine Binding Site on DNA: Molecular Dynamics Simulations and Free Energy Calculations with Full Atomistic Details. *The Journal of Physical Chemistry B*, *125*(12), 3032–3044. https://doi.org/10.1021/acs.jpcb.0c09166
Nair, M., Nagamori, I., Sun, P., Mishra, D. P., Rhéaume, C., Li, B., Sassone-Corsi, P., & Dai, X. (2008). Nuclear regulator Pygo2 controls spermiogenesis and histone H3 acetylation. *Developmental Biology*, *320*(2), 446–455. https://doi.org/10.1016/j.ydbio.2008.05.553
Nanassy, L., Liu, L., Griffin, J., & Carrell, D. (2011). The clinical utility of the protamine 1/protamine 2 ratio in sperm. *Protein and Peptide Letters*, *18*(8), 772–777. https://doi.org/10.2174/092986611795713934
Nashun, B., Yukawa, M., Liu, H., Akiyama, T., & Aoki, F. (2010). Changes in the nuclear deposition of histone H2A variants during pre-implantation development in mice. *Development*, *137*(22), 3785–3794. https://doi.org/10.1242/dev.051805
Nazarov, I. B., Shlyakhtenko, L. S., Lyubchenko, Y. L., Zalenskaya, I. A., & Zalensky, A. O. (2008). Sperm chromatin released by nucleases. *Systems Biology in Reproductive Medicine*, *54*(1), 37–46. https://doi.org/10.1080/19396360701876849
Ni, K., Spiess, A.-N., Schuppe, H.-C., & Steger, K. (2016). The impact of sperm protamine deficiency and sperm DNA damage on human male fertility: a systematic review and meta-analysis. *Andrology*, *4*(5), 789–799. https://doi.org/10.1111/andr.12216
Okada, Y., Scott, G., Ray, M. K., Mishina, Y., & Zhang, Y. (2007). Histone demethylase JHDM2A is critical for Tnp1 and Prm1 transcription and spermatogenesis. *Nature*, *450*(7166), 119–123. https://doi.org/10.1038/nature06236
Okada, Y., Tateishi, K., & Zhang, Y. (2010). Histone Demethylase JHDM2A Is Involved in Male Infertility and Obesity. *Journal of Andrology*, *31*(1), 75–78. https://doi.org/10.2164/jandrol.109.008052
Oliva, R. (2006). Protamines and male infertility. *Human Reproduction Update*, *12*(4), 417–435. https://doi.org/10.1093/humupd/dml009
Oliva, R., Bazett-Jones, D., Mezquita, C., & Dixon, G. H. (1987). Factors affecting nucleosome disassembly by protamines in vitro. Histone hyperacetylation and chromatin structure, time dependence, and the size of the sperm nuclear proteins. *Journal of Biological Chemistry*, *262*(35), 17016–17025.
Oliva, R., & Castillo, J. (2011). Proteomics and the genetics of sperm chromatin condensation. *Asian Journal of Andrology*, *13*(1), 24–30. https://doi.org/10.1038/aja.2010.65

Oliva, R., & Dixon, G. H. (1991). Vertebrate Protamine Genes and the Histone-to-Protamine Replacement Reaction. *Progress in Nucleic Acid Research and Molecular Biology*, *40*(C), 25–94. https://doi.org/10.1016/S0079-6603(08)60839-9

Oliva, R., & Mezquita, C. (1982). Histone H4 hyperacetylation and rapid turnover of its acetyl groups in transcriptionally inactive rooster testis spermatids. *Nucleic Acids Research*, *10*(24), 8049–8059. https://doi.org/10.1093/nar/10.24.8049

Oliva, R., & Mezquita, C. (1986). Marked differences in the ability of distinct protamines to disassemble nucleosomal core particles in vitro. *Biochemistry*, *25*(21), 6508–6511. https://doi.org/10.1021/bi00369a025

Orgebin-Crist, M. C. (1969). Studies on the function of the epididymis. *Biology of Reproduction*, *1*, Suppl 1:155-75. https://doi.org/10.1095/biolreprod1.supplement_1.155

Ozturk, N., Dansranjavin, T., Gies, S., Calay, D., Shiplu, S., Creppe, C., Hendrickx, J., & Schagdarsurengin, U. (2021). H4K20me3 marks distal intergenic and repetitive regions in human mature spermatozoa. *Development (Cambridge, England)*, *148*(15). https://doi.org/10.1242/dev.196477

Padavattan, S., Thiruselvam, V., Shinagawa, T., Hasegawa, K., Kumasaka, T., Ishii, S., & Kumarevel, T. (2017). Structural analyses of the nucleosome complexes with human testis-specific histone variants, hTh2a and hTh2b. *Biophysical Chemistry*, *221*, 41–48. https://doi.org/10.1016/j.bpc.2016.11.013

Papoutsopoulou, S., Nikolakaki, E., Chalepakis, G., Kruft, V., Chevaillier, P., & Giannakouros, T. (1999). SR protein-specific kinase 1 is highly expressed in testis and phosphorylates protamine 1. *Nucleic Acids Research*, *27*(14), 2972–2980. https://doi.org/10.1093/nar/27.14.2972

Pentakota, S. K., Sandhya, S., P. Sikarwar, A., Chandra, N., & Satyanarayana Rao, M. R. (2014). Mapping Post-translational Modifications of Mammalian Testicular Specific Histone Variant TH2B in Tetraploid and Haploid Germ Cells and Their Implications on the Dynamics of Nucleosome Structure. *Journal of Proteome Research*, *13*(12), 5603–5617. https://doi.org/10.1021/pr500597a

Philpott, A., & Leno, G. H. (1992). Nucleoplasmin remodels sperm chromatin in Xenopus egg extracts. *Cell*, *69*(5), 759–767. https://doi.org/10.1016/0092-8674(92)90288-N

Pirhonen, A., Linnala-Kankkunen, A., & Mäenpää, P. H. (1994). Identification of phosphoseryl residues in protamines from mature mammalian spermatozoa. *Biology of Reproduction*, *50*(5), 981–986. https://doi.org/10.1095/biolreprod50.5.981

Pirhonen, A., Linnala-Kankkunen, A., & Mënpää, P. H. (1994). P2 protamines are phosphorylated in vitro by protein kinase C, whereas P1 protamines prefer cAMP-dependent protein kinase. A comparative study of five mammalian species. *European Journal of Biochemistry*, *223*(1), 165–169. https://doi.org/10.1111/j.1432-1033.1994.tb18979.x

Pivot-Pajot, C., Caron, C., Govin, J., Vion, A., Rousseaux, S., & Khochbin, S. (2003). Acetylation-Dependent Chromatin Reorganization by BRDT, a Testis-Specific Bromodomain-Containing Protein. *Molecular and Cellular Biology*, *23*(15), 5354–5365. https://doi.org/10.1128/MCB.23.15.5354-5365.2003

Portela, J. M. D., de Winter-Korver, C. M., van Daalen, S. K. M., Meißner, A., de Melker, A. A., Repping, S., & van Pelt, A. M. M. (2019). Assessment of fresh and cryopreserved testicular tissues from (pre)pubertal boys during organ culture as a strategy for in vitro spermatogenesis. *Human Reproduction*, *34*(12), 2443–2455. https://doi.org/10.1093/humrep/dez180

Pradeepa, M. M., Nikhil, G., Hari Kishore, A., Bharath, G. N., Kundu, T. K., & Rao, M. R. S. (2009). Acetylation of transition protein 2 (TP2) by KAT3B (p300) alters its DNA condensation property and interaction with putative histone chaperone NPM3. *The Journal of Biological Chemistry*, *284*(43), 29956–29967. https://doi.org/10.1074/jbc.M109.052043

Pruslin, F. H., Imesch, E., Winston, R., & Rodman, T. C. (1987). Phosphorylation state of protamines 1 and 2 in human spermatids and spermatozoa. *Gamete Research*, *18*(2), 179–190. https://doi.org/10.1002/mrd.1120180208

Qian, M.-X., Pang, Y., Liu, C. H., Haratake, K., Du, B.-Y., Ji, D.-Y., Wang, G.-F., Zhu, Q.-Q., Song, W., Yu, Y., Zhang, X.-X., Huang, H.-T., Miao, S., Chen, L.-B., Zhang, Z.-H., Liang, Y.-N., Liu, S., Cha, H., Yang, D., … Qiu, X.-B. (2013). Acetylation-Mediated Proteasomal Degradation of Core Histones during DNA Repair and Spermatogenesis. *Cell*, *153*(5), 1012–1024. https://doi.org/10.1016/j.cell.2013.04.032

Raman, P., Rominger, M. C., Young, J. M., Molaro, A., Tsukiyama, T., & Malik, H. S. (2022). Novel Classes and Evolutionary Turnover of Histone H2B Variants in the Mammalian Germline. *Molecular Biology and Evolution*, *39*(2). https://doi.org/10.1093/molbev/msac019

Rando, O. J. (2012). Daddy issues: paternal effects on phenotype. *Cell*, *151*(4), 702–708. https://doi.org/10.1016/j.cell.2012.10.020

Rathke, C., Baarends, W. M., Awe, S., & Renkawitz-Pohl, R. (2014). Chromatin dynamics during spermiogenesis. *Biochimica et Biophysica Acta (BBA) - Gene Regulatory Mechanisms*, *1839*(3), 155–168. https://doi.org/10.1016/j.bbagrm.2013.08.004

Reda, A., Hou, M., Winton, T. R., Chapin, R. E., Söder, O., & Stukenborg, J.-B. (2016). In vitro differentiation of rat spermatogonia into round spermatids in tissue culture. *Molecular Human Reproduction*, *22*(9), 601–612. https://doi.org/10.1093/molehr/gaw047

Reynoird, N., Schwartz, B. E., Delvecchio, M., Sadoul, K., Meyers, D., Mukherjee, C., Caron, C., Kimura, H., Rousseaux, S., Cole, P. A., Panne, D., French, C. A., & Khochbin, S. (2010). Oncogenesis by sequestration

of CBP/p300 in transcriptionally inactive hyperacetylated chromatin domains. *The EMBO Journal*, *29*(17), 2943–2952. https://doi.org/10.1038/emboj.2010.176

Rezaei-Gazik, M., Vargas, A., Amiri-Yekta, A., Vitte, A.-L., Akbari, A., Barral, S., Esmaeili, V., Chuffart, F., Sadighi-Gilani, M. A., Couté, Y., Eftekhari-Yazdi, P., Khochbin, S., Rousseaux, S., & Totonchi, M. (2022). Direct visualization of pre-protamine 2 detects protamine assembly failures and predicts ICSI success. *Molecular Human Reproduction*, *28*(2). https://doi.org/10.1093/molehr/gaac004

Richer, G., Hobbs, R. M., Loveland, K. L., Goossens, E., & Baert, Y. (2021). Long-Term Maintenance and Meiotic Entry of Early Germ Cells in Murine Testicular Organoids Functionalized by 3D Printed Scaffolds and Air-Medium Interface Cultivation. *Frontiers in Physiology*, *12*, 757565. https://doi.org/10.3389/fphys.2021.757565

Roque, A., Ponte, I., & Suau, P. (2011). Secondary structure of protamine in sperm nuclei: an infrared spectroscopy study. *BMC Structural Biology*, *11*, 14. https://doi.org/10.1186/1472-6807-11-14

Royo, H., Stadler, M. B., & Peters, A. H. F. M. (2016). Alternative Computational Analysis Shows No Evidence for Nucleosome Enrichment at Repetitive Sequences in Mammalian Spermatozoa. *Developmental Cell*, *37*(1), 98–104. https://doi.org/10.1016/j.devcel.2016.03.010

Ruthenburg, A. J., Allis, C. D., & Wysocka, J. (2007). Methylation of lysine 4 on histone H3: intricacy of writing and reading a single epigenetic mark. *Molecular Cell*, *25*(1), 15–30. https://doi.org/10.1016/j.molcel.2006.12.014

Sabari, B. R., Zhang, D., Allis, C. D., & Zhao, Y. (2017). Metabolic regulation of gene expression through histone acylations. *Nature Reviews. Molecular Cell Biology*, *18*(2), 90–101. https://doi.org/10.1038/nrm.2016.140

Saida, M., Iles, D., Elnefati, A., Brinkworth, M., & Miller, D. (2011). Key gene regulatory sequences with distinctive ontological signatures associate with differentially endonuclease-accessible mouse sperm chromatin. *Reproduction (Cambridge, England)*, *142*(1), 73–86. https://doi.org/10.1530/REP-10-0536

Samans, B., Yang, Y., Krebs, S., Sarode, G. V., Blum, H., Reichenbach, M., Wolf, E., Steger, K., Dansranjavin, T., & Schagdarsurengin, U. (2014). Uniformity of nucleosome preservation pattern in Mammalian sperm and its connection to repetitive DNA elements. *Developmental Cell*, *30*(1), 23–35. https://doi.org/10.1016/j.devcel.2014.05.023

Sartori Blanc, N., Senn, A., Leforestier, A., Livolant, F., & Dubochet, J. (2001). DNA in Human and Stallion Spermatozoa Forms Local Hexagonal Packing with Twist and Many Defects. *Journal of Structural Biology*, *134*(1), 76–81. https://doi.org/10.1006/jsbi.2001.4365

Sato, T., Katagiri, K., Gohbara, A., Inoue, K., Ogonuki, N., Ogura, A., Kubota, Y., & Ogawa, T. (2011). In vitro production of functional sperm in cultured neonatal mouse testes. *Nature*, *471*(7339), 504–507. https://doi.org/10.1038/nature09850

Sato, T., Katagiri, K., Yokonishi, T., Kubota, Y., Inoue, K., Ogonuki, N., Matoba, S., Ogura, A., & Ogawa, T. (2011). In vitro production of fertile sperm from murine spermatogonial stem cell lines. *Nature Communications*, *2*(1), 472. https://doi.org/10.1038/ncomms1478

Schneider, S., Balbach, M., Jan F Jikeli, Fietz, D., Nettersheim, D., Jostes, S., Schmidt, R., Kressin, M., Bergmann, M., Wachten, D., Steger, K., & Schorle, H. (2016). Re-visiting the Protamine-2 locus: deletion, but not haploinsufficiency, renders male mice infertile. *Scientific Reports*, *6*, 36764. https://doi.org/10.1038/srep36764

Schneider, S., Shakeri, F., Trötschel, C., Arévalo, L., Kruse, A., Buness, A., Poetsch, A., Steger, K., & Schorle, H. (2020). Protamine-2 Deficiency Initiates a Reactive Oxygen Species (ROS)-Mediated Destruction Cascade during Epididymal Sperm Maturation in Mice. *Cells*, *9*(8). https://doi.org/10.3390/cells9081789

Schoysman, R. J., & Bedford, J. M. (1986). The role of the human epididymis in sperm maturation and sperm storage as reflected in the consequences of epididymovasostomy. *Fertility and Sterility*, *46*(2), 293–299. https://doi.org/10.1016/s0015-0282(16)49528-2

Shang, E., Nickerson, H. D., Wen, D., Wang, X., & Wolgemuth, D. J. (2007). The first bromodomain of Brdt, a testis-specific member of the BET sub-family of double-bromodomain-containing proteins, is essential for male germ cell differentiation. *Development*, *134*(19), 3507–3515. https://doi.org/10.1242/dev.004481

Shinagawa, T., Huynh, L. M., Takagi, T., Tsukamoto, D., Tomaru, C., Kwak, H.-G., Dohmae, N., Noguchi, J., & Ishii, S. (2015). Disruption of *Th2a* and *Th2b* genes causes defects in spermatogenesis. *Development*. https://doi.org/10.1242/dev.121830

Shinagawa, T., Takagi, T., Tsukamoto, D., Tomaru, C., Huynh, L. M., Sivaraman, P., Kumarevel, T., Inoue, K., Nakato, R., Katou, Y., Sado, T., Takahashi, S., Ogura, A., Shirahige, K., & Ishii, S. (2014). Histone Variants Enriched in Oocytes Enhance Reprogramming to Induced Pluripotent Stem Cells. *Cell Stem Cell*, *14*(2), 217–227. https://doi.org/10.1016/j.stem.2013.12.015

Shiota, H., Barral, S., Buchou, T., Tan, M., Couté, Y., Charbonnier, G., Reynoird, N., Boussouar, F., Gérard, M., Zhu, M., Bargier, L., Puthier, D., Chuffart, F., Bourova-Flin, E., Picaud, S., Filippakopoulos, P., Goudarzi, A., Ibrahim, Z., Panne, D., … Khochbin, S. (2018). Nut Directs p300-Dependent, Genome-Wide H4 Hyperacetylation in Male Germ Cells. *Cell Reports*, *24*(13), 3477-3487.e6. https://doi.org/10.1016/j.celrep.2018.08.069

Shirley, C. R., Hayashi, S., Mounsey, S., Yanagimachi, R., & Meistrich, M. L. (2004). Abnormalities and Reduced Reproductive Potential of Sperm from Tnp1- and Tnp2-Null Double Mutant Mice1. *Biology of Reproduction*, *71*(4), 1220–1229. https://doi.org/10.1095/biolreprod.104.029363

Shmueli, M. D., Sheban, D., Eisenberg-Lerner, A., & Merbl, Y. (2021). Histone degradation by the proteasome regulates chromatin and cellular plasticity. *The FEBS Journal*. https://doi.org/10.1111/febs.15903

Siklenka, K., Erkek, S., Godmann, M., Lambrot, R., McGraw, S., Lafleur, C., Cohen, T., Xia, J., Suderman, M., Hallett, M., Trasler, J., Peters, A. H. F. M., & Kimmins, S. (2015). Disruption of histone methylation in developing sperm impairs offspring health transgenerationally. *Science (New York, N.Y.)*, *350*(6261), aab2006. https://doi.org/10.1126/science.aab2006

Singh, I., & Parte, P. (2021). Heterogeneity in the Epigenetic Landscape of Murine Testis-Specific Histone Variants TH2A and TH2B Sharing the Same Bi-Directional Promoter. *Frontiers in Cell and Developmental Biology*, *9*. https://doi.org/10.3389/fcell.2021.755751

Soler-Ventura, A., Castillo, J., de la Iglesia, A., Jodar, M., Barrachina, F., Ballesca, J. L., & Oliva, R. (2018). Mammalian Sperm Protamine Extraction and Analysis: A Step-By-Step Detailed Protocol and Brief Review of Protamine Alterations. *Protein and Peptide Letters*, *25*(5), 424–433. https://doi.org/10.2174/0929866525666180412155205

Soler-Ventura, A., Gay, M., Jodar, M., Vilanova, M., Castillo, J., Arauz-Garofalo, G., Villarreal, L., Ballescà, J. L., Vilaseca, M., & Oliva, R. (2020). Characterization of Human Sperm Protamine Proteoforms through a Combination of Top-Down and Bottom-Up Mass Spectrometry Approaches. *Journal of Proteome Research*, *19*(1), 221–237. https://doi.org/10.1021/acs.jproteome.9b00499

Soupsana, K., Karanika, E., Kiosse, F., Christogianni, A., Sfikas, Y., Topalis, P., Batistatou, A., Kanaki, Z., Klinakis, A., Politou, A. S., & Georgatos, S. (2021). Distinct roles of haspin in stem cell division and male gametogenesis. *Scientific Reports*, *11*(1), 19901. https://doi.org/10.1038/s41598-021-99307-8

Steilmann, C., Paradowska, A., Bartkuhn, M., Vieweg, M., Schuppe, H.-C., Bergmann, M., Kliesch, S., Weidner, W., & Steger, K. (2011). Presence of histone H3 acetylated at lysine 9 in male germ cells and its distribution pattern in the genome of human spermatozoa. *Reproduction, Fertility and Development*, *23*(8), 997. https://doi.org/10.1071/RD10197

Strahl, B. D., & Allis, C. D. (2000). The language of covalent histone modifications. *Nature*, *403*(6765), 41–45. https://doi.org/10.1038/47412

Stukenborg, J.-B., Schlatt, S., Simoni, M., Yeung, C.-H., Elhija, M. A., Luetjens, C. M., Huleihel, M., & Wistuba, J. (2009). New horizons for in vitro spermatogenesis? An update on novel three-dimensional culture systems as tools for meiotic and post-meiotic differentiation of testicular germ cells. *Molecular Human Reproduction*, *15*(9), 521–529. https://doi.org/10.1093/molehr/gap052

Subirana, J. A. (1983). Proceedings of the Fourth International Symposium on Spermatology. In *The sperm cell* (pp. 197–213). Martinus Nijhoff Pub The Hague (The Netherlands).

Subirana, J. A. (1997). A crystallographic approach to DNA bending: prediction of nucleosome formation by DNA triple repeats and other repetitive sequences. *FEBS Letters*, *417*(3), 352–354. https://doi.org/10.1016/S0014-5793(97)01317-3

Subirana, J. A., Muñoz-Guerra, S., Aymamí, J., Radermacher, M., & Frank, J. (1985). The layered organization of nucleosomes in 30 nm chromatin fibers. *Chromosoma*, *91*(5), 377–390. https://doi.org/10.1007/BF00291012

Tachiwana, H., Kagawa, W., Osakabe, A., Kawaguchi, K., Shiga, T., Hayashi-Takanaka, Y., Kimura, H., & Kurumizaka, H. (2010). Structural basis of instability of the nucleosome containing a testis-specific histone variant, human H3T. *Proceedings of the National Academy of Sciences*, *107*(23), 10454–10459. https://doi.org/10.1073/pnas.1003064107

Takeda, N., Yoshinaga, K., Furushima, K., Takamune, K., Li, Z., Abe, S., Aizawa, S., & Yamamura, K. (2016). Viable offspring obtained from Prm1-deficient sperm in mice. *Scientific Reports*, *6*(1), 27409. https://doi.org/10.1038/srep27409

Tan, M., Luo, H., Lee, S., Jin, F., Yang, J. S., Montellier, E., Buchou, T., Cheng, Z., Rousseaux, S., Rajagopal, N., Lu, Z., Ye, Z., Zhu, Q., Wysocka, J., Ye, Y., Khochbin, S., Ren, B., & Zhao, Y. (2011). Identification of 67 Histone Marks and Histone Lysine Crotonylation as a New Type of Histone Modification. *Cell*, *146*(6), 1016–1028. https://doi.org/10.1016/j.cell.2011.08.008

Tanaka, H., Miyagawa, Y., Tsujimura, A., Matsumiya, K., Okuyama, A., & Nishimune, Y. (2003). Single nucleotide polymorphisms in the protamine-1 and -2 genes of fertile and infertile human male populations. *Molecular Human Reproduction*, *9*(2), 69–73. https://doi.org/10.1093/molehr/gag010

Tang, M. C. W., Jacobs, S. A., Mattiske, D. M., Soh, Y. M., Graham, A. N., Tran, A., Lim, S. L., Hudson, D. F., Kalitsis, P., O'Bryan, M. K., Wong, L. H., & Mann, J. R. (2015). Contribution of the Two Genes Encoding Histone Variant H3.3 to Viability and Fertility in Mice. *PLOS Genetics*, *11*(2), e1004964. https://doi.org/10.1371/journal.pgen.1004964

Teperek, M., Simeone, A., Gaggioli, V., Miyamoto, K., Allen, G. E., Erkek, S., Kwon, T., Marcotte, E. M., Zegerman, P., Bradshaw, C. R., Peters, A. H. F. M., Gurdon, J. B., & Jullien, J. (2016). Sperm is epigenetically programmed to regulate gene transcription in embryos. *Genome Research*, *26*(8), 1034–1046. https://doi.org/10.1101/gr.201541.115

Torres-Flores, U., & Hernández-Hernández, A. (2020). The Interplay Between Replacement and Retention of Histones in the Sperm Genome. *Frontiers in Genetics*, *11*, 780. https://doi.org/10.3389/fgene.2020.00780

Ueda, J., Harada, A., Urahama, T., Machida, S., Maehara, K., Hada, M., Makino, Y., Nogami, J., Horikoshi, N., Osakabe, A., Taguchi, H., Tanaka, H., Tachiwana, H., Yao, T., Yamada, M., Iwamoto, T., Isotani, A., Ikawa,

M., Tachibana, T., … Yamagata, K. (2017). Testis-Specific Histone Variant H3t Gene Is Essential for Entry into Spermatogenesis. *Cell Reports*, *18*(3), 593–600. https://doi.org/10.1016/j.celrep.2016.12.065

Urahama, T., Harada, A., Maehara, K., Horikoshi, N., Sato, K., Sato, Y., Shiraishi, K., Sugino, N., Osakabe, A., Tachiwana, H., Kagawa, W., Kimura, H., Ohkawa, Y., & Kurumizaka, H. (2016). Histone H3.5 forms an unstable nucleosome and accumulates around transcription start sites in human testis. *Epigenetics & Chromatin*, *9*(1), 2. https://doi.org/10.1186/s13072-016-0051-y

Utley, R. T., Lacoste, N., Jobin-Robitaille, O., Allard, S., & Côté, J. (2005). Regulation of NuA4 Histone Acetyltransferase Activity in Transcription and DNA Repair by Phosphorylation of Histone H4. *Molecular and Cellular Biology*, *25*(18), 8179–8190. https://doi.org/10.1128/MCB.25.18.8179-8190.2005

van der Heijden, G. W., Derijck, A. A. H. A., Ramos, L., Giele, M., van der Vlag, J., & de Boer, P. (2006). Transmission of modified nucleosomes from the mouse male germline to the zygote and subsequent remodeling of paternal chromatin. *Developmental Biology*, *298*(2), 458–469. https://doi.org/10.1016/j.ydbio.2006.06.051

van der Heijden, G. W., Dieker, J. W., Derijck, A. A. H. A., Muller, S., Berden, J. H. M., Braat, D. D. M., van der Vlag, J., & de Boer, P. (2005). Asymmetry in Histone H3 variants and lysine methylation between paternal and maternal chromatin of the early mouse zygote. *Mechanisms of Development*, *122*(9), 1008–1022. https://doi.org/10.1016/j.mod.2005.04.009

Vavouri, T., & Lehner, B. (2011). Chromatin organization in sperm may be the major functional consequence of base composition variation in the human genome. *PLoS Genetics*, *7*(4), e1002036. https://doi.org/10.1371/journal.pgen.1002036

Vilfan, I. D., Conwell, C. C., & Hud, N. V. (2004). Formation of Native-like Mammalian Sperm Cell Chromatin with Folded Bull Protamine. *Journal of Biological Chemistry*, *279*(19), 20088–20095. https://doi.org/10.1074/jbc.M312777200

Vilfan, I. D., Conwell, C. C., Sarkar, T., & Hud, N. v. (2006). Time Study of DNA Condensate Morphology: Implications Regarding the Nucleation, Growth, and Equilibrium Populations of Toroids and Rods. *Biochemistry*, *45*(26), 8174–8183. https://doi.org/10.1021/bi060396c

Vollmuth, F., & Geyer, M. (2010). Interaction of Propionylated and Butyrylated Histone H3 Lysine Marks with Brd4 Bromodomains. *Angewandte Chemie International Edition*, *49*(38), 6768–6772. https://doi.org/10.1002/anie.201002724

Wang, H., Huang, Z.-Q., Xia, L., Feng, Q., Erdjument-Bromage, H., Strahl, B. D., Briggs, S. D., Allis, C. D., Wong, J., Tempst, P., & Zhang, Y. (2001). Methylation of Histone H4 at Arginine 3 Facilitating Transcriptional Activation by Nuclear Hormone Receptor. *Science*, *293*(5531), 853–857. https://doi.org/10.1126/science.1060781

Wang, T., Gao, H., Li, W., & Liu, C. (2019). Essential Role of Histone Replacement and Modifications in Male Fertility. *Frontiers in Genetics*, *10*. https://doi.org/10.3389/fgene.2019.00962

Wang, X., Kang, J.-Y., Wei, L., Yang, X., Sun, H., Yang, S., Lu, L., Yan, M., Bai, M., Chen, Y., Long, J., Li, N., Li, D., Huang, J., Lei, M., Shao, Z., Yuan, W., Zuo, E., Lu, K., … Li, J. (2019). PHF7 is a novel histone H2A E3 ligase prior to histone-to-protamine exchange during spermiogenesis. *Development*. https://doi.org/10.1242/dev.175547

Wang, Y., Wang, H., Zhang, Y., Du, Z., Si, W., Fan, S., Qin, D., Wang, M., Duan, Y., Li, L., Jiao, Y., Li, Y., Wang, Q., Shi, Q., Wu, X., & Xie, W. (2019). Reprogramming of Meiotic Chromatin Architecture during Spermatogenesis. *Molecular Cell*, *73*(3), 547-561.e6. https://doi.org/10.1016/j.molcel.2018.11.019

Warrant, R. W., & Kim, S.-H. (1978). α-Helix–double helix interaction shown in the structure of a protamine-transfer RNA complex and a nucleoprotamine model. *Nature*, *271*(5641), 130–135. https://doi.org/10.1038/271130a0

Wike, C. L., Guo, Y., Tan, M., Nakamura, R., Shaw, D. K., Díaz, N., Whittaker-Tademy, A. F., Durand, N. C., Aiden, E. L., Vaquerizas, J. M., Grunwald, D., Takeda, H., & Cairns, B. R. (2021). Chromatin architecture transitions from zebrafish sperm through early embryogenesis. *Genome Research*, *31*(6), 981–994. https://doi.org/10.1101/gr.269860.120

Willmitzer, L., Bode, J., & Wagner, K. G. (1977a). Phosphorylated protamines. I. Binding stoichiometry and thermal stability of complexes in DNA. *Nucleic Acids Research*, *4*(1), 149–162. https://doi.org/10.1093/nar/4.1.149

Willmitzer, L., Bode, J., & Wagner, K. G. (1977b). Phosphorylated protamines. II. Circular dichroism of complexes with DNA, dependency on ionic strength. *Nucleic Acids Research*, *4*(1), 163–176. https://doi.org/10.1093/nar/4.1.163

Wu, J. Y., Ribar, T. J., Cummings, D. E., Burton, K. A., McKnight, G. S., & Means, A. R. (2000). Spermiogenesis and exchange of basic nuclear proteins are impaired in male germ cells lacking Camk4. *Nature Genetics*, *25*(4), 448–452. https://doi.org/10.1038/78153

Wykes, S. M., & Krawetz, S. A. (2003). The structural organization of sperm chromatin. *The Journal of Biological Chemistry*, *278*(32), 29471–29477. https://doi.org/10.1074/jbc.M304545200

Xia, X., Zhou, X., Quan, Y., Hu, Y., Xing, F., Li, Z., Xu, B., Xu, C., & Zhang, A. (2019). Germline deletion of Cdyl causes teratozoospermia and progressive infertility in male mice. *Cell Death & Disease*, *10*(3), 229. https://doi.org/10.1038/s41419-019-1455-y

Yamaguchi, K., Hada, M., Fukuda, Y., Inoue, E., Makino, Y., Katou, Y., Shirahige, K., & Okada, Y. (2018). Re-evaluating the Localization of Sperm-Retained Histones Revealed the Modification-Dependent Accumulation in Specific Genome Regions. *Cell Reports*, *23*(13), 3920–3932. https://doi.org/10.1016/j.celrep.2018.05.094

Yin, H., Kang, Z., Zhang, Y., Gong, Y., Liu, M., Xue, Y., He, W., Wang, Y., Zhang, S., Xu, Q., Fu, K., Zheng, B., Xie, J., Zhang, J., Wang, Y., Lin, M., Zhang, Y., Feng, H., Xin, C., … Ye, L. (2021). HDAC3 controls male fertility through enzyme-independent transcriptional regulation at the meiotic exit of spermatogenesis. *Nucleic Acids Research*, *49*(9), 5106–5123. https://doi.org/10.1093/nar/gkab313

Yokonishi, T., Sato, T., Komeya, M., Katagiri, K., Kubota, Y., Nakabayashi, K., Hata, K., Inoue, K., Ogonuki, N., Ogura, A., & Ogawa, T. (2014). Offspring production with sperm grown in vitro from cryopreserved testis tissues. *Nature Communications*, *5*(1), 4320. https://doi.org/10.1038/ncomms5320

Yoshida, K., Muratani, M., Araki, H., Miura, F., Suzuki, T., Dohmae, N., Katou, Y., Shirahige, K., Ito, T., & Ishii, S. (2018). Mapping of histone-binding sites in histone replacement-completed spermatozoa. *Nature Communications*, *9*(1), 3885. https://doi.org/10.1038/s41467-018-06243-9

Yu, Y. E., Zhang, Y., Unni, E., Shirley, C. R., Deng, J. M., Russell, L. D., Weil, M. M., Behringer, R. R., & Meistrich, M. L. (2000). Abnormal spermatogenesis and reduced fertility in transition nuclear protein 1-deficient mice. *Proceedings of the National Academy of Sciences*, *97*(9), 4683–4688. https://doi.org/10.1073/pnas.97.9.4683

Yuen, B. T. K., Bush, K. M., Barrilleaux, B. L., Cotterman, R., & Knoepfler, P. S. (2014). Histone H3.3 regulates dynamic chromatin states during spermatogenesis. *Development*, *141*(18), 3483–3494. https://doi.org/10.1242/dev.106450

Zalenskaya, I. A., Bradbury, E. M., & Zalensky, A. O. (2000). Chromatin structure of telomere domain in human sperm. *Biochemical and Biophysical Research Communications*, *279*(1), 213–218. https://doi.org/10.1006/bbrc.2000.3917

Zhao, M., Shirley, C. R., Mounsey, S., & Meistrich, M. L. (2004). Nucleoprotein Transitions During Spermiogenesis in Mice with Transition Nuclear Protein Tnp1 and Tnp2 Mutations1. *Biology of Reproduction*, *71*(3), 1016–1025. https://doi.org/10.1095/biolreprod.104.028191

Zhao, M., Shirley, C. R., Yu, Y. E., Mohapatra, B., Zhang, Y., Unni, E., Deng, J. M., Arango, N. A., Terry, N. H. A., Weil, M. M., Russell, L. D., Behringer, R. R., & Meistrich, M. L. (2001). Targeted Disruption of the Transition Protein 2 Gene Affects Sperm Chromatin Structure and Reduces Fertility in Mice. *Molecular and Cellular Biology*, *21*(21), 7243–7255. https://doi.org/10.1128/MCB.21.21.7243-7255.2001

Živković, D., Sanchez Dafun, A., Menneteau, T., Schahl, A., Lise, S., Kervarrec, C., Toste Rêgo, A., da Fonseca, P. C. A., Chavent, M., Pineau, C., Burlet-Schiltz, O., Marcoux, J., & Bousquet, M.-P. (2022). Proteasome complexes experience profound structural and functional rearrangements throughout mammalian spermatogenesis. *Proceedings of the National Academy of Sciences*, *119*(15). https://doi.org/10.1073/pnas.2116826119

Zuo, X., Rong, B., Li, L., Lv, R., Lan, F., & Tong, M.-H. (2018). The histone methyltransferase SETD2 is required for expression of acrosin-binding protein 1 and protamines and essential for spermiogenesis in mice. *Journal of Biological Chemistry*, *293*(24), 9188–9197. https://doi.org/10.1074/jbc.RA118.002851

10.

ABBREVIATIONS

A

Ac: Acetylation

A_d: A-dark type spermatogonial stem cell

A_p: A-pale type spermatogonial stem cell

ACT: activator of CREM in the testis

ART: Assisted reproduction techniques

ASF1: Histone chaperone ASF1

ASF/SF2: Serine/arginine-rich splicing factor 1

ATAC-seq: Assay for Transposase-Accessible Chromatin with high-throughput sequencing

AURKC: Aurora Kinase C

AYA: Adolescent and young adults (population)

B

BMI: Body Mass Index

BNC1: Zinc finger protein basonuclin-1

BORIS: Transcriptional repressor CTCFL

BRDT: Bromodomain-containing testis specific protein

BRWD1: Bromodomain and WD repeat-containing protein 1

Bu: Butyrylation

C

CAMK4: Calcium/calmodulin dependent protein kinase type IV

CBP: CREB binding protein

CB1: Cannabinoid receptor 1

CD45: Receptor-type tyrosine-protein phosphatase C

CHD5: Chromodomain-helicase-DNA-binding protein 5

cP2: Cleaved domain of protamine 2 precursor

CREM: cAMP-responsive element modulator

CRISPR/Cas9: Clustered Regularly Interspaced Short Palindromic Repeats and Cas9 associated endonuclease

Cro: Crotonylation

CTCF: Transcriptional repressor CTCF

D

Da: Dalton

DNA: Desoxyribonucleic acid

DICER: Endoribonuclease Dicer

DOT1L: Histone-lysine N-methyltransferase, H3 lysine-79 specific

DPY19L2: Probable C-mannosyltransferase DPY19L2

dsDNA: Double strand DNA

G

GMCL1: Germ cell-less protein-like 1

GRTH: ATP-dependent RNA helicase DDX25

H

HAT: Histone acetyltransferases

hINO80 complex: chromatin remodeling complex including INO80, RUVBL1, and RUVBL2 among others

HIRA: Protein HIRA

Hi-C: High-throughput chromosome conformation capture technique to analyze spatial genome organization and map higher-order chromosome folding

HP: Hypospermatogenesis

HPI1: Intermediate P2 form HPI1

HPI2: Intermediate P2 form HPI2

HPS1: Intermediate P2 form HPS1

HPS2: Intermediate P2 form HPS2

HP2: mature protamine 2

HP3: mature protamine 3

HP4: mature protamine 4

HSPA4L: Heat shock 70 kDa protein 4L

H2A: Canonical histone H2A

H2A.L.2: Histone H2A-Bbd type 1

H2A.Z: Histone H2A.Z

H2B: Canonical histone H2B

H2B.K: Histone H2B type 1-K

H2B.N: Histone H2B type 1-N

H2BFWT: Histone H2B type W-T

H3: Canonical histone H3

H3.3: Histone H3.3

H3.4: Histone H3.4

H4: Canonical histone H4

I

ICSI: Intra-cytoplasmic sperm injection

IGF2BP3: Insulin-like growth factor 2 mRNA-binding protein 3

IMSI: Intra-cytoplasmic morphologically selected sperm injection

IVF: *In vitro* fertilization

K

K: Lysine

KPNA6: Importin subunit alpha-7

L

L (measure): Length

LIS1: Platelet-activating factor acetylhydrolase IB subunit beta

L3MBTL2: Lethal(3)malignant brain tumor-like protein 2

M

MCM7: DNA replication licensing factor MCM7

MDA: Malondialdehyde

Me(n): Methylation (n indicates number of methyl groups)

mRNA: messenger RNA

Mz/mL: Millions of sperm per millilitre (unit)

N

NH-NP transition: Nucleo-histone to nucleo-protamine transition

NP-NH transition: Nucleo-protamine to nucleo-histone transition

NuA4: Mammalian nucleosome acetyltransferase of canonical histone H4

NUT: NUT family member 1

P

PABP1: Polyadenylate-binding protein 1

PCR: Polymerase chain reaction

PIH1D1: PIH1 domain-containing protein 1

piRNAs: Piwi-interacting RNAs

PIWI: Protein PIWI

PKA: c-AMP-dependent protein kinase A

PKC: Protein kinase C

PP1γ2: Serine/threonine-protein phosphatase PP1-gamma catalytic subunit

PPP1R7: Protein phosphatase 1 regulatory subunit 7

PPP1R11: Protein phosphatase 1 regulatory subunit 11

Pre-P2: Protamine 2 precursor

PSMA8: Proteasome subunit alpha type-8

PTM: Post-translational modification (PTMs refers to the plural)

PYGO2: Pygopus homolog 2

P1: Protamine 1

P2: Protamine 2 family

P300: Histone acetyltransferase p300

Q

***q* (SAXS)**: Scattering vector

R

R (amino acid): Arginine

RC: Round cells

R (measure): radius

Req: Equivalent radius

Rg: Radius of gyration

RFX2: DNA-binding protein RFX2

RMP: Unconventional prefoldin RPB5 interactor

RNA: Ribonucleic acid

ROS: Reactive oxygen species

RPAP3: RNA polymerase II-associated protein 3

RUVBL1: RuvB-like 1 protein

RUVBL2: RuvB-like 2 protein

R2TP complex: protein complex composed by RPAP3-PIH1D1, RUVBL1, and RUVBL2

S

S: Serine

SA: Spermatogenic arrest

SAXS: Small-Angle X-ray Scattering

SCD: Sperm chromatin dispersion (test)

SCOS: Sertoli-cell only syndrome

SCSA: Sperm chromatin structure assay

SD Standard deviation

Ser: Serine

SETD2: Histone-lysine N-methyltransferase SETD2

SLY: Sycp3-like Y-linked protein

SMRT/N-CoR complex: Nuclear receptor corepressor (NCoR) and silencing mediator for retinoid and thyroid hormone receptors (SMRT) complex

sncRNAs: Small non-coding RNAs

SOX30: Transcription factor SOX-30

SRCAP complex: protein complex composed by SRCAP, Znhit1, YL-1, and H2A.Z

SRPK1: SRSF protein kinase 1

SRSF: Serine/arginine-rich splicing factor

SRY: Sex determining region Y

ssDNA: Single strand DNA

T

TADs: Topologically associated domains

TAF7L: Transcription initiation factor TFIID subunit 7-like

TARBP2: RISC-loading complex subunit TARBP2

TBL1XR1: F-box-like/WD repeat-containing protein TBL1XR1

TGCT: Testicular germ cell tumor

TH2A: Testis-Specific Histone Variant TH2A

TH2B: Testis-Specific Histone Variant TH2B

TISP40: Cyclic AMP-responsive element-binding protein 3-like protein 4

tRNA: Transfer RNA

TSGA8: Testis-specific gene A8 protein

tsHMG: Testis-specific HMG-box protein

TSSK6: Testis-specific serine/threonine-protein kinase 6

TUNEL: Terminal deoxynucleotidyl transferase dUTP nick end labeling (assay)

TPs: Transition proteins

TP1: Transition protein 1

TP2: Transition protein 2

W

WDR92: Dynein axonemal assembly factor 10

WHO: World Health Organization

Z

ZFP628: Zinc finger protein 628

Zn^{2+}: Zinc ion

Others

3D: tridimensional

ξ: fractal cutoff

γH2AX: histone variant H2A.X phosphorylated at Ser139